Glycoprotein A repetition predominant (GARP) as a key molecule in the immunosuppressive tumor microenvironment

Glycoprotein A repetition predominant (GARP) als Schlüsselmolekül im immunsuppressiven Tumormikromilieu

Dissertation zur Erlangung des Grades
Doktor der Naturwissenschaften

Am Fachbereich Biologie
der Johannes Gutenberg-Universität Mainz

Niklas Zimmer
geboren am 04.10.1990 in Mainz

Mainz, den 07.02.2024

Dekan: Prof. Dr. Eckhard Thines

1.Berichterstatter: [redacted]

2.Berichterstatter: [redacted]

Tag der mündlichen Prüfung: 07.06.2024

DECLARATION OF AUTHORSHIP

I hereby confirm that I have authored this PhD thesis independently and without use of other than the indicated resources.

EIDESSTATTLICHE VERSICHERUNG

Hiermit bestätige ich, dass ich die vorliegende Dissertation selbstständig und ohne Zuhilfenahme von anderen als den angegebenen Quellen verfasst habe.

Mainz, 07.02.2024 _____

Niklas Zimmer

List of Contents

ZUSAMMENFASSUNG **8**

SUMMARY **11**

GRAPHICAL ABSTRACT **14**

1.0 INTRODUCTION **15**

1.1 IMMUNOTOLERANCE IN CANCER – TUMOR MICROENVIRONMENT 15
1.2 MANUSCRIPT I: OVERVIEW OF GARP - GLYCOPROTEIN A REPETITIONS PREDOMINANT 18
Summary of own contributions *18*
Zusammenfassung *18*
Abstract *18*
1.2.1 GARP expression, structure, and function *19*
1.2.1.1 LRRC32 Gene Structure 19
1.2.1.2 GARP Protein Structure 19
1.2.2 GARP Function *20*
1.2.3 GARP Regulation *20*
1.2.3.1 GARP and its regulation in Treg 20
1.2.3.2 Interplay of GARP and Foxp3 21
1.2.3.3 Pre-transcriptional Regulation of LRRC32 21
1.2.3.4 Post-transcriptional regulation of the GARP mRNA 23
1.2.3.5 Post-translational regulation of GARP 23
1.2.4 Soluble GARP (sGARP) *24*
1.2.5 Cellular GARP *25*
1.2.5.1 Regulatory T cells 25
1.2.5.2 Non-Treg cells 26
1.2.5.3 Platelets 26
1.2.5.4 Tumor cells 27

2.0 MOTIVATION AND OBJECTIVES **28**

3.0 GARP ON GLIOBLASTOMA **29**

3.1 OVERVIEW: GLIOBLASTOMA 29
3.1.1 Epidemiology *29*
3.1.2 Diagnosis & Pathology *29*
3.1.3 Therapy *31*
3.2 CANCER STEM CELLS IN GLIOBLASTOMA AND THEIR RELEVANCE IN THERAPY RESISTANCE 32
3.2.1 GSC plasticity *33*
3.2.2 GSC identification & isolation *35*
3.3 MANUSCRIPT II: GARP AS AN IMMUNE REGULATORY MOLECULE IN THE TUMOR MICROENVIRONMENT OF GLIOBLASTOMA MULTIFORME 37
Summary of own contributions *37*
Zusammenfassung *37*
Abstract *37*
3.3.1 Introduction *38*
3.3.2. Results *38*
3.3.2.1. GARP Expression on Immunohistochemistry of Glioblastoma and Low-Grade Astrocytomas 38
3.3.2.2. GARP Expressed on the Surface of GB and in the Cytoplasma and Nucleus 41
3.3.2.3. GB Cell Line T98G Suppresses T Effector Cell Function 43
3.3.3. Discussion *44*
3.3.4. Materials and Methods *46*
3.3.4.1. Cell Culture 46
3.3.4.2. Isolation and Stimulation of Human $CD4^+$ T Cells and Treg 46
3.3.4.3. Flow Cytometry 47
3.3.4.4. Confocal Microscopy 47

3.3.4.5. GARP-Immunohistochemistry ... 47
3.3.4.6. Statistics ... 48
3.3.5. Conclusions ... 48
3.3.6. Supplementary Materials ... 48
3.4 MANUSCRIPT III: NUCLEAR GLYCOPROTEIN A REPETITION PREDOMINANT IS A COMMON TRAIT OF GLIOBLASTOMA STEM-LIKE CELLS AND CORRELATES WITH POOR SURVIVAL IN GLIOBLASTOMA PATIENTS. ... 50
Summary of own contributions ... 50
Zusammenfassung ... 50
Abstract ... 51
3.4.1. Introduction ... 51
3.4.2. Materials and Methods ... 52
3.4.2.1 Cell culture ... 52
3.4.2.2 Western blot ... 52
3.4.2.3 Flow cytometry ... 52
3.4.2.4 Confocal microscopy ... 53
3.4.2.5 Animal experiments ... 53
3.4.2.6 GARP Immunohistochemistry and immunofluorescence ... 53
3.4.2.7 Cell sorting ... 54
3.4.2.8 Extreme limiting dilution assay ... 54
3.4.2.9 Bioinformatic pipeline ... 54
3.4.2.10 Statistics ... 55
3.4.3. Results ... 55
3.4.3.1. GARP expression is conserved across different types of GSC in vitro and in vivo ... 55
3.4.3.2. Intratumoral heterogeneity of subcellular distribution patterns of GARP ... 57
3.4.3.3. Relationship between GARP expression and GSC stemness ... 60
3.4.3.4. GARP mRNA and surface protein levels do not predict GB patient survival ... 62
3.4.3.5. Nuclear localization of GARP correlates with poor survival in patients with GB ... 64
3.4.4. Discussion ... 66
3.4.5. Conclusions ... 68
3.4.6. Supplementary Materials ... 69

4.0 GARP ON PLATELETS IN MALIGNANT MELANOMA ... 79

4.1 OVERVIEW: MELANOMA ... 79
4.1.1 Epidemiology ... 79
4.1.2 Diagnosis & Pathology ... 79
4.1.3 Therapy ... 80
4.2 MANUSCRIPT IV: PLATELET-DERIVED GARP INDUCES PERIPHERAL REGULATORY T CELLS—POTENTIAL IMPACT ON T CELL SUPPRESSION IN PATIENTS WITH MELANOMA-ASSOCIATED THROMBOCYTOSIS ... 82
Summary of own contributions ... 82
Zusammenfassung ... 82
Abstract ... 82
4.2.1. Introduction ... 83
4.2.2. Results ... 83
4.2.2.1. Expression of GARP on Platelets ... 83
4.2.2.2. Platelet-Derived GARP Induced Peripheral Regulatory T cells ... 84
4.2.2.3. Role of TGF-β and Platelet-Conditioned Medium in Platelet-Mediated iTreg Induction ... 88
4.2.2.4. Correlation of Thrombocytosis and Prognosis—Clinical Impact of Platelets Expressing Increased Levels of GARP ... 91
4.2.3. Discussion ... 92
4.2.4. Materials and Methods ... 95
4.2.4.1. Isolation of Pre-Activated and Resting Platelets and Preparation of Platelet-Conditioned Medium ... 95
4.2.4.2. Isolation and Stimulation of Human T Cell Populations ... 95
4.2.4.3. Enzyme-Linked Immunosorbent Assay ... 96
4.2.4.4. Flow Cytometry ... 96
4.2.4.5. Patients ... 96
4.2.4.6. Statistics ... 97
4.2.5. Conclusions ... 97

4.2.6 Appendix *98*

5.0 GENERAL DISCUSSION **104**

5.1 GARP AS A BIOMARKER 104
5.2 GARP AS A THERAPEUTIC TARGET 105
5.3 OPEN QUESTIONS AND FUTURE DIRECTIONS 107

6.0 CONCLUSION **109**

7.0 REFERENCES **110**

8.0 LIST OF FIGURES AND TABLES **133**

8.1 LIST OF FIGURES 133
8.2 LIST OF TABLES 134

9.0 ACKNOWLEDGMENTS **135**

10.0 CURICULUM VITAE **136**

11.0 APPENDIX **138**

Preface

This thesis is part of research, which was done between 2017 and 2022 in the group of Prof. Dr. med. Andrea Tüttenberg in the Department of Dermatology of the University Medical Center Mainz. Contents of this thesis were published in the following manuscripts (reverse chronological order).

1. Nuclear GARP expression is a common trait of glioblastoma stem-like cells that correlates with poor survival in glioblastoma patients. (Article)
   Zimmer N*, Trzeciak ER*, Licht P, Sprang B, Leukel P, Mailänder V, Ringel F, Sommer C, Tuettenberg J, Kim E, Tuettenberg A.
   Cancers 2023, 15(24), 5711; https://doi.org/10.3390/cancers15245711
2. GARP as a Therapeutic Target for the Modulation of Regulatory T Cells in Cancer and Autoimmunity. (Review)
   Zimmer N, Trzeciak ER, Graefen B, Satoh K, Tuettenberg A.
   Front Immunol. 2022 Jul 8;13:928450. doi: 10.3389/fimmu.2022.928450
3. Platelet-Derived GARP Induces Peripheral Regulatory T Cells-Potential Impact on T Cell Suppression in Patients with Melanoma-Associated Thrombocytosis. (Article)
   Zimmer N, Krebs FK, Zimmer S, Mitzel-Rink H, Kumm EJ, Jurk K, Grabbe S, Loquai C, Tuettenberg A.
   Cancers (Basel). 2020 Dec 5;12(12):3653. doi: 10.3390/cancers12123653
4. GARP as an Immune Regulatory Molecule in the Tumor Microenvironment of Glioblastoma Multiforme. (Article)
   Zimmer N, Kim E, Sprang B, Leukel P, Khafaji F, Ringel F, Sommer C, Tuettenberg J, Tuettenberg A.
   Int J Mol Sci. 2019 Jul 26;20(15):3676. doi: 10.3390/ijms20153676

Research based on manuscripts, which are not included in this thesis:

1. GARP Regulates the Immune Capacity of a Human Autologous Platelet Concentrate. (Article)
   Trzeciak ER*, **Zimmer N***, Kämmerer PW, Thiem D, Al-Nawas B, Tuettenberg A, Blatt S.
   Biomedicines. 2022 Dec 5;10(12):3136. doi: 10.3390/biomedicines10123136
2. Oxidative Stress Differentially Influences the Survival and Metabolism of Cells in the Melanoma Microenvironment. (Article)
   Trzeciak ER, **Zimmer N**, Gehringer I, Stein L, Graefen B, Schupp J, Stephan A, Rietz S, Prantner M, Tuettenberg A.
   Cells. 2022 Mar 8;11(6):930. doi: 10.3390/cells11060930
3. In-Depth Immune-Oncology Studies of the Tumor Microenvironment in a Humanized Melanoma Mouse Model. (Article)
   Schupp J, Christians A, **Zimmer N**, Gleue L, Jonuleit H, Helm M, Tuettenberg A.
   Int J Mol Sci. 2021 Jan 20;22(3):1011. doi: 10.3390/ijms22031011
4. Stability of Alkyl Chain-Mediated Lipid Anchoring in Liposomal Membranes. (Article)
   Gleue L, Schupp J, **Zimmer N**, Becker E, Frey H, Tuettenberg A, Helm M.
   Cells. 2020 Sep 29;9(10):2213. doi: 10.3390/cells9102213
5. Targeting myeloid cells in the tumor sustaining microenvironment. (Review)
   Schupp J*, Krebs FK*, **Zimmer N***, Trzeciak E, Schuppan D, Tuettenberg A.
   Cell Immunol. 2019 Sep;343:103713. doi: 10.1016/j.cellimm.2017.10.013

(*equal contribution)

Zusammenfassung

Bei Krebserkrankungen ist ein entscheidender Mechanismus, der einer erfolgreichen (Immun-) Therapie im Wege steht, die aktive Unterdrückung der immunologischen Abwehr bei Tumorpatienten. In diesem Zusammenhang spielen allgemeine immunologische Toleranzmechanismen eine entscheidende Rolle. So leisten beispielsweise regulatorische T-Zellen (Treg), tolerogene dendritische Zellen (tolDC) und myeloid-derived suppressor cells (MDSC) einen wichtigen Beitrag. Lösliche Faktoren wie IL-10 und TGF-β, die von Treg und tolDC produziert werden, induzieren ein immunsuppressives Tumormikromilieu (TME) und fördern das Wachstum, die Ausbreitung und die Metastasierung des Tumors.

Das Glioblastom (GB) ist der häufigste und aggressivste primäre Hirntumor bei Erwachsenen, mit einer medianen Überlebensrate von nur 15 Monaten. Die konventionelle Standardbehandlung für neu diagnostizierte primäre GB besteht aus Operation, Bestrahlung und anschließender Anwendung von Temozolomid (TMZ). Eine signifikante Tumorinfiltration in gesundes Hirngewebe schränkt die Wirksamkeit der neurochirurgischen Resektion ein. Nach einer multimodalen Behandlung ist ein GB-Rezidiv praktisch sicher. In Primärtumoren und bei Rezidiven hemmen die immunsuppressiven Eigenschaften von z. B. Tumorzellen, Mikroglia und eindringenden Treg eine wirksame Antitumorreaktion. Die Immuntherapie ist eine der vielversprechendsten Behandlungen für diese rezidivierenden GB, insbesondere, wenn sie auf die hemmende T-Zell-Signalübertragung im TME über den "programmed cell death protein 1" (PD-1), den PD-1-Rezeptor oder "cytotoxic T-lymphocyte-associated Protein 4" (CTLA-4) abzielt. Trotz umfangreicher experimenteller und klinischer Forschung ist GB nach wie vor eine der tödlichsten Krebsarten beim Menschen, mit einer Sterblichkeitsrate von nahezu 100%. Aus diesem Grund besteht ein dringender Bedarf an der Entwicklung zusätzlicher Therapien, die auf die spezifischen immunsuppressiven Signalwege von GB abzielen.

Zu dem hohen Grad an inhärenter und erworbener Therapieresistenz bei GB trägt die außergewöhnliche starke intratumorale Heterogenität bei. Diese manifestiert sich in der Vielfalt der molekularen und zellulären Subtypen/Zellzustände, die vor allem durch stammzellähnliche Glioblastomzellen (GSC) bedingt sind. GSC sind eine Subpopulation von Tumorzellen mit (Krebs-) Stammzellmerkmalen wie unbegrenzter Selbsterneuerung, abnormaler Differenzierungsreaktion und inhärenter Plastizität. GSC können auf Umwelteinflüsse reagieren, indem sie ihren zellulären Zustand ändern. Es wird angenommen, dass GSC aufgrund dieser einzigartigen Eigenschaften während oder nach zytotoxischen Therapien, die Glioblastomzellen abtöten, überleben und den Tumor wieder aufbauen können. GSC sind die Hauptursache für Therapieresistenz und Tumorrezidive bei GB. Daher sind GSC das klinisch relevanteste Ziel für GB, aber sie sind aus mehreren Gründen in Tumoren schwer zu erfassen:
(I) der relativ geringe Prozentsatz von GSC im Vergleich zum Rest der Tumorzellen, bei denen es sich vermutlich in erster Linie um Nicht-Stamm-Gliomzellen oder differenzierte Nachkommen von GSC handelt, (II) eine inhomogene Verteilung von GSC innerhalb des Tumors, die sich in spezialisierten Nischen befinden, die ein geeignetes Umfeld für die Aufrechterhaltung ihres undifferenzierten Zustands bieten, und (III) die phänotypische Vielfalt und inhärente Plastizität von GSC, die in der Lage sind, dynamisch zwischen zellulären Zuständen und morphologischen Phänotypen zu wechseln.

Darüber hinaus erschwert das Fehlen stabiler Marker bei GSC die diagnostische Klassifizierung auf der Grundlage von Tumorproben. Aufgrund der phänotypischen Variabilität von GSC wurden im Laufe der Zeit verschiedene potenzielle Marker mit GSC in Verbindung gebracht, die jedoch letztlich nicht zu einer universellen Identifizierung führen. GSC bestehen aus hierarchisch getrennten Zellen mit unterschiedlichen stammähnlichen Potenzialen. Diese phänotypische Vielfalt und die Flexibilität der GSC, sich an das Tumormilieu anzupassen, haben entscheidende Auswirkungen auf der Suche nach GSC-Markern. GSC-Marker müssen universell einsetzbar sein und verschiedene Untergruppen von GSC identifizieren, und zwar unabhängig von ihrem aktuellen Zellzustand. Ein potentieller GSC Marker ist Glykoprotein A repetition predominant (GARP).

GARP, ein Transmembranprotein vom Typ I, wurde zuerst auf der Oberfläche von Blutplättchen und auf aktivierten Treg identifiziert. GARP wird durch das Gen LRRC32 kodiert und besteht aus 662 Aminosäuren mit einer 20 Leucin-reichen externen Domäne, einer hydrophoben Transmembranregion

und einem 15 Aminosäuren langen intrazellulären Teil. Im Allgemeinen ist GARP als ein nicht-signalisierender Andockrezeptor bekannt, der für die Erzeugung und Oberflächenexpression des latenten transformierenden Wachstumsfaktors beta (TGF-β) benötigt wird. Es ist beschrieben worden, dass die Bindung und Freisetzung von TGF-β durch GARP die periphere Toleranz und die Krebsentwicklung beeinflusst. Darüber hinaus kann GARP selbst von der Oberfläche von z.B. aktivierten Treg und Thrombozyten in seiner löslichen Form, soluble GARP (sGARP), freigesetzt werden.

In der Vergangenheit hat unsere Arbeitsgruppe herausgefunden, dass sGARP in der Lage ist, periphere Toleranz zu induzieren. GARP fördert die Anhäufung von suppressiven Treg und verhindert chronische Entzündungskrankheiten in humanisierten Mäusen. Darüber hinaus ist GARP in der Lage, die Funktion zytotoxischer $CD8^+$-T-Zellen zu hemmen und die Differenzierung von Makrophagen in einen tolerogenen Phänotyp zu stimulieren. GARP ist also ein funktionelles immunsuppressives Protein, das Effektorzellreaktionen im TME verhindert und die periphere Toleranz fördert.

Kürzlich wurde GARP auf den Zellen bösartiger Tumoren wie Melanom und GB nachgewiesen. In Zimmer et al., 2019 (beschrieben in 3.3), wiesen wir GARP in GB und niedriggradigen Astrozytomen nach. Weitere durchflusszytometrische Analysen zeigten eine starke Expression von GARP auf der Oberfläche von GB-Zellen und GSC. Wir konnten zeigen, dass GB über GARP eine starke immunsuppressive Wirkung ausübt. Eine Kokultur der GB-Zelllinie T98G mit T-Zellen führte zu einer starken Unterdrückung der T-Zell-Funktion, die durch die Verwendung eines GARP-Antikörpers, der den Rezeptor blockierte, wieder aufgehoben wurde.

In Zimmer et al., 2023 (beschrieben in 3.4) konnten wir zeigen, dass die Expression von GARP in Bezug auf den Differenzierungsstatus und die Fähigkeit zur Selbsterneuerung bei verschiedenen Arten von GSC konserviert ist. Im Gegensatz zu anderen Markern wie CD133 bleibt die Expression von GARP während der gesamten Therapie erhalten, was auf eine wichtige Rolle bei der Funktion von GSC hinweist. Die Expression von GARP war in allen GSC stabil, auch wenn sie aus verschiedenen Regionen desselben Tumors stammten, was die bereits beschriebene stabile Expression von GARP in verschiedenen Tumorregionen und während der Therapie weiter untermauert. Überraschenderweise sagte die Gesamtexpression der GARP-mRNA das Überleben von Patienten mit GB nicht voraus. Neben seiner Rolle als immunsuppressives Molekül im TME und als potenzieller ergänzender Marker für die Identifizierung von GSC wurde GARP zum ersten Mal im Kern und im Zytoplasma von aktivierten Treg bzw. Tumorzellen, einschließlich GSC, lokalisiert. Diese Kernlokalisierung von GARP korrelierte mit einer schlechten Überlebensrate bei Patienten mit GB, was zeigt, dass nicht die Gesamtexpression von GARP im Tumor, sondern die Häufigkeit von GARP-positiven Kernen ein wichtiger prognostischer Marker für das Fortschreiten von Krebs ist.

Insgesamt konnten wir zeigen, dass GARP zur immunsuppressiven Mikroumgebung des Tumors beiträgt, ein potenzieller ergänzender Marker für die Charakterisierung und Identifizierung menschlicher GSC ist und durch seine Kernlokalisierung ein Marker für das Überleben der Patienten ist.

Aufgrund ihres Vorkommens in den perivaskulären und pseudopalisierenden Zonen des GB kommen die GSC mit Blutplättchen in Kontakt. In der Vergangenheit wurde eine synergetische Beziehung zwischen Thrombozyten und anderen Krebsarten beschrieben, aber detaillierte Informationen sind immer noch schwer zu finden. Kürzlich konnten Sloan et al. (2022) zeigen, dass GSC Thrombozyten aktivieren, um ihre Stammzelleneigenschaften zu erhöhen und das Tumorwachstum weiter zu fördern. Diese Effekte ließen sich durch pharmakologische Unterdrückung gezielt beeinflussen. Dies unterstreicht die Verbindung zwischen Thrombozyten und Krebs(stamm)zellen, die bösartige Erkrankungen begünstigen. Dieser Befund ist von Bedeutung, da sich bei mehreren bösartigen Erkrankungen gezeigt hat, dass eine Thrombozytose (hohe Thrombozytenzahlen) mit schlechten klinischen Ergebnissen korreliert, wie bereits beim Melanom beschrieben.

Thrombozyten gerinnen, um Blutungen zu stoppen; neue Forschungsergebnisse deuten jedoch darauf hin, dass sie auch die Anti-Tumor-Immunantwort und die Mikroumgebung des Tumors beeinflussen. Die krebsassoziierte Thrombozytose ist ein gängiger prädiktiver Marker für eine schlechte Überlebensprognose bei verschiedenen Krebsarten. Außerdem verschlimmert die Thrombozytose die Metastasierung, die Invasion und das Wachstum des Tumors. Die gezielte

Behandlung von Thrombozyten, z. B. die Thrombozytenaktivierung und/oder hohe Thrombozytenzahlen, verringert die Metastasierung. Darüber hinaus fördern Thrombozyten die Beweglichkeit von Krebszellen, den epithelial-mesenchymalen Übergang (EMT), das Überleben, die Umgehung des Immunsystems, die Adhäsion von Endothelzellen und die Extravasation.

GARP wurde Erstmals auf Blutplättchen beschrieben. Wir stellten die Hypothese auf, dass Thrombozyten zur Entwicklung einer peripheren Toleranz führen und somit durch eine Verringerung der Wirtsimmunität sowohl Malignität als auch Behandlungsresistenz fördern können. In Zimmer et al., 2021 (beschrieben in 4.2), beschrieben wir, dass Thrombozyten exprimiertes GARP zu Induktion von peripheren Treg führt. Kokulturen von $CD4^+CD25^-$T-Zellen mit Thrombozyten führten zu einem signifikanten Anstieg der Foxp3- und GARP-Expression, während die Proliferation und die Produktion der Effektorzytokine IL-2 und IFN-γ gehemmt wurden, was auf einen regulatorischen, immunsuppressiven Phänotyp hindeutet. Darüber hinaus besaßen diese "plättcheninduzierten" Treg eine signifikante Suppressionskapazität. Es zeigte sich, dass die durch Thrombozyten ausgelöste Treg-Induktion GARP-abhängig ist, da ein blockierender GARP-Antikörper die Auswirkungen der Thrombozyten-Kokultur umkehren konnte und die Induktion von Treg hemmte. Diese GARP-abhängigen Effekte konnten auch bei der Verwendung von thrombozytenkonditioniertem Medium beobachtet werden, was darauf hindeutet, dass die beobachteten Effekte zum Teil unabhängig vom Zellkontakt sind. Die GARP-abhängige Induktion von Treg stellt einen bedeutenden Beitrag zum immunsuppressiven TME dar und könnte die Korrelation zwischen Thrombozytose und schlechtem Überleben bei Krebs erklären. Die Analyse von Thrombozyten von Melanompatienten in den Stadien I und IV im Vergleich zu gesunden Spendern ergab, dass Thrombozyten von Melanompatienten im Vergleich zu gesunden Kontrollen eine signifikant erhöhte GARP-Expression und einen erhöhten Thrombozytenaktivierungsstatus aufweisen. Darüber hinaus hatten Melanompatienten im Stadium IV mit einem hohen Thrombozyten-Lymphozyten-Verhältnis ein wesentlich höheres Risiko, auf eine Therapie mit Immun-Checkpoint-Inhibitoren nicht anzusprechen.

Obwohl die Entwicklung von Immun-Checkpoint-Inhibitoren einen bedeutenden Fortschritt in der Behandlung des Melanoms darstellt und damit die Prognose der Patienten verbessert hat, sprechen viele Patienten nicht auf die Therapie an, so dass sie nur begrenzte therapeutische Alternativen haben.

Infolgedessen werden mehrere Studien durchgeführt, um neue regulatorische Moleküle und Signalwege menschlicher Melanomzellen sowie deren Bedeutung für die Mikroumgebung des Tumors zu identifizieren, um neue immuntherapeutische Ziele zu finden.

Neben den hohen Kosten ist angesichts der steigenden Zahl verfügbarer Medikamente, ihrer Nebenwirkungen und der patientenabhängigen Ansprechraten, die Entwicklung eines auf den einzelnen Patienten zugeschnittenen Behandlungskonzepts unter Verwendung von Biomarkern von entscheidender Bedeutung. Es werden zahlreiche Anstrengungen unternommen, um Faktoren auf zellulärer und löslicher Proteinebene im Gewebe und im peripheren Blut von Tumorpatienten zu identifizieren, die zur genaueren Charakterisierung der Mikroumgebung des Tumors und damit der Prognose und des Therapieansprechens des jeweiligen Patienten verwendet werden können. Dies unterstreicht das Potenzial von GARP auf Thrombozyten als möglicher Biomarker für den Therapieverlauf und seine Bedeutung als immunsuppressives Molekül im TME beim malignen Melanom.

GARP ist ein Protein, das stark in die Krebsimmunität involviert ist und ein potenzielles multifaktorielles Ziel darstellt, um mehrere tumorfördernde Wege gleichzeitig anzugehen. Ein kombinatorischer therapeutischer Ansatz würde gleichzeitig auf Thrombozyten, aktivierte Treg, $GARP^+$-Tumor(stamm)zellen und damit auf das TME abzielen, um die Therapieresistenz bei Krebs zu überwinden. Darüber hinaus könnte GARP als neuartiger Biomarker bei Patienten mit immunbedingten Krankheiten wie Krebs und Autoimmunkrankheiten nützlich sein.

Summary

In cancer, a crucial mechanism standing in the way of successful (immune-)therapy is the active suppression of the immunological defense in tumor patients. In this context, general immunological tolerance mechanisms play a crucial role. For example, regulatory T cells (Treg), tolerogenic dentritic cells (tolDC), and myeloid-derived suppressor cells (MDSC) make an important contribution. Soluble factors such as IL-10 and TGF-β produced by Treg and tolDC induce an immunosuppressive tumor micromilieu (TME) and promote tumor growth, invasion, and metastasis.

Glioblastoma (GB) is the most common and aggressive primary brain tumor in adults, with only a 15-month median survival rate. The conventional standard of care for newly diagnosed primary GB tumors is surgery, radiation, and subsequent application of temozolomide (TMZ). Significant tumor infiltration into healthy brain tissue limits the efficacy of neurosurgical resection. After multi-modal treatment, GB recurrence is practically certain. In primary tumors and in recurrence, the immunosuppressive properties of e.g. tumor cells, microglia and invading Treg inhibit an effective anti-tumor response. Immunotherapy is one of the most promising treatments for recurrent GB, especially targeting inhibitory T cell signaling in the TME via programmed cell death 1 (PD-1), the PD-1 receptor, or CTLA-4. Despite significant experimental and clinical research, GB remains one of the deadliest cancers in humans, with a near 100% mortality rate. Because of this, there is an urgent need for the development of additional therapies that target the specific immunosuppressive pathways of GB.

The high degree of therapeutic resistance in GB, either inherent or acquired by therapy, and the extraordinary intratumoral heterogeneity, manifested by the diversity of molecular and cellular subtypes/cellular states associated with glioblastoma stem-like cells (GSC), contribute to poor prognosis. GSC are a subpopulation of tumor cells that share some classical stem cell traits in a malignant form, such as unlimited self-renewal, innately slow growing, (ab-) normal differentiation response, and innate plasticity. GSC can respond to environmental inputs by switching cellular states. It is hypothesized that GSC may survive and rebuild the tumor during or after cytotoxic therapies that kill non-stem glioma cells due to these unique features. GSC are the major causes of therapeutic resistance and tumor recurrence in GB. Therefore, GSC are the most clinically relevant cellular target in GB, but they are difficult to assess in tumors due to several reasons:

(I) the relatively low percentage of GSC compared to the rest of the tumor cells, which are thought to be primarily non-stem glioma cells or differentiated progenies of GSC, (II) an inhomogeneous distribution of GSC within the tumor, which are located in specialized niches that provide a proper environment for maintaining their undifferentiated state, and (III) phenotypic diversity and inherent plasticity of GSC, that are capable of dynamically transitioning between cellular states and morphological phenotypes.

Additionally, the lack of stable markers on GSC complicates diagnostic classification based on tumor samples. Due to the phenotypic variability of GSC, various potential markers have been linked to GSC, but they ultimately fail to universally identify them. GSC consist of hierarchically separate cells with different stem-like potentials. This phenotypic variety and flexibility of GSC to adapt to the tumor milieu have crucial implications on the quest for GSC markers. GSC markers have to be universally applicable and have to identify GSC independently of their current cellular state.

Glycoprotein A repetitions predominant (GARP), a type I transmembrane protein was first identified on the surface of platelets and activated Treg. GARP is encoded by the gene LRRC32 and consists of 662 amino acids with a 20 leucine rich external domain, a hydrophobic transmembrane region, and a 15 amino acid long intracellular portion. More common, GARP is known as a non-signaling docking receptor, needed for the generation and surface expression of latent transforming growth factor beta (TGF-β). It has been described that TGF-β binding and release by GARP affects peripheral tolerance and

cancer development. Furthermore, GARP itself can be released from the surface of e.g., activated Treg, platelets and cancer cells in its soluble form sGARP.

In the past, our group found that sGARP is able to induce peripheral tolerance. GARP promotes the accumulation of suppressive Treg and prevents chronic inflammatory illness in humanized mice. Furthermore, GARP is able to inhibit $CD8^+$ cytotoxic T cell function and to stimulate macrophage differentiation into a tolerogenic phenotype. Thus, GARP is a functional immunosuppressive protein that prevents effector cell responses in the TME and promotes peripheral tolerance.

Recently, GARP has been detected on the cells of malignant tumors, like melanoma and GB. In Zimmer et al., 2019 (described in 3.3), we detected GARP in GB and low-grade astrocytoma. Further flow cytometric analyses revealed a strong expression of GARP on the surface of GB cells and GSC. We were able to show that GB exerts strong immunosuppressive effects via GARP. A coculture of the GB cell line T98G and T cells resulted in a strong suppression of T-effector cell function, which was reversed by the use of a GARP antibody that blocked the receptor.

In Zimmer et al., 2023 (described in 3.4) we were able to show that the expression of GARP is conserved across different types of GSC with regard to differentiation status and self-renewal capacity. GARP expression is conserved throughout therapy, unlike other markers like CD133, indicating an important role in GSC function. The expression of GARP was stable throughout GSC, with origins in different regions of the same tumor, further supporting the already described stable expression of GARP throughout different regions of the tumor and throughout therapy. Surprisingly, overall GARP mRNA levels did not predict survival in patients with GB. Besides its role as an immunosuppressive molecule in the TME and as a potential complementary marker for GSC identification, GARP was found to be alternatively localized in the nucleus and cytoplasm of activated Treg and tumor cells, including GSC, respectively for the first time. This nuclear localization of GARP correlated with poor survival in patients with GB, showing that the frequency of GARP positive nuclei – not GARP transcript levels – is an important prognostic marker for cancer progression.

Taken together, we were able to show that GARP is a contributor to the immunosuppressive TME, a potential complementary marker for human GSC characterization and identification, and through its nuclear localization, a possible prognostic marker for patient survival.

Due to their presence in the perivascular and pseudopalisading zones of GB, GSC come into contact with platelets. A synergetic relationship between platelets and other cancers has been described in the past, but detailed information is still elusive. Recently, Sloan et al., 2022 were able to show that GSC activate platelets to increase their stemness properties and further promote tumor growth. These effects were targetable by pharmacological suppression. This further underlines the connection between platelets and cancer (stem) cells, which foster malignancies. This finding is of importance as it has been shown in several malignancies that thrombocytosis (high platelet counts) correlates to poor clinical outcomes, as already described in melanoma.

Platelets coagulate to stop bleeding; however, emerging research suggests that they also influence anti-tumor immune responses and the tumor microenvironment. Cancer associated thrombocytosis is a common predictive marker for a poor survival prognosis in several cancers. Furthermore, thrombocytosis worsens cancer metastasis, invasion, and tumor growth. Targeting platelets, e.g., platelet activation and/or high platelet counts decreases metastasis. Furthermore, platelets promote cancer cell motility, epithelial–mesenchymal transition (EMT), survival, immune evasion, endothelial cell adhesion, and extravasation.

GARP was first described as being expressed on platelets. We hypothesized that platelets may lead to the development of peripheral tolerance and thus promote malignancy and treatment resistance by

reducing host immunity. In Zimmer et al., 2021 (described in 4.2), we described that platelet-derived GARP led to the induction of peripheral Treg. Cocultures of $CD4^+CD25^-$ T cells with platelets led to a significant increase in Foxp3 and GARP expression, while the proliferation and effector cytokine production of IL-2 and IFN-γ were inhibited, resembling a regulatory, immunosuppressive phenotype. Furthermore, these “platelet induced” Treg possessed a significant suppressive capacity. Platelet driven Treg induction was shown to be GARP dependent, as a blocking GARP antibody was able to reverse the effects of platelet coculture and inhibited the induction of Treg. These GARP dependent effects could also be observed using platelet conditioned medium, hinting that the observed effects are in part cell contact independent. The GARP dependent induction of Treg resembles a significant contribution to the immunosuppressive TME and could explain the correlation between thrombocytosis and poor survival in cancer. In support of that, the analysis of platelets from melanoma patients at stages I and IV compared to healthy donors revealed that platelets from melanoma patients show a significantly increased level of GARP expression and platelet activation status compared to healthy controls. Furthermore, stage IV melanoma patients with high platelet-to-lymphocyte ratios had a much higher chance of not responding to therapy by immune checkpoint inhibition.

Despite the fact that the development of immune checkpoint inhibitors constitutes a significant advancement in the treatment of melanoma and has thus improved patient prognosis. However, there are few other therapeutic options available to patients who do not react to therapy.

As a result, several studies are being conducted to identify new regulatory molecules and signaling pathways of human melanoma cells, as well as their significance for the tumor microenvironment, in order to identify new immunotherapeutic targets.

Given the rising number of available medication options, side effects, response rates, and costs, developing a treatment concept personalized to each patient utilizing biomarkers is crucial. Numerous efforts are being made to identify factors at both the cellular and soluble protein levels in tumor patients' tissue and peripheral blood that can be used to more precisely characterize the tumor microenvironment and thus the specific patient's prognosis and therapy response. This underlines the potential of GARP on platelets as a potential biomarker for the course of therapy and its importance as an immunosuppressive molecule in the TME in malignant melanoma.

GARP is a protein deeply involved in cancer immunity and a potential multifactorial target to address several pro-tumorigenic pathways at once. A combinatorial therapeutic approach would simultaneously target platelets, activated Treg, $GARP^+$ tumor (stem-) cells, and therefore the TME to overcome therapy resistance in cancer. Furthermore, GARP may be useful as a novel biomarker in patients with immune-related illnesses like cancer and autoimmune diseases.

Graphical Abstract

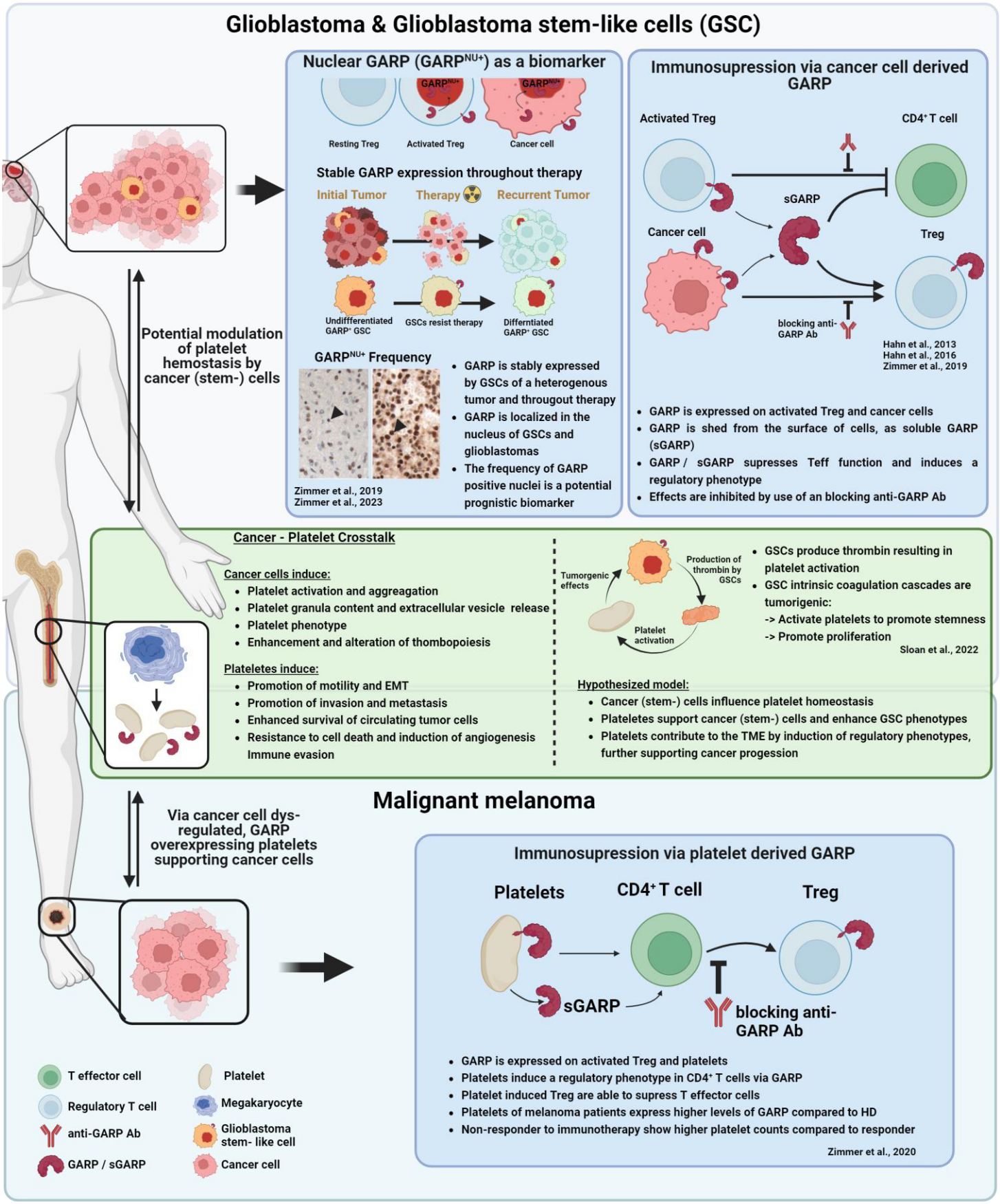

Figure 1: (A) Schematic overview of the role of GARP in the tumor microenvironment based on the findings of this work. Created with BioRender.com

1.0 Introduction

1.1 Immunotolerance in cancer – Tumor microenvironment

The tumor microenviorement (TME) describes the interaction between tumor cells, immune cells and the tissue around them.

The immune system constantly monitors the body. The creation of tumor-specific neo-antigens is a direct consequence of the accumulation of genetic changes in malignant cells. The detection of tumor neo-antigens by the monitoring immune system triggers an effective immune response that eliminates tumor cells without ever being diagnosed (1).The current concept of tumor immune editing divides the alteration of the tumor and the resulting tumor induced tolerance of the immune system into four phases: (I) initiation, (II) elimination, (III) equilibrium, and (IV) escape (see Figure 2) (2). First, malignant cells develop through genetic predisposition and/or external influences (e.g., radiation) from healthy tissue. The second phase involves the concept of immune surveillance. Due to a high burden of genomic mutations, tumor cells develop and express neo-antigens, which are unknown to the immune system. Cytotoxic $CD8^+$ T cells are able to detect these neo-antigens, when they bind to neoantigen-presenting DC in the secondary lymphoid organs (3), following invasion of the TME. Together with natural killer (NK) cells, cytotoxic $CD8^+$ T cells lyse the neo-antigen expressing cancer cell through perforins and granzymes. The third phase describes the balance between the immune response and immune tolerance. Immunological selective pressure results in the survival of tumor cells that have low T cell receptor (TCR)-binding capacity for neo-antigens (antigenicity), lower immunogenicity, and deficient antigen-processing properties due to epigenetic instability (4). Thus, human leukocyte antigen (HLA) molecules may be mutated and downregulated in tumor cells, leading to immune evasion due to reduced recognition of tumor cells by the immune system. If the balance (equilibrium) tips in favor of tumor tolerance, tumor cells are tolerated by the immune system. This marks the beginning of the fourth phase of tumor immunity: uncontrolled tumor growth. Mutations in tumor cell-intrinsic signaling pathways are an "innate" tumor strategy to evade the immune system, leading to the exclusion and suppression of immune cells in the TME.

For example, regulatory T cells (Treg) (5), tolerogenic dendritic cells (tolDC) (6), and myeloid-derived suppressor cells (MDSC) (7, 8) are recruited by the tumor and suppress the anti-tumor immune response against it (see Figure 2 V A). Soluble factors, such as interleukin 10 (IL-10) and transforming growth factor beta (TGF-β), produced by Treg and tolDC (9) induce an immunosuppressive milieu, which leads to the shutdown of the $CD4^+$ and $CD8^+$ effector cells present in the tumor and promotes tumor growth, while proangiogenic factors (Vascular endothelial growth factor - VEGF, platelet-derived growth factor - PDGF, fibroblast Growth Factor - FGF, and interleukin 8 - IL-8) play a role in the promoting tumor angiogenesis (10). Furthermore, the production of cytokines, like IL1-β, induces a phenotype switch to epithelial to mesenchymal transition (EMT), in which tumor cells change or lose their cell-specific properties and thus acquire the ability to migrate, leading to tumor promotion and metastatic expansion. These mechanisms are particularly important in patients at an advanced stage of disease, e.g., patients with a high tumor burden.

However, cell contact-dependent mechanisms such as surface molecules on Treg (Cytotoxic T-lymphocyte-associated Protein 4 - CTLA-4, glucocorticoid-induced TNFR-related protein - GITR) or cell contact-dependent transfer of cyclic adenosine monophosphate (cAMP) into or through Treg also contribute significantly to tolerance development (11, 12).

For Treg, the transcription factor Foxp3 plays a key role in their development and suppressive function (13). Furthermore, several studies have identified additional Treg molecules that contribute to the

characteristic or suppressive properties of these cells. These include CTLA-4, GITR, CD137, CD39, and CD73 (12). Interestingly, some of these "Treg molecules", such as Foxp3 or CD39/73 have been described not only in tumor-infiltrating Treg but also in tumor tissue of solid tumors, including malignant melanoma and GB (14–17), and are part of the immune escape phase. This suggests that tumor cells may have similar regulatory or inhibitory properties and molecular mechanisms as Treg ("Treg mimicry"), thus additionally contributing to the immunosuppressive effect in the immediate tumor microenvironment.

Surgical resection, radiation, and chemotherapy are the most common conventional cancer treatment methods. Surgical resection seeks to physically remove tumor tissue from the body; however, it also has the potential to overlook tumor cells in surrounding tissues or metastases. To eliminate the residual cancer cells, cytotoxic radiotherapy and chemotherapy are frequently used. These drugs work by damaging the DNA of rapidly dividing cells, resulting in cell death. These medicines also cause DNA damage in healthy proliferating cells, which is what causes the therapies' widespread side effects.

Despite the efficacy of radio- and chemotherapies, various people and malignancies respond differently. Patients frequently develop resistance to their treatment, which might result in cancer recurrence. The tremendous selective pressure these cytotoxic drugs impose on the tumor has been linked to the development of treatment resistance. Although the fast-dividing tumor cells die, the slower dividing tumor cells that remain, which are less sensitive to radiotherapy and chemotherapy, can survive treatment and give rise to a highly drug-resistant recurring tumor (18).

Immunotherapies are a relatively new and promising class of cancer therapeutics. Immunotherapies, in contrast to the medicines discussed above, have a specialized mode of action that tries to only eliminate malignant cells in the body. Immunotherapies, in general, boost and activate the immune system, which aids in the detection and elimination of cancer cells. Immune checkpoint inhibitors are the most commonly used type of cancer immunotherapy. They work by targeting immunological checkpoints or the molecular brakes on T cell activation, such as CTLA-4 and program death 1 (PD-1). When these targets are blocked, T lymphocytes become and remain activated, allowing them to recognize and destroy cancer cells. However, therapeutic resistance, as in the cases of radiotherapy and chemotherapy, lowers their efficacy and clinical success in patients (19–21). In the case of malignant melanoma, half of the patients do not react directly to checkpoint blockage ("primary resistance") or develop resistance throughout therapy (22). The underlying mechanisms of resistance include, but are not limited to, inadequate T cell infiltration, T cell exclusion, resistance to interferon gamma, and loss of T cell function or antigen presentation (23). Because naturally occurring autoreactive T cells are also boosted through therapy, autoimmunity is a common and serious side effect (24). As a result, severe side effects or immune related adverse events often lead to the early discontinuation of therapy.

To further improve patient outcomes, it is important to develop novel ways to diminish the immunosuppressive nature of TME to overcome the therapeutic resistance associated with immunotherapies by identifying new targets.

In light of the increasing number of possible therapy options coupled with their varying response rates, side effects, and costs, it is of great importance to create a treatment concept individually for each patient with the help of biomarkers. In this regard, there are numerous efforts to identify factors, both at the cellular and soluble protein level, in the tissue and peripheral blood of tumor patients, that help to characterize more precisely the tumor microenvironment and thus the prognosis and treatment response of the individual patient (25, 26). One potential novel target is the protein GARP, which is a marker for activated Treg and was also found to be expressed by cancer cells.

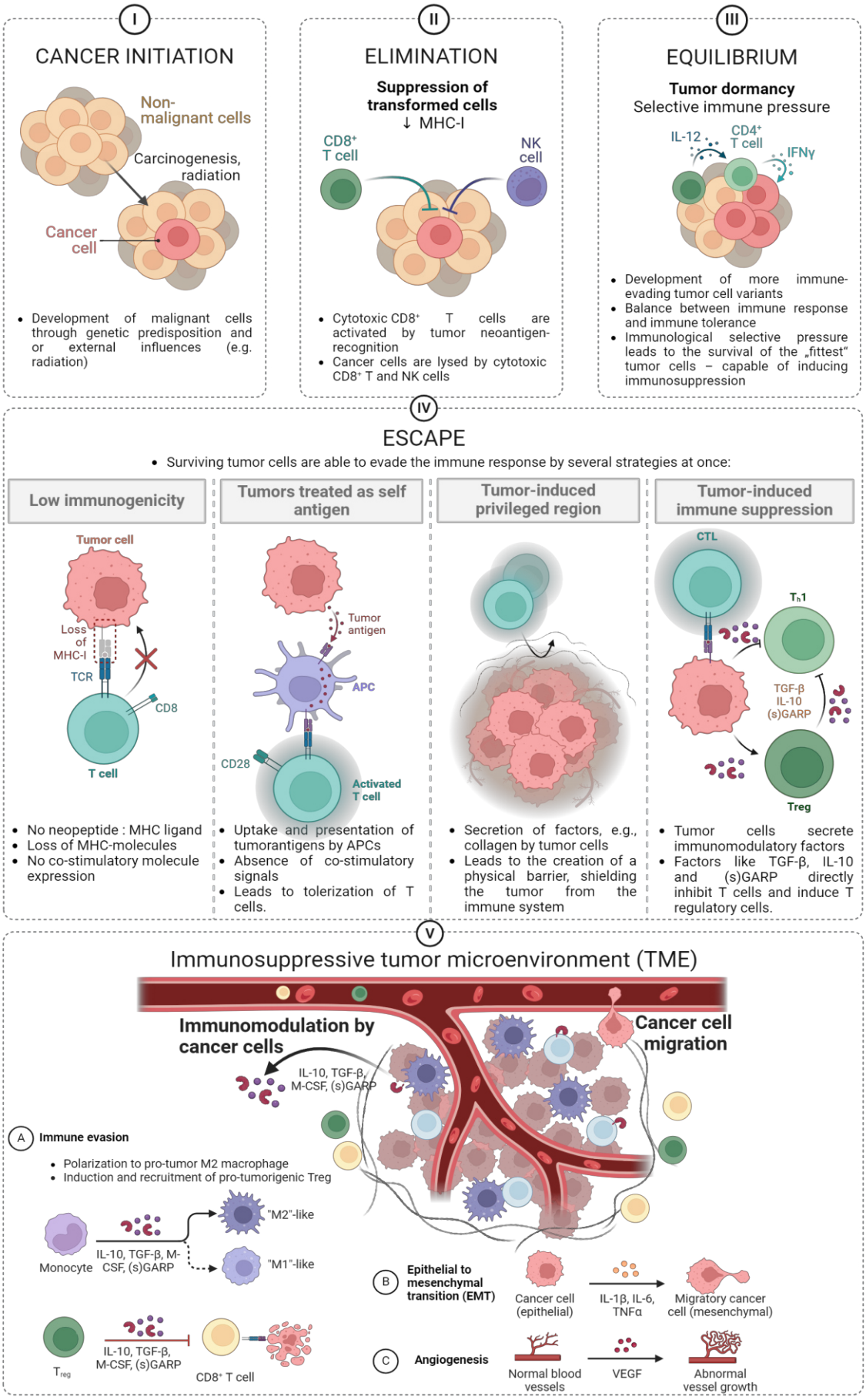

Figure 2: Overview of cancer development and the immunosuppressive tumor microenvironment. Created with BioRender.com

1.2 Manuscript I: Overview of GARP - Glycoprotein a repetitions predominant

This section is an excerpt from the following manuscript:
Manuscript I: GARP as a Therapeutic Target for the Modulation of Regulatory T Cells in Cancer and Autoimmunity. Front. Immunol. 13:928450. https://doi.org/10.3389/fimmu.2022.928450
The complete, unedited version of this manuscript can be found in the appendix I.

Summary of own contributions

NZ and AT took the lead in structuring and writing the manuscript. ET and KS wrote single sections, modified, and reviewed the manuscript. BG prepared the figure, modified, and reviewed the manuscript.

The Author took lead in the preparation of the manuscript together with Prof. Dr. med. Andrea Tüttenberg.

Keywords: LRRC32, GARP mRNA, Glycoprotein A repetitions predominant (GARP), Treg, Soluble GARP or soluble Glycoprotein A repetitions predominant (sGARP), biomarker, therapy

Citation: ***Zimmer N****, Trzeciak ER, Graefen B, Satoh K and Tuettenberg A (2022) GARP as a Therapeutic Target for the Modulation of Regulatory T Cells in Cancer and Autoimmunity. Front. Immunol. 13:928450. doi: 10.3389/fimmu.2022.928450*

Received: 25 April 2022; Accepted: 16 June 2022; Published: 08 July 2022.

Zusammenfassung

Regulatorische T-Zellen (Treg) spielen eine entscheidende Rolle in der Immunhomöostase, indem sie mehrere Aspekte der Immunantwort unterdrücken. Dabei spielt Glycoprotein A repetitions predominant (GARP) eine entscheidende Rolle bei der Aufrechterhaltung der Treg-vermittelten Immuntoleranz. Nach Aktivierung exprimieren Treg GARP auf ihrer Oberfläche. Aufgrund seiner Lage und Funktion, könnte GARP ein wichtiges Ziel für immuntherapeutische Ansätze sein, einschließlich die Hemmung der Treg vermittelten immunsuppression bei Krebs oder die Förderung der immunsuppressiven Eigenschaften im Falle von Autoimmunität. Folgend wird die zelluläre und molekulare Regulierung der GARP-Expression nicht nur in humanen Treg, sondern auch in anderen Zellen des Tumormikromilieus beschrieben. Auch wird die allgemeine Rolle von GARP bei der Regulierung des Immunsystems untersucht.

Abstract

Regulatory T cells (Treg) play a critical role in immune homeostasis by suppressing several aspects of the immune response. Herein, Glycoprotein A repetitions predominant (GARP), the docking receptor for latent transforming growth factor (LTGF-β), which promotes its activation, plays a crucial role in maintaining Treg mediated immune tolerance. After activation, Treg uniquely express GARP on their surfaces. Due to its location and function, GARP may represent an important target for immunotherapeutic approaches, including the inhibition of Treg suppression in cancer or the enhancement of suppression in autoimmunity. In the present review, we will clarify the cellular and molecular regulation of GARP expression not only in human Treg but also in other cells present in the tumor microenvironment. We will also examine the overall roles of GARP in the regulation of the immune system.

1.2.1 GARP expression, structure, and function

1.2.1.1 LRRC32 Gene Structure

The gene encoding human GARP can be referred to by various names including: LRRC32, Glycoprotein A Repetitions Predominant, GARP, Transforming Growth Factor Beta Activator LRRC32, Leucine-Rich Repeat-Containing Protein 32, Garpin, CPPRDD, and D11S833E (Gene ID: 2615). For the sake of clarity, we will specifically refer to the GARP gene as "LRRC32", its mRNA as "GARP mRNA", and the protein as "GARP" for the remainder of the manuscript.

LRRC32 was first described in the telomeric region of 11q13.5-11q14 in human (27) and mice (28). LRRC32 consists of two exons (29), and its expression is conferred by two alternative promoters (30). One exon codes for a signal peptide as well as nine amino acids, while the other codes for leucine-rich repeats (LRR). In addition, LRRC32 contains an extensive 2-kb long 3' untranslated region (UTR), that has five highly conserved regions which are of importance for the post-transcriptional regulation of the GARP mRNA (31).

So far, the GARP mRNA has been detected in various cell types and tissues of different origin, including heart, kidney, liver, lung, pancreas, placenta, skeletal muscle, and lymphoid tissues as well as in different cancer entities (e.g. melanoma, breast cancer, oral squamous cell carcinoma, prostate cancer, and glioblastoma). Although the GARP mRNA is expressed by many cell types, surface expression of the GARP protein itself has been only reported in the context of activated Treg (32, 33), activated B cells (34, 35), macrophages (36), platelets (37), mesenchymal stem cells (38), and hepatic stellate cells (34, 39). In Treg, surface GARP is considered to be an activation marker. Of note, the GARP mRNA is also expressed by human effector T cells (Teff) clones. Nevertheless, even though its expression levels in such clones are similar to levels found in some Treg clones, GARP has not been detected on the surface of either human or mouse activated Teff (40).

Interestingly, the LRRC32 gene locus is part of a chromosomal region that was described to be altered in several human cancers. In agreement with this finding, the GARP mRNA is highly amplified in tumor cells, and GARP surface expression has been detected in invasive, metastatic, and drug resistant tumors (41–43). Furthermore, in ovarian cancer, single nucleotide polymorphisms (SNP) were described in the non-coding regions of the LRRC32 (two were found in the 3' UTR, and one was found in the intron (rs3781699 and rs7944357, respectively), which have been associated with poor patient survival (44) (19). Additionally, the gene locus of LRRC32 was also identified as a risk locus for asthma (45), atopic dermatitis (46), and colitis (47).

1.2.1.2 GARP Protein Structure

GARP is an approximately 78 kDa type I transmembrane protein made-up of 662 amino acids with an extracellular region consisting of 20 LRR. In more detail, its structure has three domains: a cytoplasmic tail of 15 amino acid residues, a hydrophobic transmembrane domain, and an extracellular domain, containing the LRR, which accounts for about 70% of the protein (27). In addition, a signal peptide is located in the N-terminus, and its cleavage is required for the surface expression of GARP (29). The extracellular domain of GARP is similar to the corresponding region of other members of the LRR protein family, which in general play an important role in protein-protein interactions and signal transduction (27). It contains 20 LRR motifs, subdivided into two groups of 10 LRRs each by a proline rich domain and a C-terminal LRR (45). The proline rich region confers flexibility and supports the idea of the involvement of GARP in protein-protein interactions. The two cysteines, Cys-192 and Cys-331, located in the 7th and 12th LRR respectively, are responsible for the two disulfide bonds that form between GARP and its ligand, latency associated peptide (LAP), in the LTGF-β complex (48). Following translation, GARP undergoes N-linked glycosylation and contains five predicted glycosylation sites (27, 49).

1.2.2 GARP Function

TGF-β is a pleiotropic cytokine, that is an important mediator during the development of Treg and the maintenance of their immunoregulatory state (50). Besides Treg, TGF-β is expressed by a multitude of cell types and tissues and participates in the mediation of numerous pathways, including development, wound healing, homeostasis, and cancer (51).

GARP has been shown to be essential for the formation and surface expression of LTGF-β on Treg. GARP binds all three isoforms of TGF-β (32, 52, 53) and plays an important role in TGF-β activation, which is first synthesized as a biologically inactive homodimeric precursor protein (48, 54, 55). This proprotein consists of three distinct parts: (I) mature TGF-β, (II) LAP, and (III) a signal peptide. Following the removal of the signal peptide, via cleavage by furin proteases, inactive TGF-β becomes mature TGF-β (56). Then, mature TGF-β binds LAP through both covalent (disulfide bridges) and non-covalent interactions (57). The resulting complex of mature TGF-β and LAP is called latent TGF-β (LTGF-β) and lacks biological activity. In the absence of GARP, LTGF-β binds to the latent TGF-β binding protein (LTBP), thereby forming the large latent complex (LLC), which associates with the extracellular matrix (ECM) (58). Surface GARP inhibits the binding of LTGF-β to the LTBP due to its higher affinity and in turn, presents LTGF-β on the cell surface. GARP enables the binding of latent TGF-β to αVβ6 and αVβ8 integrins, forming a ring-like shape with TGF-β orientated towards the center. This enables the release of TGF-β from LTGF-β mediated by a protease dependent or a protease independent mechanism. Integrin recruited metalloproteinases or serine proteases may cleave LAP from the TGF-β – LAP - GARP complex. Of note, αVβ6 and αVβ8 are expressed in a cell type specific manner. In particular, Treg express αVβ8 (59). Protease independent release of TGF-β is facilitated through the binding of the respective integrins to LTGF-β and the resulting deformation of LAP, triggered by cell contraction. This results in the release of bioactive mature TGF-β into the extracellular space (59) (Figure 1.2.1B).

1.2.3 GARP Regulation

1.2.3.1 GARP and its regulation in Treg

$CD4^+CD25^+CD127^{-/low}Fox3p^+$ Treg, a highly immunosuppressive subset of $CD4^+$ T cells, play a major role in immune homeostasis by controlling immune responses through the induction and maintenance of peripheral tolerance (58). As mentioned above, GARP is expressed on the surface of activated Treg and plays a vital role in conveying their suppressive capacity. GARP expression is obligatory for the binding of TGF-β1 on their surfaces (30, 59). Until recently, the functions of GARP on Treg were described as aiding in the presentation of LTGF-β by acting as both an anchor and support protein for the activation and release of LTGF-β (30) (5). It has been shown that the expression of GARP increased the suppressive function of Treg. It has been observed that $GARP^+$ Treg in comparison to GARP- Treg displayed a greater Teff suppressive capacity in vitro. This difference was associated with a decrease in IL-2 and IFN-γ production (37, 59) and a corresponding increase in the production of TGF-β and IL-10 (60, 61). Further evidence highlighted the importance of GARP in Treg function. In a humanized mouse model of allogenic graft rejection, $CD4^+CD25^{high}CD127^{low}$ Treg and $CD4^+$ $CD25^{high}$ Treg showed a significantly lower capacity in preventing alloreactions in comparison to $CD4^+CD154^-GARP^+$ and $CD4^+CD154^-LAP^+$ Treg (62). This study concluded that LAP and GARP are specific markers for human Treg, and they have a high suppressive activity. Additionally, a complete depletion of activated GARP+ Treg in a humanized mouse model of allergen-induced gut inflammation diminished the protective effects of Treg (63).

1.2.3.2 Interplay of GARP and Foxp3

The detailed relationship between Foxp3 and GARP in Treg remains a matter of debate.

At first, it was described that the regulation of GARP is independent of Foxp3. This conclusion was based on studies, which demonstrated that TGF-β induced overexpression of Foxp3 was not sufficient enough to induce the expression of GARP (32, 60). Furthermore, it was shown that the knockout of Foxp3 in Treg did not change GARP expression, and correspondingly, the knockdown of GARP did not affect Foxp3 expression. However, a knockdown of GARP led to an impaired suppressive capacity of Treg, while silencing of Foxp3 in GARP-expressing cells did not affect their suppressive capacity, but knockdown of Foxp3 lead to an impaired Treg function (33). Interestingly, GARP is not expressed by resting $CD4^+Foxp3^+$ Treg, but it is upregulated upon Treg activation. In comparison, $CD4^+Helios^+Foxp3^-$ cells upregulate the expression of GARP/LAP upon TCR stimulation, supporting that Foxp3 and GARP are not regulated by each other (61).

In contrast to this conclusion, Probst-Kepper et al. proposed a mutual dependency of Foxp3 and GARP expression, which occurs in a positive feedback loop like manner. They were able to demonstrate that lentiviral downregulation of the GARP mRNA led to the downregulation of Foxp3 and the loss of Treg suppressive properties. Similarly, the downregulation of Foxp3 also resulted in the downregulation of GARP mRNA and impaired suppressive Treg function (40).

1.2.3.3 Pre-transcriptional Regulation of LRRC32

Haupt et al. improved our understanding of the regulation of LRRC32 by showing that the transcription factors, nuclear factor of activated T cells (NFAT) and nuclear factor kappa light chain enhancer of activated B cells (NF-kB), play an important role in the expression of LRRC32. Transcription of LRRC32 is driven by two different promoter regions, P1 and P2, which differ in their methylation status depending on the cell type examined and the surrounding environmental conditions. It was shown, that in Treg, P1 and P2 are completely demethylated. This allows Foxp3 to bind to P1, opening the promoter region via chromatin remodeling, enabling the binding of NFAT and NF-kB, resulting in the expression of LRRC32. In contrast, Th cells differ from Treg as they exhibit increased methylation of their P1 promotor, which consequently prevents the expression of LRRC32 (30).

In 2020, Nasrallah et al. were able to show that an enhancer, located at chromosome 11q13.5, is active in Treg (47). This enhancer forms conformational interactions with the promoter of LRRC32, and the enhancer risk variant, rs11236797, is associated with a reduction in histone acetylation and decreased LRRC32 expression. This is based on the recruitment of STAT5 and NF-kB (47), which in turn mediate the expression of LRRC32. Therefore, these transcription factors are vital for Treg-mediated suppression. Any disruption of LRRC32 leads to early lethality in mice. The knockout of the enhancer led to the development of Treg that did not express LRRC32/GARP, which were unable to control colitis in an adoptive transfer model. This underlines the results of previous studies, that indicated that GARP is necessary for Treg function (33, 47).

Recently, Lehmkuhl et al. demonstrated that GARP-deficient murine Treg were characterized by an unstable Treg phenotype as reflected by the decreased expression of CD25, Neuropilin-1(Nrp1), cytotoxic T-lymphocyte-associated Protein 4 (CTLA-4), Interleukin-10 (IL-10), and Histone deacetylase 9 (HDAC9), and they were characterized by impaired immunosuppressive activity (63). These alterations were due to decreased acetylation of Foxp3 in comparison to stable Treg. Interestingly, it was found that GARP could regulate the expression of HDAC9, which is responsible for Foxp3 acetylation and thus Treg stability (62, 63). Future studies are necessary to elucidate how HDAC9, NFAT, and NF-kB interact and how their interplay affects the expression of LRRC32/GARP in more detail.

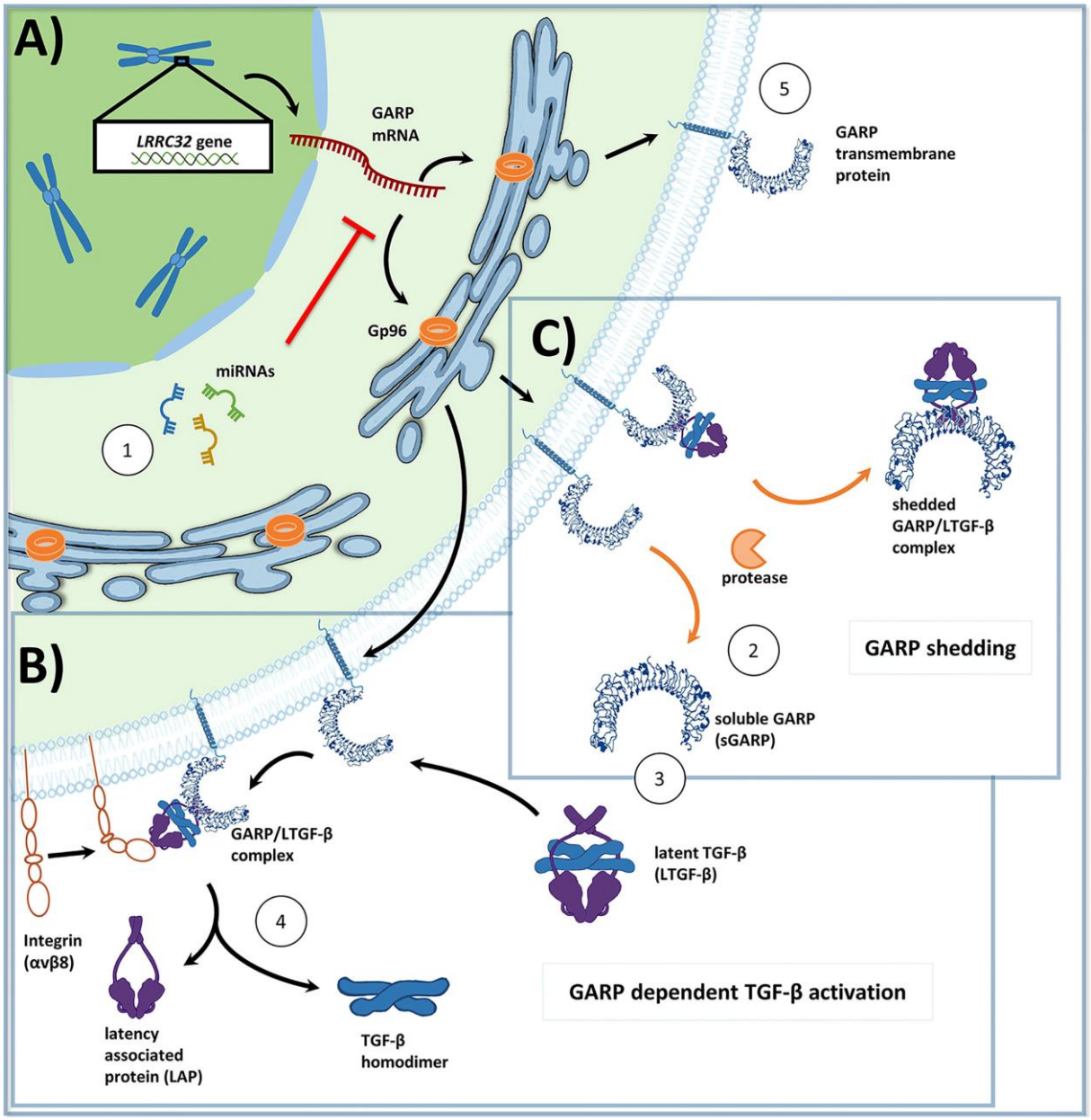

Figure 1.2.1 edited from Zimmer et al., 2022: (A) Overview of Glycoprotein a repetitions predominant (GARP) protein biosynthesis and transport to the cell membrane in activated human regulatory T cells (Treg). GP96, a chaperone found in the endoplasmic reticulum, ensures proper folding of GARP [GARP structure modified from: Liénart et al. (60)]. The GARP mRNA is targeted by miRNA, which promote its degradation, and thus lower GARP mRNA/GARP levels. (B) GARP functions as a docking receptor for biologically inactive latent transforming growth factor beta (LTGF-b), which consists of a TGF-b homodimer bound to latency associated protein (LAP), and GARP plays an important role in its activation. GARP binds LTGF-b with high affinity, forming the GARP/LTGF-b complex. Release of bioactive TGF-b can occur in both a protease independent (shown) or a protease dependent manner (not shown). For protease independent release of mature TGF-b, aVb8 integrins, expressed on the surface of Treg bind to the GARP/LTGF-b complex, resulting in a conformational change and in the subsequent release of biologically active TGF-b. Alternatively, bioactive TGF-b can be released in a protease dependent manner, in which integrin recruited metalloproteinases or serine proteases cleave LAP from the GARP/LTGF-b complex (not shown). (C) GARP can be cleaved from the surface of Treg by proteases in a form called soluble GARP (sGARP). GARP/LTGF-b complexes can also be released into the extracellular environment via proteases.

1.2.3.4 Post-transcriptional regulation of the GARP mRNA

It is becoming increasingly apparent that the expression of GARP is tightly regulated. Hereby, miRNA have been shown to play an important role. miRNA are single stranded, conserved, non-coding RNA molecules that play an essential role in post-transcriptional regulation (64). By binding to sequence complementary sites within the 3' UTR of their target mRNAs, miRNA lead to translation inhibition and mRNA degradation, which collectively leads to the suppression of gene expression. Numerous miRNA have already been found to regulate the development, differentiation, proliferation, and suppressive function of Treg, including the targeting of the GARP mRNA itself (65).

As mentioned in section 1.2.1.1, LRRC32 Structure, the 3' UTR of LRRC32 contains five evolutionary conserved regions, which are a promising indicator for potential miRNA recognition sites (31). So far, several miRNA have been found to target the 3' UTR of the GARP mRNA in human Treg. Zhou et al. found that miR-142-3p directly binds to the 3' UTR of the GARP mRNA and promotes its subsequent degradation via the Argonaute 2 pathway in primary $CD4^+CD25^+$ human T cells (31). They could also show that miR-142-3p controls the expression of GARP mRNA/GARP in activated Treg. Upon Treg activation, GARP mRNA/GARP levels are upregulated. However, the reason GARP levels subsequently decline following activation results from the upregulation of miR-142-3p, which binds to the GARP mRNA and targets it for subsequent degradation. Gauthy et al. could show that miR-185, and miR-181 a, b, c, d, in addition to miR-142-3p, target the 3' UTR of GARP mRNA in human Treg differentiated from PBMCs (56) (Figure 1.2.1A). Furthermore, they could show that these miRNA were also expressed at a lower level in human Treg when compared to Th cells. Interestingly, a study by Jebbawi et al. demonstrated that miR-24 and miR-335 directly bind to the 3' UTR of the GARP mRNA and regulate GARP levels (66). It is important to note that they examined primary human $CD8^+CD25^+$ Treg derived from cord blood in contrast to the aforementioned studies, which studied human $CD4^+$ Treg (67). These differences in cell type and tissue source may help explain in part why different sets of miRNA were detected.

1.2.3.5 Post-translational regulation of GARP

Surface expression of GARP has been found to be dependent on the heat shock protein, GP96 (GRP94) (68). GP96 is a master chaperone, which is found in the endoplasmic reticulum (ER), and its clientele consists of proteins implicated in both immune response and oncogenesis, such as toll-like receptors (TLR), integrins, Wnt co-receptor low-density lipoprotein receptor-related protein 6 (LRP6), insulin-like growth factor (IGF), platelet glycoprotein Ib-IX-V complex, and human epidermal growth factor receptor-2 (HER2) (68, 69). In a study by Zhang et al., examining the effects of GP96 knockout (KO) in Treg in vivo, it was discovered that although GP96 KO mice developed Treg, they displayed unstable Foxp3 expression, increased IFN-γ production, and impaired suppressive function, thus leading to the development of fatal autoimmunity (68). One reason for this reduction in Treg suppressive function was a decrease in surface GARP expression and mature LTGF-β levels. Loss of surface GARP and mature LTGF-β was also observed in $CD41^+$ GP96 KO platelets and GP96 deficient B cells, suggesting that GP96 acts as an obligate chaperone for GARP. Loss of surface GARP expression in GP96 deficient B cells was attributed to the inability of GARP to leave the ER and was accompanied by a decrease in the half-life of GARP. Collectively, this suggests that GP96 is required for the stable protein conformation of GARP. In addition, it was discovered that GARP interacts with the C-terminal client-binding domain of GP96 as also reported for TLRs (68).

Another protein that interacts with GARP, lysosomal associated transmembrane 4B (LAPTM4B), was identified in a yeast two hybrid assay (62). LAPTM4B expression increased upon Treg activation, and it directly decreased the surface expression of GARP and the secretion of LTGF-β1. LAPTM4B has been postulated to function as part of a negative feedback mechanism to downregulate Treg production of LTGF-β1 and surface GARP during T cell activation. Translocation of intracellular GARP to the surface

of Treg upon activation requires the cleavage of a signal peptide located in the N-terminus of GARP (29). It has also been found in a model of forced GARP overexpression in T cells, TCR activation was needed for the translocation of intracellular GARP to the cellular surface. Furthermore, in case of Treg, IL-2 signaling is able to specifically increase the surface expression of GARP (70, 71).

It has been described that activated Treg shed a soluble form of GARP (sGARP) from their surfaces (43). Shedding of GARP was first proposed by Roubin et al. in their description of the protein structure of GARP. They hypothesized, that a hydrophobic leader sequence embedded in the amino acid sequence of GARP may resemble a signal peptide for secretion (28). The shedding of GARP has been subsequently confirmed in blood plasma by mass spectrometry (72). Additionally, Metelli et al., were able to show that thrombin can cleave GARP from the surface of platelets, which is essential for the release of membrane latent TGF-β (mLTGF-β) (73). Shedding of GARP/LTGF-β1 complexes from the surfaces of stimulated Treg and GARP overexpressing Th cells has also been described and detected in cell supernatants (56) (Figure 1.2.1C). These complexes may have been shed from the membrane by proteases, and their functional significance remains unknown.

1.2.4 Soluble GARP (sGARP)

As mentioned earlier, sGARP is released by an array of different cell types, including activated Treg, activated platelets, and cancer cells. Hahn et al. could show that sGARP can modulate immune responses and has strong suppressive properties (74). In this regard, recombinant sGARP was found to suppress the proliferation and cytokine production of Teff. Exposure of naive T cells to sGARP led to an induction of Treg. This transition was accompanied by the induction of Foxp3 expression, the inhibition of cell proliferation, and a significant decrease in IL-2 and IFN-γ production. Furthermore, sGARP induced a tumor associated “M2-like” macrophage (TAM) phenotype and suppressed cytotoxic T cell function by inhibiting cell proliferation and the production of IFN-γ and Granzyme B (74).

Additionally, in a humanized mouse model of a xenogenic graft versus host disease (GvHD), the application of recombinant sGARP protected the animals from T cell mediated inflammation through Treg activation (74). It was also found that sGARP drives epithelial-mesenchymal cell transition (EMT). Cells treated with sGARP showed increased proliferation and migratory capacities in comparison to the untreated control (55). The mechanism by which sGARP induces these phenotypic changes is at least in part dependent on the TGF-β signaling pathway, as phosphorylation of Mothers against decapentaplegic homolog 2 and 3 (Smad2/3) in sGARP treated naive CD4+ T cells was observed. However, inhibition of TGF-β signaling by the use of a TGF-β receptor II blocking antibody could not fully prevent the effects of sGARP (74).

These findings could be confirmed by our group using a physiological source of sGARP (37). Activated platelets have been shown to shed GARP from their surfaces. Based on these findings, $CD4^+$ T cells were cocultured with platelet conditioned medium (PCM). PCM was able to induce Treg, characterized by a strong Foxp3 expression, while simultaneously suppressing their proliferation as well as their IL-2 and IFN-γ production when compared to the untreated control. Administration of a blocking anti-GARP antibody was able to mitigate these effects. Furthermore, it was shown that blockade of the TGF-β pathway, by applying blocking antibodies against TGF-β I-III and TGF-β RII, could not completely inhibit the effects of PCM on T cells. This indicates that sGARP mediates its effects in part through a TGF-β independent signaling pathway (37).

Furthermore, it has been shown that recombinant sGARP has a strong capability to enhance the activation of free latent TGF-β. This function further amplifies the effects of sGARP in the case of autoimmunity and cancer (75).

Collectively, this leads to the conclusion that sGARP is able to achieve two things in parallel, which may multiply its immunomodulatory effects. First, sGARP has the ability to modulate the differentiation and suppression of immune cells. Second, sGARP can enhance the activation of TGF-β and correspondingly its manifold downstream effects. Therefore, sGARP may act as an important player in both autoimmunity and the tumor microenvironment (TME). Taken together, this highlights the importance of sGARP as a potent immunoregulatory molecule on its own and in its interplay with TGF-β.

1.2.5 Cellular GARP

1.2.5.1 Regulatory T cells

$CD4^+CD25^+CD127^{low}Foxp3^+$ Treg, a highly immunosuppressive subset of $CD4^+$ T cells, play a major role in immune homeostasis by controlling immune responses through the induction and maintenance of peripheral tolerance (76). As mentioned above, GARP is expressed on the surface of activated Treg and plays a vital role in conveying their suppressive capacity (Figure 1.2.1A). GARP expression is also obligatory for the binding of TGF-β1 to the surface of Treg (32, 61).

Until recently, the functions of GARP on Treg were described as aiding in the presentation of LTGF-β by acting as both an anchor and support protein for the activation and release of LTGF-β (32). It has been shown that $GARP^+$ Treg in comparison to GARP- Treg displayed a greater suppressive capacity of Teff in vitro. This difference was associated with a decrease in the effector cytokines IL-2 and IFN-γ production (40, 61) and a corresponding increase in the production of the inhibitory cytokines TGF-β and IL-10 (76, 77).

Resting murine Treg express a low level of GARP. Upon TCR stimulation GARP gets upregulated on the cell surface of Treg, followed by an increased expression of latent TGF-β1. GARP expression can be upregulated on murine Treg via exposure to IL-2 and IL-4 without the need for TCR activation in vitro. Expression of GARP in mice was found to be independent of TGF-β1, but specific KO of GARP in murine CD4+ T cells leads to a diminished expression of TGF-β1 on the surface of activated Treg. These GARP- Treg were found to develop normally and were capable of suppressing Teff in vitro. Additionally, Treg numbers in the periphery were not affected. Treg which express GARP/LTGF-β1 on their surfaces are able to induce Treg in the presence of IL-2, while the presence of IL-6 leads to the induction of Th17 cells (31, 71).

Further evidence highlighted the importance of GARP in Treg function. In a humanized mouse model of allogenic graft rejection, $CD4^+CD25^{high}CD127^{low}$ Treg and $CD4^+CD25^{high}$ Treg showed a significantly lower capacity in preventing alloreactions in comparison to $CD4^+CD154^-GARP^+$ and $CD4^+CD154^-LAP^+$ Treg (78). This study concluded that LAP and GARP are specific markers for human Treg having a high suppressive activity. In addition, a complete depletion of activated $GARP^+$ Treg in a humanized mouse model of allergen-induced gut inflammation diminished the protective effects of Treg (79).

In Treg with mutated LRRC32, expression of GARP was reduced, resulting in an unstable Treg phenotype that led to severe immune dysregulation and an increased development of inflammatory diseases (63). In giant cell arteritis, the most common primary arteritis, based on an imbalance of activated Teff cells and dysfunctional Treg, patients' Treg showed an ineffective and reduced induction of GARP (80). In a preclinical approach, in vitro expanded Treg were isolated based on their selective surface expression of LAP. Herein, $LAP^+GARP^+Foxp3^+$ Treg showed a highly demethylated Treg-Specific Demethylated Region, indicating a stable Foxp3 expression and ultimately a stable Treg phenotype. Additionally, these cells showed a high suppressive capacity in vitro and in a GvHD in vivo model, making these cells a suitable population for the treatment of GvHD in patients (81).

Taken together, GARP expression on Treg significantly influences the immunological balance in different settings: $GARP^+$ Treg lead to immunosuppression, being of importance especially in the tumor

microenvironment. Deficiency of GARP in Treg has an impact on the development of inflammatory diseases including autoimmunity, allergy and transplant rejection.

1.2.5.2 Non-Treg cells

Besides Treg, B cells are known to express GARP when activated by TLR ligands, such as TLR4, TLR7, and TLR9 (82). Expression of GARP led to the inhibition of cell proliferation, induced a class switch to IgA production, and resulted in a more tolerogenic B cell phenotype. This has been explored especially in the context of autoimmune diseases (35, 82). Herein, GARP was upregulated on B cells in autoimmune diseases and the GARP-LTGF-β axis was shown to be an important factor for B cell tolerance and prevention of lupus-like autoimmune diseases in mice. Furthermore, hepatic stellate cells constitutively express GARP on their surfaces. A blockade or knockdown of GARP resulted in an impaired suppression of T cell proliferation and IFN-γ production. It has been described that GARP is required to anchor and activate LTGF-β. Whether the observed effects are mainly mediated by LTGF-β, a suppressive function of GARP itself, or by a release of sGARP has not yet been described (39). Nevertheless, being expressed on cells involved in fibrosis as well as in hepatic cell cancer progression, it will be of interest to further investigate influence of GARP in this context. In multipotent mesenchymal stromal cells (MSC), GARP has been shown to be important for their proliferation and survival by rendering them more resistant to DNA damage and apoptosis in a TGF-β dependent manner (83)(58). In addition, GARP is involved in the immunomodulatory activities of MSC (84).

1.2.5.3 Platelets

Expression of GARP was initially described on the surface of platelets (28). Platelets are the main cells that mediate hemostasis at the site of injury. Platelets are important modulators of both innate and adaptive immunity through their interaction with immune cells. In the case of infection, platelets become activated and are able to modulate inflammation (85, 86). In addition, recent evidence indicates that platelets are present in the TME, and cancer associated thrombocytosis has been associated with the promotion of invasion and metastasis, and thus poor clinical outcomes in different tumor entities (87). Low platelet counts and inhibited platelet activation in patient blood correlated with a lower likelihood of metastasis (88, 89). In more detail, platelets promote motility (90–92) and EMT (93). Furthermore, platelet count and activation status influenced the survival of circulating tumor cells (CTC) by shielding them from NK cells and from destruction by shear stress (94, 95). This is due to their expression of fibrinogen receptor GPIIb-IIIa and P-Selectin, which mediate the attachment of platelets onto CTCs via the binding of CD44 and avB3 integrin (94). In addition, melanoma cells express chemokines that attract and activate platelets, in a process called tumor cell-induced platelet aggregation (96), resulting in the shielding of metastasizing melanoma cells by platelets in the bloodstream. Platelet-derived TGF-β has been shown to be an important modulator of the immune system (97). Besides being known for its immunosuppressive capability, TGF-β can downregulate B-cell lymphoma 2 (Bcl-2) proteins, known for their anti-apoptotic effects, as well as natural killer group 2D (NKG2D) leading to a decrease in NK cell efficacy (98). While there is increasing evidence that GARP on platelets plays an important role in immunomodulation, GARP does not seem to play a significant role in hemostasis and thrombosis. The conditional knockout of GARP on platelets and endothelial cells in mice did not lead to any changes during agonist induced platelet activation and aggregation. Furthermore, the tail bleeding time and the FeCl3-induced thrombus formation occlusion time were not affected (99).

There has been an emerging role of platelets not only in hemostasis but also in the immunomodulation of cancer patients. Given the fact that platelets express GARP on their surfaces and connecting this to previous works describing GARP as a key molecule in inducing peripheral tolerance, several groups have shown a possible contribution of platelets to adaptive immunity, leading to a poor prognosis of cancer patients with cancer associated thrombocytosis. For example, GARP was found to be expressed

on platelets to a certain extent; however, upon platelet activation, surface GARP levels were found to be significantly increased (37). We demonstrated that, cocultures of platelets and Teff as well as Teff grown in the presence of PCM induced a regulatory phenotype, characterized by an upregulation of Foxp3, reduced proliferation, and decreased effector cytokine production, as well as an induction of suppressive capacity. This phenomenon was shown to be GARP dependent. In addition, the TGF-β signaling axis seemed to be at least in part associated to GARP mediated Treg induction (37). The cleavage of GARP by proteolysis through thrombin from the surface of platelets, has been shown to be a major contributor to cancer immune evasion. The blockade of the GARP cleavage led to an improved therapeutic efficacy of anti-PD-1 therapy (73)(47). Furthermore, activated platelets released sGARP, as shown by us and Metelli et al., which in turn induces Treg in a GARP dependent manner (37, 73).

1.2.5.4 Tumor cells

As already mentioned, GARP has been shown to be expressed by several tumor entities, like malignant melanoma (43), glioblastoma (41), bone sarcoma (42), breast cancer (100), and lung cancer (101).

It has been shown that the relation between Foxp3, GARP, and TGF-β, as thoroughly analyzed in Treg, also plays an important role in cancer progression. Tumor cells employ a form of "Treg mimicry", by utilizing specific immunosuppressive strategies, similar to Treg, to modulate their surroundings (41, 75, 102, 103). In bone sarcoma, GARP plays a vital role in cancer cell proliferation and resistance against irradiation and chemotherapy. Silencing of GARP in these cells led to a decrease in cell proliferation and an increase in apoptosis (42). Li et al., were able to show that GARP also plays an important role in the regulation of TGF-β1 in osteoblast differentiation. Downregulation of the GARP mRNA/GARP in bone marrow mesenchymal stem cells (BMSC) attenuated their differentiation into osteoblasts (104). Furthermore, normal murine mammary epithelial cells, showed an increased production of TGF-β and oncogenesis when GARP was overexpressed. Furthermore, the murine mammary gland tissue cell line, NMuMG, that was unable to form tumors in vivo, was able to do so once GARP was overexpressed (55).

In a coculture with $CD4^+$ T cells, GB cells were able to suppress the proliferation and IFN-γ production of the former. By using a blocking anti-GARP antibody, the proliferation and cytokine production of $CD4^+$ T cells could be restored (41). Malignant melanoma has been shown to release sGARP into its surroundings, suggesting a further contribution to a GARP-TGF-β mediated immunosuppressive microenvironment (43).

Zhang et al. showed that in pancreatic cancer, tumor cells were able to reprogram M1-like macrophages metabolically and functionally through a GARP-dependent and via a DNA methylation-mediated mechanism to M2 macrophages with a pro-tumorigenic phenotype (36).

All these data show that GARP on tumor cells is I) maybe involved in tumor cell proliferation and II) significantly modulates immune responses leading to an inhibitory tumor micromilieu, both facts resulting in massive tumor promotion.

2.0 Motivation and Objectives

This work is based on previous studies done in the lab of Prof. Dr. med. Andrea Tüttenberg, which was published in the following manuscripts:

Hahn, S.A.; Stahl, H.F.; Becker, C.; Correll, A.; Schneider, F.-J.; Tuettenberg, A.; Jonuleit, H. Soluble GARP has potent anti-inflammatory and immunomodulatory impact on human $CD4^+$ T cells. Blood 2013, 122, 1182–1191, https://doi.org/10.1182/blood-2012-12-474478

Hahn, S.A.; Neuhoff, A.; Landsberg, J.; Schupp, J.; Eberts, D.; Leukel, P.; Bros, M.; Weilbaecher, M.; Schuppan, D.; Grabbe, S.; et al. A key role of GARP in the immune suppressive tumor microenvironment. Oncotarget 2016, 7, 42996–43009, https://doi.org/10.18632/oncotarget.9598

Zimmer, N.; Master thesis 2016, Johannes Gutenberg-Universität Mainz, AG Prof. Dr. med. Andrea Tüttenberg; Title: *Immunoregulatorische Funktion von Thrombozyten auf den Differenzierungsprozess von $CD4^+$ T-Zellen.*

In short, the key findings were as follows: (A) soluble GARP suppresses the proliferation of $CD4^+$ and $CD8^+$ T cells and induces regulatory T cells. *In vivo*, soluble GARP inhibits the development of graft versus host disease by inducing regulatory T cells. (B) GARP is expressed by melanoma cells, and $GARP^+$ melanoma cells are able to induce a tolerogenic phenotype in T cells and macrophages. Additionally, GARP was identified in brain metastases from melanoma. (C) GARP expressing platelets are capable to significantly modulate T cell differentiation.

Based on these findings, the following questions were investigated:

Manuscript II: To investigate (I) whether GARP is expressed on primary brain tumors and (II) if so, what role does GARP play in the immunosuppressive microenvironment of brain tumors.

Manuscript III: Based on the findings of manuscript II, to investigate (I) if GARP is a suitable complementing marker for the identification of human GSC and (II) if nuclear GARP ($GARP^{NU+}$) has a potential use as a prognostic marker for patient survival.

Manuscript IV: To determine (I) if platelets are able to induce Treg via a (s)GARP dependent mechanism, and (II) if GARP on platelets could be a possible therapeutic target or biomarker for melanoma patients.

3.0 GARP on Glioblastoma

3.1 Overview: Glioblastoma

3.1.1 Epidemiology

The extremely malignant properties of GB, such as necrosis, rapid proliferation, and invasiveness into adjacent tissues, make complete surgical resection challenging. Remaining cells, missed in surgical resection, are responsible for a high recurrence rate, accompanied by a high degree of therapeutic resistance complicate GB treatment. Furthermore, considerable morphological and molecular heterogeneity hampers clinical outcome prediction.

The World Health Organization (WHO) classifies GB as a stage IV cancer. In their classification from 2021, gliomas are divided into four different subtypes based on their degree of malignancy. The diagnosis of the subtypes is determined by histopathological characteristics and molecular genetic alterations of GB (105):

- **Glioblastoma (IDH):** The wildtype of isocitratdehydrogenase (IDH) accounts for the vast majority of all GB cases and develops around age 60.
- **Glioblastoma IDH-mutant:** The second most common cases are often secondary GB that develops in younger individuals with grade I-III gliomas.
- **Glioblastoma NOS:** Not else specified (NOS) due to insufficient tissue for histological or genetic examination.
- **Glioblastoma NEC:** Not elsewhere classified (NEC) owing to inconsistent or conflicting traits, not yet categorized by the WHO.

GB is the most aggressive glioma of the astrocyte lineage and is incurable. They arise from astrocytes and oligodendrocytes (106). The median survival time is 14.6 months, and the 5 year survival rate is 5% (107). The incidence of GB is 5.0 per 100,000 people (108). GB is most commonly but not exclusively localized in the frontal lobe, supratentorial compartment, the sub tentorial compartment, and less often, in the brainstem or the cerebellum (109, 110) As it is the case with the majority of malignancies, aging plays a significant role in cancer development. The majority of GB cases occur in adults older than 40, with increasing incidence by age. Males are more likely than females to develop GB, providing evidence that gender has a prognostic significance (111–113). There is insufficient data to support a correlation between GB incidence and ethnicity. According to Ostrom et al., the incidence of GB in Caucasians is 2.97 times greater than in Asians and 1.99 times higher than in African Americans (114). Nevertheless, Fukushima et al. found no substantial molecular differences in the GB malignancies of Caucasians and Asians (115).

3.1.2 Diagnosis & Pathology

Risk factors for the development of GB remain unknown, and research addressing this topic typically lack statistical power. Increased GB incidence raises concerns about environmental risk factors, but clear evidence is still elusive (116). For instance, smoking and exposure to other carcinogens have not been demonstrated to be associated with GB (117, 118). The connection between cell phone use and the development of GB is hotly contested, and no definitive conclusion can be formed (119–121). Patients with Lynch, Turcot type 1, or Li Fraumeni syndromes are genetically predisposed to develop GB in a very small percentage of instances (1%) (122, 123). There are signs that radiation exposure at

a younger age (<5 years) increases the risk of developing a brain tumor. This appears to be both dose and volume dependent (124, 125).

The clinical appearance of a GB tumor depends on its size and location at the time of diagnosis. In the context of a large tumor or significant edema, the most prevalent symptoms at the time of diagnosis are headache and/or nausea. Clinical symptoms include cerebral hypertension, weight and condition loss, disorientation, as well as motor, visual, and/or speech deficits (126). Furthermore, epilepsy is a common symptom (127). These symptoms are frequently related and result in a diagnosis of GB within weeks or months following onset. One part of the diagnosis of GB is magnetic resonance imaging (MRI). MRI characteristics of GB are well-known and are visible as infiltrative, heterogeneous, intraparenchymal lesions (128, 129). Furthermore, tumor biopsies or material from surgical resections are used for mandatory histopathological and molecular studies (108, 123, 130).

While the therapeutic value of subtyping is still up for debate, a genome-wide transcriptome study led to the classification of GB into four more homogeneous subtypes: mesenchymal (MES), classical (CL), proneural (PN), and neural (NE) based on bulk tumor transcriptomic profiles (131–133).

One of these studies includes the analysis of IDH1/2 (isocitrate dehydrogenase (NADP(+)) 1/2), which significantly predicts patient survival (105). More than seventy percent of adult-type diffuse gliomas are caused by mutational changes in either the IDH1 gene at position 132 of the amino acid sequence or the IDH2 gene at position 172 (134). Mutations in IDH have an effect on the way in which brain cancers grow and spread. Cancers that have a mutation in the IDH gene grow more slowly than cancers that do not have this mutation. Patients diagnosed with IDH-altered gliomas are much younger than those diagnosed with IDH wild-type gliomas. Additionally, IDH-altered gliomas frequently manifest as a larger tumor at the time of diagnosis and tend to be localized in the frontal lobe of the brain (135). In addition, a more favorable prognosis is related with cancers that have pathogenic mutations in IDH1 and IDH2 as opposed to tumors that have IDH1/2 wild type (136). Approximately 40% of IDH1/2 wild-type GB show MGMT promoter methylation (136).

An additional marker, which predicts patient survival includes the analysis of O6-methylguanine-DNA methyltransferase (MGMT) gene promoter mutations. The MGMT gene encodes for a DNA-repair protein called O6-Methylguanin-DNS-Methyltransferase, which is responsible for removing alkyl groups from the position O6 of guanine in DNA. The promoter of the MGMT gene is responsible for regulating the production of the MGMT protein. It is generally agreed that increased methylation of the MGMT promoter is the primary cause of decreased MGMT protein production, and hence decreased DNA repair ability, making the tumor cells more sensitive to treatment with alkylating agents such as temozolomide (TMZ) (137).

In addition, analysis of EGFRvIII (epidermal growth factor receptor mutation type III) expression is associated with poor prognosis. In tumors with amplification of the EGFR gene, this genotype is observed in 50-60% of cases (138–140). This is in part through enhanced repair of double-strand DNA breaks and an elevated hypoxic fraction in the tumor (141, 142). Tissue hypoxia, regardless of treatment modality, has been shown to correlate with increased tumor cell invasion and poor clinical outcomes (143).

Recent research has shown that mutations in the tumor suppressor gene, phosphatase and tensin homolog (PTEN) (144) play a role in GB oncogenesis.

3.1.3 Therapy

GB remains an incurable cancer (145). Standard therapy consists of surgical resection, radiotherapy and concomitant and adjuvant chemotherapy with the alkylating agent temozolomide (TMZ). Despite treatment, tumor recurrence is inevitable, accompanied by the rise of satellite tumors in the brain.

The current goal of disease management is to prolong and improve the quality of life of the patient. The largest portion of patients are treated with multiple-modality therapy, consisting of the treatment of symptoms and surgery. While surgical resection of the tumor remains the primary treatment for disease management, the symptomatic treatment addresses the symptoms which result from the increased local pressure in the brain. A local pressure increase leads to damage in the surrounding areas, which in turn can lead to epilepsy, neurological deficiencies, and high intracranial pressure (ICP) (146). As described before, tumor recurrence is inevitable, as GB is highly invasive, and differentiation between tumor and healthy brain tissue is extremely difficult. There are multiple resection approaches to GB, but they are limited in their efficacy and safety to patients.

The removal of brain tumors can be accomplished using a surgical procedure known as supramaximal resection (SMR). It requires the removal of the tumor as well as some of the healthy tissue that is around it and extending beyond the contrast-enhanced zone. This is the portion of the tumor that stands out as bright on an MRI image. The purpose of SMR is to lessen the burden of cancer and increase patients' chances of surviving their disease in the case of GB (147, 148). Gross total resection (GTR) refers to a surgical treatment that tries to remove the entirety of the visible tumor mass, including the infiltrating edges of the tumor (149). In comparison, the GTR compared to SMR did not lead to a significant difference in disease progression (150). It is hypothesized that this is related to the imperceptible migration of tumor cells through nerve fibers (neuropils), which renders full detection of tumor cells and ultimately resection impossible. Otherwise, extensive excision of tumor and healthy tissue (SMR) has the potential to harm healthy brain areas, resulting in a substantial deterioration in the patient's quality of life. Consequently, following primary resection, adjuvant fractionated radiation remains the mainstay of treatment (130).

In recent years, novel therapeutic approaches have had some moderate success. Combining low dosed fractioned radiotherapy with the alkylating agent temozolomide (TMZ) led to an increase in therapeutic efficacy in comparison to radiotherapy alone (150).

The presence of a hypermethylated MGMT promotor, which results in the inactivation of MGMT in GB cells, increased the magnitude of the effect dramatically. The adjuvant, combined treatment of TMZ and radiation (daily for the length of the radiotherapy), followed by six recurrent treatments of 5 days every 4 weeks with TMZ, dramatically increased the two- and five-year median survival of GB patients. As only one third of patients have mutations in the MGMT gene promotor, it is one of the rarest and most accurate predictors in GB treatment (150).

Recently, it was shown that the lysosomotropic drug chloroquine (CQ), routinely used for malaria prevention and rheumatoid arthritis, had a potential synergistic impact with TMZ and radiation in tumors with an EGFRvIII mutation. In a first, initial study, the addition of chloroquine to conventional treatment increased overall survival and was well tolerated in newly diagnosed GB patients (151).

3.2 Cancer stem cells in glioblastoma and their relevance in therapy resistance

GB are highly heterogeneous tumors; it has long been recognized that GBs consist of discrete cellular populations with diverse genetic, epigenetic, and phenotypic characteristics. One small fraction of the tumor consists of highly malignant GB stem-like cells (GSC).

The theory of cancer stem cells mainly consists of two different and somewhat competing concepts.

(I) GSC, resemble a malignant version of a healthy stem cell, giving rise to different lineages of daughter cells that differentiate and maintain a healthy and functioning tissue. The malignant change in neural stem cells therefore leads to the establishment of GB. This process resembles a strict hierarchical, unidirectional differentiation and proliferation of malignant daughter cells. In this model, the heterogeneous nature of a tumor is due to cellular differentiation, mediated by cancer stem cells.

(II) A competing theory describes the development of GSC out of non-stem cell tumor cells through mutation and de-differentiation of malignant cells in an existing tumor (152, 153).

What both theories have in common is that GSC resemble unlimited self-renewing malignant cells that maintain the tumor and give rise to a slow but steady supply of high proliferating daughter cells that in turn enable fast tumor growth. Hereby, the unlimited self-renewal and slow proliferation of GSC sustains the tumor, but a rapid tumor development and expansion is reliant on more differentiated, fast dividing GSC offspring. Therefore, the heterogeneous nature of a tumor is due to cellular differentiation, mediated by cancer stem cells.

It has been described that, within one GB tumor, several subtypes of GSC, and differentiated tumor cells are present, further increasing the complexity of tumor composition in GB.

GB are divided into several molecular subgroups according to gene expression patterns or immunohistochemical findings that are present in tumors (133, 154, 155). Throughout the course of medical research, four distinct subtypes of GB have been distinguished: proneural, neural, classical, and mesenchymal. It is interesting to note that GSC may also be classified based on the molecular subtypes that they possess. It has been shown that the primary immunohistochemical subtypes of GB are closely mirrored by mesenchymal and proneural GSC (154). In addition to this, primary proneural GB may sometimes present itself as mesenchymal GB. The transition from one subtype to another is a characteristic feature of GB tumors and can be explained in two different ways: either by the occurrence of a molecular switch in proneural GSC, which results in a transformation into a mesenchymal profile, or by the greater survival of mesenchymal GSC that are present in the main proneural GB (156–158). Furthermore, GSC are heterogeneous, volatile cells that can change their phenotypic and molecular programming in response to changes in their environment. These characteristics enable GSC to contribute to tumor angiogenesis, immune evasion, therapy resistance, and recurrence.

A low abundance within the tumor, low proliferative activity, resistance to chemo- and radiotherapy, and tumor recurrence (159, 160) are attributed to GSC.

GSC attract and manipulate immune cells, such as TAMs, MDSCs, and Treg. By secreting chemokines and growth factors, these cells are able to promote angiogenesis and restrict the immune response, leading to a immunosuppressive environment (161). Immunosuppression is a hallmark characteristic of cancerous tumors, including brain neoplasms (162), where it may be further exacerbated by the characteristics of the blood–brain barrier. GSC are responsible for the immunosuppressive environment that is present in gliomas. They do this by preventing the activation of cytotoxic T lymphocytes, which in turn causes them to undergo apoptosis, and by activating Treg. Molecular

interactions between soluble galectin-3 and B7-H1 are responsible for mediating these processes (163). In addition, GSC are capable of inducing immunosuppressive M2 differentiation in TAMs by means of IL-10, TGF-β1, soluble colony-stimulating factor 1 (sCSF-1), and macrophage inhibitory cytokine-1 (MIC-1) (164).

The low mitotic activity of GSCs renders them resistant to therapeutic strategies aimed at actively dividing cells. GSC chemoresistance has been shown in cell cultures, with apoptosis escape proposed as the fundamental mechanism (159). It has also been established that the radioresistance of GB is related with GSC expressing the stem cell marker CD133 (153). Within the context of combination treatment for GB, chemotherapy based on TMZ is a recognized and approved standard. Relapses, on the other hand, are quite likely to take place during the first year after therapy. This brief period of remission lends credence to the hypothesis that some GB cells are able to survive therapy. Because of their quiescent characteristic, which indicates low proliferation and, as a result, low activity of DNA synthesis, GSC seem to be hard to treat with chemotherapy. As a matter of fact, Liu et al. analyzed the effects of chemotherapy on $CD133^+$ GSC and $CD133^-$ GB cells. When compared, $CD133^+$ GSC showed a much higher level of chemoresistance (165–167). In addition to their ability to remain dormant, GSC have a greater potential to evade apoptosis and activate intrinsic DNA repair mechanisms compared to non-stem tumor cells (156, 166, 168).

MGMT, is an enzyme that plays a significant role in the development of treatment resistance in GSC (169). When treating MGMT-positive GSC with TMZ, much greater dosages are required to achieve the desired therapeutic effect. It has been shown in patients, that dosages of TMZ that were adequate for the eradication of GSC in MGMT-negative tumors, were insufficient in MGMT-positive tumors (170).

Therapeutic irradiation is a crucial component of the protocol for treating GB; however, like TMZ, it is unable to stop GB from reoccurring after therapy. When compared with $CD133^-$ glioma cells, $CD133^+$ GSC have a much higher level of resistance in both *in vitro* and *in vivo* settings. CD133 expressing cells preferentially activate the DNA damage response and are able to quickly repair any damage that has occurred (153). Tyrosine kinase MET should also be included when talking about the signaling cascade that occurs during DNA damage repair when exposed to ionizing radiation. MET is necessary for proper cell migration during embryonic development (171), which occurs throughout the body. In cancer, it plays a role in the survival of cancer cells, the formation of new blood vessels, invasion, and metastasis (172). Through the activation of AKT kinase and the following downstream effectors of DNA repair, MET is responsible for inducing radio-resistance in cancer cells. Phosphorylation and cytoplasmic retention of the p21 protein, which has an impact that is anti-apoptotic, is the second MET-induced mechanism of radio resistance. In GSC, inhibition of MET may lead to an increase in radiosensitivity (156, 173).

Furthermore, GSC have been shown to have tumor initiating capacities. When patient-derived GSC are introduced into an animal, they are able to give rise to a heterogeneous tumor, resembling the morphology seen in the original patient (159, 160). Chen et al. demonstrated in a mouse model that a subgroup of tumor cells is the cause of GB recurrence after TMZ therapy; these cells express the stemness marker nestin and have poor Ki-67 proliferative activity (152).

3.2.1 GSC plasticity

GSC are heterogeneous, volatile cells that can change their phenotypic and molecular programming in response to changes in their environment.

Stem cells are abundant in locations containing endothelial and ependymal cells, which aid in preserving their stem cell characteristics in a synergistic and co-dependent manner (174). GSC exploit this link within the TME since their stem-like properties require a specialized niche, which enables the

following characteristics of GSC: cell division, self-renewal (175), a high rate of proliferation (176), and the multidirectional differentiation of tumor cells into differentiated tumor cells.

There are three main GSC niches: the perivascular, the invasive, and the hypoxic niche.

When GSC come in direct contact with the endothelium, perivascular niches will grow along the capillaries and arterioles of the blood vessel. Through angiogenic pathways, an abnormally formed and functional mass of blood vessels nourishing the tumor is formed. In this perivascular niche, GSC interact with their surrounding cells in a synergistic and co-dependent manner, which promotes tumor cell growth and invasion (177).

Invasive niches are distinguished from non-invasive niches by the presence of perivascular development of single invasive neoplastic cells along the capillaries, in the space between the endothelium and reactive astrocytes. The proliferation of nestin-positive GSC in the perivascular space causes the end-feet of astrocytes to detach from arteries, which in turn leads to the dissociation of pericytes. Endothelial proliferation and angiogenesis are also characteristics of GB, and both mechanisms contribute to tumor development. Necrosis is caused by vascular blockage and/or as a result of an imbalance between the rapid development of GB and the delayed proliferation of blood vessels. Necrotic areas are surrounded by highly cellular perinecrotic pseudopalisades. These regions are known to harbor increased amounts of GSC. GSC are not only able to endure hypoxia, but they are also induced by it, being triggered by the expression of hypoxia-inducible factors HIF-1 and HIF-2 (158, 178–180). GB invasion frequently occurs in the perivascular regions of healthy blood vessels, where tumor cells encircle healthy blood vessels and rob them of oxygen and nutrients through a process known as vascular co-option. In this nutrient- and oxygen-rich environment, tumor cells multiply rapidly and form a tumor. Tumor formation leads to endothelial cell death and blood vessel collapse, resulting in the development of hypoxia in the tumor core. Ultimately, this mechanism compels GSC to release VEGF and SDF-1α for angiogenesis. GSC also produce TGF-β to encourage tumor-derived pericytes to promote the function of newly formed blood vessel and therefore tumor growth (181). It has been postulated that all niches are merged into the hypoxic periarteriolar niche. This is due to the fact that the interaction between GSC and the endothelium, vascular development in GB, and necrosis are all distinct features that are reflected within the same process (156, 182).

In the perinecrotic (hypoxic niche), GSC congregate around arterioles, which do not permit oxygen exchange and hence cause hypoxia, comparable to hematopoeic stem cell niches in bone marrow. Hypoxia has long been recognized as a crucial factor in cancer stemness induction. Hypoxic niches in GB are known to include a greater number of GSC, which are maintained by HIF-2α, which is triggered by CD44. Hypoxic niches promote the essential stem cell characteristics of pluripotency, self-renewal, and tumorigenicity (183).As described above, hypoxic conditions can induce the synthesis of HIF-1 α.

The transcription factor HIF-1α plays a significant role in the regulation of the response of $CD8^+$ T lymphocytes to hypoxic circumstances. It has been demonstrated that HIF-1α has the ability to improve the effectiveness of $CD8^+$ T cells in promoting antitumor immunity. However, once it is stabilized by the binding of T cell receptors, HIF-1α limits the growth, proliferation, and generation of inflammatory cytokines by cytotoxic T lymphocytes (CTLs) (176, 184–187). Furthermore, it has been described that the IFN-γ secretion by $CD4^+$ T cells is enhanced (188). Hypoxia is a key component of the microenvironment of GB. The self-renewal of GSC is maintained by hypoxia, and the total number of GSC in the population is even increased (158). In addition to this, it ensures the continuation of malignant cell proliferation, invasive development, and survival (189–191). Hypoxia, via a variety of different processes, increases a patient's resistance to therapy. Because hypoxia prevents the production of free radicals, radiation therapy is less effective when it is administered (158).

Furthermore, hypoxia promotes the development of the multidrug resistance gene MDR1/ABCB1, which is detrimental to the effectiveness of chemotherapy.

As mentioned before, a lack of oxygen is one of the defining characteristics of GB. Hypoxic conditions increase the need for glycolysis, which is often active in tumor cells even despite being in aerobic circumstances (192). This is in addition to the regulatory influence that hypoxia has on the quantity and activity of GSC (162). The Warburg effect has also been shown to be present in glioma cells, including GSC. This is characterized by a de-prioritization of oxidative phosphorylation, which is more active in normal cells, in favor of aerobic glycolysis. This is because aerobic glycolysis provides most of the building blocks required for fast cell proliferation, while reducing oxidative stress by avoiding byproducts of the oxidative phosphorylation. Aerobic glycolysis is not as efficient as its anaerobic counterpart in terms of ATP production, but it is advantageous as a metabolic source for the production of new molecules (162). According to the "go or grow" hypothesis (193), metabolism serves as a reciprocal switch between two pathways—glycolysis, associated with invasion, and the pentose phosphate pathway (PPP) which is connected to proliferation. These two behaviors are related to the cell's ability to either proliferate or invade new territory. Under circumstances of low oxygen, glycolysis remains active, and cells continue to actively migrate and invade their surroundings. The PPP is activated and proliferation occurs when oxygen is present (164).

Because of their phenotypic flexibility due to the not yet known mode of origin, the multifactorial environmental influences, and the capacity to adjust to new circumstances, the high phenotypic flexibility of GSC makes the establishment of diagnostic and therapeutic approaches challenging. Currently, there are several markers like CD133, nestin, Sox2 and CD44 known to be expressed by GSC, but ultimately fail to identify them.

3.2.2 GSC identification & isolation

CD133 was the initial marker that allowed for the identification of GSC and continues to be one of the best characterized. CD133, also referred to as prominin-1 or AC133, is a member of the pentaspan transmembrane glycoprotein family (194). It was initially found in human hematopoietic stem cells (195). CD133 is commonly used to identify and enrich cells involved in tumor initiation and progression. In a NOD/SCID xenograft model, it has been demonstrated that $CD133^+$ cells are responsible for proliferation and resistance to therapy in GB (196). Nevertheless, the usefulness of CD133 for GSC characterization and identification is still highly debated as it has been described, that CD133 negative GB cells are also able to initiate tumors and $CD133^+$ cells are more differentiated (197). Additionally, the function of CD133 in GB is still unclear. CD133 may change depending on the interaction partners in the TME. Furthermore, there is evidence that CD133 is involved in the epithelial to mesenchymal transition (198). Due to the not yet fully understood function, the role of CD133 as a surface marker for GSC is in doubt.

Initially, the protein that is now known as nestin was discovered to be an antigen of rat-401 that was directed toward embryonic spinal cord cells. The expression of this protein has been demonstrated to occur in neuroepithelial stem cells, and it is found to be strongly expressed in a number of different forms of human cancer, including high-grade GB. Nestin has been shown to be highly related with lower cancer patient survival, but other studies have shown no correlation between nestin expression and poor prognosis in GB. Combining CD133 and nestin expression increases the accuracy of the prognosis significantly. Furthermore, the combination of nestin and CD133 has a potential as an indicator of GB invasion. Despite intensive research the description and function of nestin is still elusive. Nestin is another possible marker for the GSC phenotype, and it is highly likely that it plays a substantial part in the aggressive growth metastasis and the capacity of GSCs to expand and renew themselves. In addition to this, it plays a role in the organization of the cytoskeleton, cell signaling, organogenesis, and cell metabolism. Furthermore, it is a representation of the properties of multi-

lineage progenitor cells, including proliferation, migration, and multi-differentiation. Because of this, it is a more appropriate target molecule than CD133 for identifying GSC in GB. Consequently, the coexpression of nestin and CD133 may be a signal of the biological invasion of GB.

Markers are not yet suitable for GSC identification. Yet, confident identification of GSC is key to understanding GB. Over time, various methods have been established to analyze the properties of GSC. One common model to study GSC is to develop patient derived GSC. After undergoing tumor resection, tumor tissue is processed by enzymatic dissociation, cell filtration and subsequent cancer single cell culture in serum free media complemented by growth factors like epidermal growth factor (EGF) and basic fibroblast growth factor (bFGF) to preserve the stem cell characteristics. Cells are then cultured in ultra low attachment dishes, where the GSC are able to form neurospheres.

To verify that the isolated cell lines are GSC several assays were developed over the years. As GSC have the capacity for self-renewal, serial limiting dilution assays and sphere formation assay are performed. Hereby, GSC are still able to form neurospheres from single cells after subsequent rounds of serial limiting dilution assays. Furthermore, GSC are tested for the capacity of *in vitro* differentiation. The cells are commonly subjected to EGF and bFGF withdrawal and assessed for the expression of neural lineage specific differentiation markers. Additionally, the tumorigenic potential is evaluated in an orthotopic mouse glioma model. In this case, GSC give raise to tumors, resembling morphological criteria of GB when implanted into mice brains.

3.3 Manuscript II: GARP as an Immune Regulatory Molecule in the Tumor Microenvironment of Glioblastoma Multiforme

Summary of own contributions

Conceptualization, A.T., E.K., J.T., and C.S.; methodology, N.Z., J.S., P.L., F.K., and B.S.; validation, N.Z. and B.S.; formal analysis, F.K.; resources, A.T.; writing—original draft preparation, A.T., N.Z., and E.K.; writing—review and editing, C.S., J.T., and F.R.; supervision, A.T.; project administration, N.Z.; funding acquisition, A.T.

The author planned, designed, and performed all *in vitro* experiments and the subsequent analysis. Immunohistochemical staining of patient material by Petra Leukel. Cell lines were provided by Ella Kim. The author took lead in preparing the manuscript together with Prof. Dr. med. Andrea Tüttenberg and Ella Kim.

Keywords: glioblastoma; GARP; tumor microenvironment; immunotherapy; regulatory T cells

Citation: ***Zimmer, N.****; Kim, E.; Schupp, J.; Sprang, B.; Leukel, P.; Khafaji, F.; Ringel, F.; Sommer, C.; Tuettenberg, J.; Tuettenberg, A. GARP as an Immune Regulatory Molecule in the Tumor Microenvironment of Glioblastoma Multiforme. Int. J. Mol. Sci. 2019, 20, 3676. https://doi.org/10.3390/ijms20153676*

Received: 9 July 2019; Accepted: 23 July 2019; Published: 26 July 2019.

Zusammenfassung

Glykoprotein A repetitions predominant (GARP) ist ein spezifisches Oberflächenmolekül auf aktivierten regulatorischen T-Zellen (Treg) und trägt beim Menschen nachweislich erheblich zur Immuntoleranz bei. GARP ist in der Lage periphere Treg und regulatorische M2-Makrophagen zu induzieren und hemmt tumorantigenspezifische T-Effektorzellen. In der Vergangenheit wurde die Expression von GARP auf Treg sowie auch auf der Oberfläche verschiedener bösartiger Tumoren beschrieben. Zusätzlich konnte GARP in löslicher Form als immunsuppressives Protein nachgewiesen werden, das von der Zelloberfläche freigesetzt wird. Des Weiteren konnte eine GARP-Expression auf Hirnmetastasen vom malignen Melanom beschrieben werden. Auf der Grundlage dieser Ergebnisse wurde untersucht, ob GARP auch in primären Hirntumoren nachgewiesen werden kann. In dieser Arbeit konnte die Expression von GARP auf Glioblastom (GB)-Zelllinien, primärem GB-Gewebe sowie auf niedriggradigen Gliomen nachgewiesen werden. Dies deutet auf eine wichtige Rolle von GARP im immunsuppressiven Tumormikromilieu primärer Hirntumore hin. Es konnte gezeigt werden, dass in Kokulturexperimenten, GB-Zellen in der Lage sind, T-Effektozellen GARP-abhängig zu unterdrücken. Interessanterweise ist GARP nicht nur auf der Zelloberfläche lokalisiert, sondern kann auch im zytoplasmatischen und nukleären Kompartimenten von Tumorzellen nachgewiesen werden. Unsere Ergebnisse zeigen, dass GARP, als immunregulatorisches Molekül, sowohl auf als auch in Tumorzellen von GB und niedriggradigen Gliomen exprimiert ist und durch seine immunsuppressiven Eigenschaften einen signifikanten Beitrag zum Tumormikromilieu primärer Hirntumore leistet. Da GARP sowohl auf aktivierten Treg als auch auf Hirntumoren exprimiert wird, könnte es als Ziel für neue antikörperbasierte immuntherapeutische Ansätze dienen.

Abstract

Glycoprotein A repetition predominant (GARP), a specific surface molecule of activated regulatory T cells (Treg), has been demonstrated to significantly contribute to tolerance in humans by induction of peripheral Treg and regulatory M2-macrophages and by inhibition of (tumorantigen-specific) T

effector cells. Previous work identified GARP on Treg, and also GARP on the surface of several malignant tumors, as well as in a soluble form being shedded from their surface, contributing to tumor immune escape. Preliminary results also showed GARP expression on brain metastases of malignant melanoma. On the basis of these findings, we investigated whether GARP is also expressed on primary brain tumors. We showed GARP expression on glioblastoma (GB) cell lines and primary GB tissue, as well as on low-grade glioma, suggesting an important influence on the tumor micromilieu and the regulation of immune responses also in primary cerebral tumors. This was supported by the finding that GB cells led to a reduced, in part GARP-dependent effector T cell function (reduced proliferation and reduced cytokine secretion) in coculture experiments. Interestingly, GARP was localized not only on the cell surface but also in the cytoplasmatic, as well as nuclear compartments in tumor cells. Our findings reveal that GARP, as an immunoregulatory molecule, is located on, as well as in, tumor cells of GB and low-grade glioma, inhibiting effector T cell function, and thus contributing to the immunosuppressive tumor microenvironment of primary brain tumors. As GARP is expressed on activated Treg, as well as on brain tumors, it may be an interesting target for new immunotherapeutic approaches using antibody-based strategies as this indication.

3.3.1 Introduction

This section has been shortened to avoid any major repetition of previous chapters. The complete, unedited version of this manuscript can be found in the appendix II.

Despite extensive experimental and clinical research, GB is still one of the most fatal tumors in humans with a median progression-free interval with maximal therapy of less than 12 months and a median overall survival of up to 15 months (199). The tumor itself develops numerous so-called immune-escape mechanisms that help to shut down or prevent an efficient antitumor response. This mainly includes the genetic instability of tumor cells, which leads to changes in the surface profile or the antigenic structures on the tumor cell itself and downregulation of human leukocyte antigens(HLA) molecules (200). Furthermore, soluble factors such as IL-10 and TGF-β, as well as pro-angiogenic factors (vascular endothelial growth factor -VEGF, platelet-derived growth factor - PDGF, fibroblast growth factor -FGF, IL-8), play a role in turning off the effector cells present in the tumor and promoting tumor angiogenesis (10, 201). Therefore, many studies aim to characterize new regulatory molecules and signaling pathways of tumor cells and their impact on the tolerogenic properties of the tumor microenvironment in order to identify new targets for immunotherapeutic approaches.

We have recently shown that the specific Treg activation marker GARP (glycoprotein A repetition predominant) in its soluble form has tolerance-inducing functions (74). In addition to its expression on activated Treg, we have also shown its occurrence on cells of primary malignant melanoma and melanoma cerebral metastasis.

In the present study, we analyzed GARP as a potential marker molecule and key factor for the immunoregulatory environment in GB and investigated its relevance as a potential target for a therapeutic approach in patients with cerebral cancer.

3.3.2. Results

3.3.2.1. GARP Expression on Immunohistochemistry of Glioblastoma and Low-Grade Astrocytomas

Recent studies of our own group revealed GARP as an immunoregulatory molecule expressed on activated Treg and capable of suppressing effector cell proliferation and cytokine production and to confer suppressive activity to T effector cells. In addition, GARP has been detected on melanoma cells, as well as on brain metastasis of melanoma (43).

In order to investigate in situ GARP expression and thus its relevance on the immunosuppressive tumor microenvironment of GB, 37 patients (26 males and 11 females) with histologically proven GB between January 2009 and May 2015 were included (Table 3.3.1). The mean ± standard deviation (SD) at the onset of disease for males was 69.05 ± 11.93 years and 71.38 ± 11.72 years for females (independent t-test p >0.05). As shown in Table 3.3.1, 67.6% (17 males and eight females) had the tumor left hemispheric. The temporal lobe was the most involved part of the tumor (29.7%, Pearson Chi-square p > 0.05, Figure 3.3.1a). There were 33 subjects who underwent a surgical resection. The first histological diagnosis showed GB in 89.2% of the subjects. After surgery, 29 patients had radiation therapy, 26 had chemotherapy, and a combined chemoradiotherapy had been applied to 24 patients. The mean survival after diagnosis was 11.07 ± 13.27 months.

Glioma grade III and IV	***male***	***female***	***total***	***lost to follow up***
Number of patients	*26*	*11*	*37*	
Age at the onset mean±SD (yr.)	*69.05±11.08*	*71.38±11.72*	*68.78±13.36*	
Side hemispheric				
right	*9*	*3*	*12*	
left	*17*	*8*	*25*	
bilateral	*0*	*0*	*0*	
Surgery				
resection	*19*	*3*	*27*	
biopsy	*7*	*8*	*10*	
First histological diagnosis				
grade IV	*23*	*10*	*33*	
grade III	*3*	*1*	*4*	
Localization				
frontal	*5*	*5*	*10*	
parietal	*6*	*2*	*8*	
temporal	*9*	*2*	*11*	
thalamic	*2*	*0*	*2*	
fronto-parietal	*0*	*1*	*1*	
occipital	*2*	*0*	*2*	
perieto-occipital	*0*	*1*	*1*	
temporo-parietal	*2*	*0*	*2*	
Radiation therapy	*20*	*9*	*29*	*3*
Chemotherapy	*20*	*6*	*26*	*5*
Survival mean±SD (mon.)	*11.68±15.22*	*9.38±4.98*	*11.07±13.27*	

Table 3.3.1. Patients with glioma grade III and IV at the study center Idar-Oberstein, Germany were included. Patient characteristics (gender, age), as well as primary tumor data including localization, therapy, and follow-up are displayed.

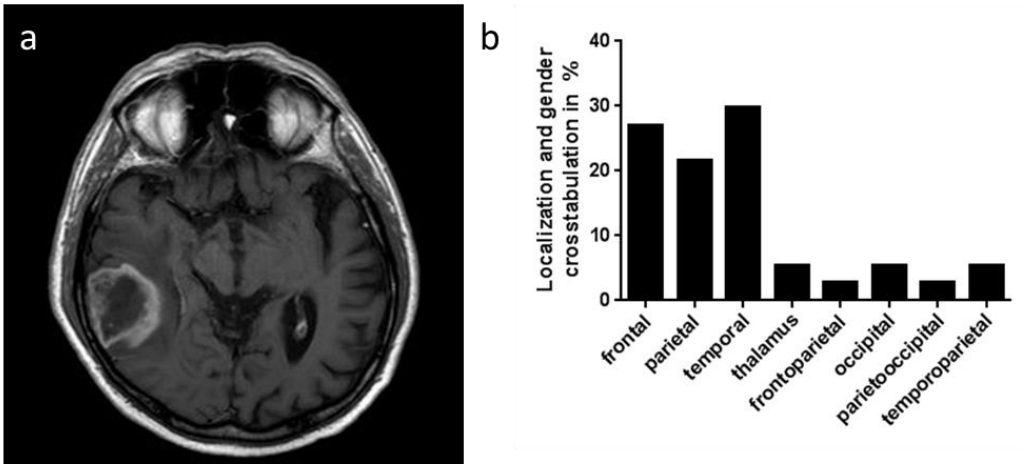

Figure 3.3.1. (**a**) T1-weighted gandolinium enhanced cranial axial image with a typical glioblastoma (GB) in the right dorsal temporal lobe. (**b**) Frequency of localization of GB in % is shown. Most tumors were found in the frontal, parietal, and temporal lobe of the patients.

In these patients we investigated the relevance of GARP in primary brain tumors such as GB and compared it to astrocytomas grade II and grade III (Table 3.3.A1, 3.3.A2). In this study, GARP immunostaining was analyzed only in tumor cells and not in inflammatory cells. Interestingly, all tumors analyzed, except one GB, showed at least 50% GARP expression (Figure 3.3.2). In detail, two of the grade II astrocytomas showed more than 50% labeled nuclei, the other two more than 90% labeled nuclei (Figure 3.3.2a, d). Five of the grade III astrocytomas showed more than 50% labeled nuclei, the other six more than 90% labeled nuclei (Figure 3.3.2e). One of the GBs was completely negative, whereas, 19 GBs showed more than 50% labeled nuclei, the remaining 16 showed more than 90% labeled nuclei (Figure 3.3.2b, f). As a control, normal brain tissue derived from the neighborhood of a glioma was stained. Single neurons, so-called dark neurons or hypoxic-ischemic damaged neurons, displayed some weak GARP staining (Figure 3.3.2c), whereas, the majority of cells did not display any GARP expression.

Taken together these data show dominant expression of the inhibitory GARP molecule also in primary brain tumors such as GB and low-grade glioma, implicating a potential relevance for the immunosuppressive tumor micromilieu.

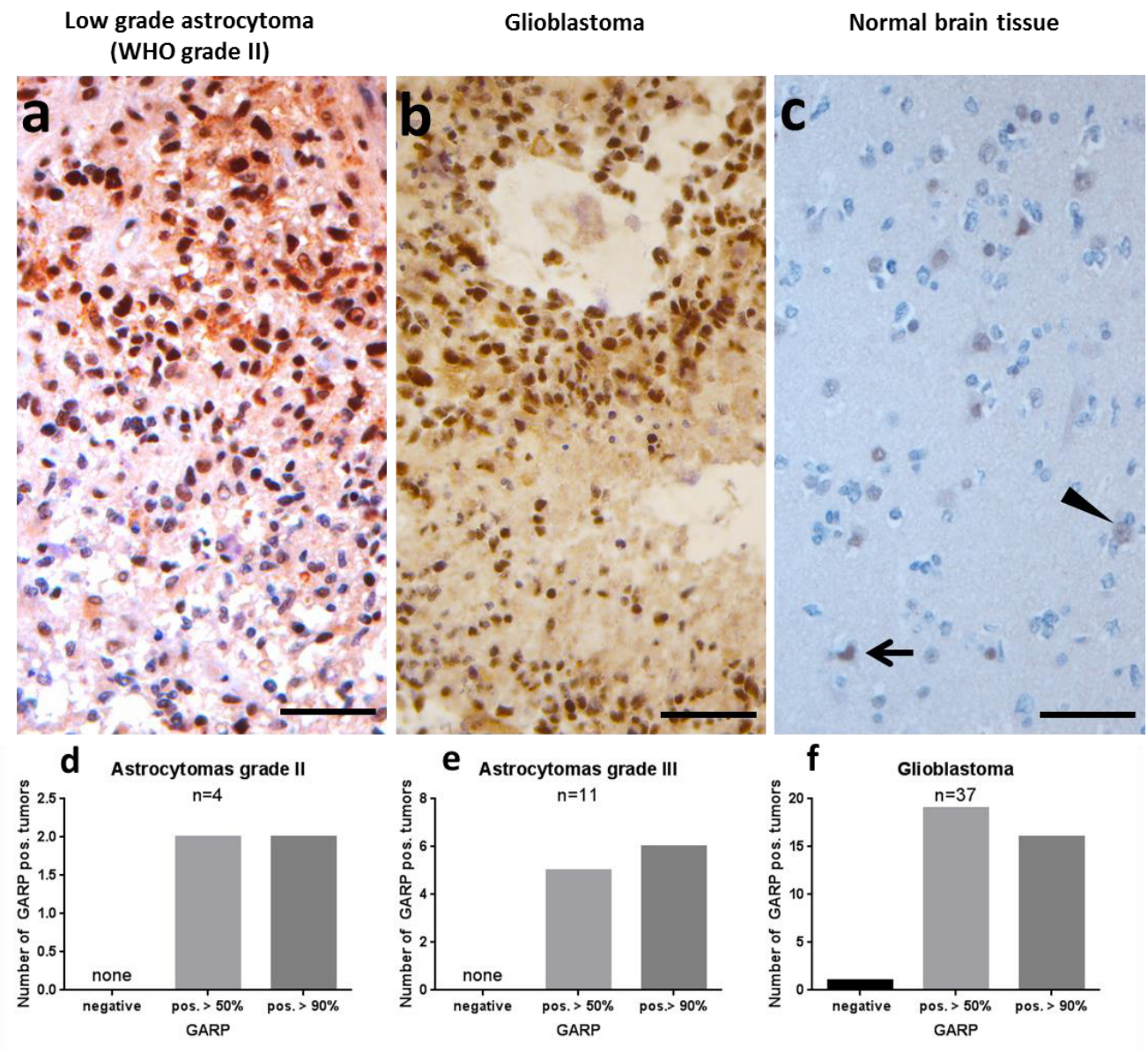

Figure 3.3.2. Glycoprotein A repetition predominant (GARP) immunohistochemistry in gliomas and astrocytomas. (**a**,**d**,**e**) Low-grade astrocytoma (WHO grade II) with more than 50% positive (pos.) labeled nuclei (magnification × 400). (**b**,**f**) GB with palisading necroses and more than 90% pos. stained tumor cells (magnification × 400). (**c**) Largely normal brain tissue in the neighborhood of a glioma with some labeled neurons (arrow) while others where unstained (arrowhead). Bar corresponds to 50 µm.

3.3.2.2. GARP Expressed on the Surface of GB and in the Cytoplasma and Nucleus

GARP is a transmembrane protein that presents latent TGF-β1 on the surface of Treg. TGF-β1 influences a variety of immune cells by conferring immune tolerance and has been shown to be present in brain tumors being associated with poor prognosis of patients with GB (202).

In order to confirm the expression of GARP on GB tumor cells, a commercially available GB cell line (T98G), three patient-derived GB cell lines (#1043, #1051, #1063), and a melanoma cell line (MaMel-19) were analyzed by flow cytometry and confocal microscopy (Figures 3.3.3 and 3.3.4). As a positive control for GARP expression, resting and activated Treg were investigated (Figure 3.3.3). Flow cytometry data showed GARP localization on the surface of Treg and all tested cell lines, confirming not only previous results but also the in situ data from primary brain tumor tissue (shown in Figure 3.3.2) (32).

Interestingly, while analyzing the expression of GARP in brain tumor cells in more detail, we detected intracellular (IC) and intranuclear (IN) localization of GARP in T98G, MaMel-19, and all three patient-derived cell lines (#1043, #1051, and #1063), as well as in resting and activated Treg. All cell lines showed a significant expression of GARP in the cytoplasma as well as in the nucleus of tumor cells. The intracellular expression of GARP was even more pronounced when compared to surface expression. This could be shown using confocal microscopy (Figures 3.3.3a, and 3.3.4a) and for the Treg, T98G, and MaMel-19 also via flow cytometry (Figure 3.3.3b).

Thus, our data show, for the first time, intracellular GARP expression in tumor cell lines of GB and melanoma, as well as in Treg.

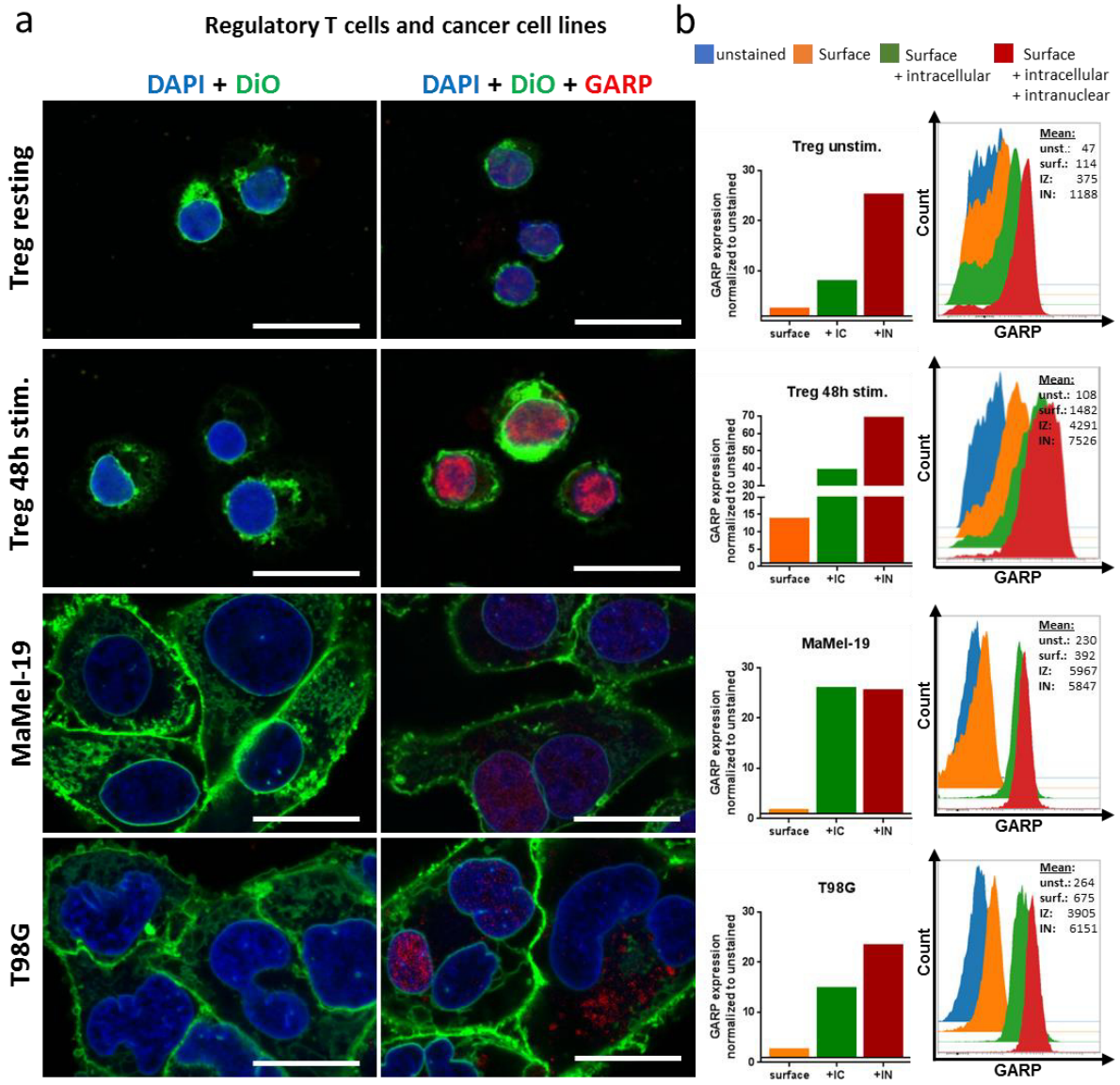

Figure 3.3.3. Analysis of the GARP localization in resting and stimulated regulatory T cells, melanoma cell line MaMel-19, and glioblastoma cell line T98G. The Treg were stimulated with 1 µg/mL anti-CD3 mAb, 1 µg/mL anti-CD28 mAb, and 10 IU/mL IL-2 for 48 h. (**a**) Cytoplasmatic and intranuclear localization of GARP shown in confocal images. The white bar corresponds to 20 µm (**b**) flow cytometric analysis GARP expression on the surface; surface and intracellular (IC); and surface, IC, and intranuclear (IN) of Treg, melanoma, and GB cell lines. Means were normalized to the unstained control.

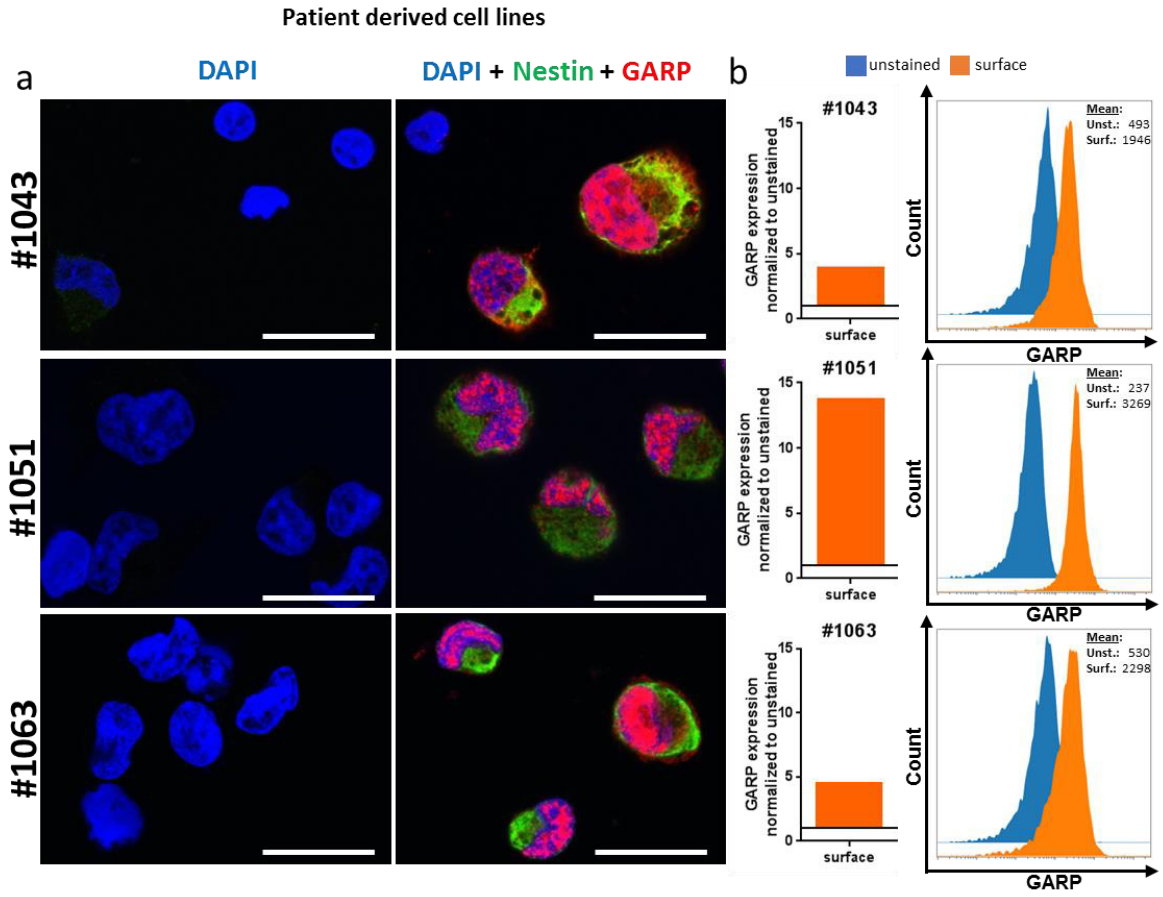

Figure 3.3.4. Flow cytometric and confocal analysis of GARP expression in patient-derived GB cell lines. (**a**) Confocal images show a strong GARP expression on the surface, intracellular (IC) and intranuclear (IN) in all tested patient-derived GB cell lines. The white bar corresponds to 20 µm (**b**) Flow cytometric analysis of the surface expression of GARP. All three cell lines showed an expression of GARP. Due to the nature of these cells, nestin instead of DiO was stained. Means were normalized to the unstained control.

3.3.2.3. GB Cell Line T98G Suppresses T Effector Cell Function

It is known that the tumor microenvironment (TME) promotes immune escape mechanisms through inhibitory cell populations such as Treg, myeloid-derived suppressor cells (MDSC), and tolerogenic dendritic cells (tolDC), as well as inhibitory factors produced by the tumor cells themselves (203–205). Furthermore, soluble factors secreted by Treg and tolDC, such as IL-10 and TGF-β, promote the immunosuppressive TME which prevents the rejection of the tumor by the immune system and results in tumor expansion and metastasis (9).

In order to analyze the effect of GB cell line T98G on T effector cells, coculture experiments were performed as described by (32, 43) and proliferation and cytokine production of T effector cells were analyzed. As shown previously, the addition of soluble GARP (sGARP, 1µg/mL) downregulated IFN-γ production in activated $CD4^+$ T effector cells (Figure 3.3.5a). Furthermore, we observed that the addition of T98G to $CD4^+$ T effector cells exerted a dose-dependent inhibition of INF-γ production (approximately 30% inhibition), which was nearly completely restored by using a blocking anti-GARP Ab. Proliferation of T effector cells was also inhibited in coculture was, in part, rescued (Figure 3.3.5b) by blocking GARP. These results are in agreement with data obtained previously, showing the T effector cell suppression by melanoma cells (43).

Taken together, our data show that GARP plays an important role in the suppressive capacities of GB on T effector cells.

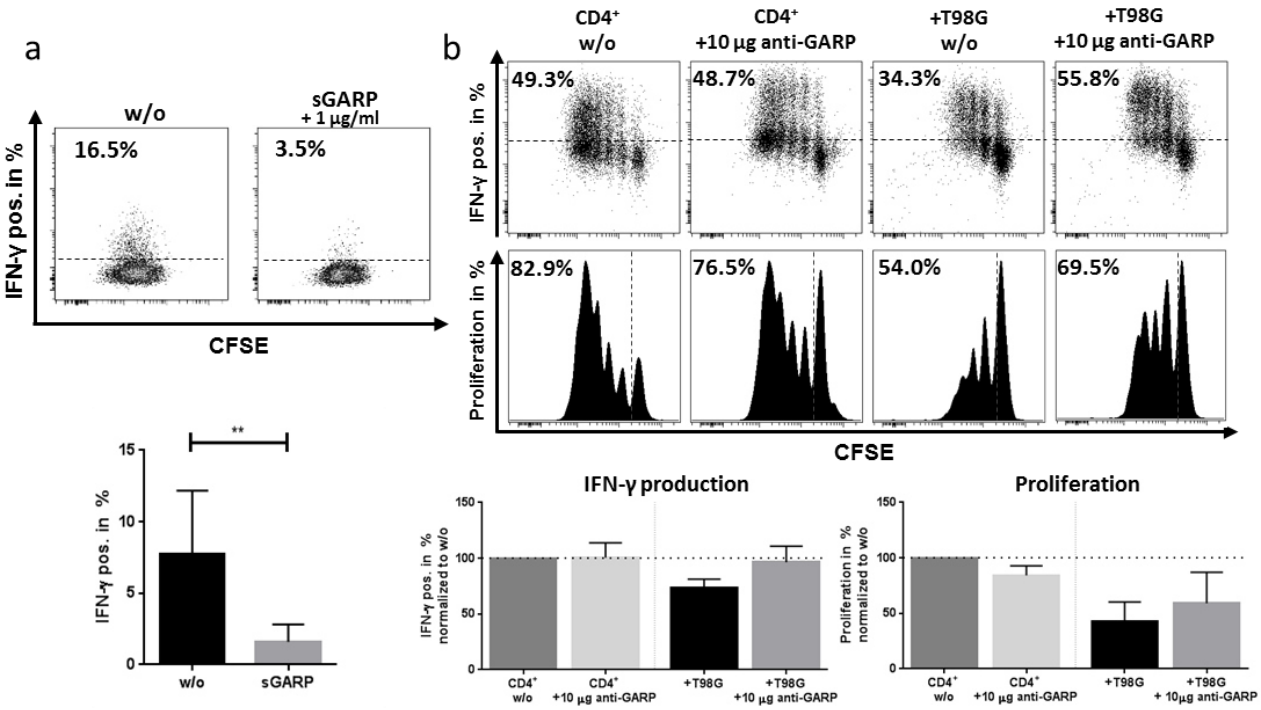

Figure 3.3.5. (**a**) Soluble GARP (sGARP) cytokine suppression. $CD4^+$ T cells were stimulated with 1 µg/mL anti-CD3 mAb, 1 µg/mL anti-CD28 mAb, and with or without 1 µg/mL sGARP for 24 h. INF-γ production was measured by intracellular staining via flow cytometry. Dot plots show one representative result of 5 independent experiments. (**b**) T98G cells suppress T cell proliferation and cytokine production. $CD4^+$ T cells were cultured together with or without (w/o) T98G cells in the ratio of 8:1 and stimulated, as described above. Additionally, either 10 µg/mL anti-GARP Ab or no Ab were added into the culture and $CD4^+$ T cells were stimulated as described before. IFN-γ production and proliferation (CFSE) were measured 4 days after stimulation by intracellular staining via flow cytometry. Dot plots show one representative result of 4 independent experiments. Data are displayed as mean values ± SEM, p-values relative to w/o ** $p < 0.01$. Dotted lines represent either unstained control (a + b IFN- γ), CFSE stained cells before stimulation or percentages normalized to the untreated control (w/o).

3.3.3. Discussion

A protein specifically expressed by activated Treg is the activation marker GARP. We have recently shown that GARP (glycoprotein A repetition predominant) has tolerance-inducing functions (inhibition of effector cell proliferation and cytokine production, induction of Treg, and induction of M2 macrophages) (74).

GARP is required for the formation and surface expression of latent TGF-β (32, 99) known to be involved in several immunoregulatory mechanisms, especially in tumor biology. The lentiviral knockdown of GARP in Treg showed decreased suppressive capacity and reduced FoxP3 expression in these cells (33). In addition to its expression on activated Treg, we also showed an occurrence on cells of the malignant melanoma, and thus a further regulatory effect in the tumor micromilieu (43).

GARP has been described by several groups as a transmembrane protein whose extracellular portion consists of 21 leucine-rich domains and is expressed on both Treg and platelets (32, 33). Leucine-rich domains (LRRs) have been identified in a variety of proteins involved in many different functions including signal transduction, cell differentiation, and migration. Those proteins are often membrane bound, can also be secreted or exhibit a cytoplasmic or nuclear localization (27), and are involved in protein–protein interactions. Amongst others, LRRs are found in molecules such as adhesion molecules, enzymes, or tyrosine kinase receptors (RTKs). Despite the localization of RTKs at the cell

surface, several are also found in the nucleus (206) being responsible for protein–protein interactions. Whether this is transferable for the intranuclear role of GARP in tumor cells as well as in Treg will be analyzed in more detail in future studies. Nevertheless, structural parallels such as LRRs suggest the possibility of comparable functions also for GARP.

Immunotherapy and targeted therapies have become increasingly important for the treatment of malignant tumors in recent years. However, only some patients respond here. Before considering the increasing number of possible therapy options, the side effects, and the response rates, as well as the costs, it is very important to create a treatment concept individually for each patient with the help of biomarkers. There are numerous efforts to identify factors at the cellular level, as well as at the level of soluble proteins, in the tissue and in the peripheral blood of tumor patients, which help to more accurately characterize the tumor microenvironment and thus the prognosis and the therapy response of an individual patient, and additionally lead to the development of new immunotherapeutic approaches (26, 207, 208). In this study, regulatory components of the tumor itself play an important role. In melanoma cells, GARP has been shown to be expressed on the surface of tumor cells, modulating and inhibiting antigen-specific T effector cell responses, and inducing peripheral Treg (43), thus, contributing to the immune-inhibitory tumor microenvironment. In order to analyze the suppressive role of GARP in GB we used a suppressor assay already published for melanoma cells (43). In this study, tumor cells were cocultured with T effector cells and IFN-γ production and proliferation of T cells were assessed. We have shown that the presence of GARP on GB cells was, in part, responsible for reduced T effector cell function also showing its immunosuppressive role in GB. The presence of GARP on GB cells may therefore be of great importance when discussing prognosis and therapeutic approaches in this tumor entity.

GB is the most common and most malignant form of intrinsic brain tumors accounting for 52% of all primary brain and central nervous system (CNS) malignancies in adults. The current standard of care for newly diagnosed GB is based on the “one-treatment-for-all” principle and consists of surgical resection followed by aggressive regimens of combined radiochemotherapy. Despite aggressive treatment, GBs have a final mortality rate close to 100%, less than a 10% five-years survival rate and a median survival of 15 months (199). The inevitable recurrence after standard therapy poses a major challenge for improving clinical outcomes of patients with GB. For recurrent GBs (recGBs), no effective therapeutic options are currently available with experimental treatments being the only option at this stage of the disease (209, 210). Currently, immunotherapy is considered among the most promising approaches for recurrent GB, particularly, the targeting of inhibitory T cell signaling mediated through programmed death 1 (PD-1), the PD-1 ligand or cytotoxic T-lymphocyte associated antigen 4 (CTLA-4) has emerged as a promising approach (210). On the basis of our findings, showing GARP being expressed on activated Treg as well as on brain tumors, it may be an interesting target for new immunotherapeutic approaches using antibody-based strategies.

In Treg, low levels of intracellular GARP were demonstrated prior to activation via the T cell receptor and CD28 (29), suggesting that low levels of GARP are sequestered intracellularly and T cell activation is necessary for the synthesis and surface expression of GARP. In addition, previous studies have shown that ectopically expressed GARP in T cells is able to upregulate Foxp3, indicating a more upstream induction of a tolerogenic phenotype (33). Interestingly, GARP has also been shown, via Northern blot, to be expressed intracellularly in different tissues such as placenta, lung, kidney, heart, liver, skeletal muscle, and pancreas but not in the brain (27).

The intranuclear localization and accumulation of GARP in cancer cells and also in Treg, as shown in our study for the first time, could be a hint for a second, TGF-β pathway independent way to exerpt its tumor immunity suppressing function. For example, RTKs, proteins containing LRRs similar to GARP protein, are mainly localized at the cell surface. Nevertheless, several RTKs, such as colony stimulating

factor 1 receptor (CSF-1R), are also found in the nucleus (206) where they interact with transcription factors regulation cell proliferation, survival, and migration. These full-length proteins translocate from the cell surface to the nucleus via the Golgi apparatus and the endoplasmatic reticulum.

Nevertheless, detailed information about a possible dynamic interaction of GARP with other proteins in the nucleus, and thus potentially regulating gene expression is still elusive and will be a topic for further research.

In the present study we describe for the first time the expression of the immunoregulatory molecule GARP in the tumor microenvironment of primary brain tumors such as GB but also astrocytoma grade II or III. Having shown previously the relevance of GARP for immunomodulation and inhibition of tumor-antigen specific effector cells (43) in melanoma patients, these findings could contribute to the understanding of tumor escape mechanisms of GB including progression and therapy resistance. Notably, GARP is known to exert its function in suppressing tumor immunity via the TGF-β pathway (74), which is one of the key pathways involved in GB progression and maintenance of self-renewal in glioma stem cells (GCS) (211). The necessity of targeting factors that contribute to the tumor immunosuppressive microenvironment has been increasingly recognized as a strategy to improve the efficacy of immunotherapy for GB (212, 213). Further studies with larger groups of patients are needed to confirm these findings.

Taken together, the present study will help to develop new immunotherapeutic approaches targeting GARP on Treg as well as on GB tumor cells as one possible factor to improve the outcome of GB patients.

3.3.4. Materials and Methods

3.3.4.1. Cell Culture

For the cell line T98G, Eagles minimum medium supplemented with 10% FCS, 1% glutamine, and 0.1% primocin was used. The MaMel-19 was cultured with RPMI-1640 supplemented with 10% FCS, 1% glutamine, and 0.1% primocin. The human melanoma cell line MaMel-19 was described previously (43). Cells were detached via Trypsin-EDTA for 5 min every 3 to 4 days. Cell lines were authenticated at Eurofins Genomics (Ebersberg, Germany) in March 2019. The resulting STR profiles were matched with the online databases of the german collection of microorganisms and cell cultures (DSMZ) (http://www.dsmz.de/de/service/services-human-and-animal-cell) and Cellosaurus database (https://web.expasy.org/cellosaurus/) references.

Human glioma cell lines #1043, #1051, and #1063 used in this study were derived from GB previously described by (214–216). The glioma cells were maintained under a serum-free culture condition that supported cell self-renewal and was based on NeuroBasal Medium supplemented with B27 supplement (Invitrogen, Darmstadt, Germany) and recombinant human cytokines basic fibroblast growth factor 2 (bFGF) and epidermal growth factor (EGF), (10 and 20 ng/mL, respectively, Biochrom GmbH, Merck KGaA, Darmstadt city, Germany).

3.3.4.2. Isolation and Stimulation of Human $CD4^+$ T Cells and Treg

Buffy coats were obtained from healthy volunteers, with approval by the local ethical committee (Landesärztekammer Rhineland Palatine No. 837.019.10 (7028), approved on 4 March 2010). The $CD4^+$ T cells were isolated via CD4 Microbeads (Miltenyi # 130-045-101). The Treg were isolated with the $CD4^+$ $CD25^+$ $CD127^{dim/-}$ isolation kit (Miltenyi #130-094-775, Bergisch Gladbach, Germany) according to the manufacturer's protocol. For proliferation assays, $CD4^+$ T cells were labeled with carboxyfluorescein succinimidyl ester (CFSE, eBioscience #65-0850-84, San Diego, CA, USA) and cultured in 48 well plates at 10^6 cells/mL, stimulated with 1 µg/mL anti-CD3 mAb (clone OKT3) plus 1 µg/mL anti-CD28 mAb (clone 28.2, eBioscience San Diego, CA, USA) in the presence or absence of T98G

in the ratio of 8:1, 10 µg/mL anti-GARP Ab (Origene AP17415PU-N, Rockland, MD, USA) and 1 µg/mL soluble GARP (recombinant human LRRC32/GARP protein #6055-LR-050, Minneapolis, MN, USA). For the activation of Treg, 1 x 10^6 cells were stimulated with 1 µg/mL anti-CD3 mAb (clone OKT3) plus 1 µg/mL anti-CD28 mAb (clone 28.2, eBioscience, San Diego, CA, USA) with 10 U/mL IL-2 (Novartis #PZN 02238131, Basel, Switzerland) for 48 h.

3.3.4.3. Flow Cytometry

For the flow cytometric analysis, the following antibodies were used: FVD506 (eBioscience #65-0866-14) and GARP (Miltenyi #130-103-820). Cells were stained with fixable viability dye prior to the antibody staining of GARP. Flow cytometry was performed on a BD LSRII flow cytometer (Heidelberg, Germany) and was analyzed using Cytobank (217).

For intracellular and intranuclear staining of GARP or intracellular staining of IFN-γ, cells were fixed and permeabilized with either the intracellular staining kit (BD Cytofix/Cytoperm Plus #555028, Heidelberg, Germany) or intranuclear with the Foxp3 / Transcription Factor Staining Buffer Kit (eBioscience #00-5523-00) and subsequently stained with anti-GARP mAb (Miltenyi #130-103-820) or anti-INF-γ (BD Biosciences #557643, Heidelberg, Germany).

3.3.4.4. Confocal Microscopy

For the confocal imaging, the Leica SP8 with HyD Detector (Wetzlar, Germany) was used. Melanoma cell line MaMel 19 and GB cell line T98G were cultured for 24 h in ibidi 15 µ-slides (Ibidi - # 80826, Gräfelfing, Germany), 25,000 cells/well each. Treg were plated on microscopyslides 100,000 each, using a Cytospin centrifuge (Cellspin II- Tharmac, Waldolms, Germany). Cells were checked for adherence and then fixed and permeabilized with a Foxp3/Transcription Factor Staining Buffer Kit (eBioscience, San Diego, CA, USA). For analysis of intracellular localization, cells were stained with anti-GARP mAb for 20 min at RT. Additionally DNA (Hoechst 33342 Solution Promokine #PK-CA707-40046, Heidelberg, Germany) and the membrane (NeuroDiO Solution #PK-CA707-30021- PromoKine, Heidelberg, Germany) were stained for 30 min at RT each.

For confocal imaging of the non-adherent human glioma cell lines #1043, #1051, and #1063, 30,000–50,000 cells were seeded on glass coverslips pre-coated with poly-L-ornithine hydrobromide (15 µg/mL, Sigma Aldrich, St. Louis, MO, USA) and cultured for 24 h. The cells were fixed with 4% paraformaldehyde/PBS (Merck KGaA, Darmstadt, Germany) for 5 min at RT followed by methanol/acetone (50% v/v) fixation at −20 °C. Cell permeabilization was performed using 0.3% Triton X-100/PBS (Sigma, St. Louis, MO, USA) for 5 min at RT. The primary antibodies used in the study included α-nestin (Abcam ab22035, Cambridge, UK), α-GARP (Origene AP17415PU-N, Rockland, MD, USA), and secondary antibodies (goat α-mouse Alexa Fluor 488 or goat α-rabbit Alexa Fluor 555, Thermo Fisher Scientific, Waltham, MA, USA). Because of their different nature as compared with the adherent T98G, MaMel-19, and non-adherent Treg, α-nestin was used instead of NeuroDiO Solution (see above). For editing, ImageJ2 (https://imagej.net/ImageJ2) was used (218).

3.3.4.5. GARP-Immunohistochemistry

Paraffin-embedded tumor samples were studied from 37 GBs (WHO grade IV), 13 anaplastic astrocytomas (WHO grade III), and 6 low-grade astrocytomas (WHO grade II) by GARP immunohistochemistry. Tumor tissue was resected in the Department of Neurosurgery in Idar-Oberstein, Germany, and completely sent for neuropathological examination to the Institute of Neuropathology, University Medical Center Mainz, Germany. Tissue not used for diagnostic proposes was used for additional GARP staining. Written informed consent of all patients was obtained for "scientific use of tumor tissue not needed for histopathological diagnosis" in the admission contract of Idar-Oberstein hospital. Immunohistochemistry was performed on 4 µm thick routinely processed formalin-fixed and paraffin-embedded tissue sections. After dewaxing, antigen retrieval using EnVision

FLEX Target Retrieval Solution, high pH (Dako #S2368 Glostrup, Denmark) was performed. Afterwards, endogenous peroxidase was blocked by peroxidase blocking solution (DAKO, Glostrup, Denmark) and sections were stained with anti-GARP primary antibody 1:100 (Origene AP17415PU-N, Rockland, MD, USA) using an immunostainer (Dako Autostainer Plus, DAKO, Glostrup, Denmark). Immunoreactivity was visualized by the universal immuno-enzyme polymer method (Nichirei Biosciences, Tokyo, Japan). Finally, sections were developed in diaminobenzidine (Lab Vision Cooperation, Fermont, CA, USA). Omission of the primary antisera in a subset of control slides resulted in no immunostaining at all. Nuclear GARP-immunostaining was semiquantitatively assessed in areas with labeled nuclei of tumor cells (more than 90%, 50%, and 10%). Immunohistochemical analysis was performed by an experienced neuropathologist (CS).

3.3.4.6. Statistics

Results represent the mean ± standard error of the mean (SEM). Statistical significance was determined using the Student's t-test with * p <0.05, ** p < 0.01, *** p < 0.001 and n.s. (not significant) as indicated.

3.3.5. Conclusions

Our data indicate for the first time a key role of the immunoregulatory molecule GARP in the tumor microenvironment of primary brain tumors such as GB and low-grade gliomas inducing and promoting tumor immune tolerance via multiple pathways. Moreover, since GARP is not only expressed by activated Treg but also by brain tumor cells, it may serve as a potential target for an immunotherapeutic approach in patients with cerebral cancer.

3.3.6. Supplementary Materials

Low grade Astrocytomas II	**male**	**female**	**total**	**lost to follow up**
Number of patients	3	3	6	
Age at the onset mean±SD (yr.)	60±17.7	55.66±7.6	57.83±12.4	
Side hemispheric **right** **left** **bilateral**	 3 0 0	 1 2 0	 4 2 0	
Surgery **resection** **biopsy**	 1 2	 2 1	 3 3	
Localization				
midbrain	1	0	1	
Front/temp/insular	1	0	1	
hemispheric	1	0	1	
temporal	0	2	2	
frontal	0	1	1	
Radiation therapy	1	0	1	1
Chemotherapy	1	0	1	1
Survival mean±SD (mon.)	14±15.55	13.5±14.84	13.75±12.41	3

Table 3.3.A1. Characteristics of astrocytoma grade II patients at the study center Idar-Oberstein, Germany. Patient characteristics (gender, age), primary tumor data including localization, therapy, and follow-up are displayed.

Low grade Astrocytomas III	**male**	**female**	**total**	**lost to follow up**
Number of patients	6	5	11	
Age at the onset mean±SD (yr.)	53.33±13.27	64.2±17.94	58.27±15.7	
Side hemispheric **right** **left** **bilateral**	 3 3 0	 3 0 2	 6 3 2	
Surgery **resection** **biopsy**	 4 2	 1 4	 5 6	
Localization				
frontal	3	1	4	
temporal	3	1	4	
bifrontal	0	2	2	
hemispheric	0	1	1	
Radiation therapy	5	3	8	2
Chemotherapy	4	2	6	1
Survival mean±SD (mon.)	17.8±12.43	5.0	15.66±12.29	4 female

Table 3.3.A2. Characteristics of astrocytoma grade III patients at the study center Idar-Oberstein, Germany. Patient characteristics (gender, age), primary tumor data including localization, therapy, and follow-up are displayed.

3.4 Manuscript III: Nuclear Glycoprotein A repetition predominant is a common trait of glioblastoma stem-like cells and correlates with poor survival in glioblastoma patients.

Summary of own contributions
Conceptualization: N.Z., A.T., E.K., J.T., F.R., V.M. and C.S.; methodology: N.Z., E.R.T., A.M., P.L. (Philipp Licht), P.L. (Petra Leukel) and B.S.; validation: N.Z. and E.R.T.; formal analysis: N.Z., E.R.T., A.M. and P.L. (Philipp Licht); resources: A.T. and E.K.; writing—original draft: N.Z., E.R.T., A.T. and E.K.; writing—review and editing: all authors; visualization, N.Z.; project administration: N.Z.; supervision: A.T. and E.K.; funding acquisition: A.T. and E.K. All authors have read and agreed to the published version of the manuscript.

The author planned, designed, and performed most of the *in vitro* experiments and the subsequent analysis in the main manuscript. Bioinformatic analysis was performed by Philipp Licht, Western Blot antibody validation (suppl. Material), $GARP^{+}$ cell line generation and ELDA by Emily R. Trzeciak, immunohistochemistry staining of patient material by Petra Leukel. Mouse data and cell lines were provided by Ella Kim. The author took lead in preparing the manuscript together with Prof. Dr. med. Andrea Tüttenberg, Emily R. Trzeciak and Ella Kim.

Keywords: glioblastoma; GARP; tumor microenvironment; immunotherapy; regulatory T cells

Citation: ***Zimmer, N.****; *Trzeciak, ER.**; *Licht, P.; Sprang, B.; Leukel, P.; Mailänder, V.; Ringel, F.; Sommer, C.; Tuettenberg, J.; Kim, E.; Tuettenberg, Nuclear Glycoprotein A repetition predominant is a common trait of glioblastoma stem-like cells and correlates with poor survival in glioblastoma patients*

** These authors contributed equally to this work.*

Original submission received: 17 March 2023 / Resubmission received: 20 October 2023 / Revised: 17 November 2023 / Accepted: 1 December 2023 / Published: 5 December 2023

Zusammenfassung

Das Glioblastom (GB) ist bekanntermaßen therapieresistent. Es wird angenommen, dass die Entstehung und das Fortschreiten von GB durch stammzell-ähnliche Zellen (GSC) vor und nach der Therapie vorangetrieben wird. Das vorrangige Ziel zur Verbesserung der Wirksamkeit der Behandlung und der Behandlungsergebnisse ist die Bekämpfung dieser Tumorstammzellen im GB. Derzeit gibt es keine gemeinsamen Marker für die Identifizierung von GSC. Glykoprotein A repetitions predominant (GARP), ein entzündungshemmendes Protein, das von aktivierten regulatorischen T-Zellen und Blutplättchen exprimiert wird, wurde als möglicher Marker für humane GSC identifiziert. In dieser Studie wurde die Eignung von GARP für die Erkennung menschlicher GSC anhand eines mehrdimensionalen Versuchsplans untersucht, der mehrere Merkmale von GB nachbildete, darunter: (1) intratumorale Heterogenität, (2) zelluläre Hierarchie (GSC-Linien mit unterschiedlichen Graden der Selbsterneuerung und Differenzierung) und (3) longitudinale GSC-Evolution während eines GB-Rezidivs (GSC-Linien aus patientengleichen neu diagnostizierten oder rezidivierten GB). Unsere Ergebnisse deuten darauf hin, dass GARP in GSC über verschiedene zelluläre Zustände und Krankheitsstadien hinweg stabiler exprimiert wird als der gemeinsame GSC-Marker CD133. Wir zeigen die nukleäre Lokalisierung von GARP in menschlichen GSC und die erste Korrelation von nukleärem GARP ($GARP^{NU+}$) mit dem Überleben der Patienten. Die Gleichförmigkeit und Stabilität der GARP/$GARP^{NU+}$ Expression in verschiedenen Arten von menschlichen GSC legen eine mögliche Verwendung von GARP als prognostischen Biomarker für GB nahe.

Abstract

Glioblastoma (GB) is notoriously resistant to therapy. GB genesis and progression are driven by glioblastoma stem-like cells (GSC). One goal for improving treatment efficacy and patient outcomes is targeting GSC. Currently, there are no universal markers for GSC. Glycoprotein A repetitions predominant (GARP), an anti-inflammatory protein expressed by activated Treg, was identified as a possible marker for GSC. This study evaluated GARP for the detection of human GSC utilizing a multidimensional experimental design that replicated several features of GB: (1) intratumoral heterogeneity, (2) cellular hierarchy (GSC with varied degrees of self-renewal and differentiation), and (3) longitudinal GSC evolution during GB recurrence (GSC from patient-matched newly diagnosed and recurrent GB). Our results indicate that GARP is expressed by GSC across various cellular states and disease stages. GSC with an increased GARP expression had reduced self-renewal but no alterations in proliferative capacity or differentiation commitment. Rather, GARP correlated inversely with the expression of GFAP and PDGFR-α, markers of astrocyte or oligodendrocyte differentiation. GARP had an abnormal nuclear localization ($GARP^{NU+}$) in GSC and was negatively associated with patient survival. The uniformity of GARP/ $GARP^{NU+}$ expression across different types of GSC suggests a potential use of GARP as a marker to identify GSC.

3.4.1. Introduction

This section has been shortened to avoid any major repetition of previous chapters. The complete, unedited version of this manuscript can be found in the appendix III.

As described in 3.2., GSC possess a high degree of plasticity, which renders them capable of switching between different cellular states and distinct morphological phenotypes. Lack of definitive markers that are stably expressed on GSC poses a further challenge to the diagnostic stratification of GB based on the evaluation of GSC content in tumor specimens (159).

Although a range of molecules like CD15, SOX2, and Prominin1/CD133 have been implicated as identification markers of GSC, their diagnostic utility has been limited due to the phenotypic heterogeneity within the GSC compartment, constituted by cells in hierarchically distinct states (167, 197, 219–222). For example, expression of Prominin1/CD133, historically one of the most investigated and arguably the best validated GSC marker, is sample specific, being restricted to only a subset of GSC (153, 223–225). Considering that the tumor-propagating capacity of CD133− GSC is comparable to that of $CD133^{+}$ GSC (223), the diagnostic utility of CD133 remains uncertain (226). Phenotypic diversity and plasticity of GSC as a means of adaptation to the tumor microenvironment have important implications for the continuing search for GSC markers that would be universally applicable for different subsets of GSC and would be expressed unambiguously, regardless of cellular state.

In this regard, Glycoprotein A repetitions predominant (GARP) has recently emerged as a potential marker of human GSC (41, 227). Recently, we have found that GARP is also expressed by different types of GB cells, including GSC, where it shows an atypical pattern of subcellular distribution characterized by GARP localization on both the cell surface and within the nucleus ($GARP^{NU+}$) (41). Up until now, GARP expression in GSC has only been shown in vitro, with several open-ended questions remaining. Namely, is GARP/$GARP^{NU+}$ expression associated with a particular cellular state (self-renewal or differentiation) or a particular subtype of GSC? Does the associated expression of GARP/$GARP^{NU+}$ in GSC persist during GB progression after therapy?

In the present study, these questions were addressed in vitro and in vivo by analyzing the expression of GARP/$GARP^{NU+}$ in different subtypes of patient-derived GSC with consideration of intratumoral heterogeneity and the longitudinal changes accompanying GB recurrence. For the first time, the present study examined the potential link of nuclear GARP expression with patient outcomes.

3.4.2. Materials and Methods

3.4.2.1 Cell culture

The human GB cell line T98G was purchased from the ATCC (CRL-1690) and was cultured in Minimum Essential Medium Eagle supplemented with 10% FCS, 1% Glutamine, and 0.1% Primocin. The human melanoma cell lines, Mewo and Ma-Mel-19, were obtained from Dr. Daniela Kramer (Mewo, RRID:CVCL_0445, Cellosaurus) in Mainz, Germany, in 2021 and from Dr. Annette Paschen (Ma-Mel-19, RRID:CVCL_A156, Cellosaurus) in Essen, Germany, in 2014. Mewo cells were cultured in Dulbecco's Modified Eagle Medium supplemented with 10% FCS and 0.1% Primocin. Ma-Mel-19 cells were grown in RPMI 1640 supplemented with 10% FCS, 1% Glutamine, and 0.1% Primocin. T98G, Mewo, and Ma-Mel-19 cells were passed every 2 to 3 days by using Trypsin-EDTA. The cell lines T98G and Ma-Mel-19 were authenticated in August 2022 by PCR single locus technology. The results were compared to the online databases of the DSMZ and Cellosaurus (Eurofins Genomics Europe). Patient-derived GSC lines used in this study were established as previously described and have been well characterized in previous studies, in terms of their stem cell frequency (SCF) and expression of various GSC markers (214, 215, 228, 229). Additional information regarding their origin, SCF, predominant phenotype (nestin^{+}/$^{-}$, GFAP^{+}/$^{-}$), and percentage of CD133-positive cells, as well as an exemplary analysis of the GSC markers, CD133, platelet-derived growth factor receptor alpha (PDGFR-α), and aldehyde dehydrogenase 1 family member A3 (ALDH1A3), can be found in Figure 3.4.S1 (214, 215, 230). In brief, excess GB tumor tissue was obtained from patients operated on at the Department of Neurosurgery of the Johannes Gutenberg University Medical Center Mainz (JG-UMC), with informed consent. The use of tumor tissue for research purposes was approved by the JG-UMC Institutional Review Board (permission 08.06.2017 #837.211.12(8312-F). For GSC isolation, a combined enzymatic and mechanical titration procedure was used as previously described (215). To promote self-renewal, glioma cells were cultured in serum-free NeuroBasal (NB) medium supplemented with the following factors: B27 supplement (Invitrogen, Darmstadt, Germany) and the recombinant human cytokines, basic fibroblast growth factor 2 (bFGF) (10 ng/mL) and epidermal growth factor (EGF), (20 ng/mL) (Biochrom GmbH, Merck KGaA, Darmstadt, Germany). For in vitro differentiation, cells were subjected to EGF and bFGF withdrawal and assessed for the expression of neural lineage specific markers after 7 days. Self-renewal promoting conditions are hence referred to as "NB+bFGF/+EGF" whereas differentiation is indicated by "NB-bFGF/-EGF" in the manuscript.

3.4.2.2 Western blot

Protein preparation and Western blotting were performed as previously described in Müller et al., 2023 (231). Membranes were probed with the following antibodies: anti-CD133/1 (clone: W6B3C1), anti-PDFGR-α (D13C6) (Cell Signaling, #5241T, Danvers, MA, USA), anti-ALDH1A3 (Thermo Fischer Scientific, MA5-25528, Waltham, MA, USA), anti-p53 (DO-1) (Cell Signaling, #18032), anti-actin (C4) (Santa Cruz Biotechnology, sc-47778, Dallas, TX, USA), anti-glial fibrillary acidic protein (GFAP) (DAKO, Z0334, Santa Clara, CA, USA), anti-p21 (Cell Signaling, #2947), anti-phosphorylated-histone H3 (Ser28) (Cell Signaling, #9713S), anti-HSP70 (Enzo Life Sciences Inc., Farmingdale, NY, USA), anti-mouse IgGκ light chain-binding protein horseradish peroxidase (Santa Cruz Biotechnology, sc-516102), goat anti-rabbit IgG H&L horseradish peroxidase (Abcam, ab205718, Cambridge, UK), goat anti-mouse IgG horseradish peroxidase (Santa Cruz Biotechnology, sc-2055), and goat anti-rabbit horseradish peroxidase (Santa Cruz Biotechnology, sc-2054). Signal intensity was analyzed via densitometry (https://imagej.nih.gov, accessed on 17 October 2023) (232).

3.4.2.3 Flow cytometry

For flow cytometric analysis, the following fixable viability dye and antibodies were used: FVD506 (eBioscience #65-0866-14, San Diego, CA, USA), anti-GARP (Miltenyi #130-103-820 and 130-103-890, updated ordering numbers: 130-125-511 and 130-125-532, Bergisch Gladbach, Germany), anti-CD133 (epitope AC133, Miltenyi # 130-113-111), and their respective isotype controls (Miltenyi #130-113-434

and Miltenyi #130-113-200). Cells were stained with fixable viability dye prior to surface antibody staining of anti-GARP and anti-CD133. Cells were not fixed for the analysis.

Extensive validation of the anti-GARP antibodies mentioned above and a demonstration of their specificity can be found in Figures 3.4.S2 and 3.4.S3 as well as in previous work by Zimmer et al., 2019 (41). In more detail, the anti-GARP antibodies from Miltenyi were validated against two other flow cytometry certified antibodies (Biolegend, 352506, San Diego, CA, USA; Origene, TA337028, Rockland, MD, USA) (Figure 3.4.S3) and against the polyclonal anti-GARP antibody used in this study (Origene, AP17415PU-N) (Figure 3.4.S2). Antibody specificity was demonstrated using GARP-overexpressing Mewo cells, resulting from transient transfection using the LOX-IMVI Cell Avalanche Transfection Reagent (EZ Biosystems, EZT-LOXI-1, College Park, MD, USA) as well as a LRRC32 overexpression plasmid (Origene, SC116699) and an empty vector control plasmid (Origene, PS100001) (Figure 3.4.S3). Transfection was performed in accordance with the manufacturer's recommendations. Cells were stained with fixable viability dye and for surface GARP as described above 48 h post-transfection.

Flow cytometry was performed on a BD LSRII flow cytometer (Heidelberg, Germany) and was analyzed using Cytobank (217). Doublets, debris, and dead cells were excluded from analysis (Figure 3.4.S4).

3.4.2.4 Confocal microscopy

Confocal imaging was performed on a Leica SP8 with HyD detector (Wetzlar, Germany) at the Imaging Core Facility (ICF) of the Forschungszentrum für Immuntherapie (FZI) of the University Medical Center Mainz as described before (41). The following antibodies were used in the study: anti-nestin (Abcam, ab22035), anti-GARP (Origene, AP17415PU-N), and secondary antibodies goat anti-mouse Alexa Fluor 488 or goat anti-rabbit Alexa Fluor 555 (both Thermo Fisher Scientific, Waltham, MA, USA). Validation and specificity of the anti-GARP antibody (Origene AP17415PU-N) for its use in confocal microscopy can be found in Figure 3.4.S5 and in previous work by Zimmer et al., 2019 (41).

3.4.2.5 Animal experiments

Animal experiments were performed at the Translational Animal Research Facility (TARC) of the JG-UMC, Germany, in accordance with the guidelines of the European Convention for the Protection of Vertebrates Used for Scientific Purposes and under the approval of the State Office of Chemical Investigations of Rhineland-Palatinate (permission #23 177-07/G12-1-020). Immunodeficient mice (strain NMRI) were purchased from a commercial supplier (Charles River Laboratories Germany). After an adaptation period of one to two weeks, mice were subjected to intracerebral injection of GSC using a standardized procedure as described previously (230, 233). In brief, single-cell suspensions were prepared from glioma sphere cultures by using a combined trypsin/mechanical titration procedure. Cells were washed twice in PBS and re-suspended in PBS at 2 × 104 cells/µL. Cell viability was determined by trypan blue staining. Single-cell suspensions were injected at 5 µL into the caudato-putamen of the right hemisphere using a stereotactic frame (TSE Systems, Bad Homburg, Germany) and the following stereotactic coordinates in reference to the bregma: 1 mm (anteroposterior axis), 3 mm (lateromedial axis), 2.5 mm (vertical axis). Mice were sacrificed at the first manifestation of tumor-associated neurological symptoms.

3.4.2.6 GARP Immunohistochemistry and immunofluorescence

Tumor-bearing mouse brains were extracted and fixed in 4% paraformaldehyde in PBS for at least 24 h at 4 °C as described previously (233). Briefly, after fixation, brains were paraffin-embedded, dissected into 1–3 µm thick coronal sections and analyzed by immunohistochemical or immunofluorescence staining using antibodies specific to human nestin (R&D Systems GmbH, Wiesbaden-Nordenstadt, Germany), GFAP (DAKO, Z0334), or GARP (Origene, AP17415PU-N). Previous work has demonstrated the specificity of the anti-GARP antibody (Origene, AP17415PU-N) for its use in immunohistochemistry

and immunofluorescence (41, 43). For analysis, ImageJ2 (Available online: https://imagej.net/ImageJ2, accessed on 16 August 2021) was used (234).

A GB patient cohort from Zimmer et al., 2019 (41), was reanalyzed to correlate the frequency of $GARP^{NU+}$ cells in tumor tissue to patient overall survival regardless of IDH status. Patient characteristics are described in detail in Figure 3.4.1 of Zimmer et al., 2019 (41). In brief, the patient cohort consisted of 35 newly diagnosed (WHO stage IV) GB patients from the Department of Neurosurgery in Idar-Oberstein, Germany, between January 2009 and May 2015. The median high and low survival times were 12 and 4 months. Primary tumor tissue was resected and stained for GARP via immunohistochemistry. Description of the immunohistochemical staining process can be found in Zimmer et al., 2019 (41). The frequency of $GARP^{NU+}$ was semi-quantified in tumor tissue with regions of labeled nuclei (categorized as >90%, >50%, >10% $GARP^{NU+}$ cells) at the Institute of Neuropathology, University Medical Center Mainz, Germany (41).

3.4.2.7 Cell sorting

Single-cell suspensions of the GSC line, #1095, were stained sequentially with the following: fixable viability dye FVD780 (eBioscience #65-0865-14), unconjugated anti-GARP antibody (Origene, AP17415PU-N) or a control unconjugated IgG rabbit isotype antibody (R&D Systems, AB-105-C), followed by a PE-conjugated goat anti-rabbit secondary antibody (Invitrogen, P2771MP). Cells were sorted into GARPlow and GARPhigh populations. Cell sorting gates were defined as the lower 10th (GARPlow) and upper 90th percentiles (GARPhigh) of all cells. An example gating strategy and proof of positive GARP staining can be found in Figure 3.4.S6. Debris, doublets, and dead cells were excluded from analysis. Sorting was performed using BD Aria II and III cell sorters at the Core Facility Flow Cytometry (CFFC) of the Forschungszentrum für Immuntherapie (FZI) of the University Medical Center Mainz.

3.4.2.8 Extreme limiting dilution assay

The self-renewal capacity of GSC lines was analyzed by extreme limiting dilution assay (ELDA). In brief, single-cell suspensions were serially diluted in self-renewal promoting medium (NB+bFGF/+EGF) and seeded into 24 well plates. The number of replicates used for each serial dilution are indicated as follows: 12 for 100 cells/well, 18 for 50 cells/well, 24 for 25 cells/well, 58 for 12.5 cells/well, 24 for 6.25 cells/well, 18 for 3.125 cells/well, and 12 for 1.56 cells/well. Cells were incubated for three weeks to develop neurospheres. Wells were assessed for neurosphere formation; a positive result was recorded for each dose (number of seeded cells/well) if the examined well contained at least one neurosphere. Each experiment was repeated independently three times. Stem cell frequency (SCF) was calculated using the ELDA: Extreme Limiting Dilution Analysis webtool from the Walter and Eliza Hall Institute of Medical Research (https://bioinf.wehi.edu.au/software/elda/, accessed on 6 September 2023) (235).

3.4.2.9 Bioinformatic pipeline

In a previous work, Kim et al., 2020, performed Illumina RNA-Sequencing on a total of 155 GB samples derived from 28 patients (229). These consisted of primary, recurrent, and secondary recurrent tumors (128 samples) as well as GSC cultures developed from freshly resected tumor tissue (27 samples). We obtained unnormalized gene counts through the Gene Expression Omnibus database (GEO) under the accession number: GSE139533. Gene counts were normalized with DESeq2 and analyzed using the likelihood ratio test to decipher the effect of progressing tumor stages on transcript levels within the same patient (236). Normalized counts for CD133 and GARP were plotted with GraphPad Prism version 9.3.1 for Windows, GraphPad Software, San Diego, CA, USA, www.graphpad.com. Survival analysis of CD133 and GARP was performed using OncoLnc (http://www.oncolnc.org/, accessed on 8 July 2023) which is based upon data generated by The Cancer Genome Atlas (TCGA) Research Network (https://www.cancer.gov/tcga, accessed on 8 July 2023) (237–239).

3.4.2.10 Statistics

Statistical analysis was performed with Student's t-test, the likelihood ratio test, the chi-squared test, or two-way ANOVA as indicated. Data are displayed as mean values ± SEM or ±SD as indicated. Survival curve comparison was analyzed using the log-rank (Mantel–Cox) test using GraphPad Prism. Statistical significance is indicated as follows: * $p < 0.05$, ** $p < 0.01$, *** $p < 0.001$, **** $p < 0.001$, and ns (not significant).

3.4.3. Results

3.4.3.1. GARP expression is conserved across different types of GSC in vitro and in vivo

We have previously shown that GARP is expressed by three human GSC lines and by the conventional human glioblastoma cell line, T98G (41). The questions that remained were whether GARP expression is restricted to a particular type of GSC or if it represents a common phenotypic trait shared by different subsets of GSC. To address these questions, we analyzed the expression of GARP in a panel of heterologous GSC lines, differing in their self-renewal capacity, degree of differentiation, and expression of CD133, a proposed marker for GSC in the past (Figure 3.4.S1A). All GSC used in this study invariably expressed nestin, a neural stem cell marker, but they varied in their expression of the astrocyte differentiation marker, GFAP, and CD133, a putative GSC marker (Figure 3.4.S1A). A non-stem glioblastoma cell line, T98G, (ATCC CRL-1690) was analyzed in parallel as a control. Flow cytometry revealed that the surface expression of GARP varied across heterologous GSC (Figure 3.4.1A). Notably, variations in GARP expression paralleled variations in CD133 levels indicating that GARP and CD133 are not mutually exclusive markers (Figure 3.4.1A). Line-dependent variations in GARP expression were also confirmed by microscopic evaluation of intracellular GARP (Figure 3.4.1B,C). Confirming our previous observations, microscopic analysis revealed that GARP localization in GSC is not restricted to the cell membrane, a normal localization site for GARP, but it also extends to the nuclear compartment (Figure 3.4.1B) (41, 227). The nuclear localization of GARP was evident in confocal microscopy with co-staining for nestin, an established marker of neural stem/progenitor cells expressed in the cytoplasm. The prevalence of cells with nuclear GARP (termed hereafter as "$GARP^{NU+}$") varied between different GSC lines (Figure 3.4.1B,C) and mirrored the levels of surface-expressed GARP (Figure 3.4.1A), indicating a possible relationship between the two forms. For example, the GSC lines #1051 and #1095 had the highest levels of surface-membrane-associated GARP (Figure 3.4.1A), and they also exhibited a high proportion of cells with $GARP^{NU+}$ (92.1% and 87.2%, Figure 3.4.1B,C). Vice versa, GSC with moderate levels of surface GARP (#1043 and #1063, Figure 3.4.1A) had lower proportions of cells with $GARP^{NU+}$ (40.9% and 29.7%, Figure 3.4.1C).

Our in vitro findings prompted us to test if GARP/$GARP^{NU+}$ expression is sustained in vivo in GSC involved in tumor propagation. To this end, we analyzed xenograft tumors grown from two GSC lines that express the lowest (line #1043) and highest (line #1051) levels of GARP in vitro (Figure 3.4.1). Both lines gave rise to highly invasive brain tumors as ascertained by immunohistochemical staining with an antibody specific for human nestin (Figure 3.4.S7) and had comparable rates of tumor growth (230). Immunofluorescence staining for GARP revealed its expression in both #1051 and #1043 xenografts (Figure 3.4.S8). Notably, GARP expression in #1043 xenograft (low expressor in vitro, Figure 3.4.1) was comparable with that in #1051 xenograft (high expressor in vitro, Figure 3.4.1), suggesting that GARP expression in GSC might be even more profound in the tumor context. Concordant with our in vitro findings, tumor-propagating GSC also showed GARP localization in both the cytoplasm and nucleus (Figure 3.4.S8). Additionally, $GARP^{NU+}$ was observed to be co-expressed with nestin (Figure 3.4.S8). These results further support the conclusion that GARP/$GARP^{NU+}$ expression might be a common trait stably sustained (or even augmented) in GSC involved in tumor propagation.

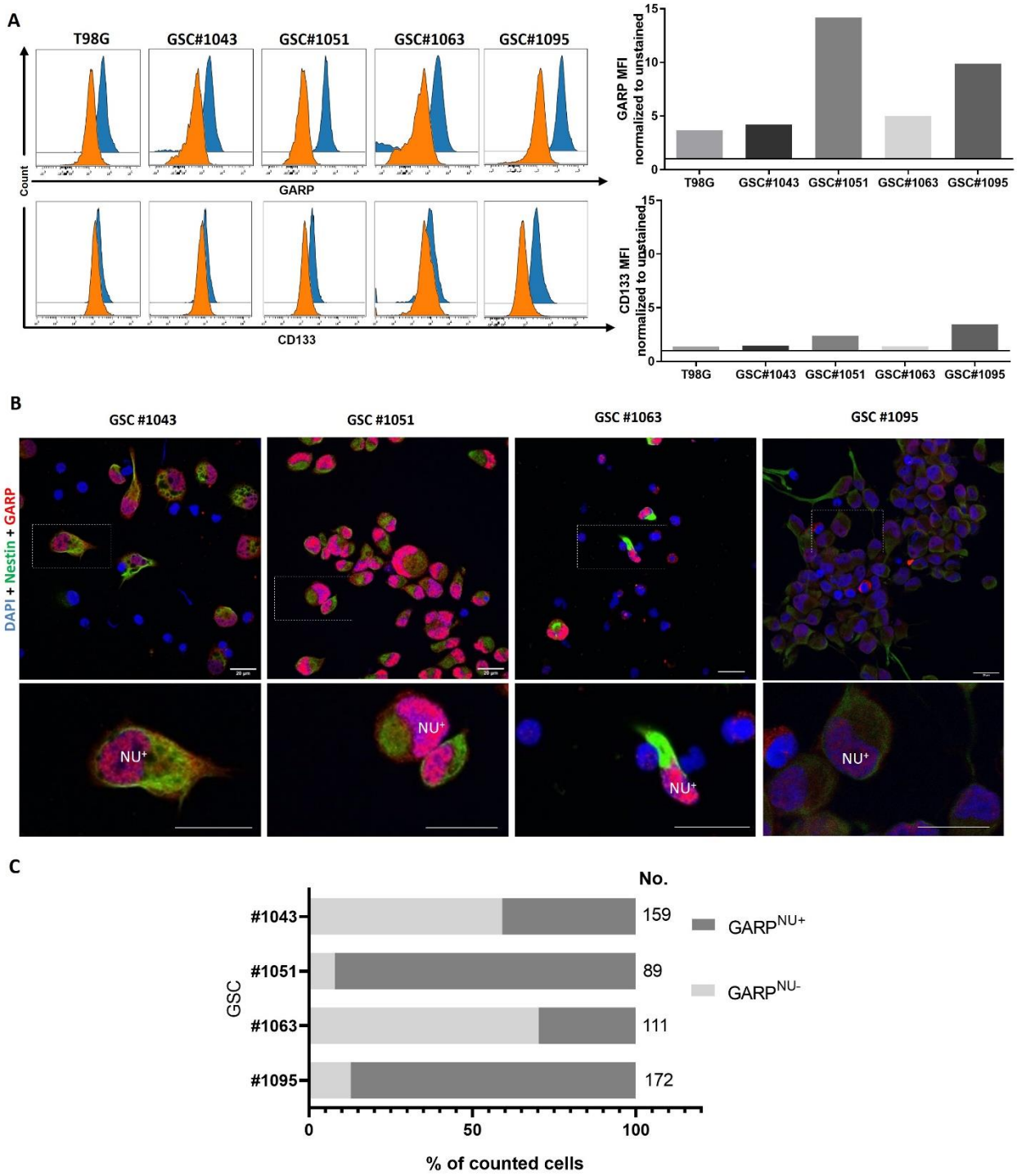

Figure 3.4.1. (A) Flow cytometric analysis of surface GARP and CD133 on different GSC and the control, non-stem, GB cell line, T98G. Doublets, debris, and dead cells were excluded from the analysis. Mean fluorescence intensity (MFI) was normalized to the MFI of the respective unstained control. (B) Confocal images of GARP- and nestin-expressing GSC and T98G. Cells were stained for GARP (red) and nestin (green). Cells were counterstained for their nuclei with Hoechst (blue). Note the intranuclear localization of GARP ($^{NU+}$). Scale bar corresponds to 20 µm. (C) Percentage of GARP^{NU+} cells were determined by counting GARP stained nuclei. "No." indicates the number of counted cells for the analysis.

3.4.3.2. Intratumoral heterogeneity of subcellular distribution patterns of GARP

GBs are known for their high degree of intratumoral heterogeneity, which is thought to reflect the hierarchical diversity of cellular states generated by GSC (240, 241). Our observation that heterologous GSC vary in their levels of GARP/GARP^{NU+} (Figure 3.4.1 and Figure 3.4.S8) prompted us to check if this is a mere reflection of intertumoral diversity, GARP/GARP^{NU+} association with a particular GSC subtype or cellular state, or a hierarchical diversification taking place during tumor growth. To address these questions, we made use of isogenic GSC (lines IT-726-#1, IT-726-#2, IT-726-#3a, IT-726-#3b, and IT-726-#4) that have been isolated from different regions of the same tumor (Figure 3.4.S9—Cohort 2"—comparison line 1) and provide a unique model for analyzing the impact of intratumoral heterogeneity in an isogenic background (228, 229). Indeed, despite their identical genetic background, isogenic GSC from the IT-726 set displayed notable morphological differences, considerable variations in their self-renewal capacity, and expression of GSC-associated markers CD133, ALDH1 A3, and PDGFR-α (Figure3.4.S1) (228, 229).

Interestingly, we found no apparent correlation between CD133 expression and the degree of self-renewal activity. For example, the lines IT-726-1 and IT-726-3B had comparable degrees of self-renewal activity (Figure 3.4.S1A), but they differed profoundly in the expression of surface CD133 (glycosylated epitope AC133) (Figure 3.4.2). Vice versa, the line IT-726-4 expressed similar levels of surface CD133 as the lines IT-726-2, IT-726-3A, and IT-726-3B, (Figure 3.4.2), but it stood out markedly from the other lines in terms of its extremely low self-renewal capacity (Figure 3.4.S1A). In contrast to CD133, the expression of surface GARP was very similar across isogenic lines, and it did not parallel the striking difference in CD133 expression between the IT-726-1 line and its isogenic counterparts (Figure 3.4.2). In comparison to the uniform expression of surface GARP, the patterns of GARP subcellular distribution between IT-726 lines were heterogeneous, with the proportion of GARP^{NU+} cells varying across different isogenic lines (Figure 3.4.3A). The highest level of GARP^{NU+} was found in line IT-726-2, which had a prominent expression of nuclear GARP in nearly every cell (Figure 3.4.3B, IT-726-2 upper panel). GARP expression was also examined on IT-726 cell lines grown in self-renewal-promoting (NB+bFGF/+EGF) versus differentiation-promoting (NB$^-$bFGF/-EGF) conditions. Interestingly, IT-726-2 displayed a prominent expression of nuclear GARP in almost every cell regardless of culture condition. In contrast, other isogenic IT-726 lines exhibited a mixed pattern of GARP localization in both nuclear and cytoplasmic compartments in self-renewal-promoting conditions (NB+bFGF/+EGF) (Figure 3.4.3B, shown for IT-726-4). Notably, the nuclear localization of GARP appeared to be more profound when cells were grown in differentiation-promoting conditions (NB-bFGF/-EGF), suggesting an inverse correlation between GARP^{NU+} and self-renewal capacity. The IT-726-2 line, in which the GARP^{NU+} pattern was predominant (Figure 3.4.3B), had a lower self-renewal capacity when compared to the other isogenic counterparts (Figure 3.4.S1A), consistent with this interpretation.

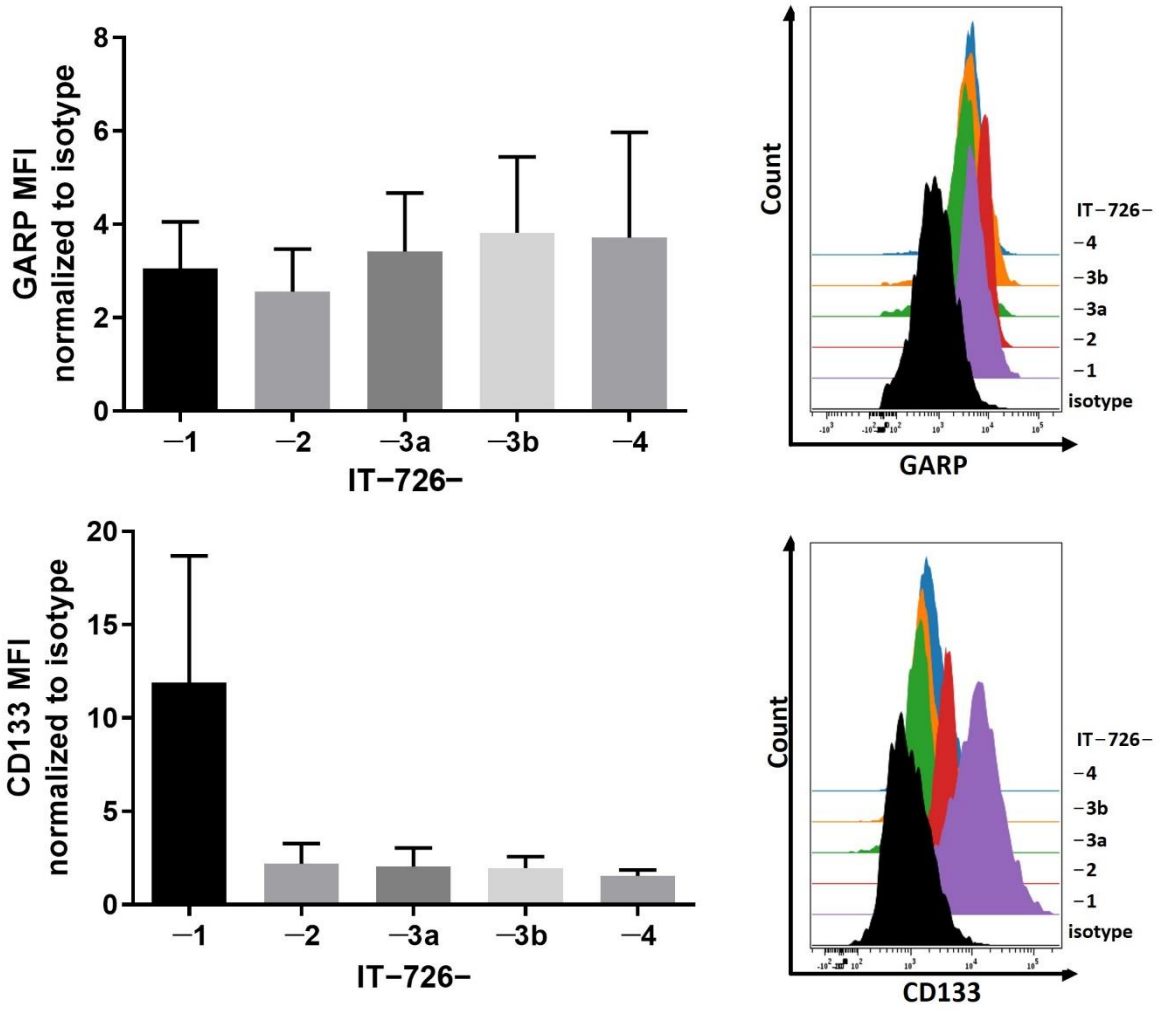

Figure 3.4.2. GARP expression in isogenic GSC derived from newly diagnosed GB IT-726. Flow cytometric analysis of IT-726-1, -2, -3a, -3b, and -4. Doublets, debris, and dead cells were excluded from analysis. Mean fluorescence intensity (MFI) was normalized to the MFI of the unstained control. Histograms display one representative result of three independent measurements. Data are displayed as mean values ± SEM.

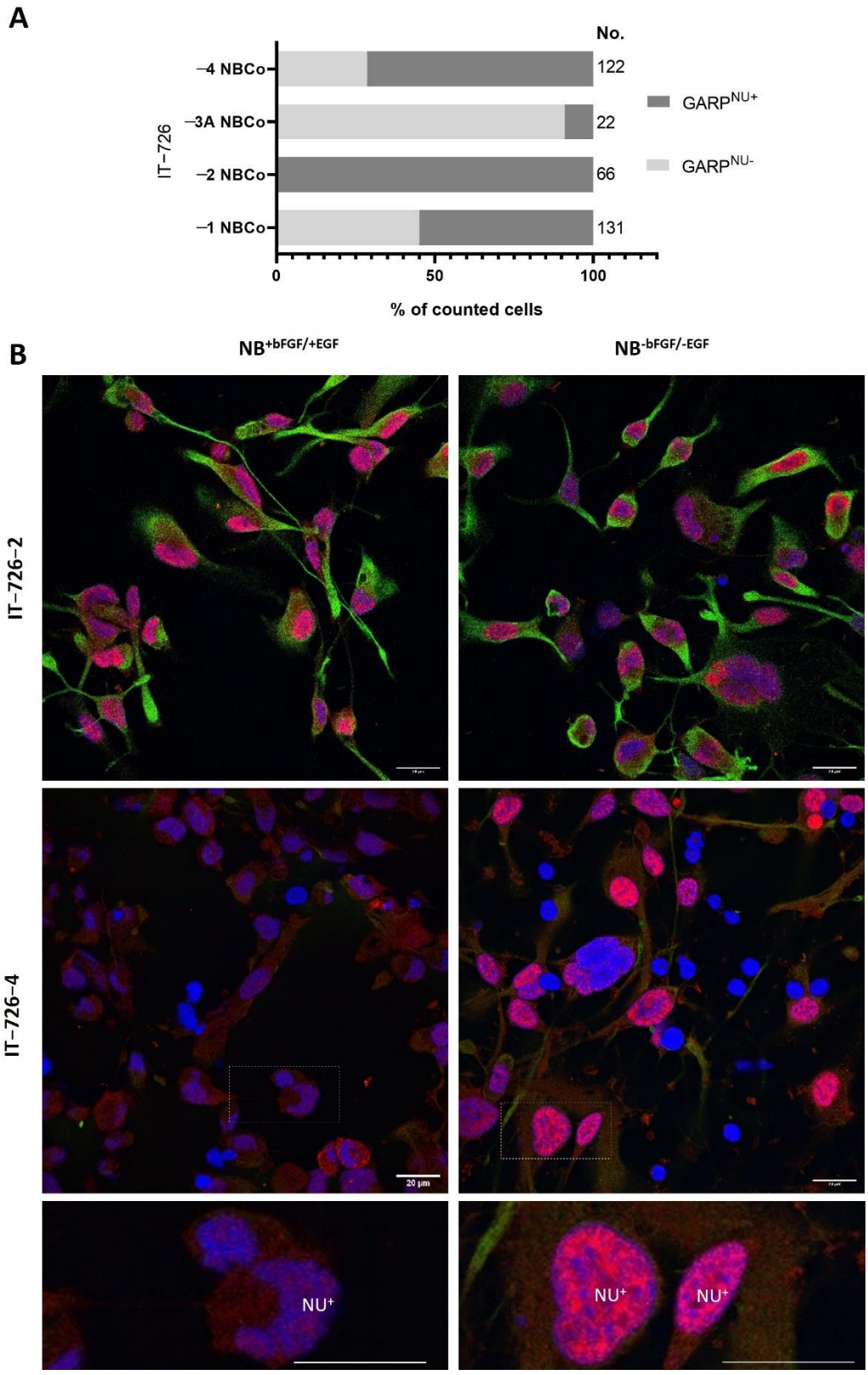

Figure 3.4.3. Analysis of expression and localization of GARP in isogenic GSC cell lines, which vary in differentiation states derived from different regions of the same tumor. (A) Number of GARP positive nuclei for GSC lines IT-726—1, -2, -3A, and -4 were analyzed by counting double positive (Hoechst and GARP) cell nuclei ($^{NU+}$). "No." indicates the number of counted cells for the analysis. (B) Confocal images of GARP- and nestin-expressing GSC IT-726 -2 and -4. Cells were stained for their nuclei with Hoechst (blue), GARP (red), and nestin (green). Note the intranuclear localization of GARP. Scale bar corresponds to 20 µm.

3.4.3.3. Relationship between GARP expression and GSC stemness

The dual capacity of self-renewal and differentiation are the fundamental and unique properties of stem cells. We therefore sought to determine if there is an association between GARP expression and self-renewal. To this end, cell populations differing in GARP expression ($GARP^{high}$ or $GARP^{low}$) were FACS sorted from the GSC line #1095 and compared with respect to self-renewal activity by ELDA. A demonstration of the sorting efficacy and quantification of surface GARP expression on $GARP^{high}$ vs. $GARP^{low}$ sorted cells via flow cytometry can be found in Figure 3.4.S6A. The GSC line #1095 was chosen for these investigations because of its well-established stemness attributes as well as molecular and cellular responses to clinically relevant treatments in vitro and in vivo (214, 215, 230, 231). The results of ELDA assessments revealed that $GARP^{high}$ and $GARP^{low}$ populations of GSC differ in their self-renewal propensity, which was significantly (p = 2.48 × 10−16) lower in the $GARP^{high}$ subpopulation compared to $GARP^{low}$ subpopulation (Figure 3.4.4).

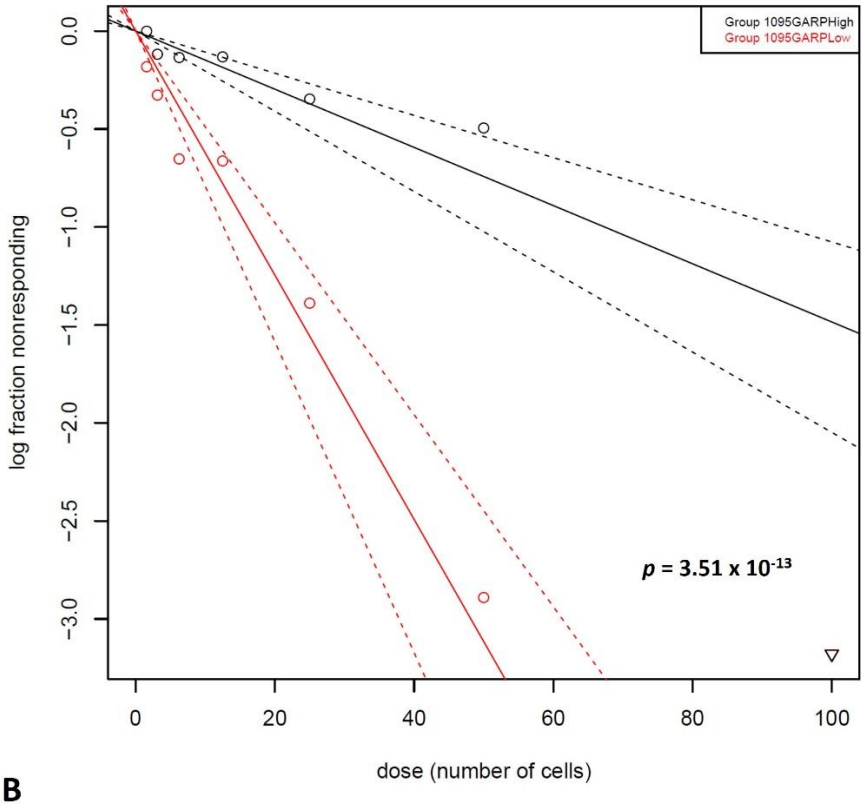

B

1095 subline	Stem cell frequency (1/SCF)			*p* value
	Lower	Estimated	Upper	
$GARP^{High}$	18.75	16.30	14.16	2.48×10^{-16}
$GARP^{Low}$	8.58	7.49	6.53	

Figure 3.4.4. Quantitative assessments of self-renewal capacity by extreme limiting dilution assay (ELDA). (A) Representative results. (B) The pooled results from three independent experiments are indicated in the table. $GARP^{high}$ and $GARP^{low}$ correspond to isogenic GSC differing in their GARP expression, which were FACs sorted from the GSC line #1095. Estimates of the stem cell frequency (SCF) are framed in red, while lower and upper indicate the confidence intervals for 1/SCF. Statistical significance between groups was calculated by chi-squared tests.

As loss of self-renewal is a prerequisite for stem cell differentiation, the outcome of the ELDA experiments raised the possibility that GARP expression may be related to differentiation of GSC. To address this question, GARP^{high} and GARP^{low} GSC were subjected to comparative assessments for the differentiation-inducing factor p21 and the differentiation-associated markers, GFAP and PDGFRα, activated during astrocyte or oligodendrocyte differentiation. The results showed that GARP^{high} GSC had considerably higher steady-state levels of p21 compared to GARP^{low} GSC, which seems consistent with the interpretation that increased expression of GARP is associated with a more differentiated state. However, an elevated level of p21 was unaccompanied by increased expression of GFAP or PDFGRα in GARP^{high} GSC. Quite the contrary, the expression of either GFAP or PDFGRα was found to be lower in GARP^{high} GSC than in GARP^{low} GSC (Figure 3.4.5) with the difference in PDGFRα levels being especially profound (Figure 3.4.5B). Although the difference in GFAP expression between GARP^{high} and GARP^{low} GSC was less profound, it was also confirmed by using a different approach, namely the estimation of GFAP-positive differentiating cells by immunofluorescence staining (Figure 3.4.S10). A decline in proliferative activity is an important functional hallmark of normal stem cell differentiation. Deviating from this rule, GARP^{high} GSC, which had a reduced self-renewal capacity in comparison to GARP^{low} GSC (Figure 3.4.4), had comparable levels of the proliferation marker PHH3 (Figure 3.4.5). Collectively, our data indicate that increased expression of GARP correlates with reduced self-renewal but not with the cessation of proliferation or induction of phenotypic traits of neural differentiation.

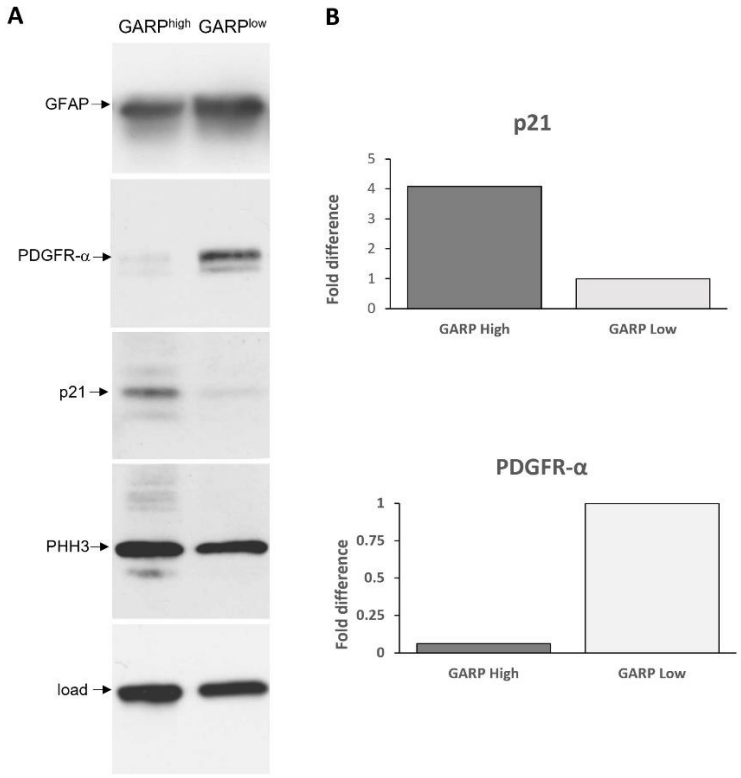

Figure 3.4.5. Comparative assessments of glial fibrillary acidic protein (GFAP), platelet-derived growth factor receptor alpha (PDGFR-α), p21, and phosphorylated histone H3 (PHH3) in FACs-sorted GARP^{high} and GARP^{low} isogenic GSC (#1095) by Western blot. (A) Representative results. HSP70 was used as a loading control. The following antibodies were used to probe the membranes: anti-GFAP (DAKO, Z0334), anti-PDFGR-α (D13C6) (Cell Signaling, #5241T), anti-p21 (Cell Signaling, #2947), anti-phospho-histone H3 (Ser28) (Cell Signaling, #9713S), anti-HSP70 (Enzo Life Sciences Inc.), anti-mouse IgGκ light chain-binding protein horseradish peroxidase (Santa Cruz Biotechnology, sc-516102), and goat anti-rabbit IgG H&L horseradish peroxidase (Abcam, ab205718). (B) PDGFR-α and p21 bands were quantified by densitometry.

3.4.3.4. GARP mRNA and surface protein levels do not predict GB patient survival

Having established that GARP is expressed in patient-derived GSC, we sought to determine whether a correlation exists between GARP expression and GB patient survival. To address this question, gene expression and survival data from the TCGA database were analyzed for GARP and CD133 by using OncoLnc.org (Figure 3.4.S9—Cohort 1) (237–239). Based on the TCGA dataset, consisting of 152 patients with newly diagnosed GB, all patients analyzed were stratified by their expression levels of GARP into either "GARP-high" (upper 50%) or "GARP-low" (lower 50%) groups and were analyzed for their survival rates via the online tool OncoLnc (237). We could not find any significant difference in survival between GARP-high and GARP-low groups (Figure 3.4.6A). Similarly, no significant correlation was found between survival and CD133 expression (Figure 3.4.6A). In a second approach, GARP and CD133 transcript levels were compared between newly diagnosed glioblastomas (ndGB) and progressed recurrent glioblastomas (recGB) as depicted in Figure 3.4.S9—Cohort 2—comparison line 2. To this end, we retroactively analyzed RNAseq data from a database that compiles RNAseq data for ndGBs (23 patients) or recGBs (21 patients) as well as 27 primary cultures derived from either ndGB (ndGB-GSC, 17 cultures) or recGB (recGB-GSC, 10 cultures) (230). GARP and CD133 mRNA expression were compared between ndGB samples (ndGB tissues and ndGB-GSC cultures) and recGB samples (recGB tissues and recGB-GSC). The results showed that expression levels of GARP do not differ significantly between ndGB and recGB samples whereas CD133 levels were found to be significantly reduced in recGB samples compared to ndGB samples (Figure 3.4.6B). In a third approach, surface GARP expression was compared between isogenic ndGB-GSC and recGB-GSC isolated from ndGB and recGB tumors of the same patient (Figure 3.4.S9—Cohort 2—comparison line 3). Both ndGB-GSC and recGB-GSC showed virtually the same levels of surface GARP expression, whereas the level of CD133 was significantly lower in recGB-GSC in comparison to ndGB-GSC (Figure 3.4.6C). This agreed with the results of the RNAseq analysis (Figure 3.4.6B) as both GARP transcript and surface GARP (Figure 3.4.6C) levels were consistently expressed regardless of disease progression. Interestingly, in contrast to GARP transcript and surface GARP levels, it was found that the percentage of $GARP^{NU+}$ cells were elevated in the recurrent GSC line, IT-654 (Figure 3.4.6D).

Collectively, these results obtained via different experimental approaches indicate that expression of GARP mRNA and surface protein remain at a constant level throughout GB progression and after therapy—in contrast to the fluctuating expression of CD133. This sustained expression of surface GARP and GARP transcript levels in ndGBs and recGBs suggests the potential utility of GARP as a reliable GSC biomarker, which persists at different tumor stages, possibly allowing for the detection of potential residual disease of a remarkably invasive cancer type.

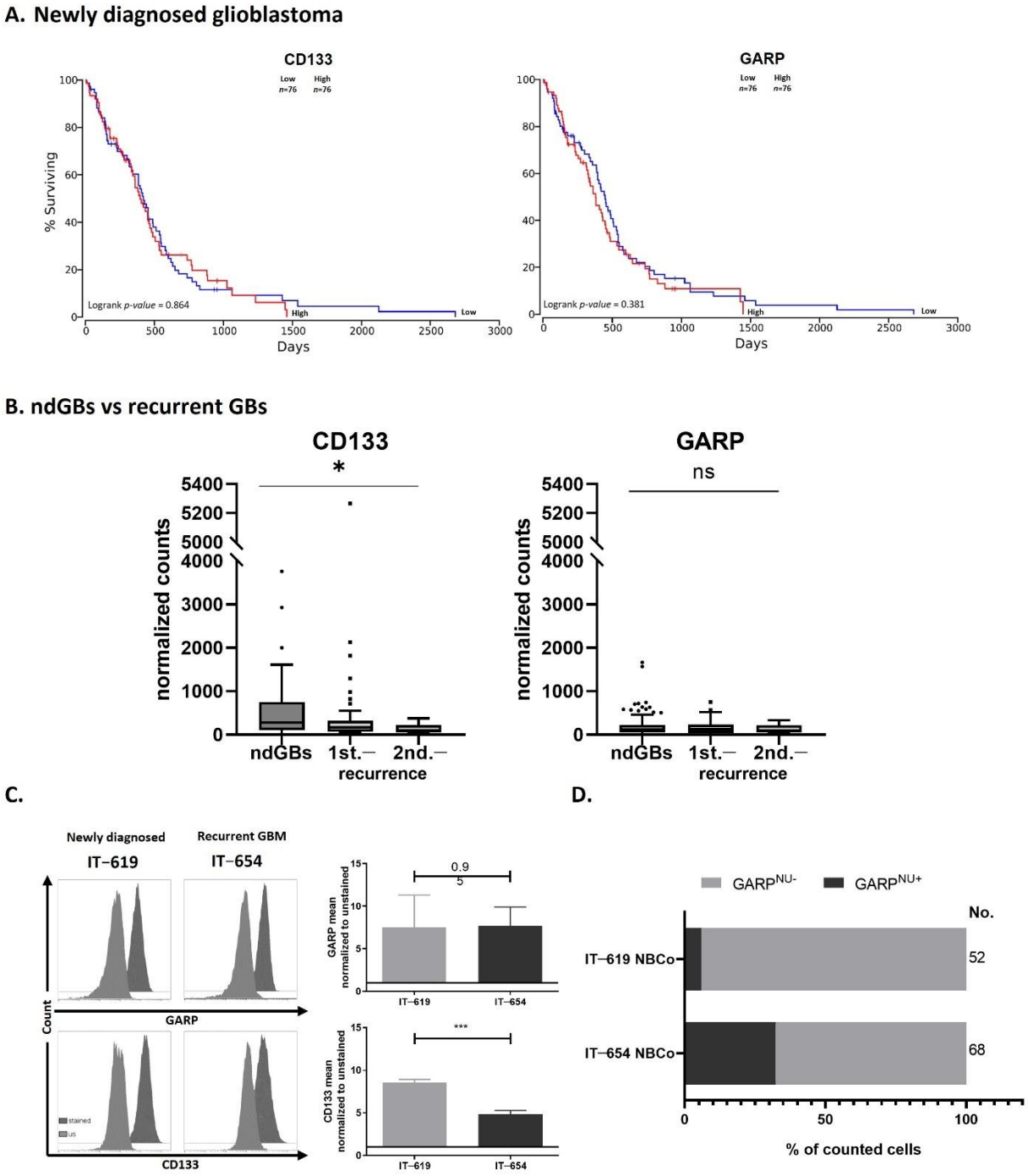

Figure 3.4.6. GARP expression in GB is unaffected throughout therapy. (A) Survival analysis of GARP and CD133 based on data available through The Cancer Genome Atlas (TCGA). GARP and CD133 mRNA expression data of 152 primary glioblastomas were divided 50/50 into either “low” expression or “high” expression and were analyzed for patient survival. (B) Retrospective analysis of transcriptomic data of 155 GB samples from 28 patients of Kim et al., 2020 (229). ndGBs, first, and second recurrent tumors were analyzed for their GARP and CD133 mRNA levels across tumor stages. (C) Flow cytometric analysis of IT-619 and IT-654. Doublets, debris, and dead cells were excluded from analysis. Recurrent IT-654 GSC exhibited stable surface GARP levels after TMZ and radiotherapy, whereas expression of CD133 decreased after treatment. The MFIs were normalized to the unstained control. n = 3. Significance was calculated by Student´s t-test and is indicated as follows: * $p < 0.05$, *** $p < 0.001$, and ns (not significant). (D) Number of GARP-positive nuclei for GSC IT-619 and IT-654 were analyzed by counting double-positive (Hoechst and GARP) cell nuclei. “No.” indicates the number of counted cells for the analysis.

3.4.3.5. Nuclear localization of GARP correlates with poor survival in patients with GB

As we observed an upregulation of the percentage of $GARP^{NU+}$ cells in the recurrent GSC line, IT-654 (Figure 3.4.6D), we wanted to explore a possible link between $GARP^{NU+}$ and the survival rate of GB patients (Figure 3.4.S9—Cohort 3). Therefore, we retroactively assessed $GARP^{NU+}$ levels in tumor tissue from a cohort of 35 newly diagnosed GB patients (WHO stage IV) and correlated them to patient overall survival (Figure 3.4.7, representative images) (41).

Notably, all GB patients in the cohort were found to express $GARP^{NU+}$ but varied in their frequency of $GARP^{NU+}$ cells. Therefore, we divided the cohort into two groups based on their frequency of $GARP^{NU+}$ expression. The first group encompassed 19 GB patients with tumors having a low frequency (~50%) of $GARP^{NU+}$ cells. The other group included 16 patients with a high frequency (>90%) of $GARP^{NU+}$ cells. In striking contrast with the transcriptomic analysis, which showed a consistent lack of correlation between GARP mRNA levels and patient survival (Figure 3.4.6A), stratification by $GARP^{NU+}$ revealed a significant correlation between $GARP^{NU+}$ and GB patient survival (Figure 3.4.7B). The results showed that patients with a low frequency of $GARP^{NU+}$ had a significantly longer overall survival in comparison to patients with a high frequency of $GARP^{NU+}$ (medians low: 12 months, high: 4 months; $p = 0.0026$, Figure 3.4.7B). These results indicate that the abundance of the GARP protein in the nuclear compartment—not GARP transcript levels—is associated with survival in patients with GB.

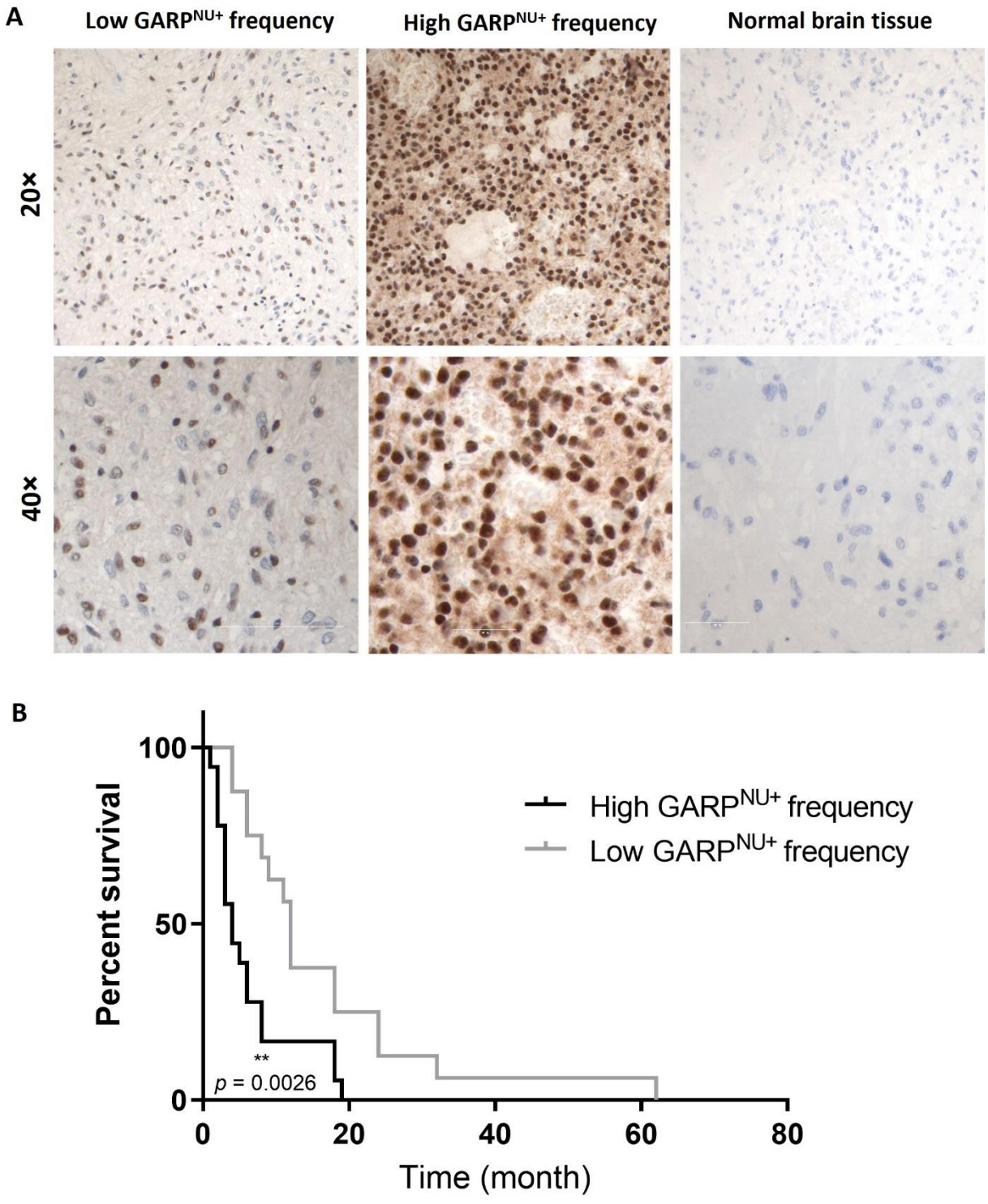

Figure 3.4.7. Nuclear GARP is a potential new prognostic biomarker for GB patient survival. (A) Immunohistochemistry of GARP in glioblastoma. GB (WHO grade IV) with low frequency of labeled nuclei (magnification ×20 and ×40) and GB with palisading necroses and a high frequency of stained nuclei (magnification ×20 and ×40). Normal brain tissue had no detectable GARP expression. Bar corresponds to 50 µm (40×) and 200 µm (20×), respectively. (B) Survival analysis of 35 GB patients based on their GARP-positive nuclei counts (1: high frequency, n = 16 and 2: low frequency, n = 19). Comparison of survival curves was performed by log-rank (Mantel–Cox) test (** $p < 0.01$).

3.4.4. Discussion

GSC comprise a heterogenous and highly volatile group of cells, which can switch between different phenotypes and molecular programs in response to environmental changes. The high degree of phenotypic plasticity displayed by GSC poses a challenge in the development of GSC-based diagnostic and GSC-targeting therapeutic strategies. The continuing search for GSC-associated markers has led to the identification of several molecules expressed in some but not all subtypes of human GSC or associated with some but not all cellular states (241, 242). One approach to counterbalance the phenotypic diversity of GSC is to simultaneously target multiple markers associated with different types of GSC, in order to increase the diagnostic coverage of the GSC content in a highly heterogeneous milieu of GBs (215, 229, 242–244). An alternative possibility is that some phenotypic traits may be conserved across heterogeneous GSC. Our data indicate that expression of GARP/GARP^{NU+} may be one such trait. We provide several lines of evidence that GARP/GARP^{NU+} is expressed in otherwise phenotypically distinct GSC (Figure 3.4.1 and Figure 3.4.3) and persists invariably across different cellular states (Figure 3.4.3). In the past, several groups have tried to identify universal GSC markers. One challenge is that most of the previously identified putative markers of GSC, e.g., CD133, are not universally expressed in all types of GSC, which limits the diagnostic utility of such markers for estimating GSC content in tumors (153). In this regard, both surface GARP and GARP^{NU+} expression appear to be invariably expressed in phenotypically distinct GSC including CD133^{+} and CD133– subtypes, under in vitro and in vivo experimental conditions (Figure 3.4.1, Figure 3.4.3, and Figure 3.4.S8) and in different stages of GB progression (ndGBs or recGBs) (Figure 3.4.6).

Our data indicate that GSC-associated expression of GARP persists in different cellular states. However, the degree of GARP expression varies between different cellular states. Interestingly, we find that expression of GARP is elevated in the state associated with a reduced self-renewal but not proliferative capacity and in conjunction with loss of differentiation-associated traits (Figure 3.4.4, Figure 3.4.5 and Figure 3.4.S10). Such a pattern is reminiscent of the transit-amplifying state during neurogenesis whereby slow-cycling neural stem cells must first exit from the state of self-renewal and convert into more differentiated but uncommitted and fast-proliferating transit-amplifying progenitors, prior to entering the lineage-commitment stage and differentiation (245). The simultaneous reduction in self-renewal and differentiation-associated traits without loss of the proliferation activity seen in GARPhigh GSC suggests that GARP may have a role in GSC' transition from the slow-cycling self-renewal state to a more differentiated and proliferation-competent state similar to that of transit-amplifying progenitors. It should be noted that even the complete loss of self-renewal does not lead to a loss of the tumor-propagating capacity of GSC, and recent evidence indicates that GB propagation is driven primarily not by self-renewing GSC but their non-self-renewing progenies (246).

It is important to note that GARP expression is not limited to GSC alone. Cancer cells, including GB (as shown in this work with T98G in Figure 3.4.1A), activated Treg and B cells, and platelets are all known to express GARP on their surfaces (215). Therefore, GARP alone cannot be used to identify GSC but rather in combination with a panel of other markers to better distinguish between GSC and other GARP-positive cells in the tumor microenvironment. In this regard, our finding that elevated GARP expression coincides with a significant increase in p21 expression suggests that dual assessments for GARP and p21 may enable a distinguishment between GSC and non-GSC cells. Considering that p21 plays important roles in the maintenance of neural stem cells and is one of the factors implicated in GB radioresistance, the concomitant elevation of p21 and GARP in GSC further supports the potential merits of GARP as a predictive and prognostic biomarker for GB (247, 248). A limitation of this exploratory work is that it mainly analyzed the expression of GARP in comparison to one GSC reference marker, CD133. Future studies are needed to analyze in depth the association of GARP expression with an expanded panel of putative GSC markers to further evaluate how universally and stably expressed

GARP is on GSC, and on different cellular components of the tumor microenvironment, especially those that are known to express GARP, like activated Treg and platelets.

Intriguingly, whereas GARP mRNA levels are comparable between ndGBs and recGBs, the level of $GARP^{NU+}$ protein correlated with poor survival in patients with GB (Figure 3.4.7). Notably, the critical cutoff for $GARP^{NU+}$ was >90% (Figure 3.4.7), which is significantly higher than the 10% cutoff for CD133 expression implicated as a predictive marker for GB recurrence (249).

Although the link between a high frequency of nuclear GARP and poor outcomes of GB patients provides a novel and intriguing insight into the previously unsuspected role of $GARP^{NU+}$ in GB, it is important to also acknowledge the limitations of this exploratory study. One is the small patient cohort size (n = 35). The relationship between $GARP^{NU+}$ and clinical outcome from GB must be validated in future studies using larger datasets. A further confirmation in larger follow-up studies is a prerequisite for the conclusion on the diagnostic value of $GARP^{NU+}$ as a prognostic biomarker for GB.

Cancer stem cells are related to reduced survival in GB patients (241, 242). Therefore, it was surprising to see that a high frequency of $GARP^{NU+}$ tumor cells was linked to reduced overall survival, despite the observed upregulation of $GARP^{NU+}$ in differentiation-promoting conditions (NB-bFGF/-EGF) (Figure 3.4.3B). One possible explanation for this is that elevated GARP levels are linked to enhanced immunosuppression in the tumor microenvironment (41, 43). In more detail, previously, we demonstrated both in melanoma (43) and in GB (41) that tumor cells upregulate the expression of GARP and thus gain tolerogenic potential. This in turn aids in the suppression of effector $CD4^+$ and $CD8^+$ T cell function, required for anti-tumor immune responses, and correspondingly induces suppressive Treg, which further contribute to the suppression of effective anti-tumor immune responses. Furthermore, the upregulation of GARP, an inhibitory protein, upon the differentiation process of cancer stem cells is consistent with previous reports by Ullah et al., 2020, who similarly demonstrated that the immune checkpoints PD-L1 and HLA-G are upregulated by cancer stem cells upon differentiation (250). The principal binding partner of GARP, TGF-β, has been shown to induce the expression of PD-L1, but it remains unclear if GARP expression can as well (251, 252). It is worth noting that the simultaneous targeting of GARP, TGF-β1, and PD-1 has been shown to be an effective combination therapy, capable of restoring T effector cell function and overcoming resistance to PD-1/PD-L1 blockade (253, 254). Future studies are planned to clarify the relationship between GARP, PD-L1, and differentiation to determine if their contribution to immune suppression is responsible for the observed reduction in patient survival.

Interestingly, we found a discrepancy between RNAseq data from primary tumor tissue samples (Figure 3.4.6A) and our histological analysis of the frequency of $GARP^{NU+}$-positive cells in GB patient samples (Figure 3.4.7). Whereas no relationship between GARP transcript levels and patient survival was detectable in the TCGA data (Figure 3.4.6A), the frequency of $GARP^{NU+}$ GB cells seems to be a suitable prognostic marker for patient survival. It should be considered that the tissue samples used for TCGA RNAseq analysis (Figure 3.4.6A) presumably consisted of tumor lysates, which contain a multitude of cell types, ranging from tumor cells to immune cells, up to healthy tissue. As information on the cellular origin of the transcripts is missing due to the bulk sequencing, otherwise significant differences between donors can be diluted into insignificant results based on the individual composition and frequencies of cell types included in the analysis. In addition, GARP mRNA can be detected in many tissues, e.g., heart, kidney, liver, and lung, whereas surface expression of the GARP protein itself seems to be limited to only a number of cell types, e.g., activated Treg (74), platelets (37), various cancers like GB and malignant melanoma (41, 43), and mesenchymal stem cells (38), further contributing to a decreasing validity. Therefore, the identification of the cell type analyzed in RNAseq is key to interpreting and understanding future datasets.

More advanced methods like spatial transcriptomics, multiplex immunofluorescence, and spatial multi-omics single-cell imaging are more fitting to further enhance our understanding of GARP transcript and protein levels in GB cells and their surrounding microenvironment, as well as their distribution within subcellular compartments (255). The additional information gained by these techniques would enable the identification of different cell types, their localization within the tumor and relation to other cells of the tumor microenvironment, and the determination of whether a surface or intranuclear localization of the GARP protein is present in these cells. Furthermore, the exclusion of certain cell types (e.g., Treg or platelets) from the analysis would enable a better understanding of GARP and its subcellular localization on patient outcomes.

Our data suggest that nuclear localization of the GARP protein—rather than abundance of the GARP transcript—is a factor associated with GB progression after therapy. Our finding that GARP is localized to the nucleus is novel and intriguing, as GARP has previously been characterized only as a surface and secreted protein, which currently has no annotated nuclear localization signal (NLS). Interestingly, the use of nuclear localization of an otherwise surface-associated protein as a prognostic marker has been described before (256–258). One such example is the protein Src, which plays a key role in cell morphology, motility, proliferation, and survival (259). Urciuoli et al., 2017, was able to show in human osteosarcoma that nuclear localization of Src correlates with overall survival and therefore has relevance as a prognostic marker for osteosarcoma patients (257). Likewise, it has also been described that PD-L1, a T cell inhibitory molecule in cancer, shows a nuclear localization as a reaction to therapy. In more detail, PD-L1 is translocated from the cell surface into the nucleus as a reaction to high-dose doxorubicin therapy regimens. The nuclear localization of PD-L1 was described as a prognostic biomarker, as patients with low PD-L1 nuclear expression had significantly fewer circulating cancer cells and exhibited a longer overall survival (256, 258). While the mechanisms of GARP nuclear localization in GSC still have to be elucidated, the potential clinical implications of this previously unknown phenomenon are clear given the critical role of GARP in the activation of TGF-β, one of the key factors (260) contributing to GB progression particularly via the maintenance of GSC via the induction of, e.g., Sox2 and LIF expression (261, 262). Considering that targeting TGF-β-activating ligands in GB has been intensively explored as a promising therapeutic strategy (260, 263), the clarification of $GARP^{NU+}$ activities in GSC may provide novel insights into the interaction of GARP and TGF-β, as TGF-β activation is known to trigger the nuclear localization of proteins like Smad and Smad4 (264). Further pointing to the potential merit of GARP as a diagnostic and therapeutic target is the dual impact of GARP on cancer progression—via the modulation of Treg and through the direct activities of GARP exerted on cancer (stem) cells themselves.

3.4.5. Conclusions

The scope of the present study was to evaluate GARP as a biomarker for heterogeneous GSC and to determine the effects of GARP on GB patient outcomes. Based on our data, we propose that $GARP^{NU+}$ could potentially serve, in combination with existing GSC markers, as a universal and stably expressed marker for different subsets and cellular states of GSC as well as a possible prognostic marker for patient outcomes in GB. We propose that GARP assessments may provide the means to identify not only self-renewing GSC but also their progenies that exit from self-renewal but retain proliferative activity. Further validation of this hypothesis in future studies will require analyses of larger patient cohorts using an extended panel of markers associated with GSC and GB progression. Future investigations should focus on addressing mechanistic questions, such as the functional significance of GARP in regulating GSC-specific functions, by employing knockdown and/or overexpressing lines, as well as further investigating the role of nuclear GARP, its nuclear retention, and functional relevance.

A

line	origin	SCF	predominant phenotype	CD133, %	ref
#1051	ndGB	1/3	Nestin^{+}/GFAP^{-}	<1	Barrantes-Freer 2013[29], 2015[26]
#1063	ndGB	1/4	Nestin^{+}/GFAP^{-}	2.4	Barrantes-Freer 2013[29]
#1095	ndGB	1/4	Nestin^{+}/GFAP^{-}	<1	Barrantes-Freer 2013[29], 2015[26]
#1043	ndGB	1/3	Nestin^{+}/GFAP^{+}	<15	this study
IT-726-1	ndGB	1/8	Nestin^{+}/GFAP^{+}	<80	this study
IT-726-2	ndGB	1/30	Nestin^{+}/GFAP^{+}	<1	this study
IT-726-3A	ndGB	1/25	Nestin^{+}/GFAP^{+}	<5	this study
IT-726-3B	ndGB	1/3	Nestin^{+}/GFAP^{+}	<7	this study
IT-726-4	ndGB	1/59	Nestin^{+}/GFAP^{+}	<3	this study
IT-619	ndGB	1/15	Nestin^{+}/GFAP^{+}	>90	this study
IT-654	recGB	1/80	Nestin^{+}/GFAP^{+}	<70	this study

SCF, stem cell frequency

B

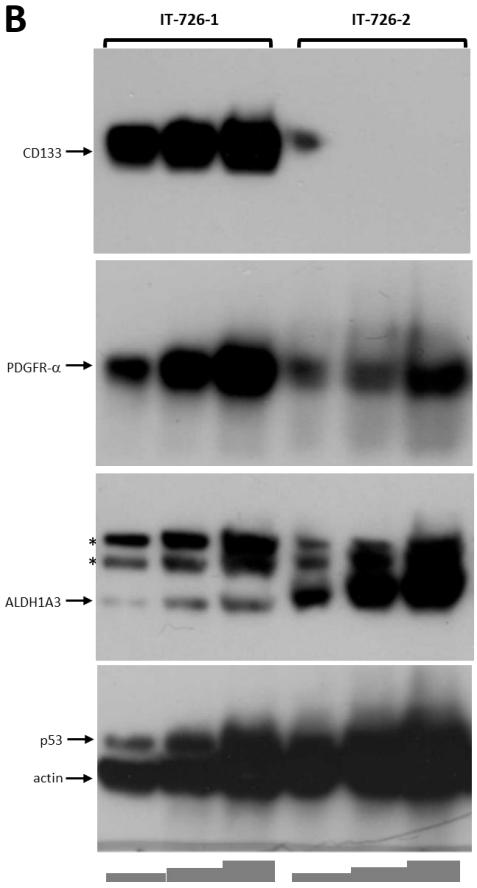

*, unspecific bands

Figure. 3.4.S1: Heterologous GSC lines differing in their self-renewal capacity. Previous characterization of the heterologous patient derived GSC lines used in this work (A,B) (225, 226, 253, 254). Considerable variation in the expression of several GSC markers, including glial fibrillary acidic protein (GFAP), CD133, platelet-derived growth factor receptor alpha (PDGFR-α), and aldehyde dehydrogenase 1 family member A3 (ALDH1A3), was observed in both heterologous and isogenic GSC lines. (B) Example analysis of several GSC markers, including CD133, PDGFR-α, and ALDH1A3, in the isogenic GSC lines, IT-726-1 and IT-726-2 (GSC lines featured in figure S1A indicated by red arrows), via western blot using the following antibodies: anti-CD133/1 (clone: W6B3C1), anti-PDFGR-α (D13C6) (Cell Signaling, #5341), anti-ALDH1A3 (Thermo Fischer Scientific, MA5-25528), anti-p53 (DO-1) (Cell Signaling, #18032), anti-actin (C4) (Santa Cruz Biotechnology, sc-47778), goat anti-mouse IgG horseradish peroxidase (Santa Cruz Biotechnology, sc-2055), goat anti-rabbit horseradish peroxidase (Santa Cruz Biotechnology, sc-2054) (B). Cell lysates were loaded in increasing volumes, and actin was used as a loading control.

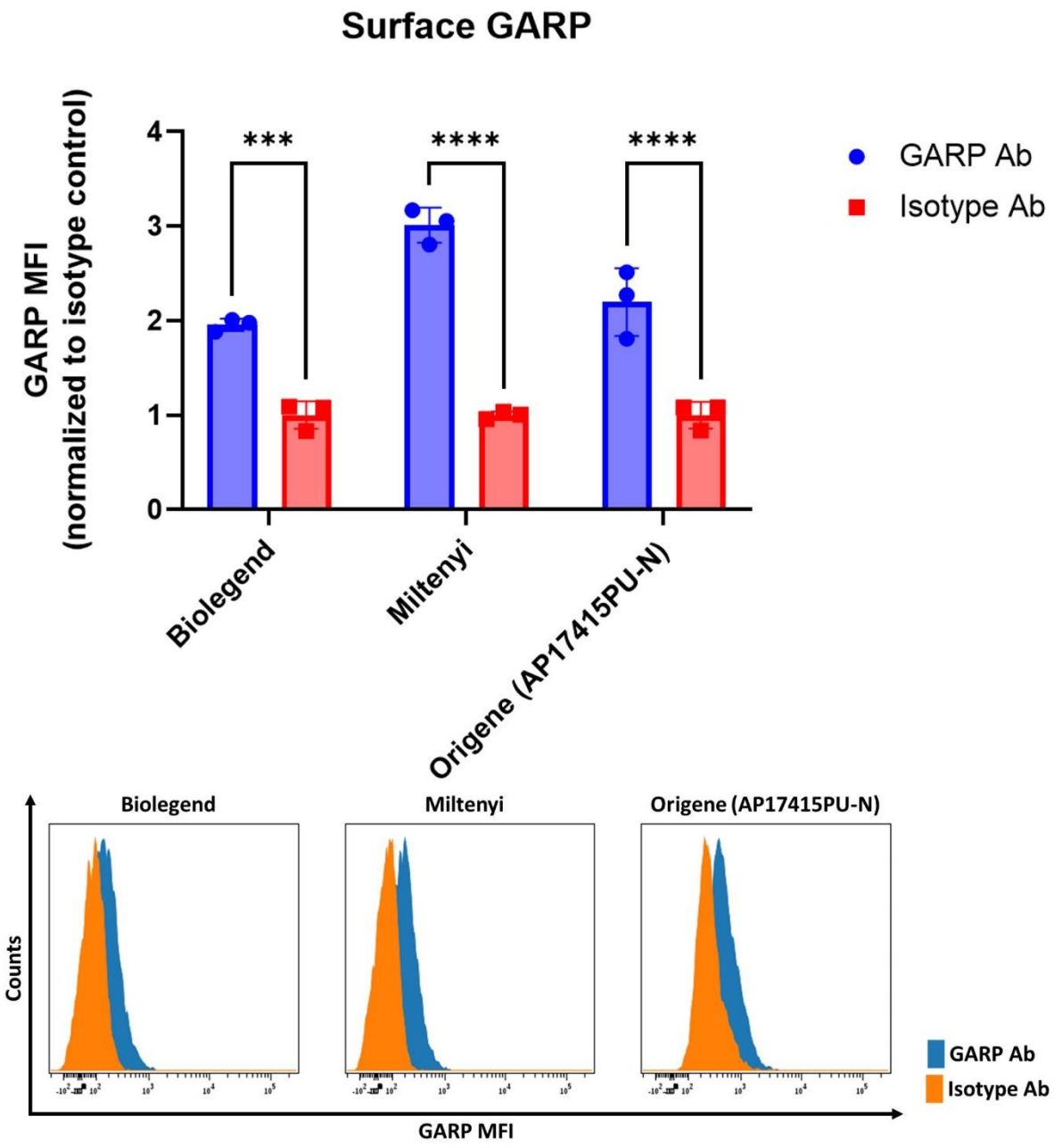

Figure 3.4.S2: Anti-GARP antibody validation for flow cytometry. Comparative flow cytometric analysis of surface GARP levels on a control human melanoma cell line, Mewo, using three different human anti-GARP antibodies. The following antibodies were analyzed: Miltenyi (130-103-890), Biolegend (352502), Origene (AP17415PU-N). Doublets, debris, and dead cells were excluded from the analysis. Graph shows the mean fluorescence intensity (MFI) normalized to the MFI of the respective isotype control, whereas histograms display one representative result (n=3, ± SD, *** $p < 0.001$, and **** $p < 0.0001$ determined by two-way ANOVA).

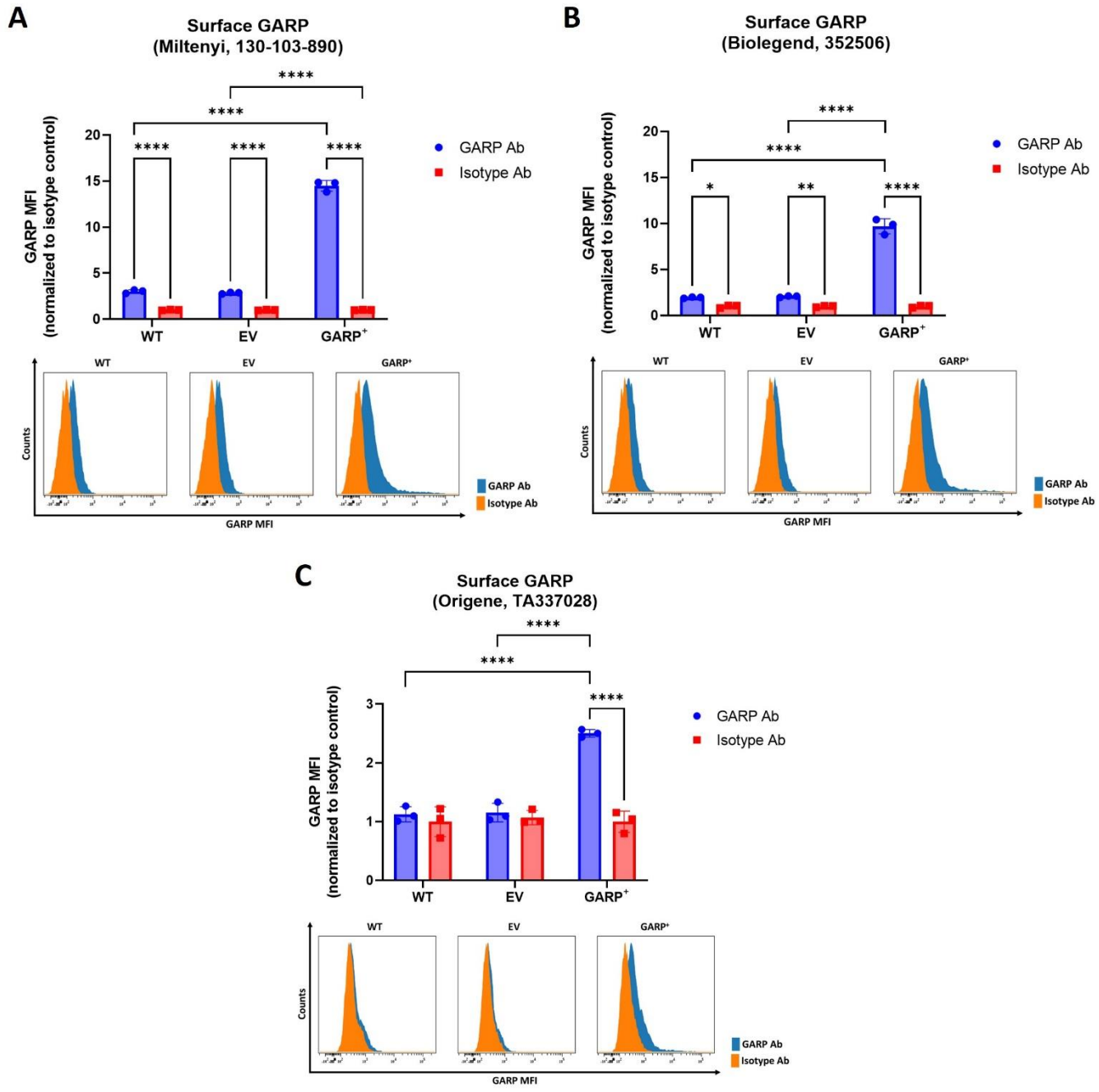

Figure 3.4.S3: Specificity demonstration and validation of anti-GARP antibodies. Comparative flow cytometric analysis of surface GARP levels on wildtype (WT) and transfected (GARP overexpression (GARP$^+$), empty vector control (EV)) Mewo cells using three different human anti-GARP antibodies. The following antibodies were analyzed: Miltenyi (130-103-890) (A), Biolegend (352502) (B), Origene (TA337028) (C). Doublets, debris, and dead cells were excluded from the analysis. Graph shows the mean fluorescence intensity (MFI) normalized to the MFI of the respective isotype control, whereas histograms display one representative result (n=3, ± SD, * $p < 0.05$, ** $p < 0.01$, and **** $p < 0.0001$ determined by two-way ANOVA).

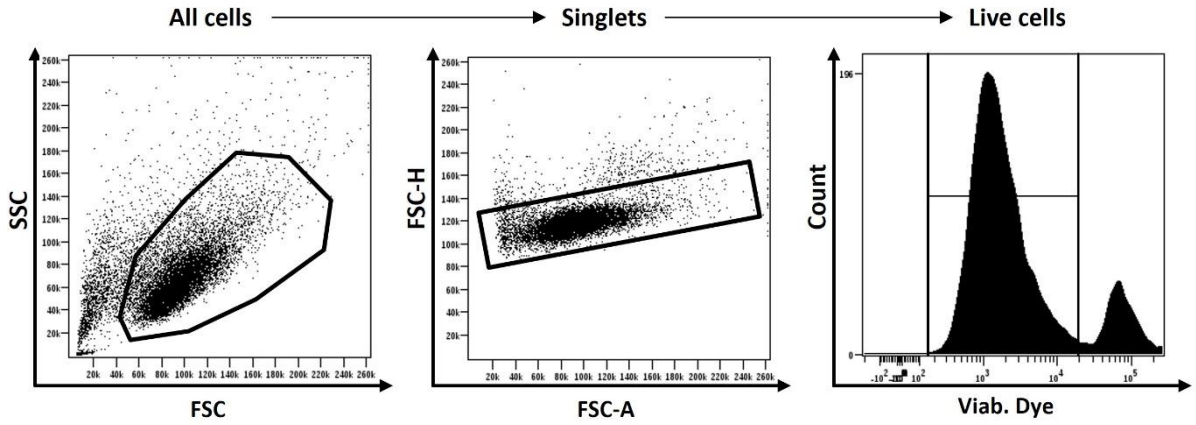

Figure 3.4.S4: Flow cytometric gating strategy for GSC. Representative flow cytometric gating strategies used for GSC. Debris, doublets, and dead cells were excluded from analysis.

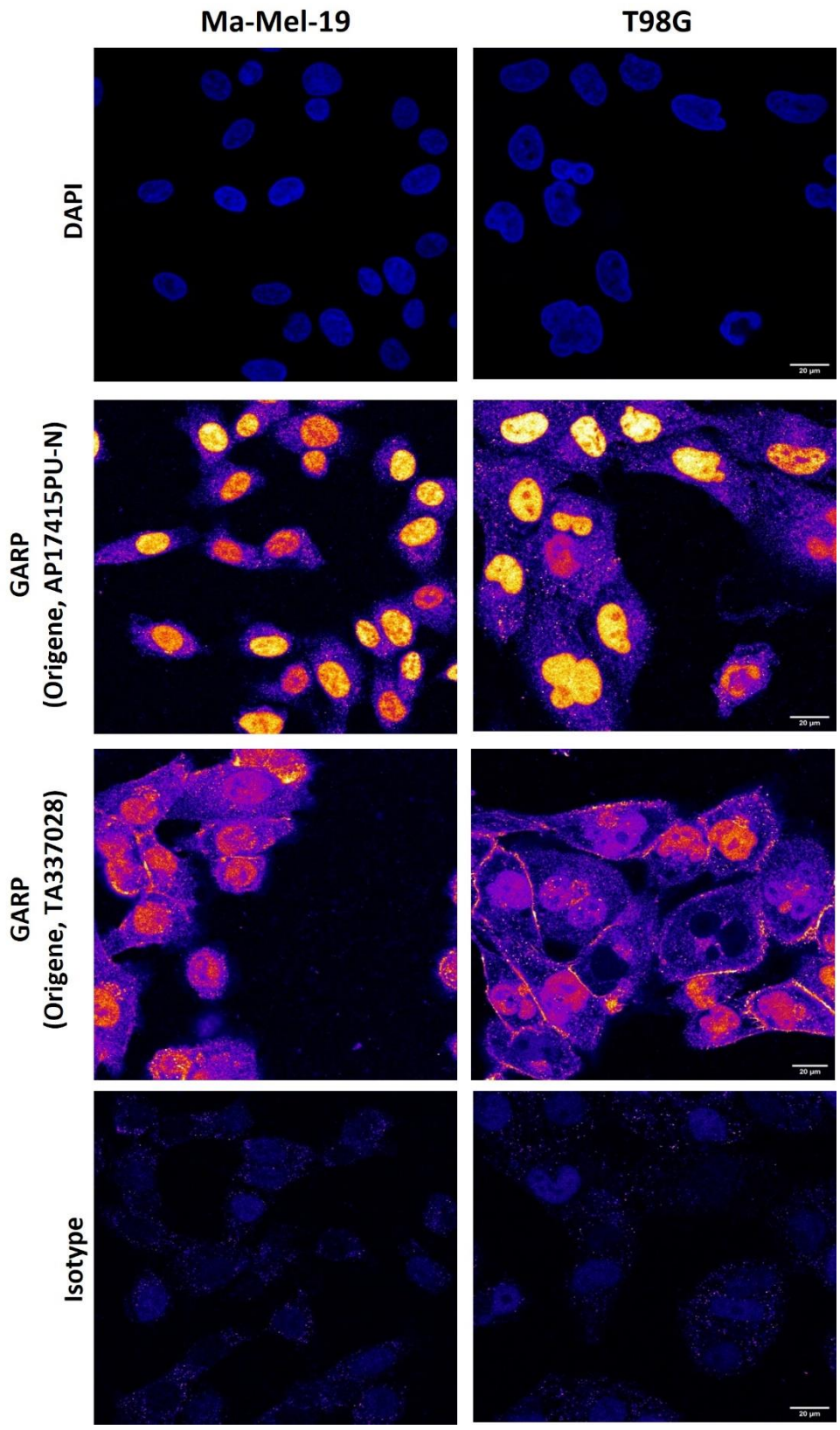

Figure 3.4.S5: Anti-GARP antibody validation for confocal microscopy. Confocal images of the human GARP expressing cell lines, Ma-Mel-19 and T98G. Cells were stained for GARP using two different antibodies (Origene, AP17415PU-N; Origene, TA337028) as seen in orange. Cells were counterstained for their nuclei with Hoechst (blue). Note the intranuclear localization of GARP ($GARP^{NU+}$) detectable with both antibodies. Scale bar corresponds to 20 µm.

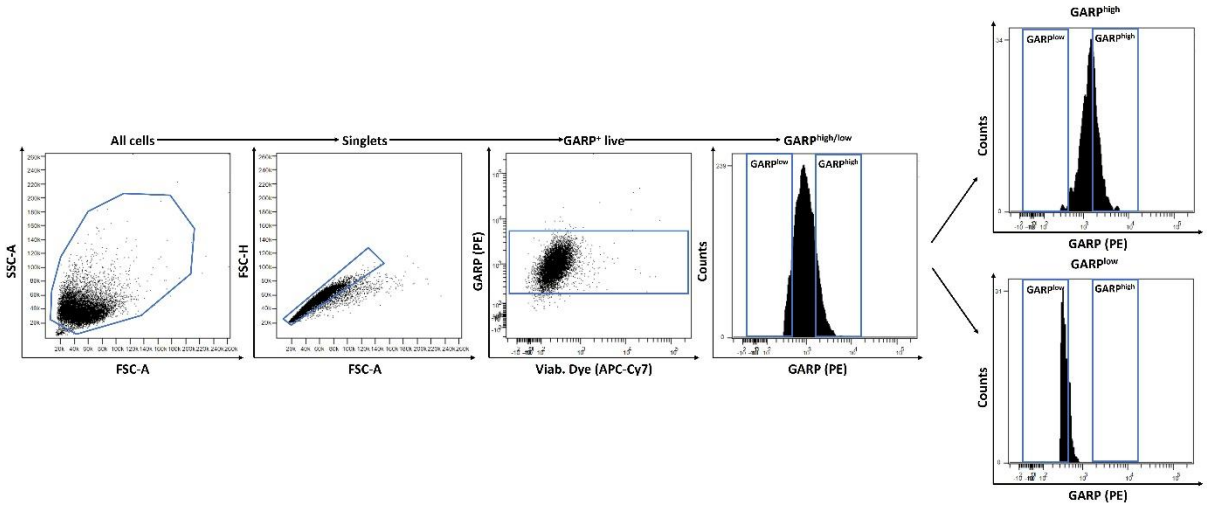

Figure 3.4.S6: Flow cytometric gating strategy for GARP^{high} and GARP^{low} sorted GSC. (A) Representative flow cytometric gating strategy used for sorting GARP^{high} and GARP^{low} GSC. Sorted cells were re-measured via flow cytometry to confirm sorting efficacy. (B) Example GARP staining of GSC (mean fluorescence intensity shown) compared to its respective isotype and unstained controls. Debris, doublets, and dead cells were excluded from analysis.

#1051

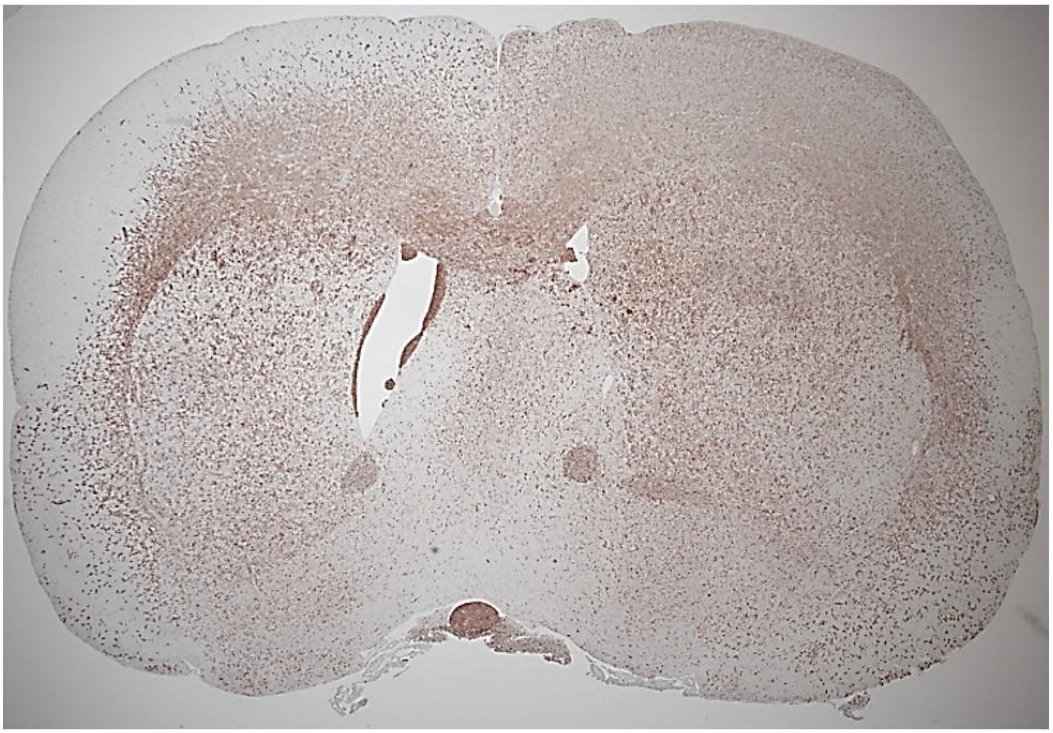

#1043

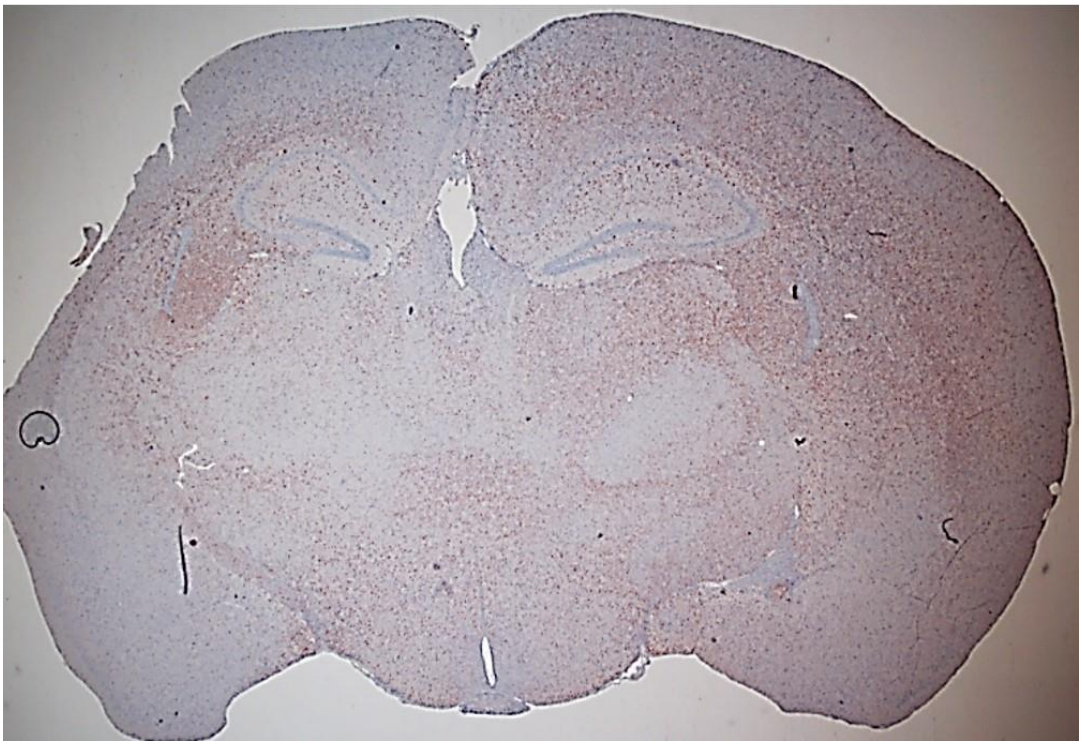

Figure 3.4.S7: Invasive xenograft tumors arisen from GSC lines, #1051 and #1043. Representative images of xenograft tumors grown from human GSC in an orthotopic mouse model for brain tumors. Immunohistochemistry stainings for human nestin (anti-human nestin antibody PA5-82905, 1:100, Life Technologies).

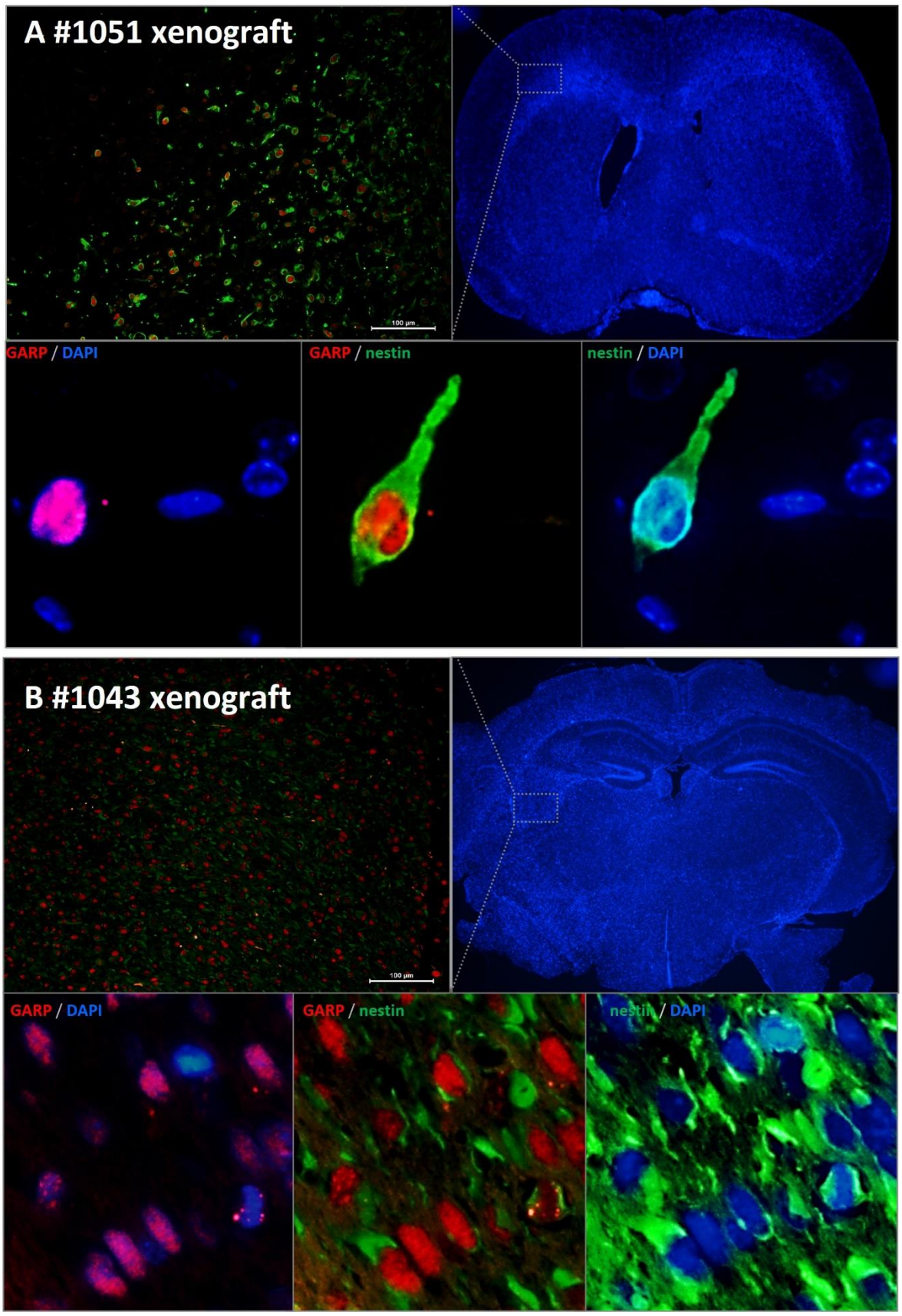

Figure 3.4.S8: GARP is expressed in xenograft tumors arisen from GSC lines, #1051 and #1043. Immunofluorescence of GARP and nestin of (A) #1051 and (B) #1043 xenograft tumors. GARP seems to be exclusively expressed on GSC cells. Confocal images of GARP and nestin expressing GSC stained for GARP and nestin. Cells were stained for their nuclei. Nuclear counterstaining with Hoechst (blue), GARP (red), and nestin (green). Scale bar corresponds to 100 µm.

Cohort 1:

TCGA-Databases → **OncoLnc**
J. Anaya., 2016
https://doi.org/10.7717/peerj-cs.67

Brennan *et al.*, 2013
https://doi.org/10.1016/j.cell.2013.09.034

Cohort 2:

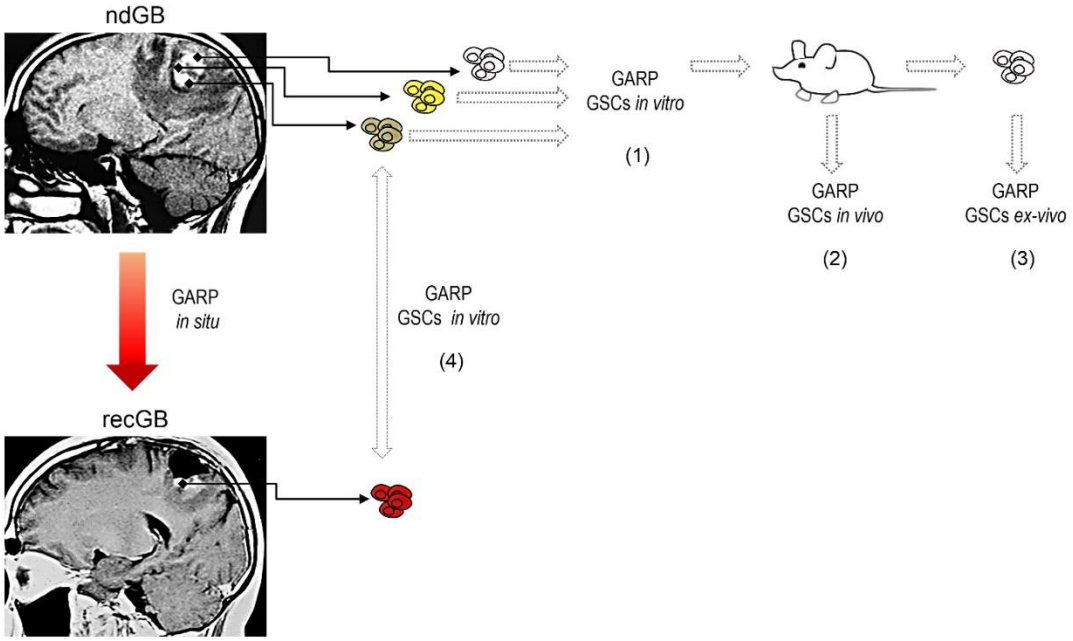

Cohort 3:

35 patients with glioma grade IV at the study center Idar-Oberstein, Germany (Zimmer *et al.*, 2019)

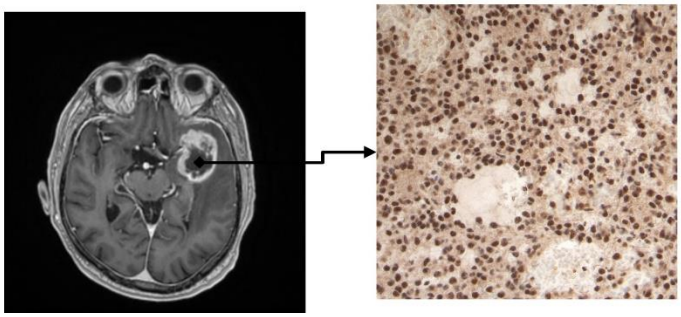

Figure 3.4.S9: Study design and models used for the assessment of GARP. Cohort 1: For the analysis of GARP and CD133 expression in GB, the online tool OncoLnc was used. Based on 152 complete data sets, including complete survival data, patients were divided 50/50 into "low" or "high" groups based off their mRNA expression of GARP and CD133 and were analyzed for their survival. The results shown are in whole or part based upon data generated by the TCGA Research Network: https://www.cancer.gov/tcga and were analyzed using OncoLnc (237) . Cohort 2: „GARP in situ" corresponds to GARP assessments in tumor specimens from newly diagnosed or recurrent GBs. Investigation track (1) corresponds to *in vitro* assessments in GSC either isogenic or heterogenic originating from ndGBs. Track (2) corresponds to *in vivo* assessments of GARP in tumor xenografts grown from orthotopically implanted GSC. Track (3) corresponds to GARP assessments in GSC explanted from tumor xenografts. Track (4) corresponds to tumor-matched GSC isolated from the same patient at the ndGB or recGB stage. Furthermore, retrospective analysis of transcriptome data of 155 GB samples from 28 patients of Kim et al., 2020. ndGBs, first and second recurrent tumors were analyzed for their GARP and CD133 expression levels across tumor stages (229). Cohort 3: A cohort of 35 patients with (WHO grade IV) glioblastoma (Zimmer et al., 2019) were analyzed for their GARP expression by immunohistochemistry and analyzed for their survival (41).

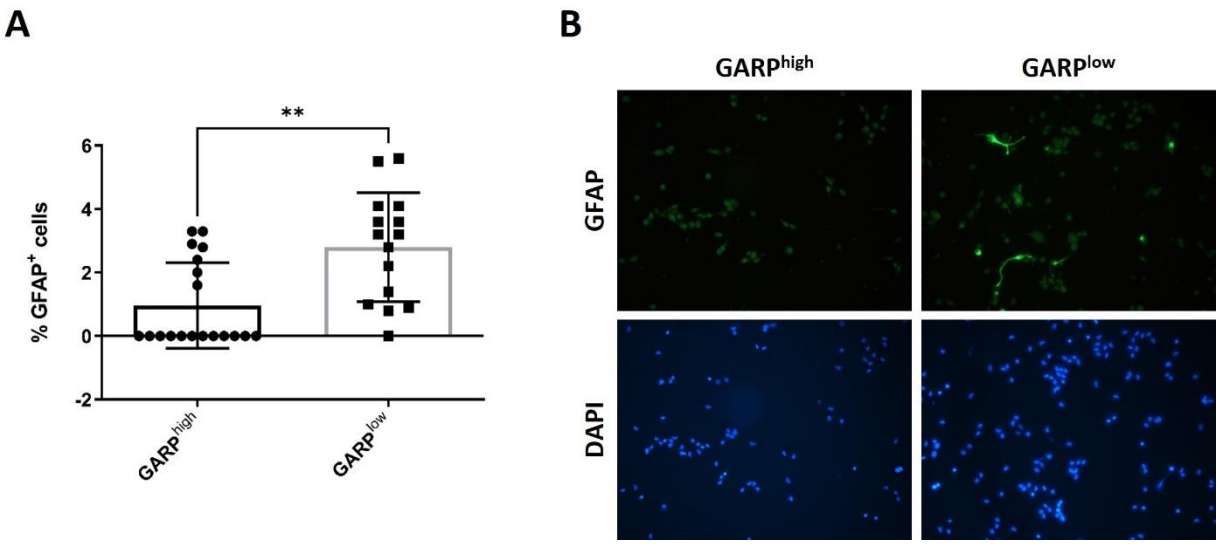

Figure 3.4.S10: Frequency of GFAP^{+} GARP^{high} and GARP^{low} GSC. The GSC line, #1095, was sorted into GARP^{high} and GARP^{low} populations. Cells were cultured in self-renewal promoting conditions (NB^{+}bFGF/$^{+}$EGF) and assessed for their frequency of glial fibrillary acidic protein (GFAP), an astrocyte differentiation associated marker, via immunofluorescence. (A) The percentage of GFAP^{+} cells was quantified from the total cells counted. (B) Representative images of GFAP (green) stained GARP^{high} and GARP^{low} GSC with paired DAPI (blue) controls. The white scale bar corresponds to 50 µm.

4.0 GARP on Platelets in malignant melanoma

4.1 Overview: Melanoma

4.1.1 Epidemiology

The deadliest and most dangerous type of skin cancer is malignant melanoma (265). Melanoma accounts for 65% of skin cancer-related mortality although accounting for fewer than 5% of skin cancer diagnoses (266). The prevalence of cutaneous melanoma is rising globally, and this rise is happening more quickly than that of other cancers (267). While some estimates for the western world claim that one in every 50 persons are at risk of acquiring cutaneous melanoma, estimations from the United States place the average lifetime risk of the disease at one in 56 for men and one in 37 for women (268, 269). Malignant melanoma is more frequently diagnosed in females than in males between the ages of 20 and 24 (4:10), but as people get older, men become far more likely to get the disease (17:10, over the age of 65). Secondary to this, there has been a dramatic rise in the prevalence of males who are roughly in the middle of their sixth decade of life (270). Men with cutaneous melanoma have poorer clinical outcomes, higher rates of recurrence, progression, and mortality, possibly due to less self-examination, delayed presentation, and advanced disease stages (271, 272).

Malignant melanoma arises from melanocytes, which produce melanin. Melanocytes are found in the eye, meninges, hair follicles, mucosal tissue, and in large numbers in the basal epidermal layer. Melanoma can be separated based on their diverse origin, genetic composition and its own treatment guidelines into three subgroups, the cutaneous, mucosal, and uveal malignant melanoma (273).

UV radiation is one of the most prevalent risk factors for DNA damage in the skin and is thus a significant factor in the development of malignant melanoma (274, 275). UV exposure has genotoxic effects that can cause melanocyte somatic mutations. Accumulation of mutations can result in unregulated cell division, leading to the formation of a malignant tumor. In an attempt to counteract this process, the body induces inflammatory responses and death in the damaged cells, resulting in the well-known sunburn. Malignant melanoma is characterized by a high mutational burden, particularly in gene areas that control cell cycle, proliferation, and metabolism. As demonstrated by the success of Australia, a country with a high incidence of melanoma, the focus of skin cancer prevention should be on reducing high UV-exposure (276). As the occurrence of melanoma in sun-protected areas demonstrates, UV light is not the only known cause of melanoma. Other recognized risk factors include genetic susceptibility and the density of preexisting moles (277).

4.1.2 Diagnosis & Pathology

Suspicious naevi are classified by a dermatologist, utilizing a dermatoscope. The ABCD rule is a key set of guidelines for visually detecting naevi that are likely cancerous (278). Hereby represents A - Asymmetry, B - Border, C - Color, D - Diameter, and E – Elevation of the naevi. This is reinforced by regular photo documentation, which enables the assessment of major morphological changes in suspicious naevi over time (279–281). According to the TNM-categorization, which is recommended by the American Joint Committee on Cancer (AJCC), the categorization of malignant melanoma tumors is determined by the results of tumor biopsies (276, 282). In the early stages of illness, the thickness T, which ranges from T0/T is (not detectable) to T4 (more than 4.0 mm), is especially significant. The N classification is determined by the number of metastatic lymph nodes and the presence of in-transit, satellite, and/or microsatellite metastases. M describes the severity of metastatic occurrence ranging from M0 (no metastases) to M1a-d in various organs such as the skin and lung. The TNM-Classification is summarized in stages ranging from 0 to IV when viewed in its entirety. Tumors that are non-

metastatic and have a thickness that increases from Tis (0) to T4 are classified as stages 0 to II (II). Regional metastases are present at the tumor site or draining lymph nodes in stage III cancers. Stage IV tumors are characterized by distant metastases.

With approximately 15 mutations per mega base pair, melanoma exhibits a significant mutation burden (283, 284). In 50-70 percent and 15-30% of melanomas, respectively, the primary mutations impact cell division-regulating genes such as the B-RAF and N-RAS proto-oncogenes, and the tumor suppressor gene neurofibromin 1 in 10-20% of cases (285, 286). Other mutations impact genes that regulate cell metabolism, including the anti-oncogene PTEN (phosphatase and tensin homolog) and the proto-oncogene KIT (receptor tyrosine kinase). TP53 (tumor protein p53) mutations hinder cell death and result in uncontrolled cell division (CDKN2A, cyclin-dependent kinase inhibitor-2A aka p16). Mutations in the TERT gene (telomerase reverse transcriptase) boost telomerase activity, which can exceed the number of natural cell divisions (Hayflick limit) (287). Mutations result in the overexpression of the MAPK and (PI3K)/AKT signaling pathways (288). In stage IV, the mutations serve as targets for molecularly targeted therapy involving RAS/BRAF/MEK/mTOR/PI3K and AKT inhibitors.

4.1.3 Therapy

The first-line treatment is surgical excision of the tumor, affected lymph nodes, and metastases.

Mortality is therefore directly proportional to tumor thickness, as resectable tumors devoid of metastases are treatable, if not curable (282). In malignant melanoma, conventional chemo-, and radiotherapy have proven less effective than in other cancers. Tumor recurrence is often inevitable. For the treatment of advanced, non-resectable melanoma stage IV, novel systemic treatments such as tyrosine kinase and checkpoint inhibitors have been on the market since 2011 (289, 290).

Melanoma cells containing mutations in the MAPK/ERK and PI3K/Akt pathways multiply more rapidly. In 90% of melanomas, the tyrosine kinases of the MAPK pathway are mutated. BRAF and MEK signal transduction inhibitors inhibit the tyrosine kinases BRAF and MEK (mitogen-activated protein kinase) in the MAPK pathway. 80% -90% of BRAF mutations are point mutations at codon 600, resulting in the substitution of valine for glutamic acid (BRAFV600E mutation) (287, 291). There are several approved drugs targeting BRAF on the market. Dabrafenib inhibits serine-threonine (RAF) kinases (such as B-RAF and C-RAF), whereas vemurafenib inhibits mutant BRAF kinases, namely BRAFV600 mutations. In 2012, the European Medicines Agency (EMA) approved vemurafenib for monotherapy and in 2015 for combination therapy with cobimetinib in BRAFV600-mutated, non-resectable, metastatic melanoma. Dabrafenib was licensed in 2013 as a monotherapy and in combination with trametinib as adjuvant therapy for stage III melanoma. The guidelines urge prescribing combination medicines since patients often acquire resistance to kinase inhibitor monotherapy after six months while living 12 months progression-free and attaining a 70% response with combination medications (292–295).

With the introduction of checkpoint inhibitors into clinical practice, patients have shown significant improvement. Introduced first, was the antibody Ipilimumab. It is directed against cytotoxic T-lymphocyte-associated protein 4, also known as CTLA-4, which is a protein that is involved in the negative feedback loop of activated T cells. Activation of T cells causes an increase in the production of CTLA-4, which then attaches to CD80 and CD86 on antigen-presenting cells or tumor cells, where it acts as a signal for deactivation. However, the actual mechanism of downregulation and the immune response to the tumor remain unclear (296). Ipilimumab's binding to CTLA-4 inhibits the function of the receptor and leads to an overall increase in T cell responses. The greater proliferation of tumor antigen reactive $CD8^+$ T lymphocytes, is the impact that is most beneficial for cancer patients. Since autoreactive T cells are also stimulated, it is obvious that autoimmunity is a common, serious adverse effect (19, 24).

Humanized antibodies against programmed cell death protein 1 (PD-1), were the second immune checkpoint inhibitors that have been established as therapy. T cells express PD-1 on their surface, where it binds to its ligands, PD-L1 and PD-L2 which are expressed on a variety of cell types, including myeloid immune cells (297). PD-1 inhibition largely stimulates proliferation of tumor-infiltrating $CD8^+$ T cells that appear exhausted (296).

T cell exhaustion describes a decrease in reactivity to external factors, that occurs with persistent antigen stimulation like cancer (298). When it comes to patients with inoperable stages III to IV melanoma, the first-line treatment in Europe and Germany is either monotherapy with anti-PD-1 antibodies or combination therapy with anti-CTLA-4 and anti-PD-1 antibodies (297). The introduction of these therapies represents a paradigm shift in the treatment of melanoma, as the overall survival rates for patients undergoing combination therapy range from approximately 50% (for all patients) to 60% (for patients with BRAF mutation) after five years of follow-up. This represents a significant increase in the patient's chance of survival.

Nevertheless, 50% of patients do not react to checkpoint blockage immediately ("primary resistance") or develop resistance throughout treatment (22). Inadequate T cell infiltration, T cell exclusion, IFN-γ resistance, or loss of T cell function or antigen presentation are underlying mechanisms (23). Currently, clinical studies are being conducted to investigate the potential benefits of combining checkpoint inhibitors with BRAF and MEK inhibitors for the treatment of malignancies that are positive for BRAFV600E/K.(295).

Cancer vaccines are another option that are being evaluated for people who do not respond to checkpoint inhibitors. In order to combat cancer, cancer vaccines are designed to make use of the immune system and to stimulate a cellular and humoral immune response that specifically targets the tumor.

Tumor cells are not being recognized as “foreign” by the immune system, leading to an inadequate immune response. Therefore, targeting antigens that are overexpressed by the tumor by vaccination might result in autoimmunity as well as a quick reduction of expression by the tumor as a result of selection pressure. Because of this, previous approaches to vaccinate against a tumor by a single antigen have failed (299). The development of novel therapies takes advantage of a tumor cell characteristic that differentiates them from healthy tissue. During the development of cancer, tumor cells have a greater likelihood of undergoing mutations, and essential genes that control tumor growth are changed. As a consequence of these changes, neoepitopes, which are modifications of epitopes or proteins that are known to the immune system, are made. Since there is no tolerance or expression by cells other than tumors, they constitute a potential vector of attack. As a result, contemporary technologies assess each patient's mutatome in order to create tailored immunizations against newly developed neoepitopes or to combine several antigens associated with the tumor (300–302).

4.2 Manuscript IV: Platelet-Derived GARP Induces Peripheral Regulatory T Cells—Potential Impact on T Cell Suppression in Patients with Melanoma-Associated Thrombocytosis

Summary of own contributions

Conceptualization, A.T., K.J. and N.Z.; methodology, N.Z., F.K.K., S.Z., H.M.-R. and E.J.K.; validation, N.Z.; formal analysis, F.K.K., S.Z. and N.Z.; resources, A.T.; writing—original draft preparation, A.T. and N.Z.; writing—review and editing, K.J., F.K.K., C.L. and S.G.; supervision, A.T.; project administration, N.Z.; funding acquisition, A.T.

The author planned, designed and performed all *in vitro* experiments and the subsequent analysis. Analysis of patient cohort II was supported by Franziska K. Krebs. Furthermore, the author took lead in the preparation of the manuscript together with Prof. Dr. med. Andrea Tüttenberg.

Keywords: glioblastoma; GARP; tumor microenvironment; immunotherapy; regulatory T cells

Citation: ***Zimmer, N.****; Krebs, F.K.; Zimmer, S.; Mitzel-Rink, H.; Kumm, E.J.; Jurk, K.; Grabbe, S.; Loquai, C.; Tuettenberg, A. Platelet-Derived GARP Induces Peripheral Regulatory T Cells—Potential Impact on T Cell Suppression in Patients with Melanoma-Associated Thrombocytosis. Cancers 2020, 12, 3653. https://doi.org/10.3390/cancers12123653*

Received: 26 November 2020; Accepted: 3 December 2020; Published: 5 December 2020.

Zusammenfassung

Thrombozyten wurden kürzlich als wichtiger Bestandteil der angeborenen und adaptiven Immunität durch ihre Interaktion mit Immunzellen beschrieben. Die Informationen über die Interaktion wischen Thrombozyten und T-Zellen bei immunvermittelten Krankheiten sind jedoch nach wie vor begrenzt. *Glycoprotein A repetitions predominant* (GARP), das auf Thrombozyten und auf aktivierten regulatorischen T-Zellen (Treg) exprimiert wird, ist an der Regulierung der peripheren Immunantwort beteiligt, indem es die Bioverfügbarkeit des transformierenden Wachstumsfaktors (TGF-β) reguliert. Lösliches GARP (sGARP) weist sowohl in vitro als auch in vivo starke regulatorische und entzündungshemmende Fähigkeiten auf, was zur Induktion von peripheren Treg führt. Wir untersuchten die Auswirkung von aus Blutplättchen gewonnenem GARP auf die Differenzierung, den Phänotyp und die Funktion von T-Effektorzellen. $CD4^+CD25^-$ T-Zellen, die mit Blutplättchen kokultiviert wurden, exprimierten FoxP3, waren anergisch und stark suppressiv. Diese Wirkungen wurden durch die Verwendung eines blockierenden Anti-GARP-Antikörpers aufgehoben, was auf eine Abhängigkeit von GARP hinweist. Wichtig ist, dass Melanompatienten in verschiedenen Krankheitsstadien eine signifikante Hochregulierung von GARP auf der Thrombozytenoberfläche aufwiesen, was mit einem geringeren Ansprechen auf die Immuntherapie korreliert. Zusammenfassend zeigen unsere Daten, dass Thrombozyten periphere Treg über GARP induzieren. Diese Erkenntnisse könnten zu Krankheiten wie Krebs-assoziierten Thrombozytose beitragen, bei der eine schlechte Prognose und Metastasierung mit hohen zirkulierenden Thrombozyten verbunden sind.

Abstract

Platelets have been recently described as an important component of the innate and adaptive immunity through their interaction with immune cells. However, information on the platelet–T cell interaction in immune-mediated diseases remains limited. Glycoprotein A repetitions predominant (GARP) expressed on platelets and on activated regulatory T cells (Treg) is involved in the regulation of peripheral immune responses by modulating the bioavailability of transforming growth factor β (TGF-

β). Soluble GARP (sGARP) exhibits strong regulatory and anti-inflammatory capacities both in vitro and in vivo, leading to the induction of peripheral Treg. Herein, we investigated the effect of platelet-derived GARP on the differentiation, phenotype, and function of T effector cells. $CD4^+CD25^-$ T cells cocultured with platelets upregulated Foxp3, the master transcription factor for Treg, were anergic, and were strongly suppressive. These effects were reversed by using a blocking anti-GARP antibody, indicating a dependency on GARP. Importantly, melanoma patients in different stages of disease showed a significant upregulation of GARP on the platelet surface, correlating to a reduced responsiveness to immunotherapy. In conclusion, our data indicate that platelets induce peripheral Treg via GARP. These findings might contribute to diseases such as cancer-associated thrombocytosis, wherein poor prognosis and metastasis are associated with high counts of circulating platelets.

4.2.1. Introduction

This section has been shortened to avoid any major repetition of previous chapters. The complete, unedited version of this manuscript can be found in the appendix IV.

As described in 1.2.5.3, platelets exhibit important immunomodulatory functions, especially on T cells (303, 304). However, how platelets regulate T cell immunity is far from being completely understood. Given the fact that platelets express GARP on their surfaces and linking this to our previous work describing GARP as a key molecule in inducing peripheral tolerance, we hypothesized that platelets may be involved in the induction of peripheral tolerance and thus the promotion of malignancy and resistance to therapy by inhibiting host immunity. The present study investigated the effect of platelets on T effector cell function and clearly demonstrated that platelets led to the induction of Treg in a GARP-dependent manner. Melanoma patients showed significantly higher levels of GARP on the surface of platelets and an increase in platelet surface expression of the platelet activation marker CD62P (P-selectin). Late-stage melanoma patients with an overall increased frequency of platelets showed a decreased response rate to their applied immunotherapy.

Our data showed a possible contribution of platelets to the adaptive immunity, leading to a poor prognosis of cancer patients with cancer-associated thrombocytosis. Additionally, this opens up new possibilities to target platelets as a therapeutic option for the treatment of cancer.

4.2.2. Results

4.2.2.1. Expression of GARP on Platelets

GARP was initially described as being expressed on the surface of platelets (48). Therefore, GARP expression was analyzed on resting and pre-activated platelets in combination with the platelet activation marker CD62P. In accordance with the literature, we detected GARP expression on resting platelets. Nevertheless, platelet activation led to a significant increase in the frequency of $GARP^+$ platelets as well as the overall GARP expression (MFI) on platelets (Figure 4.2.1A). As we have demonstrated before, GARP can be shed from and found in the supernatants of either activated Treg or tumor cells, leading to the immunomodulation of T effector cells and macrophages (Figure 4.2.A1). We investigated whether this process is also true for platelets. Pre-activated platelets were isolated from peripheral blood of healthy donors (HD) and cultured in X-VIVO 15, as described in the method section. Supernatants (platelet-conditioned medium, PCM) were collected after 16 h of culture and analyzed in an ELISA for GARP content. In all samples, analyzed GARP was detectable when compared to the medium control (X-VIVO-15) (Figure 4.2.1B). Importantly, no cellular contaminants (determined by microscopy and flow cytometry) were detectable.

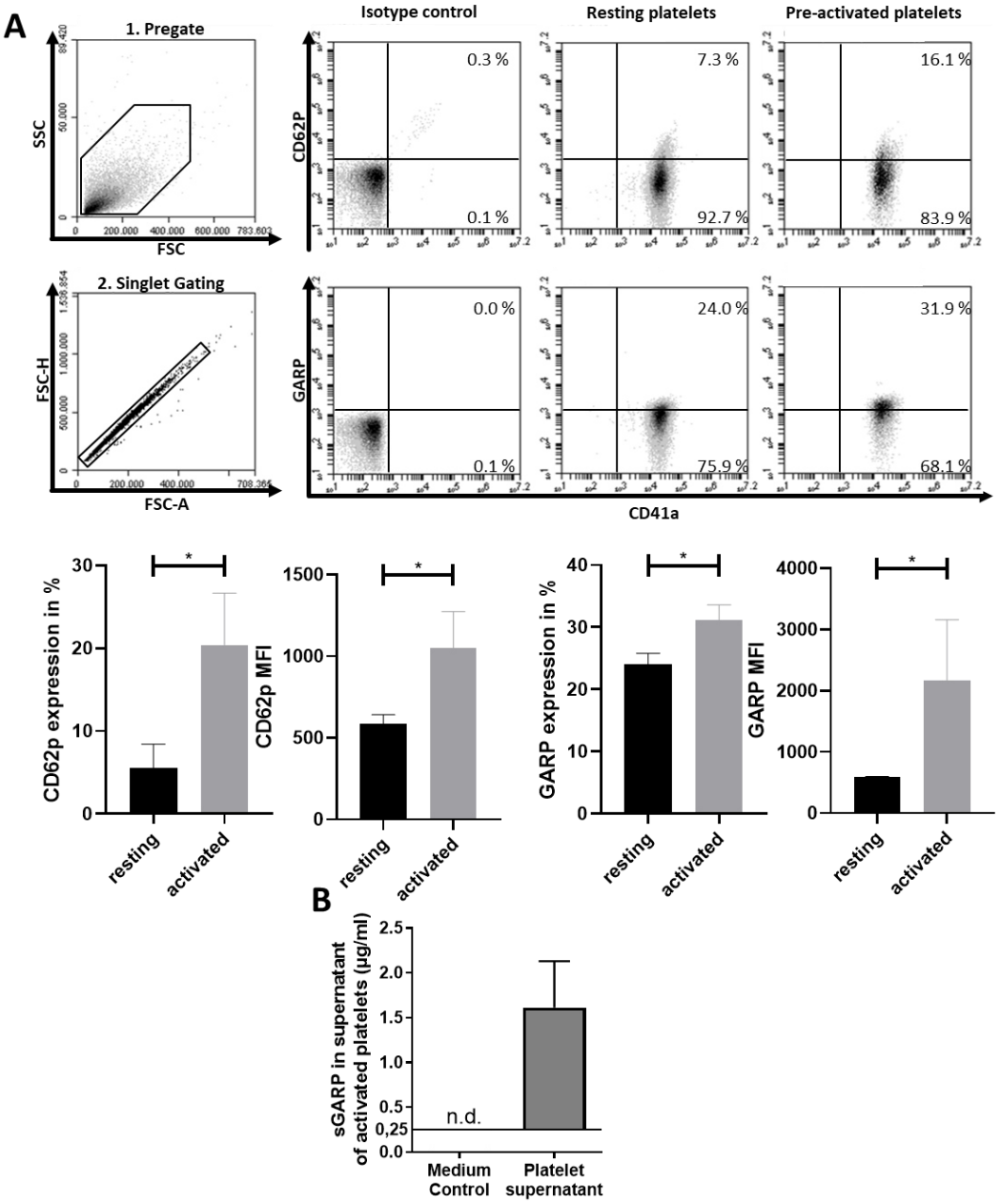

Figure 4.2.1. Glycoprotein A repetitions predominant (GARP) was expressed on the surface of platelets and was detectable in the supernatant of activated platelets. (**A**) Flow cytometric analysis of CD62P and GARP expression levels in resting and pre-activated platelets. Only singlets were used in the analysis. Isotype controls are shown. Bar diagrams of CD62P and GARP expression show pooled data of percentages (%) of positive cells and raw means (n = 3, means ± SD * $p < 0.05$, ** $p \leq 0.01$, *** $p \leq 0.001$, and n.s. determined by Student's t-test). (**B**) Presence of soluble GARP (sGARP) in the supernatant of pre-activated platelets. sGARP content of the supernatant of 2×10^9 activated platelets after 16 h compared to a negative medium control (n.d. = not detected). sGARP levels were determined by ELISA from three different healthy donors (HD).

4.2.2.2. Platelet-Derived GARP Induced Peripheral Regulatory T cells

We next investigated the effect of platelet-derived GARP on peripheral blood $CD4^+CD25^-$ T cells. $CD4^+CD25^-$ T effector cells (Teff) and platelets were cocultured in different ratios, ranging from 1:15, 1:30, 1:50 to 1:100 Teff/platelets. With increasing platelet numbers, we detected a significant increase in Foxp3 and GARP expression on Teff (Figure 4.2.2A), whereas proliferation and effector cytokine

production of Interleukin 2 (IL-2) and Interferon γ (IFN-γ) decreased (Figure 4.2.2B). To exclude the fact that the displayed GARP upregulation on Teff was due to contaminating adhering platelets on the Teff surface, we performed flow cytometry using a co-staining with anti-CD4 (Teff) and anti-CD41a (platelets) Abs. Within the first 24 h of coculture, about 25% of $CD4^+$ T cells were also positive for the platelet marker CD41a, indicating adherence of platelets on the surface of Teff. This percentage significantly decreased within 6 days ($CD4^+CD41a^+$ 4.8%), as demonstrated by flow cytometry (Figure 4.2.A2), showing that only a minor fraction of cells were $CD4^+CD41a^+$ double-positive. Notably, GARP expression on T cells increased over time. Because platelet effects on $CD4^+CD25^-$ T cells were most prominent at a ratio of 1:50, we used this ratio in the following experiments.

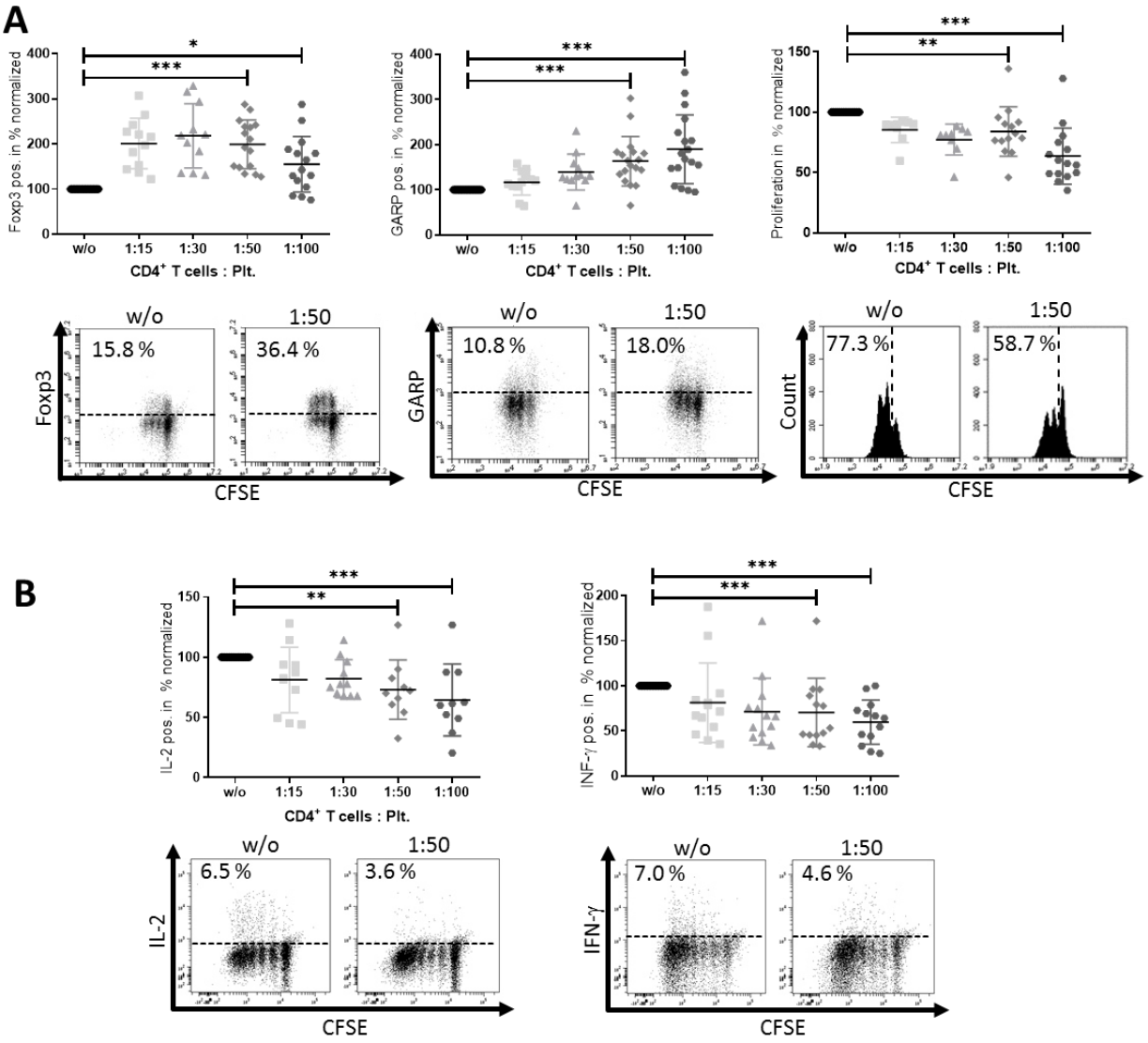

Figure 4.2.2. Platelets induce peripheral regulatory T cells (iTreg). (**A**) $CD4^+$ $CD25^-$ T cells and platelets were cocultured as indicated. Herein, carboxyfluorescein succinimidyl ester (CFSE)-labeled $CD4^+CD25^-$ T cells were stimulated with 0.5 µg/mL anti-CD3 mAb and 1.0 µg/mL anti-CD28 mAb with or without different ratios of platelets. The expression of Foxp3, GARP and the proliferation of cells were analyzed via flow cytometry on day 3 after stimulation. (**B**) Effector cytokine production of Interferon (IFN)-γ and interleukin (IL)-2 was analyzed using intracellular flow cytometry on day 6. Only live $CD4^+CD25^-$ T cells were included into the analysis. Representative dot plots of 12 independent experiments are shown. The graphs show cells cultured in the presence of platelets normalized to $CD4^+CD25^-$ T cells without platelets (expression levels were normalized to 100) (n = 12, means ± SD, * $p < 0.05$, ** $p \leq 0.01$, *** $p \leq 0.001$, and n.s. determined by Kruskal–Wallis test).

Having thus far used a non-canonical activation method, we next wanted to investigate a canonical, agonist-induced platelet activation, e.g., by thrombin being clinically more relevant. Therefore, we added 10 U/mL thrombin to the coculture. In comparison to the coculture without thrombin, this led to similar results, with increased Foxp3 and GARP expression and decreased cytokine production. Nevertheless, as described by Metelli et al. (73), thrombin leads to the cleavage of GARP on thrombocytes, which might partially explain the slightly reduced significances in the thrombin treated versus the 1:50 coculture control group (Figure 4.2.A4). Therefore, we used TRAP-6, an additional canonical platelet activator, in our coculture. Here, we could again see similar results without any significant difference between TRAP-6-activated platelets (canonical activation) and the 1:50 coculture control group (non-canonical activation, Figure 4.2.A5).

In sum, platelet-cocultured Teff displayed typical characteristics of induced peripheral Treg (iTreg), namely, reduced proliferation and effector cytokine production and increased Foxp3 expression.

To analyze whether these phenotypically altered anergic T cells resembling iTreg also had a suppressive function, we used them in a conventional suppressor assay. In detail, $CD4^+Foxp3^+$ iTreg (T cells pre-cultured with platelets for 6 days at the ratio 1:50) were harvested, washed, and then cultured together with untreated Teff (Figure 4.2.A3) to investigate their suppressive function. Herein, platelet-induced Treg showed a significant suppressive capacity (Figure 4.2.3), as demonstrated by the reduced proliferation of T cells by Ki-67 staining in the suppression assay. Herein, decreasing numbers of platelet-induced Treg in the culture led to an increased proliferation of T cells, showing a dose-dependent suppression by the iTreg.

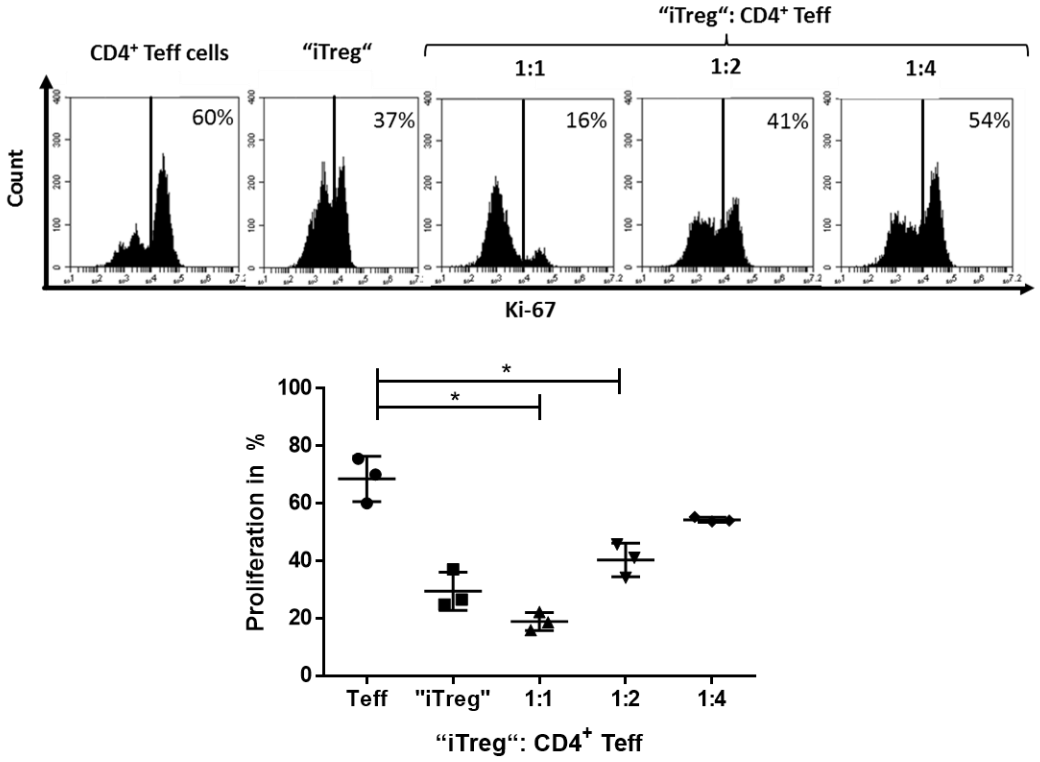

Figure 4.2.3. Platelet-induced iTreg suppressed T effector cells (Teff) cells. To analyze iTreg induction by platelets, we expanded $CD4^+CD25^-$ T cells for 6 days in the presence of platelets at the ratio of 1:50, as described previously, and were subsequently incubated at various ratios with 0.5×10^5 $CD4^+CD25^-$ T cells and restimulated with 1×10^5 irradiated peripheral blood mononuclear cells (PBMC) and 0.5 µg/mL anti-CD3 mAb. Proliferation was determined on day 3 of culture by Ki-67 staining ($n = 3$, means ± SD, * $p < 0.05$, ** $p \leq 0.01$, *** $p \leq 0.001$, and n.s. determined by one-way ANOVA).

In order to determine whether the induction of iTreg is GARP-dependent, we added 10 µg/mL of a blocking anti-GARP Ab to the cocultures and again analyzed Foxp3 and GARP expression, proliferation, (Figure 4.2.4A) and cytokine production (Figure 4.2.4B). As demonstrated, addition of the blocking Ab led to a significant normalization of Foxp3 expression and restored the production of the effector cytokine IFN-γ to a normal level, indicating an induction of iTreg that was at least in part GARP-dependent.

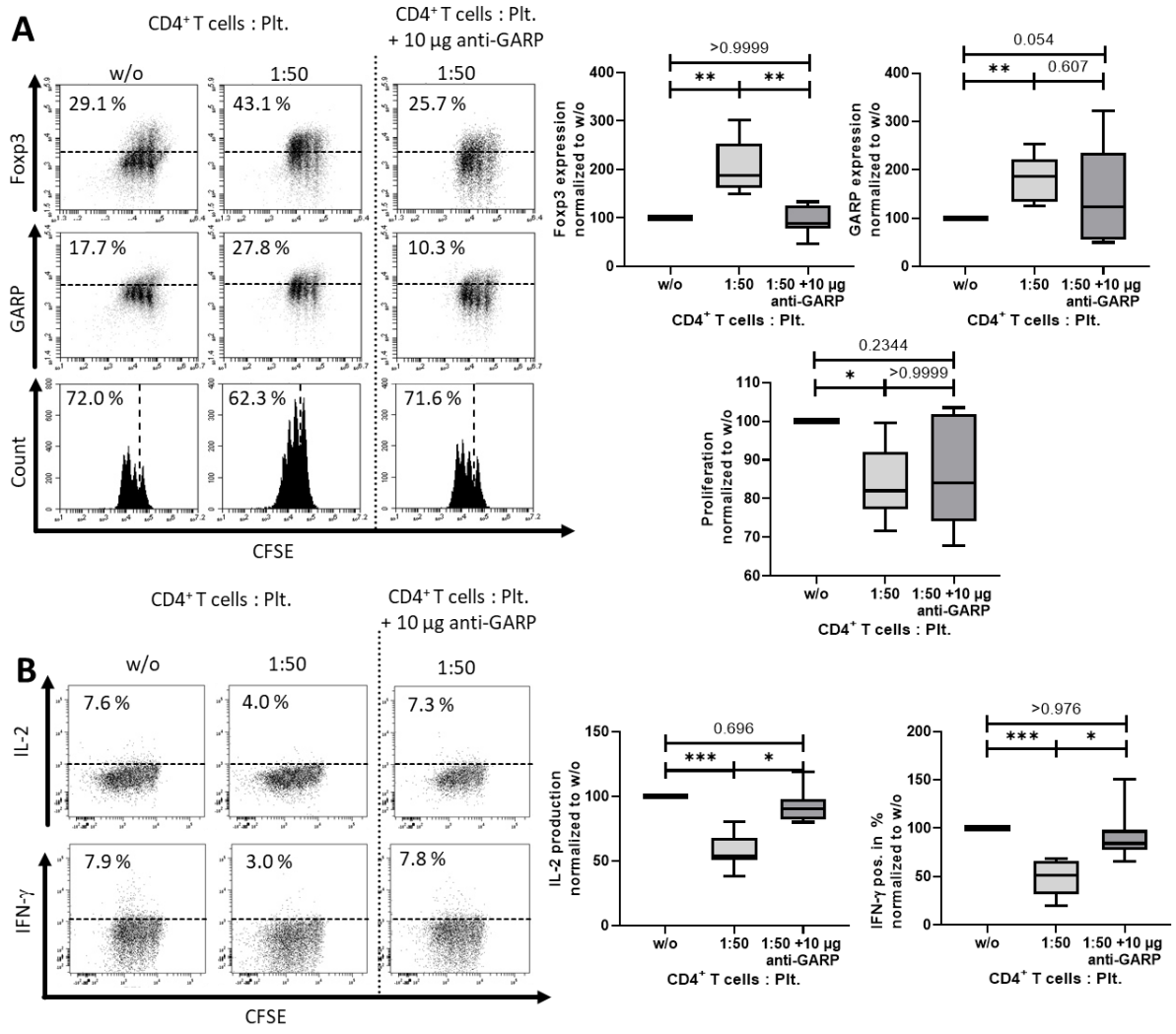

Figure 4.2.4. Platelets induced iTreg in a mainly GARP-dependent manner. (**A**) Blocking anti-GARP antibody inhibited platelet-induced effects on Foxp3 and GARP expression, as well as proliferation. CFSE-labeled $CD4^+CD25^-$ T cells were stimulated with 0.5 µg/mL anti-CD3 mAb and 1.0 µg/mL CD28 mAb with different ratios of platelets. In coculture, 10 µg/mL blocking anti-GARP Ab was added at day 0, as indicated. Foxp3 and GARP expression and proliferation is shown on day 3 after stimulation. (**B**) Cytokine production is shown on day 6. The graphs show cells cultured in the presence of platelets normalized to $CD4^+CD25^-$ T cells without platelets. For analysis, only live cells were included. Representative dot plots of eight independent experiments are shown (n = 9, box and whiskers, medians ± min/max, * $p < 0.05$, ** $p \leq 0.01$, *** $p \leq 0.001$, and n.s. determined by one-way ANOVA).

4.2.2.3. Role of TGF-β and Platelet-Conditioned Medium in Platelet-Mediated iTreg Induction

GARP is known to be a surface docking receptor for TGF-β, and plays a dominant role in its activation and release. Thus, we next assessed the impact of TGF-β in the regulatory activity of platelet-derived GARP. Herein, the blockade of TGF-β signaling with blocking antibodies against TGF-β I-III showed a partial inhibition of the modulatory effects of platelet-derived GARP on Foxp3 regulation (Figure 4.2.5A) and IL-2 (Figure 4.2.5B) production, whereas proliferation and IFN-γ production was not affected. Using a blocking antibody against TGF-β receptor II (TGF-β RII), we had similar results, as Foxp3 and GARP were upregulated, whereas the production of IFN-γ and IL-2 were only partially inhibited. Only proliferation was strongly affected by the TGF-β RII blocking antibody, which was consequently restored to a normal level.

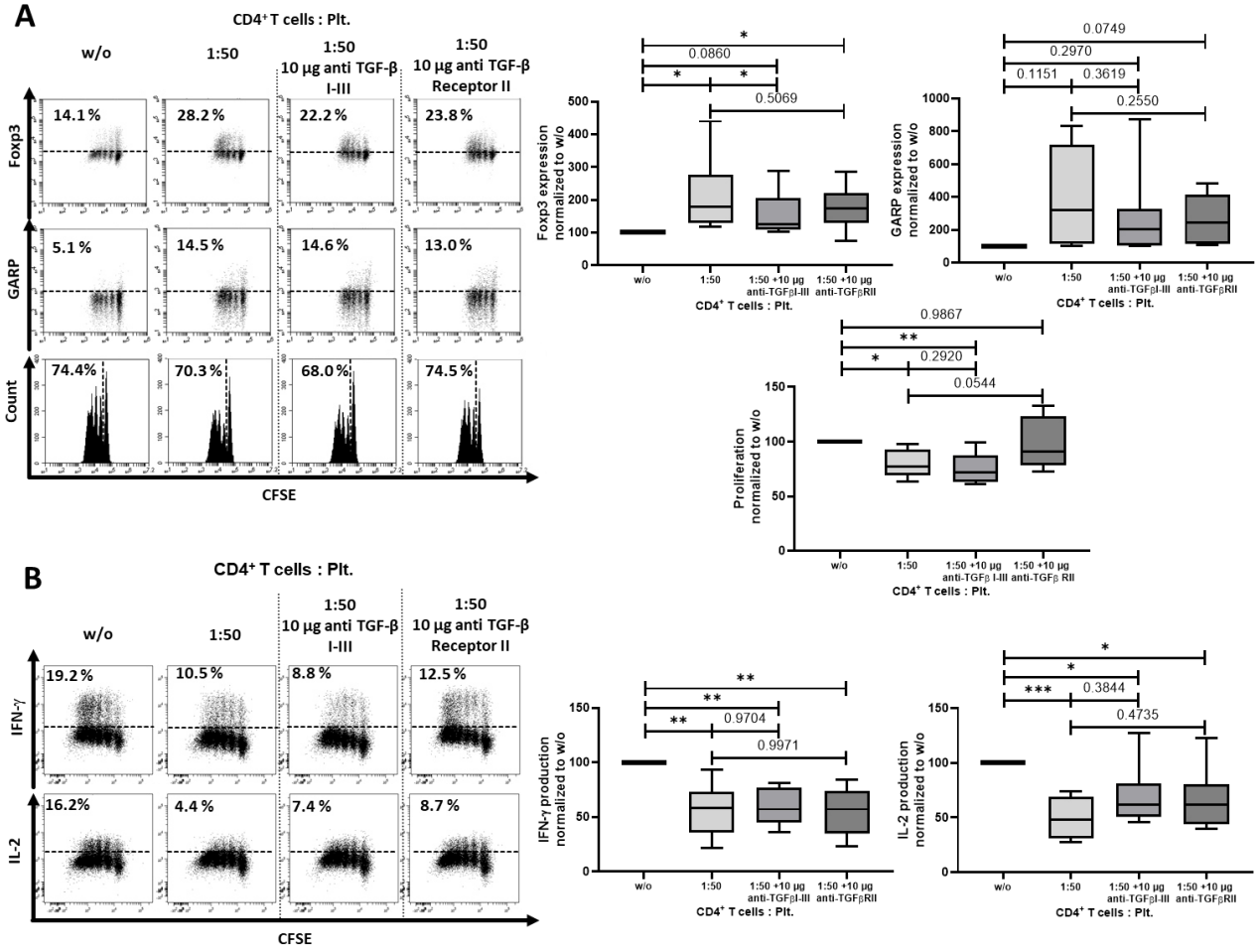

Figure 4.2.5. Blockade of transforming growth factor (TGF)-β I-III did in part prevent regulatory T cells (Treg) induction. (**A**) CFSE-labeled $CD4^+CD25^-$ T cells were cocultured with platelets in the ratio of 1:50 and were stimulated with anti-CD3 mAb (0.5 µg/mL) and anti-CD28 mAb (1.0 µg/mL) in the presence of either anti-TGF-β I-III (10 µg/mL) or anti-TGF-β receptor II (10 µg/mL) antibodies. Antibodies were added at day 0. The expression of Foxp3 and GARP and cell proliferation were determined on day 3 via flow cytometry. (**B**) Production of IL-2 and IFN-γ was assessed by intracellular flow cytometry on day 6. The graphs show cells cultured in the presence of platelets normalized to $CD4^+CD25^-$ T cells without platelets. Dot plots show one representative result of 10 independent experiments (n = 10, box and whiskers, medians ± min/max, * $p < 0.05$, ** $p \leq 0.01$, *** $p \leq 0.001$, and n.s. determined by one-way ANOVA).

To gain more insight into the relationship between TGF-β and GARP, we performed an additional experiment where the TGF-β receptor II was blocked on $CD4^+CD25^-$ T cells before coculture. The subsequent addition of either anti-TGF-β I-III Ab, anti-GARP Ab, or both only led to a complete inhibition of platelet effects in the samples with an anti-GARP Ab present. The combination of anti-TGF-β RII Ab, anti-TGF-β I-III Ab, and anti-GARP Ab showed the strongest effects on Foxp3, IL-2, and IFN-γ production, which were brought back to untreated levels. Anti-TGF-β RII Ab combined with anti-GARP Ab had the second strongest effect, followed by anti-TGF-β I-III Ab combined anti-GARP Ab and the use of only the anti-GARP Ab itself. The blockade of TGF-β alone by a combination of anti-TGF-β RII and anti-TGF-β I-III was not sufficient to inhibit platelet effects on T cells (Figure 4.2.6A,B).

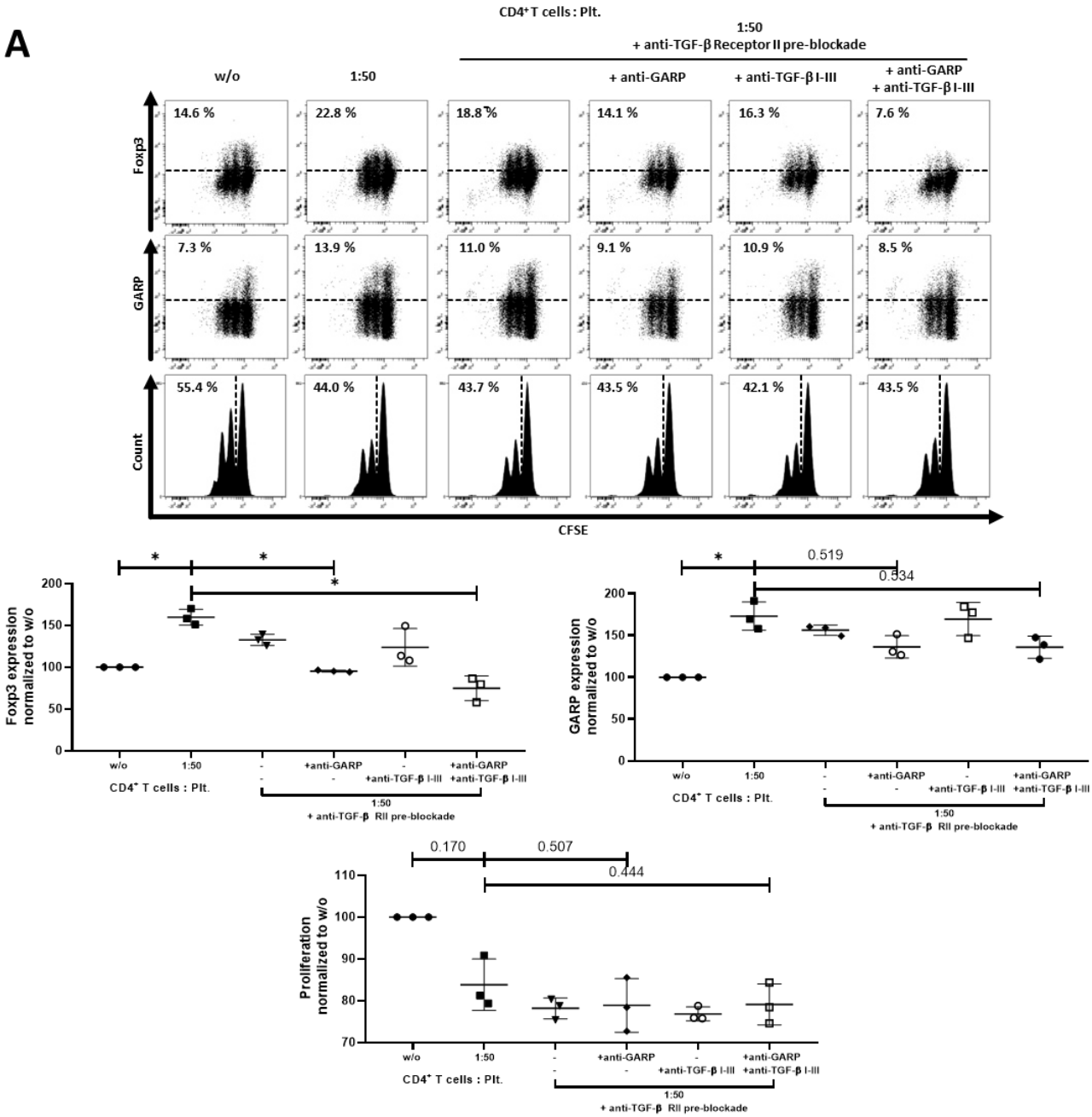

Figure 4.2.6. *Continued on the next page.*

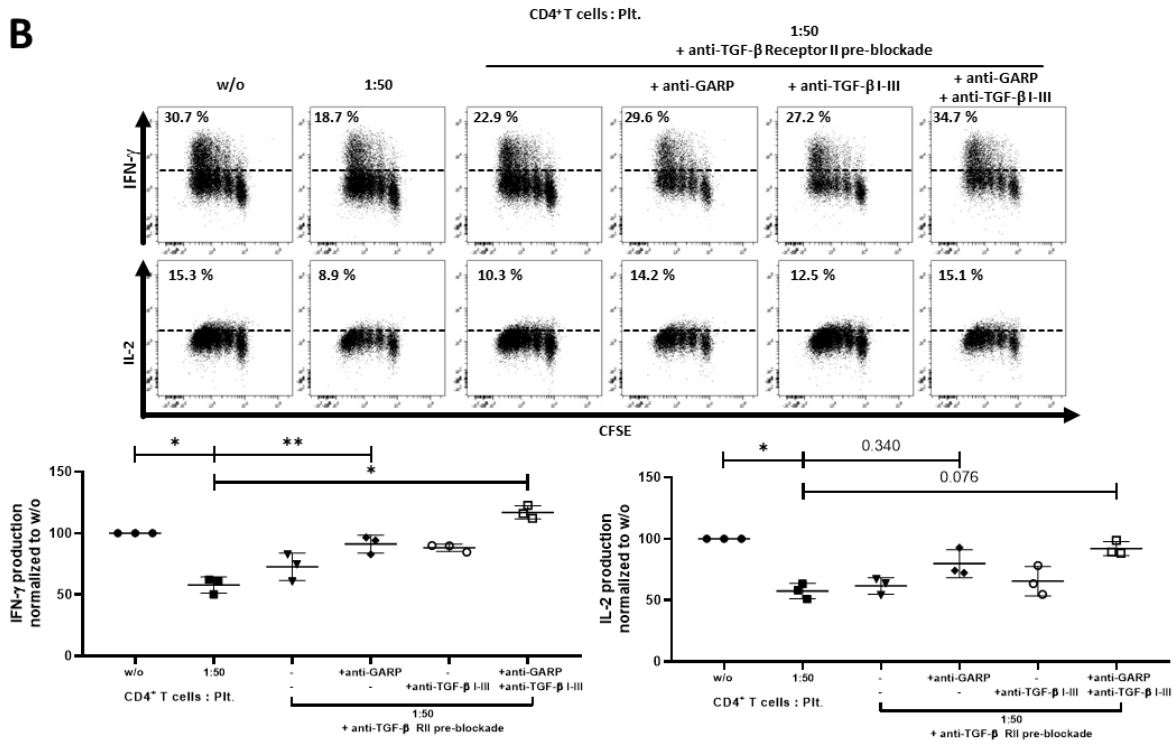

Figure 4.2.6. Combining blockade of TGF-β signaling and GARP led to a complete inhibition of platelet effects**.** (**A**) CFSE-labeled $CD4^+CD25^-$ T cells were cocultured with platelets in the ratio of 1:50 and were stimulated with anti-CD3 mAb (0.5 µg/mL) and anti-CD28 mAb (1.0 µg/mL). $CD4^+CD25^-$ T cells were incubated for 15 min with TGF-β receptor II (10 µg/mL) antibody prior to coculture, as indicated. Excess antibody was removed. Pre-treated $CD4^+CD25^-$ T cells were cultured in the presence of either anti-TGF-β I–III (10 µg/mL) and/or anti-GARP Ab (10 µg/mL) antibodies. Antibodies were added at day 0. The expression of Foxp3, GARP and cell proliferation were determined on day 3 via flow cytometry. (**B**) Production of IL-2 and IFN-γ was assessed by intracellular flow cytometry on day 6. The graphs show cells cultured in the presence of platelets normalized to $CD4^+CD25^-$ T cells without platelets. Dot plots show 1 representative result of 10 independent experiments (n = 3, means ± SD, * $p < 0.05$, ** $p \leq 0.01$, *** $p \leq 0.001$, and n.s. determined by one-way ANOVA).

These results demonstrate that the T cell modulating impact of platelet-derived GARP is in part but not completely associated with TGF-β signaling.

As shown in Figure 4.2.1B, soluble GARP (sGARP) was detected in PCM. To further assess the effects of PCM on the differentiation process of T cells, we cultured T cells with PCM. Addition of PCM to T cells resulted in a tendency of an upregulation of Foxp3, an inhibition of proliferation (Figure 4.2.7A), and a significantly lower production of the effector cytokine IFN-γ (Figure 4.2.7B). The addition of the blocking anti-GARP Ab lead to a normalization of the Foxp3 expression level and the IFN-γ and IL-2 production, whereas proliferation and GARP expression did not normalize.

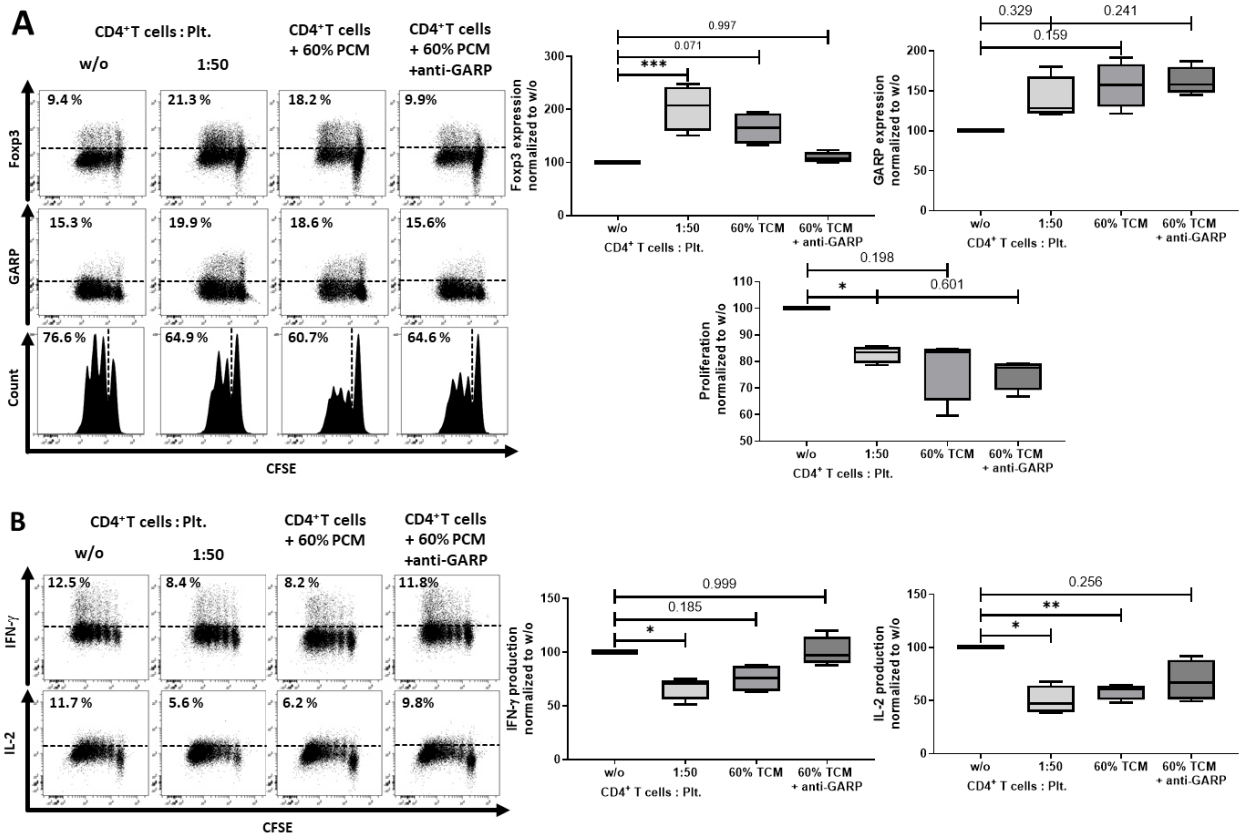

Figure 4.2.7. Platelet-conditioned medium (PCM) inhibited IFN-γ production but failed to induce a Treg phenotype. (**A**) $CD4^+CD25^-$ T cells were cultured in X-Vivo 15 (Lonza, Basel, Switzerland) with 60% PCM content, with or without 10 µg/mL anti-GARP Ab and stimulated with 0.5 µg/mL anti-CD3 mAb and 1.0 µg/mL anti-CD28 mAb. Antibodies were added at day 0. The expression of Foxp3, GARP and cell proliferation were determined at day 3 with flow cytometry. (**B**) Cytokine production of IL-2 and IFN-γ was measured by intracellular flow cytometry on day 6. Dot plots show one representative result of five independent experiments (n = 5, box and whiskers, medians ± min/max, * $p < 0.05$, ** $p \leq 0.01$, *** $p \leq 0.001$, and n.s. determined by one-way ANOVA).

4.2.2.4. Correlation of Thrombocytosis and Prognosis—Clinical Impact of Platelets Expressing Increased Levels of GARP

By analyzing GARP expression on platelets from patients out of our first, initial cohort (n = 35) in both early and late-stage melanoma patients, we could detect increased GARP levels in comparison with HD controls. Nevertheless, GARP expression slightly differed between early stage I and late stage IV melanoma patients (Figure 4.2.8A). Additionally, platelets of stage I melanoma patients showed a stronger activation status compared to HD controls.

Several studies in different tumor entities indicate that cancer patients with thrombocytosis have poor prognoses (305). In order to interpret these findings in the context of our own results, we analyzed a second, retrospective cohort of stage IV melanoma patients (n = 36) for their platelet counts and platelet–lymphocyte ratios (PLR) and correlated them to progression versus stable disease during therapy with checkpoint inhibitors (Figure 4.2.8B). Herein, non-responders to therapy with progressive disease showed significantly higher PLR and platelet counts than patients with stable disease, which responded to immunotherapeutic approaches.

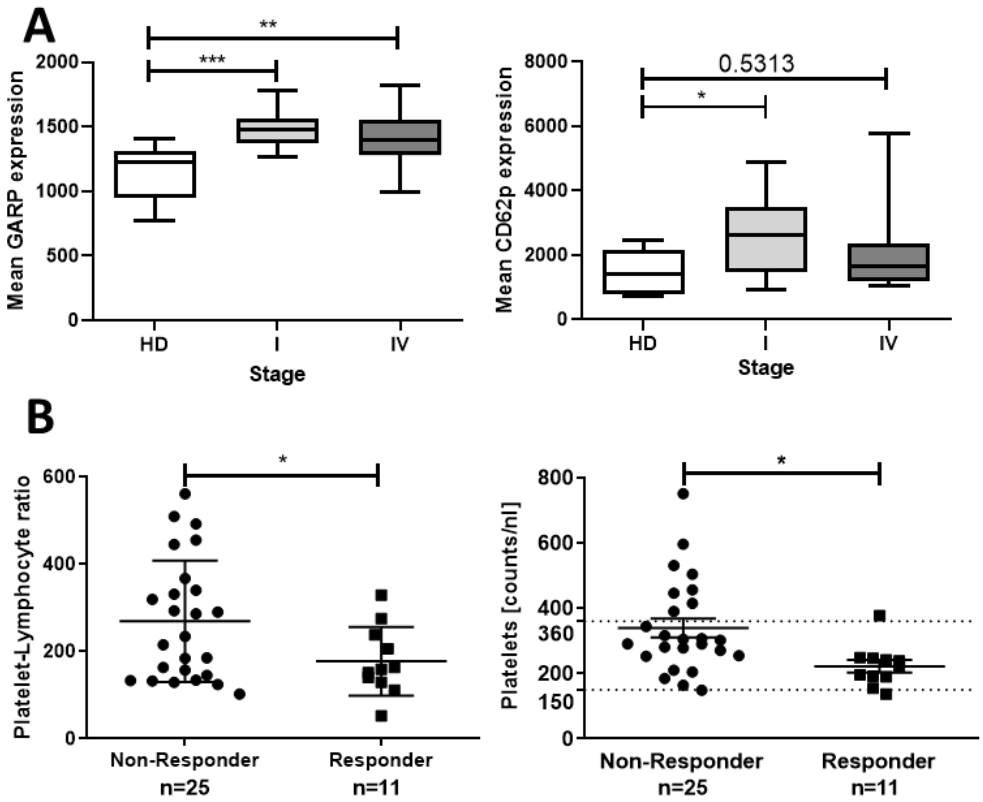

Figure 4.2.8. Increased platelet surface GARP levels in stage I/IV melanoma patient stage**.** (**A**) Comparison of platelet GARP and CD62P surface levels between HD (*n* = 8), stage I (*n* = 18), and stage IV (*n* = 17) melanoma patients assessed via flow cytometry. Means for GARP expression for HD = 1161, stage I = 1489, and stage IV = 1418. Means for CD62P expression are HD = 1470, stage I = 2611, and stage IV = 1977 (box and whiskers, medians ± min/max, * $p < 0.05$, ** $p < .01$, *** $p < .001$, and n.s. determined by unpaired *t*-test). (**B**) The platelet count in melanoma patients before starting immunotherapy using checkpoint inhibitors was measured as part of the routine blood tests. Platelet counts and the platelet–lymphocyte ratios of non-responders (*n* = 25) and responders (*n* = 11; staging results after 6 months of therapy) were compared. Means of platelet counts (PC) and the platelet–lymphocyte ratio (PLR) were as follows: progression: PC = 339.8, PLR = 269.0; stable disease: PC = 222.3, PLR = 177.5 (means ± SD, * $p < 0.05$, ** $p \leq 0.01$, *** $p \leq 0.001$, and n.s. determined by unpaired *t*-test).

4.2.3. Discussion

There has been an emerging role of platelets in the immunomodulation of cancer patients. Recent studies have indicated that platelets are present in the tumor microenvironment, and cancer-associated thrombocytosis has been linked to the promotion of metastasis, invasiveness, and tumor development and thus to poor clinical outcome in different tumor entities (87, 306). Tumors constantly activate the coagulation pathways, resulting in the generation of thrombin and consequently chronic platelet activation. Correlations between high platelet counts and shorter disease-specific survival are described for several tumor entities including lung, colon, breast, pancreatic, kidney, and gynecologic cancers. Platelets promote motility (90–92) and epithelial–mesenchymal cell transition, and readily bind to the surface of melanoma cells, thus protecting them from immunological clearance and/or chemotherapy-induced apoptosis (93).

The present study demonstrates a new and important role of platelets in mediating Teff inhibition by induction of Treg via a GARP-dependent mechanism. In agreement with the literature (99), GARP was found to be expressed on platelets to a certain extent and increased upon platelet activation, with a

significant amount of GARP detected in the supernatants of activated platelets. This finding is of special interest for its implications on the tumor microenvironment as it is described that tumor cells lead to the chronic activation of platelets (307). Coculture of platelets and Teff cells but also culture of Teff in the presence of PCM induced cells with a regulatory phenotype. This included upregulation of the Treg master regulator Foxp3, reduced proliferation, and decreased effector cytokine production, as well as induction of suppressive capacity. Our study did not exclude other platelet-derived factors that could mediate the described effects. Nevertheless, blocking experiments showed that a significant part of the immunomodulatory effects of platelets or PCM can be contributed to their GARP expression. The platelet numbers chosen for our coculture experiments resulted in a lower platelet/Teff-ratio (50:1) than usually present in peripheral blood (approximately 500:1). Despite this, GARP effects were already detectable at these lower platelet numbers, with no changes at higher-tested ratios (i.e., 100:1). Limitations in cell culture prevented detailed analysis of more physiological ratios at 500:1. In addition, the TGF-β signaling axis seemed to be at least in part associated to the investigated GARP effect in inducing iTreg, thus contributing to a rather inhibitory tumor micromilieu. In former studies, our group demonstrated that sGARP induced Treg through TGF-β receptor II (Figure 4.2.A1) (74). This is in agreement with recent studies. A deletion of GARP on platelets of mice showed a blunted TGF-β activity, which improved the $CD4^+$ and $CD8^+$ T cell immune response at the site of the tumor (308). As described above, we could show that the observed effect by Rachidi et al. is not only TGF-β -dependent but also GARP dependent. The complete blockade of TGF-β signaling in combination with the blockade of GARP led to almost complete inhibition of platelet effects. This effect could not be achieved by the combination of anti-TGF-β I-III and anti-TGF-β receptor II alone, indicating that GARP plays an important role in the induction of Treg by platelets, which is in part independent of TGF-β signaling. This was supported by further studies, as deletion of GARP in mice led to an increase in $CD4^+$ and $CD8^+$ T cell anti-tumor activity. Another study analyzed the role of GARP in hemostasis and thrombosis. Herein, it was demonstrated that GARP-deficient mouse platelets showed normal activation responses in vitro. Moreover, megakaryocyte/platelet-specific GARP knock-out in mice did not affect the tail bleeding time or the occlusion time in the carotid and mesenteric arteries after FeCl3-induced thrombus formation, indicating no essential role of GARP in hemostasis and thrombosis (99).

Interestingly, the melanoma patients of the first cohort, independent of their tumor stage, expressed higher amounts of GARP on their platelets as well as exhibited higher platelet activation statuses. As described earlier, GARP is associated with inhibitory effects on immune cells in the tumor microenvironment. One could reasonably speculate then that GARP expression on platelets may differ between stage IV patients with poorer prognoses and stage I patients, as a further increase in GARP expression in stage IV patients could be expected. Nevertheless, a closer look into Figure 4.2.8b shows that there was a detectable minor shift of GARP expression levels from stage IV patients in comparison to stage I patients in the direction of HD GARP levels. This was supported by a decrease in significance of stage IV patients (*p*-value HD-stage I: 0.0005 ***) compared to stage I patients (*p*-value HD-stage IV: 0.0068 **). Whether this was due to response to immunotherapy (16 out of 17 patients of stage IV in our rather small first cohort were responders) must be analyzed in future studies with representative control groups. In several studies, including different tumor entities, such as ovarian, GB, head and neck, colorectal, and non-small cell lung cancer, it has been described that patients with thrombocytosis often have an advanced tumor stage, a higher tumor grade, and lower progression-free and median overall survival, and thus have a poorer prognosis. Collectively, this indicates thrombocytosis as an adverse prognostic factor in various tumor entities (309–314). Our study (second cohort) is in agreement with these previous studies as it shows that reduced response to immunotherapy correlated to higher platelet counts/PLR.

Platelets may promote carcinogenesis in several ways. First, circulating tumor cells may use platelets as protective barriers in a complex system of evasion from the attack of immune cells, as well as

possibly as mediators for attachment to endothelial cells when initiating extravasation at metastatic sites (315). Furthermore, platelets have a role in the prevention of hemorrhage in newly formed tumor vasculature, which is structurally abnormal and lacks the stability of local resident vasculature (316). Several cytokines and growth factors contained in the alpha granules of platelets, such as vascular endothelial growth factor (VEGF), epidermal growth factor (EGF), platelet-derived growth factor (PDGF), transforming growth factor β (TGF-β), interleukin 1β (IL-1β), IL-8, and CXC motif containing ligand 12 (CXCL12) may play diverse roles in the tumor micro-environment, including the promotion of invasion and metastasis through a positive regulation of the epithelial–mesenchymal transition (EMT) process and immune evasion (317–319).

The present study provides new insights into how platelets could promote tumor progression through the induction of Treg via GARP. A recent study by Metelli et al. (2020) showed that thrombin contributes to cancer immune evasion by proteolysis/cleavage of GARP and subsequent liberation of TGF-β. The authors proposed that blockade of GARP cleavage is a valuable therapeutic strategy to overcome resistance to immunotherapy. This paper supports our data, wherein we showed that GARP plays an important role in the inhibitory tumor microenvironment (73).

Nevertheless, we postulate that not only the soluble (cleaved) form of GARP but also the membrane-bound and thus contact-dependent GARP can mediate suppressive effects through induction of iTreg. In our study, addition of thrombin to the platelet–Teff coculture and thus potential GARP cleavage even slightly reduced the capacity of Treg induction by platelets. One possible explanation for this would be that thrombin-cleaved GARP is impaired in function and has decreased immunosuppressive capacity. Another explanation, which is supported by the weaker effect of PCM compared to platelet–Teff cocultures, could be that sGARP is less potent at inducing Treg in contrast to surface-expressed GARP. Using TRAP-6 as a platelet activator in this context did not lead to the possible cleavage of GARP from the surface of platelets, and therefore it had no impact on platelet effects on $CD4^+CD25^-$ T cells. Whether this effect can be attributed to a truncated form of GARP after thrombin cleavage or that sGARP has a decreased immunomodulatory capacity must be further investigated. In our hands, it was shown for the first time that this effect on tolerance induction via GARP could be due to the induction of T cells with a regulatory phenotype. This is of great importance as Treg play a major role in the suppression of anti-tumor immunity.

Platelets are the second most abundant cell type in peripheral blood and thus are easy to isolate, count, and analyze. Furthermore, they contain large amounts of TGF-β and are positive for GARP, which contributes to a large extent towards immune inhibition, as described in our work. Therefore, the analysis of platelets, including their frequency and GARP expression levels, could serve as predictive or prognostic biomarkers in relation to potential for immune evasion and reduced responses to immunotherapies and thus to poor prognosis. Certainly, this has to be verified in a future larger study. Another important implication that arises from our data is the concept of implementing platelet-modulating therapies within oncology and investing new therapeutic strategies that target platelets and/or GARP. For instance, this could be achieved with GARP-specific antibodies targeting different immune as well as tumor cells and platelets within the tumor microenvironment.

In conclusion, our study describes for the first time in the human system the mechanism of GARP-dependent, platelet-mediated T cell suppression. Our study linked platelets to immune inhibition and explained, at least in part, why cancer patients with cancer-associated thrombocytosis have poor prognoses. This makes platelets an additional attractive target in combinatorial cancer immunotherapy treatments, mainly through the development of new (antibody-based) anti-GARP therapeutic approaches. This strategy would not only target platelets but also activated Treg and $GARP^+$ tumor cells, leading to the modulation of the inhibitory tumor microenvironment with the overall aim to overcome cancer's resistance to immunotherapy through this combinatorial approach.

4.2.4. Materials and Methods

4.2.4.1. Isolation of Pre-Activated and Resting Platelets and Preparation of Platelet-Conditioned Medium

Pre-activated platelets: Blood bags were obtained from healthy donors (HD), with approval of the local ethical committee (Landesaerztekammer Rheinland-Pfalz, No.837.019.10 (7028)). Blood bags were transferred to conical tubes (Greiner bio-one, Kremsmünster, Austria #227261) and subsequently centrifuged for 15 min at 160 × *g* at room temperature (RT). The resulting platelet-rich plasma (PRP) supernatant was collected and centrifuged for another 15 min at 200 × *g* at RT in order to deplete potential leukocyte contamination. Next, the PRP supernatant was washed with 1× Phosphate-buffered saline (PBS) at a ratio of 1:1 and centrifuged for 5 min at 2000 × *g* at RT. The resulting pellet containing platelets was resuspended, and platelets were counted and added in different ratios to the coculture experiments. These platelets had a higher CD62P expression as measured in flow cytometry compared to "resting platelets" (see below) and were therefore referred to as "pre-activated platelets". Platelet-conditioned medium (PCM) was prepared by culturing 2×10^9 pre-activated platelets for 16 h in 2 mL of cell culture medium at RT (X-Vivo 15, Lonza, Basel Switzerland, #BE02-060F), and, as a control, were either activated with 10 U/mL thrombin or TRAP-6, as indicated. Subsequently, platelets were centrifuged at 2000 × *g* for 5 min at RT. The resulting supernatant was isolated and immediately used for analysis as well as for coculture experiments. The PCM was checked for cell residues by conventional microscopy and flow cytometry.

Resting platelets: In contrast, "resting platelets", which showed a lower CD62P expression as measured in flow cytometry, were isolated at RT by first generating PRP. Citrated blood was supplemented with 2 mM EGTA and centrifuged for 10 min at 200 × *g*. The resulting PRP was diluted with CGS buffer (120 mM NaCl, 12.9 mM trisodium citrate dihydrate, 30 mM d-glucose, pH 6.5) at a ratio of 1:1. For leukocyte depletion, the PRP was centrifuged for 10 min at 69 × *g*. The resulting supernatant was subsequent centrifuged for 10 min at 400 × *g*. The resulting pellet was resuspended in CGS buffer and again centrifuged for 10 min at 400 × *g*. The platelets were resuspended in 1× PBS for flow cytometry (320).

4.2.4.2. Isolation and Stimulation of Human T Cell Populations

$CD4^+CD25^-$ T cells were isolated from buffy coat, as previously described (321). The purity of the isolated $CD4^+CD25^-$T cells was around 98%, as checked by flow cytometry (Figure 4.2.A6). For proliferation assays, cells were labeled with carboxyfluorescein succinimidyl ester (CFSE) and cultured in 48 well plates at 10^6 cells/mL in X-Vivo 15 (Lonza, #BE02-060F, Basel, Switzerland). Percentage of proliferating cells was defined as cells with less CFSE signal than the initial signal strength of the unstimulated cells at the start of the assay. Cells were stimulated with 0.5 µg/mL anti-CD3 mAb (Clone OKT3) and 1 µg/mL anti-CD28 mAb (Clone 28.2, BD Pharmingen #555725, Heidelberg, Germany) in the presence or absence of different ratios of platelets and 10 µg/mL anti-GARP Ab (Origene AP17415PU-N, Rockland, MD, USA), 10 U/mL thrombin (Sigma-Aldrich #T7009-250UN, Munich, Germany), 10 µM TRAP-6 (H-Ser-Phe-Leu-Leu-Ag-Asn-OH trifluoroacetate salt (#4017752), Bachem Holding AG, Bubendorf, Switzerland), 10 µg/mL anti-TGF-β I-III (R&D Systems #MAB1835R), and anti-TGF-β receptor II (R&D Systems #AF-241-NA) at day 0, as indicated. For pre-blockade of TGF-β receptor II on $CD4^+CD25^-$ T cells, we incubated T cells with 10 µg/mL anti-TGF-β receptor II Ab for 15 min. The remaining unbound antibody was removed by washing cells with X-Vivo (Lonza, #BE02-060F, Basel, Switzerland)15 for 5 min at 400 × *g*, twice. Alternatively, T cells were cocultured with PCM at the ratio indicated and proliferation was analyzed as described. For suppression assays, platelet-conditioned T cells (iTreg) were isolated from culture after 6 days, washed, and cocultured in a new assay with $CD4^+$ T effector cells (Teff) for an additional 3 days at the ratio indicated. Cells were restimulated with 0.5 µg/mL anti-CD3 plus irradiated (90Gy) peripheral blood mononuclear cells PBMC. Proliferation was

measured by Ki-67 staining via flow cytometry. Positive Ki-67 resembles proliferating cells instead of Ki-67 low cells.

4.2.4.3. Enzyme-Linked Immunosorbent Assay

Soluble GARP was analyzed by enzyme-linked immunosorbent assay (ELISA), according to the manufacturer's protocol (R&D Systems #DY6055, Wiesbaden, Germany).

4.2.4.4. Flow Cytometry

For flow cytometric analysis, cells were stained with fixable viability dye (Thermo Fisher #65-0865-14, Dreieich, Germany) prior to the antibody surface staining of anti-CD4 (BD Pharmingen #555348, Heidelberg, Germany), anti-CD41a (eBioscience #11-0419-42, Dreieich, Germany), anti-CD62P (ImmunoTools #21270624, Friesoythe, Germany), and anti-GARP (Miltenyi #130-103-820, Bergisch Gladbach, Germany). For intranuclear staining of Foxp3 or intracellular staining of IFN-γ and IL-2, cells were fixed and permeabilized with the Foxp3/Transcription Factor Staining Buffer Kit (eBioscience #00-5523-00, Dreieich, Germany) and subsequently stained with anti-Foxp3 (BioLegend #320208, San Diego, USA), anti-IL-2 (eBioscience #17-7049-42, Dreieich, Germany), and anti- IFN-γ (BD Biosciences #557643, Heidelberg, Germany). After 6 days of culture, T cells were harvested and expression of the cytokines IL-2 and IFN-γ were analyzed in T cells stimulated with 50 ng/mL phorbol 12-myristate 13-acetate (PMA; Sigma Aldrich #P1585-1MG, Munich, Germany) and 1 µg/mL ionomycin (Enzo Life Sciences #ALX-450-006-M001, Lörrach, Germany) in the presence of monensin (1.3 µM) (BD,#554724, Heidelberg, Germany) for 5 h. Cells were then permeabilized as described above and stained. Only live cells were included into the analysis (Figure 4.2.A7). Flow cytometry was performed on an BD LSRII and BD Accuri C6 flow cytometer (BD Biosciences, Heidelberg, Germany) and analyzed using Cytobank software (Cytobank.org, Santa Clara, USA; (217) and the FACSVia Software (BD Biosciences, Heidelberg, Germany).

4.2.4.5. Patients

Patient samples were obtained from melanoma patients at different stages of disease after informed written consent. The study protocol (837.226.05 (4884)) was approved by the local ethics committee of Rhineland-Palatinate and Hessen (Landesärztekammer). All procedures in studies involving human participants were performed in accordance with the 1964 Declaration of Helsinki and its later amendments or comparable ethical standards. In the initial primary cohort, GARP expression on platelets and platelet activation status was measured from the blood of stage I (n = 18) and stage IV (n = 17) melanoma patients, of which 16 out of 17 patients responded to immunotherapy, by using flow cytometry. Therein, PRP was isolated as described, and platelets were stained for GARP and CD62P using flow cytometry. Next, platelet counts of the second retrospective cohort of stage IV melanoma patients undergoing checkpoint inhibitor treatment were analyzed in order to investigate platelet numbers, platelet–lymphocyte ratios, and therapy outcome in these patients (Table 4.2.1). Therefore, routine blood tests were performed during follow-up. Therapies included the checkpoint inhibitors ipilimumab (Yervoy, BMS, New York, USA), nivolumab (Opdivo, BMS, New York, USA), and pembrolizumab (Keytruda, MSD, Haar, Germany). Patients were divided into non-responders (progressive disease) and responders (complete response, partial response, or stable disease) according to Response Evaluation Criteria in Solid Tumors (RECIST) criteria in routine staging.

Table 4.2.1. Patient characteristics.

Cohort 1. Analysis of Platelet GARP and CD62p Expression Levels	**n**	**%**
Patients	35	100
Stage I	18	51
Stage IV (responders)	17 (16)	49
Cohort 2. Retrospective Analysis of Platelet Count and PLR	***n***	***%***
Patients	39	100
Responder	11	28
Non-responder	25	64
Unknown outcome, lost to follow-up	3	8

4.2.4.6. Statistics

Statistical analysis was performed using GraphPad Prism version 8.0.0 for Windows (GraphPad Software, San Diego, California, USA, www.graphpad.com). Results were normalized to the untreated (w/o) samples as indicated. Bar diagrams and scatter plots display mean ± standard deviation (SD). Box and whiskers plots display median with the 25th and 75th percentiles and minimum to maximum whiskers. Statistical significance was determined using one-way ANOVA, Kruskal–Wallis test, and unpaired Student's *t*-test, as indicated in the figure legends with * $p < 0.05$, ** $p \leq 0.01$, *** $p \leq 0.001$, and not significant. Not significant is indicated by *p*-values > 0.05.

4.2.5. Conclusions

Our data show, for the first time, that platelets are able to induce Treg in a GARP-dependent manner. Furthermore, melanoma patients with a high platelet count showed a reduced responsiveness to immunotherapy and a significantly increased expression of GARP on platelets. This could be of great importance, as thrombocytosis is associated with poor prognosis and metastasis in cancer. Our data implicate that the targeting of platelets in cancer could be a potential impactful new supplementary approach in addition to standard immunotherapy.

4.2.6 Appendix

Appendix 4.2.A

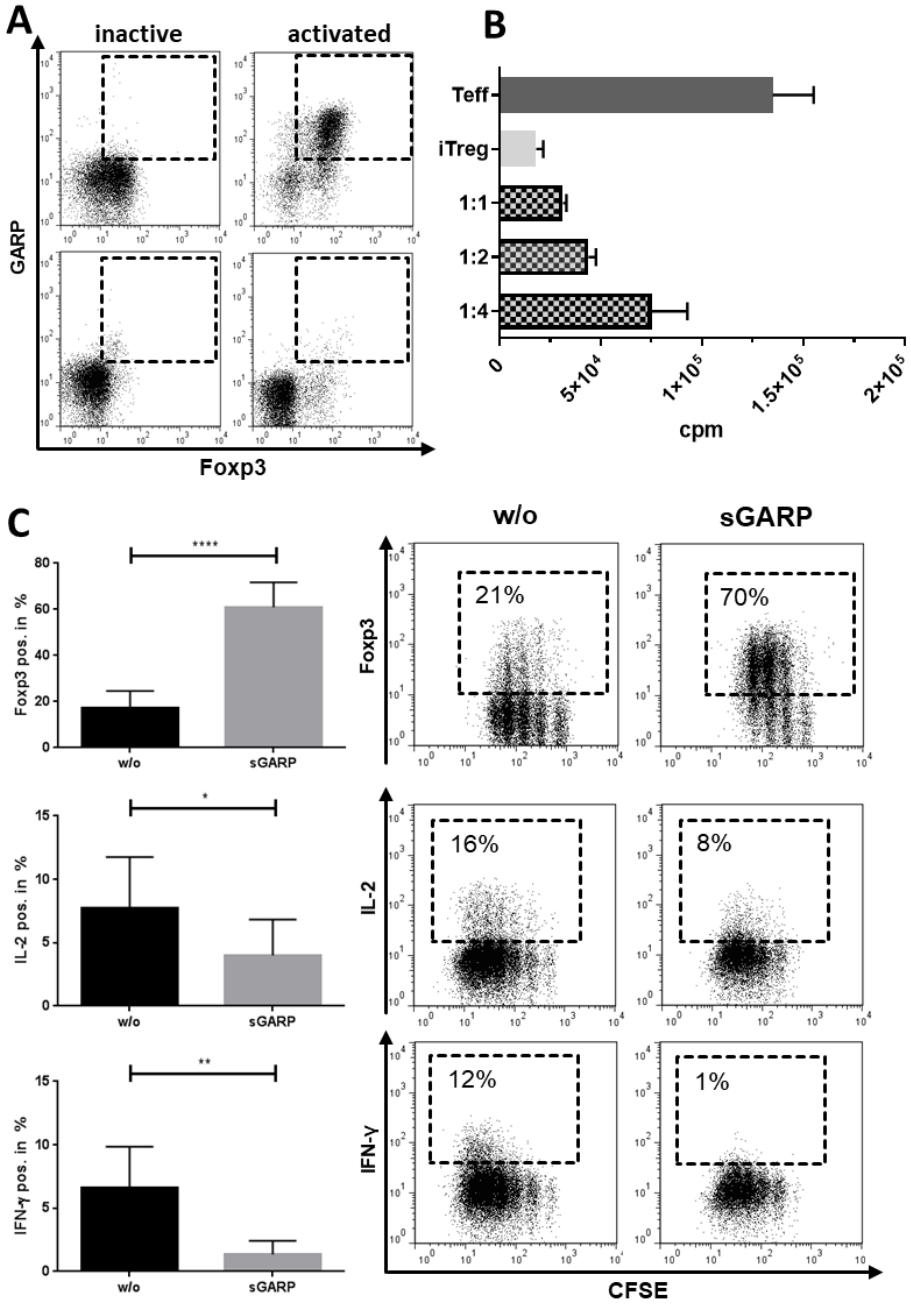

Figure 4.2.A1. sGARP induced Treg**.** (**A**) GARP expression on Treg vs. Teff: GARP is an activation marker on Treg. 16h after stimulation, $CD4^+$ $CD25^+$ Treg showed a strong GARP expression compared to $CD4^+CD25^-$ Teff. One representative dot plot of four different experiments is shown. (**B**) Suppressive capacity of sGARP-conditioned T cells. $CD4^+CD25^-$ T cells were stimulated with 0.5 µg/mL anti-CD3 mAb and 1.0 µg/mL anti-CD28 mAb for 6 days in the presence of 10 µg/mL sGARP, resulting in Treg. Simultaneously, allogenic Teff were generated without the use of sGARP. After 6 days of stimulation, Teff and titrated Treg were cocultured and re-stimulated with anti-CD3 mAb and irradiated PBMC. After 4 days, proliferation was determined by tritiated thymidine (^{3}H TdR) pulse. Results show the pooled data of three independent experiments. (**C**) sGARP induction of Foxp3, inhibition of proliferation, and inhibition of effector cytokine production in $CD4^+$ T cells (n = 3, means ± SD, * p < 0.05, ** $p \leq 0.01$, *** $p \leq 0.001$, and n.s. determined by one-way ANOVA).

Appendix 4.2.B

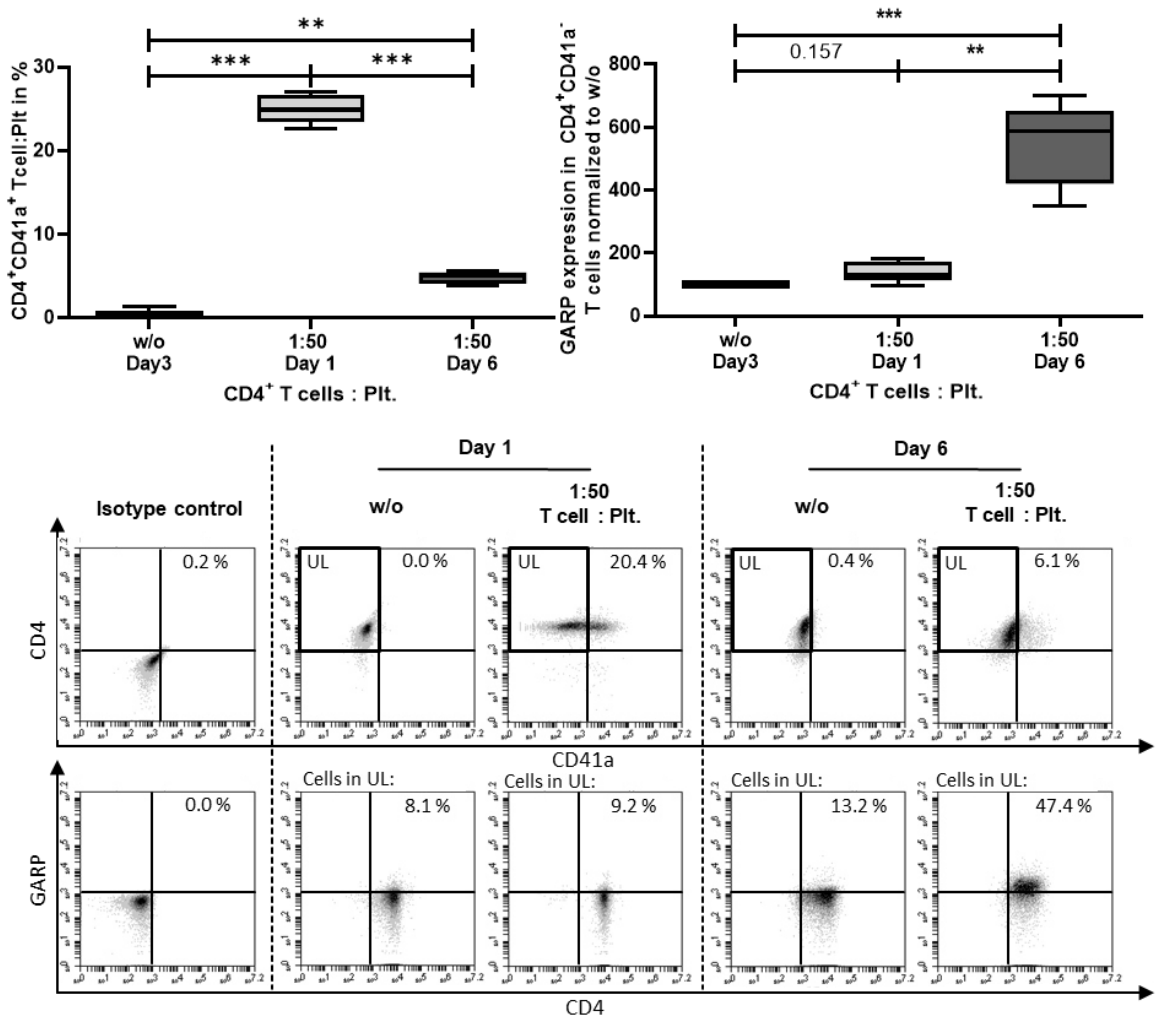

Figure 4.2.A2. Platelets bound to T cells upon activation in coculture**.** $CD4^+CD25^-$ T cells were cocultured with or without platelets at the ratio of 1:50 and stimulated with 0.5 µg/mL anti-CD3 mAb and 1.0 µg/mL anti-CD28 mAb for 6 days. At day 1 and 6, platelet–T cell conjugates ($CD41a^+CD4^+$ double-positive cells) were analyzed via flow cytometry. For assessment of GARP expression, only $CD4^+$CD41a- cells were included in the analysis (indicated by the pregating on the upper left (UL)). GARP expression was normalized to the untreated (w/o) control. Dot plots show one representative result of five independent experiments. Isotype controls are shown (n = 5, box and whiskers, medians + min/max, * $p < 0.05$, ** $p \leq 0.01$, *** $p \leq 0.001$, and n.s. determined by one-way ANOVA).

Appendix 4.2.C

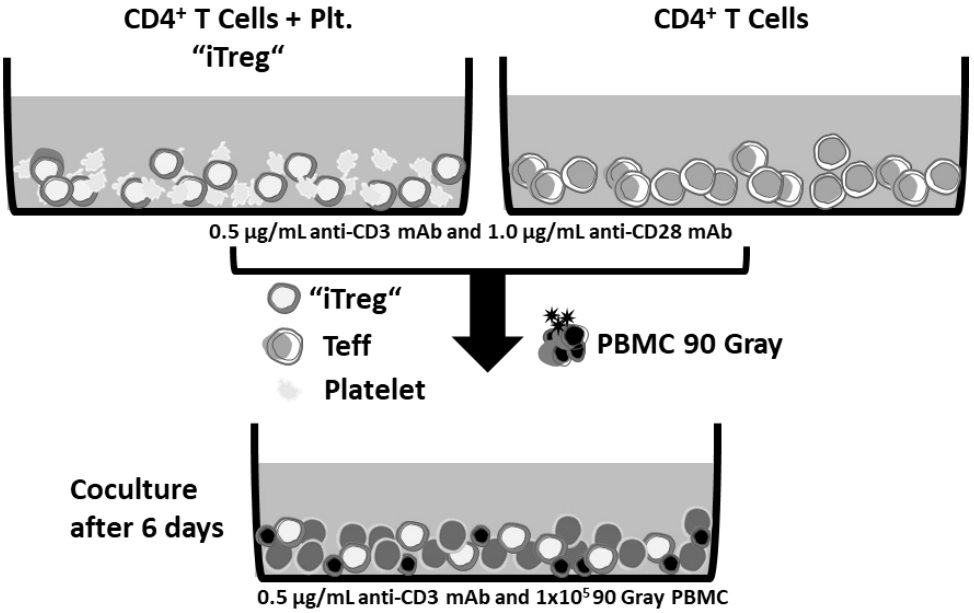

Figure 4.2.A3. Experimental setup of a platelet-conditioned T cell suppression assay**.** 1×10^6 $CD4^+CD25^-$ T cells were stimulated with 0.5 µg/mL anti-CD3 mAb and 1.0 µg/mL anti-CD28 mAb with or without 50×10^6 platelets for 6 days. T cells cocultured with platelets developed an iTreg-like phenotype, whereas T cells cultured without platelets displayed a Teff phenotype. Next, iTreg and Teff were cultured at different ratios (iTreg/Teff: 1:1, 1:2, 1:4, and the corresponding controls) and restimulated with 0.5 µg/mL anti-CD3 mAb and 90Gy irradiated PBMC. Proliferation (Ki-67) was measured via flow cytometry 3 days after restimulation.

Appendix 4.2.D

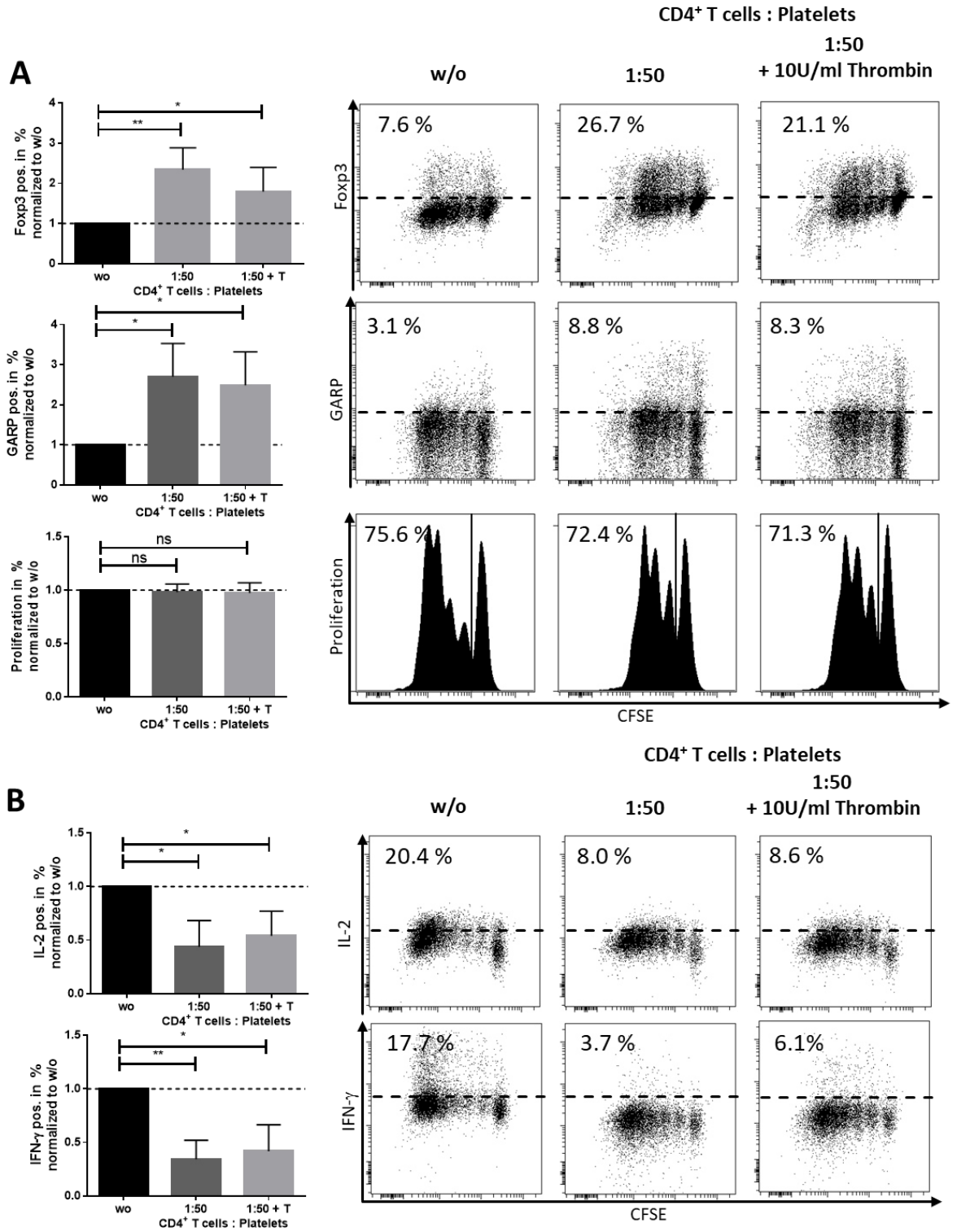

Figure 4.2.A4. Thrombin-activated platelets induced a regulatory phenotype in $CD4^+CD25^-$ T cells**.** 1 × 10^6 $CD4^+CD25^-$ T cells were stimulated with 0.5 µg/mL anti-CD3 mAb and 1.0 µg/mL anti-CD28 mAb with or without 50 × 10^6 platelets for 6 days and treated with or without 10 U/mL thrombin. (**A**) Foxp3 and GARP expression and proliferation were determined at day 3 via flow cytometry. (**B**) Using intracellular flow cytometry, we analyzed cytokine production of IL-2 and IFN-γ on day 6. Dot plots show one representative result of five independent experiments (n = 5, box and whiskers, medians ± min/max, * $p < 0.05$, ** $p \leq 0.01$, *** $p \leq 0.001$, and n.s. determined by one-way ANOVA).

Appendix 4.2.E

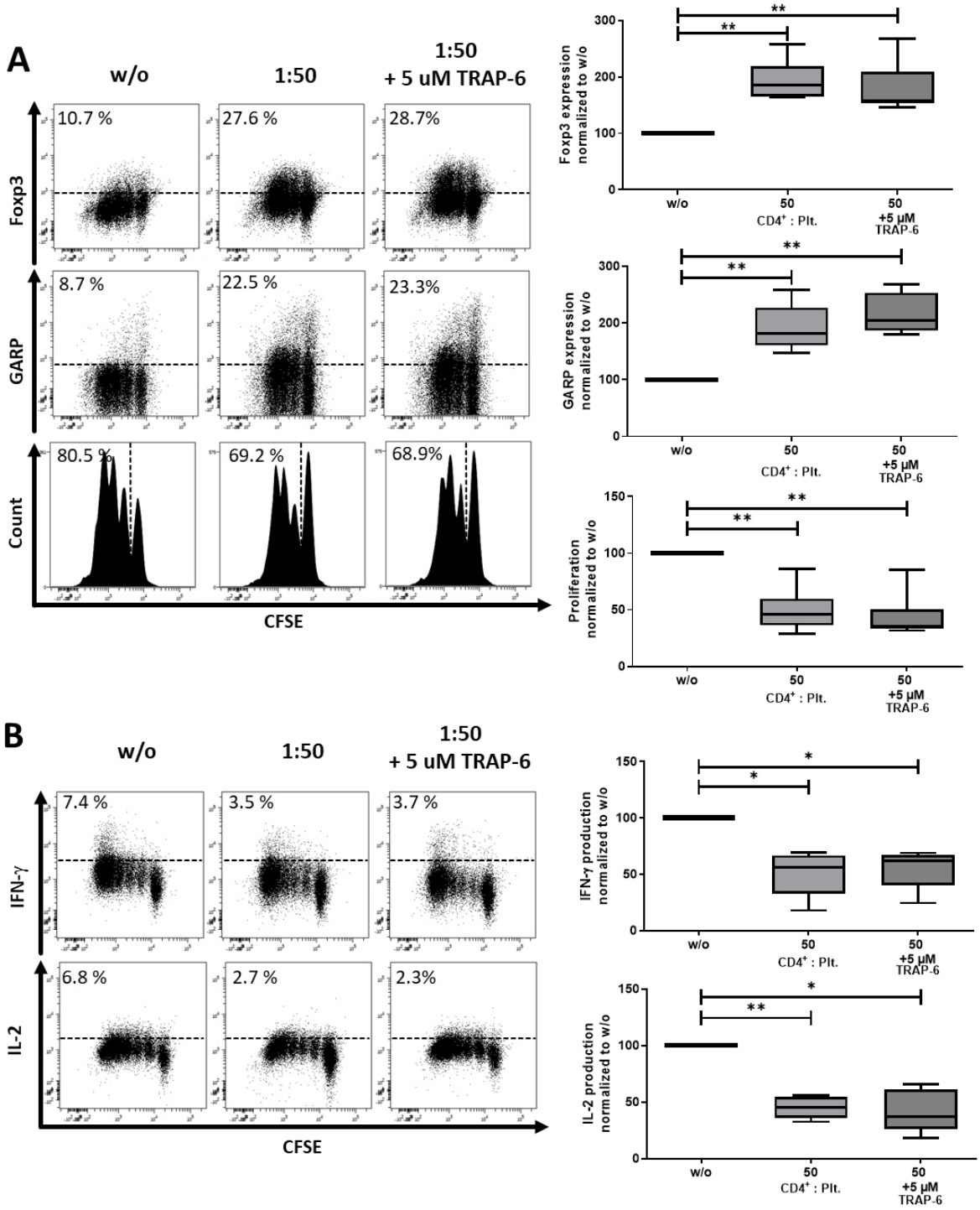

Figure 4.2.A5. TRAP-6-activated platelets induced a regulatory phenotype in $CD4^+CD25^-$ T cells**.** 1×10^6 $CD4^+CD25^-$ T cells were stimulated with 0.5 µg/mL anti-CD3 mAb and 1.0 µg/mL anti-CD28 mAb with or without 50×10^6 platelets for 6 days and treated with or without 5 µM TRAP-6. (**A**) Foxp3 and GARP expression and proliferation were determined at day 3 via flow cytometry. (**B**) Using intracellular flow cytometry, we analyzed cytokine production of IL-2 and IFN-γ on day 6. Dot plots show one representative result of five independent experiments (n = 5, box and whiskers, medians ± min/max, * $p < 0.05$, ** $p \leq 0.01$, *** $p \leq 0.001$, and n.s. determined by one-way ANOVA).

Appendix 4.2.F

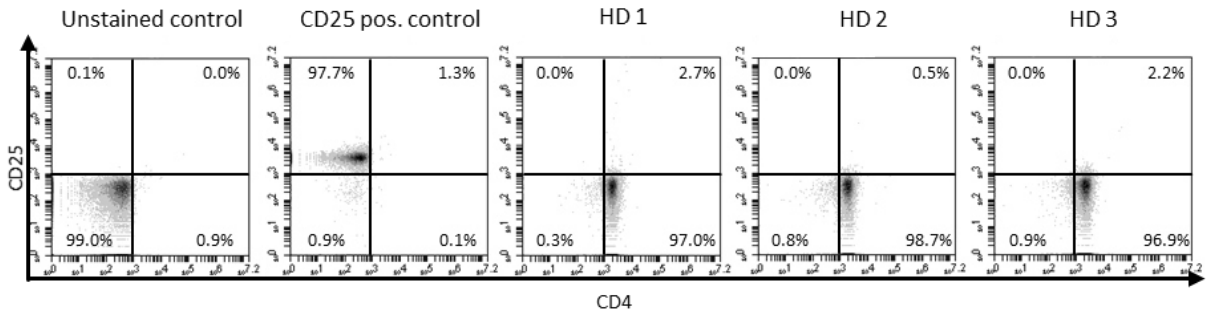

Figure 4.2.A6. Flow cytometric analysis of T cell purity**.** $CD4^+CD25^-$ cells showed a purity of around 98% after isolation. $CD4^+CD25^-$ T cells were isolated as described in the manuscript. Shown are the unstained control, the CD25-positive staining control, and successful $CD4^+CD25^-$ isolations of three different healthy donors.

Appendix 4.2.G

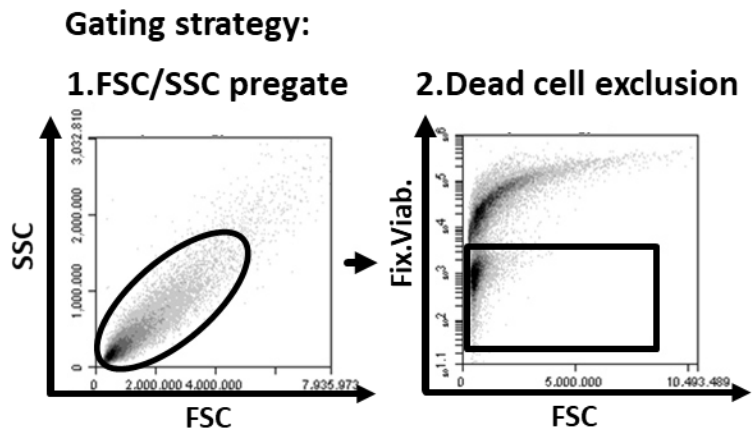

Figure 4.2.A7. Gating strategy**.** Cells were pregated via forward- and side scatter (FSC/SSC) following a dead cell exclusion via fixable viability dye.

5.0 General discussion

This discussion will set all manuscripts into the greater context and therefore, will not repeat each manuscript discussion. Furthermore, this part is largely based on Zimmer et al., 2022, (227) which was in part updated to incorporate some of the latest key findings. This section addresses the function of GARP as a biomarker and prospective therapeutic target and identifies outstanding questions in the field that need to be addressed.

5.1 GARP as a Biomarker

Examining sGARP levels in easily accessible specimens, like serum and plasma from routine blood tests, and correlating their content to patient diagnoses and clinical outcomes is a novel approach to evaluate the potential of sGARP as a diagnostic and prognostic biomarker. This information would be highly valuable for clinicians as it is not only a more practical, time efficient, and cost-effective approach than screening for GARP expressing cells in the TME, but it is also a less invasive procedure for patients. Reliable assessment of the concentration of sGARP in patient blood could be of high importance as even low levels of sGARP are capable of greatly enhancing the activation of TGF-β (75). Therefore, elevated sGARP levels in cancer patients could have a great impact on the disease development, leading to unfavorable patient outcomes. Metelli et al. were able to detect high levels of sGARP and sGARP/LTGF-β1 complexes in the blood plasma of prostate cancer patients. Increased amounts of sGARP correlated with increased likelihood of metastasis in these patients (73). Some studies have indicated that TGF-β, which is regulated by GARP, plays an important role in DNA repair, and may protect cells from ionizing radiation. Kim et al. could show that pretreatment of human epidermoid carcinoma cells with TGF-β reduced g-radiation induced apoptosis (97). However, to the best of our knowledge, no known study has examined the possibility of GARP as a predictive marker for radiation sensitivity in cancer cells yet.

GARP is an enticing potential diagnostic biomarker for cancer as it is highly upregulated on the surface of both tumor cells and suppressive immune cells found in the TME (41, 43). Nevertheless, only a few studies have examined the possibility of GARP as a diagnostic biomarker in further detail. One study by Jin et al., examined the potential of GARP on Treg as a diagnostic biomarker in both the tumor tissue and peripheral blood of lung cancer patients. They found that frequencies of GARP-expressing Treg were higher in the tumor tissue of early stage (I-II) versus late stage (III- IV) patients but not in their peripheral blood (101). Furthermore, Zimmer et al., 2023 could show for the first time, that GARP is stably expressed throughout GSC, (I) isolated from a heterogenous tumor, (II) different levels of stemness in the cellular hierarchy and (III) longitudinal evolution throughout therapy. This uniformity and stability of the GARP expression across different types of human GSC suggests a potential use of GARP as a prognostic biomarker for GB. Additionally, they were able to find that the frequency of nuclear GARP positive GB ($GARP^{NU+}$) cells correlates with patient survival. Here, a high frequency of $GARP^{NU+}$ cells lead to a significant decrease in survival, compared to a low frequency (322).

Additionally, they could show that melanoma patients, who do not respond to immunotherapy, showed a longer overall survival, when they had a low percentage of $GARP^{+}$ Treg (323). This was also the case in hepatocellular carcinoma, as a high frequency of $Foxp3^{+}GARP^{+}$ Treg correlated with a more aggressive phenotype and a TME with enhanced suppressive properties (324). A study by Metelli et al. showed that high GARP expression in lung cancer versus healthy adjacent tissue correlated with a reduced overall survival (55). The same observation was also described in bone sarcoma (42). Furthermore, it has been shown that GARP expression is increased in gastric cancer (325). Here, increased levels of $CD4^{+}GARP^{+}$ T cells in the tumor vicinity correlated with poor overall survival. Interestingly, elevated expression of GARP also correlated with the expression of CTLA-4 and PD-L1 (325). Correlation data listed by the Human Protein Atlas, based on the TCGA data set, show that renal

and urothelial cancer patients with elevated GARP mRNA levels have a significantly lower overall survival when compared to patients with lower GARP mRNA concentrations (proteinatlas.org/ENSG00000137507- LRRC32). This was not observed though for human lung cancer. As mentioned before, it has been described that GARP expression was increased on the platelets of melanoma patients, but there were no differences between stage I and stage IV patients (37). One potential limitation of this study was the composition of the patient cohort, as 15 out of 16 patients responded to immunotherapy, potentially impacting the GARP expression levels found on platelets. Nevertheless, a potential use of GARP as a biomarker on platelets should be analyzed in a larger patient cohort (37). As outlined above, an increased platelet count in malignant melanoma patients is associated with poor prognosis. Furthermore, patients, who did not respond to immunotherapy, had an increased platelet to lymphocyte ratio as compared to responders to immunotherapy (37, 305, 323). Elevated platelet counts, increased expression of GARP on platelets, and shedding of GARP from their surfaces, combined with the fact that platelets are able to GARP dependently induce Treg, may be a highly disadvantageous combination that negatively affects patient survival. However, future studies must be conducted to evaluate platelet counts and their GARP levels as potential predictive and prognostic biomarkers for immunotherapy response and disease progression in melanoma.

Interestingly a recent study concluded that GSC manipulate platelets in their close surrounding through their endogenous coagulation cascade, leading to platelet activation and ultimately to an increase in GSC characteristics like stemness and proliferation (326). This manipulation of platelets by GARP expressing cancer (stem-) cells and the ability of platelets to contribute to an immunosuppressive TME via GARP indicates a complex interaction. Here an autocrine-like manipulation of the platelet function by cancer (stem-) cells leads to GSC promoting micromilieu in the tumor and further tampering of platelet homeostasis.

In patients with inflammatory diseases, GARP has begun to be evaluated as a potential biomarker. For example, in patients with primary biliary cholangitis, an autoimmune biliary disease, GARP was found to be upregulated on cholangiocytes and was also detected on biliary duct cells (327). Herein, GARP expression was increased in response to biliary salts and released under cholestatic conditions via apoptosis of cholangiocytes. Atopic dermatitis patients showed a significantly reduced surface expression of GARP on Treg (46). Furthermore, patients with psoriasis, who received systemic therapy, had higher frequencies of activated $GARP^+$ Treg than patients, who were only treated with topical therapy (328). Research in mice revealed that there is an increased expression of GARP on B cells in murine models of lupus (82). Whether these findings can be translated into the human setting has to be investigated in future trials. Taken together, it will be interesting to validate GARP, either in its soluble or in its cell-associated form, as a predictive and prognostic biomarker in patients with immune mediated diseases in future clinical trials and to investigate whether GARP could be used as an early indicator for therapy response.

5.2 GARP as a Therapeutic Target

As described in section 1.2.5, Cellular GARP, GARP is expressed by a variety of cells in the TME and plays a prominent role in immunosuppression and cancer progression. Drugs that modulate the expression of GARP may be useful for the treatment of various disease indications. Enhancing GARP expression, and its accompanying immunosuppression, may be beneficial for the treatment of autoimmunity and transplant rejection, whereas downregulating GARP expression may aid in the improvement of anti-tumor immune responses. Herein, several strategies are possible. On one hand, increased and long-lasting expression of GARP on Treg could lead to $GARP^+$ Treg, which are more potent in inhibiting the proliferation and function of conventional Teff. This approach of improving Treg efficiency could be used in the treatment of autoimmunity and allergic diseases in order to modulate and downregulate overshooting immune or inflammatory processes.

Inhibition of miRNA, through the use of so called antagomirs, might be one possibility to induce elevated and long lasting GARP expression in Treg (Figure 1.2.1A). Antagomirs are oligonucleotides complementary to the mature form of specific miRNA. They easily penetrate into cells, and they inhibit the activity of their target miRNA, both in vitro and in vivo (329). Thus, they could represent a novel class of therapeutic molecules, leading to a sustained expression of GARP on Treg. Of note, transfer of miR-142-3p into Treg impaired their suppressive function (330). Importantly, Krützfeld et al. showed that antagomirs can be utilized as a systemic treatment and are resistant to degradation by RNases following injection into an organism (329). This approach should be further evaluated in future studies. One example would be to improve the clinical efficacy of human adoptive Treg transfer by enhancing the suppressive function and/or stability of Treg in an autoimmune or GvHD setting. Furthermore, in case of cancer and metabolic disease, the application of antagomir loaded nanoparticles to target unfavorable miRNA has already been demonstrated in several mouse studies (331, 332), supporting the potential of antagomirs to be used in novel therapeutic approaches.

As demonstrated earlier, sGARP can have a beneficial effect in the induction of peripheral Treg and can help sustain Treg differentiation. Additionally, sGARP can inhibit Teff functions by reducing their proliferation and inflammatory cytokine production (43, 75). When sGARP was applied in vivo, it was shown to inhibit overshooting immune responses in a humanized mouse model of allergy (333) as well as of transplant rejection and in GvHD (74). This opens up further strategies in using sGARP as an immunomodulatory agent, such as in transplantation or autoimmune diseases (Figure 1.2.1C). Furthermore, the simultaneous administration of sGARP and LTGF-β could also be a promising treatment approach (Figure 1.2.1B, C). Herein, GARP could bind LTGF-β and enhance its activation. Since integrins are necessary for the final activation step of TGF-β, this would minimize the risk of putative side effects of exaggerated TGF-β activation. This approach was already proposed by Fridrich et al. in 2016 (75). In more detail, they were able to show that even small doses of sGARP could greatly enhance the activation of LTGF-β. This could have implications for autoimmune diseases, as a low dose combination application of sGARP and LTGF-β may mitigate the potential side effects of high dosages of pre-activated TGF-β (75).

On the one hand, Treg cellular therapies have been shown to ameliorate autoimmune diseases, graft rejections, and GvHD (334, 335). Elevating GARP expression levels on Treg to increase and prolong their activation status or using sGARP to increase the number of Treg could contribute to the suppression of autoimmune responses by restoring T cell tolerance. On the other hand, targeting of GARP on activated Treg through the use of blocking antibodies could enhance anti-tumor immunity. Several studies have reported that targeting GARP provided protective immunity against melanoma and colon cancer and the depletion of GARP on platelets did not lead to changes in hemostasis and thrombosis (99, 308). Currently, two therapeutic antibody products are in phase 1 clinical trials: ABBV-151 (NCT03821935) and DS-1055 (NCT04419532). Both antibodies aim for the reactivation of anti-tumor immunity by specifically inhibiting Treg in malignant solid tumors. However, they differ in their mechanism of action by several points. ABBV-151 is a human IgG4 monoclonal antibody (mAb) that specifically binds to the GARP/LTGF-β 1 complex to inhibit the release of mature TGF-β1 from LTGF-β1 (Figure 1.2.1B) (336). This results in a Treg specific blocking effect on functional TGFb1 release. This leads to the inhibition of TGF-β1 signaling in Treg and Teff, which in turn decreases the suppressive effects by Treg and restores Teff functions in the TME. In a preclinical study, a mouse surrogate antibody that targeted the GARP/ LTGF-β1 complex improved anti-tumor effects in a combination setting with an anti-mouse programmed cell death protein 1 (PD-1) antibody when compared with the anti–PD-1 treatment alone. However, the former antibody did not display anti-tumor activity when administered as a monotherapy alone in a CT26 tumor mouse model (253). The anti-tumor combination effects of the anti-GARP-TGF-β1 antibody did not require FcγR-mediated effector functions. In the current clinical study ABBV-151 is applied in parallel as a monotherapy and in

combination with an anti-PD-1 antibody. DS-1055a is an anti-GARP afucosylated human IgG1 mAb, that aims for the efficient depletion of GARP$^+$ Treg via antibody-dependent cellular cytotoxicity (Figure 1.2.1A) (337). This prevents Treg-mediated suppression of immune effector cells and thereby results in the reactivation of anti-tumor activities in the TME.

In preclinical settings, DS-1055a treatment resulted in the depletion of GARP$^+$ Treg and increased Teff functions in vitro and exerted anti-tumor effects in HT-29 tumor bearing humanized mice. In addition, combined treatment of DS-1055a with an anti-PD-1 antibody yielded in a combination effect since the proliferation of Teff increased in comparison to treatment with either agent alone. GARP targeting antibodies can be described as a kind of Treg-specific treatment approach. In immune cells of the TME, GARP expression is almost completely limited to activated Treg. Unlike other targeted Treg-associated proteins, this specificity in GARP expression on activated Treg is considered to be critical for the recovery of intrinsic anti-tumor activities without affecting effector immune functions. It is important to await the results of the aforementioned phase 1 clinical trials to determine whether the inhibition of Treg function or the removal of Treg themselves from the TME can lead to the revival and activation of Teff from their immunosuppressive dormant state, and thus result in tumor eradication. Since, at least in preclinical models, the effects of combined treatment with an anti-PD-1 antibody have been confirmed. There is a rationale that GARP targeting antibodies have the potential to improve insufficient immune responses and decrease resistance to immune checkpoint inhibitors (ICI), like PD-1, programmed cell death protein ligand 1 (PD-L1), and CTLA-4, in clinical settings. In addition, the fact that GARP is expressed only by activated — not resting Treg, suggests that the actions of these antibodies should mainly occur in the highly immunosuppressive TME and should hopefully not lead to an increase in immune-related adverse events when used in combination with ICI. In this regard, it has been shown that antibody-mediated blockade or deletion of GARP did not alter innate or adaptive immune responses (338). Therefore, antibody therapies targeting GARP represent promising approaches in order to restore anti-tumor immunity without severely impairing other immunological defenses.

5.3 Open Questions and future directions

GARP presents a promising target molecule in different disease settings. Of note, it is tightly associated to TGF-β and its functions. TGF-β is a pleiotropic cytokine and as such, a key mediator of many, often opposing biological processes. In cancer, TGF-β is a double-edged sword. It exerts potent cytostatic and pro-apoptotic activities in early stages of disease, but it can also paradoxically favor EMT and metastasis at later stages of malignant transformation, thus shifting from tumor inhibition to tumor promotion during the progression of cancer. In addition, it modulates the proliferation and function of different immune cells necessary for building a potent anti-tumor immune response, making it a difficult target for anti-cancer therapies. Therefore, due to this lack of specificity (in targeted function and cell type) resulting from the pleiotropic nature of TGF-β, combined with insufficient therapeutic efficacy, therapies directly targeting TGF-β have not entered the clinic for routine applications yet. In addition, clinical trials, which target TGF-β signaling, must be considered in combination with other therapies, including immune checkpoint blockade, chemotherapy, and radiotherapy.

One novel approach to address a particular function of TGF-β, is through the blockade of TGF-β1 activation by GARP expressing Treg using an anti-GARP:LTGF-β1 mAb. This would specifically prevent the release of TGF-β1 that is in complex with GARP. Whereas blocking of GARP:LTGF-β1 would decrease immunosuppression via Treg, another novel approach targets GARP itself. This might delete important inhibitory cellular components of the TME, such as Treg and tumor cells. It can be argued that targeting and blocking GARP is a more promising upstream target, as GARP itself exerts a

suppressive function on other cells as described above. Furthermore, cell surface complexation and soluble GARP have been shown to enhance TGF-β activation (75). Therefore, targeting GARP could lead to a simultaneous inhibition of TGF-β activation and function as well as the inhibition of the suppressive functions of GARP and sGARP. Whether an anti-GARP: TGF-β1 mAb is superior to using an anti-GARP mAb for blocking immune suppression in the TME will have to be analyzed in future studies. Both approaches have the potential to boost intrinsic anti-tumor activities and to show encouraging results in mouse models; however, a clinical validation is still awaited. Nevertheless, one challenge for the use of this therapeutic target could be the need for sufficient amounts of GARP on the surface of the mentioned cell types above. In addition, non-Treg side effects have to be taken into account, when using an anti-GARP antibody, as GARP is also expressed e.g. on activated platelets in peripheral blood (37). However, a GARP knockdown in platelets did not show any negative effects on hemostasis (99), and it also promoted antitumor immunity by inhibiting of TGF-β signaling in different cancer entities (308). Additionally, these findings point out a possible novel therapeutic approach in cancer based on the combination of GARP inhibition with platelet modulating agents, such as ticagrelor and aspirin (339). This is further supported by Sloan et al., where the therapeutic modulation of platelets led to the inhibition of tumor development in a GSC / GB disease setting underlining the existence of a therapeutically targetable connection between platelet and cancer (326).

It was shown by several groups (63) that GARP deficiency in Treg led to increased susceptibility to inflammatory diseases through the induction of immune dysregulation. Thus, GARP is somehow required to maintain immune homeostasis. It will be very interesting to investigate in more detail if and to what extend GARP alone contributes as an important molecule to Treg generation, stability, and function or whether GARP effects are solely modulated via regulation of TGF-β bioavailability. In this context, the link between GARP and Foxp3 remains elusive. On the one hand, several publications support the idea that GARP and Foxp3 expression is independent of one and other (33, 61, 62, 71). On the other hand, it has been described that Treg-specific transcription of LRRC32 is Foxp3 mediated, resulting from the synergistic interaction of Foxp3 with NFAT (30). Additionally, it has been suggested that there is a mutual dependency of Foxp3 and GARP expression, which influence Treg suppressive function. Future studies must be conducted to better understand the interdependence of GARP and Foxp3 expression in different cell types. In most studies, GARP has been described as a surface molecule involved in the processing and maturation of TGF-β. Nevertheless, there are some reports showing cytoplasmatic and nuclear GARP expression as well (40).

As previously described, the nuclear localization of GARP in GB cells could be useful as a prognostic marker for patient survival. In addition, $GARP^{NU+}$ was stably expressed in every GSC examined, which were (I) derived from a heterogeneous tumor, (II) with varying degrees of stemness in the cellular hierarchy, and (III) evolving longitudinally throughout treatment, indicating a pivotal role for nuclear localized GARP in these cells. How and to what purpose does GARP, an otherwise surface expressed protein, become localized into the nucleus of tumor cells remains unclear. Whether $GARP^{NU+}$ undergoes additional post-translational modifications and what its exact method of intranuclear localization and size must be determined in future studies. Computational analysis from databases like gene card shows 5 potential proteins which interact with GARP. For example, GP96 is involved in the folding of the protein, possibly leading to a posttranslational modification of GARP enabling an active / passive nuclear localization of GARP. Nuclear localisation of a cytoplasmic protein is not an uncommon phenomenon. However, GARP may be interacting with the nuclear localized transcription factor, STAT3, as shown by initial affinity capture mass spectrometry studies in HCT116 and 293T cells (340). As STAT3 has been implicated in maintaining tumorigenicity and self-renewal in GSC (341), this could explain why GARP was observed to be stably expressed by GSC, but this interaction and its subsequent characterization has yet to be confirmed in GB or GSC.

However, the function of this intracellular GARP and the significance of its intracellular localization need to be further characterized in future studies. These studies will help to clarify if GARP does have the same function on Treg, on platelets, and in cancer cells in means of the above-described functions, including suppressive capacity, proliferation, and therapy resistance.

Besides being a relevant therapeutic target, the use of GARP as a prognostic and predictive biomarker should be transferred into clinical routine. Quantification of GARP on peripheral blood cells, in serum, and on tumor tissue could potentially be used to reflect the immunosuppressive burden present in tumor patients. Up until now, there has been only little correlation between GARP expression and clinical tumor stages of patients. To gain more insight and to define a potential application of GARP as a biomarker, future studies should quantify GARP levels on blood cells, in serum, and on tumor tissues. Ideally, this should be performed with the use of multiplex approaches (342) in order to investigate in more detail the distribution and complex spatial interactions of $GARP^+$ cells in the TME. These results can then be correlated back to clinical data. Most data up until now has been generated from in vitro and in vivo (in mice) experimental models. There is an urgent need to translate and validate these results in the human system through clinical trials, as the findings of GARP (i.e. regulation) seem to be similar — but not identical to the murine setting.

6.0 Conclusion

GARP is a highly promising target molecule in diverse disease settings, and it is expressed by different cells and tissues that exert immunomodulatory functions. As such, it could serve as a relevant new biomarker in patients with immune related diseases, such as cancer and autoimmunity. In addition, targeting of membrane GARP as well as the use of soluble GARP are attractive therapeutic approaches for the treatment of a wide variety of malignant, autoimmune, and inflammatory diseases. Of note, one cannot consider the contribution of GARP to the immunosuppressive function of Treg in the absence of its key partner: LTGF-β. Nevertheless, novel approaches are needed as LTGF-β is produced and expressed ubiquitously, whereas cellular GARP expression is much more restricted.

7.0 REFERENCES

1. BURNET M. Cancer; a biological approach. I. The processes of control. *Br Med J* (1957) **1**:779–86. doi:10.1136/bmj.1.5022.779
2. Mittal D, Gubin MM, Schreiber RD, Smyth MJ. New insights into cancer immunoediting and its three component phases--elimination, equilibrium and escape. *Curr Opin Immunol* (2014) **27**:16–25. doi:10.1016/j.coi.2014.01.004
3. Wang Y, Xiang Y, Xin VW, Wang X-W, Peng X-C, Liu X-Q, et al. Dendritic cell biology and its role in tumor immunotherapy. *J Hematol Oncol* (2020) **13**:107. doi:10.1186/s13045-020-00939-6
4. Iorgulescu JB, Braun D, Oliveira G, Keskin DB, Wu CJ. Acquired mechanisms of immune escape in cancer following immunotherapy. *Genome Med* (2018) **10**:87. doi:10.1186/s13073-018-0598-2
5. Jonuleit H, Schmitt E. Regulatory T-cells in antitumor therapy: isolation and functional testing of CD4+CD25+ regulatory T-cells. *Methods Mol Med* (2005) **109**:285–96. doi:10.1385/1-59259-862-5:285
6. Steinbrink K, Jonuleit H, Müller G, Schuler G, Knop J, Enk AH. Interleukin-10-treated human dendritic cells induce a melanoma-antigen-specific anergy in CD8(+) T cells resulting in a failure to lyse tumor cells. *Blood* (1999) **93**:1634–42.
7. Poschke I, Mougiakakos D, Hansson J, Masucci GV, Kiessling R. Immature immunosuppressive CD14+HLA-DR-/low cells in melanoma patients are Stat3hi and overexpress CD80, CD83, and DC-sign. *Cancer Res* (2010) **70**:4335–45. doi:10.1158/0008-5472.CAN-09-3767
8. Schupp J, Krebs FK, Zimmer N, Trzeciak E, Schuppan D, Tuettenberg A. Targeting myeloid cells in the tumor sustaining microenvironment. *Cell Immunol* (2019) **343**:103713. doi:10.1016/j.cellimm.2017.10.013
9. Roncarolo MG, Gregori S, Battaglia M, Bacchetta R, Fleischhauer K, Levings MK. Interleukin-10-secreting type 1 regulatory T cells in rodents and humans. *Immunol Rev* (2006) **212**:28–50. doi:10.1111/j.0105-2896.2006.00420.x.
10. Gajewski TF. Identifying and overcoming immune resistance mechanisms in the melanoma tumor microenvironment. *Clin Cancer Res* (2006) **12**:2326s-2330s. doi:10.1158/1078-0432.CCR-05-2517.
11. Bopp T, Becker C, Klein M, Klein-Hessling S, Palmetshofer A, Serfling E, et al. Cyclic adenosine monophosphate is a key component of regulatory T cell-mediated suppression. *J Exp Med* (2007) **204**:1303–10. doi:10.1084/jem.20062129
12. Sakaguchi S. Regulatory T cells: history and perspective. *Methods Mol Biol* (2011) **707**:3–17. doi:10.1007/978-1-61737-979-6_1
13. Sadlon TJ, Wilkinson BG, Pederson S, Brown CY, Bresatz S, Gargett T, et al. Genome-wide identification of human FOXP3 target genes in natural regulatory T cells. *J Immunol* (2010) **185**:1071–81. doi:10.4049/jimmunol.1000082
14. Niu J, Jiang C, Li C, Liu L, Li K, Jian Z, et al. Foxp3 expression in melanoma cells as a possible mechanism of resistance to immune destruction. *Cancer Immunol Immunother* (2011) **60**:1109–18. doi:10.1007/s00262-011-1025-3
15. Redpath M, Xu B, van Kempen LC, Spatz A. The dual role of the X-linked FoxP3 gene in human cancers. *Mol Oncol* (2011) **5**:156–63. doi:10.1016/j.molonc.2011.03.001
16. Stagg J, Divisekera U, Duret H, Sparwasser T, Teng MW, Darcy PK, et al. CD73-deficient mice have increased antitumor immunity and

are resistant to experimental metastasis. *Cancer Res* (2011) **71**:2892–900. doi:10.1158/0008-5472.CAN-10-4246

17. Stagg J, Smyth MJ. Extracellular adenosine triphosphate and adenosine in cancer. *Oncogene* (2010) **29**:5346–58. doi:10.1038/onc.2010.292
18. Housman G, Byler S, Heerboth S, Lapinska K, Longacre M, Snyder N, et al. Drug resistance in cancer: an overview. *Cancers (Basel)* (2014) **6**:1769–92. doi:10.3390/cancers6031769
19. Marin-Acevedo JA, Dholaria B, Soyano AE, Knutson KL, Chumsri S, Lou Y. Next generation of immune checkpoint therapy in cancer: new developments and challenges. *J Hematol Oncol* (2018) **11**:39. doi:10.1186/s13045-018-0582-8
20. Ha D, Tanaka A, Kibayashi T, Tanemura A, Sugiyama D, Wing JB, et al. Differential control of human Treg and effector T cells in tumor immunity by Fc-engineered anti-CTLA-4 antibody. *Proc Natl Acad Sci U S A* (2019) **116**:609–18. doi:10.1073/pnas.1812186116
21. Sharma A, Subudhi SK, Blando J, Scutti J, Vence L, Wargo J, et al. Anti-CTLA-4 Immunotherapy Does Not Deplete FOXP3+ Regulatory T Cells (Tregs) in Human Cancers. *Clin Cancer Res* (2019) **25**:1233–8. doi:10.1158/1078-0432.CCR-18-0762
22. Bagchi S, Yuan R, Engleman EG. Immune Checkpoint Inhibitors for the Treatment of Cancer: Clinical Impact and Mechanisms of Response and Resistance. *Annu Rev Pathol* (2021) **16**:223–49. doi:10.1146/annurev-pathol-042020-042741
23. Nowicki TS, Hu-Lieskovan S, Ribas A. Mechanisms of Resistance to PD-1 and PD-L1 Blockade. *Cancer J* (2018) **24**:47–53. doi:10.1097/PPO.0000000000000303.
24. Simeone E, Grimaldi AM, Festino L, Trojaniello C, Vitale MG, Vanella V, et al. Immunotherapy in metastatic melanoma: a novel scenario of new toxicities and their management. *Melanoma Manag* (2019) **6**:MMT30. doi:10.2217/mmt-2019-0005.
25. Weide B, Martens A, Hassel JC, Berking C, Postow MA, Bisschop K, et al. Baseline Biomarkers for Outcome of Melanoma Patients Treated with Pembrolizumab. *Clin Cancer Res* (2016) **22**:5487–96. doi:10.1158/1078-0432.CCR-16-0127.
26. Martens A, Wistuba-Hamprecht K, Geukes Foppen M, Yuan J, Postow MA, Wong P, et al. Baseline Peripheral Blood Biomarkers Associated with Clinical Outcome of Advanced Melanoma Patients Treated with Ipilimumab. *Clin Cancer Res* (2016) **22**:2908–18. doi:10.1158/1078-0432.CCR-15-2412
27. Ollendorff V, Noguchi T, deLapeyriere O, Birnbaum D. The GARP gene encodes a new member of the family of leucine-rich repeat-containing proteins. *Cell Growth Differ* (1994) **5**:213–9.
28. Roubin R, Pizette S, Ollendorff V, Planche J, Birnbaum D, deLapeyriere O. Structure and developmental expression of mouse Garp, a gene encoding a new leucine-rich repeat-containing protein. *Int J Dev Biol* (1996) **40**:545–55.
29. Chan DV, Somani A-K, Young AB, Massari JV, Ohtola J, Sugiyama H, et al. Signal peptide cleavage is essential for surface expression of a regulatory T cell surface protein, leucine rich repeat containing 32 (LRRC32). *BMC Biochem* (2011) **12**:27. doi:10.1186/1471-2091-12-27
30. Haupt S, Söntgerath VS, Leipe J, Schulze-Koops H, Skapenko A. Methylation of an intragenic alternative promoter regulates transcription of GARP. *Biochim Biophys Acta* (2016) **1859**:223–34. doi:10.1016/j.bbagrm.2015.11.003
31. Zhou Q, Haupt S, Prots I, Thümmler K, Kremmer E, Lipsky PE, et al. miR-142-3p is involved in CD25+ CD4 T cell proliferation by

targeting the expression of glycoprotein A repetitions predominant. *J Immunol* (2013) **190**:6579–88. doi:10.4049/jimmunol.1202993

32. Tran DQ, Andersson J, Wang R, Ramsey H, Unutmaz D, Shevach EM. GARP (LRRC32) is essential for the surface expression of latent TGF-beta on platelets and activated FOXP3+ regulatory T cells. *Proc Natl Acad Sci U S A* (2009) **106**:13445–50. doi:10.1073/pnas.0901944106
33. Wang R, Wan Q, Kozhaya L, Fujii H, Unutmaz D. Identification of a regulatory T cell specific cell surface molecule that mediates suppressive signals and induces Foxp3 expression. *PLoS One* (2008) **3**:e2705. doi:10.1371/journal.pone.0002705
34. Stanic B, van de Veen W, Wirz OF, Rückert B, Morita H, Söllner S, et al. IL-10-overexpressing B cells regulate innate and adaptive immune responses. *J Allergy Clin Immunol* (2015) **135**:771-80.e8. doi:10.1016/j.jaci.2014.07.041
35. Dedobbeleer O, Stockis J, van der Woning B, Coulie PG, Lucas S. Cutting Edge: Active TGF-β1 Released from GARP/TGF-β1 Complexes on the Surface of Stimulated Human B Lymphocytes Increases Class-Switch Recombination and Production of IgA. *J Immunol* (2017) **199**:391–6. doi:10.4049/jimmunol.1601882.
36. Zhang M, Pan X, Fujiwara K, Jurcak N, Muth S, Zhou J, et al. Pancreatic cancer cells render tumor-associated macrophages metabolically reprogrammed by a GARP and DNA methylation-mediated mechanism. *Signal Transduct Target Ther* (2021) **6**:366. doi:10.1038/s41392-021-00769-z
37. Zimmer N, Krebs FK, Zimmer S, Mitzel-Rink H, Kumm EJ, Jurk K, et al. Platelet-Derived GARP Induces Peripheral Regulatory T Cells-Potential Impact on T Cell Suppression in Patients with Melanoma-Associated Thrombocytosis. *Cancers (Basel)* (2020) **12**. doi:10.3390/cancers12123653
38. Xing H, Liang C, Xu X, Sun H, Ma X, Jiang Z. Mesenchymal stroma/stem-like cells of GARP knockdown inhibits cell proliferation and invasion of mouse colon cancer cells (MC38) through exosomes. *J Cell Mol Med* (2020) **24**:13984–90. doi:10.1111/jcmm.16008
39. Li Y, Kim B-G, Qian S, Letterio JJ, Fung JJ, Lu L, et al. Hepatic Stellate Cells Inhibit T Cells through Active TGF-β1 from a Cell Surface-Bound Latent TGF-β1/GARP Complex. *J Immunol* (2015) **195**:2648–56. doi:10.4049/jimmunol.1500139
40. Probst-Kepper M, Geffers R, Kröger A, Viegas N, Erck C, Hecht H-J, et al. GARP: a key receptor controlling FOXP3 in human regulatory T cells. *J Cell Mol Med* (2009) **13**:3343–57. doi:10.1111/j.1582-4934.2009.00782.x
41. Zimmer N, Kim E, Sprang B, Leukel P, Khafaji F, Ringel F, et al. GARP as an Immune Regulatory Molecule in the Tumor Microenvironment of Glioblastoma Multiforme. *Int J Mol Sci* (2019) **20**. doi:10.3390/ijms20153676
42. Carrillo-Gálvez AB, Quintero JE, Rodríguez R, Menéndez ST, Victoria González M, Blanco-Lorenzo V, et al. GARP promotes the proliferation and therapeutic resistance of bone sarcoma cancer cells through the activation of TGF-β. *Cell Death Dis* (2020) **11**:985. doi:10.1038/s41419-020-03197-z
43. Hahn SA, Neuhoff A, Landsberg J, Schupp J, Eberts D, Leukel P, et al. A key role of GARP in the immune suppressive tumor microenvironment. *Oncotarget* (2016) **7**:42996–3009. doi:10.18632/oncotarget.9598
44. Derycke MS, Charbonneau B, Preston CC, Kalli KR, Knutson KL, Rider DN, et al. Toward

understanding the genetics of regulatory T cells in ovarian cancer. *Oncoimmunology* (2013) **2**:e24535. doi:10.4161/onci.24535

45. Ferreira MA, Matheson MC, Duffy DL, Marks GB, Hui J, Le Souëf P, et al. Identification of IL6R and chromosome 11q13.5 as risk loci for asthma. *Lancet* (2011) **378**:1006–14. doi:10.1016/S0140-6736(11)60874-X
46. Manz J, Rodríguez E, ElSharawy A, Oesau E-M, Petersen B-S, Baurecht H, et al. Targeted Resequencing and Functional Testing Identifies Low-Frequency Missense Variants in the Gene Encoding GARP as Significant Contributors to Atopic Dermatitis Risk. *J Invest Dermatol* (2016) **136**:2380–6. doi:10.1016/j.jid.2016.07.009
47. Nasrallah R, Imianowski CJ, Bossini-Castillo L, Grant FM, Dogan M, Placek L, et al. A distal enhancer at risk locus 11q13.5 promotes suppression of colitis by Treg cells. *Nature* (2020) **583**:447–52. doi:10.1038/s41586-020-2296-7
48. Wang R, Zhu J, Dong X, Shi M, Lu C, Springer TA. GARP regulates the bioavailability and activation of TGFβ. *Mol Biol Cell* (2012) **23**:1129–39. doi:10.1091/mbc.E11-12-1018
49. Sun L, Jin H, Li H. GARP: a surface molecule of regulatory T cells that is involved in the regulatory function and TGF-β releasing. *Oncotarget* (2016) **7**:42826–36. doi:10.18632/oncotarget.8753
50. Choi G, Na H, Kuen D-S, Kim B-S, Chung Y. Autocrine TGF-β1 Maintains the Stability of Foxp3+ Regulatory T Cells via IL-12Rβ2 Downregulation. *Biomolecules* (2020) **10**. doi:10.3390/biom10060819
51. Gordon KJ, Blobe GC. Role of transforming growth factor-beta superfamily signaling pathways in human disease. *Biochim Biophys Acta* (2008) **1782**:197–228. doi:10.1016/j.bbadis.2008.01.006
52. Wu BX, Li A, Lei L, Kaneko S, Wallace C, Li X, et al. Glycoprotein A repetitions predominant (GARP) positively regulates transforming growth factor (TGF) β3 and is essential for mouse palatogenesis. *J Biol Chem* (2017) **292**:18091–7. doi:10.1074/jbc.M117.797613
53. Stockis J, Colau D, Coulie PG, Lucas S. Membrane protein GARP is a receptor for latent TGF-beta on the surface of activated human Treg. *Eur J Immunol* (2009) **39**:3315–22. doi:10.1002/eji.200939684
54. Stockis J, Dedobbeleer O, Lucas S. Role of GARP in the activation of latent TGF-β1. *Mol Biosyst* (2017) **13**:1925–35. doi:10.1039/c7mb00251c
55. Metelli A, Wu BX, Fugle CW, Rachidi S, Sun S, Zhang Y, et al. Surface Expression of TGFβ Docking Receptor GARP Promotes Oncogenesis and Immune Tolerance in Breast Cancer. *Cancer Res* (2016) **76**:7106–17. doi:10.1158/0008-5472.CAN-16-1456
56. Gauthy E, Cuende J, Stockis J, Huygens C, Lethé B, Collet J-F, et al. GARP is regulated by miRNAs and controls latent TGF-β1 production by human regulatory T cells. *PLoS One* (2013) **8**:e76186. doi:10.1371/journal.pone.0076186
57. Derynck R, Budi EH. Specificity, versatility, and control of TGF-β family signaling. *Sci Signal* (2019) **12**. doi:10.1126/scisignal.aav5183
58. Annes JP, Munger JS, Rifkin DB. Making sense of latent TGFbeta activation. *J Cell Sci* (2003) **116**:217–24. doi:10.1242/jcs.00229
59. Edwards JP, Thornton AM, Shevach EM. Release of active TGF-β1 from the latent TGF-β1/GARP complex on T regulatory cells is mediated by integrin β8. *J Immunol* (2014) **193**:2843–9. doi:10.4049/jimmunol.1401102
60. Liénart S, Merceron R, Vanderaa C, Lambert F, Colau D, Stockis J, et al. Structural basis of latent TGF-β1 presentation and activation by GARP on human regulatory T cells. *Science*

(2018) **362**:952–6. doi:10.1126/science.aau2909

61. Wang R, Kozhaya L, Mercer F, Khaitan A, Fujii H, Unutmaz D. Expression of GARP selectively identifies activated human FOXP3+ regulatory T cells. *Proc Natl Acad Sci U S A* (2009) **106**:13439–44. doi:10.1073/pnas.0901965106
62. Elkord E, Abd Al Samid M, Chaudhary B. Helios, and not FoxP3, is the marker of activated Tregs expressing GARP/LAP. *Oncotarget* (2015) **6**:20026–36. doi:10.18632/oncotarget.4771
63. Lehmkuhl P, Gentz M, Garcia de Otezya AC, Grimbacher B, Schulze-Koops H, Skapenko A. Dysregulated immunity in PID patients with low GARP expression on Tregs due to mutations in LRRC32. *Cell Mol Immunol* (2021) **18**:1677–91. doi:10.1038/s41423-021-00701-z
64. Tao R, Zoeten EF de, Ozkaynak E, Chen C, Wang L, Porrett PM, et al. Deacetylase inhibition promotes the generation and function of regulatory T cells. *Nat Med* (2007) **13**:1299–307. doi:10.1038/nm1652
65. Pu M, Chen J, Tao Z, Miao L, Qi X, Wang Y, et al. Regulatory network of miRNA on its target: coordination between transcriptional and post-transcriptional regulation of gene expression. *Cell Mol Life Sci* (2019) **76**:441–51. doi:10.1007/s00018-018-2940-7
66. Jebbawi F, Fayyad-Kazan H, Merimi M, Lewalle P, Verougstraete J-C, Leo O, et al. A microRNA profile of human CD8(+) regulatory T cells and characterization of the effects of microRNAs on Treg cell-associated genes. *J Transl Med* (2014) **12**:218. doi:10.1186/s12967-014-0218-x
67. Liu C, Li N, Liu G. The Role of MicroRNAs in Regulatory T Cells. *J Immunol Res* (2020) **2020**:3232061. doi:10.1155/2020/3232061
68. Zhang Y, Wu BX, Metelli A, Thaxton JE, Hong F, Rachidi S, et al. GP96 is a GARP chaperone and controls regulatory T cell functions. *J Clin Invest* (2015) **125**:859–69. doi:10.1172/JCI79014
69. Duan X, Iwanowycz S, Ngoi S, Hill M, Zhao Q, Liu B. Molecular Chaperone GRP94/GP96 in Cancers: Oncogenesis and Therapeutic Target. *Front Oncol* (2021) **11**:629846. doi:10.3389/fonc.2021.629846
70. Zhou AX, Kozhaya L, Fujii H, Unutmaz D. GARP-TGF-β complexes negatively regulate regulatory T cell development and maintenance of peripheral CD4+ T cells in vivo. *J Immunol* (2013) **190**:5057–64. doi:10.4049/jimmunol.1300065
71. Edwards JP, Fujii H, Zhou AX, Creemers J, Unutmaz D, Shevach EM. Regulation of the expression of GARP/latent TGF-β1 complexes on mouse T cells and their role in regulatory T cell and Th17 differentiation. *J Immunol* (2013) **190**:5506–15. doi:10.4049/jimmunol.1300199
72. Qian W-J, Monroe ME, Liu T, Jacobs JM, Anderson GA, Shen Y, et al. Quantitative proteome analysis of human plasma following in vivo lipopolysaccharide administration using 16O/18O labeling and the accurate mass and time tag approach. *Mol Cell Proteomics* (2005) **4**:700–9. doi:10.1074/mcp.M500045-MCP200
73. Metelli A, Wu BX, Riesenberg B, Guglietta S, Huck JD, Mills C, et al. Thrombin contributes to cancer immune evasion via proteolysis of platelet-bound GARP to activate LTGF-β. *Sci Transl Med* (2020) **12**. doi:10.1126/scitranslmed.aay4860
74. Hahn SA, Stahl HF, Becker C, Correll A, Schneider F-J, Tuettenberg A, et al. Soluble GARP has potent antiinflammatory and immunomodulatory impact on human $CD4^+$ T

cells. *Blood* (2013) **122**:1182–91. doi:10.1182/blood-2012-12-474478

75. Fridrich S, Hahn SA, Linzmaier M, Felten M, Zwarg J, Lennerz V, et al. How Soluble GARP Enhances TGFβ Activation. *PLoS One* (2016) **11**:e0153290. doi:10.1371/journal.pone.0153290
76. Rappl G, Pabst S, Riemann D, Schmidt A, Wickenhauser C, Schütte W, et al. Regulatory T cells with reduced repressor capacities are extensively amplified in pulmonary sarcoid lesions and sustain granuloma formation. *Clin Immunol* (2011) **140**:71–83. doi:10.1016/j.clim.2011.03.015
77. Zhong Y, Tang H, Wang X, Zeng Q, Liu Y, Zhao XI, et al. Intranasal immunization with heat shock protein 60 induces CD4(+) CD25(+) GARP(+) and type 1 regulatory T cells and inhibits early atherosclerosis. *Clin Exp Immunol* (2016) **183**:452–68. doi:10.1111/cei.12726
78. Noyan F, Lee Y-S, Zimmermann K, Hardtke-Wolenski M, Taubert R, Warnecke G, et al. Isolation of human antigen-specific regulatory T cells with high suppressive function. *Eur J Immunol* (2014) **44**:2592–602. doi:10.1002/eji.201344381
79. Eschborn M, Weigmann B, Reissig S, Waisman A, Saloga J, Bellinghausen I. Activated glycoprotein A repetitions predominant (GARP)-expressing regulatory T cells inhibit allergen-induced intestinal inflammation in humanized mice. *J Allergy Clin Immunol* (2015) **136**:159–68. doi:10.1016/j.jaci.2015.04.020
80. Adriawan IR, Atschekzei F, Dittrich-Breiholz O, Garantziotis P, Hirsch S, Risser LM, et al. Novel aspects of regulatory T cell dysfunction as a therapeutic target in giant cell arteritis. *Ann Rheum Dis* (2022) **81**:124–31. doi:10.1136/annrheumdis-2021-220955
81. Wang H, Song H, Pham AV, Cooper LJ, Schulze JJ, Olek S, et al. Human LAP+GARP+FOXP3+ regulatory T cells attenuate xenogeneic graft versus host disease. *Theranostics* (2019) **9**:2315–24. doi:10.7150/thno.30254
82. Wallace CH, Wu BX, Salem M, Ansa-Addo EA, Metelli A, Sun S, et al. B lymphocytes confer immune tolerance via cell surface GARP-TGF-β complex. *JCI Insight* (2018) **3**. doi:10.1172/jci.insight.99863
83. Carrillo-Gálvez AB, Gálvez-Peisl S, González-Correa JE, Haro-Carrillo M de, Ayllón V, Carmona-Sáez P, et al. GARP is a key molecule for mesenchymal stromal cell responses to TGF-β and fundamental to control mitochondrial ROS levels. *Stem Cells Transl Med* (2020) **9**:636–50. doi:10.1002/sctm.19-0372
84. Carrillo-Galvez AB, Cobo M, Cuevas-Ocaña S, Gutiérrez-Guerrero A, Sánchez-Gilabert A, Bongarzone P, et al. Mesenchymal stromal cells express GARP/LRRC32 on their surface: effects on their biology and immunomodulatory capacity. *Stem Cells* (2015) **33**:183–95. doi:10.1002/stem.1821
85. Huong PT, Nguyen LT, Nguyen X-B, Lee SK, Bach D-H. The Role of Platelets in the Tumor-Microenvironment and the Drug Resistance of Cancer Cells. *Cancers (Basel)* (2019) **11**. doi:10.3390/cancers11020240
86. Yap ML, McFadyen JD, Wang X, Ziegler M, Chen Y-C, Willcox A, et al. Activated platelets in the tumor microenvironment for targeting of antibody-drug conjugates to tumors and metastases. *Theranostics* (2019) **9**:1154–69. doi:10.7150/thno.29146
87. McAllister SS, Weinberg RA. The tumour-induced systemic environment as a critical regulator of cancer progression and metastasis. *Nat Cell Biol* (2014) **16**:717–27. doi:10.1038/ncb3015

88. Camerer E, Qazi AA, Duong DN, Cornelissen I, Advincula R, Coughlin SR. Platelets, protease-activated receptors, and fibrinogen in hematogenous metastasis. *Blood* (2004) **104**:397–401. doi:10.1182/blood-2004-02-0434
89. Palumbo JS, Talmage KE, Massari JV, La Jeunesse CM, Flick MJ, Kombrinck KW, et al. Tumor cell-associated tissue factor and circulating hemostatic factors cooperate to increase metastatic potential through natural killer cell-dependent and-independent mechanisms. *Blood* (2007) **110**:133–41. doi:10.1182/blood-2007-01-065995
90. Karpatkin S, Pearlstein E, Ambrogio C, Coller BS. Role of adhesive proteins in platelet tumor interaction in vitro and metastasis formation in vivo. *J Clin Invest* (1988) **81**:1012–9. doi:10.1172/JCI113411
91. Sierko E, Wojtukiewicz MZ. Platelets and angiogenesis in malignancy. *Semin Thromb Hemost* (2004) **30**:95–108. doi:10.1055/s-2004-822974
92. Stone RL, Nick AM, McNeish IA, Balkwill F, Han HD, Bottsford-Miller J, et al. Paraneoplastic thrombocytosis in ovarian cancer. *N Engl J Med* (2012) **366**:610–8. doi:10.1056/NEJMoa1110352.
93. Schumacher D, Strilic B, Sivaraj KK, Wettschureck N, Offermanns S. Platelet-derived nucleotides promote tumor-cell transendothelial migration and metastasis via P2Y2 receptor. *Cancer Cell* (2013) **24**:130–7. doi:10.1016/j.ccr.2013.05.008
94. Leblanc R, Peyruchaud O. Metastasis: new functional implications of platelets and megakaryocytes. *Blood* (2016) **128**:24–31. doi:10.1182/blood-2016-01-636399
95. Cravioto-Villanueva A, Luna-Perez P, La Gutierrez-de Barrera M, Martinez-Gómez H, Maffuz A, Rojas-Garcia P, et al. Thrombocytosis as a predictor of distant recurrence in patients with rectal cancer. *Arch Med Res* (2012) **43**:305–11. doi:10.1016/j.arcmed.2012.06.008
96. Honn KV, Tang D. Hemostasis and malignancy: an overview. *Cancer Metastasis Rev* (1992) **11**:223–6. doi:10.1007/BF01307178
97. Kim E-S, Kim M-S, Moon A. Transforming growth factor (TGF)-beta in conjunction with H-ras activation promotes malignant progression of MCF10A breast epithelial cells. *Cytokine* (2005) **29**:84–91. doi:10.1016/j.cyto.2004.10.001
98. Guo S-W, Du Y, Liu X. Platelet-derived TGF-β1 mediates the down-modulation of NKG2D expression and may be responsible for impaired natural killer (NK) cytotoxicity in women with endometriosis. *Hum Reprod* (2016) **31**:1462–74. doi:10.1093/humrep/dew057
99. Vermeersch E, Denorme F, Maes W, Meyer SF de, Vanhoorelbeke K, Edwards J, et al. The role of platelet and endothelial GARP in thrombosis and hemostasis. *PLoS One* (2017) **12**:e0173329. doi:10.1371/journal.pone.0173329
100. Szepetowski P, Ollendorff V, Grosgeorge J, Courseaux A, Birnbaum D, Theillet C, et al. DNA amplification at 11q13.5-q14 in human breast cancer. *Oncogene* (1992) **7**:2513–7.
101. Jin H, Sun L, Tang L, Yu W, Li H. Expression of GARP Is Increased in Tumor-Infiltrating Regulatory T Cells and Is Correlated to Clinicopathology of Lung Cancer Patients. *Front Immunol* (2017) **8**:138. doi:10.3389/fimmu.2017.00138
102. Zhang L, Xu J, Zhang X, Zhang Y, Wang L, Huang X, et al. The Role of Tumoral FOXP3 on Cell Proliferation, Migration, and Invasion in Gastric Cancer. *Cell Physiol Biochem* (2017) **42**:1739–54. doi:10.1159/000479442
103. Karanikas V, Speletas M, Zamanakou M, Kalala F, Loules G, Kerenidi T, et al. Foxp3

expression in human cancer cells. *J Transl Med* (2008) **6**:19. doi:10.1186/1479-5876-6-19

104. Li R, Sun J, Yang F, Sun Y, Wu X, Zhou Q, et al. Effect of GARP on osteogenic differentiation of bone marrow mesenchymal stem cells via the regulation of TGFβ1 in vitro. *PeerJ* (2019) **7**:e6993. doi:10.7717/peerj.6993
105. Wen PY, Packer RJ. The 2021 WHO Classification of Tumors of the Central Nervous System: clinical implications. *Neuro Oncol* (2021) **23**:1215–7. doi:10.1093/neuonc/noab120
106. Goodman CC. *Pathology: Implications for the physical therapist*. St. Louis, Mo: Saunders (2009). 1738 p.
107. Holland EC. Glioblastoma multiforme: the terminator. *Proc Natl Acad Sci U S A* (2000) **97**:6242–4. doi:10.1073/pnas.97.12.6242
108. Stupp R, Tonn J-C, Brada M, Pentheroudakis G. High-grade malignant glioma: ESMO Clinical Practice Guidelines for diagnosis, treatment and follow-up. *Ann Oncol* (2010) **21 Suppl 5**:v190-3. doi:10.1093/annonc/mdq187
109. Lam S, Lin Y, Zinn P, Su J, Pan I-W. Patient and treatment factors associated with survival among pediatric glioblastoma patients: A Surveillance, Epidemiology, and End Results study. *J Clin Neurosci* (2018) **47**:285–93. doi:10.1016/j.jocn.2017.10.041
110. Ghosh M, Shubham S, Mandal K, Trivedi V, Chauhan R, Naseera S. Survival and prognostic factors for glioblastoma multiforme: Retrospective single-institutional study. *Indian J Cancer* (2017) **54**:362–7. doi:10.4103/ijc.IJC_157_17
111. Li K, Lu D, Guo Y, Wang C, Liu X, Liu Y, et al. Trends and patterns of incidence of diffuse glioma in adults in the United States, 1973-2014. *Cancer Med* (2018) **7**:5281–90. doi:10.1002/cam4.1757
112. Tian M, Ma W, Chen Y, Yu Y, Zhu D, Shi J, et al. Impact of gender on the survival of patients with glioblastoma. *Biosci Rep* (2018) **38**. doi:10.1042/BSR20180752
113. Gittleman H, Boscia A, Ostrom QT, Truitt G, Fritz Y, Kruchko C, et al. Survivorship in adults with malignant brain and other central nervous system tumor from 2000-2014. *Neuro Oncol* (2018) **20**:vii6-vii16. doi:10.1093/neuonc/noy090
114. Ostrom QT, Price M, Neff C, Cioffi G, Waite KA, Kruchko C, et al. CBTRUS Statistical Report: Primary Brain and Other Central Nervous System Tumors Diagnosed in the United States in 2016-2020. *Neuro Oncol* (2023) **25**:iv1-iv99. doi:10.1093/neuonc/noad149
115. Fukushima T, Favereaux A, Huang H, Shimizu T, Yonekawa Y, Nakazato Y, et al. Genetic alterations in primary glioblastomas in Japan. *J Neuropathol Exp Neurol* (2006) **65**:12–8. doi:10.1097/01.jnen.0000196132.66464.96
116. Philips A, Henshaw DL, Lamburn G, O'Carroll MJ. Brain Tumours: Rise in Glioblastoma Multiforme Incidence in England 1995-2015 Suggests an Adverse Environmental or Lifestyle Factor. *J Environ Public Health* (2018) **2018**:7910754. doi:10.1155/2018/7910754
117. Benke G, Turner MC, Fleming S, Figuerola J, Kincl L, Richardson L, et al. Occupational solvent exposure and risk of glioma in the INTEROCC study. *Br J Cancer* (2017) **117**:1246–54. doi:10.1038/bjc.2017.285
118. Parent M-E, Turner MC, Lavoué J, Richard H, Figuerola J, Kincl L, et al. Lifetime occupational exposure to metals and welding fumes, and risk of glioma: a 7-country population-based case-control study. *Environ Health* (2017) **16**:90. doi:10.1186/s12940-017-0300-y
119. Yang M, Guo W, Yang C, Tang J, Huang Q, Feng S, et al. Mobile phone use and glioma risk: A systematic review and meta-analysis. *PLoS*

One (2017) **12**:e0175136. doi:10.1371/journal.pone.0175136

120. Karipidis K, Elwood M, Benke G, Sanagou M, Tjong L, Croft RJ. Mobile phone use and incidence of brain tumour histological types, grading or anatomical location: a population-based ecological study. *BMJ Open* (2018) **8**:e024489. doi:10.1136/bmjopen-2018-024489
121. Repacholi MH, Lerchl A, Röösli M, Sienkiewicz Z, Auvinen A, Breckenkamp J, et al. Systematic review of wireless phone use and brain cancer and other head tumors. *Bioelectromagnetics* (2012) **33**:187–206. doi:10.1002/bem.20716
122. Rice T, Lachance DH, Molinaro AM, Eckel-Passow JE, Walsh KM, Barnholtz-Sloan J, et al. Understanding inherited genetic risk of adult glioma - a review. *Neurooncol Pract* (2016) **3**:10–6. doi:10.1093/nop/npv026
123. Gilard V, Tebani A, Dabaj I, Laquerrière A, Fontanilles M, Derrey S, et al. Diagnosis and Management of Glioblastoma: A Comprehensive Perspective. *J Pers Med* (2021) **11**. doi:10.3390/jpm11040258.
124. Wingren C, James P, Borrebaeck CA. Strategy for surveying the proteome using affinity proteomics and mass spectrometry. *Proteomics* (2009) **9**:1511–7. doi:10.1002/pmic.200800802
125. Yamanaka R, Hayano A, Kanayama T. Radiation-induced gliomas: a comprehensive review and meta-analysis. *Neurosurg Rev* (2018) **41**:719–31. doi:10.1007/s10143-016-0786-8
126. Yuile P, Dent O, Cook R, Biggs M, Little N. Survival of glioblastoma patients related to presenting symptoms, brain site and treatment variables. *J Clin Neurosci* (2006) **13**:747–51. doi:10.1016/j.jocn.2005.10.011
127. Vecht CJ, Kerkhof M, Duran-Pena A. Seizure prognosis in brain tumors: new insights and evidence-based management. *Oncologist* (2014) **19**:751–9. doi:10.1634/theoncologist.2014-0060
128. Wirsching H-G, Galanis E, Weller M. Glioblastoma. *Handb Clin Neurol* (2016) **134**:381–97. doi:10.1016/b978-0-12-802997-8.00023-2
129. Yan J-L, Li C, Boonzaier NR, Fountain DM, Larkin TJ, Matys T, et al. Multimodal MRI characteristics of the glioblastoma infiltration beyond contrast enhancement. *Ther Adv Neurol Disord* (2019) **12**:1756286419844664. doi:10.1177/1756286419844664
130. Stupp R, Brada M, van den Bent MJ, Tonn J-C, Pentheroudakis G. High-grade glioma: ESMO Clinical Practice Guidelines for diagnosis, treatment and follow-up. *Ann Oncol* (2014) **25 Suppl 3**:iii93-101. doi:10.1093/annonc/mdu050
131. Garofano L, Migliozzi S, Oh YT, D'Angelo F, Najac RD, Ko A, et al. Pathway-based classification of glioblastoma uncovers a mitochondrial subtype with therapeutic vulnerabilities. *Nat Cancer* (2021) **2**:141–56. doi:10.1038/s43018-020-00159-4
132. Teo W-Y, Sekar K, Seshachalam P, Shen J, Chow W-Y, Lau CC, et al. Relevance of a TCGA-derived Glioblastoma Subtype Gene-Classifier among Patient Populations. *Sci Rep* (2019) **9**:7442. doi:10.1038/s41598-019-43173-y.
133. Verhaak RG, Hoadley KA, Purdom E, Wang V, Qi Y, Wilkerson MD, et al. Integrated genomic analysis identifies clinically relevant subtypes of glioblastoma characterized by abnormalities in PDGFRA, IDH1, EGFR, and NF1. *Cancer Cell* (2010) **17**:98–110. doi:10.1016/j.ccr.2009.12.020.
134. Murugan AK, Alzahrani AS. Isocitrate Dehydrogenase IDH1 and IDH2 Mutations in Human Cancer: Prognostic Implications for Gliomas. *Br J Biomed Sci* (2022) **79**:10208. doi:10.3389/bjbs.2021.10208

135. Miller JJ, Gonzalez Castro LN, McBrayer S, Weller M, Cloughesy T, Portnow J, et al. Isocitrate dehydrogenase (IDH) mutant gliomas: A Society for Neuro-Oncology (SNO) consensus review on diagnosis, management, and future directions. *Neuro Oncol* (2023) **25**:4–25. doi:10.1093/neuonc/noac207
136. Melhem JM, Detsky J, Lim-Fat MJ, Perry JR. Updates in IDH-Wildtype Glioblastoma. *Neurotherapeutics* (2022) **19**:1705–23. doi:10.1007/s13311-022-01251-6
137. Hegi ME, Diserens A-C, Gorlia T, Hamou M-F, Tribolet N de, Weller M, et al. MGMT gene silencing and benefit from temozolomide in glioblastoma. *N Engl J Med* (2005) **352**:997–1003. doi:10.1056/NEJMoa043331
138. Maire CL, Ligon KL. Molecular pathologic diagnosis of epidermal growth factor receptor. *Neuro Oncol* (2014) **16 Suppl 8**:viii1-6. doi:10.1093/neuonc/nou294
139. Brennan CW, Verhaak RG, McKenna A, Campos B, Noushmehr H, Salama SR, et al. The somatic genomic landscape of glioblastoma. *Cell* (2013) **155**:462–77. doi:10.1016/j.cell.2013.09.034.
140. Shinojima N, Tada K, Shiraishi S, Kamiryo T, Kochi M, Nakamura H, et al. Prognostic value of epidermal growth factor receptor in patients with glioblastoma multiforme. *Cancer Res* (2003) **63**:6962–70.
141. Jutten B, Keulers TG, Peeters HJ, Schaaf MB, Savelkouls KG, Compter I, et al. EGFRvIII expression triggers a metabolic dependency and therapeutic vulnerability sensitive to autophagy inhibition. *Autophagy* (2018) **14**:283–95. doi:10.1080/15548627.2017.1409926
142. Theys J, Jutten B, Dubois L, Rouschop KM, Chiu RK, Li Y, et al. The deletion mutant EGFRvIII significantly contributes to stress resistance typical for the tumour microenvironment. *Radiother Oncol* (2009) **92**:399–404. doi:10.1016/j.radonc.2009.06.017
143. Heddleston JM, Li Z, McLendon RE, Hjelmeland AB, Rich JN. The hypoxic microenvironment maintains glioblastoma stem cells and promotes reprogramming towards a cancer stem cell phenotype. *Cell Cycle* (2009) **8**:3274–84. doi:10.4161/cc.8.20.9701
144. Choi SW, Lee Y, Shin K, Koo H, Kim D, Sa JK, et al. Mutation-specific non-canonical pathway of PTEN as a distinct therapeutic target for glioblastoma. *Cell Death Dis* (2021) **12**:374. doi:10.1038/s41419-021-03657-0
145. Tran B, Rosenthal MA. Survival comparison between glioblastoma multiforme and other incurable cancers. *J Clin Neurosci* (2010) **17**:417–21. doi:10.1016/j.jocn.2009.09.004
146. Ohka F, Natsume A, Wakabayashi T. Current trends in targeted therapies for glioblastoma multiforme. *Neurol Res Int* (2012) **2012**:878425. doi:10.1155/2012/878425
147. Di L, Shah AH, Mahavadi A, Eichberg DG, Reddy R, Sanjurjo AD, et al. Radical supramaximal resection for newly diagnosed left-sided eloquent glioblastoma: safety and improved survival over gross-total resection. *J Neurosurg* (2023) **138**:62–9. doi:10.3171/2022.3.JNS212399
148. Que T, Huang G, Tan J-E, Zhang P, Li Z, Yi G, et al. Supramaximal resection based on en-bloc technique reduces tumor burden and prolongs survival in primary supratentorial lobar glioblastoma. *J Neurooncol* (2023) **164**:557–68. doi:10.1007/s11060-023-04399-z
149. Mier-García JF, Ospina-Santa S, Orozco-Mera J, Ma R, Plaha P. Supramaximal versus gross total resection in Glioblastoma, IDH wild-type and Astrocytoma, IDH-mutant, grade 4, effect on overall and progression free survival: systematic review and meta-analysis. *J*

Neurooncol (2023) **164**:31–41. doi:10.1007/s11060-023-04409-0

150. Roh TH, Kang S-G, Moon JH, Sung KS, Park HH, Kim SH, et al. Survival benefit of lobectomy over gross-total resection without lobectomy in cases of glioblastoma in the noneloquent area: a retrospective study. *J Neurosurg* (2019) **132**:895–901. doi:10.3171/2018.12.JNS182558
151. Compter I, Eekers DB, Hoeben A, Rouschop KM, Reymen B, Ackermans L, et al. Chloroquine combined with concurrent radiotherapy and temozolomide for newly diagnosed glioblastoma: a phase IB trial. *Autophagy* (2021) **17**:2604–12. doi:10.1080/15548627.2020.1816343
152. Chen J, Li Y, Yu T-S, McKay RM, Burns DK, Kernie SG, et al. A restricted cell population propagates glioblastoma growth after chemotherapy. *Nature* (2012) **488**:522–6. doi:10.1038/nature11287
153. Bao S, Wu Q, McLendon RE, Hao Y, Shi Q, Hjelmeland AB, et al. Glioma stem cells promote radioresistance by preferential activation of the DNA damage response. *Nature* (2006) **444**:756–60. doi:10.1038/nature05236
154. Jakovlevs A, Vanags A, Gardovskis J, Strumfa I. Molecular classification of diffuse gliomas. *Pol J Pathol* (2019) **70**:246–58. doi:10.5114/pjp.2019.93126
155. Popova SN, Bergqvist M, Dimberg A, Edqvist P-H, Ekman S, Hesselager G, et al. Subtyping of gliomas of various WHO grades by the application of immunohistochemistry. *Histopathology* (2014) **64**:365–79. doi:10.1111/his.12252
156. Biserova K, Jakovlevs A, Uljanovs R, Strumfa I. Cancer Stem Cells: Significance in Origin, Pathogenesis and Treatment of Glioblastoma. *Cells* (2021) **10**. doi:10.3390/cells10030621
157. Āboliņš A, Vanags A, Trofimovičs G, Miklaševičs E, Gardovskis J, Štrumfa I. Molecular subtype shift in breast cancer upon trastuzumab treatment: a case report. *Pol J Pathol* (2011) **62**:65–8.
158. Guardia GD, Correa BR, Araujo PR, Qiao M, Burns S, Penalva LO, et al. Proneural and mesenchymal glioma stem cells display major differences in splicing and lncRNA profiles. *NPJ Genom Med* (2020) **5**:2. doi:10.1038/s41525-019-0108-5
159. Lathia JD, Mack SC, Mulkearns-Hubert EE, Valentim CL, Rich JN. Cancer stem cells in glioblastoma. *Genes Dev* (2015) **29**:1203–17. doi:10.1101/gad.261982.115
160. Eramo A, Ricci-Vitiani L, Zeuner A, Pallini R, Lotti F, Sette G, et al. Chemotherapy resistance of glioblastoma stem cells. *Cell Death Differ* (2006) **13**:1238–41. doi:10.1038/sj.cdd.4401872
161. Nizet V, Johnson RS. Interdependence of hypoxic and innate immune responses. *Nat Rev Immunol* (2009) **9**:609–17. doi:10.1038/nri2607
162. Carruthers RD, Ahmed SU, Ramachandran S, Strathdee K, Kurian KM, Hedley A, et al. Replication Stress Drives Constitutive Activation of the DNA Damage Response and Radioresistance in Glioblastoma Stem-like Cells. *Cancer Res* (2018) **78**:5060–71. doi:10.1158/0008-5472.CAN-18-0569
163. Wei J, Barr J, Kong L-Y, Wang Y, Wu A, Sharma AK, et al. Glioblastoma cancer-initiating cells inhibit T-cell proliferation and effector responses by the signal transducers and activators of transcription 3 pathway. *Mol Cancer Ther* (2010) **9**:67–78. doi:10.1158/1535-7163.MCT-09-0734
164. Wu A, Wei J, Kong L-Y, Wang Y, Priebe W, Qiao W, et al. Glioma cancer stem cells induce immunosuppressive macrophages/microglia.

Neuro Oncol (2010) **12**:1113–25. doi:10.1093/neuonc/noq082

165. Liu G, Yuan X, Zeng Z, Tunici P, Ng H, Abdulkadir IR, et al. Analysis of gene expression and chemoresistance of CD133+ cancer stem cells in glioblastoma. *Mol Cancer* (2006) **5**:67. doi:10.1186/1476-4598-5-67
166. Ahmed SI, Javed G, Laghari AA, Bareeqa SB, Farrukh S, Zahid S, et al. CD133 Expression in Glioblastoma Multiforme: A Literature Review. *Cureus* (2018) **10**:e3439. doi:10.7759/cureus.3439
167. Chen R, Nishimura MC, Bumbaca SM, Kharbanda S, Forrest WF, Kasman IM, et al. A hierarchy of self-renewing tumor-initiating cell types in glioblastoma. *Cancer Cell* (2010) **17**:362–75. doi:10.1016/j.ccr.2009.12.049
168. Annovazzi L, Mellai M, Schiffer D. Chemotherapeutic Drugs: DNA Damage and Repair in Glioblastoma. *Cancers (Basel)* (2017) **9**. doi:10.3390/cancers9060057
169. Beier D, Schulz JB, Beier CP. Chemoresistance of glioblastoma cancer stem cells--much more complex than expected. *Mol Cancer* (2011) **10**:128. doi:10.1186/1476-4598-10-128
170. Beier D, Röhrl S, Pillai DR, Schwarz S, Kunz-Schughart LA, Leukel P, et al. Temozolomide preferentially depletes cancer stem cells in glioblastoma. *Cancer Res* (2008) **68**:5706–15. doi:10.1158/0008-5472.CAN-07-6878
171. Todorova PK, Mukherjee B, Burma S. MET signaling promotes DNA repair and radiation resistance in glioblastoma stem-like cells. *Ann Transl Med* (2017) **5**:61. doi:10.21037/atm.2017.01.67
172. Gherardi E, Birchmeier W, Birchmeier C, Vande Woude G. Targeting MET in cancer: rationale and progress. *Nat Rev Cancer* (2012) **12**:89–103. doi:10.1038/nrc3205
173. Bacco F de, D'Ambrosio A, Casanova E, Orzan F, Neggia R, Albano R, et al. MET inhibition overcomes radiation resistance of glioblastoma stem-like cells. *EMBO Mol Med* (2016) **8**:550–68. doi:10.15252/emmm.201505890
174. Chen J, McKay RM, Parada LF. Malignant glioma: lessons from genomics, mouse models, and stem cells. *Cell* (2012) **149**:36–47. doi:10.1016/j.cell.2012.03.009
175. Knudsen AM, Halle B, Cédile O, Burton M, Baun C, Thisgaard H, et al. Surgical resection of glioblastomas induces pleiotrophin-mediated self-renewal of glioblastoma stem cells in recurrent tumors. *Neuro Oncol* (2022) **24**:1074–87. doi:10.1093/neuonc/noab302
176. Fan X, Khaki L, Zhu TS, Soules ME, Talsma CE, Gul N, et al. NOTCH pathway blockade depletes CD133-positive glioblastoma cells and inhibits growth of tumor neurospheres and xenografts. *Stem Cells* (2010) **28**:5–16. doi:10.1002/stem.254
177. Jhaveri N, Chen TC, Hofman FM. Tumor vasculature and glioma stem cells: Contributions to glioma progression. *Cancer Lett* (2016) **380**:545–51. doi:10.1016/j.canlet.2014.12.028
178. Qiang L, Wu T, Zhang H-W, Lu N, Hu R, Wang Y-J, et al. HIF-1α is critical for hypoxia-mediated maintenance of glioblastoma stem cells by activating Notch signaling pathway. *Cell Death Differ* (2012) **19**:284–94. doi:10.1038/cdd.2011.95
179. Serocki M, Bartoszewska S, Janaszak-Jasiecka A, Ochocka RJ, Collawn JF, Bartoszewski R. miRNAs regulate the HIF switch during hypoxia: a novel therapeutic target. *Angiogenesis* (2018) **21**:183–202. doi:10.1007/s10456-018-9600-2
180. Troise D, Infante B, Mercuri S, Netti GS, Ranieri E, Gesualdo L, et al. Hypoxic State of Cells and Immunosenescence: A Focus on the Role of the HIF Signaling Pathway. *Biomedicines* (2023) **11**. doi:10.3390/biomedicines11082163

181. Cheng L, Huang Z, Zhou W, Wu Q, Donnola S, Liu JK, et al. Glioblastoma stem cells generate vascular pericytes to support vessel function and tumor growth. *Cell* (2013) **153**:139–52. doi:10.1016/j.cell.2013.02.021
182. Breznik B, Limbaeck Stokin C, Kos J, Khurshed M, Hira VV, Bošnjak R, et al. Cysteine cathepsins B, X and K expression in peri-arteriolar glioblastoma stem cell niches. *J Mol Histol* (2018) **49**:481–97. doi:10.1007/s10735-018-9787-y
183. Colwell N, Larion M, Giles AJ, Seldomridge AN, Sizdahkhani S, Gilbert MR, et al. Hypoxia in the glioblastoma microenvironment: shaping the phenotype of cancer stem-like cells. *Neuro Oncol* (2017) **19**:887–96. doi:10.1093/neuonc/now258
184. Nakamura H, Makino Y, Okamoto K, Poellinger L, Ohnuma K, Morimoto C, et al. TCR engagement increases hypoxia-inducible factor-1 alpha protein synthesis via rapamycin-sensitive pathway under hypoxic conditions in human peripheral T cells. *J Immunol* (2005) **174**:7592–9. doi:10.4049/jimmunol.174.12.7592
185. Doedens AL, Phan AT, Stradner MH, Fujimoto JK, Nguyen JV, Yang E, et al. Hypoxia-inducible factors enhance the effector responses of CD8(+) T cells to persistent antigen. *Nat Immunol* (2013) **14**:1173–82. doi:10.1038/ni.2714
186. Chen J. HIF1α or HIF2α: Enhancing CD8+ T-cell Fitness for Antitumor Immunity. *Cancer Immunol Res* (2021) **9**:364. doi:10.1158/2326-6066.CIR-21-0114
187. Tran CW, Gold MJ, Garcia-Batres C, Tai K, Elford AR, Himmel ME, et al. Hypoxia-inducible factor 1 alpha limits dendritic cell stimulation of CD8 T cell immunity. *PLoS One* (2020) **15**:e0244366. doi:10.1371/journal.pone.0244366
188. Roman J, Rangasamy T, Guo J, Sugunan S, Meednu N, Packirisamy G, et al. T-cell activation under hypoxic conditions enhances IFN-gamma secretion. *Am J Respir Cell Mol Biol* (2010) **42**:123–8. doi:10.1165/rcmb.2008-0139OC
189. Hanahan D, Weinberg RA. Hallmarks of cancer: the next generation. *Cell* (2011) **144**:646–74. doi:10.1016/j.cell.2011.02.013
190. Fischer U, Radermacher J, Mayer J, Mehraein Y, Meese E. Tumor hypoxia: Impact on gene amplification in glioblastoma. *Int J Oncol* (2008) **33**:509–15.
191. Binello E, Germano IM. Targeting glioma stem cells: a novel framework for brain tumors. *Cancer Sci* (2011) **102**:1958–66. doi:10.1111/j.1349-7006.2011.02064.x
192. Li Z, Bao S, Wu Q, Wang H, Eyler C, Sathornsumetee S, et al. Hypoxia-inducible factors regulate tumorigenic capacity of glioma stem cells. *Cancer Cell* (2009) **15**:501–13. doi:10.1016/j.ccr.2009.03.018
193. Kathagen A, Schulte A, Balcke G, Phillips HS, Martens T, Matschke J, et al. Hypoxia and oxygenation induce a metabolic switch between pentose phosphate pathway and glycolysis in glioma stem-like cells. *Acta Neuropathol* (2013) **126**:763–80. doi:10.1007/s00401-013-1173-y
194. Glumac PM, LeBeau AM. The role of CD133 in cancer: a concise review. *Clin Transl Med* (2018) **7**:18. doi:10.1186/s40169-018-0198-1
195. Weigmann A, Corbeil D, Hellwig A, Huttner WB. Prominin, a novel microvilli-specific polytopic membrane protein of the apical surface of epithelial cells, is targeted to plasmalemmal protrusions of non-epithelial cells. *Proc Natl Acad Sci U S A* (1997) **94**:12425–30. doi:10.1073/pnas.94.23.12425
196. Kang M-K, Kang S-K. Tumorigenesis of chemotherapeutic drug-resistant cancer stem-like cells in brain glioma. *Stem Cells Dev*

(2007) **16**:837–47. doi:10.1089/scd.2007.0006

197. Ludwig K, Kornblum HI. Molecular markers in glioma. *J Neurooncol* (2017) **134**:505–12. doi:10.1007/s11060-017-2379-y

198. Ding Q, Miyazaki Y, Tsukasa K, Matsubara S, Yoshimitsu M, Takao S. CD133 facilitates epithelial-mesenchymal transition through interaction with the ERK pathway in pancreatic cancer metastasis. *Mol Cancer* (2014) **13**:15. doi:10.1186/1476-4598-13-15

199. Stupp R, Mason WP, van den Bent MJ, Weller M, Fisher B, Taphoorn MJ, et al. Radiotherapy plus concomitant and adjuvant temozolomide for glioblastoma. *New England Journal of Medicine* (2005) **352**:987–96. doi:10.1056/NEJMoa043330

200. Perea F, Bernal M, Sánchez-Palencia A, Carretero J, Torres C, Bayarri C, et al. The absence of HLA class I expression in non-small cell lung cancer correlates with the tumor tissue structure and the pattern of T cell infiltration. *Int J Cancer* (2017) **140**:888–99. doi:10.1002/ijc.30489

201. Nduom EK, Weller M, Heimberger AB. Immunosuppressive mechanisms in glioblastoma. *Neuro Oncol* (2015) **17 Suppl 7**:vii9-vii14. doi:10.1093/neuonc/nov151

202. Guo S-K, Shen M-F, Yao H-W, Liu Y-S. Enhanced Expression of TGFBI Promotes the Proliferation and Migration of Glioma Cells. *Cell Physiol Biochem* (2018) **49**:1097–109. doi:10.1159/000493293

203. Ahmad F, Mani J, Kumar P, Haridas S, Upadhyay P, Bhaskar S. Activation of anti-tumor immune response and reduction of regulatory T cells with Mycobacterium indicus pranii (MIP) therapy in tumor bearing mice. *PLoS One* (2011) **6**:e25424. doi:10.1371/journal.pone.0025424

204. Tucci M, Stucci S, Passarelli A, Giudice G, Dammacco F, Silvestris F. The immune escape in melanoma: role of the impaired dendritic cell function. *Expert Rev Clin Immunol* (2014) **10**:1395–404. doi:10.1586/1744666X.2014.955851

205. Umansky V, Sevko A. Melanoma-induced immunosuppression and its neutralization. *Semin Cancer Biol* (2012) **22**:319–26. doi:10.1016/j.semcancer.2012.02.003

206. Bencheikh L, Diop MK, Rivière J, Imanci A, Pierron G, Souquere S, et al. Dynamic gene regulation by nuclear colony-stimulating factor 1 receptor in human monocytes and macrophages. *Nature Communications* (2019) **10**:1935. doi:10.1038/s41467-019-09970-9

207. Groot JF de, Piao Y, Tran H, Gilbert M, Wu H-K, Liu J, et al. Myeloid biomarkers associated with glioblastoma response to anti-VEGF therapy with aflibercept. *Clin Cancer Res* (2011) **17**:4872–81. doi:10.1158/1078-0432.CCR-11-0271

208. Ilhan-Mutlu A, Wagner L, Wöhrer A, Jungwirth S, Marosi C, Fischer P, et al. Blood alterations preceding clinical manifestation of glioblastoma. *Cancer Invest* (2012) **30**:625–9. doi:10.3109/07357907.2012.725443

209. Weller M, Cloughesy T, Perry JR, Wick W. Standards of care for treatment of recurrent glioblastoma--are we there yet? *Neuro Oncol* (2013) **15**:4–27. doi:10.1093/neuonc/nos273.

210. Seystahl K, Wick W, Weller M. Therapeutic options in recurrent glioblastoma--An update. *Crit Rev Oncol Hematol* (2016) **99**:389–408. doi:10.1016/j.critrevonc.2016.01.018

211. Han J, Alvarez-Breckenridge CA, Wang Q-E, Yu J. TGF-β signaling and its targeting for glioma treatment. *Am J Cancer Res* (2015) **5**:945–55.

212. Lim M, Xia Y, Bettegowda C, Weller M. Current state of immunotherapy for glioblastoma. *Nat Rev Clin Oncol* (2018) **15**:422–42. doi:10.1038/s41571-018-0003-5

213. Xue S, Hu M, Iyer V, Yu J. Blocking the PD-1/PD-L1 pathway in glioma: a potential new

treatment strategy. *J Hematol Oncol* (2017) **10**:81. doi:10.1186/s13045-017-0455-6

214. Barrantes-Freer A, Kim E, Bielanska J, Giese A, Mortensen LS, Schulz-Schaeffer WJ, et al. Human glioma-initiating cells show a distinct immature phenotype resembling but not identical to NG2 glia. *J Neuropathol Exp Neurol* (2013) **72**:307–24. doi:10.1097/NEN.0b013e31828afdbd

215. Barrantes-Freer A, Renovanz M, Eich M, Braukmann A, Sprang B, Spirin P, et al. CD133 Expression Is Not Synonymous to Immunoreactivity for AC133 and Fluctuates throughout the Cell Cycle in Glioma Stem-Like Cells. *PLoS One* (2015) **10**:e0130519. doi:10.1371/journal.pone.0130519

216. Fischer U, Kim E, Keller A, Meese E. Specific amplifications and copy number decreases during human neural stem cells differentiation towards astrocytes, neurons and oligodendrocytes. *Oncotarget* (2017) **8**:25872–84. doi:10.18632/oncotarget.15980

217. Kotecha N, Krutzik PO, Irish JM. Web-based analysis and publication of flow cytometry experiments. *Current Protocols in Cytometry* (2010) **Chapter 10**:Unit10.17. doi:10.1002/0471142956.cy1017s53

218. Rueden CT, Schindelin J, Hiner MC, DeZonia BE, Walter AE, Arena ET, et al. ImageJ2: ImageJ for the next generation of scientific image data. *BMC Bioinformatics* (2017) **18**:529. doi:10.1186/s12859-017-1934-z

219. Günther HS, Schmidt NO, Phillips HS, Kemming D, Kharbanda S, Soriano R, et al. Glioblastoma-derived stem cell-enriched cultures form distinct subgroups according to molecular and phenotypic criteria. *Oncogene* (2008) **27**:2897–909. doi:10.1038/sj.onc.1210949

220. Singh SK, Hawkins C, Clarke ID, Squire JA, Bayani J, Hide T, et al. Identification of human brain tumour initiating cells. *Nature* (2004) **432**:396–401. doi:10.1038/nature03128

221. Lee J, Kotliarova S, Kotliarov Y, Li A, Su Q, Donin NM, et al. Tumor stem cells derived from glioblastomas cultured in bFGF and EGF more closely mirror the phenotype and genotype of primary tumors than do serum-cultured cell lines. *Cancer Cell* (2006) **9**:391–403. doi:10.1016/j.ccr.2006.03.030

222. Son MJ, Woolard K, Nam D-H, Lee J, Fine HA. SSEA-1 is an enrichment marker for tumor-initiating cells in human glioblastoma. *Cell Stem Cell* (2009) **4**:440–52. doi:10.1016/j.stem.2009.03.003

223. Beier D, Hau P, Proescholdt M, Lohmeier A, Wischhusen J, Oefner PJ, et al. CD133(+) and CD133(-) glioblastoma-derived cancer stem cells show differential growth characteristics and molecular profiles. *Cancer Res* (2007) **67**:4010–5. doi:10.1158/0008-5472.CAN-06-4180

224. Ogden AT, Waziri AE, Lochhead RA, Fusco D, Lopez K, Ellis JA, et al. Identification of A2B5+CD133- tumor-initiating cells in adult human gliomas. *Neurosurgery* (2008) **62**:505-14; discussion 514-5. doi:10.1227/01.neu.0000316019.28421.95

225. Tang X, Zuo C, Fang P, Liu G, Qiu Y, Huang Y, et al. Targeting Glioblastoma Stem Cells: A Review on Biomarkers, Signal Pathways and Targeted Therapy. *Front Oncol* (2021) **11**:701291. doi:10.3389/fonc.2021.701291

226. Bidlingmaier S, Zhu X, Liu B. The utility and limitations of glycosylated human CD133 epitopes in defining cancer stem cells. *J Mol Med (Berl)* (2008) **86**:1025–32. doi:10.1007/s00109-008-0357-8

227. Zimmer N, Trzeciak ER, Graefen B, Satoh K, Tuettenberg A. GARP as a Therapeutic Target for the Modulation of Regulatory T Cells in Cancer and Autoimmunity. *Front Immunol*

(2022) **13**:928450. doi:10.3389/fimmu.2022.928450

228. Fauß J, Sprang B, Leukel P, Sommer C, Nikolova T, Ringel F, et al. ALDH1A3 Segregated Expression and Nucleus-Associated Proteasomal Degradation Are Common Traits of Glioblastoma Stem Cells. *Biomedicines* (2021) **10**:7. doi:10.3390/biomedicines10010007
229. Kim EL, Sorokin M, Kantelhardt SR, Kalasauskas D, Sprang B, Fauss J, et al. Intratumoral Heterogeneity and Longitudinal Changes in Gene Expression Predict Differential Drug Sensitivity in Newly Diagnosed and Recurrent Glioblastoma. *Cancers (Basel)* (2020) **12**:520. doi:10.3390/cancers12020520
230. Kalasauskas D, Sorokin M, Sprang B, Elmasri A, Viehweg S, Salinas G, et al. Diversity of Clinically Relevant Outcomes Resulting from Hypofractionated Radiation in Human Glioma Stem Cells Mirrors Distinct Patterns of Transcriptomic Changes. *Cancers (Basel)* (2020) **12**:570. doi:10.3390/cancers12030570
231. Müller A, Weyerhäuser P, Berte N, Jonin F, Lyubarskyy B, Sprang B, et al. Concurrent Activation of Both Survival-Promoting and Death-Inducing Signaling by Chloroquine in Glioblastoma Stem Cells: Implications for Potential Risks and Benefits of Using Chloroquine as Radiosensitizer. *Cells* (2023) **12**:1290. doi:10.3390/cells12091290
232. Schneider CA, Rasband WS, Eliceiri KW. NIH Image to ImageJ: 25 years of image analysis. *Nature Methods* (2012) **9**:671–5. doi:10.1038/nmeth.2089
233. Kim EL, Wüstenberg R, Rübsam A, Schmitz-Salue C, Warnecke G, Bücker E-M, et al. Chloroquine activates the p53 pathway and induces apoptosis in human glioma cells. *Neuro Oncol* (2010) **12**:389–400. doi:10.1093/neuonc/nop046
234. Schindelin J, Arganda-Carreras I, Frise E, Kaynig V, Longair M, Pietzsch T, et al. Fiji: an open-source platform for biological-image analysis. *Nature Methods* (2012) **9**:676–82. doi:10.1038/nmeth.2019
235. Hu Y, Smyth GK. ELDA: extreme limiting dilution analysis for comparing depleted and enriched populations in stem cell and other assays. *J Immunol Methods* (2009) **347**:70–8. doi:10.1016/j.jim.2009.06.008
236. Love MI, Huber W, Anders S. Moderated estimation of fold change and dispersion for RNA-seq data with DESeq2. *Genome Biology* (2014) **15**:550. doi:10.1186/s13059-014-0550-8
237. Anaya J. OncoLnc: linking TCGA survival data to mRNAs, miRNAs, and lncRNAs. *PeerJ Computer Science* (2016) **2**:e67. doi:10.7717/peerj-cs.67
238. Brat DJ, Verhaak RG, Aldape KD, Yung WK, Salama SR, Cooper LA, et al. Comprehensive, Integrative Genomic Analysis of Diffuse Lower-Grade Gliomas. *New England Journal of Medicine* (2015) **372**:2481–98. doi:10.1056/NEJMoa1402121
239. Ciriello G, Miller ML, Aksoy BA, Senbabaoglu Y, Schultz N, Sander C. Emerging landscape of oncogenic signatures across human cancers. *Nat Genet* (2013) **45**:1127–33. doi:10.1038/ng.2762
240. Bradshaw. Cancer Stem Cell Hierarchy in Glioblastoma Multiforme. *Front. Surg.* (2016) **3**:21.
241. Gimple RC, Bhargava S, Dixit D, Rich JN. Glioblastoma stem cells: lessons from the tumor hierarchy in a lethal cancer. *Genes Dev* (2019) **33**:591–609. doi:10.1101/gad.324301.119
242. Dirkse A, Golebiewska A, Buder T, Nazarov PV, Muller A, Poovathingal S, et al. Stem cell-associated heterogeneity in Glioblastoma results from intrinsic tumor plasticity shaped

by the microenvironment. *Nat Commun* (2019) **10**:1787. doi:10.1038/s41467-019-09853-z

243. Lan X, Jörg DJ, Cavalli FM, Richards LM, Nguyen LV, Vanner RJ, et al. Fate mapping of human glioblastoma reveals an invariant stem cell hierarchy. *Nature* (2017) **549**:227–32. doi:10.1038/nature23666

244. Silver A, Feier D, Ghosh T, Rahman M, Huang J, Sarkisian MR, et al. Heterogeneity of glioblastoma stem cells in the context of the immune microenvironment and geospatial organization. *Front Oncol* (2022) **12**:1022716. doi:10.3389/fonc.2022.1022716

245. Miyashita S, Hoshino M. Transit Amplifying Progenitors in the Cerebellum: Similarities to and Differences from Transit Amplifying Cells in Other Brain Regions and between Species. *Cells* (2022) **11**:726. doi:10.3390/cells11040726

246. Barrett LE, Granot Z, Coker C, Iavarone A, Hambardzumyan D, Holland EC, et al. Self-renewal does not predict tumor growth potential in mouse models of high-grade glioma. *Cancer Cell* (2012) **21**:11–24. doi:10.1016/j.ccr.2011.11.025

247. Jin X, Kuang Y, Li L, Li H, Zhao T, He Y, et al. A positive feedback circuit comprising p21 and HIF-1α aggravates hypoxia-induced radioresistance of glioblastoma by promoting Glut1/LDHA-mediated glycolysis. *The FASEB Journal* (2022) **36**:e22229. doi:10.1096/fj.202101736R

248. Marqués-Torrejón MÁ, Porlan E, Banito A, Gómez-Ibarlucea E, Lopez-Contreras AJ, Fernández-Capetillo O, et al. Cyclin-dependent kinase inhibitor p21 controls adult neural stem cell expansion by regulating Sox2 gene expression. *Cell Stem Cell* (2013) **12**:88–100. doi:10.1016/j.stem.2012.12.001

249. Abdoli Shadbad M, Hosseinkhani N, Asadzadeh Z, Brunetti O, Silvestris N, Baradaran B. The Prognostic Value of CD133 in Predicting the Relapse and Recurrence Pattern of High-Grade Gliomas on MRI: A Meta-Analysis. *Front Oncol* (2021) **11**:722833. doi:10.3389/fonc.2021.722833

250. Ullah. Differentiation of cancer cells upregulates HLA-G and PD-L1. *Oncol. Rep.* (2020) **43**:1797.

251. NI XY, Sui HX, Liu Y, Ke SZ, Wang YN, GAO FG. TGF-β of lung cancer microenvironment upregulates B7H1 and GITRL expression in dendritic cells and is associated with regulatory T cell generation. *Oncology Reports* (2012) **28**:615–21. doi:10.3892/or.2012.1822

252. Song S, Yuan P, Wu H, Chen J, Fu J, Li P, et al. Dendritic cells with an increased PD-L1 by TGF-β induce T cell anergy for the cytotoxicity of hepatocellular carcinoma cells. *International Immunopharmacology* (2014) **20**:117–23. doi:10.1016/j.intimp.2014.02.027

253. Streel G de, Bertrand C, Chalon N, Liénart S, Bricard O, Lecomte S, et al. Selective inhibition of TGF-β1 produced by GARP-expressing Tregs overcomes resistance to PD-1/PD-L1 blockade in cancer. *Nat Commun* (2020) **11**:4545. doi:10.1038/s41467-020-17811-3

254. Bertrand C, van Meerbeeck P, Streel G de, Vaherto-Bleeckx N, Benhaddi F, Rouaud L, et al. Combined Blockade of GARP:TGF-β1 and PD-1 Increases Infiltration of T Cells and Density of Pericyte-Covered GARP+ Blood Vessels in Mouse MC38 Tumors. *Front Immunol* (2021) **12**:704050. doi:10.3389/fimmu.2021.704050

255. Asp M, Bergenstråhle J, Lundeberg J. Spatially Resolved Transcriptomes-Next Generation Tools for Tissue Exploration. *BioEssays* (2020) **42**:e1900221. doi:10.1002/bies.201900221

256. Ghebeh H, Lehe C, Barhoush E, Al-Romaih K, Tulbah A, Al-Alwan M, et al. Doxorubicin

downregulates cell surface B7-H1 expression and upregulates its nuclear expression in breast cancer cells: role of B7-H1 as an anti-apoptotic molecule. *Breast Cancer Research* (2010) **12**:R48. doi:10.1186/bcr2605

257. Urciuoli E, Coletta I, Rizzuto E, Vito R de, Petrini S, D'Oria V, et al. Src nuclear localization and its prognostic relevance in human osteosarcoma. *Journal of Cellular Physiology* (2018) **233**:1658–70. doi:10.1002/jcp.26079
258. Satelli A, Batth IS, Brownlee Z, Rojas C, Meng QH, Kopetz S, et al. Potential role of nuclear PD-L1 expression in cell-surface vimentin positive circulating tumor cells as a prognostic marker in cancer patients. *Sci Rep* (2016) **6**:28910. doi:10.1038/srep28910
259. Roskoski R. Src protein-tyrosine kinase structure and regulation. *Biochemical and Biophysical Research Communications* (2004) **324**:1155–64. doi:10.1016/j.bbrc.2004.09.171
260. Han. TGF-β signaling and its targeting for glioma treatment. *Am. J. Cancer Res.* (2015) **5**:945.
261. Ikushima H, Todo T, Ino Y, Takahashi M, Miyazawa K, Miyazono K. Autocrine TGF-beta signaling maintains tumorigenicity of glioma-initiating cells through Sry-related HMG-box factors. *Cell Stem Cell* (2009) **5**:504–14. doi:10.1016/j.stem.2009.08.018
262. Peñuelas S, Anido J, Prieto-Sánchez RM, Folch G, Barba I, Cuartas I, et al. TGF-beta increases glioma-initiating cell self-renewal through the induction of LIF in human glioblastoma. *Cancer Cell* (2009) **15**:315–27. doi:10.1016/j.ccr.2009.02.011
263. Shaim H, Shanley M, Basar R, Daher M, Gumin J, Zamler DB, et al. Targeting the αv integrin/TGF-β axis improves natural killer cell function against glioblastoma stem cells. *Journal of Clinical Investigation* (2021) **131**. doi:10.1172/JCI142116
264. Golestaneh N, Mishra B. TGF-beta, neuronal stem cells and glioblastoma. *Oncogene* (2005) **24**:5722–30. doi:10.1038/sj.onc.1208925
265. Rigel DS. Epidemiology of melanoma. *Semin Cutan Med Surg* (2010) **29**:204–9. doi:10.1016/j.sder.2010.10.005
266. Dzwierzynski WW. Managing malignant melanoma. *Plast Reconstr Surg* (2013) **132**:446e-460e. doi:10.1097/PRS.0b013e31829ad411
267. Kohler BA, Ward E, McCarthy BJ, Schymura MJ, Ries LA, Eheman C, et al. Annual report to the nation on the status of cancer, 1975-2007, featuring tumors of the brain and other nervous system. *J Natl Cancer Inst* (2011) **103**:714–36. doi:10.1093/jnci/djr077
268. Giblin A-V, Thomas JM. Incidence, mortality and survival in cutaneous melanoma. *J Plast Reconstr Aesthet Surg* (2007) **60**:32–40. doi:10.1016/j.bjps.2006.05.008
269. Jemal A, Siegel R, Xu J, Ward E. Cancer statistics, 2010. *CA Cancer J Clin* (2010) **60**:277–300. doi:10.3322/caac.20073
270. Yuan T-A, Lu Y, Edwards K, Jakowatz J, Meyskens FL, Liu-Smith F. Race-, Age-, and Anatomic Site-Specific Gender Differences in Cutaneous Melanoma Suggest Differential Mechanisms of Early- and Late-Onset Melanoma. *Int J Environ Res Public Health* (2019) **16**. doi:10.3390/ijerph16060908
271. Geller J, Swetter SM, Leyson J, Miller DR, Brooks K, Geller AC. Crafting a melanoma educational campaign to reach middle-aged and older men. *J Cutan Med Surg* (2006) **10**:259–68. doi:10.2310/7750.2006.00066
272. Wang Y, Freemantle N, Nazareth I, Hunt K. Gender differences in survival and the use of primary care prior to diagnosis of three cancers: an analysis of routinely collected UK general practice data. *PLoS One* (2014)

9:e101562. doi:10.1371/journal.pone.0101562

273. Schank, Hassel. Immunotherapies for the Treatment of Uveal Melanoma—History and Future. *Cancers (Basel)* (2019) **11**:1048. doi:10.3390/cancers11081048
274. Garland CF, Garland FC, Gorham ED. Rising trends in melanoma. An hypothesis concerning sunscreen effectiveness. *Ann Epidemiol* (1993) **3**:103–10. doi:10.1016/1047-2797(93)90017-x
275. Tucker MA, Goldstein AM. Melanoma etiology: where are we? *Oncogene* (2003) **22**:3042–52. doi:10.1038/sj.onc.1206444
276. Deutsche Krebsgesellschaft DK. *Leitlinienprogramm Onkologie 12/2023*.
277. Merkel EA, Gerami P. Malignant melanoma of sun-protected sites: a review of clinical, histological, and molecular features. *Lab Invest* (2017) **97**:630–5. doi:10.1038/labinvest.2016.147.
278. Grob JJ, Bonerandi JJ. The 'ugly duckling' sign: identification of the common characteristics of nevi in an individual as a basis for melanoma screening. *Arch Dermatol* (1998) **134**:103–4. doi:10.1001/archderm.134.1.103-a
279. Michielin O, van Akkooi AC, Ascierto PA, Dummer R, Keilholz U. Cutaneous melanoma: ESMO Clinical Practice Guidelines for diagnosis, treatment and follow-up†. *Ann Oncol* (2019) **30**:1884–901. doi:10.1093/annonc/mdz411.
280. Haenssle HA, Fink C, Schneiderbauer R, Toberer F, Buhl T, Blum A, et al. Man against machine: diagnostic performance of a deep learning convolutional neural network for dermoscopic melanoma recognition in comparison to 58 dermatologists. *Ann Oncol* (2018) **29**:1836–42. doi:10.1093/annonc/mdy166
281. Salerni G, Carrera C, Lovatto L, Puig-Butille JA, Badenas C, Plana E, et al. Benefits of total body photography and digital dermatoscopy ("two-step method of digital follow-up") in the early diagnosis of melanoma in patients at high risk for melanoma. *J Am Acad Dermatol* (2012) **67**:e17-27. doi:10.1016/j.jaad.2011.04.008
282. Balch CM, Gershenwald JE, Soong S-J, Thompson JF, Atkins MB, Byrd DR, et al. Final version of 2009 AJCC melanoma staging and classification. *J Clin Oncol* (2009) **27**:6199–206. doi:10.1200/JCO.2009.23.4799
283. Hugo W, Zaretsky JM, Sun L, Song C, Moreno BH, Hu-Lieskovan S, et al. Genomic and Transcriptomic Features of Response to Anti-PD-1 Therapy in Metastatic Melanoma. *Cell* (2016) **165**:35–44. doi:10.1016/j.cell.2016.02.065
284. van Allen EM, Miao D, Schilling B, Shukla SA, Blank C, Zimmer L, et al. Genomic correlates of response to CTLA-4 blockade in metastatic melanoma. *Science* (2015) **350**:207–11. doi:10.1126/science.aad0095
285. Curtin JA, Fridlyand J, Kageshita T, Patel HN, Busam KJ, Kutzner H, et al. Distinct sets of genetic alterations in melanoma. *N Engl J Med* (2005) **353**:2135–47. doi:10.1056/nejmoa050092
286. Maertens O, Johnson B, Hollstein P, Frederick DT, Cooper ZA, Messiaen L, et al. Elucidating distinct roles for NF1 in melanomagenesis. *Cancer Discov* (2013) **3**:338–49. doi:10.1158/2159-8290.cd-12-0313
287. Leonardi GC, Falzone L, Salemi R, Zanghì A, Spandidos DA, Mccubrey JA, et al. Cutaneous melanoma: From pathogenesis to therapy (Review). *Int J Oncol* (2018) **52**:1071–80. doi:10.3892/ijo.2018.4287
288. Chappell WH, Steelman LS, Long JM, Kempf RC, Abrams SL, Franklin RA, et al. Ras/Raf/MEK/ERK and PI3K/PTEN/Akt/mTOR

inhibitors: rationale and importance to inhibiting these pathways in human health. *Oncotarget* (2011) **2**:135–64. doi:10.18632/oncotarget.240

289. Testori AA, Ribero S, Indini A, Mandalà M. Adjuvant Treatment of Melanoma: Recent Developments and Future Perspectives. *Am J Clin Dermatol* (2019) **20**:817–27. doi:10.1007/s40257-019-00456-4
290. Weiss SA, Wolchok JD, Sznol M. Immunotherapy of Melanoma: Facts and Hopes. *Clin Cancer Res* (2019) **25**:5191–201. doi:10.1158/1078-0432.CCR-18-1550
291. Lovly CM, Dahlman KB, Fohn LE, Su Z, Dias-Santagata D, Hicks DJ, et al. Routine multiplex mutational profiling of melanomas enables enrollment in genotype-driven therapeutic trials. *PLoS One* (2012) **7**:e35309. doi:10.1371/journal.pone.0035309
292. Flaherty KT, Puzanov I, Kim KB, Ribas A, McArthur GA, Sosman JA, et al. Inhibition of mutated, activated BRAF in metastatic melanoma. *N Engl J Med* (2010) **363**:809–19. doi:10.1056/NEJMoa1002011
293. Long GV, Flaherty KT, Stroyakovskiy D, Gogas H, Levchenko E, Braud F de, et al. Dabrafenib plus trametinib versus dabrafenib monotherapy in patients with metastatic BRAF V600E/K-mutant melanoma: long-term survival and safety analysis of a phase 3 study. *Ann Oncol* (2017) **28**:1631–9. doi:10.1093/annonc/mdx176
294. Robert C, Karaszewska B, Schachter J, Rutkowski P, Mackiewicz A, Stroiakovski D, et al. Improved overall survival in melanoma with combined dabrafenib and trametinib. *N Engl J Med* (2015) **372**:30–9. doi:10.1056/NEJMoa1412690
295. Ascierto PA, Ferrucci PF, Fisher R, Del Vecchio M, Atkinson V, Schmidt H, et al. Dabrafenib, trametinib and pembrolizumab or placebo in BRAF-mutant melanoma. *Nat Med* (2019) **25**:941–6. doi:10.1038/s41591-019-0448-9
296. Wei SC, Levine JH, Cogdill AP, Zhao Y, Anang N-AA, Andrews MC, et al. Distinct Cellular Mechanisms Underlie Anti-CTLA-4 and Anti-PD-1 Checkpoint Blockade. *Cell* (2017) **170**:1120-1133.e17. doi:10.1016/j.cell.2017.07.024
297. Larkin J, Chiarion-Sileni V, Gonzalez R, Grob J-J, Rutkowski P, Lao CD, et al. Five-Year Survival with Combined Nivolumab and Ipilimumab in Advanced Melanoma. *N Engl J Med* (2019) **381**:1535–46. doi:10.1056/NEJMoa1910836.
298. Blank CU, Haining WN, Held W, Hogan PG, Kallies A, Lugli E, et al. Defining 'T cell exhaustion'. *Nat Rev Immunol* (2019) **19**:665–74. doi:10.1038/s41577-019-0221-9
299. Vyas M, Müller R, Pogge von Strandmann E. Antigen Loss Variants: Catching Hold of Escaping Foes. *Front Immunol* (2017) **8**:175. doi:10.3389/fimmu.2017.00175
300. Sahin U, Türeci Ö. Personalized vaccines for cancer immunotherapy. *Science* (2018) **359**:1355–60. doi:10.1126/science.aar7112
301. Scheetz L, Park KS, Li Q, Lowenstein PR, Castro MG, Schwendeman A, et al. Engineering patient-specific cancer immunotherapies. *Nat Biomed Eng* (2019) **3**:768–82. doi:10.1038/s41551-019-0436-x.
302. Peng M, Mo Y, Wang Y, Wu P, Zhang Y, Xiong F, et al. Neoantigen vaccine: an emerging tumor immunotherapy. *Mol Cancer* (2019) **18**:128. doi:10.1186/s12943-019-1055-6
303. Koupenova M, Clancy L, Corkrey HA, Freedman JE. Circulating Platelets as Mediators of Immunity, Inflammation, and Thrombosis. *Circulation Research* (2018) **122**:337–51. doi:10.1161/CIRCRESAHA.117.310795
304. Gaertner F, Massberg S. Patrolling the vascular borders: platelets in immunity to infection and cancer. *Nature Reviews*

Immunology (2019) **19**:747–60. doi:10.1038/s41577-019-0202-z

305. Erpenbeck L, Schön MP. Deadly allies: the fatal interplay between platelets and metastasizing cancer cells. *Blood* (2010) **115**:3427–36. doi:10.1182/blood-2009-10-247296
306. Cao W, Yao X, Cen D, Zhi Y, Zhu N, Xu L. Prognostic role of pretreatment thrombocytosis on survival in patients with cervical cancer: a systematic review and meta-analysis. *World Journal of Surgical Oncology* (2019) **17**:132. doi:10.1186/s12957-019-1676-7
307. Palacios-Acedo AL, Mège D, Crescence L, Dignat-George F, Dubois C, Panicot-Dubois L. Platelets, Thrombo-Inflammation, and Cancer: Collaborating With the Enemy. *Front Immunol* (2019) **10**:1805. doi:10.3389/fimmu.2019.01805
308. Rachidi S, Metelli A, Riesenberg B, Wu BX, Nelson MH, Wallace C, et al. Platelets subvert T cell immunity against cancer via GARP-TGFβ axis. *Sci Immunol* (2017) **2**. doi:10.1126/sciimmunol.aai7911
309. Wang Z, Fang M, Li J, Yang R, Du J, Luo Y. High Platelet Levels Attenuate the Efficacy of Platinum-Based Treatment in Non-Small Cell Lung Cancer. *Cellular Physiology and Biochemistry* (2018) **48**:2456–69. doi:10.1159/000492683
310. Mercier J, Voutsadakis IA. The platelets-neutrophils to lymphocytes ratio: a new prognostic marker in metastatic colorectal cancer. *Journal of Gastrointestinal Oncology* (2018) **9**:478–86. doi:10.21037/jgo.2018.03.13
311. Takenaka Y, Oya R, Kitamiura T, Ashida N, Shimizu K, Takemura K, et al. Platelet count and platelet-lymphocyte ratio as prognostic markers for head and neck squamous cell carcinoma: Meta-analysis. *Head & Neck* (2018) **40**:2714–23. doi:10.1002/hed.25366
312. Brockmann MA, Giese A, Mueller K, Kaba Fj, Lohr F, Weiss C, et al. Preoperative thrombocytosis predicts poor survival in patients with glioblastoma. *Neuro Oncol* (2007) **9**:335–42. doi:10.1215/15228517-2007-013
313. Hefler-Frischmuth K, Grimm C, Gensthaler L, Reiser E, Schwameis R, Hefler LA. Prognostic value of preoperative hyponatremia and thrombocytosis in patients with epithelial ovarian cancer. *Wiener klinische Wochenschrift* (2018) **130**:575–80. doi:10.1007/s00508-018-1388-y
314. Davis AN, Afshar-Kharghan V, Sood AK. Platelet effects on ovarian cancer. *Seminars in Oncology* (2014) **41**:378–84. doi:10.1053/j.seminoncol.2014.04.004
315. Buergy D, Wenz F, Groden C, Brockmann MA. Tumor-platelet interaction in solid tumors. *Int J Cancer* (2012) **130**:2747–60. doi:10.1002/ijc.27441
316. Ho-Tin-Noé B, Carbo C, Demers M, Cifuni SM, Goerge T, Wagner DD. Innate immune cells induce hemorrhage in tumors during thrombocytopenia. *The American Journal of Pathology* (2009) **175**:1699–708. doi:10.2353/ajpath.2009.090460
317. Labelle M, Begum S, Hynes RO. Direct signaling between platelets and cancer cells induces an epithelial-mesenchymal-like transition and promotes metastasis. *Cancer Cell* (2011) **20**:576–90. doi:10.1016/j.ccr.2011.09.009
318. Kopp H-G, Placke T, Salih HR. Platelet-derived transforming growth factor-beta down-regulates NKG2D thereby inhibiting natural killer cell antitumor reactivity. *Cancer Res* (2009) **69**:7775–83. doi:10.1158/0008-5472.CAN-09-2123

319. Labelle M, Hynes RO. The initial hours of metastasis: the importance of cooperative host-tumor cell interactions during hematogenous dissemination. *Cancer Discov* (2012) **2**:1091–9. doi:10.1158/2159-8290.CD-12-0329
320. Kumm EJ, Pagel O, Gambaryan S, Walter U, Zahedi RP, Smolenski A, et al. The Cell Cycle Checkpoint System MAST(L)-ENSA/ARPP19-PP2A is Targeted by cAMP/PKA and cGMP/PKG in Anucleate Human Platelets. *Cells* (2020) **9**:472. doi:10.3390/cells9020472
321. Tuettenberg A, Huter E, Hubo M, Horn J, Knop J, Grimbacher B, et al. The role of ICOS in directing T cell responses: ICOS-dependent induction of T cell anergy by tolerogenic dendritic cells. *The Journal of Immunology* (2009) **182**:3349–56. doi:10.4049/jimmunol.0802733
322. Zimmer N, Trzeciak ER, Müller A, Licht P, Sprang B, Leukel P, et al. Nuclear Glycoprotein A Repetitions Predominant (GARP) Is a Common Trait of Glioblastoma Stem-like Cells and Correlates with Poor Survival in Glioblastoma Patients. *Cancers (Basel)* (2023) **15**:5711. doi:10.3390/cancers15245711
323. Krebs FK, Trzeciak ER, Zimmer S, Özistanbullu D, Mitzel-Rink H, Meissner M, et al. Immune signature as predictive marker for response to checkpoint inhibitor immunotherapy and overall survival in melanoma. *Cancer Med* (2021) **10**:1562–75. doi:10.1002/cam4.3710
324. Kalathil S, Lugade AA, Miller A, Iyer R, Thanavala Y. Higher frequencies of GARP(+)CTLA-4(+)Foxp3(+) T regulatory cells and myeloid-derived suppressor cells in hepatocellular carcinoma patients are associated with impaired T-cell functionality. *Cancer Res* (2013) **73**:2435–44. doi:10.1158/0008-5472.CAN-12-3381
325. Jiang S, Zhang Y, Zhang X, Lu B, Sun P, Wu Q, et al. GARP Correlates With Tumor-Infiltrating T-Cells and Predicts the Outcome of Gastric Cancer. *Front Immunol* (2021) **12**:660397. doi:10.3389/fimmu.2021.660397
326. Sloan AR, Lee-Poturalski C, Hoffman HC, Harris PL, Elder TE, Richardson B, et al. Glioma stem cells activate platelets by plasma-independent thrombin production to promote glioblastoma tumorigenesis. *Neurooncol Adv* (2022) **4**:vdac172. doi:10.1093/noajnl/vdac172
327. Bombaci M, Pesce E, Torri A, Carpi D, Crosti M, Lanzafame M, et al. Novel biomarkers for primary biliary cholangitis to improve diagnosis and understand underlying regulatory mechanisms. *Liver Int* (2019) **39**:2124–35. doi:10.1111/liv.14128
328. Wegner J, Krebs FK, Tuettenberg A, Stebut E von. Treg activation status depends on psoriasis therapy regime. *J Dtsch Dermatol Ges* (2020) **18**:1481–4. doi:10.1111/ddg.14368
329. Krützfeldt J, Rajewsky N, Braich R, Rajeev KG, Tuschl T, Manoharan M, et al. Silencing of microRNAs in vivo with 'antagomirs'. *Nature* (2005) **438**:685–9. doi:10.1038/nature04303
330. Huang B, Zhao J, Lei Z, Shen S, Li D, Shen G-X, et al. miR-142-3p restricts cAMP production in CD4+CD25- T cells and CD4+CD25+ TREG cells by targeting AC9 mRNA. *EMBO Rep* (2009) **10**:180–5. doi:10.1038/embor.2008.224
331. Ha J, Kim M, Lee Y, Lee M. Intranasal delivery of self-assembled nanoparticles of therapeutic peptides and antagomirs elicits anti-tumor effects in an intracranial glioblastoma model. *Nanoscale* (2021) **13**:14745–59. doi:10.1039/d1nr03455c
332. Tao Y, Xu S, Wang J, Xu L, Zhang C, Chen K, et al. Delivery of microRNA-33 Antagomirs by Mesoporous Silica Nanoparticles to Ameliorate Lipid Metabolic Disorders. *Front Pharmacol* (2020) **11**:921. doi:10.3389/fphar.2020.00921

333. Meyer-Martin H, Hahn SA, Beckert H, Belz C, Heinz A, Jonuleit H, et al. GARP inhibits allergic airway inflammation in a humanized mouse model. *Allergy* (2016) **71**:1274–83. doi:10.1111/all.12883
334. Schlöder J, Berges C, Tuettenberg A, Jonuleit H. Novel Concept of CD4-Mediated Activation of Regulatory T Cells for the Treatment of Graft-Versus-Host Disease. *Front Immunol* (2017) **8**:1495. doi:10.3389/fimmu.2017.01495
335. Martin H, Reuter S, Dehzad N, Heinz A, Bellinghausen I, Saloga J, et al. CD4-mediated regulatory T-cell activation inhibits the development of disease in a humanized mouse model of allergic airway disease. *J Allergy Clin Immunol* (2012) **129**:521-8, 528.e1-7. doi:10.1016/j.jaci.2011.09.038
336. Powderly J, Shimizu T, LoRusso P, Razak A, Miller K, Balar A, et al. Abstract CT207: Phase 1 first-in-human study of ABBV-151 as monotherapy or in combination with budigalimab in patients with locally advanced or metastatic solid tumors. *Cancer Res* (2021) **81**:CT207-CT207. doi:10.1158/1538-7445.AM2021-CT207
337. Satoh K, Kobayashi Y, Fujimaki K, Hayashi S, Ishida S, Sugiyama D, et al. Novel anti-GARP antibody DS-1055a augments anti-tumor immunity by depleting highly suppressive GARP+ regulatory T cells. *Int Immunol* (2021) **33**:435–46. doi:10.1093/intimm/dxab027
338. Gaignage M, Zhang X, Stockis J, Dedobbeleer O, Michiels C, Cochez P, et al. Blocking GARP-mediated activation of TGF-β1 did not alter innate or adaptive immune responses to bacterial infection or protein immunization in mice. *Cancer Immunol Immunother* (2022). doi:10.1007/s00262-021-03119-8
339. Cho MS, Gonzalez-Pagan O, Court Pinto K, Sood A, Afshar-Kharghan V. The Inhibition of Platelets Restore Anti-Tumor Immune Response to Ovarian Cancer and Its Therapeutic Implication. *Blood* (2018) **132**:3698. doi:10.1182/blood-2018-99-116530
340. Huttlin EL, Bruckner RJ, Navarrete-Perea J, Cannon JR, Baltier K, Gebreab F, et al. Dual proteome-scale networks reveal cell-specific remodeling of the human interactome. *Cell* (2021) **184**:3022-3040.e28. doi:10.1016/j.cell.2021.04.011.
341. Gong A-H, Wei P, Zhang S, Yao J, Yuan Y, Zhou A-D, et al. FoxM1 Drives a Feed-Forward STAT3-Activation Signaling Loop That Promotes the Self-Renewal and Tumorigenicity of Glioblastoma Stem-like Cells. *Cancer Res* (2015) **75**:2337–48. doi:10.1158/0008-5472.CAN-14-2800
342. Schupp J, Christians A, Zimmer N, Gleue L, Jonuleit H, Helm M, et al. In-Depth Immune-Oncology Studies of the Tumor Microenvironment in a Humanized Melanoma Mouse Model. *Int J Mol Sci* (2021) **22**. doi:10.3390/ijms22031011

8.0 List of figures and tables

8.1 List of figures

Figure 1: Schematic overview of the role of GARP in the tumor microenvironment based on the findings of this work. **14**
Figure 2: Overview of cancer development and the immunosuppressive tumor microenvironment **17**

Manuscript I
Figure 1.2.1 edited from Zimmer et al., 2022: Overview of Glycoprotein a repetitions predominant (GARP) protein biosynthesis and transport to the cell membrane in activated human regulatory T cells (Treg). **22**

Manuscript II
Figure 3.3.1. T1-weighted gandolinium enhanced cranial axial image with a typical glioblastoma (GB) in the right dorsal temporal lobe. **40**
Figure 3.3.2. Glycoprotein A repetition predominant (GARP) immunohistochemistry in gliomas and astrocytomas. **41**
Figure 3.3.3. Analysis of the GARP localization in resting and stimulated regulatory T cells, melanoma cell line MaMel-19, and glioblastoma cell line T98G. **42**
Figure 3.3.4. Flow cytometric and confocal analysis of GARP expression in patient-derived GB cell lines. **43**
Figure 3.3.5. (**a**) Soluble GARP (sGARP) cytokine suppression. **44**

Manuscript III
Figure 3.4.1. (A) Flow cytometric analysis of surface GARP and CD133 on different GSC and the control, non-stem, GB cell line, T98G. **56**
Figure 3.4.2. GARP expression in isogenic GSC derived from newly diagnosed GB IT-726. **58**
Figure 3.4.3. Analysis of expression and localization of GARP in isogenic GSC cell lines, which vary in differentiation states derived from different regions of the same tumor. **59**
Figure 3.4.4. Quantitative assessments of self-renewal capacity by extreme limiting dilution assay (ELDA). **60**
Figure 3.4.5. Comparative assessments of glial fibrillary acidic protein (GFAP), platelet-derived growth factor receptor alpha (PDGFR-α), p21, and phosphorylated histone H3 (PHH3) in FACs-sorted $GARP^{high}$ and $GARP^{low}$ isogenic GSC (#1095) by Western blot. **61**
Figure 3.4.6. GARP expression in GB is unaffected throughout therapy. **63**
Figure 3.4.7. Nuclear GARP is a potential new prognostic biomarker for GB patient survival. **65**
Figure 3.4.S1: Heterologous GSC lines differing in their self-renewal capacity. **69**
Figure 3.4.S2: Anti-GARP antibody validation for flow cytometry. **70**
Figure 3.4.S3: Specificity demonstration and validation of anti-GARP antibodies. **71**
Figure 3.4.S4: Flow cytometric gating strategy for GSC. **72**
Figure 3.4.S5: Anti-GARP antibody validation for confocal microscopy. **73**
Figure 3.4.S6: Flow cytometric gating strategy for $GARP^{high}$ and $GARP^{low}$ sorted GSC. **74**
Figure 3.4.S7: Invasive xenograft tumors arisen from GSC lines, #1051 and #1043. **75**
Figure 3.4.S8: GARP is expressed in xenograft tumors arisen from GSC lines, #1051 and #1043. **76**
Figure 3.4.S9: Study design and models used for the assessment of GARP. **77**
Figure 3.4.S10: Frequency of $GFAP^{+}$ $GARP^{high}$ and $GARP^{low}$ GSC. **78**

Manuscript IV

Figure 4.2.1. Glycoprotein A repetitions predominant (GARP) was expressed on the surface of platelets and was detectable in the supernatant of activated platelets. **84**
Figure 4.2.2. Platelets induce peripheral regulatory T cells (iTreg). **85**
Figure 4.2.3. Platelet-induced iTreg suppressed T effector cells (Teff) cells. **86**
Figure 4.2.4. Platelets induced iTreg in a mainly GARP-dependent manner. **87**
Figure 4.2.5. Blockade of transforming growth factor (TGF)-β I-III did in part prevent regulatory T cells (Treg) induction. **88**
Figure 4.2.6. Combining blockade of TGF-β signaling and GARP led to a complete inhibition of platelet effects**.** **89-90**
Figure 4.2.7. Platelet-conditioned medium (PCM) inhibited IFN-γ production but failed to induce a Treg phenotype. **91**
Figure 4.2.8. Increased platelet surface GARP levels in stage I/IV melanoma patient stage**.** **92**
Figure 4.2.A1. sGARP induced Treg**.** **98**
Figure 4.2.A2. Platelets bound to T cells upon activation in coculture**.** **99**
Figure 4.2.A3. Experimental setup of a platelet-conditioned T cell suppression assay**.** **100**
Figure 4.2.A4. Thrombin-activated platelets induced a regulatory phenotype in $CD4^{+}CD25^{-}$ T cells**.** **101**
Figure 4.2.A5. TRAP-6-activated platelets induced a regulatory phenotype in $CD4^{+}CD25^{-}$ T cells**.** **102**
Figure 4.2.A6. Flow cytometric analysis of T cell purity**.** **103**
Figure 4.2.A7. Gating strategy**.** **103**

8.2 List of tables

Manuscript I

Table 3.4.1. Patients with glioma grade III and IV at the study center Idar-Oberstein, Germany. **39**
Table 3.4.A1. Characteristics of astrocytoma grade II patients at the study center Idar-Oberstein, Germany. **48**
Table 3.4.A2. Characteristics of astrocytoma grade III patients at the study center Idar-Oberstein, Germany. **49**

Manuscript III

Table 4.2.1. Patient characteristics. **97**

9.0 Acknowledgments

10.0 Curiculum Vitae

Publikationen (*equal contribution)

- Nuclear GARP expression is a common trait of glioblastoma stem-like cells that correlates with poor survival in glioblastoma patients. (Article)
  Zimmer N*, Trzeciak ER*, Licht P, Sprang B, Leukel P, Mailänder V, Ringel F, Sommer C, Tuettenberg J, Kim E, Tuettenberg A. Cancers 2023, 15(24), 5711; doi:10.3390/cancers15245711

- GARP Regulates the Immune Capacity of a Human Autologous Platelet Concentrate. (Article)
  Trzeciak ER*, **Zimmer N***, Kämmerer PW, Thiem D, Al-Nawas B, Tuettenberg A, Blatt S. Biomedicines. 2022 Dec 5;10(12):3136. doi: 10.3390/biomedicines10123136

- GARP as a Therapeutic Target for the Modulation of Regulatory T Cells in Cancer and Autoimmunity. (Review)
  Zimmer N, Trzeciak ER, Graefen B, Satoh K, Tuettenberg A.
  Front Immunol. 2022 Jul 8;13:928450. doi: 10.3389/fimmu.2022.928450

- Oxidative Stress Differentially Influences the Survival and Metabolism of Cells in the Melanoma Microenvironment. (Article)
  Trzeciak ER, **Zimmer N**, Gehringer I, Stein L, Graefen B, Schupp J, Stephan A, Rietz S, Prantner M, Tuettenberg A. Cells. 2022 Mar 8;11(6):930. doi: 10.3390/cells11060930

- In-Depth Immune-Oncology Studies of the Tumor Microenvironment in a Humanized Melanoma Mouse Model. (Article)
  Schupp J, Christians A, **Zimmer N**, Gleue L, Jonuleit H, Helm M, Tuettenberg A.
  Int J Mol Sci. 2021 Jan 20;22(3):1011. doi: 10.3390/ijms22031011

- Platelet-Derived GARP Induces Peripheral Regulatory T Cells-Potential Impact on T Cell Suppression in Patients with Melanoma-Associated Thrombocytosis. (Article)
  Zimmer N, Krebs FK, Zimmer S, Mitzel-Rink H, Kumm EJ, Jurk K, Grabbe S, Loquai C, Tuettenberg A. Cancers (Basel). 2020 Dec 5;12(12):3653. doi: 10.3390/cancers12123653

- Stability of Alkyl Chain-Mediated Lipid Anchoring in Liposomal Membranes. (Article)
  Gleue L, Schupp J, **Zimmer N**, Becker E, Frey H, Tuettenberg A, Helm M.
  Cells. 2020 Sep 29;9(10):2213. doi: 10.3390/cells9102213

- GARP as an Immune Regulatory Molecule in the Tumor Microenvironment of Glioblastoma Multiforme. (Article)
  Zimmer N, Kim E, Sprang B, Leukel P, Khafaji F, Ringel F, Sommer C, Tuettenberg J, Tuettenberg A.Int J Mol Sci. 2019 Jul 26;20(15):3676. doi: 10.3390/ijms20153676

- Targeting myeloid cells in the tumor sustaining microenvironment. (Review)
  Schupp J*, Krebs FK*, **Zimmer N***, Trzeciak E, Schuppan D, Tuettenberg A.
  Cell Immunol. 2019 Sep; 343:103713. doi: 10.1016/j.cellimm.2017.10.013

11.0 Appendix

Manuscript I: GARP as a Therapeutic Target for the Modulation of Regulatory T Cells in Cancer and Autoimmunity. 14 pages

Manuscript II: GARP as an Immune Regulatory Molecule in the Tumor Microenvironment of Glioblastoma Multiforme. 15 pages
Supplementary material. 2 pages

Manuscript III: Nuclear GARP expression is a common trait of glioblastoma stem-like cells that correlates with poor survival in glioblastoma patients. 22 pages
Supplementary material. 11 pages

Manuscript IV: Platelet-Derived GARP Induces Peripheral Regulatory T Cells-Potential Impact on T Cell Suppression in Patients with Melanoma-Associated Thrombocytosis. 24 pages

frontiers | Frontiers in Immunology

REVIEW
published: 08 July 2022
doi: 10.3389/fimmu.2022.928450

GARP as a Therapeutic Target for the Modulation of Regulatory T Cells in Cancer and Autoimmunity

Niklas Zimmer[1], *Emily R. Trzeciak*[1], *Barbara Graefen*[1], *Kazuki Satoh*[2] *and Andrea Tuettenberg*[1,3*]

[1] Department of Dermatology, University Medical Center Mainz, Johannes Gutenberg University Mainz, Mainz, Germany, [2] Early Clinical Development Department, Daiichi Sankyo Co., Ltd., Tokyo, Japan, [3] Research Center for Immunotherapy, University Medical Center Mainz, Johannes Gutenberg University Mainz, Mainz, Germany

Regulatory T cells (Treg) play a critical role in immune homeostasis by suppressing several aspects of the immune response. Herein, Glycoprotein A repetitions predominant (GARP), the docking receptor for latent transforming growth factor (LTGF-β), which promotes its activation, plays a crucial role in maintaining Treg mediated immune tolerance. After activation, Treg uniquely express GARP on their surfaces. Due to its location and function, GARP may represent an important target for immunotherapeutic approaches, including the inhibition of Treg suppression in cancer or the enhancement of suppression in autoimmunity. In the present review, we will clarify the cellular and molecular regulation of GARP expression not only in human Treg but also in other cells present in the tumor microenvironment. We will also examine the overall roles of GARP in the regulation of the immune system. Furthermore, we will explore potential applications of GARP as a predictive and therapeutic biomarker as well as the targeting of GARP itself in immunotherapeutic approaches.

Keywords: LRRC32, GARP mRNA, Glycoprotein A repetitions predominant (GARP), Treg, Soluble GARP or soluble Glycoprotein A repetitions predominant (sGARP), biomarker, therapy

OPEN ACCESS

Edited by:
Robert Zeiser,
University of Freiburg, Germany

Reviewed by:
Hodaka Fujii,
Hirosaki University, Japan
John D. Colgan,
The University of Iowa, United States
Niklas Beyersdorf,
Julius Maximilian University of Würzburg, Germany
Hana Andrlova,
Memorial Sloan Kettering Cancer Center, United States

***Correspondence:**
Andrea Tuettenberg
antuette@uni-mainz.de

Specialty section:
This article was submitted to Vaccines and Molecular Therapeutics, a section of the journal Frontiers in Immunology

Received: *25 April 2022*
Accepted: *16 June 2022*
Published: *08 July 2022*

Citation:
Zimmer N, Trzeciak ER, Graefen B, Satoh K and Tuettenberg A (2022) GARP as a Therapeutic Target for the Modulation of Regulatory T Cells in Cancer and Autoimmunity. Front. Immunol. 13:928450. doi: 10.3389/fimmu.2022.928450

INTRODUCTION

Regulatory T cells (Treg) play an essential role in the maintenance of immune homeostasis and the induction of peripheral tolerance. They have been shown to suppress many aspects of the immune response by employing multiple immunosuppressive mechanisms. These mechanisms can be broadly classified as being either contact dependent, such as the transfer of cAMP to T effector cells (Teff) *via* gap junctions (1), or contact independent, like the secretion of suppressive cytokines. As a result, many approaches have been tested to target Treg in order to suppress autoimmune diseases or to enhance anti-tumor immunity.

In addition to the transcription factor, Forkhead box P3 (Foxp3), increased expression of Glycoprotein A repetitions predominant (GARP) has been found on the surface of activated Treg. GARP, a transmembrane protein, is the docking receptor for latent transforming growth factor (LTGF-β) and thereby plays a critical role in the production and release of active transforming growth factor beta (TGF-β). TGF-β is a pleiotropic and potent immunosuppressive cytokine known to contribute to both immune modulation and evasion. GARP is also expressed by platelets and by

tumor cells of different entities, and it has been detected as a soluble factor. Expression of GARP has been found to be tightly regulated by epigenetic modifications, microRNAs (miRNA), and the master chaperone, GP96, amongst other things.

The objectives of this review are to highlight GARP expression, regulation, and function in Treg, other immune cells, and cancer cells as well as to evaluate the potential of both surface and soluble GARP as predictive and therapeutic biomarkers. In addition, approaches that target GARP for immunotherapeutic intervention in autoimmune diseases and cancer will be discussed.

GARP EXPRESSION, STRUCTURE, AND FUNCTION

LRRC32 Structure

The gene encoding human GARP can be referred to by various names including: LRRC32, Glycoprotein A Repetitions Predominant, GARP, Transforming Growth Factor Beta Activator LRRC32, Leucine-Rich Repeat-Containing Protein 32, Garpin, CPPRDD, and D11S833E (Gene ID: 2615). For the sake of clarity, we will specifically refer to the GARP gene as "LRRC32", its mRNA as "GARP mRNA", and the protein as "GARP" for the remainder of the manuscript.

LRRC32 was first described in the telomeric region of 11q13.5-11q14 in human (2) and mice (3). LRRC32 consists of two exons (4), and its expression is conferred by two alternative promoters (5). One exon codes for a signal peptide as well as nine amino acids, while the other codes for leucine-rich repeats (LRR). In addition, LRRC32 contains an extensive 2-kb long 3′ untranslated region (UTR), that has five highly conserved regions which are of importance for the post-transcriptional regulation of the GARP mRNA (6).

So far, the GARP mRNA has been detected in various cell types and tissues of different origin, including heart, kidney, liver, lung, pancreas, placenta, skeletal muscle, and lymphoid tissues as well as in different cancer entities (e.g. melanoma, breast cancer, oral squamous cell carcinoma, prostate cancer, and glioblastoma). Although the GARP mRNA is expressed by many cell types, surface expression of the GARP protein itself has been only reported in the context of activated Treg (7, 8), activated B cells (9, 10), macrophages (11), platelets (12), mesenchymal stem cells (13), and hepatic stellate cells (9, 14). In Treg, surface GARP is considered to be an activation marker. Of note, the GARP mRNA is also expressed by human Teff clones. Nevertheless, even though its expression levels in such clones are similar to levels found in some Treg clones, GARP has not been detected on the surface of either human or mouse activated Teff (15).

Interestingly, the LRRC32 gene locus is part of a chromosomal region that was described to be altered in several human cancers. In agreement with this finding, the GARP mRNA is highly amplified in tumor cells, and GARP surface expression has been detected in invasive, metastatic, and drug resistant tumors (16–18). Furthermore, in ovarian cancer, single nucleotide polymorphisms (SNP) were described in the non-coding regions of the LRRC32 (two were found in the 3' UTR, and one was found in the intron (rs3781699 and rs7944357, respectively), which have been associated with poor patient survival (19). Additionally, the gene locus of LRRC32 was also identified as a risk locus for asthma (20), atopic dermatitis (21), and colitis (22).

GARP Structure

GARP is an approximately 78 kDa type I transmembrane protein made-up of 662 amino acids with an extracellular region consisting of 20 LRR. In more detail, its structure has three domains: a cytoplasmic tail of 15 amino acid residues, a hydrophobic transmembrane domain, and an extracellular domain, containing the LRR, which accounts for about 70% of the protein (2). In addition, a signal peptide is located in the N-terminus, and its cleavage is required for the surface expression of GARP (4). The extracellular domain of GARP is similar to the corresponding region of other members of the LRR protein family, which in general play an important role in protein-protein interactions and signal transduction (2). It contains 20 LRR motifs, subdivided into two groups of 10 LRRs each by a proline rich domain and a C-terminal LRR [20]. The proline rich region confers flexibility and supports the idea of the involvement of GARP in protein-protein interactions. The two cysteines, Cys-192 and Cys-331, located in the 7th and 12th LRR respectively, are responsible for the two disulfide bonds that form between GARP and its ligand, latency associated peptide (LAP), in the LTGF-β complex (23). Following translation, GARP undergoes N-linked glycosylation and contains five predicted glycosylation sites (2, 24).

GARP Function

TGF-β is a pleiotropic cytokine, that is an important mediator during the development of Treg and the maintenance of their immunoregulatory state (25). Besides Treg, TGF-β is expressed by a multitude of cell types and tissues and participates in the mediation of numerous pathways, including development, wound healing, homeostasis, and cancer (26).

GARP has been shown to be essential for the formation and surface expression of LTGF-β on Treg. GARP binds all three isoforms of TGF-β (7, 27, 28) and plays an important role in TGF-β activation, which is first synthesized as a biologically inactive homodimeric precursor protein (23, 29, 30). This proprotein consists of three distinct parts: (I) mature TGF-β, (II) LAP, and (III) a signal peptide. Following the removal of the signal peptide, *via* cleavage by furin proteases, inactive TGF-β becomes mature TGF-β (31). Then, mature TGF-β binds LAP through both covalent (disulfide bridges) and non-covalent interactions (32). The resulting complex of mature TGF-β and LAP is called latent TGF-β (LTGF-β) and lacks biological activity. In the absence of GARP, LTGF-β binds to the latent TGF-β binding protein (LTBP), thereby forming the large latent complex (LLC), which associates with the extracellular matrix (ECM) (33). Surface GARP inhibits the binding of LTGF-β to the LTBP due to its higher affinity and in turn, presents LTGF-β on the cell surface. GARP enables the binding of latent TGF-β to $\alpha_V\beta_6$ and $\alpha_V\beta_8$ integrins, forming a ring-like shape with TGF-β orientated towards the center. This enables the release of TGF-β

from LTGF-β mediated by a protease dependent or a protease independent mechanism. Integrin recruited metalloproteinases or serine proteases may cleave LAP from the TGF-β – LAP - GARP complex. Of note, $\alpha_V\beta_6$ and $\alpha_V\beta_8$ are expressed in a cell type specific manner. In particular, Treg express $\alpha_V\beta_8$ (34). Protease independent release of TGF-β is facilitated through the binding of the respective integrins to LTGF-β and the resulting deformation of LAP, triggered by cell contraction. This results in the release of bioactive mature TGF-β into the extracellular space (34) (**Figure 1B**).

GARP REGULATION GARP AND ITS REGULATION IN TREG

Interplay of GARP and Foxp3

The detailed relationship between Foxp3 and GARP in Treg remains a matter of debate.

At first, it was described that the regulation of GARP is independent of Foxp3. This conclusion was based on studies, which demonstrated that TGF-β induced overexpression of Foxp3 was not sufficient enough to induce the expression of GARP (7, 36). Furthermore, it was shown that the knockout of Foxp3 in Treg did not change GARP expression, and correspondingly, the knockdown of GARP did not affect Foxp3 expression. However, a knockdown of GARP led to an impaired suppressive capacity of Treg, while silencing of Foxp3 in GARP-expressing cells did not affect their suppressive capacity, but knockdown of Foxp3 lead to an impaired Treg function (8). Interestingly, GARP is not expressed by resting $CD4^+Foxp3^+$ Treg, but it is upregulated upon Treg activation. In comparison, $CD4^+Helios^+Foxp3^-$ cells upregulate the expression of GARP/LAP upon TCR stimulation, supporting that Foxp3 and GARP are not regulated by each other (37).

In contrast to this conclusion, Probst-Kepper et al. proposed a mutual dependency of Foxp3 and GARP expression, which occurs in a positive feedback loop like manner. They were able to demonstrate that lentiviral downregulation of the GARP mRNA led to the downregulation of Foxp3 and the loss of Treg suppressive properties. Similarly, the downregulation of Foxp3 also resulted in the downregulation of GARP mRNA and impaired suppressive Treg function (15).

Pre-Transcriptional Regulation of LRRC32

Haupt et al. improved our understanding of the regulation of LRRC32 by showing that the transcription factors, nuclear factor of activated T cells (NFAT) and nuclear factor kappa light chain enhancer of activated B cells (NF-κB), play an important role in the expression of LRRC32. Transcription of LRRC32 is driven by two different promoter regions, P1 and P2, which differ in their methylation status depending on the cell type examined and the surrounding environmental conditions. It was shown, that in Treg, P1 and P2 are completely demethylated. This allows Foxp3 to bind to P1, opening the promoter region *via* chromatin remodeling, enabling the binding of NFAT and NF-κB, resulting in the expression of LRRC32. In contrast, Th cells differ from Treg as they exhibit increased methylation of their P1 promotor, which consequently prevents the expression of LRRC32 (5).

In 2020, Nasrallah et al. were able to show that an enhancer, located at chromosome 11q13.5, is active in Treg (22). This enhancer forms conformational interactions with the promoter of LRRC32, and the enhancer risk variant, rs11236797, is associated with a reduction in histone acetylation and decreased LRRC32 expression. This is based on the recruitment of STAT5 and NF-κB (22), which in turn mediate the expression of LRRC32. Therefore, these transcription factors are vital for Treg-mediated suppression. Any disruption of LRRC32 leads to early lethality in mice. The knockout of the enhancer led to the development of Treg that did not express LRRC32/GARP, which were unable to control colitis in an adoptive transfer model. This underlines the results of previous studies, that indicated that GARP is necessary for Treg function (8, 22).

Recently, Lehmkuhl et al. demonstrated that GARP-deficient murine Tregs were characterized by an unstable Treg phenotype as reflected by the decreased expression of CD25, Neuropilin-1 (Nrp1), cytotoxic T-lymphocyte-associated Protein 4 (CTLA-4), Interleukin-10 (IL-10), and Histone deacetylase 9 (HDAC9), and they were characterized by impaired immunosuppressive activity (38). These alterations were due to decreased acetylation of Foxp3 in comparison to stable Treg. Interestingly, it was found that GARP could regulate the expression of HDAC9, which is responsible for Foxp3 acetylation and thus Treg stability (38, 39). Future studies are necessary to elucidate how HDAC9, NFAT, and NF-κB interact and how their interplay affects the expression of LRRC32/GARP in more detail.

Post-Transcriptional Regulation of the GARP mRNA

It is becoming increasingly apparent that the expression of GARP is tightly regulated. Hereby, miRNA have been shown to play an important role. miRNA are single stranded, conserved, non-coding RNA molecules that play an essential role in post-transcriptional regulation (40). By binding to sequence complementary sites within the 3' UTR of their target mRNAs, miRNA lead to translation inhibition and mRNA degradation, which collectively leads to the suppression of gene expression. Numerous miRNA have already been found to regulate the development, differentiation, proliferation, and suppressive function of Tregs, including the targeting of the GARP mRNA itself (41).

As mentioned in *section 2.1, LRRC32 Structure*, the 3' UTR of LRRC32 contains five evolutionary conserved regions, which are a promising indicator for potential miRNA recognition sites (6). So far, several miRNA have been found to target the 3' UTR of the GARP mRNA in human Treg. Zhou et al. found that miR-142-3p directly binds to the 3' UTR of the GARP mRNA and promotes its subsequent degradation *via* the Argonaute 2 pathway in primary $CD4^+CD25^+$ human T cells (6). They could also show that miR-142-3p controls the expression of GARP mRNA/GARP in activated Treg. Upon Treg activation, GARP mRNA/GARP levels are upregulated. However, the reason GARP levels subsequently decline following activation

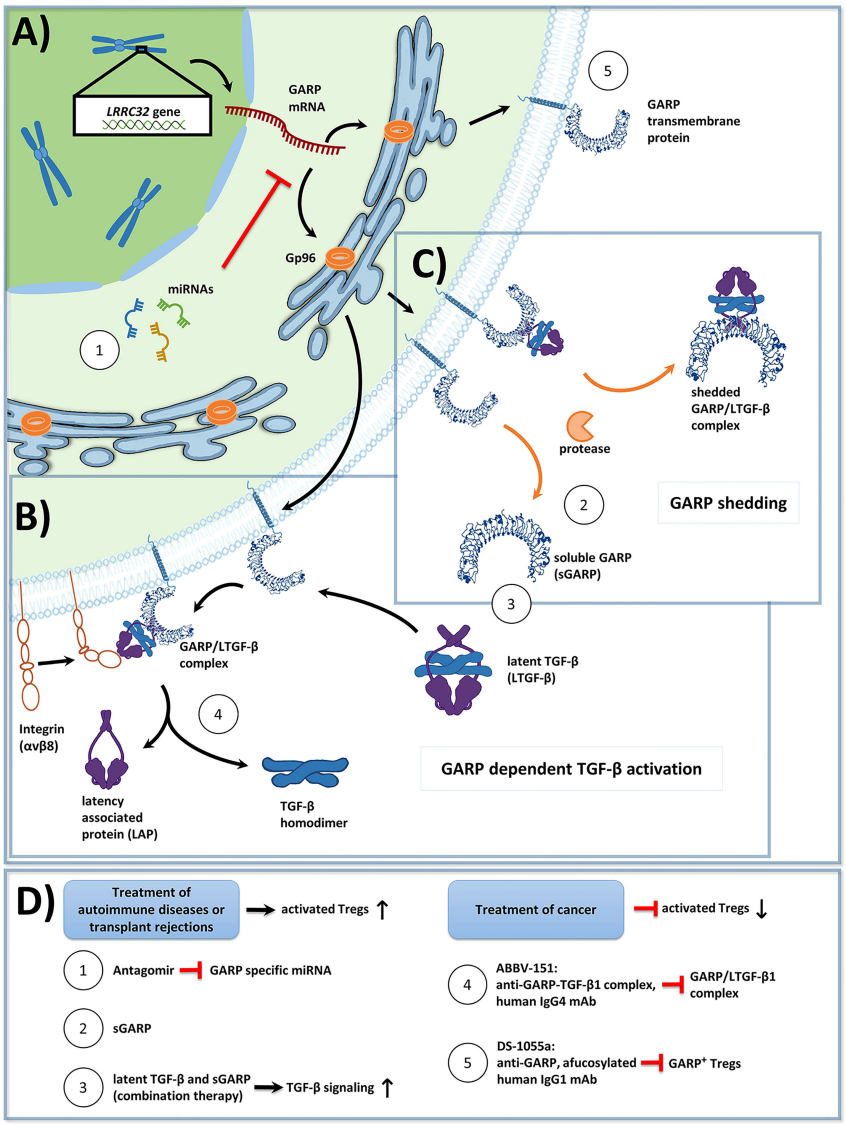

FIGURE 1 | **(A)** Overview of Glycoprotein a repetitions predominant (GARP) protein biosynthesis and transport to the cell membrane in activated human regulatory T cells (Tregs). GP96, a chaperone found in the endoplasmic reticulum, ensures proper folding of GARP [GARP structure modified from: Liénart et al. (35)]. The GARP mRNA is targeted by miRNA, which promote its degradation, and thus lower GARP mRNA/GARP levels. **(B)** GARP functions as a docking receptor for biologically inactive latent transforming growth factor beta (LTGF-β), which consists of a TGF-β homodimer bound to latency associated protein (LAP), and GARP plays an important role in its activation. GARP binds LTGF-β with high affinity, forming the GARP/LTGF-β complex. Release of bioactive TGF-β can occur in both a protease independent (shown) or a protease dependent manner (not shown). For protease independent release of mature TGF-β, $\alpha_V\beta_8$ integrins, expressed on the surface of Treg bind to the GARP/LTGF-β complex, resulting in a conformational change and in the subsequent release of biologically active TGF-β. Alternatively, bioactive TGF-β can be released in a protease dependent manner, in which integrin recruited metalloproteinases or serine proteases cleave LAP from the GARP/LTGF-β complex (not shown). **(C)** GARP can be cleaved from the surface of Treg by proteases in a form called soluble GARP (sGARP). GARP/LTGF-β complexes can also be released into the extracellular environment via proteases. **(D)** Potential methods to target GARP for the treatment of autoimmune diseases, transplant rejections, and cancer. Enhancing GARP mediated suppression by Treg offers a promising strategy for the treatment of autoimmune diseases and transplant rejections. (1) Approach 1 utilizes antagomirs, specific to miRNA, which target the GARP mRNA. This would prevent GARP mRNA degradation, and thus increase surface GARP expression and enhance the suppressive capacity of Treg. (2) Approach 2 is to apply sGARP to induce Treg. (3) Approach 3 would be to apply sGARP in combination with LTGF-β to harness both their immunosuppressive effects and to promote the activation of TGF-β in an integrin-controlled manner. For effective anti-tumor immune responses to occur, Treg mediated suppression needs to be inhibited. (4-5) Approaches 4 and 5 represent two different monoclonal antibody (mAb) therapeutic strategies, that are currently in phase 1 clinical trials. (4) Approach 4 uses an IgG4 antibody (ABBV-151) that binds to the GARP/TGF-β1 complex and prevents the release of mature TGF-β1. This results in an inhibition of TGF-β1 signaling, a subsequent decrease in the suppressive capacity of Treg, and the restoration of T effector cell (Teff) functions. (5) Approach 5 employs an afucosylated IgG1 antibody (DS-1055a), that efficiently depletes $GARP^+$ Treg via antibody-dependent cellular cytotoxicity, preventing Treg mediated suppression and restoring Teff function.

results from the upregulation of miR-142-3p, which binds to the GARP mRNA and targets it for subsequent degradation. Gauthy et al. could show that miR-185, and miR-181 a, b, c, d, in addition to miR-142-3p, target the 3' UTR of GARP mRNA in human Treg differentiated from PBMCs (31) (**Figure 1A**). Furthermore, they could show that these miRNA were also expressed at a lower level in human Treg when compared to Th cells. Interestingly, a study by Jebbawi et al. demonstrated that miR-24 and miR-335 directly bind to the 3' UTR of the GARP mRNA and regulate GARP levels (34). It is important to note that they examined primary human $CD8^+CD25^+$ Treg derived from cord blood in contrast to the aforementioned studies, which studied human $CD4^+$ Treg (42). These differences in cell type and tissue source may help explain in part why different sets of miRNA were detected.

Post-Translational Regulation of GARP

Surface expression of GARP has been found to be dependent on the heat shock protein, GP96 (GRP94) (43). GP96 is a master chaperone, which is found in the endoplasmic reticulum (ER), and its clientele consists of proteins implicated in both immune response and oncogenesis, such as toll-like receptors (TLR), integrins, Wnt co-receptor low-density lipoprotein receptor-related protein 6 (LRP6), insulin-like growth factor (IGF), platelet glycoprotein Ib-IX-V complex, and human epidermal growth factor receptor-2 (HER2) (43, 44). In a study by Zhang et al., examining the effects of GP96 knockout (KO) in Treg *in vivo*, it was discovered that although GP96 KO mice developed Treg, they displayed unstable Foxp3 expression, increased IFN-γ production, and impaired suppressive function, thus leading to the development of fatal autoimmunity (43). One reason for this reduction in Treg suppressive function was a decrease in surface GARP expression and mature LTGF-β levels. Loss of surface GARP and mature LTGF-β was also observed in $CD41^+$ GP96 KO platelets and GP96 deficient B cells, suggesting that GP96 acts as an obligate chaperone for GARP. Loss of surface GARP expression in GP96 deficient B cells was attributed to the inability of GARP to leave the ER and was accompanied by a decrease in the half-life of GARP. Collectively, this suggests that GP96 is required for the stable protein conformation of GARP. In addition, it was discovered that GARP interacts with the C-terminal client-binding domain of GP96 as also reported for TLRs (43).

Another protein that interacts with GARP, lysosomal associated transmembrane 4B (LAPTM4B), was identified in a yeast two hybrid assay (37). LAPTM4B expression increased upon Treg activation, and it directly decreased the surface expression of GARP and the secretion of LTGF-β1. LAPTM4B has been postulated to function as part of a negative feedback mechanism to downregulate Treg production of LTGF-β1 and surface GARP during T cell activation. Translocation of intracellular GARP to the surface of Treg upon activation requires the cleavage of a signal peptide located in the N-terminus of GARP (4). It has also been found in a model of forced GARP overexpression in T cells, TCR activation was needed for the translocation of intracellular GARP to the cellular surface. Furthermore, in case of Treg, IL-2 signaling is able to specifically increase the surface expression of GARP (45, 46).

It has been described that activated Treg shed a soluble form of GARP (sGARP) from their surfaces (18). Shedding of GARP was first proposed by Roubin et al. in their description of the protein structure of GARP. They hypothesized, that a hydrophobic leader sequence embedded in the amino acid sequence of GARP may resemble a signal peptide for secretion (3). The shedding of GARP has been subsequently confirmed in blood plasma by mass spectrometry (47). Additionally, Metelli et al., were able to show that thrombin can cleave GARP from the surface of platelets, which is essential for the release of membrane latent TGF-β (mLTGF-β) (48). Shedding of GARP/LTGF-β1 complexes from the surfaces of stimulated Treg and GARP overexpressing Th cells has also been described and detected in cell supernatants (31) (**Figure 1C**). These complexes may have been shed from the membrane by proteases, and their functional significance remains unknown.

SOLUBLE GARP

As mentioned earlier, sGARP is released by an array of different cell types, including activated Treg, activated platelets, and cancer cells. Hahn et al. could show that sGARP can modulate immune responses and has strong suppressive properties (49). In this regard, recombinant sGARP was found to suppress the proliferation and cytokine production of Teff. Exposure of naive T cells to sGARP led to an induction of Treg. This transition was accompanied by the induction of Foxp3 expression, the inhibition of cell proliferation, and a significant decrease in IL-2 and IFN-γ production. Furthermore, sGARP induced a tumor associated "M2-like" macrophage (TAM) phenotype and suppressed cytotoxic T cell function by inhibiting cell proliferation and the production of IFN-γ and Granzyme B (49).

Additionally, in a humanized mouse model of a xenogenic graft versus host disease (GvHD), the application of recombinant sGARP protected the animals from T cell mediated inflammation through Treg activation (49). It was also found that sGARP drives epithelial-mesenchymal cell transition (EMT). Cells treated with sGARP showed increased proliferation and migratory capacities in comparison to the untreated control (30).

The mechanism by which sGARP induces these phenotypic changes is at least in part dependent on the TGF-β signaling pathway, as phosphorylation of Mothers against decapentaplegic homolog 2 and 3 (Smad2/3) in sGARP treated naive $CD4^+$ T cells was observed. However, inhibition of TGF-β signaling by the use of a TGF-β receptor II blocking antibody could not fully prevent the effects of sGARP (49).

These findings could be confirmed by our group using a physiological source of sGARP (12). Activated platelets have been shown to shed GARP from their surfaces. Based on these findings, $CD4^+$ T cells were cocultured with platelet conditioned medium (PCM). PCM was able to induce Treg, characterized by a strong Foxp3 expression, while simultaneously suppressing their proliferation as well as their IL-2 and IFN-γ production when compared to the untreated control. Administration of a

blocking anti-GARP antibody was able to mitigate these effects. Furthermore, it was shown that blockade of the TGF-β pathway, by applying blocking antibodies against TGF-β I-III and TGF-β RII, could not completely inhibit the effects of PCM on T cells. This indicates that sGARP mediates its effects in part through a TGF-β independent signaling pathway (12).

Furthermore, it has been shown that recombinant sGARP has a strong capability to enhance the activation of free latent TGF-β. This function further amplifies the effects of sGARP in the case of autoimmunity and cancer (50).

Collectively, this leads to the conclusion that sGARP is able to achieve two things in parallel, which may multiply its immunomodulatory effects. First, sGARP has the ability to modulate the differentiation and suppression of immune cells. Second, sGARP can enhance the activation of TGF-β and correspondingly its manifold downstream effects. Therefore, sGARP may act as an important player in both autoimmunity and the tumor microenvironment (TME). Taken together, this highlights the importance of sGARP as a potent immunoregulatory molecule on its own and in its interplay with TGF-β.

CELLULAR GARP

Regulatory T Cells

$CD4^+CD25^+CD127^{low}Foxp3^+$ Treg, a highly immunosuppressive subset of $CD4^+$ T cells, play a major role in immune homeostasis by controlling immune responses through the induction and maintenance of peripheral tolerance (51). As mentioned above, GARP is expressed on the surface of activated Treg and plays a vital role in conveying their suppressive capacity (**Figure 1A**). GARP expression is also obligatory for the binding of TGF-β1 to the surface of Treg (7, 36).

Until recently, the functions of GARP on Treg were described as aiding in the presentation of LTGF-β by acting as both an anchor and support protein for the activation and release of LTGF-β (7). It has been shown that $GARP^+$ Treg in comparison to $GARP^-$ Treg displayed a greater suppressive capacity of Teff *in vitro*. This difference was associated with a decrease in the effector cytokines IL-2 and IFN-γ production (15, 36) and a corresponding increase in the production of the inhibitory cytokines TGF-β and IL-10 (52, 53).

Resting murine Treg express a low level of GARP. Upon TCR stimulation GARP gets upregulated on the cell surface of Treg, followed by an increased expression of latent TGF-β1. GARP expression can be upregulated on murine Treg *via* exposure to IL-2 and IL-4 without the need for TCR activation *in vitro*. Expression of GARP in mice was found to be independent of TGF-β1, but specific KO of GARP in murine $CD4^+$ T cells leads to a diminished expression of TGF-β1 on the surface of activated Treg. These $GARP^-$ Treg were found to develop normally and were capable of suppressing Teff *in vitro*. Additionally, Treg numbers in the periphery were not affected. Treg which express GARP/LTGF-β1 on their surfaces are able to induce Treg in the presence of IL-2, while the presence of IL-6 leads to the induction of Th17 cells (45, 46).

Further evidence highlighted the importance of GARP in Treg function. In a humanized mouse model of allogenic graft rejection, $CD4^+CD25^{high}CD127^{low}$ Treg and $CD4^+CD25^{high}$ Treg showed a significantly lower capacity in preventing alloreactions in comparison to $CD4^+CD154^-GARP^+$ and $CD4^+CD154^-LAP^+$ Treg (54). This study concluded that LAP and GARP are specific markers for human Treg having a high suppressive activity. In addition, a complete depletion of activated $GARP^+$ Treg in a humanized mouse model of allergen-induced gut inflammation diminished the protective effects of Treg (55).

In Treg with mutated LRRC32, expression of GARP was reduced, resulting in an unstable Treg phenotype that led to severe immune dysregulation and an increased development of inflammatory diseases (38). In giant cell arteritis, the most common primary arteritis, based on an imbalance of activated Teff cells and dysfunctional Treg, patients' Treg showed an ineffective and reduced induction of GARP (56).

In a preclinical approach, *in vitro* expanded Treg were isolated based on their selective surface expression of LAP. Herein, $LAP^+GARP^+Foxp3^+$ Treg showed a highly demethylated Treg-Specific Demethylated Region, indicating a stable Foxp3 expression and ultimately a stable Treg phenotype. Additionally, these cells showed a high suppressive capacity *in vitro* and in a GvHD *in vivo* model, making these cells a suitable population for the treatment of GvHD in patients (57).

Taken together, GARP expression on Treg significantly influences the immunological balance in different settings: $GARP^+$ Treg lead to immunosuppression, being of importance especially in the tumor microenvironment. Deficiency of GARP in Treg has an impact on the development of inflammatory diseases including autoimmunity, allergy and transplant rejection.

Non-Treg Cells

Besides Treg, B cells are known to express GARP when activated by TLR ligands, such as TLR4, TLR7, and TLR9 (58). Expression of GARP led to the inhibition of cell proliferation, induced a class switch to IgA production, and resulted in a more tolerogenic B cell phenotype. This has been explored especially in the context of autoimmune diseases (10, 58). Herein, GARP was upregulated on B cells in autoimmune diseases and the GARP-LTGF-β axis was shown to be an important factor for B cell tolerance and prevention of lupus-like autoimmune diseases in mice.

Furthermore, hepatic stellate cells constitutively express GARP on their surfaces. A blockade or knockdown of GARP resulted in an impaired suppression of T cell proliferation and IFN-γ production. It has been described that GARP is required to anchor and activate LTGF-β. Whether the observed effects are mainly mediated by LTGF-β, a suppressive function of GARP itself, or by a release of sGARP has not yet been described (14). Nevertheless, being expressed on cells involved in fibrosis as well as in hepatic cell cancer progression, it will be of interest to further investigate influence of GARP in this context.

In multipotent mesenchymal stromal cells (MSC), GARP has been shown to be important for their proliferation and survival by rendering them more resistant to DNA damage and apoptosis in a TGF-β dependent manner (59). In addition, GARP is involved in the immunomodulatory activities of MSC (60).

Platelets

Expression of GARP was initially described on the surface of platelets (3). Platelets are the main cells that mediate hemostasis at the site of injury. Platelets are important modulators of both innate and adaptive immunity through their interaction with immune cells. In the case of infection, platelets become activated and are able to modulate inflammation (61, 62). In addition, recent evidence indicates that platelets are present in the TME, and cancer associated thrombocytosis has been associated with the promotion of invasion and metastasis, and thus poor clinical outcomes in different tumor entities (63). Low platelet counts and inhibited platelet activation in patient blood correlated with a lower likelihood of metastasis (64, 65). In more detail, platelets promote motility (66–68) and EMT (69). Furthermore, platelet count and activation status influenced the survival of circulating tumor cells (CTC) by shielding them from NK cells and from destruction by shear stress (70, 71). This is due to their expression of fibrinogen receptor GPIIb-IIIa and P-Selectin, which mediate the attachment of platelets onto CTCs *via* the binding of CD44 and avB3 integrin (70). In addition, melanoma cells express chemokines that attract and activate platelets, in a process called tumor cell-induced platelet aggregation (72), resulting in the shielding of metastasizing melanoma cells by platelets in the bloodstream. Platelet-derived TGF-β has been shown to be an important modulator of the immune system (73). Besides being known for its immunosuppressive capability, TGF-β can downregulate B-cell lymphoma 2 (Bcl-2) proteins, known for their anti-apoptotic effects, as well as natural killer group 2D (NKG2D) leading to a decrease in NK cell efficacy (74). While there is increasing evidence that GARP on platelets plays an important role in immunomodulation, GARP does not seem to play a significant role in hemostasis and thrombosis. The conditional knockout of GARP on platelets and endothelial cells in mice did not lead to any changes during agonist induced platelet activation and aggregation. Furthermore, the tail bleeding time and the FeCl3-induced thrombus formation occlusion time were not affected (75).

There has been an emerging role of platelets not only in hemostasis but also in the immunomodulation of cancer patients. Given the fact that platelets express GARP on their surfaces and connecting this to previous works describing GARP as a key molecule in inducing peripheral tolerance, several groups have shown a possible contribution of platelets to adaptive immunity, leading to a poor prognosis of cancer patients with cancer associated thrombocytosis. For example, GARP was found to be expressed on platelets to a certain extent; however, upon platelet activation, surface GARP levels were found to be significantly increased (12). We demonstrated that, cocultures of platelets and Teff as well as Teff grown in the presence of PCM induced a regulatory phenotype, characterized by an upregulation of Foxp3, reduced proliferation, and decreased effector cytokine production, as well as an induction of suppressive capacity. This phenomenon was shown to be GARP dependent. In addition, the TGF-β signaling axis seemed to be at least in part associated to GARP mediated Treg induction (12). The cleavage of GARP by proteolysis through thrombin from the surface of platelets, has been shown to be a major contributor to cancer immune evasion. The blockade of the GARP cleavage led to an improved therapeutic efficacy of anti-PD-1 therapy (48). Furthermore, activated platelets released sGARP, as shown by us and Metelli et al., which in turn induces Treg in a GARP dependent manner (12, 48).

Tumor Cells

As already mentioned, GARP has been shown to be expressed by several tumor entities, like malignant melanoma (18), glioblastoma (16), bone sarcoma (17), breast cancer (76), and lung cancer (77).

It has been shown that the relation between Foxp3, GARP, and TGF-β, as thoroughly analyzed in Treg, also plays an important role in cancer progression. Tumor cells employ a form of "Treg mimicry", by utilizing specific immunosuppressive strategies, similar to Treg, to modulate their surroundings (16, 18, 78, 79). In bone sarcoma, GARP plays a vital role in cancer cell proliferation and resistance against irradiation and chemotherapy. Silencing of GARP in these cells led to a decrease in cell proliferation and an increase in apoptosis (17). Li et al., were able to show that GARP also plays an important role in the regulation of TGF-β1 in osteoblast differentiation. Downregulation of the GARP mRNA/GARP in bone marrow mesenchymal stem cells (BMSC) attenuated their differentiation into osteoblasts (80). Furthermore, normal murine mammary epithelial cells, showed an increased production of TGF-β and oncogenesis when GARP was overexpressed. Furthermore, the murine mammary gland tissue cell line, NMuMG, that was unable to form tumors *in vivo*, was able to do so once GARP was overexpressed (30).

In a coculture with $CD4^+$ T cells, glioblastoma cells were able to suppress the proliferation and IFN-γ production of the former. By using a blocking anti-GARP antibody, the proliferation and cytokine production of $CD4^+$ T cells could be restored (16). Malignant melanoma has been shown to release sGARP into its surroundings, suggesting a further contribution to a GARP-TGF-β mediated immunosuppressive microenvironment (18).

Zhang et al. showed that in pancreatic cancer, tumor cells were able to reprogram M1-like macrophages metabolically and functionally through a GARP-dependent and *via* a DNA methylation-mediated mechanism to M2 macrophages with a pro-tumorigenic phenotype (11).

All these data show that GARP on tumor cells is I) maybe involved in tumor cell proliferation and II) significantly modulates immune responses leading to an inhibitory tumor micromilieu, both facts resulting in massive tumor promotion.

ROLE OF GARP IN DISEASE SETTINGS

The presence of GARP as a soluble factor and as a surface marker on different cell types influences immune mediated diseases, such as cancer, allergy, and autoimmunity. The presence of GARP, e.g. in tumors, leads to a suppression of immune responses, whereas the loss of GARP, e.g. in autoimmunity, leads to spontaneous

inflammation. As such, GARP can be used as both, a biomarker and therapeutic target.

GARP as a Biomarker

Examining sGARP levels in easily accessible specimens, like serum and plasma from routine blood tests, and correlating their content to patient diagnoses and clinical outcomes is a novel approach to evaluate the potential of sGARP as a diagnostic and prognostic biomarker. This information would be highly valuable for clinicians as it is not only a more practical, time efficient, and cost-effective approach than screening for GARP expressing cells, but it is also a less invasive procedure for patients. Reliable assessment of the concentration of sGARP in patient blood could be of high importance as even low levels of sGARP are capable of greatly enhancing the activation of TGF-β (50). Therefore, elevated sGARP levels in cancer patients could have a great impact on the TME, leading to unfavorable patient outcomes.

Metelli et al., were able to detect high levels of sGARP and sGARP/LTGF-β1 complexes in the blood plasma of prostate cancer patients. Increased amounts of sGARP correlated with increased likelihood of metastasis in these patients (48).

Some studies have indicated that TGF-β, which is regulated by GARP, plays an important role in DNA repair, and may protect cells from ionizing radiation. Kim et al., could show that pretreatment of human epidermoid carcinoma cells with TGF-β reduced γ-radiation induced apoptosis (73). However, to the best of our knowledge, no known study has examined the possibility of GARP as a predictive marker for radiation sensitivity in cancer cells yet.

GARP is an enticing potential diagnostic biomarker for cancer as it is highly upregulated on the surface of both tumor cells and suppressive immune cells found in the TME (16, 18). Nevertheless, only a few studies have examined the possibility of GARP as a diagnostic biomarker in further detail. One study by Jin et al., examined the potential of GARP on Treg as a diagnostic biomarker in both the tumor tissue and peripheral blood of lung cancer patients. They found that frequencies of GARP expressing Treg were higher in the tumor tissue of early stage (I-II) versus late stage (III- IV) patients but not in their peripheral blood (77). Additionally, we could show that melanoma patients, who do not respond to immunotherapy, showed a longer overall survival, when they had a low percentage of $GARP^+$ Treg (81). This was also the case in hepatocellular carcinoma, as a high frequency of $Foxp3^+GARP^+$ Treg correlated with a more aggressive phenotype and a TME with enhanced suppressive properties (82).

A study by Metelli et al. showed that high GARP expression in lung cancer versus healthy adjacent tissue correlated with a reduced overall survival (30). The same observation was also described in bone sarcoma (17). Furthermore, it has been shown that GARP expression is increased in gastric cancer (83). Here, increased levels of $CD4^+GARP^+$ T cells in the tumor vicinity correlated with poor overall survival. Interestingly, elevated expression of GARP also correlated with the expression of CTLA-4 and PD-L1 (83).

Correlation data listed by the Human Protein Atlas, based on the TCGA data set, show that renal and urothelial cancer patients with elevated GARP mRNA levels have a significantly lower overall survival when compared to patients with lower GARP mRNA concentrations (proteinatlas.org/ENSG00000137507-LRRC32). This was not observed though for human lung cancer.

As mentioned before, it has been described that GARP expression was increased on the platelets of melanoma patients, but there were no differences between stage I and stage IV patients (12). One potential limitation of this study was the composition of the patient cohort, as 15 out of 16 patients responded to immunotherapy, potentially impacting the GARP expression levels found on platelets. Nevertheless, a potential use of GARP as a biomarker on platelets should be analyzed in a larger patient cohort (12). As outlined above, an increased platelet count in malignant melanoma patients is associated with poor prognosis. Furthermore, patients, who did not respond to immunotherapy, had an increased platelet to lymphocyte ratio as compared to responders to immunotherapy (12, 81, 84). Elevated platelet counts, increased expression of GARP on platelets, and shedding of GARP from their surfaces, combined with the fact that platelets are able to GARP dependently induce Treg, may be a highly disadvantageous combination that negatively affects patient survival. However, future studies must be conducted to evaluate platelet counts and their GARP levels as potential predictive and prognostic biomarkers for immunotherapy response and disease progression in melanoma.

In patients with inflammatory diseases, GARP has begun to be evaluated as a potential biomarker. For example, in patients with primary biliary cholangitis, an autoimmune biliary disease, GARP was found to be upregulated on cholangiocytes and was also detected on biliary duct cells (85). Herein, GARP expression was increased in response to biliary salts and released under cholestatic conditions *via* apoptosis of cholangiocytes. Atopic dermatitis patients showed a significantly reduced surface expression of GARP on Treg (21). Furthermore, patients with psoriasis, who received systemic therapy, had higher frequencies of activated $GARP^+$ Treg than patients, who were only treated with topical therapy (86). Research in mice revealed that there is an increased expression of GARP on B cells in murine models of lupus (58). Whether these findings can be translated into the human setting has to be investigated in future trials.

Taken together, it will be interesting to validate GARP, either in its soluble or in its cell-associated form, as a predictive and prognostic biomarker in patients with immune mediated diseases in future clinical trials and to investigate whether GARP could be used as an early indicator for therapy response.

GARP as a Therapeutic Target

As described in *section 5, Cellular GARP*, GARP is expressed by a variety of cells in the TME and plays a prominent role in immunosuppression and cancer progression. Drugs that modulate the expression of GARP may be useful for the treatment of various disease indications. Enhancing GARP expression, and its accompanying immunosuppression, may be beneficial for the treatment of autoimmunity and transplant rejection, whereas downregulating GARP expression may aid in the improvement of anti-tumor immune responses (**Figure 1D**).

Herein, several strategies are possible. On one hand, increased and long-lasting expression of GARP on Treg could lead to GARP$^+$ Treg, which are more potent in inhibiting the proliferation and function of conventional Teff. This approach of improving Treg efficiency could be used in the treatment of autoimmunity and allergic diseases in order to modulate and downregulate overshooting immune or inflammatory processes.

Inhibition of miRNA, through the use of so called antagomirs, might be one possibility to induce elevated and long lasting GARP expression in Treg (**Figures 1A, D**). Antagomirs are oligonucleotides complementary to the mature form of specific miRNA. They easily penetrate into cells, and they inhibit the activity of their target miRNA, both *in vitro* and *in vivo* (87). Thus, they could represent a novel class of therapeutic molecules, leading to a sustained expression of GARP on Treg. Of note, transfer of miR-142-3p into Treg impaired their suppressive function (88). Importantly, Krützfeld et al. showed that antagomirs can be utilized as a systemic treatment and are resistant to degradation by RNases following injection into an organism (87). This approach should be further evaluated in future studies. One example would be to improve the clinical efficacy of human adoptive Treg transfer by enhancing the suppressive function and/or stability of Treg in an autoimmune or GvHD setting. Furthermore, in case of cancer and metabolic disease, the application of antagomir loaded nanoparticles to target unfavorable miRNA has already been demonstrated in several mouse studies (89, 90), supporting the potential of antagomirs to be used in novel therapeutic approaches.

As demonstrated earlier, sGARP can have a beneficial effect in the induction of peripheral Treg and can help sustain Treg differentiation. Additionally, sGARP can inhibit Teff functions by reducing their proliferation and inflammatory cytokine production (18, 50). When sGARP was applied *in vivo*, it was shown to inhibit overshooting immune responses in a humanized mouse model of allergy (91) as well as of transplant rejection and in GvHD (49). This opens up further strategies in using sGARP as an immunomodulatory agent, such as in transplantation or autoimmune diseases (**Figures 1C, D**).

Furthermore, the simultaneous administration of sGARP and LTGF-β could also be a promising treatment approach (**Figures 1B-D**). Herein, GARP could bind LTGF-β and enhance its activation. Since integrins are necessary for the final activation step of TGF-β, this would minimize the risk of putative side effects of exaggerated TGF-β activation. This approach was already proposed by Fridrich et al. in 2016 (50). In more detail, they were able to show that even small doses of sGARP could greatly enhance the activation of LTGF-β. This could have implications for autoimmune diseases, as a low dose combination application of sGARP and LTGF-β may mitigate the potential side effects of high dosages of pre-activated TGF-β (50).

On the one hand, Treg cellular therapies have been shown to ameliorate autoimmune diseases, graft rejections, and GvHD (92, 93). Elevating GARP expression levels on Treg to increase and prolong their activation status or using sGARP to increase the number of Treg could contribute to the suppression of autoimmune responses by restoring T cell tolerance. On the other hand, targeting of GARP on activated Treg through the use of blocking antibodies could enhance anti-tumor immunity. Several studies have reported that targeting GARP provided protective immunity against melanoma and colon cancer and the depletion of GARP on platelets did not lead to changes in hemostasis and thrombosis (75, 94).

Currently, two therapeutic antibody products are in phase 1 clinical trials: ABBV-151 (NCT03821935) and DS-1055 (NCT04419532). Both antibodies aim for the reactivation of anti-tumor immunity by specifically inhibiting Treg in malignant solid tumors. However, they differ in their mechanism of action by several points.

ABBV-151 is a human IgG4 monoclonal antibody (mAb) that specifically binds to the GARP/LTGF-β1 complex to inhibit the release of mature TGF-β1 from LTGF-β1 (**Figures 1B, D**) (95). This results in a Treg specific blocking effect on functional TGF-β1 release. This leads to the inhibition of TGF-β1 signaling in Treg and Teff, which in turn decreases the suppressive effects by Treg and restores Teff functions in the TME. In a preclinical study, a mouse surrogate antibody that targeted the GARP/LTGF-β1 complex improved anti-tumor effects in a combination setting with an anti-mouse programmed cell death protein 1 (PD-1) antibody when compared with the anti–PD-1 treatment alone. However, the former antibody did not display anti-tumor activity when administered as a monotherapy alone in a CT26 tumor mouse model (96). The anti-tumor combination effects of the anti-GARP-TGF-β1 antibody did not require FcγR-mediated effector functions. In the current clinical study ABBV-151 is applied in parallel as a monotherapy and in combination with an anti-PD-1 antibody.

DS-1055a is an anti-GARP afucosylated human IgG1 mAb, that aims for the efficient depletion of GARP$^+$ Treg *via* antibody-dependent cellular cytotoxicity (**Figures 1A, D**) (97). This prevents Treg-mediated suppression of immune effector cells and thereby results in the reactivation of anti-tumor activities in the TME. In preclinical settings, DS-1055a treatment resulted in the depletion of GARP$^+$ Treg and increased Teff functions *in vitro* and exerted anti-tumor effects in HT-29 tumor bearing humanized mice. In addition, combined treatment of DS-1055a with an anti-PD-1 antibody yielded a combination effect since the proliferation of Teff increased in comparison to treatment with either agent alone.

GARP targeting antibodies can be described as a kind of Treg specific treatment approach. In immune cells of the TME, GARP expression is almost completely limited to activated Treg. Unlike other targeted Treg associated proteins, this specificity in GARP expression on activated Treg is considered to be critical for the recovery of intrinsic anti-tumor activities without affecting effector immune functions. It is important to await the results of the aforementioned phase 1 clinical trials to determine whether the inhibition of Treg function or the removal of Treg themselves from the TME can lead to the revival and activation of Teff from their immunosuppressive dormant state, and thus result in tumor eradication.

Since, at least in preclinical models, the effects of combined treatment with an anti-PD-1 antibody have been confirmed.

There is a rationale that GARP targeting antibodies have the potential to improve insufficient immune responses and decrease resistance to immune checkpoint inhibitors (ICI), like PD-1, programmed cell death protein ligand 1 (PD-L1), and CTLA-4, in clinical settings. In addition, the fact that GARP is expressed only by activated — not resting Treg, suggests that the actions of these antibodies should mainly occur in the highly immunosuppressive TME and should hopefully not lead to an increase in immune-related adverse events when used in combination with ICI.

In this regard, it has been shown that antibody mediated blockade or deletion of GARP did not alter innate or adaptive immune responses (98). Therefore, antibody therapies targeting GARP represent promising approaches in order to restore anti-tumor immunity without severely impairing other immunological defenses.

DISCUSSION

GARP presents as a promising target molecule in different disease settings. Of note, it is tightly associated to TGF-β and its functions. TGF-β is a pleiotropic cytokine and as such, a key mediator of many, often opposing biological processes. In cancer, TGF-β is a double-edged sword. It exerts potent cytostatic and pro-apoptotic activities in early stages of disease, but it can also paradoxically favor EMT and metastasis at later stages of malignant transformation, thus shifting from tumor inhibition to tumor promotion during the progression of cancer. In addition, it modulates the proliferation and function of different immune cells necessary for building a potent anti-tumor immune response, making it a difficult target for anti-cancer therapies. Therefore, due to this lack of specificity (in targeted function and cell type) resulting from the pleiotropic nature of TGF-β, combined with insufficient therapeutic efficacy, therapies directly targeting TGF-β have not entered the clinic for routine applications yet. In addition, clinical trials, which target TGF-β signaling, must be considered in combination with other therapies, including immune checkpoint blockade, chemotherapy, and radiotherapy.

One novel approach to address a particular function of TGF-β, is through the blockade of TGF-β1 activation by GARP expressing Treg using an anti-GARP:LTGF-β1 mAb. This would specifically prevent the release of TGF-β1 that is in complex with GARP. Whereas blocking of GARP:LTGF-β1 would decrease immunosuppression *via* Treg, another novel approach targets GARP itself.

This might delete important inhibitory cellular components of the TME, such as Treg and tumor cells. It can be argued that targeting and blocking GARP is a more promising upstream target, as GARP itself exerts a suppressive function on other cells as described above. Furthermore, cell surface complexation and soluble GARP have been shown to enhance TGF-β activation (50). Therefore, targeting GARP could lead to a simultaneous inhibition of TGF-β activation and function as well as the inhibition of the suppressive functions of GARP and sGARP. Whether an anti-GARP:TGF-β1 mAb is superior to using an anti-GARP mAb for blocking immune suppression in the TME will have to be analyzed in future studies. Both approaches have the potential to boost intrinsic anti-tumor activities and to show encouraging results in mouse models; however, a clinical validation is still awaited. Nevertheless, one challenge for the use of this therapeutic target could be the need for sufficient amounts of GARP on the surface of the mentioned cell types above. In addition, non-Treg side effects have to be taken into account, when using an anti-GARP antibody, as GARP is also expressed e.g. on activated platelets in peripheral blood (12). However, a GARP knockdown in platelets did not show any negative effects on hemostasis (75), and it also promoted anti-tumor immunity by inhibiting of TGF-β signaling in different cancer entities (94). Additionally, these findings point out a possible novel therapeutic approach in cancer based on the combination of GARP inhibition with platelet modulating agents, such as ticagrelor and aspirin (99).

It was shown by several groups (38) that GARP deficiency in Treg led to increased susceptibility to inflammatory diseases through the induction of immune dysregulation. Thus, GARP is somehow required to maintain immune homeostasis. It will be very interesting to investigate in more detail if and to what extend GARP alone contributes as an important molecule to Treg generation, stability, and function or whether GARP effects are solely modulated *via* regulation of TGF-β bioavailability.

In this context, the link between GARP and Foxp3 remains elusive. On the one hand, several publications support the idea that GARP and Foxp3 expression is independent of one and other (8, 36, 37, 46). On the other hand, it has been described that Treg specific transcription of LRRC32 is Foxp3 mediated, resulting from the synergistic interaction of Foxp3 with NFAT (5). Additionally, it has been suggested that there is a mutual dependency of Foxp3 and GARP expression, which influence Treg suppressive function. Future studies must be conducted to better understand the interdependence of GARP and Foxp3 expression in different cell types.

In most studies, GARP has been described as a surface molecule involved in the processing and maturation of TGF-β. Nevertheless, there are some reports showing cytoplasmatic and nuclear GARP expression as well (16). However, the function of this intracellular GARP and the significance of its intracellular localization need to be further characterized in future studies. These studies will help to clarify if GARP does have the same function on Treg, on platelets, and in cancer cells in means of the above-described functions, including suppressive capacity, proliferation, and therapy resistance.

Besides being a relevant therapeutic target, the use of GARP as a prognostic and predictive biomarker should be transferred into clinical routine. Quantification of GARP on peripheral blood cells, in serum, and on tumor tissue could potentially be used to reflect the immunosuppressive burden present in tumor patients. Up until now, there has been only little correlation between GARP expression and clinical tumor stages of patients. To gain more insight and to define a potential application of GARP as a biomarker, future studies should quantify GARP levels on blood cells, in serum, and on tumor tissues. Ideally, this should be performed with the use of multiplex approaches (100) in order to investigate in more detail the distribution and

complex spatial interactions of GARP$^+$ cells in the TME. These results can then be correlated back to clinical data.

Most data up until now has been generated from *in vitro* and *in vivo* (in mice) experimental models. There is an urgent need to translate and validate these results in the human system through clinical trials, as the findings of GARP (i.e. regulation) seem to be similar — but not identical to the murine setting.

CONCLUSION

GARP is a highly promising target molecule in diverse disease settings, and it is expressed by different cells and tissues that exert immunomodulatory functions. As such, it could serve as a relevant new biomarker in patients with immune related diseases, such as cancer and autoimmunity.

In addition, targeting of membrane GARP as well as the use of soluble GARP are attractive therapeutic approaches for the treatment of a wide variety of malignant, autoimmune, and inflammatory diseases. Of note, one cannot consider the contribution of GARP to the immunosuppressive function of Treg in the absence of its key partner: LTGF-β. Nevertheless, novel approaches are needed as LTGF-β is produced and expressed ubiquitously, whereas cellular GARP expression is much more restricted.

AUTHOR CONTRIBUTIONS

NZ and AT took the lead in structuring and writing the manuscript. ET and KS wrote some sections, modified, and reviewed the manuscript. BG prepared the figure, modified, and reviewed the manuscript. All authors contributed to the article and approved the submitted version.

FUNDING

This work was supported by CRC1066, TP-B14 to AT, Wilhelm-Sander-Foundation (2020.132.2) to AT, Hiege-Stiftung against skin cancer (200504) to AT, and a DAAD One-Year Research Grant for Doctoral Candidates (57552339) to ET.

ACKNOWLEDGMENTS

We thank Dr. Matthias Bros for critically reading the manuscript.

REFERENCES

1. Bopp T, Becker C, Klein M, Klein-Hessling S, Palmetshofer A, Serfling E, et al. Cyclic Adenosine Monophosphate Is a Key Component of Regulatory T Cell-Mediated Suppression. *J Exp Med* (2007) 204:1303–10. doi: 10.1084/jem.20062129
2. Ollendorff V, Noguchi T, deLapeyriere O, Birnbaum D. The GARP Gene Encodes a New Member of the Family of Leucine-Rich Repeat-Containing Proteins. *Cell Growth Differ* (1994) 5:213–9.
3. Roubin R, Pizette S, Ollendorff V, Planche J, Birnbaum D, deLapeyriere O. Structure and Developmental Expression of Mouse Garp, a Gene Encoding a New Leucine-Rich Repeat-Containing Protein. *Int J Dev Biol* (1996) 40:545–55.
4. Chan DV, Somani A-K, Young AB, Massari JV, Ohtola J, Sugiyama H, et al. Signal Peptide Cleavage is Essential for Surface Expression of a Regulatory T Cell Surface Protein, Leucine Rich Repeat Containing 32 (LRRC32). *BMC Biochem* (2011) 12:27. doi: 10.1186/1471-2091-12-27
5. Haupt S, Söntgerath VS, Leipe J, Schulze-Koops H, Skapenko A. Methylation of an Intragenic Alternative Promoter Regulates Transcription of GARP. *Biochim Biophys Acta* (2016) 1859:223–34. doi: 10.1016/j.bbagrm.2015.11.003
6. Zhou Q, Haupt S, Prots I, Thümmler K, Kremmer E, Lipsky PE, et al. miR-142-3p Is Involved in CD25+ CD4 T Cell Proliferation by Targeting the Expression of Glycoprotein A Repetitions Predominant. *J Immunol* (2013) 190:6579–88. doi: 10.4049/jimmunol.1202993
7. Tran DQ, Andersson J, Wang R, Ramsey H, Unutmaz D, Shevach EM. GARP (LRRC32) is Essential for the Surface Expression of Latent TGF-Beta on Platelets and Activated FOXP3+ Regulatory T Cells. *Proc Natl Acad Sci USA* (2009) 106:13445–50. doi: 10.1073/pnas.0901944106
8. Wang R, Wan Q, Kozhaya L, Fujii H, Unutmaz D. Identification of a Regulatory T Cell Specific Cell Surface Molecule That Mediates Suppressive Signals and Induces Foxp3 Expression. *PLoS One* (2008) 3:e2705. doi: 10.1371/journal.pone.0002705
9. Stanic B, van de Veen W, Wirz OF, Rückert B, Morita H, Söllner S, et al. IL-10-Overexpressing B Cells Regulate Innate and Adaptive Immune Responses. *J Allergy Clin Immunol* (2015) 135:771–80.e8. doi: 10.1016/j.jaci.2014.07.041
10. Dedobbeleer O, Stockis J, van der Woning B, Coulie PG, Lucas S. Cutting Edge: Active TGF-β1 Released From GARP/TGF-β1 Complexes on the Surface of Stimulated Human B Lymphocytes Increases Class-Switch Recombination and Production of IgA. *J Immunol* (2017) 199:391–6. doi: 10.4049/jimmunol.1601882
11. Zhang M, Pan X, Fujiwara K, Jurcak N, Muth S, Zhou J, et al. Pancreatic Cancer Cells Render Tumor-Associated Macrophages Metabolically Reprogrammed by a GARP and DNA Methylation-Mediated Mechanism. *Signal Transduct Target Ther* (2021) 6:366. doi: 10.1038/s41392-021-00769-z
12. Zimmer N, Krebs FK, Zimmer S, Mitzel-Rink H, Kumm EJ, Jurk K, et al. Platelet-Derived GARP Induces Peripheral Regulatory T Cells-Potential Impact on T Cell Suppression in Patients With Melanoma-Associated Thrombocytosis. *Cancers (Basel)* (2020) 12. doi: 10.3390/cancers12123653
13. Xing H, Liang C, Xu X, Sun H, Ma X, Jiang Z. Mesenchymal Stroma/Stem-Like Cells of GARP Knockdown Inhibits Cell Proliferation and Invasion of Mouse Colon Cancer Cells (MC38) Through Exosomes. *J Cell Mol Med* (2020) 24:13984–90. doi: 10.1111/jcmm.16008
14. Li Y, Kim B-G, Qian S, Letterio JJ, Fung JJ, Lu L, et al. Hepatic Stellate Cells Inhibit T Cells Through Active TGF-β1 From a Cell Surface-Bound Latent TGF-β1/GARP Complex. *J Immunol* (2015) 195:2648–56. doi: 10.4049/jimmunol.1500139
15. Probst-Kepper M, Geffers R, Kröger A, Viegas N, Erck C, Hecht H-J, et al. GARP: A Key Receptor Controlling FOXP3 in Human Regulatory T Cells. *J Cell Mol Med* (2009) 13:3343–57. doi: 10.1111/j.1582-4934.2009.00782.x
16. Zimmer N, Kim E, Sprang B, Leukel P, Khafaji F, Ringel F, et al. GARP as an Immune Regulatory Molecule in the Tumor Microenvironment of Glioblastoma Multiforme. *Int J Mol Sci* (2019) 20. doi: 10.3390/ijms20153676
17. Carrillo-Gálvez AB, Quintero JE, Rodríguez R, Menéndez ST, Victoria González M, Blanco-Lorenzo V, et al. GARP Promotes the Proliferation and Therapeutic Resistance of Bone Sarcoma Cancer Cells Through the Activation of TGF-β. *Cell Death Dis* (2020) 11:985. doi: 10.1038/s41419-020-03197-z
18. Hahn SA, Neuhoff A, Landsberg J, Schupp J, Eberts D, Leukel P, et al. A Key Role of GARP in the Immune Suppressive Tumor Microenvironment. *Oncotarget* (2016) 7:42996–3009. doi: 10.18632/oncotarget.9598
19. Derycke MS, Charbonneau B, Preston CC, Kalli KR, Knutson KL, Rider DN, et al. Toward Understanding the Genetics of Regulatory T Cells in Ovarian Cancer. *Oncoimmunology* (2013) 2:e24535. doi: 10.4161/onci.24535
20. Ferreira MA, Matheson MC, Duffy DL, Marks GB, Hui J, Le Souëf P, et al. Identification of IL6R and Chromosome 11q13.5 as Risk Loci for Asthma. *Lancet* (2011) 378:1006–14. doi: 10.1016/S0140-6736(11)60874-X
21. Manz J, Rodríguez E, ElSharawy A, Oesau E-M, Petersen B-S, Baurecht H, et al. Targeted Resequencing and Functional Testing Identifies Low-

Frequency Missense Variants in the Gene Encoding GARP as Significant Contributors to Atopic Dermatitis Risk. *J Invest Dermatol* (2016) 136:2380–6. doi: 10.1016/j.jid.2016.07.009
22. Nasrallah R, Imianowski CJ, Bossini-Castillo L, Grant FM, Dogan M, Placek L, et al. A Distal Enhancer at Risk Locus 11q13.5 Promotes Suppression of Colitis by Treg Cells. *Nature* (2020) 583:447–52. doi: 10.1038/s41586-020-2296-7
23. Wang R, Zhu J, Dong X, Shi M, Lu C, Springer TA. GARP Regulates the Bioavailability and Activation of Tgfβ. *Mol Biol Cell* (2012) 23:1129–39. doi: 10.1091/mbc.E11-12-1018
24. Sun L, Jin H, Li H. GARP: A Surface Molecule of Regulatory T Cells That is Involved in the Regulatory Function and TGF-β Releasing. *Oncotarget* (2016) 7:42826–36. doi: 10.18632/oncotarget.8753
25. Choi G, Na H, Kuen D-S, Kim B-S, Chung Y. Autocrine TGF-β1 Maintains the Stability of Foxp3+ Regulatory T Cells *via* IL-12rβ2 Downregulation. *Biomolecules* (2020) 10. doi: 10.3390/biom10060819
26. Gordon KJ, Blobe GC. Role of Transforming Growth Factor-Beta Superfamily Signaling Pathways in Human Disease. *Biochim Biophys Acta* (2008) 1782:197–228. doi: 10.1016/j.bbadis.2008.01.006
27. Stockis J, Colau D, Coulie PG, Lucas S. Membrane Protein GARP is a Receptor for Latent TGF-Beta on the Surface of Activated Human Treg. *Eur J Immunol* (2009) 39:3315–22. doi: 10.1002/eji.200939684
28. Wu BX, Li A, Lei L, Kaneko S, Wallace C, Li X, et al. Glycoprotein A Repetitions Predominant (GARP) Positively Regulates Transforming Growth Factor (TGF) β3 and Is Essential for Mouse Palatogenesis. *J Biol Chem* (2017) 292:18091–7. doi: 10.1074/jbc.M117.797613
29. Stockis J, Dedobbeleer O, Lucas S. Role of GARP in the Activation of Latent TGF-β1. *Mol Biosyst* (2017) 13:1925–35. doi: 10.1039/c7mb00251c
30. Metelli A, Wu BX, Fugle CW, Rachidi S, Sun S, Zhang Y, et al. Surface Expression of Tgfβ Docking Receptor GARP Promotes Oncogenesis and Immune Tolerance in Breast Cancer. *Cancer Res* (2016) 76:7106–17. doi: 10.1158/0008-5472.CAN-16-1456
31. Gauthy E, Cuende J, Stockis J, Huygens C, Lethé B, Collet J-F, et al. GARP Is Regulated by miRNAs and Controls Latent TGF-β1 Production by Human Regulatory T Cells. *PLoS One* (2013) 8:e76186. doi: 10.1371/journal.pone.0076186
32. Derynck R, Budi EH. Specificity, Versatility, and Control of TGF-β Family Signaling. *Sci Signal* (2019) 12. doi: 10.1126/scisignal.aav5183
33. Annes JP, Munger JS, Rifkin DB. Making Sense of Latent TGFbeta Activation. *J Cell Sci* (2003) 116:217–24. doi: 10.1242/jcs.00229
34. Edwards JP, Thornton AM, Shevach EM. Release of Active TGF-β1 From the Latent TGF-β1/GARP Complex on T Regulatory Cells is Mediated by Integrin β8. *J Immunol* (2014) 193:2843–9. doi: 10.4049/jimmunol.1401102
35. Liénart S, Merceron R, Vanderaa C, Lambert F, Colau D, Stockis J, et al. Structural Basis of Latent TGF-β1 Presentation and Activation by GARP on Human Regulatory T Cells. *Science* (2018) 362:952–6. doi: 10.1126/science.aau2909
36. Wang R, Kozhaya L, Mercer F, Khaitan A, Fujii H, Unutmaz D. Expression of GARP Selectively Identifies Activated Human FOXP3+ Regulatory T Cells. *Proc Natl Acad Sci U S A* (2009) 106:13439–44. doi: 10.1073/pnas.0901965106
37. Elkord E, Abd Al Samid M, Chaudhary B. Helios, and Not FoxP3, is the Marker of Activated Tregs Expressing GARP/LAP. *Oncotarget* (2015) 6:20026–36. doi: 10.18632/oncotarget.4771
38. Lehmkuhl P, Gentz M, Garcia de Otezya AC, Grimbacher B, Schulze-Koops H, Skapenko A. Dysregulated Immunity in PID Patients With Low GARP Expression on Tregs Due to Mutations in LRRC32. *Cell Mol Immunol* (2021) 18:1677–91. doi: 10.1038/s41423-021-00701-z
39. Tao R, de Zoeten EF, Ozkaynak E, Chen C, Wang L, Porrett PM, et al. Deacetylase Inhibition Promotes the Generation and Function of Regulatory T Cells. *Nat Med* (2007) 13:1299–307. doi: 10.1038/nm1652
40. Pu M, Chen J, Tao Z, Miao L, Qi X, Wang Y, et al. Regulatory Network of miRNA on its Target: Coordination Between Transcriptional and Post-Transcriptional Regulation of Gene Expression. *Cell Mol Life Sci* (2019) 76:441–51. doi: 10.1007/s00018-018-2940-7
41. Liu C, Li N, Liu G. The Role of MicroRNAs in Regulatory T Cells. *J Immunol Res* (2020) 2020:3232061. doi: 10.1155/2020/3232061
42. Jebbawi F, Fayyad-Kazan H, Merimi M, Lewalle P, Verougstraete J-C, Leo O, et al. A microRNA Profile of Human CD8(+) Regulatory T Cells and Characterization of the Effects of microRNAs on Treg Cell-Associated Genes. *J Transl Med* (2014) 12:218. doi: 10.1186/s12967-014-0218-x
43. Zhang Y, Wu BX, Metelli A, Thaxton JE, Hong F, Rachidi S, et al. GP96 is a GARP Chaperone and Controls Regulatory T Cell Functions. *J Clin Invest* (2015) 125:859–69. doi: 10.1172/JCI79014
44. Duan X, Iwanowycz S, Ngoi S, Hill M, Zhao Q, Liu B. Molecular Chaperone GRP94/GP96 in Cancers: Oncogenesis and Therapeutic Target. *Front Oncol* (2021) 11:629846. doi: 10.3389/fonc.2021.629846
45. Zhou AX, Kozhaya L, Fujii H, Unutmaz D. GARP-TGF-β Complexes Negatively Regulate Regulatory T Cell Development and Maintenance of Peripheral CD4+ T Cells *In Vivo*. *J Immunol* (2013) 190:5057–64. doi: 10.4049/jimmunol.1300065
46. Edwards JP, Fujii H, Zhou AX, Creemers J, Unutmaz D, Shevach EM. Regulation of the Expression of GARP/latent TGF-β1 Complexes on Mouse T Cells and Their Role in Regulatory T Cell and Th17 Differentiation. *J Immunol* (2013) 190:5506–15. doi: 10.4049/jimmunol.1300199
47. Qian W-J, Monroe ME, Liu T, Jacobs JM, Anderson GA, Shen Y, et al. Quantitative Proteome Analysis of Human Plasma Following *In Vivo* Lipopolysaccharide Administration Using 16O/18O Labeling and the Accurate Mass and Time Tag Approach. *Mol Cell Proteomics* (2005) 4:700–9. doi: 10.1074/mcp.M500045-MCP200
48. Metelli A, Wu BX, Riesenberg B, Guglietta S, Huck JD, Mills C, et al. Thrombin Contributes to Cancer Immune Evasion *via* Proteolysis of Platelet-Bound GARP to Activate LTGF-β. *Sci Transl Med* (2020) 12. doi: 10.1126/scitranslmed.aay4860
49. Hahn SA, Stahl HF, Becker C, Correll A, Schneider F-J, Tuettenberg A, et al. Soluble GARP has Potent Antiinflammatory and Immunomodulatory Impact on Human $CD4^+$ T Cells. *Blood* (2013) 122:1182–91. doi: 10.1182/blood-2012-12-474478
50. Fridrich S, Hahn SA, Linzmaier M, Felten M, Zwarg J, Lennerz V, et al. How Soluble GARP Enhances Tgfβ Activation. *PLoS One* (2016) 11:e0153290. doi: 10.1371/journal.pone.0153290
51. Sakaguchi S, Yamaguchi T, Nomura T, Ono M. Regulatory T Cells and Immune Tolerance. *Cell* (2008) 133:775–87. doi: 10.1016/j.cell.2008.05.009
52. Rappl G, Pabst S, Riemann D, Schmidt A, Wickenhauser C, Schütte W, et al. Regulatory T Cells With Reduced Repressor Capacities Are Extensively Amplified in Pulmonary Sarcoid Lesions and Sustain Granuloma Formation. *Clin Immunol* (2011) 140:71–83. doi: 10.1016/j.clim.2011.03.015
53. Zhong Y, Tang H, Wang X, Zeng Q, Liu Y, Zhao XI, et al. Intranasal Immunization With Heat Shock Protein 60 Induces CD4(+) CD25(+) GARP(+) and Type 1 Regulatory T Cells and Inhibits Early Atherosclerosis. *Clin Exp Immunol* (2016) 183:452–68. doi: 10.1111/cei.12726
54. Noyan F, Lee Y-S, Zimmermann K, Hardtke-Wolenski M, Taubert R, Warnecke G, et al. Isolation of Human Antigen-Specific Regulatory T Cells With High Suppressive Function. *Eur J Immunol* (2014) 44:2592–602. doi: 10.1002/eji.201344381
55. Eschborn M, Weigmann B, Reissig S, Waisman A, Saloga J, Bellinghausen I. Activated Glycoprotein A Repetitions Predominant (GARP)-Expressing Regulatory T Cells Inhibit Allergen-Induced Intestinal Inflammation in Humanized Mice. *J Allergy Clin Immunol* (2015) 136:159–68. doi: 10.1016/j.jaci.2015.04.020
56. Adriawan IR, Atschekzei F, Dittrich-Breiholz O, Garantziotis P, Hirsch S, Risser LM, et al. Novel Aspects of Regulatory T Cell Dysfunction as a Therapeutic Target in Giant Cell Arteritis. *Ann Rheum Dis* (2022) 81:124–31. doi: 10.1136/annrheumdis-2021-220955
57. Wang H, Song H, Pham AV, Cooper LJ, Schulze JJ, Olek S, et al. Human LAP +GARP+FOXP3+ Regulatory T Cells Attenuate Xenogeneic Graft Versus Host Disease. *Theranostics* (2019) 9:2315–24. doi: 10.7150/thno.30254
58. Wallace CH, Wu BX, Salem M, Ansa-Addo EA, Metelli A, Sun S, et al. B Lymphocytes Confer Immune Tolerance *via* Cell Surface GARP-TGF-β Complex. *JCI Insight* (2018) 3. doi: 10.1172/jci.insight.99863
59. Carrillo-Gálvez AB, Gálvez-Peisl S, González-Correa JE, de Haro-Carrillo M, Ayllón V, Carmona-Sáez P, et al. GARP is a Key Molecule for Mesenchymal Stromal Cell Responses to TGF-β and Fundamental to Control Mitochondrial ROS Levels. *Stem Cells Transl Med* (2020) 9:636–50. doi: 10.1002/sctm.19-0372
60. Carrillo-Galvez AB, Cobo M, Cuevas-Ocaña S, Gutiérrez-Guerrero A, Sánchez-Gilabert A, Bongarzone P, et al. Mesenchymal Stromal Cells

Express GARP/LRRC32 on Their Surface: Effects on Their Biology and Immunomodulatory Capacity. *Stem Cells* (2015) 33:183–95. doi: 10.1002/stem.1821
61. Huong PT, Nguyen LT, Nguyen X-B, Lee SK, Bach D-H. The Role of Platelets in the Tumor-Microenvironment and the Drug Resistance of Cancer Cells. *Cancers (Basel)* (2019) 11. doi: 10.3390/cancers11020240
62. Yap ML, McFadyen JD, Wang X, Ziegler M, Chen Y-C, Willcox A, et al. Activated Platelets in the Tumor Microenvironment for Targeting of Antibody-Drug Conjugates to Tumors and Metastases. *Theranostics* (2019) 9:1154–69. doi: 10.7150/thno.29146
63. McAllister SS, Weinberg RA. The Tumour-Induced Systemic Environment as a Critical Regulator of Cancer Progression and Metastasis. *Nat Cell Biol* (2014) 16:717–27. doi: 10.1038/ncb3015
64. Camerer E, Qazi AA, Duong DN, Cornelissen I, Advincula R, Coughlin SR. Platelets, Protease-Activated Receptors, and Fibrinogen in Hematogenous Metastasis. *Blood* (2004) 104:397–401. doi: 10.1182/blood-2004-02-0434
65. Palumbo JS, Talmage KE, Massari JV, La Jeunesse CM, Flick MJ, Kombrinck KW, et al. Tumor Cell-Associated Tissue Factor and Circulating Hemostatic Factors Cooperate to Increase Metastatic Potential Through Natural Killer Cell-Dependent and-Independent Mechanisms. *Blood* (2007) 110:133–41. doi: 10.1182/blood-2007-01-065995
66. Karpatkin S, Pearlstein E, Ambrogio C, Coller BS. Role of Adhesive Proteins in Platelet Tumor Interaction *In Vitro* and Metastasis Formation *In Vivo*. *J Clin Invest* (1988) 81:1012–9. doi: 10.1172/JCI113411
67. Stone RL, Nick AM, McNeish IA, Balkwill F, Han HD, Bottsford-Miller J, et al. Paraneoplastic Thrombocytosis in Ovarian Cancer. *N Engl J Med* (2012) 366:610–8. doi: 10.1056/NEJMoa1110352
68. Sierko E, Wojtukiewicz MZ. Platelets and Angiogenesis in Malignancy. *Semin Thromb Hemost* (2004) 30:95–108. doi: 10.1055/s-2004-822974
69. Schumacher D, Strilic B, Sivaraj KK, Wettschureck N, Offermanns S. Platelet-Derived Nucleotides Promote Tumor-Cell Transendothelial Migration and Metastasis *via* P2Y2 Receptor. *Cancer Cell* (2013) 24:130–7. doi: 10.1016/j.ccr.2013.05.008
70. Leblanc R, Peyruchaud O. Metastasis: New Functional Implications of Platelets and Megakaryocytes. *Blood* (2016) 128:24–31. doi: 10.1182/blood-2016-01-636399
71. Cravioto-Villanueva A, Luna-Perez P, La Gutierrez-de Barrera M, Martinez-Gómez H, Maffuz A, Rojas-Garcia P, et al. Thrombocytosis as a Predictor of Distant Recurrence in Patients With Rectal Cancer. *Arch Med Res* (2012) 43:305–11. doi: 10.1016/j.arcmed.2012.06.008
72. Honn KV, Tang D. Hemostasis and Malignancy: An Overview. *Cancer Metastasis Rev* (1992) 11:223–6. doi: 10.1007/BF01307178
73. Kim E-S, Kim M-S, Moon A. Transforming Growth Factor (TGF)-Beta in Conjunction With H-Ras Activation Promotes Malignant Progression of MCF10A Breast Epithelial Cells. *Cytokine* (2005) 29:84–91. doi: 10.1016/j.cyto.2004.10.001
74. Guo S-W, Du Y, Liu X. Platelet-Derived TGF-β1 Mediates the Down-Modulation of NKG2D Expression and may be Responsible for Impaired Natural Killer (NK) Cytotoxicity in Women With Endometriosis. *Hum Reprod* (2016) 31:1462–74. doi: 10.1093/humrep/dew057
75. Vermeersch E, Denorme F, Maes W, de Meyer SF, Vanhoorelbeke K, Edwards J, et al. The Role of Platelet and Endothelial GARP in Thrombosis and Hemostasis. *PLoS One* (2017) 12:e0173329. doi: 10.1371/journal.pone.0173329
76. Szepetowski P, Ollendorff V, Grosgeorge J, Courseaux A, Birnbaum D, Theillet C, et al. DNA Amplification at 11q13.5-Q14 in Human Breast Cancer. *Oncogene* (1992) 7:2513–7.
77. Jin H, Sun L, Tang L, Yu W, Li H. Expression of GARP Is Increased in Tumor-Infiltrating Regulatory T Cells and Is Correlated to Clinicopathology of Lung Cancer Patients. *Front Immunol* (2017) 8:138. doi: 10.3389/fimmu.2017.00138
78. Zhang L, Xu J, Zhang X, Zhang Y, Wang L, Huang X, et al. The Role of Tumoral FOXP3 on Cell Proliferation, Migration, and Invasion in Gastric Cancer. *Cell Physiol Biochem* (2017) 42:1739–54. doi: 10.1159/000479442
79. Karanikas V, Speletas M, Zamanakou M, Kalala F, Loules G, Kerenidi T, et al. Foxp3 Expression in Human Cancer Cells. *J Transl Med* (2008) 6:19. doi: 10.1186/1479-5876-6-19
80. Li R, Sun J, Yang F, Sun Y, Wu X, Zhou Q, et al. Effect of GARP on Osteogenic Differentiation of Bone Marrow Mesenchymal Stem Cells *via* the Regulation of Tgfβ1 *In Vitro*. *PeerJ* (2019) 7:e6993. doi: 10.7717/peerj.6993
81. Krebs FK, Trzeciak ER, Zimmer S, Özistanbullu D, Mitzel-Rink H, Meissner M, et al. Immune Signature as Predictive Marker for Response to Checkpoint Inhibitor Immunotherapy and Overall Survival in Melanoma. *Cancer Med* (2021) 10:1562–75. doi: 10.1002/cam4.3710
82. Kalathil S, Lugade AA, Miller A, Iyer R, Thanavala Y. Higher Frequencies of GARP(+)CTLA-4(+)Foxp3(+) T Regulatory Cells and Myeloid-Derived Suppressor Cells in Hepatocellular Carcinoma Patients are Associated With Impaired T-Cell Functionality. *Cancer Res* (2013) 73:2435–44. doi: 10.1158/0008-5472.CAN-12-3381
83. Jiang S, Zhang Y, Zhang X, Lu B, Sun P, Wu Q, et al. GARP Correlates With Tumor-Infiltrating T-Cells and Predicts the Outcome of Gastric Cancer. *Front Immunol* (2021) 12:660397. doi: 10.3389/fimmu.2021.660397
84. Erpenbeck L, Schön MP. Deadly Allies: The Fatal Interplay Between Platelets and Metastasizing Cancer Cells. *Blood* (2010) 115:3427–36. doi: 10.1182/blood-2009-10-247296
85. Bombaci M, Pesce E, Torri A, Carpi D, Crosti M, Lanzafame M, et al. Novel Biomarkers for Primary Biliary Cholangitis to Improve Diagnosis and Understand Underlying Regulatory Mechanisms. *Liver Int* (2019) 39:2124–35. doi: 10.1111/liv.14128
86. Wegner J, Krebs FK, Tuettenberg A, von Stebut E. Treg Activation Status Depends on Psoriasis Therapy Regime. *J Dtsch Dermatol Ges* (2020) 18:1481–4. doi: 10.1111/ddg.14368
87. Krützfeldt J, Rajewsky N, Braich R, Rajeev KG, Tuschl T, Manoharan M, et al. Silencing of microRNAs *In Vivo* With 'Antagomirs'. *Nature* (2005) 438:685–9. doi: 10.1038/nature04303
88. Huang B, Zhao J, Lei Z, Shen S, Li D, Shen G-X, et al. miR-142-3p Restricts cAMP Production in CD4+CD25- T Cells and CD4+CD25+ TREG Cells by Targeting AC9 mRNA. *EMBO Rep* (2009) 10:180–5. doi: 10.1038/embor.2008.224
89. Ha J, Kim M, Lee Y, Lee M. Intranasal Delivery of Self-Assembled Nanoparticles of Therapeutic Peptides and Antagomirs Elicits Anti-Tumor Effects in an Intracranial Glioblastoma Model. *Nanoscale* (2021) 13:14745–59. doi: 10.1039/d1nr03455c
90. Tao Y, Xu S, Wang J, Xu L, Zhang C, Chen K, et al. Delivery of microRNA-33 Antagomirs by Mesoporous Silica Nanoparticles to Ameliorate Lipid Metabolic Disorders. *Front Pharmacol* (2020) 11:921. doi: 10.3389/fphar.2020.00921
91. Meyer-Martin H, Hahn SA, Beckert H, Belz C, Heinz A, Jonuleit H, et al. GARP Inhibits Allergic Airway Inflammation in a Humanized Mouse Model. *Allergy* (2016) 71:1274–83. doi: 10.1111/all.12883
92. Schlöder J, Berges C, Tuettenberg A, Jonuleit H. Novel Concept of CD4-Mediated Activation of Regulatory T Cells for the Treatment of Graft-Versus-Host Disease. *Front Immunol* (2017) 8:1495. doi: 10.3389/fimmu.2017.01495
93. Martin H, Reuter S, Dehzad N, Heinz A, Bellinghausen I, Saloga J, et al. CD4-Mediated Regulatory T-Cell Activation Inhibits the Development of Disease in a Humanized Mouse Model of Allergic Airway Disease. *J Allergy Clin Immunol* (2012) 129:521–8,528.e1-7. doi: 10.1016/j.jaci.2011.09.038
94. Rachidi S, Metelli A, Riesenberg B, Wu BX, Nelson MH, Wallace C, et al. Platelets Subvert T Cell Immunity Against Cancer *via* GARP-Tgfβ Axis. *Sci Immunol* (2017) 2. doi: 10.1126/sciimmunol.aai7911
95. Powderly J, Shimizu T, LoRusso P, Razak A, Miller K, Balar A, et al. Abstract CT207: Phase 1 First-in-Human Study of ABBV-151 as Monotherapy or in Combination With Budigalimab in Patients With Locally Advanced or Metastatic Solid Tumors. *Cancer Res* (2021) 81:CT207–7. doi: 10.1158/1538-7445.AM2021-CT207
96. de Streel G, Bertrand C, Chalon N, Liénart S, Bricard O, Lecomte S, et al. Selective Inhibition of TGF-β1 Produced by GARP-Expressing Tregs Overcomes Resistance to PD-1/PD-L1 Blockade in Cancer. *Nat Commun* (2020) 11:4545. doi: 10.1038/s41467-020-17811-3
97. Satoh K, Kobayashi Y, Fujimaki K, Hayashi S, Ishida S, Sugiyama D, et al. Novel Anti-GARP Antibody DS-1055a Augments Anti-Tumor Immunity by Depleting Highly Suppressive GARP+ Regulatory T Cells. *Int Immunol* (2021) 33:435–46. doi: 10.1093/intimm/dxab027
98. Gaignage M, Zhang X, Stockis J, Dedobbeleer O, Michiels C, Cochez P, et al. Blocking GARP-Mediated Activation of TGF-β1 did Not Alter Innate or Adaptive Immune Responses to Bacterial Infection or Protein Immunization in Mice. *Cancer Immunol Immunother* (2022). doi: 10.1007/s00262-021-03119-8

99. Cho MS, Gonzalez-Pagan O, Court Pinto K, Sood A, Afshar-Kharghan V. The Inhibition of Platelets Restore Anti-Tumor Immune Response to Ovarian Cancer and Its Therapeutic Implication. *Blood* (2018) 132:3698. doi: 10.1182/blood-2018-99-116530
100. Schupp J, Christians A, Zimmer N, Gleue L, Jonuleit H, Helm M, et al. In-Depth Immune-Oncology Studies of the Tumor Microenvironment in a Humanized Melanoma Mouse Model. *Int J Mol Sci* (2021) 22. doi: 10.3390/ijms22031011

Conflict of Interest: KS is employed by Daiichi Sankyo Co., Ltd.

The remaining authors declare that the research was conducted in the absence of any commercial or financial relationships that could be construed as a potential conflict of interest.

Publisher's Note: All claims expressed in this article are solely those of the authors and do not necessarily represent those of their affiliated organizations, or those of the publisher, the editors and the reviewers. Any product that may be evaluated in this article, or claim that may be made by its manufacturer, is not guaranteed or endorsed by the publisher.

International Journal of
Molecular Sciences

MDPI

Article

GARP as an Immune Regulatory Molecule in the Tumor Microenvironment of Glioblastoma Multiforme

Niklas Zimmer [1], Ella Kim [2,3] Jonathan Schupp [1], Bettina Sprang [2,3], Petra Leukel [4], Fatemeh Khafaji [5], Florian Ringel [2], Clemens Sommer [4], Jochen Tuettenberg[5] and Andrea Tuettenberg [1,*]

[1] Department of Dermatology, University Medical Center Mainz, 55131 Mainz, Germany
[2] Department of Neurosurgery, University Medical Center Mainz, 55131 Mainz, Germany
[3] Translational Neurooncology Research Group, Johannes Gutenberg University, 55131 Mainz, Germany
[4] Institute of Neuropathology, University Medical Center Mainz, 55131 Mainz, Germany
[5] Department of Neurosurgery, SHG-Klinikum Idar-Oberstein, 55743 Idar-Oberstein, Germany
* Correspondence: antuette@uni-mainz.de; Tel.: +49-6131-173186, Fax: +49-6131-17473541

Received: 9 July 2019; Accepted: 23 July 2019; Published: 26 July 2019

Abstract: Glycoprotein A repetition predominant (GARP), a specific surface molecule of activated regulatory T cells, has been demonstrated to significantly contribute to tolerance in humans by induction of peripheral Treg and regulatory M2-macrophages and by inhibition of (tumorantigen-specific) T effector cells. Previous work identified GARP on Treg, and also GARP on the surface of several malignant tumors, as well as in a soluble form being shedded from their surface, contributing to tumor immune escape. Preliminary results also showed GARP expression on brain metastases of malignant melanoma. On the basis of these findings, we investigated whether GARP is also expressed on primary brain tumors. We showed GARP expression on glioblastoma (GB) cell lines and primary GB tissue, as well as on low-grade glioma, suggesting an important influence on the tumor micromilieu and the regulation of immune responses also in primary cerebral tumors. This was supported by the finding that GB cells led to a reduced, in part GARP-dependent effector T cell function (reduced proliferation and reduced cytokine secretion) in coculture experiments. Interestingly, GARP was localized not only on the cell surface but also in the cytoplasmatic, as well as nuclear compartments in tumor cells. Our findings reveal that GARP, as an immunoregulatory molecule, is located on, as well as in, tumor cells of GB and low-grade glioma, inhibiting effector T cell function, and thus contributing to the immunosuppressive tumor microenvironment of primary brain tumors. As GARP is expressed on activated Treg, as well as on brain tumors, it may be an interesting target for new immunotherapeutic approaches using antibody-based strategies as this indication.

Keywords: glioblastoma; GARP; tumor microenvironment; immunotherapy; regulatory T cells

1. Introduction

Glioblastomas (GBs) are characterized by a particularly aggressive behavior, including infiltrating tumor cells in the surrounding brain tissue. After surgical removal of the primary tumor, recurrence derived from these tumor cells nearly always occurs. In addition, tumor cells are able to suppress immune responses through regulatory cells such as microglial cells or invading regulatory T cells, especially in the relapse situation [1–3].

Immunotherapies are considered a promising method for treatment of cancer patients in general. In this study, the patient's own immune cells are conditioned to recognize and combat

structures of the tumor. The systemic effect of the immune cells also allows scattered tumor cells to be reached. However, very little is known about the factors influencing the immigration of immune cells, as well as an effective immune response, in the tumor milieu of primary brain tumors such as GB, both in the primary tumor tissue and in the recurrent tissue. Furthermore, in many tumor entities, active suppression of the immunological defense in tumor patients significantly limits the success, in particular of immunotherapies [4]. In addition to general immunological tolerance mechanisms through regulatory T cells or tolerogenic dendritic cells (tolDC), the tumor itself also develops immune escape mechanisms. Thus, by generating an inhibitory micromilieu, efficient antitumor responses are switched off or prevented, limiting the effectiveness of immunotherapeutic approaches.

Therefore, many studies aim to characterize new regulatory molecules and signaling pathways of tumor cells and their impact on the tolerogenic properties of the tumor microenvironment in order to identify new targets for immunotherapeutic approaches.

Despite extensive experimental and clinical research, GB is still one of the most fatal tumors in humans with a median progression-free interval with maximal therapy of less than 12 months and a median overall survival of up to 15 months [5].

In addition to the standard procedures of surgery and radiation, as well as concomitant chemotherapy, immunotherapy appears to be a promising therapeutic approach, for example, by vaccination [6]. It is known that GB, similar to other malignant tumors of the neuroectoderm (e.g., malignant melanoma has some very immunogenic surface molecules. Already, there is some research with different vaccination strategies [6–8] providing partly contradictory results. However, vaccination strategies have not yet been standardized or optimized, and successful phase III studies have thus far been lacking [9]. A key mechanism that usually precludes successful tumor immunotherapy is the active suppression of immunological defense [10–12]. In this context, general immunological tolerance mechanisms play an important role, for example, regulatory cells of the immune system, such as regulatory T cells (Treg) and microglia but also soluble factors such as interleukin-10 (IL-10) and transforming growth factor beta (TGF-β), induce an immunosuppressive environment and promote tumor progression, infiltrative growth/migration, and tumor recurrence [13,14].

The tumor itself also develops numerous so-called immune-escape mechanisms that help to shut down or prevent an efficient antitumor response. This mainly includes the genetic instability of tumor cells, which leads to changes in the surface profile or the antigenic structures on the tumor cell itself and downregulation of human leukocyte antigens(HLA) molecules [15]. Furthermore, soluble factors such as IL-10 and TGF-β, as well as pro-angiogenic factors (vascular endothelial growth factor -VEGF, platelet-derived growth factor - PDGF, fibroblast growth factor -FGF, IL-8), play a role in turning off the effector cells present in the tumor and promoting tumor angiogenesis [16,17].

We have recently shown that the specific Treg activation marker GARP (glycoprotein A repetition predominant) in its soluble form has tolerance-inducing functions [18]. GARP is a transmembrane protein whose extracellular portion consists of 21 leucine-rich domains and is expressed on both Treg and platelets [19,20]. GARP is required for the formation and surface expression of latent TGF-β [19]. In addition to its expression on activated Treg, we have also shown its occurrence on cells of primary malignant melanoma and melanoma cerebral metastasis.

In the present study, we analyzed GARP as a potential marker molecule and key factor for the immunoregulatory environment in GB and investigated its relevance as a potential target for a therapeutic approach in patients with cerebral cancer.

2. Results

2.1. GARP Expression on Immunohistochemistry of Glioblastoma and Low-Grade Astrocytomas

Recent studies of our own group revealed GARP as an immunoregulatory molecule expressed on activated Treg and capable of suppressing effector cell proliferation and cytokine production and

to confer suppressive activity to T effector cells. In addition, GARP has been detected on melanoma cells, as well as on brain metastasis of melanoma [21].

In order to investigate in situ GARP expression and thus its relevance on the immunosuppressive tumor microenvironment of GB, 37 patients (26 males and 11 females) with histologically proven GB between January 2009 and May 2015 were included (Table 1). The mean ± standard deviation (SD) at the onset of disease for males was 69.05 ± 11.93 years and 71.38 ± 11.72 years for females (independent t-test p >0.05). As shown in Table 1, 67.6% (17 males and eight females) had the tumor left hemispheric. The temporal lobe was the most involved part of the tumor (29.7%, Pearson Chi-square p > 0.05, Figure 1a). There were 33 subjects who underwent a surgical resection. The first histological diagnosis showed GB in 89.2% of the subjects. After surgery, 29 patients had radiation therapy, 26 had chemotherapy, and a combined chemoradiotherapy had been applied to 24 patients. The mean survival after diagnosis was 11.07 ± 13.27 months.

Table 1. Patients with glioma grade III and IV at the study center Idar-Oberstein, Germany were included. Patient characteristics (gender, age), as well as primary tumor data including localization, therapy, and follow-up are displayed.

Glioma grade III and IV	male	female	total	lost to follow up
Number of patients	26	11	37	
Age at the onset mean±SD (yr.)	69.05 ± 11.08	71.38 ± 11.72	68.78 ± 13.36	
Side hemispheric				
right	9	3	12	
left	17	8	25	
bilateral	0	0	0	
Surgery				
resection	19	3	27	
biopsy	7	8	10	
First histological diagnosis				
grade IV	23	10	33	
grade III	3	1	4	
Localization				
frontal	5	5	10	
parietal	6	2	8	
temporal	9	2	11	
thalamic	2	0	2	
fronto-parietal	0	1	1	
occipital	2	0	2	
perieto-occipital	0	1	1	
temporo-parietal	2	0	2	
Radiation therapy	20	9	29	3
Chemotherapy	20	6	26	5
Survival mean±SD (mon.)	11.68±15.22	9.38±4.98	11.07±13.27	

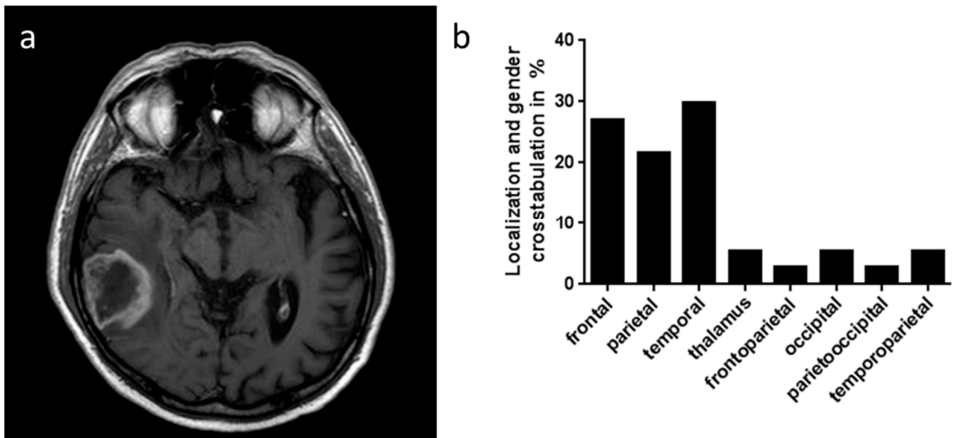

Figure 1. (**a**) T1-weighted gandolinium enhanced cranial axial image with a typical glioblastoma (GB) in the right dorsal temporal lobe. (**b**) Frequency of localization of GB in % is shown. Most tumors were found in the frontal, parietal, and temporal lobe of the patients.

In these patients we investigated the relevance of GARP in primary brain tumors such as GB and compared it to astrocytomas grade II and grade III (Supplementary Table A1,A2). In this study, GARP immunostaining was analyzed only in tumor cells and not in inflammatory cells. Interestingly, all tumors analyzed, except one GB, showed at least 50% GARP expression (Figure 2). In detail, two of the grade II astrocytomas showed more than 50% labeled nuclei, the other two more than 90% labeled nuclei (Figure 2a, d). Five of the grade III astrocytomas showed more than 50% labeled nuclei, the other six more than 90% labeled nuclei (Figure 2e). One of the GBs was completely negative, whereas, 19 GBs showed more than 50% labeled nuclei, the remaining 16 showed more than 90% labeled nuclei (Figure 2b, f). As a control, normal brain tissue derived from the neighborhood of a glioma was stained. Single neurons, so-called dark neurons or hypoxic-ischemic damaged neurons, displayed some weak GARP staining (Figure 2c), whereas, the majority of cells did not display any GARP expression.

Taken together these data show dominant expression of the inhibitory GARP molecule also in primary brain tumors such as GB and low-grade glioma, implicating a potential relevance for the immunosuppressive tumor micromilieu.

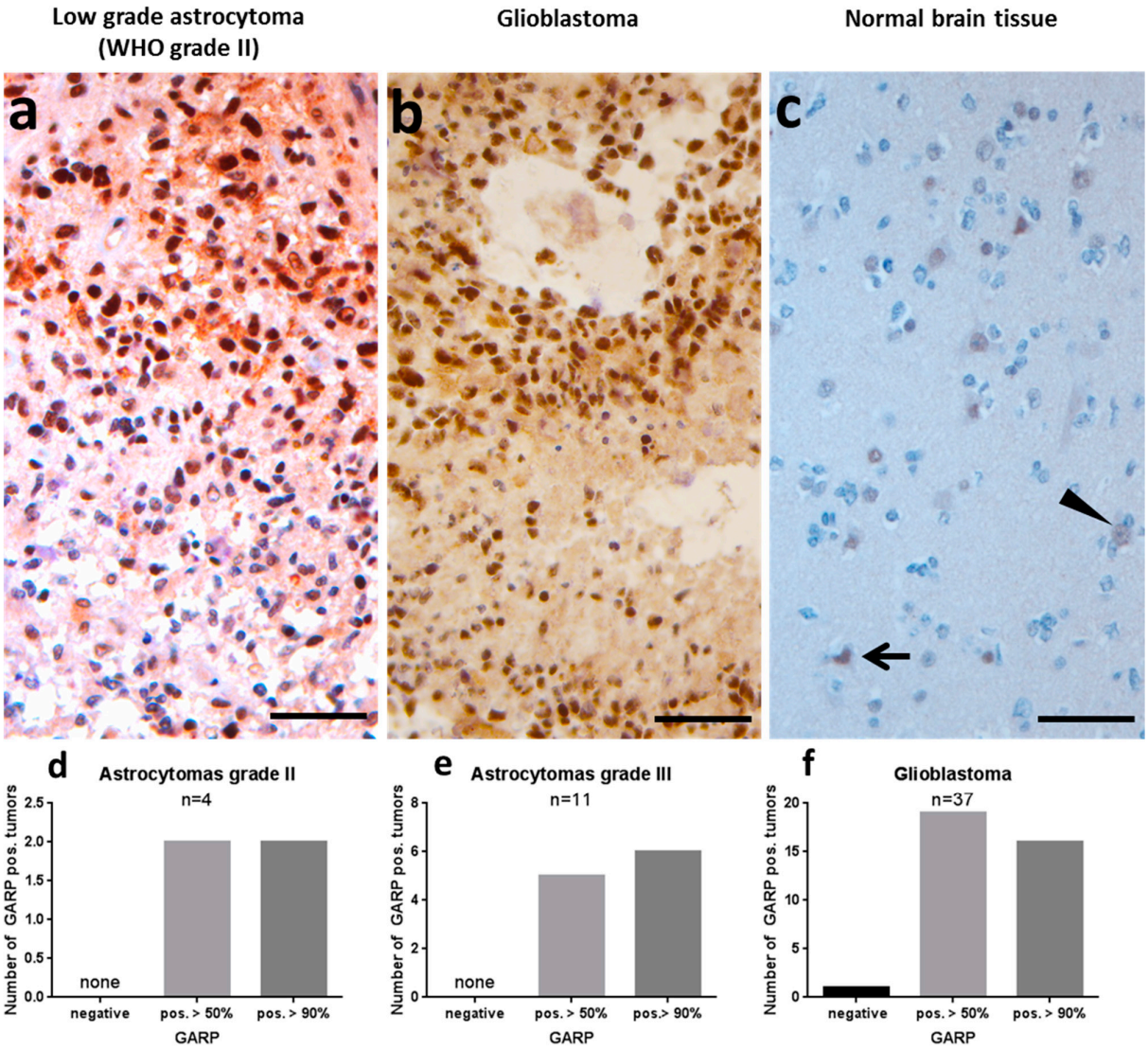

Figure 2. Glycoprotein A repetition predominant (GARP) immunohistochemistry in gliomas and astrocytomas. (**a**,**d**,**e**) Low-grade astrocytoma (WHO grade II) with more than 50% positive (pos.) labeled nuclei (magnification × 400). (**b**,**f**) GB with palisading necroses and more than 90% pos. stained tumor cells (magnification × 400). (**c**) Largely normal brain tissue in the neighborhood of a glioma with some labeled neurons (arrow) while others where unstained (arrowhead). Bar corresponds to 50 μm.

2.2. GARP Expressed on the Surface of GB and in the Cytoplasma and Nucleus

GARP is a transmembrane protein that presents latent TGF-β1 on the surface of Treg. TGF-β1 influences a variety of immune cells by conferring immune tolerance and has been shown to be present in brain tumors being associated with poor prognosis of patients with GB [22].

In order to confirm the expression of GARP on GB tumor cells, a commercially available GB cell line (T98G), three patient-derived GB cell lines (#1043, #1051, #1063), and a melanoma cell line (MaMel-19) were analyzed by flow cytometry and confocal microscopy (Figures 3 and 4). As a positive control for GARP expression, resting and activated Treg were investigated (Figure 3). Flow cytometry data showed GARP localization on the surface of Treg and all tested cell lines, confirming not only previous results but also the in situ data from primary brain tumor tissue (shown in Figure 2) [19].

Interestingly, while analyzing the expression of GARP in brain tumor cells in more detail, we detected intracellular (IC) and intranuclear (IN) localization of GARP in T98G, MaMel-19, and all three patient-derived cell lines (#1043, #1051, and #1063), as well as in resting and activated Treg. All cell lines showed a significant expression of GARP in the cytoplasma as well as in the nucleus of tumor cells. The intracellular expression of GARP was even more pronounced when compared to surface expression. This could be shown using confocal microscopy (Figures 3a, and 4a) and for the Treg, T98G, and MaMel-19 also via flow cytometry (Figure 3b).

Thus, our data show, for the first time, intracellular GARP expression in tumor cell lines of GB and melanoma, as well as in Treg.

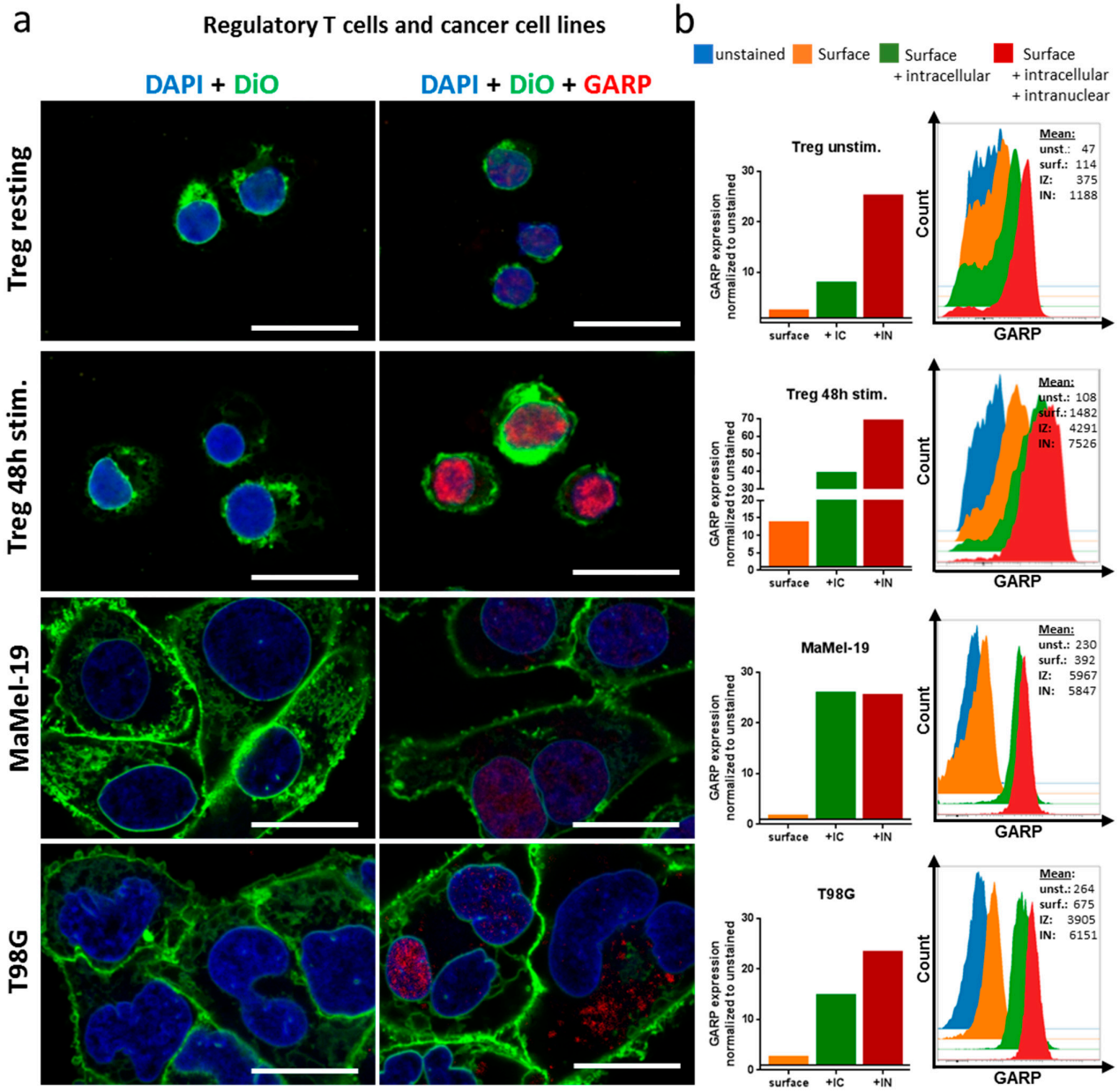

Figure 3. Analysis of the GARP localization in resting and stimulated regulatory T cells, melanoma cell line MaMel-19, and glioblastoma cell line T98G. The Treg were stimulated with 1 μg/mL anti-CD3 mAb, 1 μg/mL anti-CD28 mAb, and 10 IU/mL IL-2 for 48 h. (**a**) Cytoplasmatic and intranuclear localization of GARP shown in confocal images. The white bar corresponds to 20 μm (**b**) flow cytometric analysis GARP expression on the surface; surface and intracellular (IC); and surface, IC, and intranuclear (IN) of Treg, melanoma, and GB cell lines. Means were normalized to the unstained control.

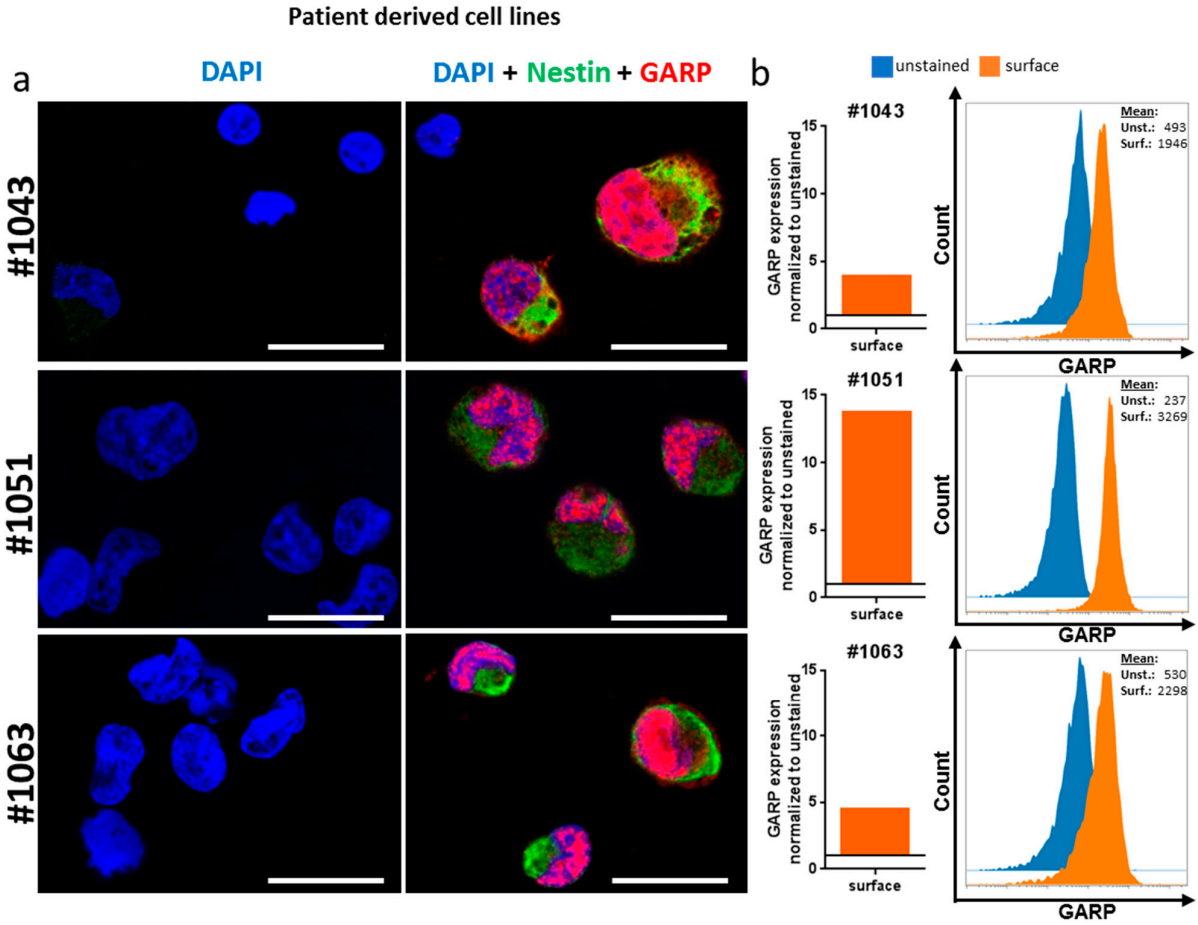

Figure 4. Flow cytometric and confocal analysis of GARP expression in patient-derived GB cell lines. (**a**) Confocal images show a strong GARP expression on the surface, intracellular (IC) and intranuclear (IN) in all tested patient-derived GB cell lines. The white bar corresponds to 20 μm (**b**) Flow cytometric analysis of the surface expression of GARP. All three cell lines showed an expression of GARP. Due to the nature of these cells, Nestin instead of DiO was stained. Means were normalized to the unstained control.

2.3. GB Cell Line T98G Suppresses T Effector Cell Function

It is known that the tumor microenvironment (TME) promotes immune escape mechanisms through inhibitory cell populations such as Treg, myeloid-derived suppressor cells (MDSC), and tolerogenic dendritic cells (tolDC), as well as inhibitory factors produced by the tumor cells themselves [23–25]. Furthermore, soluble factors secreted by Treg and tolDC, such as IL-10 and TGF-β, promote the immunosuppressive TME which prevents the rejection of the tumor by the immune system and results in tumor expansion and metastasis [26].

In order to analyze the effect of GB cell line T98G on T effector cells, coculture experiments were performed as described by [19,21] and proliferation and cytokine production of T effector cells were analyzed. As shown previously, the addition of soluble GARP (sGARP, 1μg/mL) downregulated IFN-γ production in activated $CD4^+$ T effector cells (Figure 5a). Furthermore, we observed that the addition of T98G to $CD4^+$ T effector cells exerted a dose-dependent inhibition of INF-γ production (approximately 30% inhibition), which was nearly completely restored by using a blocking anti-GARP Ab. Proliferation of T effector cells was also inhibited in coculture was, in part, rescued (Figure 5b) by blocking GARP. These results are in agreement with data obtained previously, showing the T effector cell suppression by melanoma cells [21].

Taken together, our data show that GARP plays an important role in the suppressive capacities of GB on T effector cells.

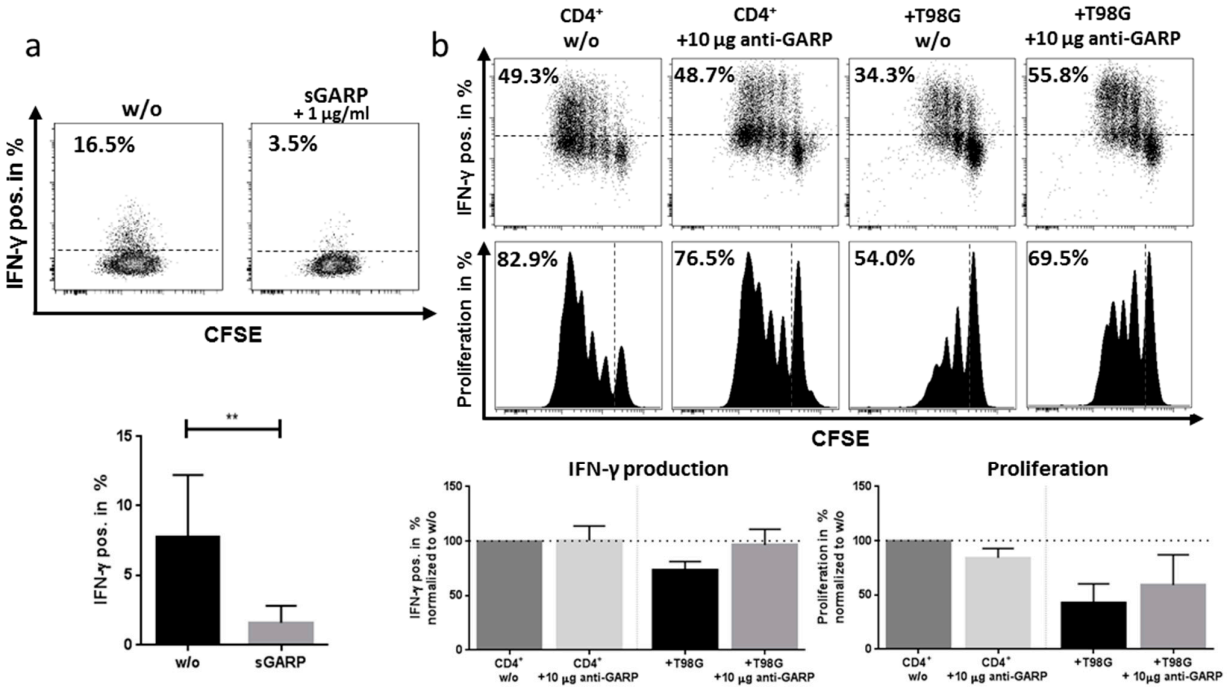

Figure

5. (**a**) Soluble GARP (sGARP) cytokine suppression. CD4+ T cells were stimulated with 1 µg/mL anti-CD3 mAb, 1 µg/mL anti-CD28 mAb, and with or without 1 µg/mL sGARP for 24 h. INF-γ production was measured by intracellular staining via flow cytometry. Dot plots show one representative result of 5 independent experiments. (**b**) T98G cells suppress T cell proliferation and cytokine production. CD4+ T cells were cultured together with or without (w/o) T98G cells in the ratio of 8:1 and stimulated, as described above. Additionally, either 10 µg/mL anti-GARP Ab or no Ab were added into the culture and CD4+ T cells were stimulated as described before. IFN-γ production and proliferation (CFSE) were measured 4 days after stimulation by intracellular staining via flow cytometry. Dot plots show one representative result of 4 independent experiments. Data are displayed as mean values ± SEM, p-values relative to w/o ** $p < 0.01$. Dotted lines represent either unstained control (a + b IFN-γ), CFSE stained cells before stimulation or percentages normalized to the untreated control (w/o).

3. Discussion

A protein specifically expressed by activated Treg is the activation marker GARP. We have recently shown that GARP (glycoprotein A repetition predominant) has tolerance-inducing functions (inhibition of effector cell proliferation and cytokine production, induction of Treg, and induction of M2 macrophages) [18].

GARP is required for the formation and surface expression of latent TGF-β [19,27] known to be involved in several immunoregulatory mechanisms, especially in tumor biology. The lentiviral knockdown of GARP in Treg showed decreased suppressive capacity and reduced FoxP3 expression in these cells [20]. In addition to its expression on activated Treg, we also showed an occurrence on cells of the malignant melanoma, and thus a further regulatory effect in the tumor micromilieu [21].

GARP has been described by several groups as a transmembrane protein whose extracellular portion consists of 21 leucine-rich domains and is expressed on both Treg and platelets [19,20]. Leucine-rich domains (LRRs) have been identified in a variety of proteins involved in many different functions including signal transduction, cell differentiation, and migration. Those proteins are often membrane bound, can also be secreted or exhibit a cytoplasmic or nuclear localization [28], and are

involved in protein–protein interactions. Amongst others, LRRs are found in molecules such as adhesion molecules, enzymes, or tyrosine kinase receptors (RTKs). Despite the localization of RTKs at the cell surface, several are also found in the nucleus [29] being responsible for protein–protein interactions. Whether this is transferable for the intranuclear role of GARP in tumor cells as well as in Treg will be analyzed in more detail in future studies. Nevertheless, structural parallels such as LRRs suggest the possibility of comparable functions also for GARP.

Immunotherapy and targeted therapies have become increasingly important for the treatment of malignant tumors in recent years. However, only some patients respond here. Before considering the increasing number of possible therapy options, the side effects, and the response rates, as well as the costs, it is very important to create a treatment concept individually for each patient with the help of biomarkers. There are numerous efforts to identify factors at the cellular level, as well as at the level of soluble proteins, in the tissue and in the peripheral blood of tumor patients, which help to more accurately characterize the tumor microenvironment and thus the prognosis and the therapy response of an individual patient, and additionally lead to the development of new immunotherapeutic approaches [30–32]. In this study, regulatory components of the tumor itself play an important role. In melanoma cells, GARP has been shown to be expressed on the surface of tumor cells, modulating and inhibiting antigen-specific T effector cell responses, and inducing peripheral regulatory T cells [21], thus, contributing to the immune-inhibitory tumor microenvironment. In order to analyze the suppressive role of GARP in GB we used a suppressor assay already published for melanoma cells [21]. In this study, tumor cells were cocultured with T effector cells and IFN-γ production and proliferation of T cells were assessed. We have shown that the presence of GARP on GB cells was, in part, responsible for reduced T effector cell function also showing its immunosuppressive role in GB. The presence of GARP on GB cells may, therefore, be of great importance when discussing prognosis and therapeutic approaches in this tumor entity.

Glioblastoma (GB) is the most common and most malignant form of intrinsic brain tumors accounting for 52% of all primary brain and central nervous system (CNS) malignancies in adults. The current standard of care for newly diagnosed GB is based on the "one-treatment-for-all" principle and consists of surgical resection followed by aggressive regimens of combined radiochemotherapy. Despite aggressive treatment, GBs have a final mortality rate close to 100%, less than a 10% five-years survival rate and a median survival of 15 months [5]. The inevitable recurrence after standard therapy poses a major challenge for improving clinical outcomes of patients with GB. For recurrent GBs (recGBs), no effective therapeutic options are currently available with experimental treatments being the only option at this stage of the disease [33,34]. Currently, immunotherapy is considered among the most promising approaches for recurrent GB, particularly, the targeting of inhibitory T cell signaling mediated through programmed death 1 (PD-1), the PD-1 ligand or cytotoxic T-lymphocyte associated antigen 4 (CTLA-4) has emerged as a promising approach [34]. On the basis of our findings, showing GARP being expressed on activated Treg as well as on brain tumors, it may be an interesting target for new immunotherapeutic approaches using antibody-based strategies.

In Treg, low levels of intracellular GARP were demonstrated prior to activation via the T cell receptor and CD28 [35], suggesting that low levels of GARP are sequestered intracellularly and T cell activation is necessary for the synthesis and surface expression of GARP. In addition, previous studies have shown that ectopically expressed GARP in T cells is able to upregulate Foxp3, indicating a more upstream induction of a tolerogenic phenotype [20]. Interestingly, GARP has also been shown, via Northern blot, to be expressed intracellularly in different tissues such as placenta, lung, kidney, heart, liver, skeletal muscle, and pancreas but not in the brain [28].

The intranuclear localization and accumulation of GARP in cancer cells and also in Treg, as shown in our study for the first time, could be a hint for a second, TGF-β pathway independent way to exerpt its tumor immunity suppressing function. For example, RTKs, proteins containing LRRs similar to GARP protein, are mainly localized at the cell surface. Nevertheless, several RTKs, such as colony stimulating factor 1 receptor (CSF-1R), are also found in the nucleus [29] where they interact with transcription factors regulation cell proliferation, survival, and migration. These full-length

proteins translocate from the cell surface to the nucleus via the Golgi apparatus and the endoplasmatic reticulum.

Nevertheless, detailed information about a possible dynamic interaction of GARP with other proteins in the nucleus, and thus potentially regulating gene expression is still elusive and will be a topic for further research.

In the present study we describe for the first time the expression of the immunoregulatory molecule GARP in the tumor microenvironment of primary brain tumors such as GB but also astrocytoma grade II or III. Having shown previously the relevance of GARP for immunomodulation and inhibition of tumor-antigen specific effector cells [21] in melanoma patients, these findings could contribute to the understanding of tumor escape mechanisms of GB including progression and therapy resistance. Notably, GARP is known to exert its function in suppressing tumor immunity via the TGF-β pathway [18], which is one of the key pathways involved in GB progression and maintenance of self-renewal in glioma stem cells (GCS) [36]. The necessity of targeting factors that contribute to the tumor immunosuppressive microenvironment has been increasingly recognized as a strategy to improve the efficacy of immunotherapy for GB [37,38]. Further studies with larger groups of patients are needed to confirm these findings.

Taken together, the present study will help to develop new immunotherapeutic approaches targeting GARP on Treg as well as on GB tumor cells as one possible factor to improve the outcome of GB patients.

4. Materials and Methods

4.1. Cell Culture

For the cell line T98G, Eagles minimum medium supplemented with 10% FCS, 1% glutamine, and 0.1% primocin was used. The MaMel-19 was cultured with RPMI-1640 supplemented with 10% FCS, 1% glutamine, and 0.1% primocin. The human melanoma cell line MaMel-19 was described previously [21]. Cells were detached via Trypsin-EDTA for 5 min every 3 to 4 days. Cell lines were authenticated at Eurofins Genomics (Ebersberg, Germany) in March 2019. The resulting STR profiles were matched with the online databases of the german collection of microorganisms and cell cultures (DSMZ) (Available online: http://www.dsmz.de/de/service/services-human-and-animal-cell) and Cellosaurus database (Available online: https://web.expasy.org/cellosaurus/) references.

Human glioma cell lines #1043, #1051, and #1063 used in this study were derived from glioblastoma previously described by [39–41]. The glioma cells were maintained under a serum-free culture condition that supported cell self-renewal and was based on NeuroBasal Medium supplemented with B27 supplement (Invitrogen, Darmstadt, Germany) and recombinant human cytokines basic fibroblast growth factor 2 (bFGF) and epidermal growth factor (EGF), (10 and 20 ng/mL, respectively, Biochrom GmbH, Merck KGaA, Darmstadt, Germany).

4.2. Isolation and Stimulation of Human CD4⁺ T Cells and Treg

Buffy coats were obtained from healthy volunteers, with approval by the local ethical committee (Landesärztekammer Rhineland Palatine No. 837.019.10 (7028), approved on 4 March 2010). The $CD4^+$ T cells were isolated via CD4 Microbeads (Miltenyi # 130-045-101). The regulatory T cells were isolated with the $CD4^+$ $CD25^+$ $CD127^{dim/-}$ isolation kit (Miltenyi #130-094-775, Bergisch Gladbach, Germany) according to the manufacturer's protocol. For proliferation assays, $CD4^+$ T cells were labeled with carboxyfluorescein succinimidyl ester (CFSE, eBioscience #65-0850-84, San Diego, CA, USA) and cultured in 48 well plates at 10^6 cells/mL, stimulated with 1 μg/mL anti-CD3 mAb (clone OKT3) plus 1 μg/mL anti-CD28 mAb (clone 28.2, eBioscience San Diego, CA, USA) in the presence or absence of T98G in the ratio of 8:1, 10 μg/mL anti-GARP Ab (Origene AP17415PU-N, Rockland, MD, USA) and 1 μg/mL soluble GARP (recombinant human LRRC32/GARP protein #6055-LR-050, Minneapolis, MN, USA). For the activation of Treg, 1 x 10^6 cells were stimulated with

1 μg/mL anti-CD3 mAb (clone OKT3) plus 1 μg/mL anti-CD28 mAb (clone 28.2, eBioscience, San Diego, CA, USA) with 10 U/mL IL-2 (Novartis #PZN 02238131, Basel, Switzerland) for 48 h.

4.3. Flow Cytometry

For the flow cytometric analysis, the following antibodies were used: FVD506 (eBioscience #65-0866-14) and GARP (Miltenyi #130-103-820). Cells were stained with fixable viability dye prior to the antibody staining of GARP. Flow cytometry was performed on a BD LSRII flow cytometer (Heidelberg, Germany) and was analyzed using Cytobank [42].

For intracellular and intranuclear staining of GARP or intracellular staining of IFN-γ, cells were fixed and permeabilized with either the intracellular staining kit (BD Cytofix/Cytoperm Plus #555028, Heidelberg, Germany) or intranuclear with the Foxp3 / Transcription Factor Staining Buffer Kit (eBioscience #00-5523-00) and subsequently stained with anti-GARP mAb (Miltenyi #130-103-820) or anti-INF-γ (BD Biosciences #557643, Heidelberg, Germany).

4.4. Confocal Microscopy

For the confocal imaging, the Leica SP8 with HyD Detector (Wetzlar, Germany) was used. Melanoma cell line MaMel 19 and GB cell line T98G were cultured for 24 h in ibidi 15 μ-slides (Ibidi - # 80826, Gräfelfing, Germany), 25,000 cells/well each. Treg were plated on microscopyslides 100,000 each, using a Cytospin centrifuge (Cellspin II- Tharmac, Waldolms, Germany). Cells were checked for adherence and then fixed and permeabilized with a Foxp3/Transcription Factor Staining Buffer Kit (eBioscience, San Diego, CA, USA). For analysis of intracellular localization, cells were stained with anti-GARP mAb for 20 min at RT. Additionally DNA (Hoechst 33342 Solution Promokine #PK-CA707-40046, Heidelberg, Germany) and the membrane (NeuroDiO Solution #PK-CA707-30021- PromoKine, Heidelberg, Germany) were stained for 30 min at RT each.

For confocal imaging of the non-adherent human glioma cell lines #1043, #1051, and #1063, 30,000–50,000 cells were seeded on glass coverslips pre-coated with poly-L-ornithine hydrobromide (15 μg/mL, Sigma Aldrich, St. Louis, MO, USA) and cultured for 24 h. The cells were fixed with 4% paraformaldehyde/PBS (Merck KGaA, Darmstadt, Germany) for 5 min at RT followed by methanol/acetone (50% v/v) fixation at −20 °C. Cell permeabilization was performed using 0.3% Triton X-100/PBS (Sigma, St. Louis, MO, USA) for 5 min at RT. The primary antibodies used in the study included α-nestin (Abcam ab22035, Cambridge, UK), α-GARP (Origene AP17415PU-N, Rockland, MD, USA), and secondary antibodies (goat α-mouse Alexa Fluor 488 or goat α-rabbit Alexa Fluor 555, Thermo Fisher Scientific, Waltham, MA, USA). Because of their different nature as compared with the adherent T98G, MaMel-19, and non-adherent Treg, α-nestin was used instead of NeuroDiO Solution (see above). For editing, ImageJ2 (Available online: https://imagej.net/ImageJ2) was used [43].

4.5. GARP-Immunohistochemistry

Paraffin-embedded tumor samples were studied from 37 GBs (WHO grade IV), 13 anaplastic astrocytomas (WHO grade III), and 6 low-grade astrocytomas (WHO grade II) by GARP immunohistochemistry. Tumor tissue was resected in the Department of Neurosurgery in Idar-Oberstein, Germany, and completely sent for neuropathological examination to the Institute of Neuropathology, University Medical Center Mainz, Germany. Tissue not used for diagnostic proposes was used for additional GARP staining. Written informed consent of all patients was obtained for "scientific use of tumor tissue not needed for histopathological diagnosis" in the admission contract of Idar-Oberstein hospital. Immunohistochemistry was performed on 4 μm thick routinely processed formalin-fixed and paraffin-embedded tissue sections. After dewaxing, antigen retrieval using EnVision FLEX Target Retrieval Solution (), high pH (Dako #S2368 Glostrup, Denmark) was performed. Afterwards, endogenous peroxidase was blocked by peroxidase blocking solution (DAKO, Glostrup, Denmark) and sections were stained with anti-GARP primary antibody 1:100 (Origene AP17415PU-N, Rockland, MD, USA) using an immunostainer (Dako Autostainer

Plus, DAKO, Glostrup, Denmark). Immunoreactivity was visualized by the universal immuno-enzyme polymer method (Nichirei Biosciences, Tokyo, Japan). Finally, sections were developed in diaminobenzidine (Lab Vision Cooperation, Fermont, CA, USA). Omission of the primary antisera in a subset of control slides resulted in no immunostaining at all. Nuclear GARP-immunostaining was semiquantitatively assessed in areas with labeled nuclei of tumor cells (more than 90%, 50%, and 10%). Immunohistochemical analysis was performed by an experienced neuropathologist (CS).

4.6. Statistics

Results represent the mean ± standard error of the mean (SEM). Statistical significance was determined using the Student's t-test with * $p < 0.05$, ** $p < 0.01$, *** $p < 0.001$ and n.s. (not significant) as indicated.

5. Conclusions

Our data indicate for the first time a key role of the immunoregulatory molecule GARP in the tumor microenvironment of primary brain tumors such as GB and low-grade gliomas inducing and promoting tumor immune tolerance via multiple pathways. Moreover, since GARP is not only expressed by activated Treg but also by brain tumor cells, it may serve as a potential target for an immunotherapeutic approach in patients with cerebral cancer.

Supplementary Materials: Supplementary materials are found at www.mdpi.com/xxx/s1.

Author Contributions: Conceptualization, A.T., E.K., J.T., and C.S.; methodology, N.Z., J.S., P.L., F.K., and B.S.; validation, N.Z. and B.S.; formal analysis, F.K.; resources, A.T.; writing—original draft preparation, A.T., N.Z., and E.K.; writing—review and editing, C.S., J.T., and F.R.; supervision, A.T.; project administration, N.Z.; funding acquisition, A.T.

Funding: This research was funded by Wilhelm-Sander Stiftung and CRC 1066 to AT.

Acknowledgments: We thank Janine Schlöder for critically reading and discussing the manuscript. We thank the molecular signaling unit of Krishnaraj Rajalingam in the PKZI Mainz for providing the Leica SP8 microscope.

Conflicts of Interest: The authors declare no conflict of interest.

Abbreviations

Treg	Regulatory T cells
GARP	Glycoprotein A repetition domain
GB	Glioblastoma
IC	Intracellular
IN	Intranuclear
sGARP	Soluble GARP
tolDC	Tolerogenic dendritic cells
MDSC	Myeloid-derived suppressor cells
GSC	Glioma stem cells
TME	Tumor microenvironment
LRR	Leucine-rich domains
RTK	Tyrosine kinase receptors
PD-1	Programmed death 1
CTLA-4	Cytotoxic T-lymphocyte associated antigen 4
CFSE	Carboxyfluorescein succinimidyl ester

References

1. Quail, D.F.; Joyce, J.A. The Microenvironmental Landscape of Brain Tumors. *Cancer Cell* **2017**, *31*, 326–341, doi:10.1016/j.ccell.2017.02.009.

2. Roesch, S.; Rapp, C.; Dettling, S.; Herold-Mende, C. When Immune Cells Turn Bad-Tumor-Associated Microglia/Macrophages in Glioma. *Int. J. Mol. Sci.* **2018**, *19*, 436, doi:10.3390/ijms19020436.
3. See, A.P.; Parker, J.J.; Waziri, A. The role of regulatory T cells and microglia in glioblastoma-associated immunosuppression. *J. Neurooncol.* **2015**, *123*, 405–412, doi:10.1007/s11060-015-1849-3.
4. Davis, R.J.; van Waes, C.; Allen, C.T. Overcoming barriers to effective immunotherapy: MDSCs, TAMs, and Tregs as mediators of the immunosuppressive microenvironment in head and neck cancer. *Oral Oncol.* **2016**, *58*, 59–70, doi:10.1016/j.oraloncology.2016.05.002.
5. Stupp, R.; Mason, W.P.; van den Bent, M.J.; Weller, M.; Fisher, B.; Taphoorn, M.J.B.; Belanger, K.; Brandes, A.A.; Marosi, C.; Bogdahn, U.; et al. Radiotherapy plus concomitant and adjuvant temozolomide for glioblastoma. *N. Engl. J. Med.* **2005**, *352*, 987–996, doi:10.1056/NEJMoa043330.
6. Hilf, N.; Kuttruff-Coqui, S.; Frenzel, K.; Bukur, V.; Stevanović, S.; Gouttefangeas, C.; Platten, M.; Tabatabai, G.; Dutoit, V.; van der Burg, Sjoerd, H.; et al. Actively personalized vaccination trial for newly diagnosed glioblastoma. *Nature* **2019**, *565*, 240–245, doi:10.1038/s41586-018-0810-y.
7. Calinescu, A.-A.; Kamran, N.; Baker, G.; Mineharu, Y.; Lowenstein, P.R.; Castro, M.G. Overview of current immunotherapeutic strategies for glioma. *Immunotherapy* **2015**, *7*, 1073–1104, doi:10.2217/imt.15.75.
8. Thomas, R.P.; Recht, L.; Nagpal, S. Advances in the management of glioblastoma: The role of temozolomide and MGMT testing. *Clin. Pharmacol.* **2013**, *5*, 1–9, doi:10.2147/CPAA.S26586.
9. Sampson, J.H.; Maus, M.V.; June, C.H. Immunotherapy for Brain Tumors. *J. Clin. Oncol.* **2017**, *35*, 2450–2456, doi:10.1200/JCO.2017.72.8089.
10. Mangani, D.; Weller, M.; Roth, P. The network of immunosuppressive pathways in glioblastoma. *Biochem. Pharmacol.* **2017**, *130*, 1–9, doi:10.1016/j.bcp.2016.12.011.
11. Lucca, L.E.; Hafler, D.A. Co-inhibitory blockade while preserving tolerance: Checkpoint inhibitors for glioblastoma. *Immunol. Rev.* **2017**, *276*, 9–25, doi:10.1111/imr.12529.
12. Kesarwani, P.; Kant, S.; Prabhu, A.; Chinnaiyan, P. The interplay between metabolic remodeling and immune regulation in glioblastoma. *Neuro-Oncology* **2017**, *19*, 1308–1315, doi:10.1093/neuonc/nox079.
13. Wesolowska, A.; Kwiatkowska, A.; Slomnicki, L.; Dembinski, M.; Master, A.; Sliwa, M.; Franciszkiewicz, K.; Chouaib, S.; Kaminska, B. Microglia-derived TGF-β as an important regulator of glioblastoma invasion—An inhibition of TGF-β-dependent effects by shRNA against human TGF-β type II receptor. *Oncogene* **2007**, *27*, 918, doi:10.1038/sj.onc.1210683.
14. Razavi, S.-M.; Lee, K.E.; Jin, B.E.; Aujla, P.S.; Gholamin, S.; Li, G. Immune Evasion Strategies of Glioblastoma. *Front. Surg.* **2016**, *3*, 11, doi:10.3389/fsurg.2016.00011.
15. Perea, F.; Bernal, M.; Sánchez-Palencia, A.; Carretero, J.; Torres, C.; Bayarri, C.; Gómez-Morales, M.; Garrido, F.; Ruiz-Cabello, F. The absence of HLA class I expression in non-small cell lung cancer correlates with the tumor tissue structure and the pattern of T cell infiltration. *Int. J. Cancer* **2017**, *140*, 888–899, doi:10.1002/ijc.30489.
16. Gajewski, T.F. Identifying and overcoming immune resistance mechanisms in the melanoma tumor microenvironment. *Clin. Cancer Res.* **2006**, *12*, 2326s–2330s, doi:10.1158/1078-0432.CCR-05-2517.
17. Nduom, E.K.; Weller, M.; Heimberger, A.B. Immunosuppressive mechanisms in glioblastoma. *Neuro-Oncology* **2015**, *17* (Suppl. 7), vii9–vii14, doi:10.1093/neuonc/nov151.
18. Hahn, S.A.; Stahl, H.F.; Becker, C.; Correll, A.; Schneider, F.-J.; Tuettenberg, A.; Jonuleit, H. Soluble GARP has potent antiinflammatory and immunomodulatory impact on human $CD4^+$ T cells. *Blood* **2013**, *122*, 1182–1191, doi:10.1182/blood-2012-12-474478.
19. Tran, D.Q.; Andersson, J.; Wang, R.; Ramsey, H.; Unutmaz, D.; Shevach, E.M. GARP (LRRC32) is essential for the surface expression of latent TGF-beta on platelets and activated FOXP3+ regulatory T cells. *Proc. Natl. Acad. Sci. USA* **2009**, *106*, 13445–13450, doi:10.1073/pnas.0901944106.
20. Wang, R.; Wan, Q.; Kozhaya, L.; Fujii, H.; Unutmaz, D. Identification of a regulatory T cell specific cell surface molecule that mediates suppressive signals and induces Foxp3 expression. *PLoS ONE* **2008**, *3*, e2705, doi:10.1371/journal.pone.0002705.
21. Hahn, S.A.; Neuhoff, A.; Landsberg, J.; Schupp, J.; Eberts, D.; Leukel, P.; Bros, M.; Weilbaecher, M.; Schuppan, D.; Grabbe, S.; et al. A key role of GARP in the immune suppressive tumor microenvironment. *Oncotarget* **2016**, *7*, 42996–43009, doi:10.18632/oncotarget.9598.
22. Guo, S.-K.; Shen, M.-F.; Yao, H.-W.; Liu, Y.-S. Enhanced Expression of TGFBI Promotes the Proliferation and Migration of Glioma Cells. *Cell. Physiol. Biochem.* **2018**, *49*, 1097–1109, doi:10.1159/000493293.

23. Ahmad, F.; Mani, J.; Kumar, P.; Haridas, S.; Upadhyay, P.; Bhaskar, S. Activation of anti-tumor immune response and reduction of regulatory T cells with Mycobacterium indicus pranii (MIP) therapy in tumor bearing mice. *PLoS ONE* **2011**, *6*, e25424, doi:10.1371/journal.pone.0025424.
24. Tucci, M.; Stucci, S.; Passarelli, A.; Giudice, G.; Dammacco, F.; Silvestris, F. The immune escape in melanoma: Role of the impaired dendritic cell function. *Expert Rev. Clin. Immunol.* **2014**, *10*, 1395–1404, doi:10.1586/1744666X.2014.955851.
25. Umansky, V.; Sevko, A. Melanoma-induced immunosuppression and its neutralization. *Semin. Cancer Biol.* **2012**, *22*, 319–326, doi:10.1016/j.semcancer.2012.02.003.
26. Roncarolo, M.G.; Gregori, S.; Battaglia, M.; Bacchetta, R.; Fleischhauer, K.; Levings, M.K. Interleukin-10-secreting type 1 regulatory T cells in rodents and humans. *Immunol. Rev.* **2006**, *212*, 28–50, doi:10.1111/j.0105-2896.2006.00420.x.
27. Vermeersch, E.; Denorme, F.; Maes, W.; Meyer, S.F. de; Vanhoorelbeke, K.; Edwards, J.; Shevach, E.M.; Unutmaz, D.; Fujii, H.; Deckmyn, H.; et al. The role of platelet and endothelial GARP in thrombosis and hemostasis. *PLoS ONE* **2017**, *12*, e0173329, doi:10.1371/journal.pone.0173329.
28. Ollendorff, V.; Noguchi, T.; deLapeyriere, O.; Birnbaum, D. The GARP gene encodes a new member of the family of leucine-rich repeat-containing proteins. *Cell Growth Differ.* **1994**, *5*, 213–219.
29. Bencheikh, L.; Diop, M.B.K.; Rivière, J.; Imanci, A.; Pierron, G.; Souquere, S.; Naimo, A.; Morabito, M.; Dussiot, M.; de Leeuw, F.; et al. Dynamic gene regulation by nuclear colony-stimulating factor 1 receptor in human monocytes and macrophages. *Nat. Commun.* **2019**, *10*, 1935, doi:10.1038/s41467-019-09970-9.
30. Groot, J.F. de; Piao, Y.; Tran, H.; Gilbert, M.; Wu, H.-K.; Liu, J.; Bekele, B.N.; Cloughesy, T.; Mehta, M.; Robins, H.I.; et al. Myeloid biomarkers associated with glioblastoma response to anti-VEGF therapy with aflibercept. *Clin. Cancer Res.* **2011**, *17*, 4872–4881, doi:10.1158/1078-0432.CCR-11-0271.
31. Ilhan-Mutlu, A.; Wagner, L.; Wöhrer, A.; Jungwirth, S.; Marosi, C.; Fischer, P.; Preusser, M. Blood alterations preceding clinical manifestation of glioblastoma. *Cancer Investig.* **2012**, *30*, 625–629, doi:10.3109/07357907.2012.725443.
32. Martens, A.; Wistuba-Hamprecht, K.; Geukes Foppen, M.; Yuan, J.; Postow, M.A.; Wong, P.; Romano, E.; Khammari, A.; Dreno, B.; Capone, M.; et al. Baseline Peripheral Blood Biomarkers Associated with Clinical Outcome of Advanced Melanoma Patients Treated with Ipilimumab. *Clin. Cancer Res.* **2016**, *22*, 2908–2918, doi:10.1158/1078-0432.CCR-15-2412.
33. Weller, M.; Cloughesy, T.; Perry, J.R.; Wick, W. Standards of care for treatment of recurrent glioblastoma—Are we there yet? *Neuro-Oncology* **2013**, *15*, 4–27, doi:10.1093/neuonc/nos273.
34. Seystahl, K.; Wick, W.; Weller, M. Therapeutic options in recurrent glioblastoma—An update. *Crit. Rev. Oncol. Hematol.* **2016**, *99*, 389–408, doi:10.1016/j.critrevonc.2016.01.018.
35. Chan, D.V.; Somani, A.-K.; Young, A.B.; Massari, J.V.; Ohtola, J.; Sugiyama, H.; Garaczi, E.; Babineau, D.; Cooper, K.D.; McCormick, T.S. Signal peptide cleavage is essential for surface expression of a regulatory T cell surface protein, leucine rich repeat containing 32 (LRRC32). *BMC Biochem.* **2011**, *12*, 27, doi:10.1186/1471-2091-12-27.
36. Han, J.; Alvarez-Breckenridge, C.A.; Wang, Q.-E.; Yu, J. TGF-β signaling and its targeting for glioma treatment. *Am. J. Cancer Res.* **2015**, *5*, 945–955.
37. Lim, M.; Xia, Y.; Bettegowda, C.; Weller, M. Current state of immunotherapy for glioblastoma. *Nat. Rev. Clin. Oncol.* **2018**, *15*, 422–442, doi:10.1038/s41571-018-0003-5.
38. Xue, S.; Hu, M.; Iyer, V.; Yu, J. Blocking the PD-1/PD-L1 pathway in glioma: A potential new treatment strategy. *J. Hematol. Oncol.* **2017**, *10*, 81, doi:10.1186/s13045-017-0455-6.
39. Barrantes-Freer, A.; Kim, E.; Bielanska, J.; Giese, A.; Mortensen, L.S.; Schulz-Schaeffer, W.J.; Stadelmann, C.; Brück, W.; Pardo, L.A. Human glioma-initiating cells show a distinct immature phenotype resembling but not identical to NG2 glia. *J. Neuropathol. Exp. Neurol.* **2013**, *72*, 307–324, doi:10.1097/NEN.0b013e31828afdbd.
40. Barrantes-Freer, A.; Renovanz, M.; Eich, M.; Braukmann, A.; Sprang, B.; Spirin, P.; Pardo, L.A.; Giese, A.; Kim, E.L. CD133 Expression Is Not Synonymous to Immunoreactivity for AC133 and Fluctuates throughout the Cell Cycle in Glioma Stem-Like Cells. *PLoS ONE* **2015**, *10*, e0130519, doi:10.1371/journal.pone.0130519.
41. Fischer, U.; Kim, E.; Keller, A.; Meese, E. Specific amplifications and copy number decreases during human neural stem cells differentiation towards astrocytes, neurons and oligodendrocytes. *Oncotarget* **2017**, *8*, 25872–25884, doi:10.18632/oncotarget.15980.

42. Kotecha, N.; Krutzik, P.O.; Irish, J.M. Web-based analysis and publication of flow cytometry experiments. *Curr. Protoc. Cytom.* **2010**, *53*, doi:10.1002/0471142956.cy1017s53.
43. Rueden, C.T.; Schindelin, J.; Hiner, M.C.; DeZonia, B.E.; Walter, A.E.; Arena, E.T.; Eliceiri, K.W. ImageJ2: ImageJ for the next generation of scientific image data. *BMC Bioinform.* 2017, *18*, 529, doi:10.1186/s12859-017-1934-z.

Table S1. Characteristics of astrocytoma grade II patients at the study center Idar-Oberstein, Germany. Patient characteristics (gender, age), primary tumor data including localization, therapy, and follow-up are displayed.

Low grade Astrocytomas II	male	female	total	lost to follow up
Number of patients	3	3	6	
Age at the onset mean±SD (yr.)	60±17.7	55.66±7.6	57.83±12.4	
Side hemispheric				
right	3	1	4	
left	0	2	2	
bilateral	0	0	0	
Surgery				
resection	1	2	3	
biopsy	2	1	3	
Localization				
midbrain	1	0	1	
Front/temp/insular	1	0	1	
hemispheric	1	0	1	
temporal	0	2	2	
frontal	0	1	1	
Radiation therapy	1	0	1	1
Chemotherapy	1	0	1	1
Survival mean±SD (mon.)	14±15.55	13.5±14.84	13.75±12.41	3

Table S2. Characteristics of astrocytoma grade III patients at the study center Idar-Oberstein, Germany. Patient characteristics (gender, age), primary tumor data including localization, therapy, and follow-up are displayed.

Low grade Astrocytomas III	male	female	total	lost to follow up
Number of patients	6	5	11	
Age at the onset mean±SD (yr.)	53.33±13.27	64.2±17.94	58.27±15.7	
Side hemispheric				
right	3	3	6	
left	3	0	3	
bilateral	0	2	2	
Surgery				
resection	4	1	5	
biopsy	2	4	6	
Localization				
frontal	3	1	4	
temporal	3	1	4	
bifrontal	0	2	2	
hemispheric	0	1	1	
Radiation therapy	5	3	8	2
Chemotherapy	4	2	6	1

Survival mean±SD (mon.)	17.8±12.43	5.0	15.66±12.29	4 female

cancers

MDPI

Article

Nuclear Glycoprotein A Repetitions Predominant (GARP) Is a Common Trait of Glioblastoma Stem-like Cells and Correlates with Poor Survival in Glioblastoma Patients

Niklas Zimmer [1,†], Emily R. Trzeciak [1,†], Andreas Müller [2,3], Philipp Licht [1], Bettina Sprang [2,3], Petra Leukel [4], Volker Mailänder [1,5], Clemens Sommer [4], Florian Ringel [2], Jochen Tuettenberg [6], Ella Kim [2,3,‡] and Andrea Tuettenberg [1,5,*,‡]

1 Department of Dermatology, University Medical Center Mainz, 55131 Mainz, Germany; plicht@uni-mainz.de (P.L.)
2 Department of Neurosurgery, University Medical Center Mainz, 55131 Mainz, Germany
3 Laboratory of Experimental Neurooncology, University Medical Center Mainz, 55131 Mainz, Germany
4 Institute of Neuropathology, University Medical Center Mainz, 55131 Mainz, Germany
5 Research Center for Immunotherapy, University Medical Center Mainz, 55131 Mainz, Germany
6 Department of Neurosurgery, SHG-Klinikum Idar-Oberstein, 55743 Idar-Oberstein, Germany; j.tuettenberg@io.shg-kliniken.de
* Correspondence: antuette@uni-mainz.de
† These authors contributed equally to this work.
‡ Joint Senior Authors.

Simple Summary: Glioblastoma (GB) is the most common primary brain tumor in adults, but it remains incurable due to its high degree of therapy resistance. Glioblastoma stem-like cells (GSCs) are believed to drive the initiation, progression, and therapy resistance of GB, making them an ideal therapeutic target to improve patient outcomes. However, due to their heterogeneity, there are no universal markers to identify GSCs. We evaluated GARP as a novel marker for GSCs and found that GARP is more stably and uniformly expressed by human GSCs, across cellular states and disease stages, than the commonly used GSC marker, CD133. Additionally, we showed that GARP is intranuclearly localized in GSCs, and we are the first to show that nuclear GARP levels ($GARP^{NU+}$) are associated with poor patient survival. Our findings indicate that GARP/$GARP^{NU+}$ expression is an improved marker for GSCs and suggest a potential application of GARP as a prognostic biomarker for GB.

Abstract: Glioblastoma (GB) is notoriously resistant to therapy. GB genesis and progression are driven by glioblastoma stem-like cells (GSCs). One goal for improving treatment efficacy and patient outcomes is targeting GSCs. Currently, there are no universal markers for GSCs. Glycoprotein A repetitions predominant (GARP), an anti-inflammatory protein expressed by activated regulatory T cells, was identified as a possible marker for GSCs. This study evaluated GARP for the detection of human GSCs utilizing a multidimensional experimental design that replicated several features of GB: (1) intratumoral heterogeneity, (2) cellular hierarchy (GSCs with varied degrees of self-renewal and differentiation), and (3) longitudinal GSC evolution during GB recurrence (GSCs from patient-matched newly diagnosed and recurrent GB). Our results indicate that GARP is expressed by GSCs across various cellular states and disease stages. GSCs with an increased GARP expression had reduced self-renewal but no alterations in proliferative capacity or differentiation commitment. Rather, GARP correlated inversely with the expression of GFAP and PDGFR-α, markers of astrocyte or oligodendrocyte differentiation. GARP had an abnormal nuclear localization ($GARP^{NU+}$) in GSCs and was negatively associated with patient survival. The uniformity of GARP/$GARP^{NU+}$ expression across different types of GSCs suggests a potential use of GARP as a marker to identify GSCs.

Keywords: GARP; nuclear GARP; $GARP^{NU+}$; LRRC32; glioblastoma; glioblastoma stem-like cells

Citation: Zimmer, N.; Trzeciak, E.R.; Müller, A.; Licht, P.; Sprang, B.; Leukel, P.; Mailänder, V.; Sommer, C.; Ringel, F.; Tuettenberg, J.; et al. Nuclear Glycoprotein A Repetitions Predominant (GARP) Is a Common Trait of Glioblastoma Stem-like Cells and Correlates with Poor Survival in Glioblastoma Patients. *Cancers* **2023**, *15*, 5711. https://doi.org/10.3390/cancers15245711

Academic Editors: Martine L. M. Lamfers, Ander Matheu and Benedikt Linder

Received: 20 October 2023
Revised: 17 November 2023
Accepted: 1 December 2023
Published: 5 December 2023

1. Introduction

Glioblastoma (GB) is one of the most aggressive tumors, with an overall survival rate of approximately 15 months [1,2]. The current standard therapy consists of surgical removal of the primary tumor, radiation, and treatment with the chemotherapeutic agent, temozolomide (TMZ) [3]. A high degree of tumor infiltration into the surrounding tissue is a characteristic feature of GB, limiting the clinical efficacy of neurosurgical resection. Despite multi-modal therapy, GB recurrence after initial treatment is almost inevitable [4–6]. Besides the immunosuppressive properties of tumor cells, which suppress anti-tumor immune responses through microglial cells or regulatory T cells, poor prognosis is also attributed to a high degree of therapeutic resistance, either inherent or acquired by therapy, and the extraordinary intratumoral heterogeneity of GB, manifesting via the diversity of molecular and cellular subtypes/cellular states associated with GSCs [7–10].

The notorious therapeutic resistance of GB has been attributed to glioblastoma stem-like cells (GSCs), which comprise a subset of tumor cells that possess some fundamental properties of cancer stem cells, including unlimited self-renewal, aberrant differentiation response, and inherent plasticity. These characteristics enable GSCs to undergo reversible transitions between distinct cellular states in response to environmental signals [11,12].

These unique properties render GSCs capable of adapting to and surviving cytotoxic treatments that are otherwise lethal to non-stem glioma cells, thereby endowing them with the potential to reconstitute the tumor during or after therapy. GSCs are currently considered the main determinants of therapy resistance and drivers of tumor recurrence in GB. Therefore, they are arguably the most clinically relevant cellular target in gliomas. Assessments of GSCs in tumor specimens face several methodological challenges. These include: (I) the relatively low percentage of GSCs compared to the rest of the tumor cells, which are thought to be comprised primarily of non-stem glioma cells or differentiated progenies of GSCs [13,14], (II) an inhomogeneous distribution of GSCs within the tumor, which are located in specialized niches that provide a proper environment for maintaining their undifferentiated state [14], and (III) the phenotypic diversity and inherent high plasticity of GSCs, enabling dynamic transitions between different cell states accompanied by morphological alterations and changes in their phenotypic make-up [15,16]. Furthermore, GSCs possess a high degree of plasticity, which renders them capable of switching between different cellular states and distinct morphological phenotypes. Lack of definitive markers that are stably expressed on GSCs poses a further challenge to the diagnostic stratification of GB based on the evaluation of GSC content in tumor specimens [17].

Although a range of molecules like CD15, L1CAM, SOX2, and Prominin1/CD133 have been implicated as identification markers of GSCs, their diagnostic utility has been limited due to the phenotypic heterogeneity within the GSC compartment, constituted by cells in hierarchically distinct states [18–23]. For example, expression of Prominin1/CD133, historically one of the most investigated and arguably the best validated GSC marker, is sample specific, being restricted to only a subset of GSCs [24–27], and fluctuates significantly during cell cycle [28]. Furthermore, a reversible loss of CD133 expression in $CD133^+$ GSCs was shown to accompany tumor propagation, as revealed in an experimental in vivo model of GB [24]. Considering that the tumor-propagating capacity of $CD133^-$ GSCs is comparable to that of $CD133^+$ GSCs [24], the diagnostic utility of CD133 remains uncertain [29]. Phenotypic diversity and plasticity of GSCs as a means of adaptation to the tumor microenvironment have important implications for the continuing search for GSCs markers that would be universally applicable for different subsets of GSCs and would be expressed unambiguously, regardless of cellular state.

In this regard, Glycoprotein A repetitions predominant (GARP) has recently emerged as a potential marker of human GSCs [7,30]. GARP is a type I transmembrane protein normally expressed on the surface of activated regulatory T cells, where it mediates tolerogenic functions in the tumor microenvironment of GB [7]. GARP consists of 662 amino acids and is composed of an extracellular domain with 20 leucine rich repeats, a hydrophobic transmembrane domain, and a 15 amino acid intracellular part. Recently, we have found

that GARP is also expressed by different types of GB cells, including GSCs, where it shows an atypical pattern of subcellular distribution characterized by GARP localization on both the cell surface and within the nucleus ($GARP^{NU+}$) [7]. Up until now, GARP expression in GSCs has only been shown in vitro, with several open-ended questions remaining. Namely, is GARP/$GARP^{NU+}$ expression associated with a particular cellular state (self-renewal or differentiation) or a particular subtype of GSCs? Does the associated expression of GARP/$GARP^{NU+}$ in GSCs persist during GB progression after therapy?

In the present study, these questions were addressed in vitro and in vivo by analyzing the expression of GARP/$GARP^{NU+}$ in different subtypes of patient-derived GSCs with consideration of intratumoral heterogeneity and the longitudinal changes accompanying GB recurrence. For the first time, the present study examined the potential link of nuclear GARP expression with patient outcomes.

2. Materials and Methods

2.1. Cell Culture

The human glioblastoma cell line T98G was purchased from the ATCC (CRL-1690) and was cultured in Minimum Essential Medium Eagle supplemented with 10% FCS, 1% Glutamine, and 0.1% Primocin. The human melanoma cell lines, Mewo and Ma-Mel-19, were obtained from Dr. Daniela Kramer (Mewo, RRID:CVCL_0445, Cellosaurus) in Mainz, Germany, in 2021 and from Dr. Annette Paschen (Ma-Mel-19, RRID:CVCL_A156, Cellosaurus) in Essen, Germany, in 2014. Mewo cells were cultured in Dulbecco's Modified Eagle Medium supplemented with 10% FCS and 0.1% Primocin. Ma-Mel-19 cells were grown in RPMI 1640 supplemented with 10% FCS, 1% Glutamine, and 0.1% Primocin. T98G, Mewo, and Ma-Mel-19 cells were passed every 2 to 3 days by using Trypsin-EDTA. The cell lines T98G and Ma-Mel-19 were authenticated in August 2022 by PCR single locus technology. The results were compared to the online databases of the DSMZ and Cellosaurus (Eurofins Genomics Europe). Patient-derived GSC lines used in this study were established as previously described and have been well characterized in previous studies, in terms of their stem cell frequency (SCF) and expression of various GSC markers [28,31–33]. Additional information regarding their origin, SCF, predominant phenotype ($Nestin^{+/-}$, $GFAP^{+/-}$), and percentage of CD133-positive cells, as well as an exemplary analysis of the GSC markers, CD133, platelet-derived growth factor receptor alpha (PDGFR-α), and aldehyde dehydrogenase 1 family member A3 (ALDH1A3), can be found in Figure S1 [28,33,34]. In brief, excess glioblastoma tumor tissue was obtained from patients operated on at the Department of Neurosurgery of the Johannes Gutenberg University Medical Center Mainz (JG-UMC), with informed consent. The use of tumor tissue for research purposes was approved by the JG-UMC Institutional Review Board (permission 08.06.2017 #837.211.12(8312-F). For GSC isolation, a combined enzymatic and mechanical titration procedure was used as previously described [28]. To promote self-renewal, glioma cells were cultured in serum-free NeuroBasal (NB) medium supplemented with the following factors: B27 supplement (Invitrogen, Darmstadt, Germany) and the recombinant human cytokines, basic fibroblast growth factor 2 (bFGF) (10 ng/mL) and epidermal growth factor (EGF), (20 ng/mL) (Biochrom GmbH, Merck KGaA, Darmstadt, Germany). For in vitro differentiation, cells were subjected to EGF and bFGF withdrawal and assessed for the expression of neural lineage specific markers after 7 days. Self-renewal promoting conditions are hence referred to as "NB+bFGF/+EGF" whereas differentiation is indicated by "NB-bFGF/-EGF" in the manuscript.

2.2. Western Blot

Protein preparation and Western blotting were performed as previously described in Müller et al., 2023 [35]. Membranes were probed with the following antibodies: anti-CD133/1 (clone: W6B3C1), anti-PDFGR-α (D13C6) (Cell Signaling, #5241T, Danvers, MA, USA), anti-ALDH1A3 (Thermo Fischer Scientific, MA5-25528, Waltham, MA, USA), anti-p53 (DO-1) (Cell Signaling, #18032), anti-actin (C4) (Santa Cruz Biotechnology, sc-47778,

Dallas, TX, USA), anti-glial fibrillary acidic protein (GFAP) (DAKO, Z0334, Santa Clara, CA, USA), anti-p21 (Cell Signaling, #2947), anti-phosphorylated-histone H3 (Ser28) (Cell Signaling, #9713S), anti-HSP70 (Enzo Life Sciences Inc., Farmingdale, NY, USA), anti-mouse IgGκ light chain-binding protein horseradish peroxidase (Santa Cruz Biotechnology, sc-516102), goat anti-rabbit IgG H&L horseradish peroxidase (Abcam, ab205718, Cambridge, UK), goat anti-mouse IgG horseradish peroxidase (Santa Cruz Biotechnology, sc-2055), and goat anti-rabbit horseradish peroxidase (Santa Cruz Biotechnology, sc-2054). Signal intensity was analyzed via densitometry (https://imagej.nih.gov, accessed on 17 October 2023) [36].

2.3. Flow Cytometry

For flow cytometric analysis, the following fixable viability dye and antibodies were used: FVD506 (eBioscience #65-0866-14, San Diego, CA, USA), anti-GARP (Miltenyi #130-103-820 and 130-103-890, updated ordering numbers: 130-125-511 and 130-125-532, Bergisch Gladbach, Germany), anti-CD133 (epitope AC133, Miltenyi # 130-113-111), and their respective isotype controls (Miltenyi #130-113-434 and Miltenyi #130-113-200). Cells were stained with fixable viability dye prior to surface antibody staining of anti-GARP and anti-CD133. Cells were not fixed for the analysis.

Extensive validation of the anti-GARP antibodies mentioned above and a demonstration of their specificity can be found in Figures S2 and S3 as well as in previous work by Zimmer et al., 2019 [7]. In more detail, the anti-GARP antibodies from Miltenyi were validated against two other flow cytometry certified antibodies (Biolegend, 352506, San Diego, CA, USA; Origene, TA337028, Rockland, MD, USA) (Figure S3) and against the polyclonal anti-GARP antibody used in this study (Origene, AP17415PU-N) (Figure S2). Antibody specificity was demonstrated using GARP-overexpressing Mewo cells, resulting from transient transfection using the LOX-IMVI Cell Avalanche Transfection Reagent (EZ Biosystems, EZT-LOXI-1, College Park, MD, USA) as well as a LRRC32 overexpression plasmid (Origene, SC116699) and an empty vector control plasmid (Origene, PS100001) (Figure S3). Transfection was performed in accordance with the manufacturer's recommendations. Cells were stained with fixable viability dye and for surface GARP as described above 48 h post-transfection.

Flow cytometry was performed on a BD LSRII flow cytometer (Heidelberg, Germany) and was analyzed using Cytobank [37]. Doublets, debris, and dead cells were excluded from analysis (Figure S4).

2.4. Confocal Microscopy

Confocal imaging was performed on a Leica SP8 with HyD detector (Wetzlar, Germany) at the Imaging Core Facility (ICF) of the Forschungszentrum für Immuntherapie (FZI) of the University Medical Center Mainz as described before [7]. The following antibodies were used in the study: anti-nestin (Abcam, ab22035), anti-GARP (Origene, AP17415PU-N), and secondary antibodies goat anti-mouse Alexa Fluor 488 or goat anti-rabbit Alexa Fluor 555 (both Thermo Fisher Scientific, Waltham, MA, USA). Validation and specificity of the anti-GARP antibody (Origene AP17415PU-N) for its use in confocal microscopy can be found in Figure S5 and in previous work by Zimmer et al., 2019 [7].

2.5. Animal Experiments

Animal experiments were performed at the Translational Animal Research Facility (TARC) of the JG-UMC, Germany, in accordance with the guidelines of the European Convention for the Protection of Vertebrates Used for Scientific Purposes and under the approval of the State Office of Chemical Investigations of Rhineland-Palatinate (permission #23 177-07/G12-1-020). Immunodeficient mice (strain NMRI) were purchased from a commercial supplier (Charles River Laboratories Germany). After an adaptation period of one to two weeks, mice were subjected to intracerebral injection of GSCs using a standardized procedure as described previously [34,38]. In brief, single-cell suspensions were prepared

from glioma sphere cultures by using a combined trypsin/mechanical titration procedure. Cells were washed twice in PBS and re-suspended in PBS at 2 × 10^4 cells/µL. Cell viability was determined by trypan blue staining. Single-cell suspensions were injected at 5 µL into the caudato-putamen of the right hemisphere using a stereotactic frame (TSE Systems, Bad Homburg, Germany) and the following stereotactic coordinates in reference to the bregma: 1 mm (anteroposterior axis), 3 mm (lateromedial axis), 2.5 mm (vertical axis). Mice were sacrificed at the first manifestation of tumor-associated neurological symptoms.

2.6. GARP Immunohistochemistry and Immunofluorescence

Tumor-bearing mouse brains were extracted and fixed in 4% paraformaldehyde in PBS for at least 24 h at 4 °C as described previously [38]. Briefly, after fixation, brains were paraffin-embedded, dissected into 1–3 µm thick coronal sections and analyzed by immunohistochemical or immunofluorescence staining using antibodies specific to human nestin (R&D Systems GmbH, Wiesbaden-Nordenstadt, Germany), GFAP (DAKO, Z0334), or GARP (Origene, AP17415PU-N). Previous work has demonstrated the specificity of the anti-GARP antibody (Origene, AP17415PU-N) for its use in immunohistochemistry and immunofluorescence [7,39]. For analysis, ImageJ2 (Available online: https://imagej.net/ImageJ2, accessed on 16 August 2021) was used [40].

A GB patient cohort from Zimmer et al., 2019 [7], was reanalyzed to correlate the frequency of $GARP^{NU+}$ cells in tumor tissue to patient overall survival regardless of IDH status. Patient characteristics are described in detail in Figure 1 of Zimmer et al., 2019 [7]. In brief, the patient cohort consisted of 35 newly diagnosed (WHO stage IV) GB patients from the Department of Neurosurgery in Idar-Oberstein, Germany, between January 2009 and May 2015. The median high and low survival times were 12 and 4 months. Primary tumor tissue was resected and stained for GARP via immunohistochemistry. Description of the immunohistochemical staining process can be found in Zimmer et al., 2019 [7]. The frequency of $GARP^{NU+}$ was semi-quantified in tumor tissue with regions of labeled nuclei (categorized as >90%, >50%, >10% $GARP^{NU+}$ cells) at the Institute of Neuropathology, University Medical Center Mainz, Germany [7].

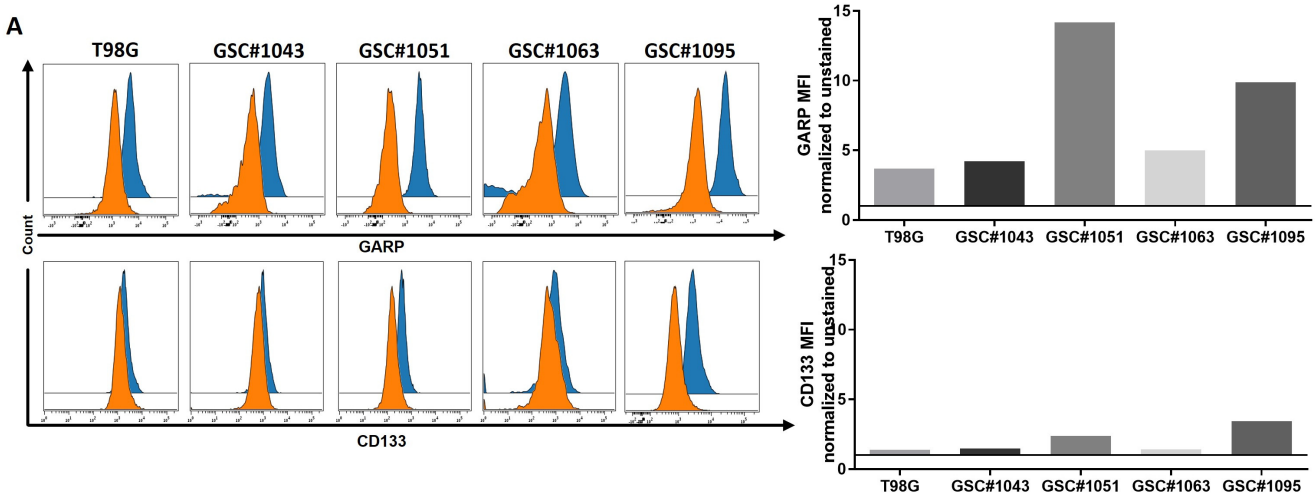

Figure 1. *Cont.*

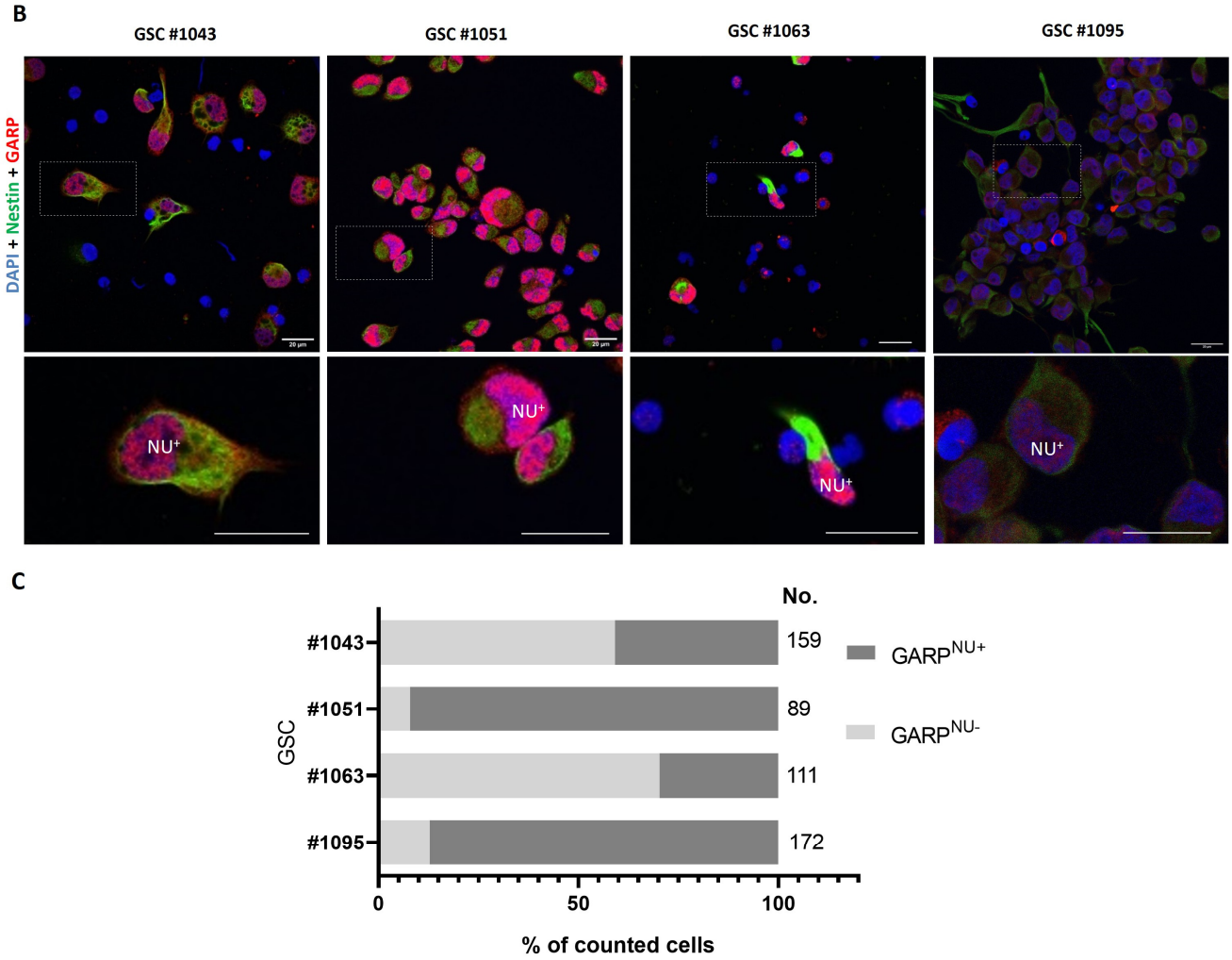

Figure 1. (**A**) Flow cytometric analysis of surface GARP and CD133 on different GSCs and the control, non-stem, GB cell line, T98G. Doublets, debris, and dead cells were excluded from the analysis. Mean fluorescence intensity (MFI) was normalized to the MFI of the respective unstained control. (**B**) Confocal images of GARP- and nestin-expressing GSCs and T98G. Cells were stained for GARP (red) and nestin (green). Cells were counterstained for their nuclei with Hoechst (blue). Note the intranuclear localization of GARP (NU^+). Scale bar corresponds to 20 µm. (**C**) Percentage of $GARP^{NU+}$ cells were determined by counting GARP stained nuclei. "No." indicates the number of counted cells for the analysis.

2.7. Cell Sorting

Single-cell suspensions of the GSC line, #1095, were stained sequentially with the following: fixable viability dye FVD780 (eBioscience #65-0865-14), unconjugated anti-GARP antibody (Origene, AP17415PU-N) or a control unconjugated IgG rabbit isotype antibody (R&D Systems, AB-105-C), followed by a PE-conjugated goat anti-rabbit secondary antibody (Invitrogen, P2771MP). Cells were sorted into $GARP^{low}$ and $GARP^{high}$ populations. Cell sorting gates were defined as the lower 10th ($GARP^{low}$) and upper 90th percentiles ($GARP^{high}$) of all cells. An example gating strategy and proof of positive GARP staining can be found in Figure S6. Debris, doublets, and dead cells were excluded from analysis. Sorting was performed using BD Aria II and III cell sorters at the Core Facility Flow Cytometry (CFFC) of the Forschungszentrum für Immuntherapie (FZI) of the University Medical Center Mainz.

2.8. Extreme Limiting Dilution Assay

The self-renewal capacity of GSC lines was analyzed by extreme limiting dilution assay (ELDA). In brief, single-cell suspensions were serially diluted in self-renewal promoting medium (NB+bFGF/+EGF) and seeded into 24 well plates. The number of replicates used for each serial dilution are indicated as follows: 12 for 100 cells/well, 18 for 50 cells/well, 24 for 25 cells/well, 58 for 12.5 cells/well, 24 for 6.25 cells/well, 18 for 3.125 cells/well, and 12 for 1.56 cells/well. Cells were incubated for three weeks to develop neurospheres. Wells were assessed for neurosphere formation; a positive result was recorded for each dose (number of seeded cells/well) if the examined well contained at least one neurosphere. Each experiment was repeated independently three times. Stem cell frequency (SCF) was calculated using the ELDA: Extreme Limiting Dilution Analysis webtool from the Walter and Eliza Hall Institute of Medical Research (https://bioinf.wehi.edu.au/software/elda/, accessed on 6 September 2023) [41].

2.9. Bioinformatic Pipeline

In a previous work, Kim et al., 2020, performed Illumina RNA-Sequencing on a total of 155 glioblastoma samples derived from 28 patients [32]. These consisted of primary, recurrent, and secondary recurrent tumors (128 samples) as well as GSC cultures developed from freshly resected tumor tissue (27 samples). We obtained unnormalized gene counts through the Gene Expression Omnibus database (GEO) under the accession number: GSE139533. Gene counts were normalized with DESeq2 and analyzed using the likelihood ratio test to decipher the effect of progressing tumor stages on transcript levels within the same patient [42]. Normalized counts for CD133 and GARP were plotted with GraphPad Prism version 9.3.1 for Windows, GraphPad Software, San Diego, CA, USA, www.graphpad.com.

Survival analysis of CD133 and GARP was performed using OncoLnc (http://www.oncolnc.org/, accessed on 8 July 2023) which is based upon data generated by The Cancer Genome Atlas (TCGA) Research Network (https://www.cancer.gov/tcga, accessed on 8 July 2023) [43–45].

2.10. Statistics

Statistical analysis was performed with Student's *t*-test, the likelihood ratio test, the chi-squared test, or two-way ANOVA as indicated. Data are displayed as mean values ± SEM or ±SD as indicated. Survival curve comparison was analyzed using the log-rank (Mantel–Cox) test using GraphPad Prism. Statistical significance is indicated as follows: * $p < 0.05$, ** $p < 0.01$, *** $p < 0.001$, **** $p < 0.001$, and ns (not significant).

3. Results

3.1. GARP Expression Is Conserved across Different Types of GSCs In Vitro and In Vivo

We have previously shown that GARP is expressed by three human GSC lines and by the conventional human glioblastoma cell line, T98G [7]. The questions that remained were whether GARP expression is restricted to a particular type of GSCs or if it represents a common phenotypic trait shared by different subsets of GSCs. To address these questions, we analyzed the expression of GARP in a panel of heterologous GSC lines, differing in their self-renewal capacity, degree of differentiation, and expression of CD133, a proposed marker for GSCs in the past (Figure S1A). All GSCs used in this study invariably expressed nestin, a neural stem cell marker, but they varied in their expression of the astrocyte differentiation marker, GFAP, and CD133, a putative GSC marker (Figure S1A). A non-stem glioblastoma cell line, T98G, (ATCC CRL-1690) was analyzed in parallel as a control. Flow cytometry revealed that the surface expression of GARP varied across heterologous GSCs (Figure 1A). Notably, variations in GARP expression paralleled variations in CD133 levels indicating that GARP and CD133 are not mutually exclusive markers (Figure 1A). Line-dependent variations in GARP expression were also confirmed by microscopic evaluation of intracellular GARP (Figure 1B,C). Confirming our previous observations, microscopic analysis

revealed that GARP localization in GSCs is not restricted to the cell membrane, a normal localization site for GARP, but it also extends to the nuclear compartment (Figure 1B) [7,30]. The nuclear localization of GARP was evident in confocal microscopy with co-staining for nestin, an established marker of neural stem/progenitor cells expressed in the cytoplasm. The prevalence of cells with nuclear GARP (termed hereafter as "GARP^{NU+}") varied between different GSC lines (Figure 1B,C) and mirrored the levels of surface-expressed GARP (Figure 1A), indicating a possible relationship between the two forms. For example, the GSC lines #1051 and #1095 had the highest levels of surface-membrane-associated GARP (Figure 1A), and they also exhibited a high proportion of cells with GARP^{NU+} (92.1% and 87.2%, Figure 1B,C). Vice versa, GSCs with moderate levels of surface GARP (#1043 and #1063, Figure 1A) had lower proportions of cells with GARP^{NU+} (40.9% and 29.7%, Figure 1C).

Our in vitro findings prompted us to test if GARP/GARP^{NU+} expression is sustained in vivo in GSCs involved in tumor propagation. To this end, we analyzed xenograft tumors grown from two GSC lines that express the lowest (line #1043) and highest (line #1051) levels of GARP in vitro (Figure 1). Both lines gave rise to highly invasive brain tumors as ascertained by immunohistochemical staining with an antibody specific for human nestin (Figure S7) and had comparable rates of tumor growth [34]. Immunofluorescence staining for GARP revealed its expression in both #1051 and #1043 xenografts (Figure S8). Notably, GARP expression in #1043 xenograft (low expressor in vitro, Figure 1) was comparable with that in #1051 xenograft (high expressor in vitro, Figure 1), suggesting that GARP expression in GSCs might be even more profound in the tumor context. Concordant with our in vitro findings, tumor-propagating GSCs also showed GARP localization in both the cytoplasm and nucleus (Figure S8). Additionally, GARP^{NU+} was observed to be co-expressed with nestin (Figure S8). These results further support the conclusion that GARP/GARP^{NU+} expression might be a common trait stably sustained (or even augmented) in GSCs involved in tumor propagation.

3.2. Intratumoral Heterogeneity of Subcellular Distribution Patterns of GARP

GBs are known for their high degree of intratumoral heterogeneity, which is thought to reflect the hierarchical diversity of cellular states generated by GSCs [12,46]. Our observation that heterologous GSCs vary in their levels of GARP/GARP^{NU+} (Figures 1 and S8) prompted us to check if this is a mere reflection of intertumoral diversity, GARP/GARP^{NU+} association with a particular GSC subtype or cellular state, or a hierarchical diversification taking place during tumor growth. To address these questions, we made use of isogenic GSCs (lines IT-726-#1, IT-726-#2, IT-726-#3a, IT-726-#3b, and IT-726-#4) that have been isolated from different regions of the same tumor (Figure S9—Cohort 2"—comparison line 1) and provide a unique model for analyzing the impact of intratumoral heterogeneity in an isogenic background [31,32]. Indeed, despite their identical genetic background, isogenic GSCs from the IT-726 set displayed notable morphological differences, considerable variations in their self-renewal capacity, and expression of GSC-associated markers CD133, ALDH1 A3, and PDGFR-α (Figure S1) [31,32].

Interestingly, we found no apparent correlation between CD133 expression and the degree of self-renewal activity. For example, the lines IT-726-1 and IT-726-3B had comparable degrees of self-renewal activity (Figure S1A), but they differed profoundly in the expression of surface CD133 (glycosylated epitope AC133) (Figure 2). Vice versa, the line IT-726-4 expressed similar levels of surface CD133 as the lines IT-726-2, IT-726-3A, and IT-726-3B, (Figure 2), but it stood out markedly from the other lines in terms of its extremely low self-renewal capacity (Figure S1A). In contrast to CD133, the expression of surface GARP was very similar across isogenic lines, and it did not parallel the striking difference in CD133 expression between the IT-726-1 line and its isogenic counterparts (Figure 2). In comparison to the uniform expression of surface GARP, the patterns of GARP subcellular distribution between IT-726 lines were heterogeneous, with the proportion of GARP^{NU+} cells varying across different isogenic lines (Figure 3A). The highest level of GARP^{NU+}

was found in line IT-726-2, which had a prominent expression of nuclear GARP in nearly every cell (Figure 3B, IT-726-2 upper panel). GARP expression was also examined on IT-726 cell lines grown in self-renewal-promoting (NB+bFGF/+EGF) versus differentiation-promoting (NB-bFGF/-EGF) conditions. Interestingly, IT-726-2 displayed a prominent expression of nuclear GARP in almost every cell regardless of culture condition. In contrast, other isogenic IT-726 lines exhibited a mixed pattern of GARP localization in both nuclear and cytoplasmic compartments in self-renewal-promoting conditions (NB+bFGF/+EGF) (Figure 3B, shown for IT-726-4). Notably, the nuclear localization of GARP appeared to be more profound when cells were grown in differentiation-promoting conditions (NB-bFGF/-EGF), suggesting an inverse correlation between $GARP^{NU+}$ and self-renewal capacity. The IT-726-2 line, in which the $GARP^{NU+}$ pattern was predominant (Figure 3B), had a lower self-renewal capacity when compared to the other isogenic counterparts (Figure S1A), consistent with this interpretation.

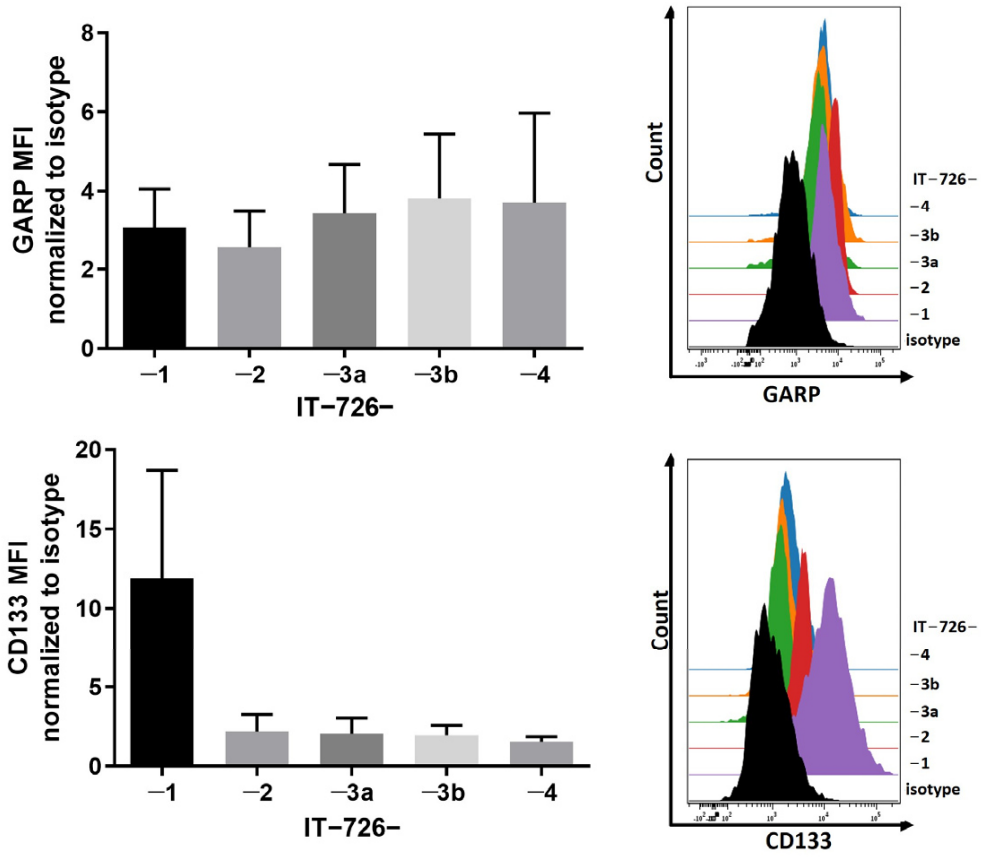

Figure 2. GARP expression in isogenic GSCs derived from newly diagnosed GB IT-726. Flow cytometric analysis of IT-726-1, -2, -3a, -3b, and -4. Doublets, debris, and dead cells were excluded from analysis. Mean fluorescence intensity (MFI) was normalized to the MFI of the unstained control. Histograms display one representative result of three independent measurements. Data are displayed as mean values ± SEM.

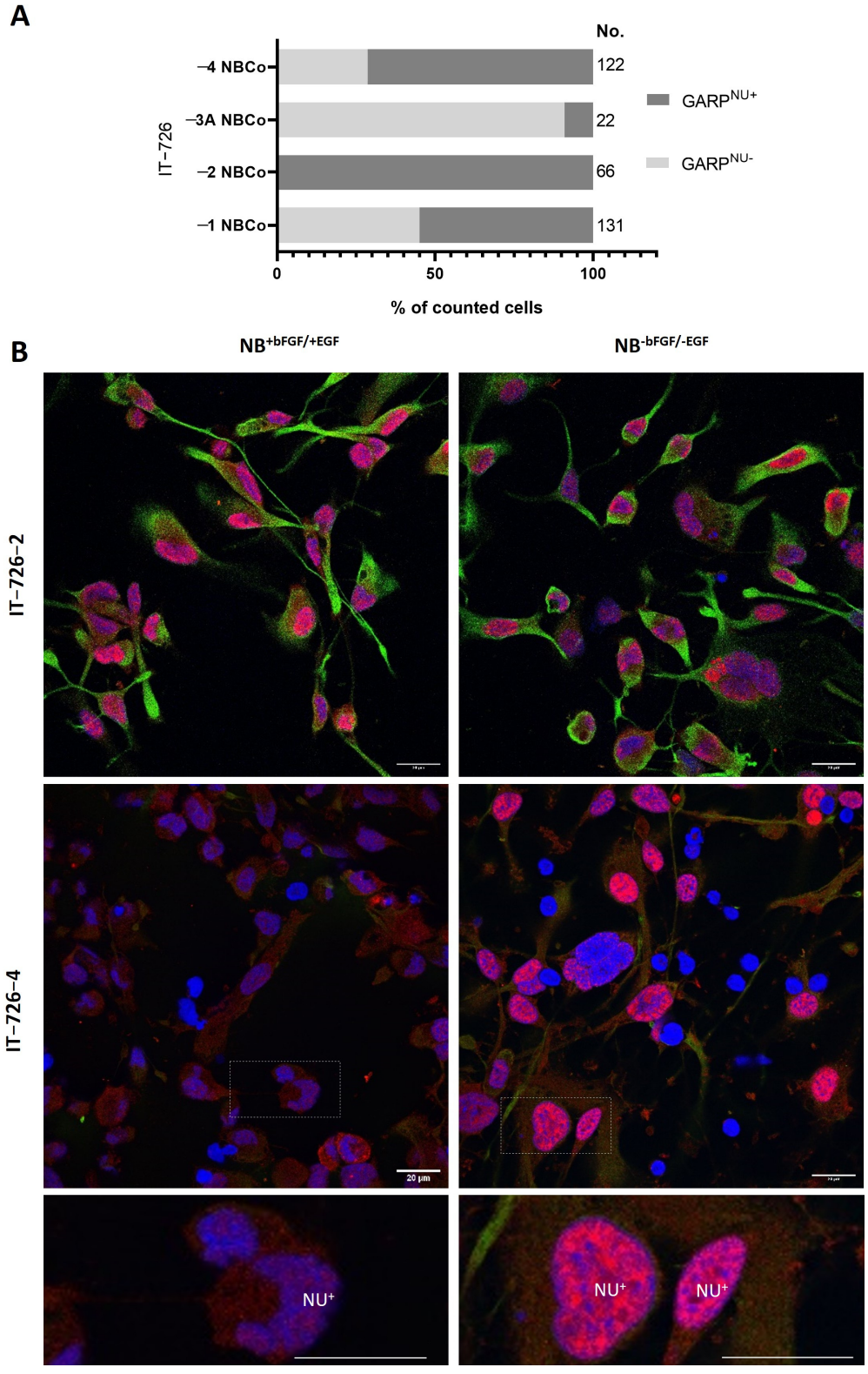

Figure 3. Analysis of expression and localization of GARP in isogenic GSC cell lines, which vary in differentiation states derived from different regions of the same tumor. (**A**) Number of GARP positive nuclei for GSC lines IT-726—1, -2, -3A, and -4 were analyzed by counting double positive (Hoechst and GARP) cell nuclei (NU^+). "No." indicates the number of counted cells for the analysis. (**B**) Confocal images of GARP- and nestin-expressing GSC IT-726 -2 and -4. Cells were stained for their nuclei with Hoechst (blue), GARP (red), and nestin (green). Note the intranuclear localization of GARP. Scale bar corresponds to 20 µm.

3.3. Relationship between GARP Expression and GSCs Stemness

The dual capacity of self-renewal and differentiation are the fundamental and unique properties of stem cells. We therefore sought to determine if there is an association between GARP expression and self-renewal. To this end, cell populations differing in GARP expression ($GARP^{high}$ or $GARP^{low}$) were FACS sorted from the GSC line #1095 and compared with respect to self-renewal activity by ELDA. A demonstration of the sorting efficacy and quantification of surface GARP expression on $GARP^{high}$ vs. $GARP^{low}$ sorted cells via flow cytometry can be found in Figure S6A. The GSC line #1095 was chosen for these investigations because of its well-established stemness attributes as well as molecular and cellular responses to clinically relevant treatments in vitro and in vivo [28,33–35]. The results of ELDA assessments revealed that $GARP^{high}$ and $GARP^{low}$ populations of GSCs differ in their self-renewal propensity, which was significantly ($p = 2.48 \times 10^{-16}$) lower in the $GARP^{high}$ subpopulation compared to $GARP^{low}$ subpopulation (Figure 4).

As loss of self-renewal is a prerequisite for stem cell differentiation, the outcome of the ELDA experiments raised the possibility that GARP expression may be related to differentiation of GSCs. To address this question, $GARP^{high}$ and $GARP^{low}$ GSCs were subjected to comparative assessments for the differentiation-inducing factor p21 and the differentiation-associated markers, GFAP and PDGFRα, activated during astrocyte or oligodendrocyte differentiation. The results showed that $GARP^{high}$ GSCs had considerably higher steady-state levels of p21 compared to $GARP^{low}$ GSCs, which seems consistent with the interpretation that increased expression of GARP is associated with a more differentiated state. However, an elevated level of p21 was unaccompanied by increased expression of GFAP or PDFGRα in $GARP^{high}$ GSCs. Quite the contrary, the expression of either GFAP or PDFGRα was found to be lower in $GARP^{high}$ GSCs than in $GARP^{low}$ GSCs (Figure 5) with the difference in PDGFRα levels being especially profound (Figure 5B). Although the difference in GFAP expression between $GARP^{high}$ and $GARP^{low}$ GSCs was less profound, it was also confirmed by using a different approach, namely the estimation of GFAP-positive differentiating cells by immunofluorescence staining (Figure S10). A decline in proliferative activity is an important functional hallmark of normal stem cell differentiation. Deviating from this rule, $GARP^{high}$ GSCs, which had a reduced self-renewal capacity in comparison to $GARP^{low}$ GSCs (Figure 4), had comparable levels of the proliferation marker PHH3 (Figure 5). Collectively, our data indicate that increased expression of GARP correlates with reduced self-renewal but not with the cessation of proliferation or induction of phenotypic traits of neural differentiation.

3.4. GARP mRNA and Surface Protein Levels Do Not Predict GB Patient Survival

Having established that GARP is expressed in patient-derived GSCs, we sought to determine whether a correlation exists between GARP expression and GB patient survival. To address this question, gene expression and survival data from the TCGA database were analyzed for GARP and CD133 by using OncoLnc.org (Figure S9—Cohort 1) [43–45]. Based on the TCGA dataset, consisting of 152 patients with newly diagnosed glioblastomas, all patients analyzed were stratified by their expression levels of GARP into either "GARP-high" (upper 50%) or "GARP-low" (lower 50%) groups and were analyzed for their survival rates via the online tool OncoLnc [43]. We could not find any significant difference in survival between GARP-high and GARP-low groups (Figure 6A). Similarly, no significant correlation was found between survival and CD133 expression (Figure 6A). In a second approach, GARP and CD133 transcript levels were compared between newly diagnosed glioblastomas (ndGB) and progressed recurrent glioblastomas (recGB) as depicted in Figure S9—Cohort 2—comparison line 2. To this end, we retroactively analyzed RNAseq data from a database that compiles RNAseq data for ndGBs (23 patients) or recGBs (21 patients) as well as 27 primary cultures derived from either ndGB (ndGB-GSCs, 17 cultures) or recGB (recGB-GSCs, 10 cultures) [34]. GARP and CD133 mRNA expression were compared between ndGB samples (ndGB tissues and ndGB-GSC cultures) and recGB samples (recGB tissues and recGB-GSCs). The results showed that expression levels of GARP do not differ

significantly between ndGB and recGB samples whereas CD133 levels were found to be significantly reduced in recGB samples compared to ndGB samples (Figure 6B). In a third approach, surface GARP expression was compared between isogenic ndGB-GSCs and recGB-GSCs isolated from ndGB and recGB tumors of the same patient (Figure S9—Cohort 2—comparison line 3). Both ndGB-GSCs and recGB-GSCs showed virtually the same levels of surface GARP expression, whereas the level of CD133 was significantly lower in recGB-GSCs in comparison to ndGB-GSCs (Figure 6C). This agreed with the results of the RNAseq analysis (Figure 6B) as both GARP transcript and surface GARP (Figure 6C) levels were consistently expressed regardless of disease progression. Interestingly, in contrast to GARP transcript and surface GARP levels, it was found that the percentage of GARP^{NU+} cells were elevated in the recurrent GSC line, IT-654 (Figure 6D).

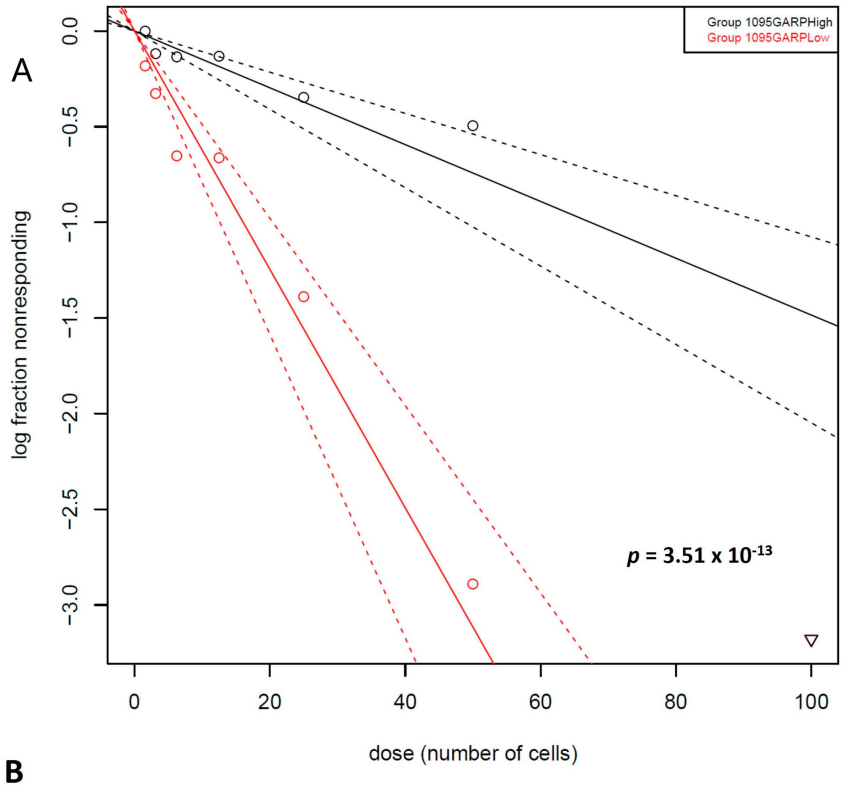

B

1095 subline	Stem cell frequency (1/SCF)			*p* value
	Lower	Estimated	Upper	
GARP^{High}	18.75	16.30	14.16	2.48×10^{-16}
GARP^{Low}	8.58	7.49	6.53	

Figure 4. Quantitative assessments of self-renewal capacity by extreme limiting dilution assay (ELDA). (**A**) Representative results. (**B**) The pooled results from three independent experiments are indicated in the table. GARP^{high} and GARP^{low} correspond to isogenic GSCs differing in their GARP expression, which were FACs sorted from the GSC line #1095. Estimates of the stem cell frequency (SCF) are framed in red, while lower and upper indicate the confidence intervals for 1/SCF. Statistical significance between groups was calculated by chi-squared tests.

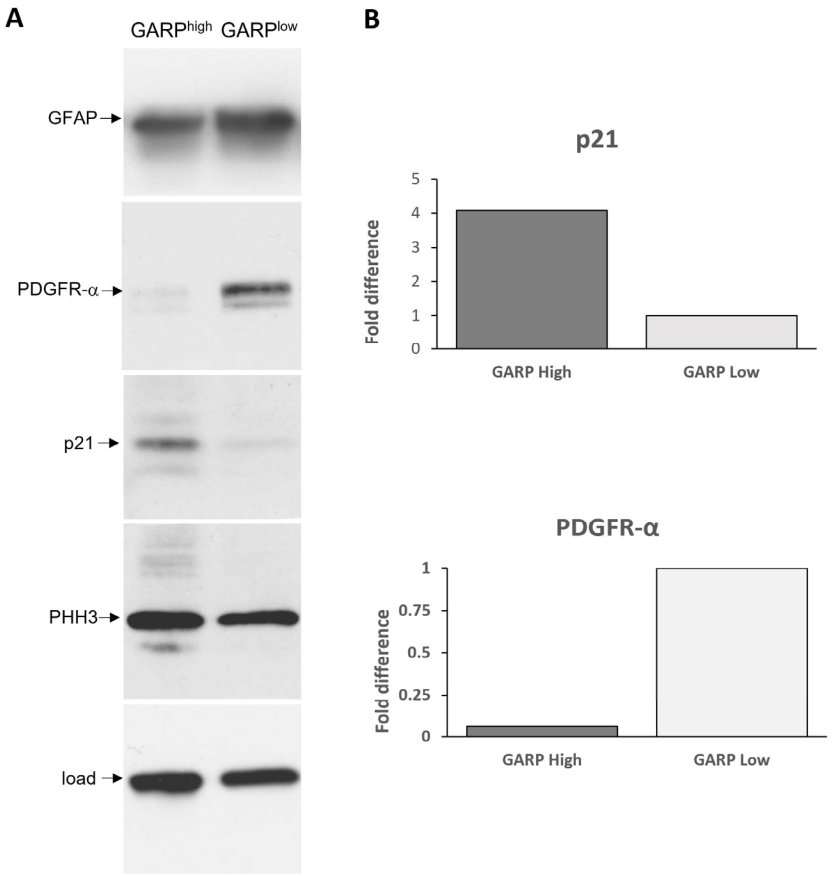

Figure 5. Comparative assessments of glial fibrillary acidic protein (GFAP), platelet-derived growth factor receptor alpha (PDGFR-α), p21, and phosphorylated histone H3 (PHH3) in FACs-sorted $GARP^{high}$ and $GARP^{low}$ isogenic GSCs (#1095) by Western blot. (**A**) Representative results. HSP70 was used as a loading control. The following antibodies were used to probe the membranes: anti-GFAP (DAKO, Z0334), anti-PDFGR-α (D13C6) (Cell Signaling, #5241T), anti-p21 (Cell Signaling, #2947), anti-phospho-histone H3 (Ser28) (Cell Signaling, #9713S), anti-HSP70 (Enzo Life Sciences Inc.), anti-mouse IgGκ light chain-binding protein horseradish peroxidase (Santa Cruz Biotechnology, sc-516102), and goat anti-rabbit IgG H&L horseradish peroxidase (Abcam, ab205718). (**B**) PDGFR-α and p21 bands were quantified by densitometry.

Collectively, these results obtained via different experimental approaches indicate that expression of GARP mRNA and surface protein remain at a constant level throughout GB progression and after therapy—in contrast to the fluctuating expression of CD133. This sustained expression of surface GARP and GARP transcript levels in ndGBs and recGBs suggests the potential utility of GARP as a reliable GSC biomarker, which persists at different tumor stages, possibly allowing for the detection of potential residual disease of a remarkably invasive cancer type.

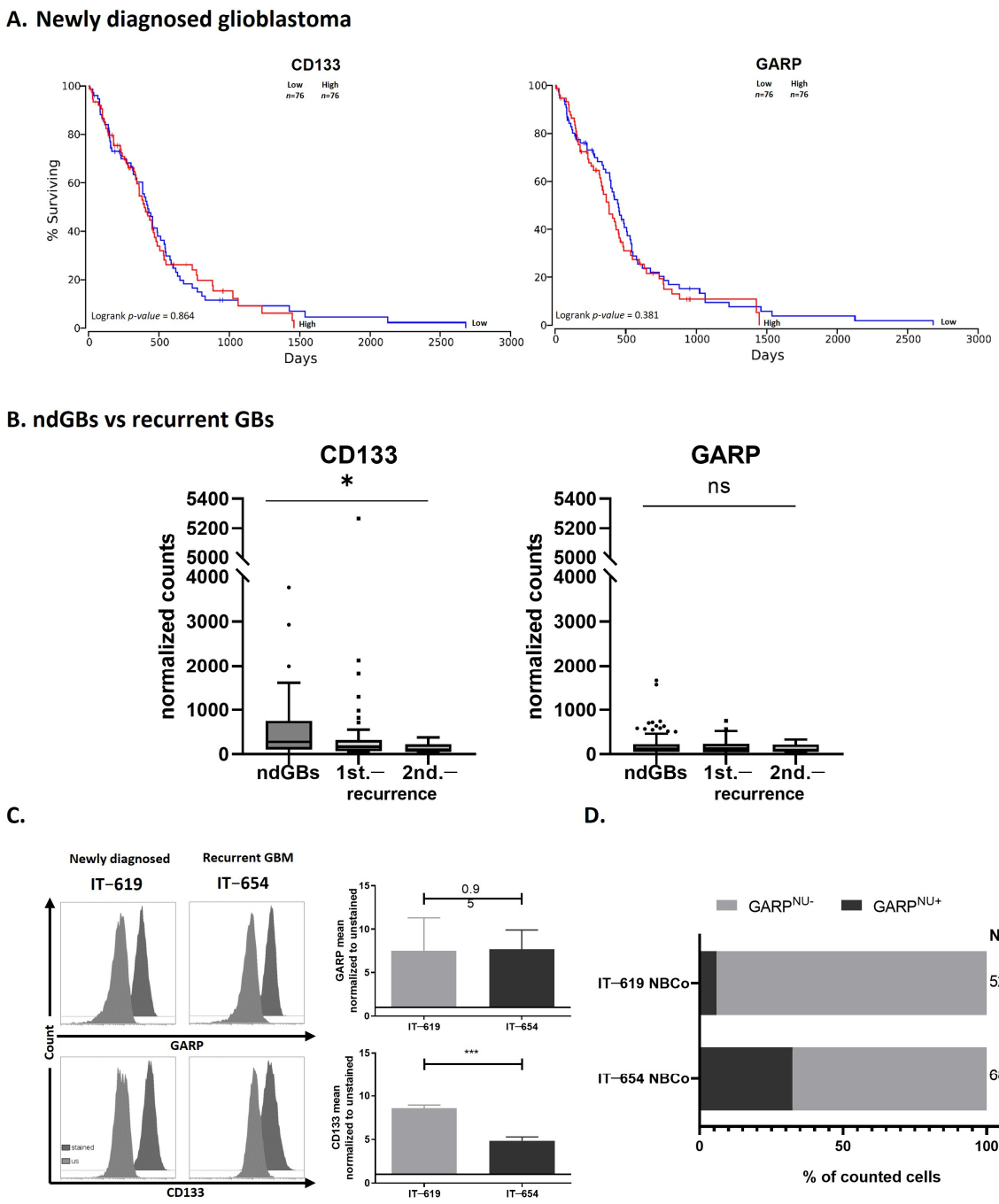

Figure 6. GARP expression in GB is unaffected throughout therapy. (**A**) Survival analysis of GARP and CD133 based on data available through The Cancer Genome Atlas (TCGA). GARP and CD133 mRNA expression data of 152 primary glioblastomas were divided 50/50 into either "low" expression or "high" expression and were analyzed for patient survival. (**B**) Retrospective analysis of transcriptomic data of 155 GB samples from 28 patients of Kim et al., 2020 [32]. ndGBs, first, and second recurrent tumors were analyzed for their GARP and CD133 mRNA levels across tumor stages. (**C**) Flow cytometric analysis of IT-619 and IT-654. Doublets, debris, and dead cells were excluded from analysis. Recurrent IT-654 GSCs exhibited stable surface GARP levels after TMZ and radiotherapy, whereas expression of CD133 decreased after treatment. The MFIs were normalized to the unstained control. $n = 3$. Significance was calculated by Student´s t-test and is indicated as follows: * $p < 0.05$, *** $p < 0.001$, and ns (not significant). (**D**) Number of GARP-positive nuclei for GSC IT-619 and IT-654 were analyzed by counting double-positive (Hoechst and GARP) cell nuclei. "No." indicates the number of counted cells for the analysis.

3.5. Nuclear Localization of GARP Correlates with Poor Survival in Patients with GB

As we observed an upregulation of the percentage of GARP^{NU+} cells in the recurrent GSC line, IT-654 (Figure 6D), we wanted to explore a possible link between GARP^{NU+} and the survival rate of GB patients (Figure S9—Cohort 3). Therefore, we retroactively assessed GARP^{NU+} levels in tumor tissue from a cohort of 35 newly diagnosed GB patients (WHO stage IV) and correlated them to patient overall survival (Figure 7, representative images) [7].

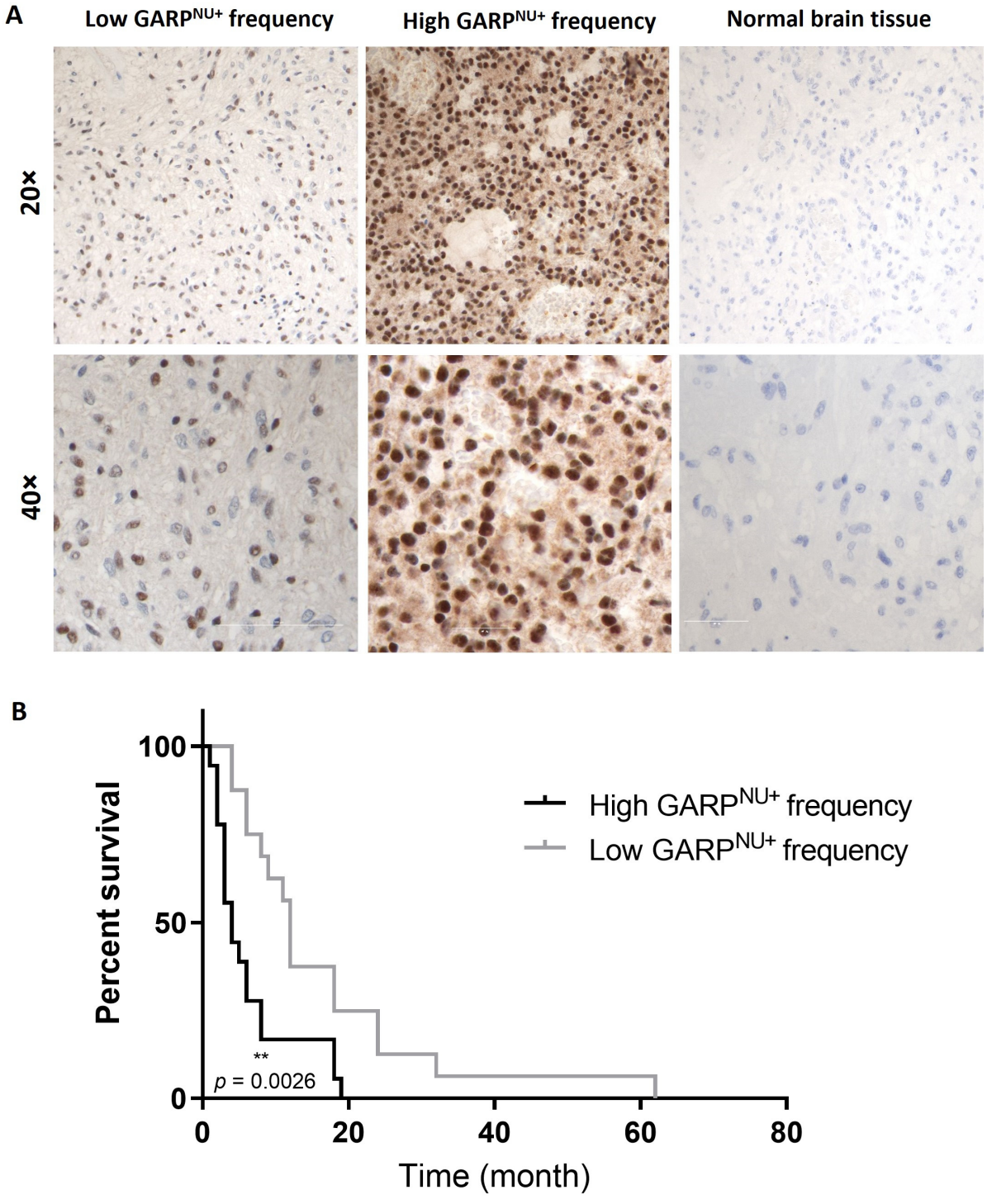

Figure 7. Nuclear GARP is a potential new prognostic biomarker for GB patient survival. (**A**) Immunohistochemistry of GARP in glioblastoma. GB (WHO grade IV) with low frequency of labeled

nuclei (magnification ×20 and ×40) and GB with palisading necroses and a high frequency of stained nuclei (magnification ×20 and ×40). Normal brain tissue had no detectable GARP expression. Bar corresponds to 50 µm (40×) and 200 µm (20×), respectively. (**B**) Survival analysis of 35 GB patients based on their GARP-positive nuclei counts (1: high frequency, n = 16 and 2: low frequency, n = 19). Comparison of survival curves was performed by log-rank (Mantel–Cox) test (** $p < 0.01$).

Notably, all GB patients in the cohort were found to express $GARP^{NU+}$ but varied in their frequency of $GARP^{NU+}$ cells. Therefore, we divided the cohort into two groups based on their frequency of $GARP^{NU+}$ expression. The first group encompassed 19 GB patients with tumors having a low frequency (~50%) of $GARP^{NU+}$ cells. The other group included 16 patients with a high frequency (>90%) of $GARP^{NU+}$ cells. In striking contrast with the transcriptomic analysis, which showed a consistent lack of correlation between GARP mRNA levels and patient survival (Figure 6A), stratification by $GARP^{NU+}$ revealed a significant correlation between $GARP^{NU+}$ and GB patient survival (Figure 7B). The results showed that patients with a low frequency of $GARP^{NU+}$ had a significantly longer overall survival in comparison to patients with a high frequency of $GARP^{NU+}$ (medians low: 12 months, high: 4 months; p = 0.0026, Figure 7B). These results indicate that the abundance of the GARP protein in the nuclear compartment—not GARP transcript levels—is associated with survival in patients with GB.

4. Discussion

GSCs comprise a heterogenous and highly volatile group of cells, which can switch between different phenotypes and molecular programs in response to environmental changes. The high degree of phenotypic plasticity displayed by GSCs poses a challenge in the development of GSC-based diagnostic and GSC-targeting therapeutic strategies. The continuing search for GSC-associated markers has led to the identification of several molecules expressed in some but not all subtypes of human GSCs or associated with some but not all cellular states [11,12]. One approach to counterbalance the phenotypic diversity of GSCs is to simultaneously target multiple markers associated with different types of GSCs, in order to increase the diagnostic coverage of the GSC content in a highly heterogeneous milieu of GBs [11,28,32,47,48]. An alternative possibility is that some phenotypic traits may be conserved across heterogeneous GSCs. Our data indicate that expression of GARP/ $GARP^{NU+}$ may be one such trait. We provide several lines of evidence that GARP/$GARP^{NU+}$ is expressed in otherwise phenotypically distinct GSCs (Figures 1 and 3) and persists invariably across different cellular states (Figure 3). In the past, several groups have tried to identify universal GSC markers. One challenge is that most of the previously identified putative markers of GSCs, e.g., CD133, are not universally expressed in all types of GSCs, which limits the diagnostic utility of such markers for estimating GSC content in tumors [26]. In this regard, both surface GARP and $GARP^{NU+}$ expression appear to be invariably expressed in phenotypically distinct GSCs including $CD133^{+}$ and $CD133^{-}$ subtypes, under in vitro and in vivo experimental conditions (Figures 1, 3 and S8) and in different stages of GB progression (ndGBs or recGBs) (Figure 6).

Our data indicate that GSC-associated expression of GARP persists in different cellular states. However, the degree of GARP expression varies between different cellular states. Interestingly, we find that expression of GARP is elevated in the state associated with a reduced self-renewal but not proliferative capacity and in conjunction with loss of differentiation-associated traits (Figures 4, 5 and S10). Such a pattern is reminiscent of the transit-amplifying state during neurogenesis whereby slow-cycling neural stem cells must first exit from the state of self-renewal and convert into more differentiated but uncommitted and fast-proliferating transit-amplifying progenitors, prior to entering the lineage-commitment stage and differentiation [49]. The simultaneous reduction in self-renewal and differentiation-associated traits without loss of the proliferation activity seen in $GARP^{high}$ GSCs suggests that GARP may have a role in GSCs' transition from the

slow-cycling self-renewal state to a more differentiated and proliferation-competent state similar to that of transit-amplifying progenitors. It should be noted that even the complete loss of self-renewal does not lead to a loss of the tumor-propagating capacity of GSCs, and recent evidence indicates that GB propagation is driven primarily not by self-renewing GSCs but their non-self-renewing progenies [50].

It is important to note that GARP expression is not limited to GSCs alone. Cancer cells, including glioblastoma (as shown in this work with T98G in Figure 1A), activated regulatory T cells and B cells, and platelets are all known to express GARP on their surfaces [28]. Therefore, GARP alone cannot be used to identify GSCs but rather in combination with a panel of other markers to better distinguish between GSCs and other GARP-positive cells in the tumor microenvironment. In this regard, our finding that elevated GARP expression coincides with a significant increase in p21 expression suggests that dual assessments for GARP and p21 may enable a distinguishment between GSC and non-GSC cells. Considering that p21 plays important roles in the maintenance of neural stem cells and is one of the factors implicated in GB radioresistance, the concomitant elevation of p21 and GARP in GSCs further supports the potential merits of GARP as a predictive and prognostic biomarker for GB [51,52]. A limitation of this exploratory work is that it mainly analyzed the expression of GARP in comparison to one GSC reference marker, CD133. Future studies are needed to analyze in depth the association of GARP expression with an expanded panel of putative GSC markers to further evaluate how universally and stably expressed GARP is on GSCs, and on different cellular components of the tumor microenvironment, especially those that are known to express GARP, like activated regulatory T cells and platelets.

Intriguingly, whereas GARP mRNA levels are comparable between ndGBs and recGBs, the level of $GARP^{NU+}$ protein correlated with poor survival in patients with GB (Figure 7). Notably, the critical cutoff for $GARP^{NU+}$ was >90% (Figure 7), which is significantly higher than the 10% cutoff for CD133 expression implicated as a predictive marker for GB recurrence [53].

Although the link between a high frequency of nuclear GARP and poor outcomes of GB patients provides a novel and intriguing insight into the previously unsuspected role of $GARP^{NU}$ in GB, it is important to also acknowledge the limitations of this exploratory study. One is the small patient cohort size (n = 35). The relationship between $GARP^{NU+}$ and clinical outcome from GB must be validated in future studies using larger datasets. A further confirmation in larger follow-up studies is a prerequisite for the conclusion on the diagnostic value of $GARP^{NU+}$ as a prognostic biomarker for GB.

Cancer stem cells are related to reduced survival in glioblastoma patients [11,12]. Therefore, it was surprising to see that a high frequency of $GARP^{NU+}$ tumor cells was linked to reduced overall survival, despite the observed upregulation of $GARP^{NU+}$ in differentiation-promoting conditions (NB-bFGF/-EGF) (Figure 3B). One possible explanation for this is that elevated GARP levels are linked to enhanced immunosuppression in the tumor microenvironment [7,39]. In more detail, previously, we demonstrated both in melanoma [39] and in glioblastoma [7] that tumor cells upregulate the expression of GARP and thus gain tolerogenic potential. This in turn aids in the suppression of effector $CD4^+$ and $CD8^+$ T cell function, required for anti-tumor immune responses, and correspondingly induces suppressive regulatory T cells, which further contribute to the suppression of effective anti-tumor immune responses. Furthermore, the upregulation of GARP, an inhibitory protein, upon the differentiation process of cancer stem cells is consistent with previous reports by Ullah et al., 2020, who similarly demonstrated that the immune checkpoints PD-L1 and HLA-G are upregulated by cancer stem cells upon differentiation [54]. The principal binding partner of GARP, TGF-β, has been shown to induce the expression of PD-L1, but it remains unclear if GARP expression can as well [55,56]. It is worth noting that the simultaneous targeting of GARP, TGF-β1, and PD-1 has been shown to be an effective combination therapy, capable of restoring T effector cell function and overcoming resistance to PD-1/PD-L1 blockade [57,58]. Future studies are planned to clarify the relationship

between GARP, PD-L1, and differentiation to determine if their contribution to immune suppression is responsible for the observed reduction in patient survival.

Interestingly, we found a discrepancy between RNAseq data from primary tumor tissue samples (Figure 6A) and our histological analysis of the frequency of $GARP^{NU+}$-positive cells in GB patient samples (Figure 7). Whereas no relationship between GARP transcript levels and patient survival was detectable in the TCGA data (Figure 6A), the frequency of $GARP^{NU+}$ GB cells seems to be a suitable prognostic marker for patient survival. It should be considered that the tissue samples used for TCGA RNAseq analysis (Figure 6A) presumably consisted of tumor lysates, which contain a multitude of cell types, ranging from tumor cells to immune cells, up to healthy tissue. As information on the cellular origin of the transcripts is missing due to the bulk sequencing, otherwise significant differences between donors can be diluted into insignificant results based on the individual composition and frequencies of cell types included in the analysis. In addition, GARP mRNA can be detected in many tissues, e.g., heart, kidney, liver, and lung, whereas surface expression of the GARP protein itself seems to be limited to only a number of cell types, e.g., activated regulatory T cells [59], platelets [60], various cancers like GB and malignant melanoma [7,39], and mesenchymal stem cells [61], further contributing to a decreasing validity. Therefore, the identification of the cell type analyzed in RNAseq is key to interpreting and understanding future datasets.

More advanced methods like spatial transcriptomics, multiplex immunofluorescence, and spatial multi-omics single-cell imaging are more fitting to further enhance our understanding of GARP transcript and protein levels in glioblastoma cells and their surrounding microenvironment, as well as their distribution within subcellular compartments [62]. The additional information gained by these techniques would enable the identification of different cell types, their localization within the tumor and relation to other cells of the tumor microenvironment, and the determination of whether a surface or intranuclear localization of the GARP protein is present in these cells. Furthermore, the exclusion of certain cell types (e.g., regulatory T cells or platelets) from the analysis would enable a better understanding of GARP and its subcellular localization on patient outcomes.

Our data suggest that nuclear localization of the GARP protein—rather than abundance of the GARP transcript—is a factor associated with GB progression after therapy. Our finding that GARP is localized to the nucleus is novel and intriguing, as GARP has previously been characterized only as a surface and secreted protein, which currently has no annotated nuclear localization signal (NLS). Interestingly, the use of nuclear localization of an otherwise surface-associated protein as a prognostic marker has been described before [63–65]. One such example is the protein Src, which plays a key role in cell morphology, motility, proliferation, and survival [66]. Urciuoli et al., 2017, was able to show in human osteosarcoma that nuclear localization of Src correlates with overall survival and therefore has relevance as a prognostic marker for osteosarcoma patients [64]. Likewise, it has also been described that PD-L1, a T cell inhibitory molecule in cancer, shows a nuclear localization as a reaction to therapy. In more detail, PD-L1 is translocated from the cell surface into the nucleus as a reaction to high-dose doxorubicin therapy regimens. The nuclear localization of PD-L1 was described as a prognostic biomarker, as patients with low PD-L1 nuclear expression had significantly fewer circulating cancer cells and exhibited a longer overall survival [63,65]. While the mechanisms of GARP nuclear localization in GSCs still have to be elucidated, the potential clinical implications of this previously unknown phenomenon are clear given the critical role of GARP in the activation of TGF-β, one of the key factors [67] contributing to GB progression particularly via the maintenance of GSCs via the induction of, e.g., Sox2 and LIF expression [68,69]. Considering that targeting TGF-β-activating ligands in GB has been intensively explored as a promising therapeutic strategy [67,70], the clarification of $GARP^{NU+}$ activities in GSCs may provide novel insights into the interaction of GARP and TGF-β, as TGF-β activation is known to trigger the nuclear localization of proteins like Smad and Smad4 [71]. Further pointing to the potential merit of GARP as a diagnostic and therapeutic target is the dual impact of GARP on cancer

progression—via the modulation of regulatory T cells and through the direct activities of GARP exerted on cancer (stem) cells themselves.

5. Conclusions

The scope of the present study was to evaluate GARP as a biomarker for heterogeneous GSCs and to determine the effects of GARP on GB patient outcomes. Based on our data, we propose that $GARP^{NU+}$ could potentially serve, in combination with existing GSC markers, as a universal and stably expressed marker for different subsets and cellular states of GSCs as well as a possible prognostic marker for patient outcomes in GB. We propose that GARP assessments may provide the means to identify not only self-renewing GSCs but also their progenies that exit from self-renewal but retain proliferative activity. Further validation of this hypothesis in future studies will require analyses of larger patient cohorts using an extended panel of markers associated with GSCs and GB progression. Future investigations should focus on addressing mechanistic questions, such as the functional significance of GARP in regulating GSC-specific functions, by employing knockdown and/or overexpressing lines, as well as further investigating the role of nuclear GARP, its nuclear retention, and functional relevance.

Supplementary Materials: The following supporting information can be downloaded at: https://www.mdpi.com/article/10.3390/cancers15245711/s1, Figure S1: Heterologous GSC lines differing in their self-renewal capacity, Figure S2: Anti-GARP antibody validation for flow cytometry, Figure S3: Specificity demonstration and validation of anti-GARP antibodies, Figure S4: Flow cytometric gating strategy for GSCs, Figure S5: Anti-GARP antibody validation for confocal microscopy, Figure S6: Flow cytometric gating strategy for $GARP^{high}$ and $GARP^{low}$ sorted GSCs, Figure S7: Invasive xenograft tumors arisen from GSC lines, #1051 and #1043, Figure S8: GARP is expressed in xenograft tumors arisen from GSC lines, #1051 and #1043, Figure S9: Study design and models used for the assessment of GARP, Figure S10: Frequency of $GFAP^{+}$ $GARP^{high}$ and $GARP^{low}$ GSCs.

Author Contributions: Conceptualization: N.Z., A.T., E.K., J.T., F.R., V.M. and C.S.; methodology: N.Z., E.R.T., A.M., P.L. (Philipp Licht), P.L. (Petra Leukel) and B.S.; validation: N.Z. and E.R.T.; formal analysis: N.Z., E.R.T., A.M. and P.L. (Philipp Licht); resources: A.T. and E.K.; writing—original draft: N.Z., E.R.T., A.T. and E.K.; writing—review and editing: all authors; visualization, N.Z.; project administration: N.Z.; supervision: A.T. and E.K.; funding acquisition: A.T. and E.K. All authors have read and agreed to the published version of the manuscript.

Funding: This research was funded by CRC1066, TP-B14 to A.T., Wilhelm-Sander-Foundation (2020.132.2) to A.T., and Hiege-Stiftung against skin cancer (200504) to A.T., a DAAD One-Year Research Grant for Doctoral Candidates (57552339) to E.R.T., and a FAZIT PhD Fellowship (090892021) to A.M.

Institutional Review Board Statement: The use of tumor tissue for research purposes was approved by the JG-UMC Institutional Review Board (permission 08.06.2017 #837.211.12(8312-F) and patients' informed consent. Animal experiments were performed in the Translational Animal Research Facility (TARC) of the JG-UMC, Germany, in accordance with the guidelines of the European Convention for the Protection of Vertebrates Used for Scientific Purposes and under the approval from the State Office of Chemical Investigations of Rhineland-Palatinate (permission #23 177-07/G12-1-020).

Informed Consent Statement: Written informed consent of all patients was obtained for "scientific use of tumor tissue not needed for histopathological diagnosis" in the admission contract of Idar-Oberstein hospital.

Data Availability Statement: Data are available in a publicly accessible repository that does not issue DOIs. Publicly available datasets were analyzed in this study. This data can be found here: https://www.ncbi.nlm.nih.gov/geo/query/acc.cgi?acc=GSE139533 and here: http://www.oncolnc.org/ (accessed on 9 April 2021).

Acknowledgments: We thank the Imaging Core Facility of the Cell Biology Unit (CBU) of Krishnaraj Rajalingam in the PKZI Mainz for providing the Leica SP8 microscope. We thank Kristian Schuetze, manager of the Flow Cytometry Core Facility (CFFC) of the PKZI Mainz, for his technical assistance in cell sorting. We thank the CFFC for providing the BD Aria II and III cell sorters.

Conflicts of Interest: The authors declare no conflict of interest.

References

1. Wen, P.Y.; Weller, M.; Lee, E.Q.; Alexander, B.M.; Barnholtz-Sloan, J.S.; Barthel, F.P.; Batchelor, T.T.; Bindra, R.S.; Chang, S.M.; Chiocca, E.A.; et al. Glioblastoma in adults: A Society for Neuro-Oncology (SNO) and European Society of Neuro-Oncology (EANO) consensus review on current management and future directions. *Neuro Oncol.* **2020**, *22*, 1073–1113. [CrossRef] [PubMed]
2. Louis, D.N.; Perry, A.; Reifenberger, G.; von Deimling, A.; Figarella-Branger, D.; Cavenee, W.K.; Ohgaki, H.; Wiestler, O.D.; Kleihues, P.; Ellison, D.W. The 2016 World Health Organization Classification of Tumors of the Central Nervous System: A summary. *Acta Neuropathol.* **2016**, *131*, 803–820. [CrossRef] [PubMed]
3. Stupp, R.; Mason, W.P.; van den Bent, M.J.; Weller, M.; Fisher, B.; Taphoorn, M.J.B.; Belanger, K.; Brandes, A.A.; Marosi, C.; Bogdahn, U.; et al. Radiotherapy plus concomitant and adjuvant temozolomide for glioblastoma. *N. Engl. J. Med.* **2005**, *352*, 987–996. [CrossRef] [PubMed]
4. Campos, B.; Olsen, L.R.; Urup, T.; Poulsen, H.S. A comprehensive profile of recurrent glioblastoma. *Oncogene* **2016**, *35*, 5819–5825. [CrossRef] [PubMed]
5. Gallego, O. Nonsurgical treatment of recurrent glioblastoma. *Curr. Oncol.* **2015**, *22*, e273–e281. [CrossRef] [PubMed]
6. Lim, M.; Xia, Y.; Bettegowda, C.; Weller, M. Current state of immunotherapy for glioblastoma. *Nat. Rev. Clin. Oncol.* **2018**, *15*, 422–442. [CrossRef] [PubMed]
7. Zimmer, N.; Kim, E.; Sprang, B.; Leukel, P.; Khafaji, F.; Ringel, F.; Sommer, C.; Tuettenberg, J.; Tuettenberg, A. GARP as an Immune Regulatory Molecule in the Tumor Microenvironment of Glioblastoma Multiforme. *Int. J. Mol. Sci.* **2019**, *20*, 3676. [CrossRef]
8. Cai, X.; Sughrue, M.E. Glioblastoma: New therapeutic strategies to address cellular and genomic complexity. *Oncotarget* **2018**, *9*, 9540–9554. [CrossRef]
9. Ghosh, D.; Nandi, S.; Bhattacharjee, S. Combination therapy to checkmate Glioblastoma: Clinical challenges and advances. *Clin. Transl. Med.* **2018**, *7*, 33. [CrossRef]
10. Bonavia, R.; Inda, M.-M.; Cavenee, W.K.; Furnari, F.B. Heterogeneity maintenance in glioblastoma: A social network. *Cancer Res.* **2011**, *71*, 4055–4060. [CrossRef]
11. Dirkse, A.; Golebiewska, A.; Buder, T.; Nazarov, P.V.; Muller, A.; Poovathingal, S.; Brons, N.H.C.; Leite, S.; Sauvageot, N.; Sarkisjan, D.; et al. Stem cell-associated heterogeneity in Glioblastoma results from intrinsic tumor plasticity shaped by the microenvironment. *Nat. Commun.* **2019**, *10*, 1787. [CrossRef] [PubMed]
12. Gimple, R.C.; Bhargava, S.; Dixit, D.; Rich, J.N. Glioblastoma stem cells: Lessons from the tumor hierarchy in a lethal cancer. *Genes Dev.* **2019**, *33*, 591–609. [CrossRef] [PubMed]
13. Kolenda, J.; Jensen, S.S.; Aaberg-Jessen, C.; Christensen, K.; Andersen, C.; Brünner, N.; Kristensen, B.W. Effects of hypoxia on expression of a panel of stem cell and chemoresistance markers in glioblastoma-derived spheroids. *J. Neurooncol.* **2011**, *103*, 43–58. [CrossRef] [PubMed]
14. Schiffer, D.; Mellai, M.; Annovazzi, L.; Caldera, V.; Piazzi, A.; Denysenko, T.; Melcarne, A. Stem cell niches in glioblastoma: A neuropathological view. *Biomed Res. Int.* **2014**, *2014*, 725921. [CrossRef] [PubMed]
15. Ivanov, V.N.; Hei, T.K. Induction of apoptotic death and retardation of neuronal differentiation of human neural stem cells by sodium arsenite treatment. *Exp. Cell Res.* **2013**, *319*, 875–887. [CrossRef] [PubMed]
16. Natsume, A.; Ito, M.; Katsushima, K.; Ohka, F.; Hatanaka, A.; Shinjo, K.; Sato, S.; Takahashi, S.; Ishikawa, Y.; Takeuchi, I.; et al. Chromatin regulator PRC2 is a key regulator of epigenetic plasticity in glioblastoma. *Cancer Res.* **2013**, *73*, 4559–4570. [CrossRef] [PubMed]
17. Lathia, J.D.; Mack, S.C.; Mulkearns-Hubert, E.E.; Valentim, C.L.L.; Rich, J.N. Cancer stem cells in glioblastoma. *Genes Dev.* **2015**, *29*, 1203–1217. [CrossRef] [PubMed]
18. Günther, H.S.; Schmidt, N.O.; Phillips, H.S.; Kemming, D.; Kharbanda, S.; Soriano, R.; Modrusan, Z.; Meissner, H.; Westphal, M.; Lamszus, K. Glioblastoma-derived stem cell-enriched cultures form distinct subgroups according to molecular and phenotypic criteria. *Oncogene* **2008**, *27*, 2897–2909. [CrossRef]
19. Chen, R.; Nishimura, M.C.; Bumbaca, S.M.; Kharbanda, S.; Forrest, W.F.; Kasman, I.M.; Greve, J.M.; Soriano, R.H.; Gilmour, L.L.; Rivers, C.S.; et al. A hierarchy of self-renewing tumor-initiating cell types in glioblastoma. *Cancer Cell* **2010**, *17*, 362–375. [CrossRef]
20. Singh, S.K.; Hawkins, C.; Clarke, I.D.; Squire, J.A.; Bayani, J.; Hide, T.; Henkelman, R.M.; Cusimano, M.D.; Dirks, P.B. Identification of human brain tumour initiating cells. *Nature* **2004**, *432*, 396–401. [CrossRef]
21. Lee, J.; Kotliarova, S.; Kotliarov, Y.; Li, A.; Su, Q.; Donin, N.M.; Pastorino, S.; Purow, B.W.; Christopher, N.; Zhang, W.; et al. Tumor stem cells derived from glioblastomas cultured in bFGF and EGF more closely mirror the phenotype and genotype of primary tumors than do serum-cultured cell lines. *Cancer Cell* **2006**, *9*, 391–403. [CrossRef] [PubMed]
22. Son, M.J.; Woolard, K.; Nam, D.-H.; Lee, J.; Fine, H.A. SSEA-1 is an enrichment marker for tumor-initiating cells in human glioblastoma. *Cell Stem Cell* **2009**, *4*, 440–452. [CrossRef]
23. Ludwig, K.; Kornblum, H.I. Molecular markers in glioma. *J. Neurooncol.* **2017**, *134*, 505–512. [CrossRef] [PubMed]
24. Beier, D.; Hau, P.; Proescholdt, M.; Lohmeier, A.; Wischhusen, J.; Oefner, P.J.; Aigner, L.; Brawanski, A.; Bogdahn, U.; Beier, C.P. CD133(+) and CD133(-) glioblastoma-derived cancer stem cells show differential growth characteristics and molecular profiles. *Cancer Res.* **2007**, *67*, 4010–4015. [CrossRef] [PubMed]

25. Ogden, A.T.; Waziri, A.E.; Lochhead, R.A.; Fusco, D.; Lopez, K.; Ellis, J.A.; Kang, J.; Assanah, M.; McKhann, G.M.; Sisti, M.B.; et al. Identification of A2B5+CD133- tumor-initiating cells in adult human gliomas. *Neurosurgery* **2008**, *62*, 505–514. [CrossRef]
26. Bao, S.; Wu, Q.; McLendon, R.E.; Hao, Y.; Shi, Q.; Hjelmeland, A.B.; Dewhirst, M.W.; Bigner, D.D.; Rich, J.N. Glioma stem cells promote radioresistance by preferential activation of the DNA damage response. *Nature* **2006**, *444*, 756–760. [CrossRef]
27. Tang, X.; Zuo, C.; Fang, P.; Liu, G.; Qiu, Y.; Huang, Y.; Tang, R. Targeting Glioblastoma Stem Cells: A Review on Biomarkers, Signal Pathways and Targeted Therapy. *Front. Oncol.* **2021**, *11*, 701291. [CrossRef]
28. Barrantes-Freer, A.; Renovanz, M.; Eich, M.; Braukmann, A.; Sprang, B.; Spirin, P.; Pardo, L.A.; Giese, A.; Kim, E.L. CD133 Expression Is Not Synonymous to Immunoreactivity for AC133 and Fluctuates throughout the Cell Cycle in Glioma Stem-Like Cells. *PLoS ONE* **2015**, *10*, e0130519. [CrossRef]
29. Bidlingmaier, S.; Zhu, X.; Liu, B. The utility and limitations of glycosylated human CD133 epitopes in defining cancer stem cells. *J. Mol. Med.* **2008**, *86*, 1025–1032. [CrossRef]
30. Zimmer, N.; Trzeciak, E.R.; Graefen, B.; Satoh, K.; Tuettenberg, A. GARP as a Therapeutic Target for the Modulation of Regulatory T Cells in Cancer and Autoimmunity. *Front. Immunol.* **2022**, *13*, 928450. [CrossRef]
31. Faußß, J.; Sprang, B.; Leukel, P.; Sommer, C.; Nikolova, T.; Ringel, F.; Kim, E.L. ALDH1A3 Segregated Expression and Nucleus-Associated Proteasomal Degradation Are Common Traits of Glioblastoma Stem Cells. *Biomedicines* **2021**, *10*, 7. [CrossRef] [PubMed]
32. Kim, E.L.; Sorokin, M.; Kantelhardt, S.R.; Kalasauskas, D.; Sprang, B.; Fauss, J.; Ringel, F.; Garazha, A.; Albert, E.; Gaifullin, N.; et al. Intratumoral Heterogeneity and Longitudinal Changes in Gene Expression Predict Differential Drug Sensitivity in Newly Diagnosed and Recurrent Glioblastoma. *Cancers* **2020**, *12*, 520. [CrossRef] [PubMed]
33. Barrantes-Freer, A.; Kim, E.; Bielanska, J.; Giese, A.; Mortensen, L.S.; Schulz-Schaeffer, W.J.; Stadelmann, C.; Brück, W.; Pardo, L.A. Human glioma-initiating cells show a distinct immature phenotype resembling but not identical to NG2 glia. *J. Neuropathol. Exp. Neurol.* **2013**, *72*, 307–324. [CrossRef] [PubMed]
34. Kalasauskas, D.; Sorokin, M.; Sprang, B.; Elmasri, A.; Viehweg, S.; Salinas, G.; Opitz, L.; Rave-Fraenk, M.; Schulz-Schaeffer, W.; Kantelhardt, S.R.; et al. Diversity of Clinically Relevant Outcomes Resulting from Hypofractionated Radiation in Human Glioma Stem Cells Mirrors Distinct Patterns of Transcriptomic Changes. *Cancers* **2020**, *12*, 570. [CrossRef]
35. Müller, A.; Weyerhäuser, P.; Berte, N.; Jonin, F.; Lyubarskyy, B.; Sprang, B.; Kantelhardt, S.R.; Salinas, G.; Opitz, L.; Schulz-Schaeffer, W.; et al. Concurrent Activation of Both Survival-Promoting and Death-Inducing Signaling by Chloroquine in Glioblastoma Stem Cells: Implications for Potential Risks and Benefits of Using Chloroquine as Radiosensitizer. *Cells* **2023**, *12*, 1290. [CrossRef] [PubMed]
36. Schneider, C.A.; Rasband, W.S.; Eliceiri, K.W. NIH Image to ImageJ: 25 years of image analysis. *Nat. Methods* **2012**, *9*, 671–675. [CrossRef] [PubMed]
37. Kotecha, N.; Krutzik, P.O.; Irish, J.M. Web-based analysis and publication of flow cytometry experiments. *Curr. Protoc. Cytom.* **2010**, *53*, 10–17. [CrossRef]
38. Kim, E.L.; Wüstenberg, R.; Rübsam, A.; Schmitz-Salue, C.; Warnecke, G.; Bücker, E.-M.; Pettkus, N.; Speidel, D.; Rohde, V.; Schulz-Schaeffer, W.; et al. Chloroquine activates the p53 pathway and induces apoptosis in human glioma cells. *Neuro Oncol.* **2010**, *12*, 389–400. [CrossRef]
39. Hahn, S.A.; Neuhoff, A.; Landsberg, J.; Schupp, J.; Eberts, D.; Leukel, P.; Bros, M.; Weilbaecher, M.; Schuppan, D.; Grabbe, S.; et al. A key role of GARP in the immune suppressive tumor microenvironment. *Oncotarget* **2016**, *7*, 42996–43009. [CrossRef]
40. Schindelin, J.; Arganda-Carreras, I.; Frise, E.; Kaynig, V.; Longair, M.; Pietzsch, T.; Preibisch, S.; Rueden, C.; Saalfeld, S.; Schmid, B.; et al. Fiji: An open-source platform for biological-image analysis. *Nat. Methods* **2012**, *9*, 676–682. [CrossRef]
41. Hu, Y.; Smyth, G.K. ELDA: Extreme limiting dilution analysis for comparing depleted and enriched populations in stem cell and other assays. *J. Immunol. Methods* **2009**, *347*, 70–78. [CrossRef]
42. Love, M.I.; Huber, W.; Anders, S. Moderated estimation of fold change and dispersion for RNA-seq data with DESeq2. *Genome Biol.* **2014**, *15*, 550. [CrossRef] [PubMed]
43. Anaya, J. OncoLnc: Linking TCGA survival data to mRNAs, miRNAs, and lncRNAs. *PeerJ Comput. Sci.* **2016**, *2*, e67. [CrossRef]
44. Brat, D.J.; Verhaak, R.G.W.; Aldape, K.D.; Yung, W.K.A.; Salama, S.R.; Cooper, L.A.D.; Rheinbay, E.; Miller, C.R.; Vitucci, M.; Morozova, O.; et al. Comprehensive, Integrative Genomic Analysis of Diffuse Lower-Grade Gliomas. *N. Engl. J. Med.* **2015**, *372*, 2481–2498. [CrossRef] [PubMed]
45. Ciriello, G.; Miller, M.L.; Aksoy, B.A.; Senbabaoglu, Y.; Schultz, N.; Sander, C. Emerging landscape of oncogenic signatures across human cancers. *Nat. Genet.* **2013**, *45*, 1127–1133. [CrossRef] [PubMed]
46. Bradshaw, A.; Wickremsekera, A.; Tan, S.T.; Peng, L.; Davis, P.F.; Itinteang, T. Cancer Stem Cell Hierarchy in Glioblastoma Multiforme. *Front. Surg.* **2016**, *3*, 21. [CrossRef] [PubMed]
47. Lan, X.; Jörg, D.J.; Cavalli, F.M.G.; Richards, L.M.; Nguyen, L.V.; Vanner, R.J.; Guilhamon, P.; Lee, L.; Kushida, M.M.; Pellacani, D.; et al. Fate mapping of human glioblastoma reveals an invariant stem cell hierarchy. *Nature* **2017**, *549*, 227–232. [CrossRef] [PubMed]
48. Silver, A.; Feier, D.; Ghosh, T.; Rahman, M.; Huang, J.; Sarkisian, M.R.; Deleyrolle, L.P. Heterogeneity of glioblastoma stem cells in the context of the immune microenvironment and geospatial organization. *Front. Oncol.* **2022**, *12*, 1022716. [CrossRef]
49. Miyashita, S.; Hoshino, M. Transit Amplifying Progenitors in the Cerebellum: Similarities to and Differences from Transit Amplifying Cells in Other Brain Regions and between Species. *Cells* **2022**, *11*, 726. [CrossRef]

50. Barrett, L.E.; Granot, Z.; Coker, C.; Iavarone, A.; Hambardzumyan, D.; Holland, E.C.; Nam, H.; Benezra, R. Self-renewal does not predict tumor growth potential in mouse models of high-grade glioma. *Cancer Cell* **2012**, *21*, 11–24. [CrossRef]
51. Jin, X.; Kuang, Y.; Li, L.; Li, H.; Zhao, T.; He, Y.; Di, C.; Kang, J.; Yuan, L.; Yu, B.; et al. A positive feedback circuit comprising p21 and HIF-1α aggravates hypoxia-induced radioresistance of glioblastoma by promoting Glut1/LDHA-mediated glycolysis. *FASEB J.* **2022**, *36*, e22229. [CrossRef] [PubMed]
52. Marqués-Torrejón, M.Á.; Porlan, E.; Banito, A.; Gómez-Ibarlucea, E.; Lopez-Contreras, A.J.; Fernández-Capetillo, O.; Vidal, A.; Gil, J.; Torres, J.; Fariñas, I. Cyclin-dependent kinase inhibitor p21 controls adult neural stem cell expansion by regulating Sox2 gene expression. *Cell Stem Cell* **2013**, *12*, 88–100. [CrossRef] [PubMed]
53. Abdoli Shadbad, M.; Hosseinkhani, N.; Asadzadeh, Z.; Brunetti, O.; Silvestris, N.; Baradaran, B. The Prognostic Value of CD133 in Predicting the Relapse and Recurrence Pattern of High-Grade Gliomas on MRI: A Meta-Analysis. *Front. Oncol.* **2021**, *11*, 722833. [CrossRef] [PubMed]
54. Ullah, M.; Meziani, S.; Shah, S.; Kaci, R.; Pimpie, C.; Pocard, M.; Mirshahi, M. Differentiation of cancer cells upregulates HLA-G and PD-L1. *Oncol. Rep.* **2020**, *43*, 1797–1804. [CrossRef] [PubMed]
55. Ni, X.Y.; Sui, H.X.; Liu, Y.; Ke, S.Z.; Wang, Y.N.; Gao, F.G. TGF-β of lung cancer microenvironment upregulates B7H1 and GITRL expression in dendritic cells and is associated with regulatory T cell generation. *Oncol. Rep.* **2012**, *28*, 615–621. [CrossRef] [PubMed]
56. Song, S.; Yuan, P.; Wu, H.; Chen, J.; Fu, J.; Li, P.; Lu, J.; Wei, W. Dendritic cells with an increased PD-L1 by TGF-β induce T cell anergy for the cytotoxicity of hepatocellular carcinoma cells. *Int. Immunopharmacol.* **2014**, *20*, 117–123. [CrossRef] [PubMed]
57. De Streel, G.; Bertrand, C.; Chalon, N.; Liénart, S.; Bricard, O.; Lecomte, S.; Devreux, J.; Gaignage, M.; de Boeck, G.; Mariën, L.; et al. Selective inhibition of TGF-β1 produced by GARP-expressing Tregs overcomes resistance to PD-1/PD-L1 blockade in cancer. *Nat. Commun.* **2020**, *11*, 4545. [CrossRef]
58. Bertrand, C.; van Meerbeeck, P.; de Streel, G.; Vaherto-Bleeckx, N.; Benhaddi, F.; Rouaud, L.; Noël, A.; Coulie, P.G.; van Baren, N.; Lucas, S. Combined Blockade of GARP:TGF-β1 and PD-1 Increases Infiltration of T Cells and Density of Pericyte-Covered GARP+ Blood Vessels in Mouse MC38 Tumors. *Front. Immunol.* **2021**, *12*, 704050. [CrossRef]
59. Hahn, S.A.; Stahl, H.F.; Becker, C.; Correll, A.; Schneider, F.-J.; Tuettenberg, A.; Jonuleit, H. Soluble GARP has potent antiinflammatory and immunomodulatory impact on human $CD4^+$ T cells. *Blood* **2013**, *122*, 1182–1191. [CrossRef]
60. Zimmer, N.; Krebs, F.K.; Zimmer, S.; Mitzel-Rink, H.; Kumm, E.J.; Jurk, K.; Grabbe, S.; Loquai, C.; Tuettenberg, A. Platelet-Derived GARP Induces Peripheral Regulatory T Cells-Potential Impact on T Cell Suppression in Patients with Melanoma-Associated Thrombocytosis. *Cancers* **2020**, *12*, 3653. [CrossRef]
61. Xing, H.; Liang, C.; Xu, X.; Sun, H.; Ma, X.; Jiang, Z. Mesenchymal stroma/stem-like cells of GARP knockdown inhibits cell proliferation and invasion of mouse colon cancer cells (MC38) through exosomes. *J. Cell. Mol. Med.* **2020**, *24*, 13984–13990. [CrossRef]
62. Asp, M.; Bergenstråhle, J.; Lundeberg, J. Spatially Resolved Transcriptomes-Next Generation Tools for Tissue Exploration. *Bioessays* **2020**, *42*, e1900221. [CrossRef] [PubMed]
63. Ghebeh, H.; Lehe, C.; Barhoush, E.; Al-Romaih, K.; Tulbah, A.; Al-Alwan, M.; Hendrayani, S.-F.; Manogaran, P.; Alaiya, A.; Al-Tweigeri, T.; et al. Doxorubicin downregulates cell surface B7-H1 expression and upregulates its nuclear expression in breast cancer cells: Role of B7-H1 as an anti-apoptotic molecule. *Breast Cancer Res.* **2010**, *12*, R48. [CrossRef]
64. Urciuoli, E.; Coletta, I.; Rizzuto, E.; de Vito, R.; Petrini, S.; D'Oria, V.; Pezzullo, M.; Milano, G.M.; Cozza, R.; Locatelli, F.; et al. Src nuclear localization and its prognostic relevance in human osteosarcoma. *J. Cell. Physiol.* **2018**, *233*, 1658–1670. [CrossRef] [PubMed]
65. Satelli, A.; Batth, I.S.; Brownlee, Z.; Rojas, C.; Meng, Q.H.; Kopetz, S.; Li, S. Potential role of nuclear PD-L1 expression in cell-surface vimentin positive circulating tumor cells as a prognostic marker in cancer patients. *Sci. Rep.* **2016**, *6*, 28910. [CrossRef] [PubMed]
66. Roskoski, R. Src protein-tyrosine kinase structure and regulation. *Biochem. Biophys. Res. Commun.* **2004**, *324*, 1155–1164. [CrossRef] [PubMed]
67. Han, J.; Alvarez-Breckenridge, C.A.; Wang, Q.-E.; Yu, J. TGF-β signaling and its targeting for glioma treatment. *Am. J. Cancer Res.* **2015**, *5*, 945–955. [PubMed]
68. Ikushima, H.; Todo, T.; Ino, Y.; Takahashi, M.; Miyazawa, K.; Miyazono, K. Autocrine TGF-beta signaling maintains tumorigenicity of glioma-initiating cells through Sry-related HMG-box factors. *Cell Stem Cell* **2009**, *5*, 504–514. [CrossRef]
69. Peñuelas, S.; Anido, J.; Prieto-Sánchez, R.M.; Folch, G.; Barba, I.; Cuartas, I.; García-Dorado, D.; Poca, M.A.; Sahuquillo, J.; Baselga, J.; et al. TGF-beta increases glioma-initiating cell self-renewal through the induction of LIF in human glioblastoma. *Cancer Cell* **2009**, *15*, 315–327. [CrossRef]
70. Shaim, H.; Shanley, M.; Basar, R.; Daher, M.; Gumin, J.; Zamler, D.B.; Uprety, N.; Wang, F.; Huang, Y.; Gabrusiewicz, K.; et al. Targeting the αv integrin/TGF-β axis improves natural killer cell function against glioblastoma stem cells. *J. Clin. Investig.* **2021**, *131*, e142116. [CrossRef]
71. Golestaneh, N.; Mishra, B. TGF-beta, neuronal stem cells and glioblastoma. *Oncogene* **2005**, *24*, 5722–5730. [CrossRef]

A

line	origin	SCF	predominant phenotype	CD133, %	ref
#1051	ndGB	1/3	Nestin$^+$/GFAP$^-$	<1	Barrantes-Freer 2013[29], 2015[26]
#1063	ndGB	1/4	Nestin$^+$/GFAP$^-$	2.4	Barrantes-Freer 2013[29]
#1095	ndGB	1/4	Nestin$^+$/GFAP$^-$	<1	Barrantes-Freer 2013[29], 2015[26]
#1043	ndGB	1/3	Nestin$^+$/GFAP$^+$	<15	this study
IT-726-1	ndGB	1/8	Nestin$^+$/GFAP$^+$	<80	this study
IT-726-2	ndGB	1/30	Nestin$^+$/GFAP$^+$	<1	this study
IT-726-3A	ndGB	1/25	Nestin$^+$/GFAP$^+$	<5	this study
IT-726-3B	ndGB	1/3	Nestin$^+$/GFAP$^+$	<7	this study
IT-726-4	ndGB	1/59	Nestin$^+$/GFAP$^+$	<3	this study
IT-619	ndGB	1/15	Nestin$^+$/GFAP$^+$	>90	this study
IT-654	recGB	1/80	Nestin$^+$/GFAP$^+$	<70	this study

SCF, stem cell frequency

B

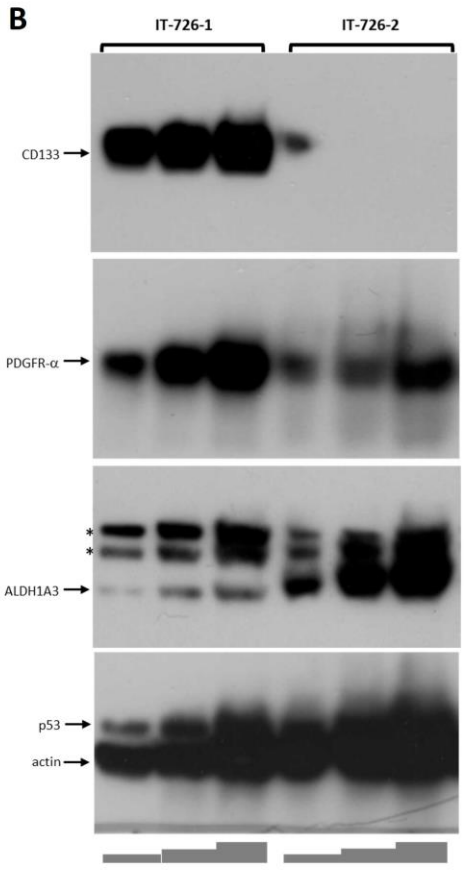

*, unspecific bands

Fig. S1: Heterologous GSC lines differing in their self-renewal capacity. Previous characterization of the heterologous patient derived GSC lines used in this work (A,B) [28,31-33]. Considerable variation in the expression of several GSC markers, including glial fibrillary acidic protein (GFAP), CD133, platelet-derived growth factor receptor alpha (PDGFR-α), and aldehyde dehydrogenase 1 family member A3 (ALDH1A3), was observed in both heterologous and isogenic GSC lines. (B) Example analysis of several GSC markers, including CD133, PDGFR-α, and ALDH1A3, in the isogenic GSC lines, IT-726-1 and IT-726-2 (GSC lines featured in Fig. S1A indicated by red arrows), via western blot using the following antibodies: anti-CD133/1 (clone: W6B3C1), anti-PDFGR-α (D13C6) (Cell Signaling, #5341), anti-ALDH1A3 (Thermo Fischer Scientific, MA5-25528), anti-p53 (DO-1) (Cell Signaling, #18032), anti-actin (C4) (Santa Cruz Biotechnology, sc-47778), goat anti-mouse IgG horseradish peroxidase (Santa Cruz Biotechnology, sc-2055), goat anti-rabbit horseradish peroxidase (Santa Cruz Biotechnology, sc-2054) (B). Cell lysates were loaded in increasing volumes, and actin was used as a loading control.

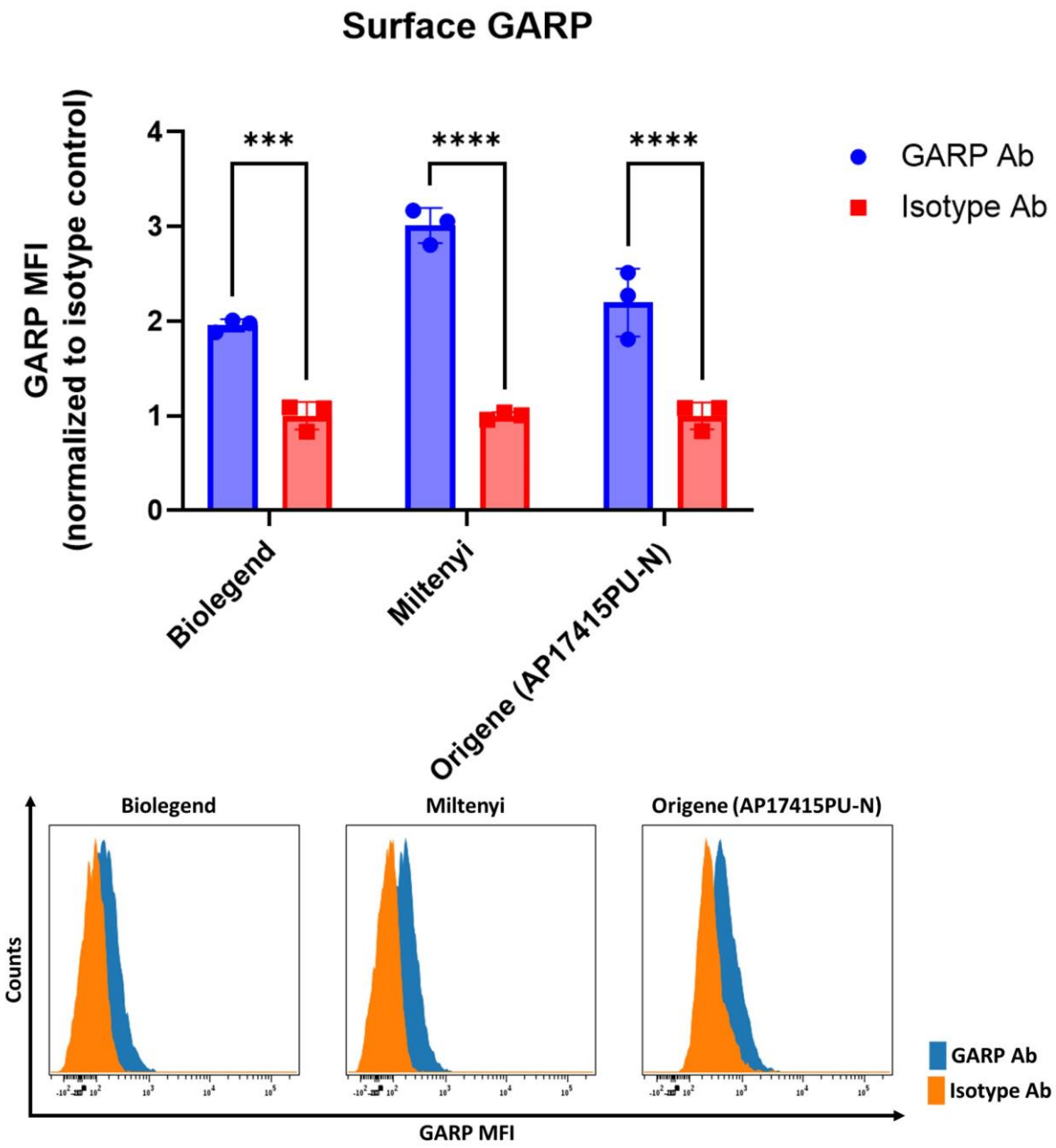

Figure S2: Anti-GARP antibody validation for flow cytometry. Comparative flow cytometric analysis of surface GARP levels on a control human melanoma cell line, Mewo, using three different human anti-GARP antibodies. The following antibodies were analyzed: Miltenyi (130-103-890), Biolegend (352502), Origene (AP17415PU-N). Doublets, debris, and dead cells were excluded from the analysis. Graph shows the mean fluorescence intensity (MFI) normalized to the MFI of the respective isotype control, whereas histograms display one representative result (n=3, ± SD, *** $p < 0.001$, and **** $p < 0.0001$ determined by two-way ANOVA).

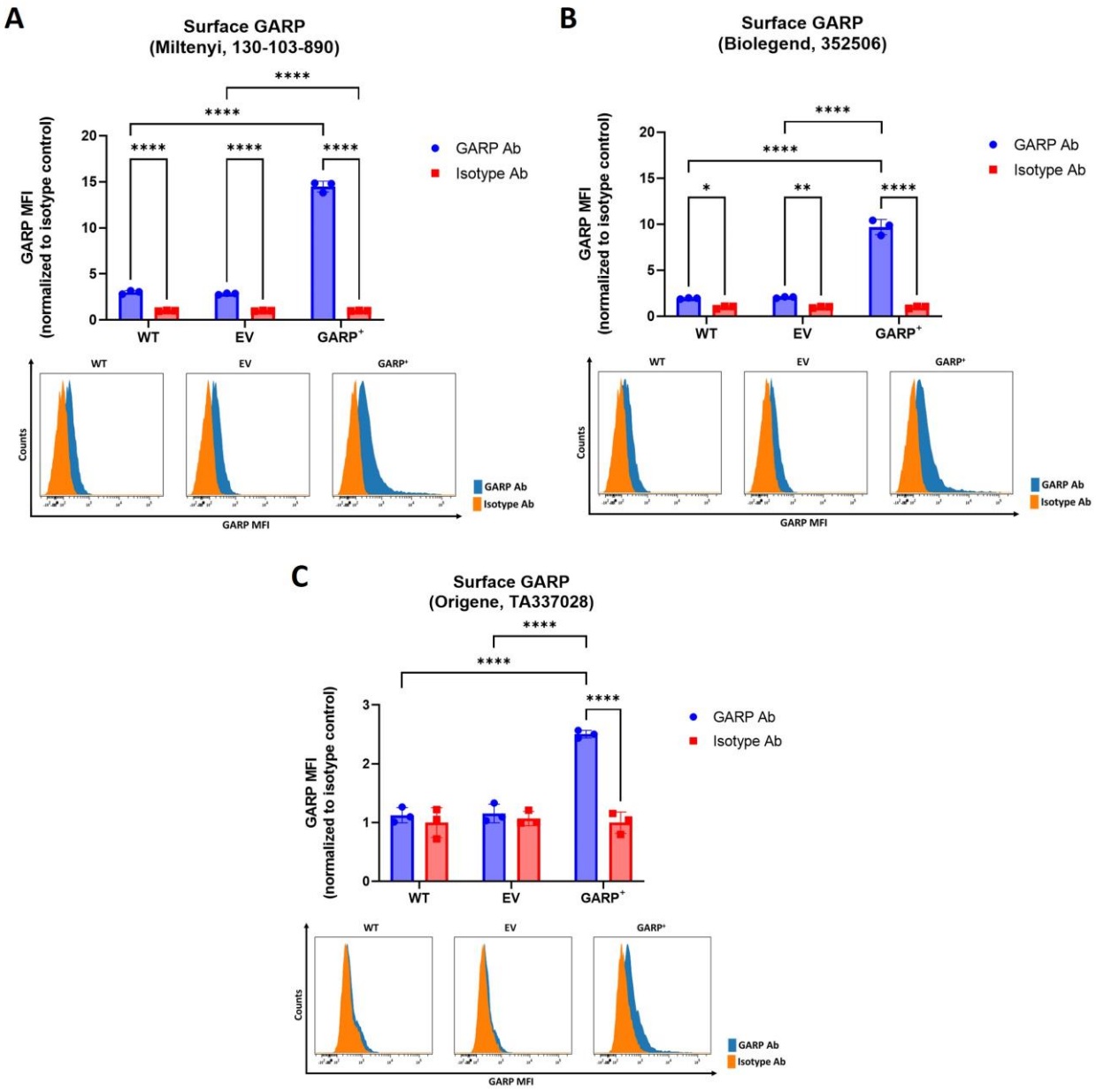

Figure S3: Specificity demonstration and validation of anti-GARP antibodies. Comparative flow cytometric analysis of surface GARP levels on wildtype (WT) and transfected (GARP overexpression (GARP$^+$), empty vector control (EV)) Mewo cells using three different human anti-GARP antibodies. The following antibodies were analyzed: Miltenyi (130-103-890) (A), Biolegend (352502) (B), Origene (TA337028) (C). Doublets, debris, and dead cells were excluded from the analysis. Graph shows the mean fluorescence intensity (MFI) normalized to the MFI of the respective isotype control, whereas histograms display one representative result (n=3, ± SD, * $p < 0.05$, ** $p < 0.01$, and **** $p < 0.0001$ determined by two-way ANOVA).

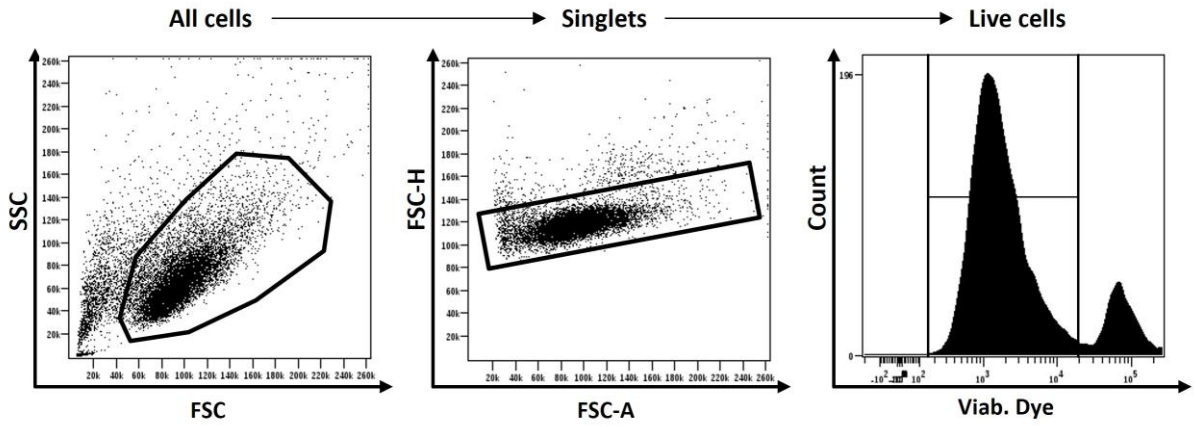

Figure S4: Flow cytometric gating strategy for GSCs. Representative flow cytometric gating strategies used for GSCs. Debris, doublets, and dead cells were excluded from analysis.

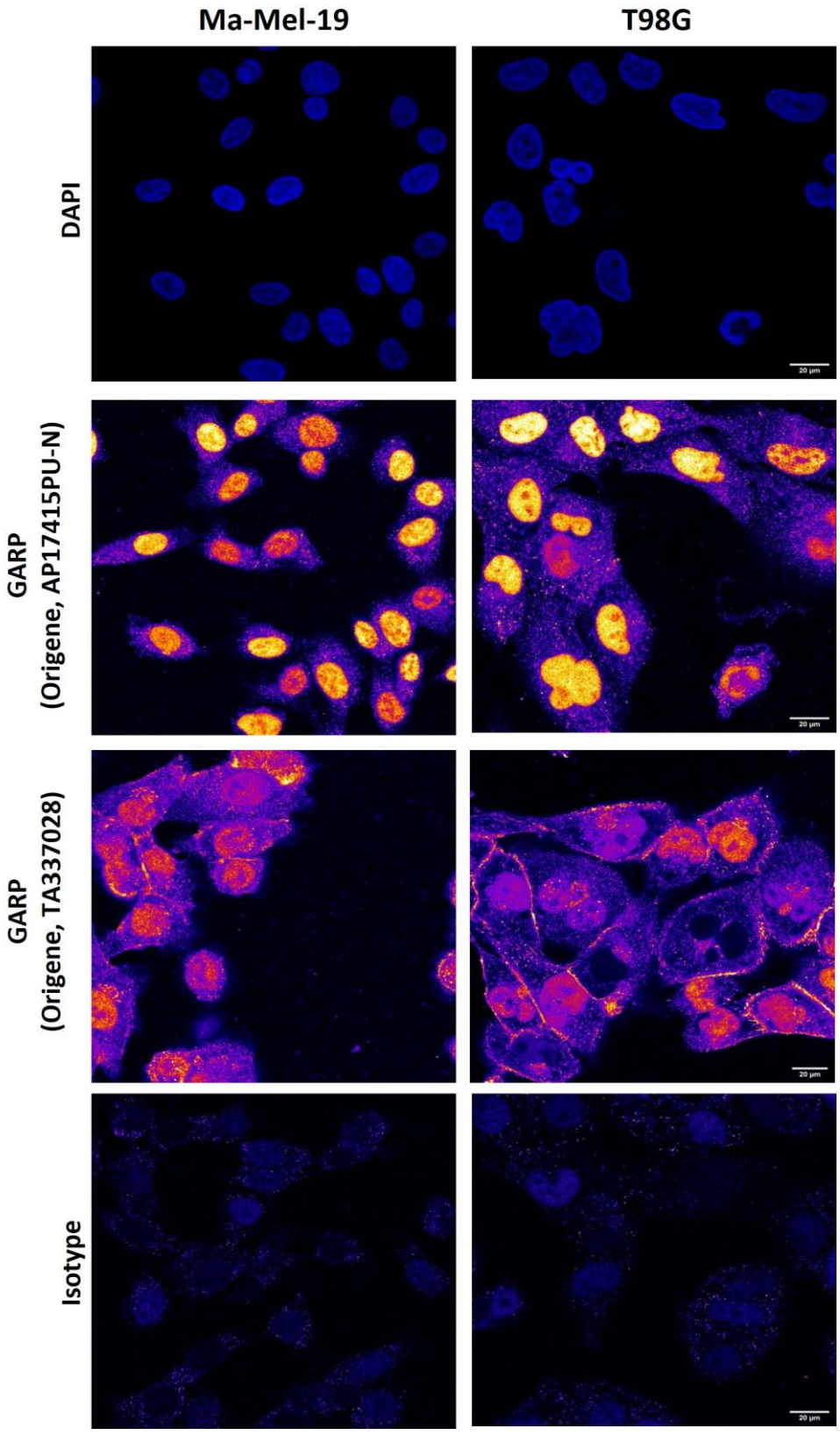

Figure S5: Anti-GARP antibody validation for confocal microscopy. Confocal images of the human GARP expressing cell lines, Ma-Mel-19 and T98G. Cells were stained for GARP using two different antibodies (Origene, AP17415PU-N; Origene, TA337028) as seen in orange. Cells were counterstained for their nuclei with Hoechst (blue). Note the intranuclear localization of GARP ($GARP^{NU+}$) detectable with both antibodies. Scale bar corresponds to 20 µm.

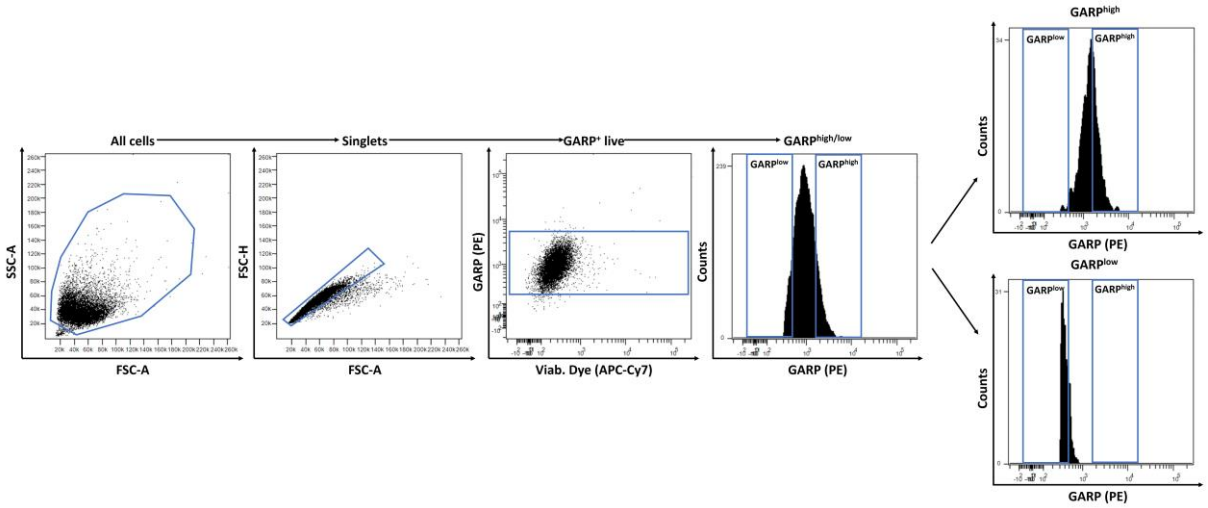

Figure S6: Flow cytometric gating strategy for GARP^{high} and GARP^{low} sorted GSCs. (A) Representative flow cytometric gating strategy used for sorting GARP^{high} and GARP^{low} GSCs. Sorted cells were re-measured via flow cytometry to confirm sorting efficacy. (B) Example GARP staining of GSCs (mean fluorescence intensity shown) compared to its respective isotype and unstained controls. Debris, doublets, and dead cells were excluded from analysis.

#1051

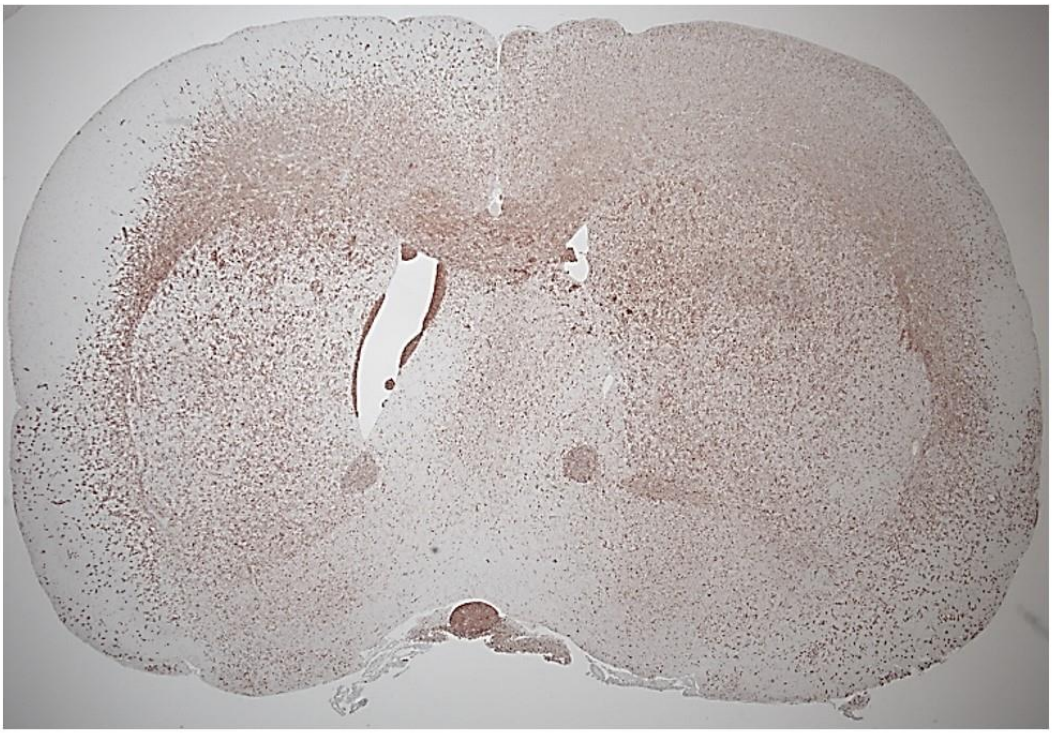

#1043

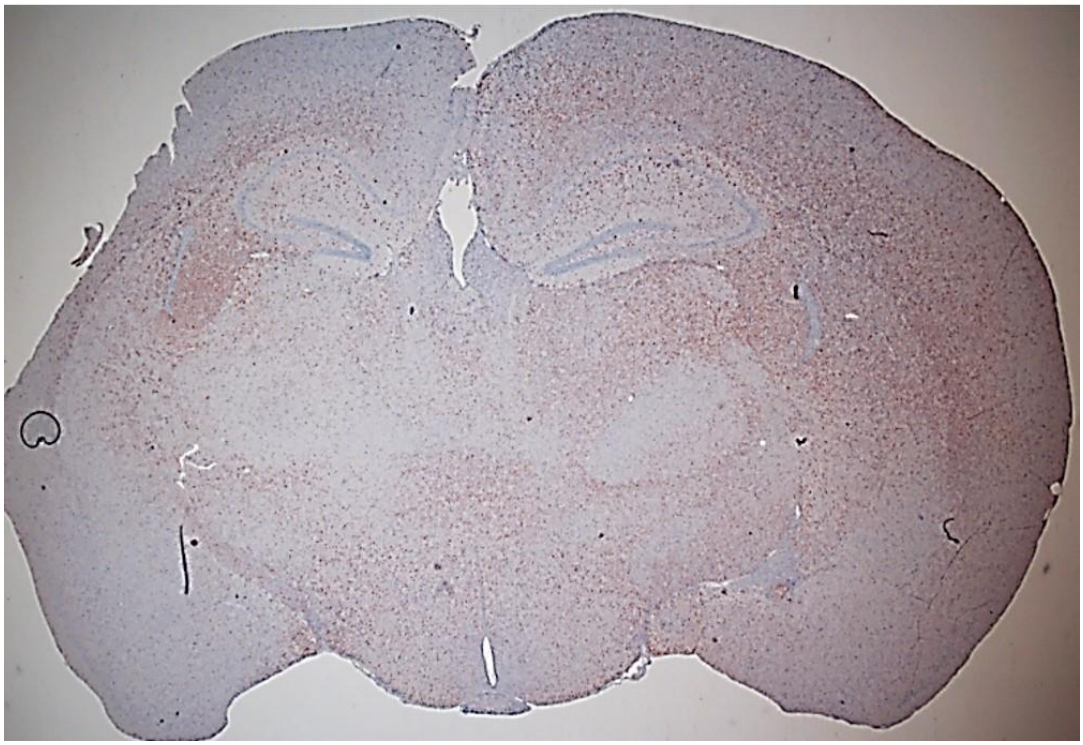

Figure S7: Invasive xenograft tumors arisen from GSC lines, #1051 and #1043. Representative images of xenograft tumors grown from human GSCs in an orthotopic mouse model for brain tumors. Immunohistochemistry stainings for human nestin (anti-human nestin antibody PA5-82905, 1:100, Life Technologies).

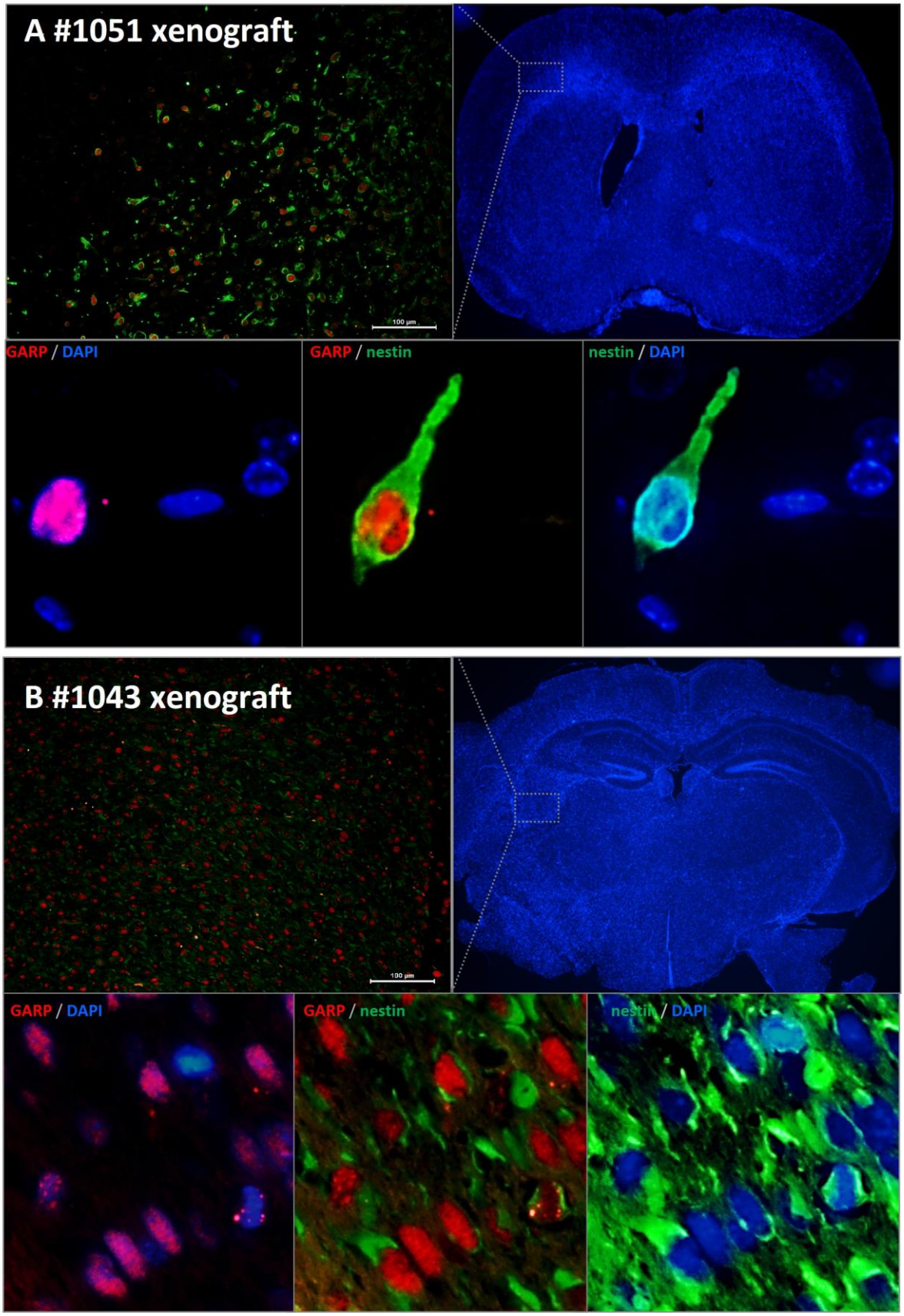

Figure S8: GARP is expressed in xenograft tumors arisen from GSC lines, #1051 and #1043. Immunofluorescence of GARP and nestin of (A) #1051 and (B) #1043 xenograft tumors. GARP seems to be exclusively expressed on GSC cells. Confocal images of GARP and nestin expressing GSCs stained for GARP and nestin. Cells were stained for their nuclei. Nuclear counterstaining with Hoechst (blue), GARP (red), and nestin (green). Scale bar corresponds to 100 μm.

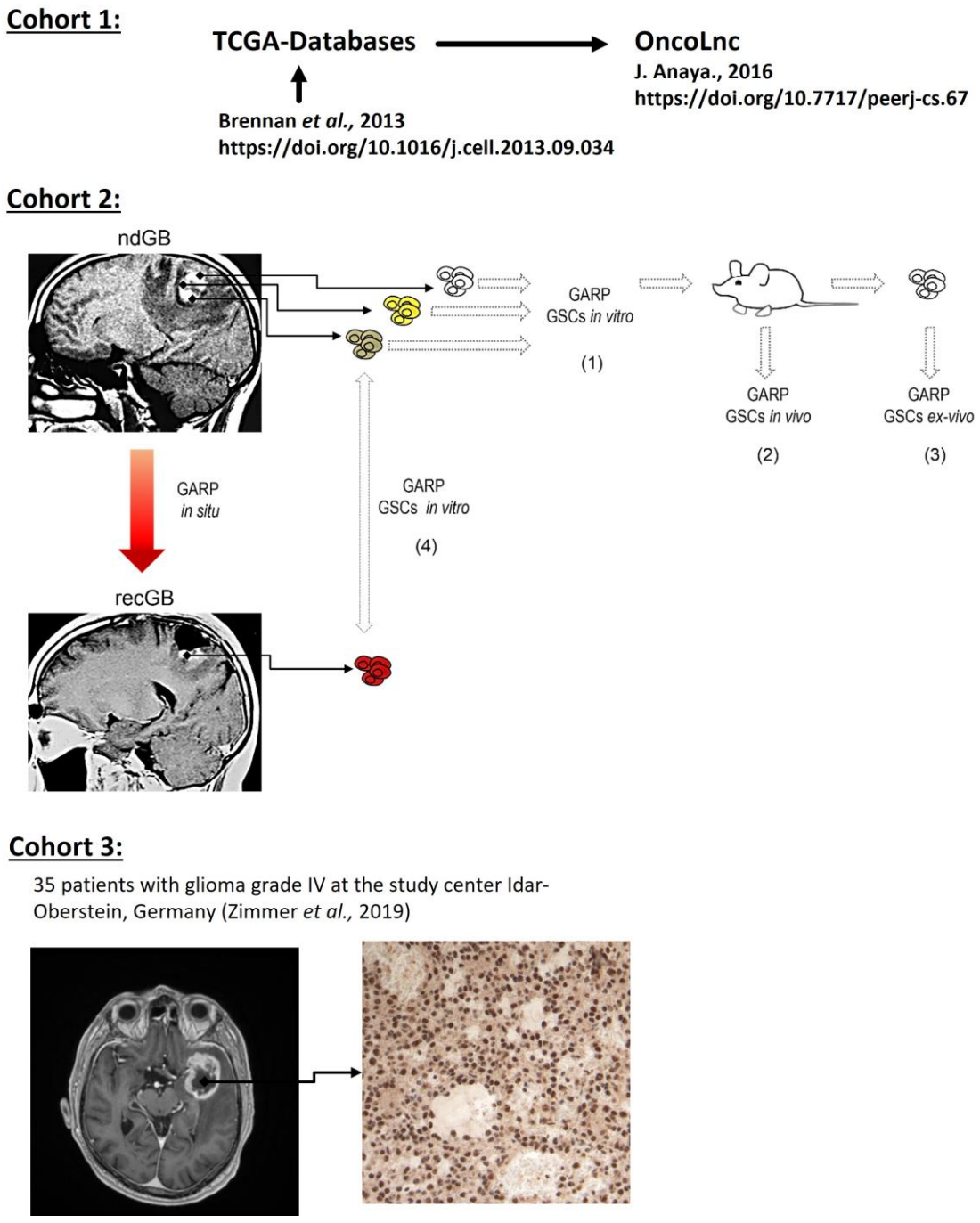

Figure S9: Study design and models used for the assessment of GARP. Cohort 1: For the analysis of GARP and CD133 expression in GB, the online tool OncoLnc was used. Based on 152 complete data sets, including complete survival data, patients were divided 50/50 into "low" or "high" groups based off their mRNA expression of GARP and CD133 and were analyzed for their survival. The results shown are in whole or part based upon data generated by the TCGA Research Network: https://www.cancer.gov/tcga and were analyzed using OncoLnc [43]. Cohort 2: „GARP in situ" corresponds to GARP assessments in tumor specimens from newly diagnosed or recurrent GBs. Investigation track (1) corresponds to *in vitro* assessments in GSCs either isogenic or heterogenic originating from ndGBs. Track (2) corresponds to *in vivo* assessments of GARP in tumor xenografts grown from orthotopically implanted GSCs. Track (3) corresponds to GARP assessments in GSCs explanted from tumor xenografts. Track (4) corresponds to tumor-matched GSCs isolated from the same patient at the ndGB or recGB stage. Furthermore, retrospective analysis of transcriptome data of 155 GB samples from 28 patients of Kim et al., 2020. ndGBs, first and second recurrent tumors were analyzed for their GARP and CD133 expression levels across tumor stages [32]. Cohort 3: A cohort of 35 patients with (WHO grade IV) glioblastoma (Zimmer et al., 2019) were analyzed for their GARP expression by immunohistochemistry and analyzed for their survival [7].

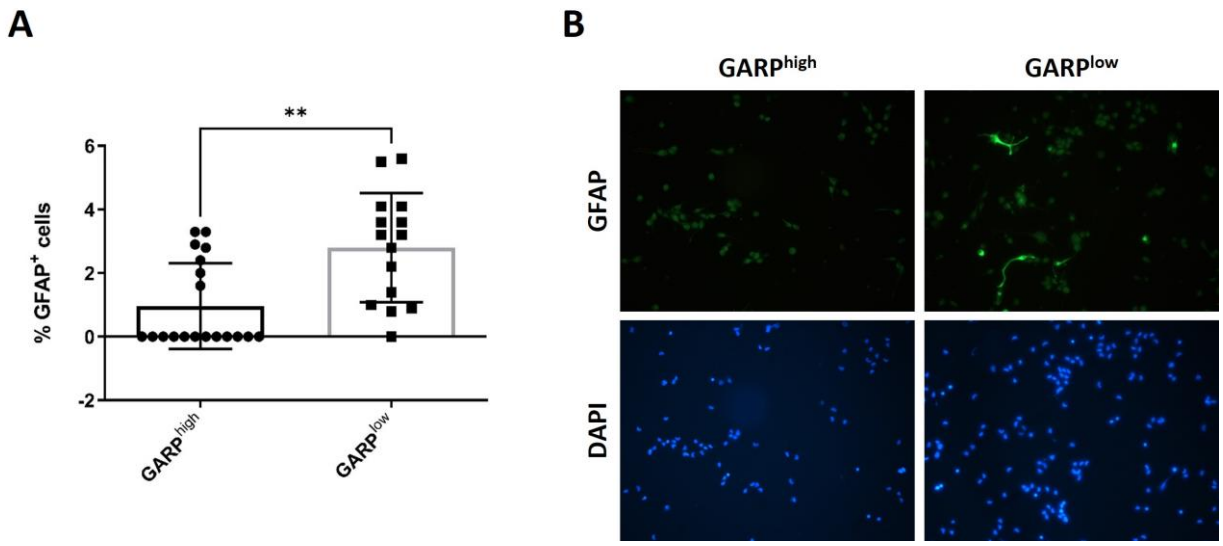

Figure S10: Frequency of GFAP$^+$ GARP^{high} and GARP^{low} GSCs. The GSC line, #1095, was sorted into GARP^{high} and GARP^{low} populations. Cells were cultured in self-renewal promoting conditions (NB+bFGF/+EGF) and assessed for their frequency of glial fibrillary acidic protein (GFAP), an astrocyte differentiation associated marker, via immunofluorescence. (A) The percentage of GFAP$^+$ cells was quantified from the total cells counted. (B) Representative images of GFAP (green) stained GARP^{high} and GARP^{low} GSCs with paired DAPI (blue) controls. The white scale bar corresponds to 50 μm.

Original Images for Blots (Figure 5)

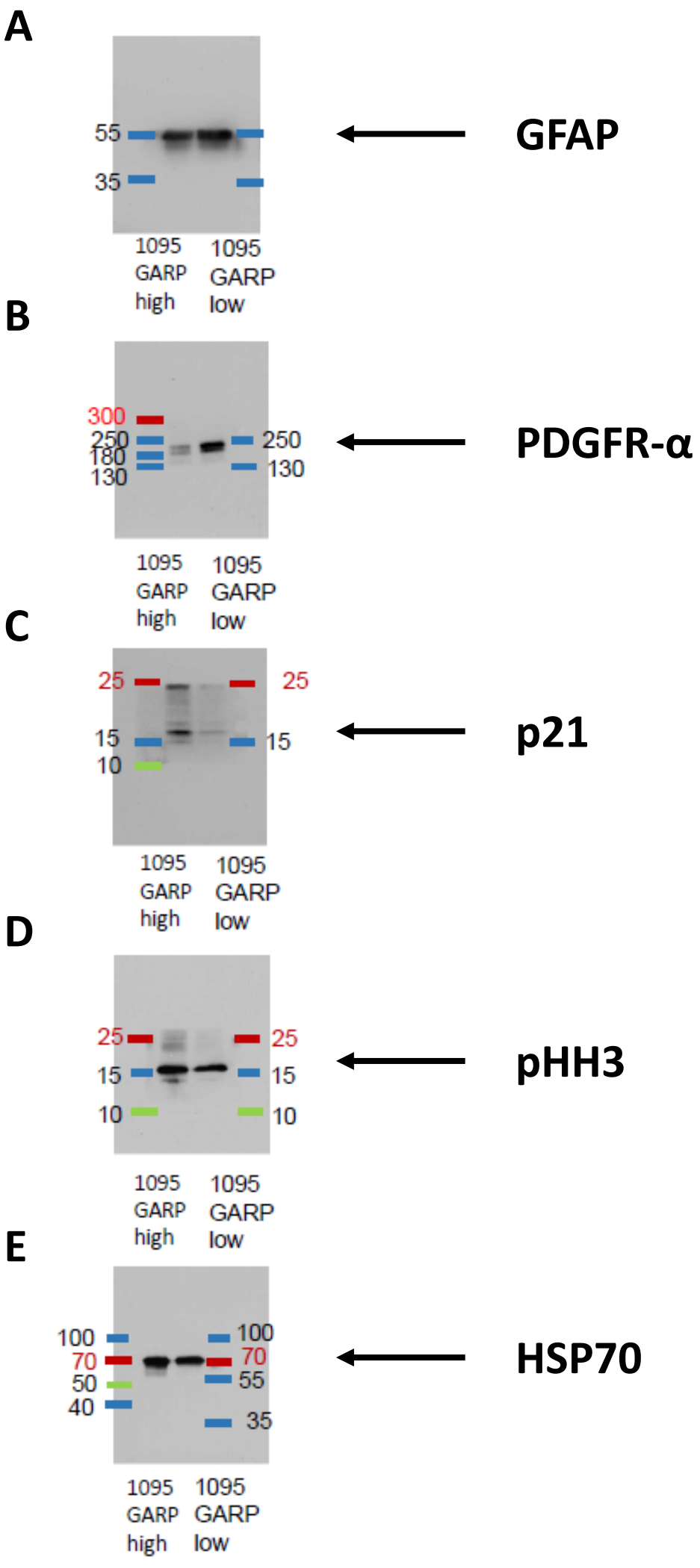

Original Images for Blots (Figure 5): Original, uncropped, and unadjusted blot images shown in Figure 5. The following proteins were analyzed: (A) glial fibrillary acidic protein (GFAP), (B) platelet-derived growth factor receptor alpha (PDGFR-α), (C) p21, (D) phosphorylated histone H3 (PHH3), and (E) HSP70 was used as a loading control. Protein size (kDa) is indicated by the ladders on the left and right sides of the membranes.

cancers

MDPI

Article

Platelet-Derived GARP Induces Peripheral Regulatory T Cells—Potential Impact on T Cell Suppression in Patients with Melanoma-Associated Thrombocytosis

Niklas Zimmer [1], Franziska K. Krebs [1], Sophia Zimmer [1], Heidrun Mitzel-Rink [1], Elena J. Kumm [2], Kerstin Jurk [2], Stephan Grabbe [1], Carmen Loquai [1] and Andrea Tuettenberg [1,*]

[1] Department of Dermatology, University Medical Center Mainz, 55131 Mainz, Germany; niklas.zimmer@unimedizin-mainz.de (N.Z.); franziska.krebs@unimedizin-mainz.de (F.K.K.); sophia.zimmer@gmx.net (S.Z.); heidrun.mitzel@unimedizin-mainz.de (H.M.-R.); stephan.grabbe@unimedizin-mainz.de (S.G.); carmen.loquai@unimedizin-mainz.de (C.L.)

[2] Center for Thrombosis and Hemostasis (CTH), University Medical Center Mainz, 55131 Mainz, Germany; elena.kumm@unimedizin-mainz.de (E.J.K.); kerstin.jurk@uni-mainz.de (K.J.)

* Correspondence: antuette@uni-mainz.de

Received: 26 November 2020; Accepted: 3 December 2020; Published: 5 December 2020

Simple Summary: Thrombocytosis correlates with poor prognosis for treatment of malignant melanoma. Detailed information on how platelets modify the anti-tumoral immune response is still elusive. Analyzing the immunomodulatory capacities of platelets on huCD4$^+$ T cells in vitro, we were able to show that platelets are able to induce regulatory T cells by the expression of glycoprotein A repetitions predominant (GARP), thus indicating a potential contribution to the immunosuppressive tumor microenvironment. Furthermore, we analyzed platelets of melanoma patients in stage I and IV. Melanoma patients with poor prognosis showed, besides an increased platelet count, a significant increase in GARP expression on platelets. This study suggests the contribution of platelets on the immune evasion in melanoma patients, opening a new potential way to target the immunosuppressive TME.

Abstract: Platelets have been recently described as an important component of the innate and adaptive immunity through their interaction with immune cells. However, information on the platelet–T cell interaction in immune-mediated diseases remains limited. Glycoprotein A repetitions predominant (GARP) expressed on platelets and on activated regulatory T cells (Treg) is involved in the regulation of peripheral immune responses by modulating the bioavailability of transforming growth factor β (TGF-β). Soluble GARP (sGARP) exhibits strong regulatory and anti-inflammatory capacities both in vitro and in vivo, leading to the induction of peripheral Treg. Herein, we investigated the effect of platelet-derived GARP on the differentiation, phenotype, and function of T effector cells. CD4$^+$CD25$^-$ T cells cocultured with platelets upregulated FoxP3, the master transcription factor for Treg, were anergic, and were strongly suppressive. These effects were reversed by using a blocking anti-GARP antibody, indicating a dependency on GARP. Importantly, melanoma patients in different stages of disease showed a significant upregulation of GARP on the platelet surface, correlating to a reduced responsiveness to immunotherapy. In conclusion, our data indicate that platelets induce peripheral Treg via GARP. These findings might contribute to diseases such as cancer-associated thrombocytosis, wherein poor prognosis and metastasis are associated with high counts of circulating platelets.

Keywords: GARP; platelets; Treg; melanoma; thrombocytosis

1. Introduction

In cancer patients, one of the main reasons for tumor immune escape and therapy failure is the immunosuppressive tumor microenvironment. Herein, suppressive immune cells as well as inhibitory factors secreted by the tumor itself play a central role [1].

Whereas platelets are primarily known for initiating hemostasis by clotting at the site of injury, recent evidence indicates that they also influence tumor immune responses and the tumor microenvironment [2,3]. Cancer-associated thrombocytosis has been linked to the promotion of metastasis, invasion, tumor development, and consequently to poor clinical outcomes in various tumor entities [4]. Lower platelet activation statuses and counts in patient blood correlate with decreased metastasis [5,6]. This can be explained in further detail as platelets promote motility [7–10], epithelial–mesenchymal cell transition (EMT) [11], tumor cell survival [12–14], immune evasion [15], increased adhesion of tumor cells to the endothelium [16–18], and subsequent extravasation [11,19–22].

Platelet-derived transforming growth factor β (TGF-β) is an important immunomodulator with a multi-faceted role in the promotion of EMT and metastasis. It has been found to enhance metastasis in vivo by directly inducing the transition of cancer cells into a mesenchymal-like phenotype through the Smad and NFkB pathways [23]. Platelet-derived TGF-β also promotes metastasis indirectly through myeloid cells and fibroblasts by encouraging the remodeling of the extracellular matrix. Additionally, it is known to affect myeloid cells via TGF-β receptor II signaling, resulting in upregulation of TGF-β1, arginase, and inducible nitric oxide synthase (iNOS). Altogether, this leads to inhibition of effector cell functions, which further contributes to metastasis [24,25].

Once metastasized, tumor cells enter the bloodstream as circulating tumor cells (CTC), being faced with extreme shear stress and attack from immune cells. Herein, melanoma cells express chemokines, which attract and activate platelets (tumor cell induced platelet aggregation, TCIPA). Platelets adhere to tumor cells due to their expression of primary fibrinogen receptor αIIbβ3 integrin and P-selectin, which bind to CD44 and αvβ3 integrin on the surface of tumor cells [26,27]. These adhered platelets act as a protective shield for CTC against extreme sheer stress and facilitate and increase extravasation [28–30].

As mentioned above, CTC must also evade attack from immune cells in the blood stream in order to survive. One mechanism is by impairing the killing efficiency of natural killer (NK) cells. TGF-β, derived from activated and shielding platelets, antagonizes the interleukin-15 (IL-15) pathway that is responsible for NK cell proliferation and activation. In addition, it downregulates NKG2D, leading to a decreased natural killer (NK) cell efficacy. Collectively, this results in a decreased killing efficiency of NK cells and increased tumor cell survival [31–33]. It has also been shown that the attachment of platelets onto CTC leads to the transfer of platelet-derived surface molecules, such as MHCI, to the surface of CTC, effectively "disguising" CTC and thus preventing attack by NK cells [34].

GARP (glycoprotein A repetitions predominant) is encoded by leucine-rich repeat containing protein 32 gene (LRRC32) and represents a non-signaling docking receptor for latent TGF-β. The expression of GARP was initially described on the surface of platelets, but it has also been found on activated regulatory T cells (Treg) and on tumor cells, such as melanoma and glioblastoma [35–37]. GARP is recognized as playing an important role in the binding and release of TGF-β and hence in peripheral tolerance and progression of cancer.

In the past, our group defined an important role for GARP itself in the induction of peripheral tolerance [38]. GARP induces Treg with strong suppressive capacity and prevents chronic inflammatory disease in a humanized mouse model [37]. It also suppresses the effector function of $CD8^+$ cytotoxic T cells and alternatively activates macrophages to favor tolerance induction [38]. Therefore, GARP represents a functionally relevant immunosuppressive molecule that contributes to peripheral tolerance by significantly preventing effector cell responses in the tumor microenvironment [36,38].

As described above, platelets exhibit important immunomodulatory functions, especially on T cells [39,40]. However, how platelets regulate T cell immunity is far from being completely understood. Given the fact that platelets express GARP on their surfaces and linking this to our previous work describing GARP as a key molecule in inducing peripheral tolerance, we hypothesized that platelets

may be involved in the induction of peripheral tolerance and thus the promotion of malignancy and resistance to therapy by inhibiting host immunity. The present study investigated the effect of platelets on T effector cell function and clearly demonstrated that platelets led to the induction of Treg in a GARP-dependent manner. Melanoma patients showed significantly higher levels of GARP on the surface of platelets and an increase in platelet surface expression of the platelet activation marker CD62P (P-selectin). Late-stage melanoma patients with an overall increased frequency of platelets showed a decreased response rate to their applied immunotherapy.

Our data showed a possible contribution of platelets to the adaptive immunity, leading to a poor prognosis of cancer patients with cancer-associated thrombocytosis. Additionally, this opens up new possibilities to target platelets as a therapeutic option for the treatment of cancer.

2. Results

2.1. Expression of GARP on Platelets

GARP was initially described as being expressed on the surface of platelets [35]. Therefore, GARP expression was analyzed on resting and pre-activated platelets in combination with the platelet activation marker CD62P. In accordance with the literature, we detected GARP expression on resting platelets. Nevertheless, platelet activation led to a significant increase in the frequency of $GARP^+$ platelets as well as the overall GARP expression (MFI) on platelets (Figure 1A). As we have demonstrated before, GARP can be shed from and found in the supernatants of either activated Treg or tumor cells, leading to the immunomodulation of T effector cells and macrophages (Figure A1). We investigated whether this process is also true for platelets. Pre-activated platelets were isolated from peripheral blood of healthy donors (HD) and cultured in X-VIVO 15, as described in the method section. Supernatants (platelet-conditioned medium, PCM) were collected after 16 h of culture and analyzed in an ELISA for GARP content. In all samples, analyzed GARP was detectable when compared to the medium control (X-VIVO-15) (Figure 1B). Importantly, no cellular contaminants (determined by microscopy and flow cytometry) were detectable.

2.2. Platelet-Derived GARP Induced Peripheral Regulatory T cells

We next investigated the effect of platelet-derived GARP on peripheral blood $CD4^+CD25^-$ T cells. $CD4^+CD25^-$ T effector cells (Teff) and platelets were cocultured in different ratios, ranging from 1:15, 1:30, 1:50 to 1:100 Teff/platelets. With increasing platelet numbers, we detected a significant increase in Foxp3 and GARP expression on Teff (Figure 2A), whereas proliferation and effector cytokine production of Interleukin 2 (IL-2) and Interferon γ (IFN-γ) decreased (Figure 2B). To exclude the fact that the displayed GARP upregulation on Teff was due to contaminating adhering platelets on the Teff surface, we performed flow cytometry using a co-staining with anti-CD4 (Teff) and anti-CD41a (platelets) Abs. Within the first 24 h of coculture, about 25% of $CD4^+$ T cells were also positive for the platelet marker CD41a, indicating adherence of platelets on the surface of Teff. This percentage significantly decreased within 6 days ($CD4^+CD41a^+$ 4.8%), as demonstrated by flow cytometry (Figure A2), showing that only a minor fraction of cells were $CD4^+CD41a^+$ double-positive. Notably, GARP expression on T cells increased over time. Because platelet effects on $CD4^+CD25^-$ T cells were most prominent at a ratio of 1:50, we used this ratio in the following experiments.

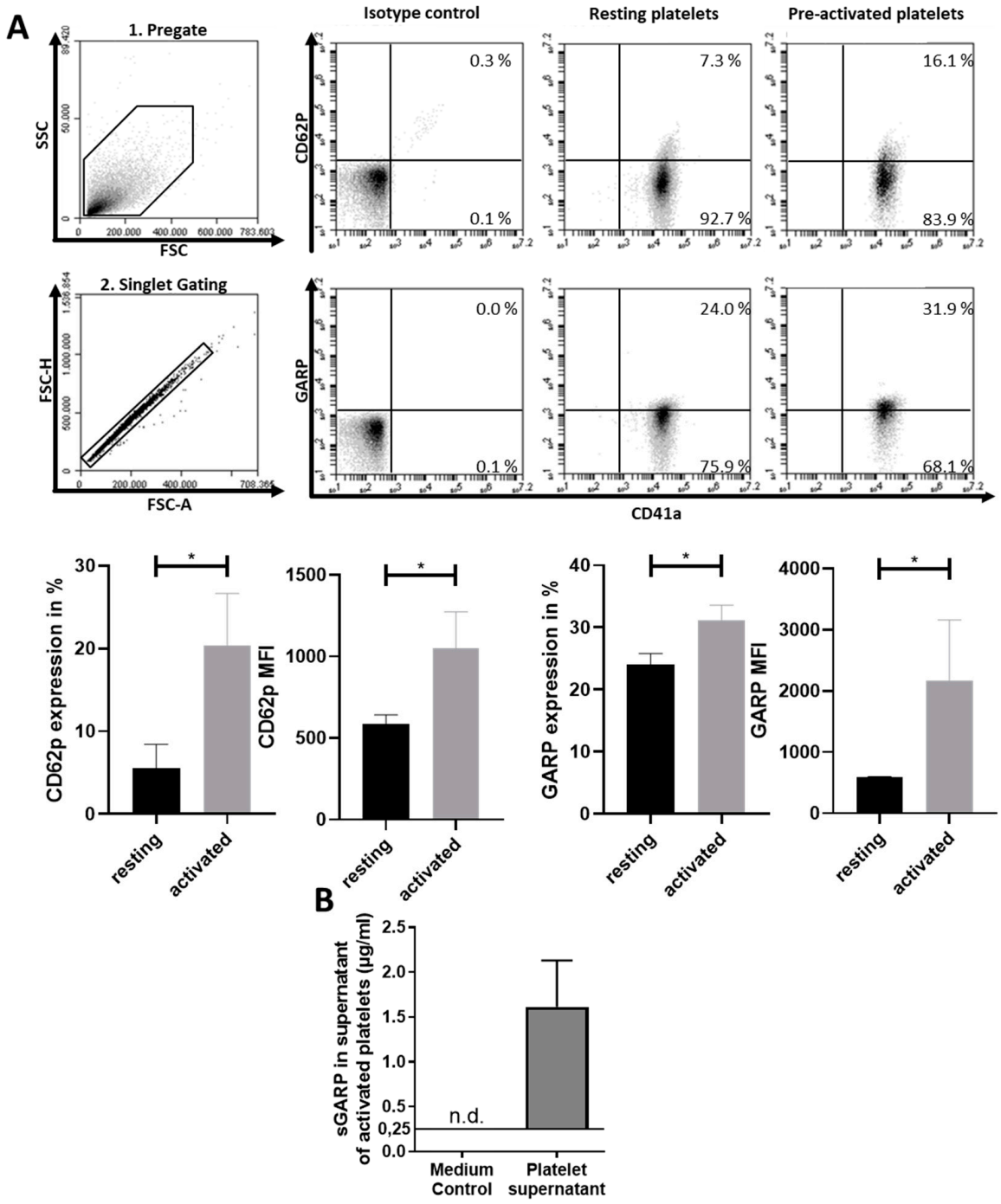

Figure 1. Glycoprotein A repetitions predominant (GARP) was expressed on the surface of platelets and was detectable in the supernatant of activated platelets. (**A**) Flow cytometric analysis of CD62P and GARP expression levels in resting and pre-activated platelets. Only singlets were used in the analysis. Isotype controls are shown. Bar diagrams of CD62P and GARP expression show pooled data of percentages (%) of positive cells and raw means ($n = 3$, means ± SD * $p < 0.05$, and n.s. determined by Student's *t*-test). (**B**) Presence of soluble GARP (sGARP) in the supernatant of pre-activated platelets. sGARP content of the supernatant of 2×10^9 activated platelets after 16 h compared to a negative medium control (n.d. = not detected). sGARP levels were determined by ELISA from three different healthy donors (HD).

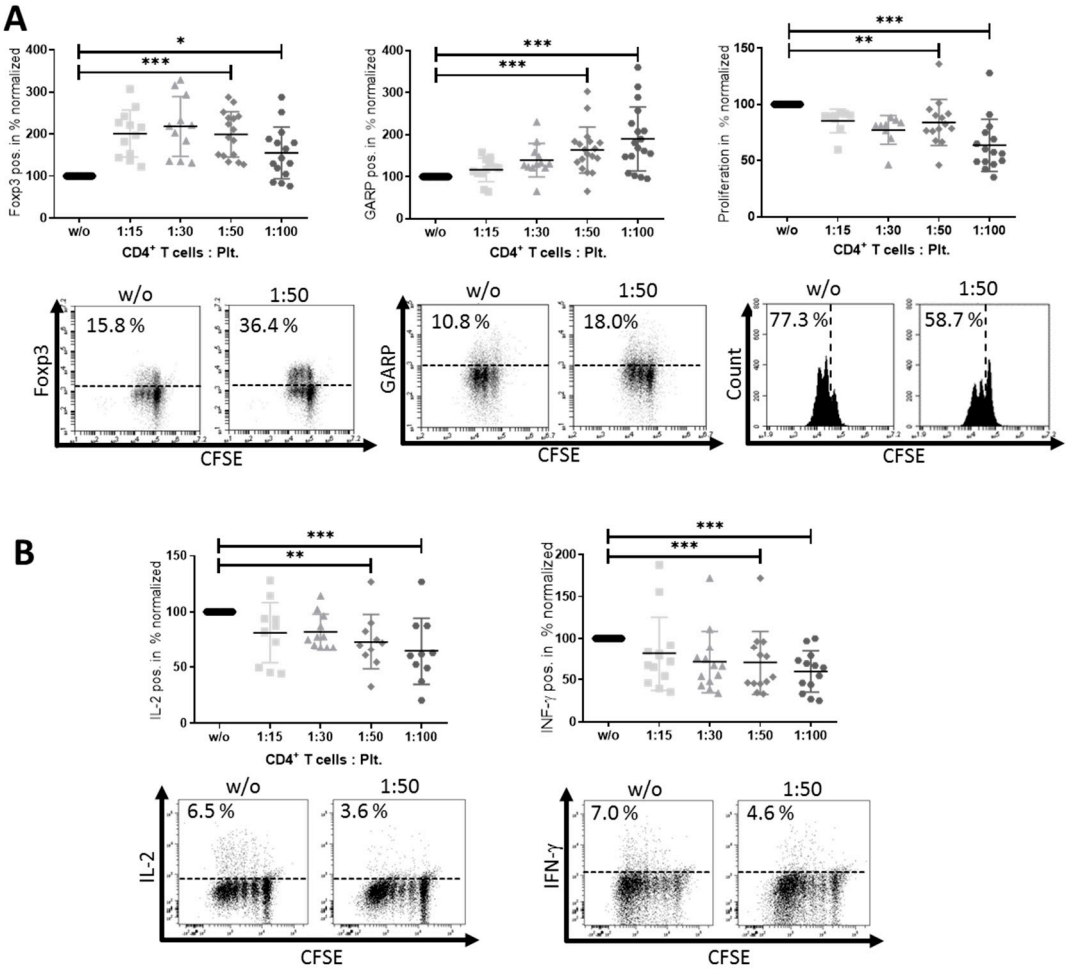

Figure 2. Platelets induce peripheral regulatory T cells (iTreg). (**A**) $CD4^+$ $CD25^-$ T cells and platelets were cocultured as indicated. Herein, carboxyfluorescein succinimidyl ester (CFSE)-labeled $CD4^+CD25^-$ T cells were stimulated with 0.5 µg/mL anti-CD3 mAb and 1.0 µg/mL anti-CD28 mAb with or without different ratios of platelets. The expression of Foxp3, GARP and the proliferation of cells were analyzed via flow cytometry on day 3 after stimulation. (**B**) Effector cytokine production of Interferon(IFN)-γ and interleukin (IL)-2 was analyzed using intracellular flow cytometry on day 6. Only live $CD4^+CD25^-$ T cells were included into the analysis. Representative dot plots of 12 independent experiments are shown. The graphs show cells cultured in the presence of platelets normalized to $CD4^+CD25^-$ T cells without platelets (expression levels were normalized to 100) (n = 12, means ± SD, * $p < 0.05$, ** $p \leq 0.01$, *** $p \leq 0.001$, and n.s. determined by Kruskal–Wallis test).

Having thus far used a non-canonical activation method, we next wanted to investigate a canonical, agonist-induced platelet activation, e.g., by thrombin being clinically more relevant. Therefore, we added 10 U/mL thrombin to the coculture. In comparison to the coculture without thrombin, this led to similar results, with increased Foxp3 and GARP expression and decreased cytokine production. Nevertheless, as described by Metelli et al. [41], thrombin leads to the cleavage of GARP on thrombocytes, which might partially explain the slightly reduced significances in the thrombin treated versus the 1:50 coculture control group (Figure A4). Therefore, we used TRAP-6, an additional canonical platelet activator, in our coculture. Here, we could again see similar results without any significant difference between TRAP-6-activated platelets (canonical activation) and the 1:50 coculture control group (non-canonical activation, Figure A5).

In sum, platelet-cocultured Teff displayed typical characteristics of induced peripheral Treg (iTreg), namely, reduced proliferation and effector cytokine production and increased FoxP3 expression.

To analyze whether these phenotypically altered anergic T cells resembling iTreg also had a suppressive function, we used them in a conventional suppressor assay. In detail, $CD4^+FoxP3^+$ iTreg (T cells pre-cultured with platelets for 6 days at the ratio 1:50) were harvested, washed, and then cultured together with untreated Teff (Figure A3) to investigate their suppressive function. Herein, platelet-induced Treg showed a significant suppressive capacity (Figure 3), as demonstrated by the reduced proliferation of T cells by Ki-67 staining in the suppression assay. Herein, decreasing numbers of platelet-induced Treg in the culture led to an increased proliferation of T cells, showing a dose-dependent suppression by the iTreg.

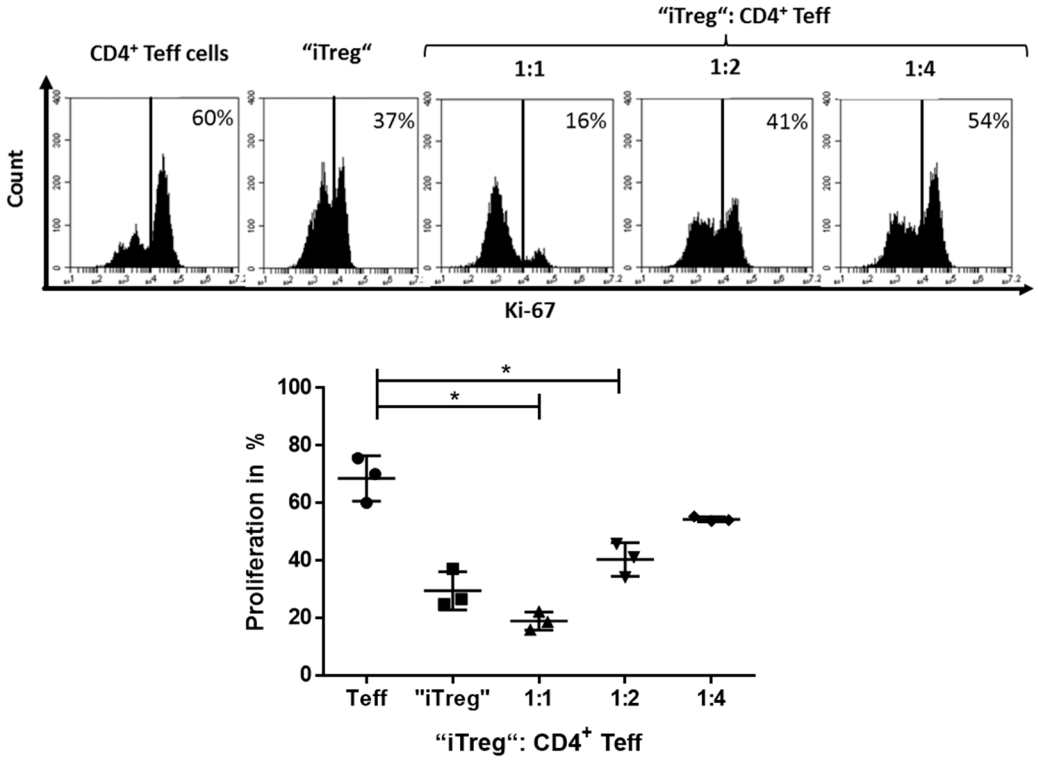

Figure 3. Platelet-induced iTreg suppressed T effector cells (Teff) cells. To analyze iTreg induction by platelets, we expanded $CD4^+CD25^-$ T cells for 6 days in the presence of platelets at the ratio of 1:50, as described previously, and were subsequently incubated at various ratios with 0.5×10^5 $CD4^+CD25^-$ T cells and restimulated with 1×10^5 irradiated peripheral blood mononuclear cells (PBMC) and 0.5 µg/mL anti-CD3 mAb. Proliferation was determined on day 3 of culture by Ki-67 staining ($n = 3$, means ± SD, * $p < 0.05$, and n.s. determined by one-way ANOVA).

In order to determine whether the induction of iTreg is GARP-dependent, we added 10 µg/mL of a blocking anti-GARP Ab to the cocultures and again analyzed Foxp3 and GARP expression, proliferation, (Figure 4A) and cytokine production (Figure 4B). As demonstrated, addition of the blocking Ab led to a significant normalization of Foxp3 expression and restored the production of the effector cytokine IFN-γ to a normal level, indicating an induction of iTreg that was at least in part GARP-dependent.

2.3. Role of TGF-βand Platelet-Conditioned Medium in Platelet-Mediated iTreg Induction

GARP is known to be a surface docking receptor for TGF-β, and plays a dominant role in its activation and release. Thus, we next assessed the impact of TGF-β in the regulatory activity of platelet-derived GARP. Herein, the blockade of TGF-β signaling with blocking antibodies against TGF-β I-III showed a partial inhibition of the modulatory effects of platelet-derived GARP on Foxp3 regulation (Figure 5A) and IL-2 (Figure 5B) production, whereas proliferation and IFN-γ production was not affected. Using a blocking antibody against TGF-β receptor II (TGF-β RII), we had similar

results, as Foxp3 and GARP were upregulated, whereas the production of IFN-γ and IL-2 were only partially inhibited. Only proliferation was strongly affected by the TGF-β RII blocking antibody, which was consequently restored to a normal level.

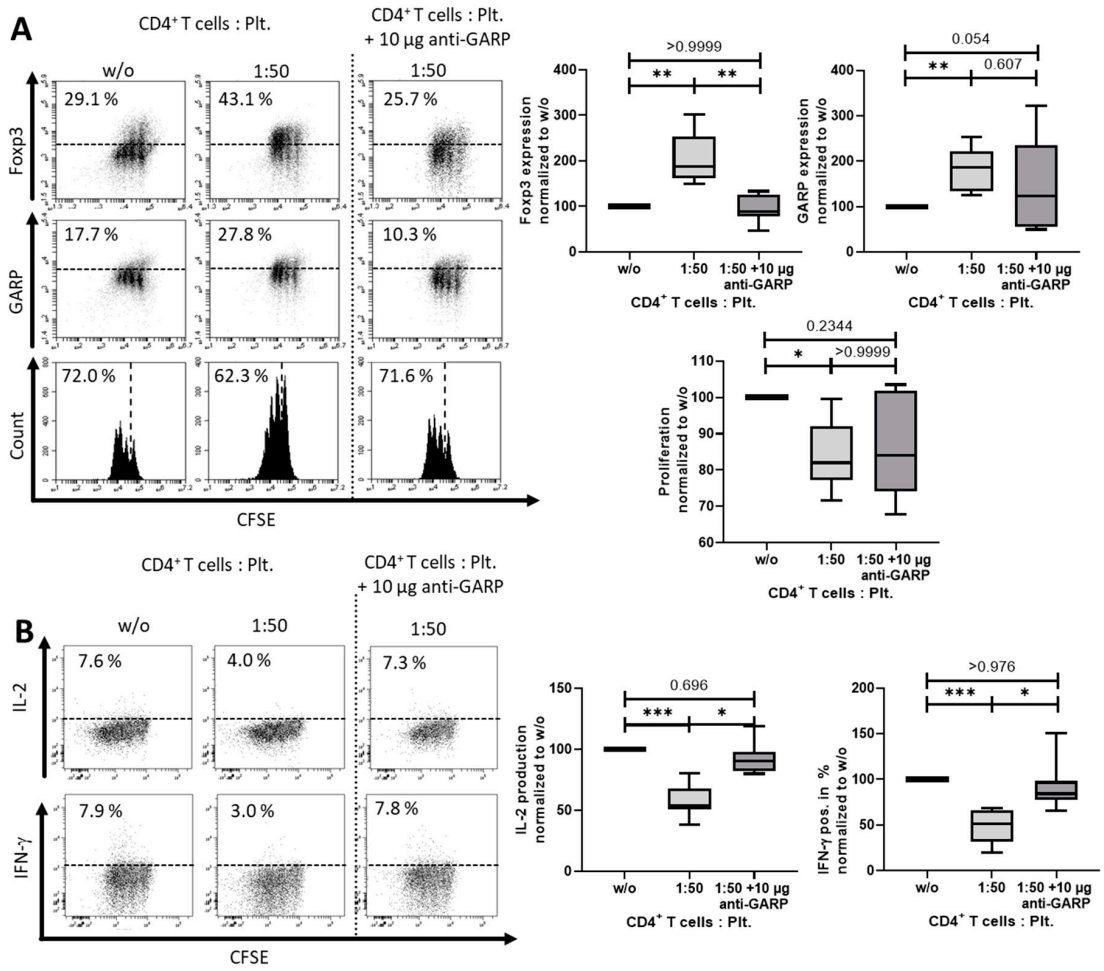

Figure 4. Platelets induced iTreg in a mainly GARP-dependent manner. (**A**) Blocking anti-GARP antibody inhibited platelet-induced effects on FoxP3 and GARP expression, as well as proliferation. CFSE-labeled $CD4^+CD25^-$ T cells were stimulated with 0.5 µg/mL anti-CD3 mAb and 1.0 µg/mL CD28 mAb with different ratios of platelets. In coculture, 10 µg/mL blocking anti-GARP Ab was added at day 0, as indicated. Foxp3 and GARP expression and proliferation is shown on day 3 after stimulation. (**B**) Cytokine production is shown on day 6. The graphs show cells cultured in the presence of platelets normalized to $CD4^+CD25^-$ T cells without platelets. For analysis, only live cells were included. Representative dot plots of eight independent experiments are shown ($n = 9$, box and whiskers, medians ± min/max, * $p < 0.05$, *** $p \leq 0.001$, and n.s. determined by one-way ANOVA).

To gain more insight into the relationship between TGF-β and GARP, we performed an additional experiment where the TGF-β receptor II was blocked on $CD4^+CD25^-$ T cells before coculture. The subsequent addition of either anti-TGF-β I-III Ab, anti-GARP Ab, or both only led to a complete inhibition of platelet effects in the samples with an anti-GARP Ab present. The combination of anti-TGF-β RII Ab, anti-TGF-β I-III Ab, and anti-GARP Ab showed the strongest effects on Foxp3, IL-2, and IFN-γ production, which were brought back to untreated levels. Anti-TGF-β RII Ab combined with anti-GARP Ab had the second strongest effect, followed by anti-TGF-β I-III Ab combined anti-GARP Ab and the use of only the anti-GARP Ab itself. The blockade of TGF-β alone by a combination of anti-TGF-β RII and anti-TGF-β I-III was not sufficient to inhibit platelet effects on T cells (Figure 6A,B).

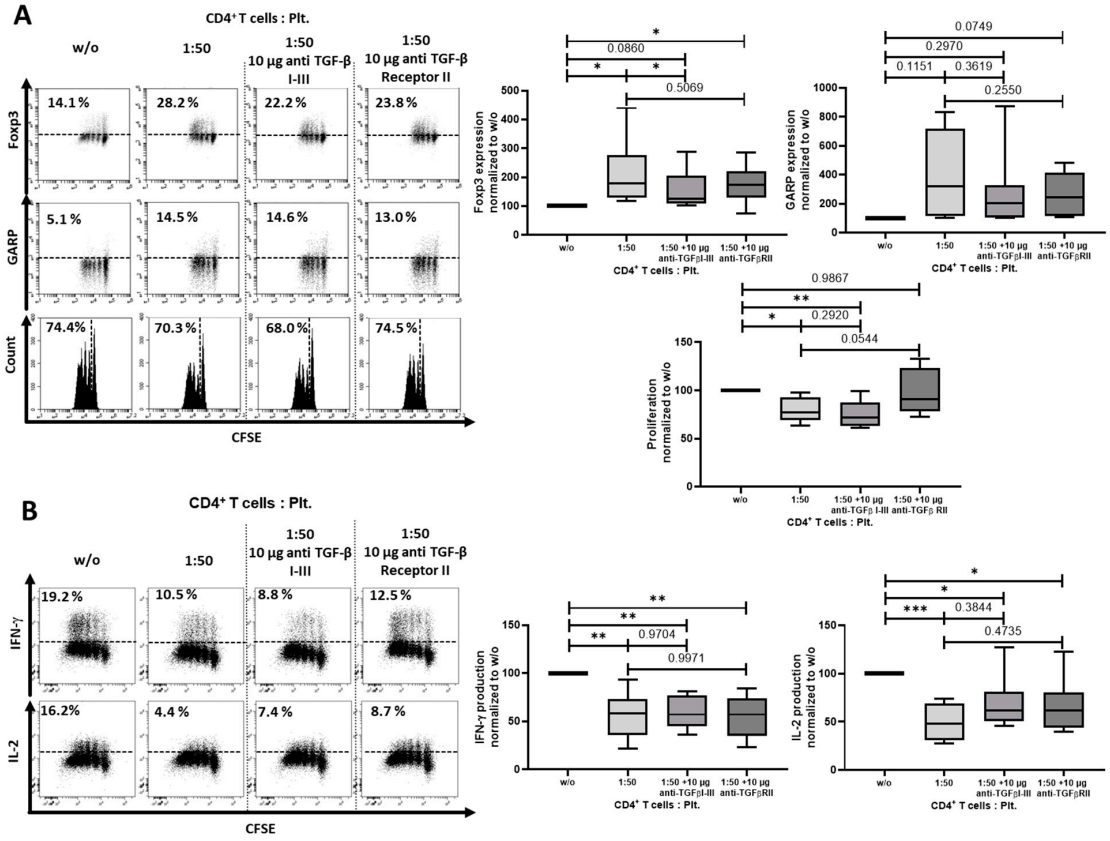

Figure 5. Blockade of transforming growth factor (TGF)-β I-III did in part prevent regulatory T cells (Treg) induction. (**A**) CFSE-labeled $CD4^+CD25^-$ T cells were cocultured with platelets in the ratio of 1:50 and were stimulated with anti-CD3 mAb (0.5 µg/mL) and anti-CD28 mAb (1.0 µg/mL) in the presence of either anti-TGF-β I-III (10 µg/mL) or anti-TGF-β receptor II (10 µg/mL) antibodies. Antibodies were added at day 0. The expression of Foxp3 and GARP and cell proliferation were determined on day 3 via flow cytometry. (**B**) Production of IL-2 and IFN-γ was assessed by intracellular flow cytometry on day 6. The graphs show cells cultured in the presence of platelets normalized to $CD4^+CD25^-$ T cells without platelets. Dot plots show one representative result of 10 independent experiments (n = 10, box and whiskers, medians ± min/max, * $p < 0.05$, ** $p \leq 0.01$, *** $p \leq 0.001$, and n.s. determined by one-way ANOVA).

These results demonstrate that the T cell modulating impact of platelet-derived GARP is in part but not completely associated with TGF-β signaling.

As shown in Figure 1B, soluble GARP (sGARP) was detected in PCM. To further assess the effects of PCM on the differentiation process of T cells, we cultured T cells with PCM. Addition of PCM to T cells resulted in a tendency of an upregulation of Foxp3, an inhibition of proliferation (Figure 7A), and a significantly lower production of the effector cytokine IFN-γ (Figure 7B). The addition of the blocking anti-GARP Ab lead to a normalization of the Foxp3 expression level and the IFN-γ and IL-2 production, whereas proliferation and GARP expression did not normalize.

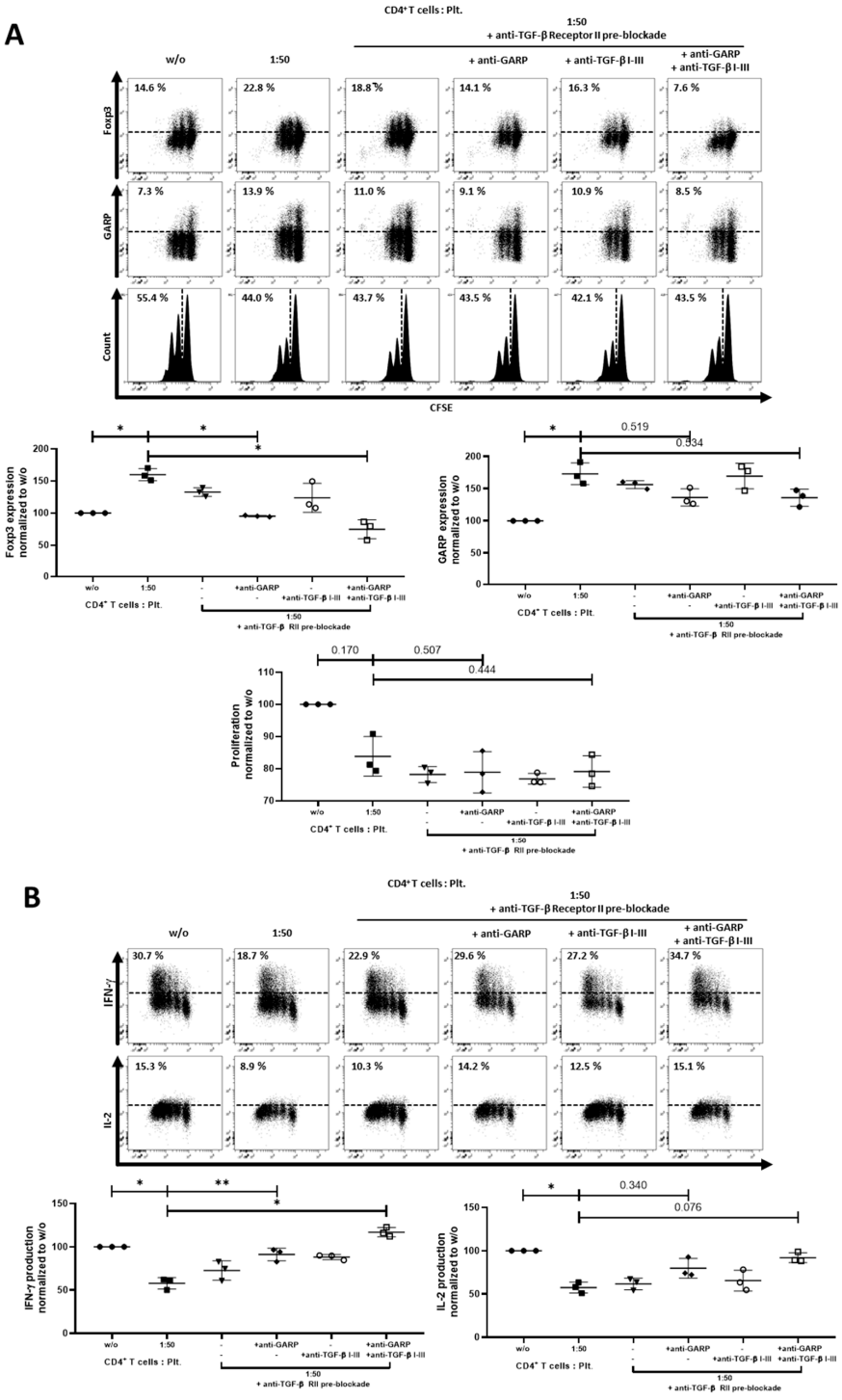

Figure 6. Combining blockade of TGF-β signaling and GARP led to a complete inhibition of platelet effects. (**A**) CFSE-labeled $CD4^+CD25^-$ T cells were cocultured with platelets in the ratio of 1:50 and were stimulated with anti-CD3 mAb (0.5 µg/mL) and anti-CD28 mAb (1.0 µg/mL). $CD4^+CD25^-$ T cells were incubated for 15 min with TGF-β receptor II (10 µg/mL) antibody prior to coculture, as indicated. Excess antibody was removed. Pre-treated $CD4^+CD25^-$ T cells were cultured in the presence of either anti-TGF-β I–III (10 µg/mL) and/or anti-GARP Ab (10 µg/mL) antibodies. Antibodies were added at day 0. The expression of Foxp3, GARP and cell proliferation were determined on day 3 via flow cytometry. (**B**) Production of IL-2 and IFN-γ was assessed by intracellular flow cytometry on day 6. The graphs show cells cultured in the presence of platelets normalized to $CD4^+CD25^-$ T cells without platelets. Dot plots show 1 representative result of 10 independent experiments ($n = 3$, means ± SD, * $p < 0.05$, ** $p \leq 0.01$, and n.s. determined by one-way ANOVA).

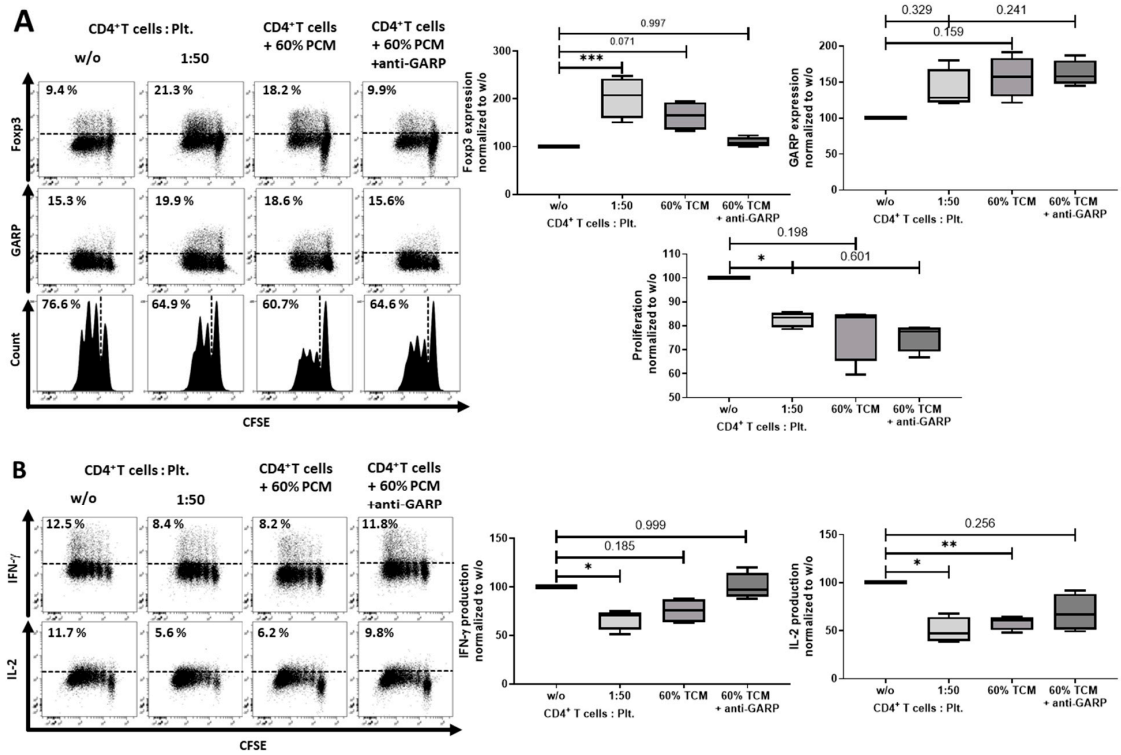

Figure 7. Platelet-conditioned medium (PCM) inhibited IFN-γ production, but failed to induce a Treg phenotype. (**A**) $CD4^+CD25^-$ T cells were cultured in X-Vivo 15 (Lonza, Basel, Switzerland) with 60% PCM content, with or without 10 µg/mL anti-GARP Ab and stimulated with 0.5 µg/mL anti-CD3 mAb and 1.0 µg/mL anti-CD28 mAb. Antibodies were added at day 0. The expression of Foxp3, GARP and cell proliferation were determined at day 3 with flow cytometry. (**B**) Cytokine production of IL-2 and IFN-γ was measured by intracellular flow cytometry on day 6. Dot plots show one representative result of five independent experiments ($n = 5$, box and whiskers, medians ± min/max, * $p < 0.05$, ** $p \leq 0.01$, *** $p \leq 0.001$, and n.s. determined by one-way ANOVA).

2.4. Correlation of Thrombocytosis and Prognosis—Clinical Impact of Platelets Expressing Increased Levels of GARP

By analyzing GARP expression on platelets from patients out of our first, initial cohort ($n = 35$) in both early and late-stage melanoma patients, we could detect increased GARP levels in comparison with HD controls. Nevertheless, GARP expression slightly differed between early stage I and late stage IV melanoma patients (Figure 8A). Additionally, platelets of stage I melanoma patients showed a stronger activation status compared to HD controls.

Several studies in different tumor entities indicate that cancer patients with thrombocytosis have poor prognoses [42]. In order to interpret these findings in the context of our own results, we analyzed a second, retrospective cohort of stage IV melanoma patients ($n = 36$) for their platelet counts and platelet–lymphocyte ratios (PLR) and correlated them to progression versus stable disease during therapy with checkpoint inhibitors (Figure 8B). Herein, non-responders to therapy with progressive disease showed significantly higher PLR and platelet counts than patients with stable disease, which responded to immunotherapeutic approaches.

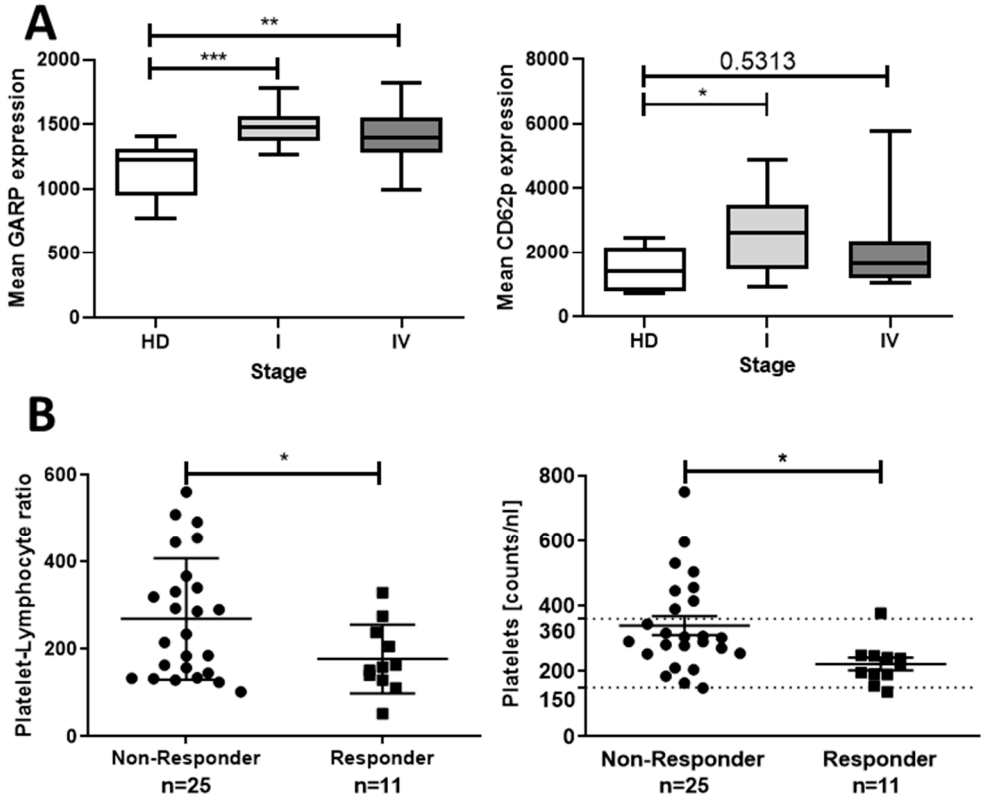

Figure 8. Increased platelet surface GARP levels in stage I/IV melanoma patient stage. (**A**) Comparison of platelet GARP and CD62P surface levels between HD (n = 8), stage I (n = 18), and stage IV (n = 17) melanoma patients assessed via flow cytometry. Means for GARP expression for HD = 1161, stage I = 1489, and stage IV = 1418. Means for CD62P expression are HD = 1470, stage I = 2611, and stage IV = 1977 (box and whiskers, medians ± min/max, * $p < 0.05$, ** p <.01, *** p <.001, and n.s. determined by unpaired t-test). (**B**) The platelet count in melanoma patients before starting immunotherapy using checkpoint inhibitors was measured as part of the routine blood tests. Platelet counts and the platelet–lymphocyte ratios of non-responders (n = 25) and responders (n = 11; staging results after 6 months of therapy) were compared. Means of platelet counts (PC) and the platelet–lymphocyte ratio (PLR) were as follows: progression: PC = 339.8, PLR = 269.0; stable disease: PC = 222.3, PLR = 177.5 (means ± SD, * $p < 0.05$, ** $p \leq 0.01$, *** $p \leq 0.001$, and n.s. determined by unpaired t-test).

3. Discussion

There has been an emerging role of platelets in the immunomodulation of cancer patients. Recent studies have indicated that platelets are present in the tumor microenvironment, and cancer-associated thrombocytosis has been linked to the promotion of metastasis, invasiveness, and tumor development and thus to poor clinical outcome in different tumor entities [4,43]. Tumors constantly activate the coagulation pathways, resulting in the generation of thrombin and consequently chronic platelet activation. Correlations between high platelet counts and shorter disease-specific survival are described for several tumor entities including lung, colon, breast, pancreatic, kidney, and gynecologic cancers. Platelets promote motility [8–10] and epithelial–mesenchymal cell transition, and readily bind to the surface of melanoma cells, thus protecting them from immunological clearance and/or chemotherapy-induced apoptosis [11].

The present study demonstrates a new and important role of platelets in mediating Teff inhibition by induction of Treg via a GARP-dependent mechanism. In agreement with the literature [44], GARP was found to be expressed on platelets to a certain extent and increased upon platelet activation, with a significant amount of GARP detected in the supernatants of activated platelets. This finding is of special interest for its implications on the tumor microenvironment as it is described that tumor cells

lead to the chronic activation of platelets [45]. Coculture of platelets and Teff cells but also culture of Teff in the presence of PCM induced cells with a regulatory phenotype. This included upregulation of the Treg master regulator Foxp3, reduced proliferation, and decreased effector cytokine production, as well as induction of suppressive capacity. Our study did not exclude other platelet-derived factors that could mediate the described effects. Nevertheless, blocking experiments showed that a significant part of the immunomodulatory effects of platelets or PCM can be contributed to their GARP expression. The platelet numbers chosen for our coculture experiments resulted in a lower platelet/Teff-ratio (50:1) than usually present in peripheral blood (approximately 500:1). Despite this, GARP effects were already detectable at these lower platelet numbers, with no changes at higher-tested ratios (i.e., 100:1). Limitations in cell culture prevented detailed analysis of more physiological ratios at 500:1. In addition, the TGF-β signaling axis seemed to be at least in part associated to the investigated GARP effect in inducing iTreg, thus contributing to a rather inhibitory tumor micromilieu. In former studies, our group demonstrated that sGARP induced Treg through TGF-β receptor II (Figure A1) [37]. This is in agreement with recent studies. A deletion of GARP on platelets of mice showed a blunted TGF-β activity, which improved the $CD4^+$ and $CD8^+$ T cell immune response at the site of the tumor [46]. As described above, we could show that the observed effect by Rachidi et al. is not only TGF-β -dependent but also GARP dependent. The complete blockade of TGF-β signaling in combination with the blockade of GARP led to almost complete inhibition of platelet effects. This effect could not be achieved by the combination of anti-TGF-β I–III and anti-TGF-β receptor II alone, indicating that GARP plays an important role in the induction of Treg by platelets, which is in part independent of TGF-β signaling. This was supported by further studies, as deletion of GARP in mice led to an increase in $CD4^+$ and $CD8^+$ T cell anti-tumor activity. Another study analyzed the role of GARP in hemostasis and thrombosis. Herein, it was demonstrated that GARP-deficient mouse platelets showed normal activation responses in vitro. Moreover, megakaryocyte/platelet-specific GARP knock-out in mice did not affect the tail bleeding time or the occlusion time in the carotid and mesenteric arteries after FeCl3-induced thrombus formation, indicating no essential role of GARP in hemostasis and thrombosis [44].

Interestingly, the melanoma patients of the first cohort, independent of their tumor stage, expressed higher amounts of GARP on their platelets as well as exhibited higher platelet activation statuses. As described earlier, GARP is associated with inhibitory effects on immune cells in the tumor microenvironment. One could reasonably speculate then that GARP expression on platelets may differ between stage IV patients with poorer prognoses and stage I patients, as a further increase in GARP expression in stage IV patients could be expected. Nevertheless, a closer look into Figure 8b shows that there was a detectable minor shift of GARP expression levels from stage IV patients in comparison to stage I patients in the direction of HD GARP levels. This was supported by a decrease in significance of stage IV patients (p-value HD-stage I: 0.0005 ***) compared to stage I patients (p-value HD-stage IV: 0.0068 **). Whether this was due to response to immunotherapy (16 out of 17 patients of stage IV in our rather small first cohort were responders) must be analyzed in future studies with representative control groups. In several studies, including different tumor entities, such as ovarian, glioblastoma, head and neck, colorectal, and non-small cell lung cancer, it has been described that patients with thrombocytosis often have an advanced tumor stage, a higher tumor grade, and lower progression-free and median overall survival, and thus have a poorer prognosis. Collectively, this indicates thrombocytosis as an adverse prognostic factor in various tumor entities [47–52]. Our study (second cohort) is in agreement with these previous studies as it shows that reduced response to immunotherapy correlated to higher platelet counts/PLR.

Platelets may promote carcinogenesis in several ways. First, circulating tumor cells may use platelets as protective barriers in a complex system of evasion from the attack of immune cells, as well as possibly as mediators for attachment to endothelial cells when initiating extravasation at metastatic sites [16]. Furthermore, platelets have a role in the prevention of hemorrhage in newly formed tumor vasculature, which is structurally abnormal and lacks the stability of local resident vasculature [53].

Several cytokines and growth factors contained in the alpha granules of platelets, such as vascular endothelial growth factor (VEGF), epidermal growth factor (EGF), platelet-derived growth factor (PDGF), transforming growth factor β (TGF-β), interleukin 1β (IL-1β), IL-8, and CXC motif containing ligand 12 (CXCL12) may play diverse roles in the tumor micro-environment, including the promotion of invasion and metastasis through a positive regulation of the epithelial–mesenchymal transition (EMT) process and immune evasion [23,54,55].

The present study provides new insights into how platelets could promote tumor progression through the induction of Treg via GARP. A recent study by Metelli et al. (2020) showed that thrombin contributes to cancer immune evasion by proteolysis/cleavage of GARP and subsequent liberation of TGF-β. The authors proposed that blockade of GARP cleavage is a valuable therapeutic strategy to overcome resistance to immunotherapy. This paper supports our data, wherein we showed that GARP plays an important role in the inhibitory tumor microenvironment [41].

Nevertheless, we postulate that not only the soluble (cleaved) form of GARP but also the membrane-bound and thus contact-dependent GARP can mediate suppressive effects through induction of iTreg. In our study, addition of thrombin to the platelet–Teff coculture and thus potential GARP cleavage even slightly reduced the capacity of Treg induction by platelets. One possible explanation for this would be that thrombin-cleaved GARP is impaired in function and has decreased immunosuppressive capacity. Another explanation, which is supported by the weaker effect of PCM compared to platelet–Teff cocultures, could be that sGARP is less potent at inducing Treg in contrast to surface-expressed GARP. Using TRAP-6 as a platelet activator in this context did not lead to the possible cleavage of GARP from the surface of platelets, and therefore it had no impact on platelet effects on $CD4^+CD25^-$ T cells. Whether this effect can be attributed to a truncated form of GARP after thrombin cleavage or that sGARP has a decreased immunomodulatory capacity must be further investigated. In our hands, it was shown for the first time that this effect on tolerance induction via GARP could be due to the induction of T cells with a regulatory phenotype. This is of great importance as Treg play a major role in the suppression of anti-tumor immunity.

Platelets are the second most abundant cell type in peripheral blood and thus are easy to isolate, count, and analyze. Furthermore, they contain large amounts of TGF-β and are positive for GARP, which contributes to a large extent towards immune inhibition, as described in our work. Therefore, the analysis of platelets, including their frequency and GARP expression levels, could serve as predictive or prognostic biomarkers in relation to potential for immune evasion and reduced responses to immunotherapies and thus to poor prognosis. Certainly, this has to be verified in a future larger study. Another important implication that arises from our data is the concept of implementing platelet-modulating therapies within oncology and investing new therapeutic strategies that target platelets and/or GARP. For instance, this could be achieved with GARP-specific antibodies targeting different immune as well as tumor cells and platelets within the tumor microenvironment.

In conclusion, our study describes for the first time in the human system the mechanism of GARP-dependent, platelet-mediated T cell suppression. Our study linked platelets to immune inhibition and explained, at least in part, why cancer patients with cancer-associated thrombocytosis have poor prognoses. This makes platelets an additional attractive target in combinatorial cancer immunotherapy treatments, mainly through the development of new (antibody-based) anti-GARP therapeutic approaches. This strategy would not only target platelets but also activated Treg and GARP+ tumor cells, leading to the modulation of the inhibitory tumor microenvironment with the overall aim to overcome cancer's resistance to immunotherapy through this combinatorial approach.

4. Materials and Methods

4.1. Isolation of Pre-Activated and Resting Platelets and Preparation of Platelet-Conditioned Medium

Pre-activated platelets: Blood bags were obtained from healthy donors (HD), with approval of the local ethical committee (Landesaerztekammer Rheinland-Pfalz, No.837.019.10 (7028)). Blood bags

were transferred to conical tubes (Greiner bio-one, Kremsmünster, Austria #227261) and subsequently centrifuged for 15 min at 160× *g* at room temperature (RT). The resulting platelet-rich plasma (PRP) supernatant was collected and centrifuged for another 15 min at 200× *g* at RT in order to deplete potential leukocyte contamination. Next, the PRP supernatant was washed with 1× Phosphate-buffered saline (PBS) at a ratio of 1:1 and centrifuged for 5 min at 2000× *g* at RT. The resulting pellet containing platelets was resuspended, and platelets were counted and added in different ratios to the coculture experiments. These platelets had a higher CD62P expression as measured in flow cytometry compared to "resting platelets" (see below) and were therefore referred to as "pre-activated platelets". Platelet-conditioned medium (PCM) was prepared by culturing 2×10^9 pre-activated platelets for 16 h in 2 mL of cell culture medium at RT (X-Vivo 15, Lonza, Basel Switzerland, #BE02-060F), and, as a control, were either activated with 10 U/mL thrombin or TRAP-6, as indicated. Subsequently, platelets were centrifuged at 2000× *g* for 5 min at RT. The resulting supernatant was isolated and immediately used for analysis as well as for coculture experiments. The PCM was checked for cell residues by conventional microscopy and flow cytometry.

Resting platelets: In contrast, "resting platelets", which showed a lower CD62P expression as measured in flow cytometry, were isolated at RT by first generating PRP. Citrated blood was supplemented with 2 mM EGTA and centrifuged for 10 min at 200× *g*. The resulting PRP was diluted with CGS buffer (120 mM NaCl, 12.9 mM trisodium citrate dihydrate, 30 mM d-glucose, pH 6.5) at a ratio of 1:1. For leukocyte depletion, the PRP was centrifuged for 10 min at 69× *g*. The resulting supernatant was subsequent centrifuged for 10 min at 400× *g*. The resulting pellet was resuspended in CGS buffer and again centrifuged for 10 min at 400× *g*. The platelets were resuspended in 1× PBS for flow cytometry [56].

4.2. Isolation and Stimulation of Human T Cell Populations

$CD4^+CD25^-$ T cells were isolated from buffy coat, as previously described [57]. The purity of the isolated $CD4^+CD25^-$T cells was around 98%, as checked by flow cytometry (Figure A6). For proliferation assays, cells were labeled with carboxyfluorescein succinimidyl ester (CFSE) and cultured in 48 well plates at 10^6 cells/mL in X-Vivo 15 (Lonza, #BE02-060F, Basel, Switzerland). Percentage of proliferating cells was defined as cells with less CFSE signal than the initial signal strength of the unstimulated cells at the start of the assay. Cells were stimulated with 0.5 µg/mL anti-CD3 mAb (Clone OKT3) and 1 µg/mL anti-CD28 mAb (Clone 28.2, BD Pharmingen #555725, Heidelberg, Germany) in the presence or absence of different ratios of platelets and 10 µg/mL anti-GARP Ab (Origene AP17415PU-N, Rockland, MD, USA), 10 U/mL thrombin (Sigma-Aldrich #T7009-250UN, Munich, Germany), 10 µM TRAP-6 (H-Ser-Phe-Leu-Leu-Ag-Asn-OH trifluoroacetate salt (#4017752), Bachem Holding AG, Bubendorf, Switzerland), 10 µg/mL anti-TGF-β I-III (R&D Systems #MAB1835R), and anti-TGF-β receptor II (R&D Systems #AF-241-NA) at day 0, as indicated. For pre-blockade of TGF-β receptor II on $CD4^+CD25^-$ T cells, we incubated T cells with 10 µg/mL anti-TGF-β receptor II Ab for 15 min. The remaining unbound antibody was removed by washing cells with X-Vivo (Lonza, #BE02-060F, Basel, Switzerland)15 for 5 min at 400× *g*, twice. Alternatively, T cells were cocultured with PCM at the ratio indicated and proliferation was analyzed as described. For suppression assays, platelet-conditioned T cells (iTreg) were isolated from culture after 6 days, washed, and cocultured in a new assay with $CD4^+$ T effector cells (Teff) for an additional 3 days at the ratio indicated. Cells were restimulated with 0.5 µg/mL anti-CD3 plus irradiated (90Gy) peripheral blood mononuclear cells PBMC. Proliferation was measured by Ki-67 staining via flow cytometry. Positive Ki-67 resembles proliferating cells instead of Ki-67 low cells.

4.3. Enzyme-Linked Immunosorbent Assay

Soluble GARP was analyzed by enzyme-linked immunosorbent assay (ELISA), according to the manufacturer's protocol (R&D Systems #DY6055, Wiesbaden, Germany).

4.4. Flow Cytometry

For flow cytometric analysis, cells were stained with fixable viability dye (Thermo Fisher #65-0865-14, Dreieich, Germany) prior to the antibody surface staining of anti-CD4 (BD Pharmingen #555348, Heidelberg, Germany), anti-CD41a (eBioscience #11-0419-42, Dreieich, Germany), anti-CD62P (ImmunoTools #21270624, Friesoythe, Germany), and anti-GARP (Miltenyi #130-103-820, Bergisch Gladbach, Germany). For intranuclear staining of FoxP3 or intracellular staining of IFN-γ and IL-2, cells were fixed and permeabilized with the Foxp3/Transcription Factor Staining Buffer Kit (eBioscience #00-5523-00, Dreieich, Germany) and subsequently stained with anti-Foxp3 (BioLegend #320208, San Diego, USA), anti-IL-2 (eBioscience #17-7049-42, Dreieich, Germany), and anti- IFN-γ (BD Biosciences #557643, Heidelberg, Germany). After 6 days of culture, T cells were harvested and expression of the cytokines IL-2 and IFN-γ were analyzed in T cells stimulated with 50 ng/mL phorbol 12-myristate 13-acetate (PMA; Sigma Aldrich #P1585-1MG, Munich, Germany) and 1 µg/mL ionomycin (Enzo Life Sciences #ALX-450-006-M001, Lörrach, Germany) in the presence of monensin (1.3 µM) (BD,#554724, Heidelberg, Germany) for 5 h. Cells were then permeabilized as described above and stained. Only live cells were included into the analysis (Figure A7). Flow cytometry was performed on an BD LSRII and BD Accuri C6 flow cytometer (BD Biosciences, Heidelberg, Germany) and analyzed using Cytobank software (Cytobank.org, Santa Clara, USA; [58] and the FACSVia Software (BD Biosciences, Heidelberg, Germany).

4.5. Patients

Patient samples were obtained from melanoma patients at different stages of disease after informed written consent. The study protocol (837.226.05 (4884)) was approved by the local ethics committee of Rhineland-Palatinate and Hessen (Landesärztekammer). All procedures in studies involving human participants were performed in accordance with the 1964 Declaration of Helsinki and its later amendments or comparable ethical standards. In the initial primary cohort, GARP expression on platelets and platelet activation status was measured from the blood of stage I (n = 18) and stage IV (n = 17) melanoma patients, of which 16 out of 17 patients responded to immunotherapy, by using flow cytometry. Therein, PRP was isolated as described, and platelets were stained for GARP and CD62P using flow cytometry. Next, platelet counts of the second retrospective cohort of stage IV melanoma patients undergoing checkpoint inhibitor treatment were analyzed in order to investigate platelet numbers, platelet–lymphocyte ratios, and therapy outcome in these patients (Table 1). Therefore, routine blood tests were performed during follow-up. Therapies included the checkpoint inhibitors ipilimumab (Yervoy, BMS, New York, USA), nivolumab (Opdivo, BMS, New York, NY, USA), and pembrolizumab (Keytruda, MSD, Haar, Germany). Patients were divided into non-responders (progressive disease) and responders (complete response, partial response, or stable disease) according to Response Evaluation Criteria in Solid Tumors (RECIST) criteria in routine staging.

4.6. Statistics

Statistical analysis was performed using GraphPad Prism version 8.0.0 for Windows (GraphPad Software, San Diego, CA, USA, www.graphpad.com). Results were normalized to the untreated (*w/o*) samples as indicated. Bar diagrams and scatter plots display mean ± standard deviation (SD). Box and whiskers plots display median with the 25th and 75th percentiles and minimum to maximum whiskers. Statistical significance was determined using one-way ANOVA, Kruskal–Wallis test, and unpaired Student's t-test, as indicated in the figure legends with * $p < 0.05$, ** $p \leq 0.01$, *** $p \leq 0.001$, and not significant. Not significant is indicated by p-values > 0.05.

Table 1. Patient characteristics.

Cohort 1. Analysis of Platelet GARP and CD62p Expression Levels	***n***	**%**
Patients	35	100
Stage I	18	51
Stage IV (responders)	17 (16)	49
Cohort 2. Retrospective Analysis of Platelet Count and PLR	***n***	**%**
Patients	39	100
Responder	11	28
Non-responder	25	64
Unknown outcome, lost to follow-up	3	8

5. Conclusions

Our data show, for the first time, that platelets are able to induce regulatory T cells in a GARP-dependent manner. Furthermore, melanoma patients with a high platelet count showed a reduced responsiveness to immunotherapy and a significantly increased expression of GARP on platelets. This could be of great importance, as thrombocytosis is associated with poor prognosis and metastasis in cancer. Our data implicate that the targeting of platelets in cancer could be a potential impactful new supplementary approach in addition to standard immunotherapy.

Author Contributions: Conceptualization, A.T., K.J. and N.Z.; methodology, N.Z., F.K.K., S.Z., H.M.-R. and E.J.K.; validation, N.Z.; formal analysis, F.K.K., S.Z. and N.Z.; resources, A.T.; writing—original draft preparation, A.T. and N.Z.; writing—review and editing, K.J., F.K.K., C.L. and S.G.; supervision, A.T.; project administration, N.Z.; funding acquisition, A.T. All authors have read and agreed to the published version of the manuscript.

Funding: This work was supported by the Wilhelm-Sander Stiftung and SFB 1066-B3 to A.T.

Acknowledgments: Results are part of the doctoral thesis of N.Z. We thank E. Trzeciak for critically revising the manuscript. Figure A3 was adapted from Servier Medical Art (https://smart.servier.com/) under CC BY 3.0 license (https://creativecommons.org/licenses/by/3.0/legalcode).

Conflicts of Interest: The authors declare no conflict of interest.

Appendix A.

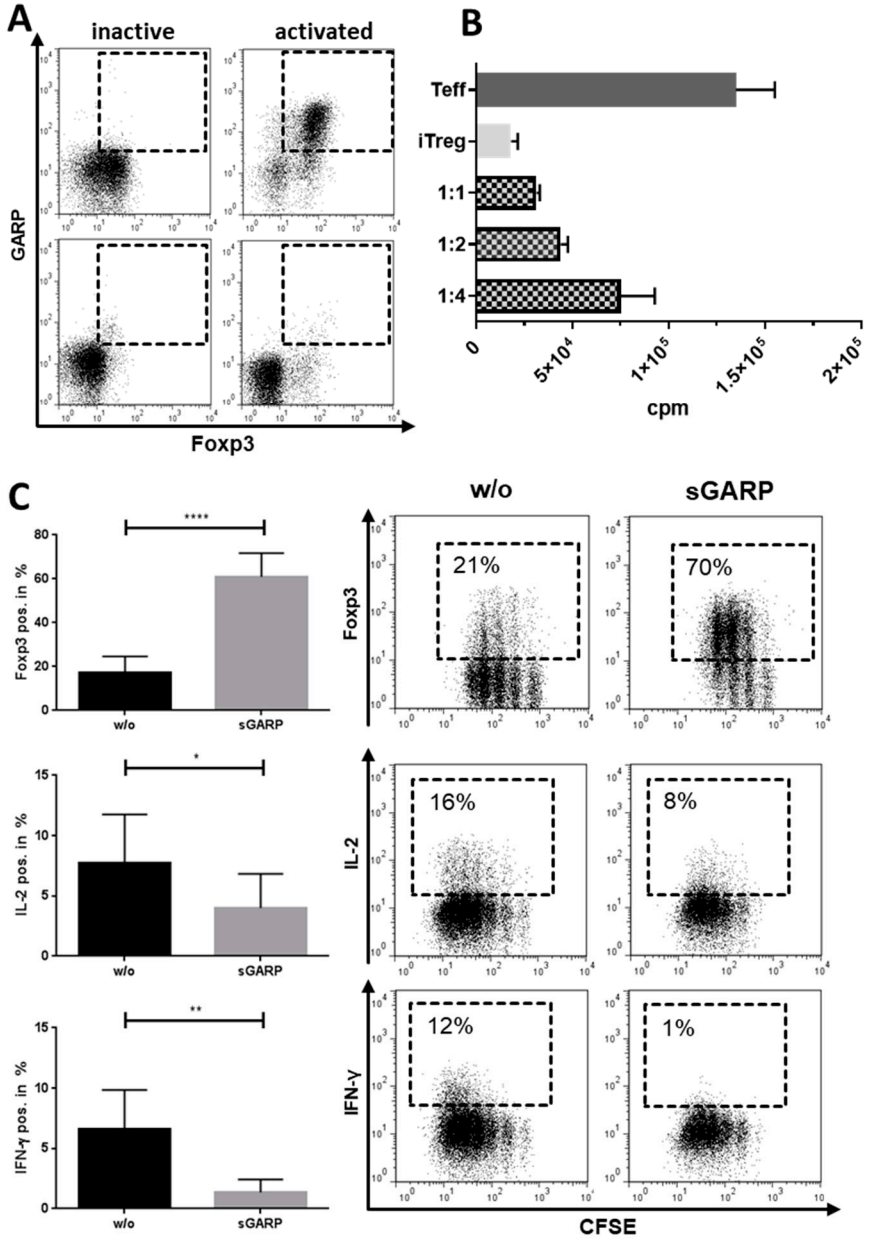

Figure A1. sGARP induced Treg. (**A**) GARP expression on Treg vs. Teff: GARP is an activation marker on Treg. 16h after stimulation, $CD4^+$ $CD25^+$ Treg showed a strong GARP expression compared to $CD4^+CD25^-$ Teff. One representative dot plot of four different experiments is shown. (**B**) Suppressive capacity of sGARP-conditioned T cells. $CD4^+CD25^-$ T cells were stimulated with 0.5 µg/mL anti-CD3 mAb and 1.0 µg/mL anti-CD28 mAb for 6 days in the presence of 10 µg/mL sGARP, resulting in Treg. Simultaneously, allogenic Teff were generated without the use of sGARP. After 6 days of stimulation, Teff and titrated Treg were cocultured and re-stimulated with anti-CD3 mAb and irradiated PBMC. After 4 days, proliferation was determined by tritiated thymidine (^{3}H TdR) pulse. Results show the pooled data of three independent experiments. (**C**) sGARP induction of FoxP3, inhibition of proliferation, and inhibition of effector cytokine production in $CD4^+$ T cells (n = 3, means ± SD, * $p < 0.05$, ** $p \leq 0.01$, **** $p \leq 0.0001$, and n.s. determined by one-way ANOVA).

Appendix B.

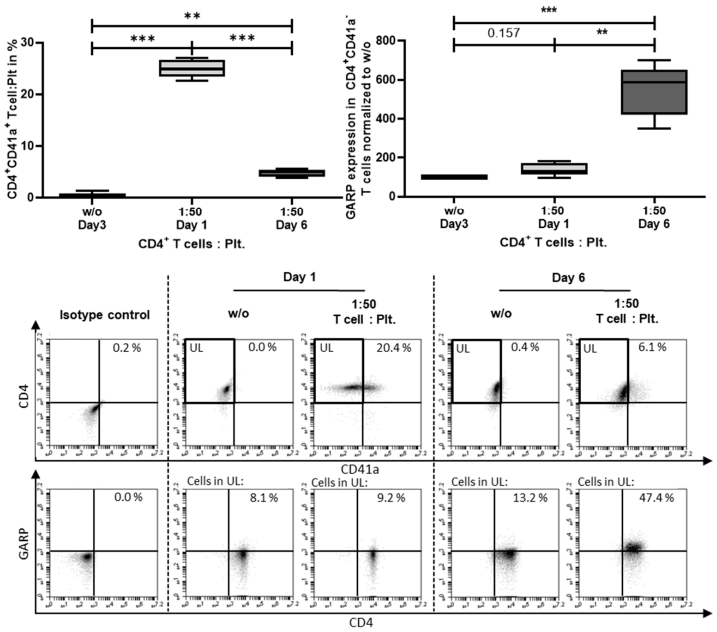

Figure A2. Platelets bound to T cells upon activation in coculture. $CD4^+CD25^-$ T cells were cocultured with or without platelets at the ratio of 1:50 and stimulated with 0.5 µg/mL anti-CD3 mAb and 1.0 µg/mL anti-CD28 mAb for 6 days. At day 1 and 6, platelet–T cell conjugates ($CD41a^+CD4^+$ double-positive cells) were analyzed via flow cytometry. For assessment of GARP expression, only $CD4^+$CD41a- cells were included in the analysis (indicated by the pregating on the upper left (UL)). GARP expression was normalized to the untreated (w/o) control. Dot plots show one representative result of five independent experiments. Isotype controls are shown ($n = 5$, box and whiskers, medians + min/max, ** $p \leq 0.01$, *** $p \leq 0.001$, and n.s. determined by one-way ANOVA).

Appendix C.

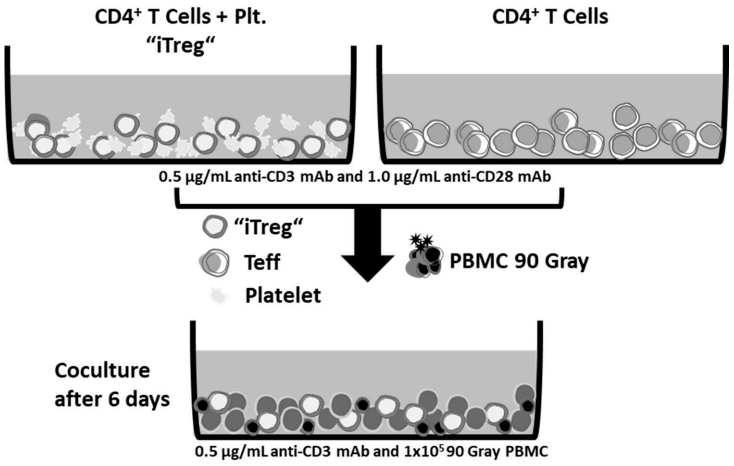

Figure A3. Experimental setup of a platelet-conditioned T cell suppression assay. 1×10^6 $CD4^+CD25^-$ T cells were stimulated with 0.5 µg/mL anti-CD3 mAb and 1.0 µg/mL anti-CD28 mAb with or without 50×10^6 platelets for 6 days. T cells cocultured with platelets developed an iTreg-like phenotype, whereas T cells cultured without platelets displayed a Teff phenotype. Next, iTreg and Teff were cultured at different ratios (iTreg/Teff: 1:1, 1:2, 1:4, and the corresponding controls) and restimulated with 0.5 µg/mL anti-CD3 mAb and 90Gy irradiated PBMC. Proliferation (Ki-67) was measured via flow cytometry 3 days after restimulation.

Appendix D.

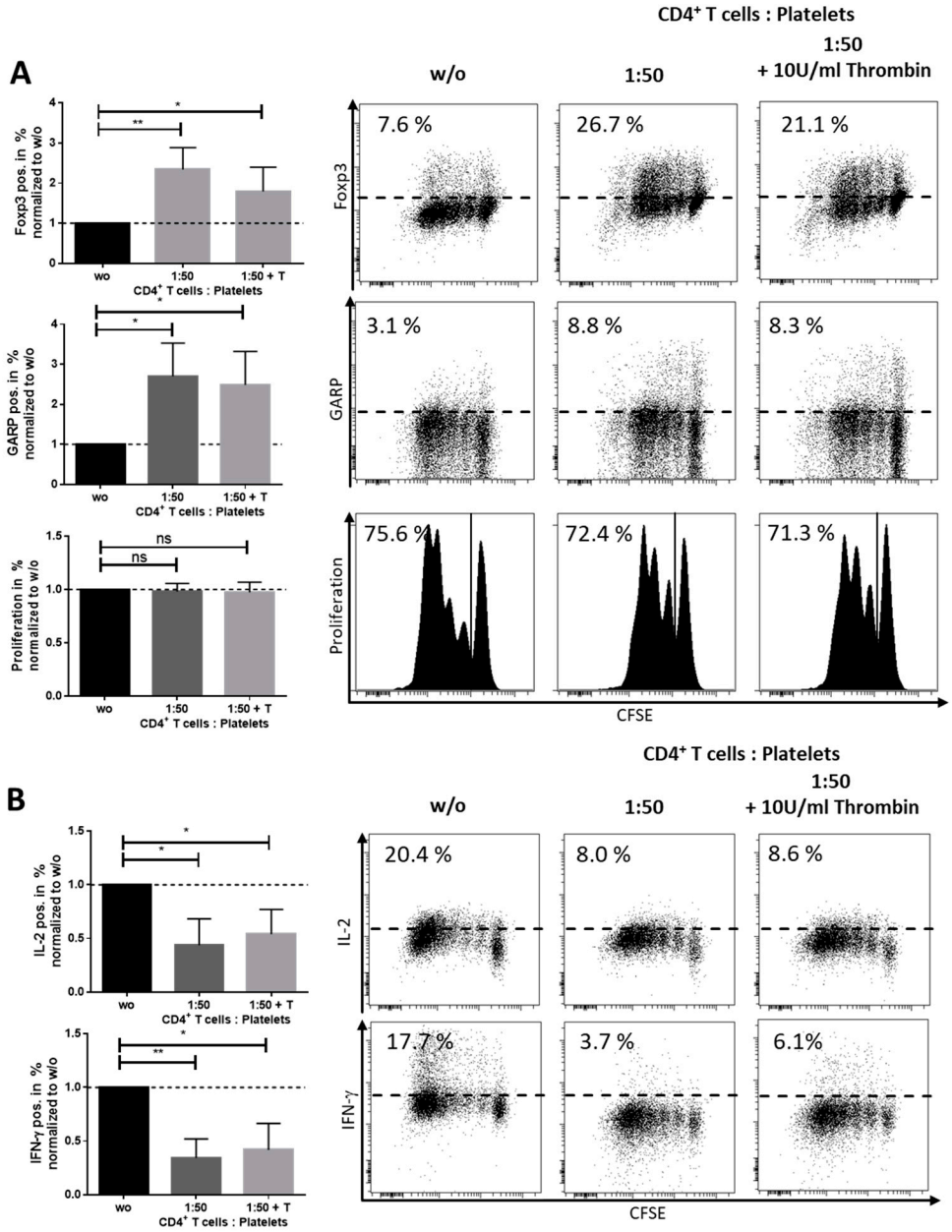

Figure A4. Thrombin-activated platelets induced a regulatory phenotype in $CD4^+CD25^-$ T cells. 1×10^6 $CD4^+CD25^-$ T cells were stimulated with 0.5 µg/mL anti-CD3 mAb and 1.0 µg/mL anti-CD28 mAb with or without 50×10^6 platelets for 6 days and treated with or without 10 U/mL thrombin. (**A**) Foxp3 and GARP expression and proliferation were determined at day 3 via flow cytometry. (**B**) Using intracellular flow cytometry, we analyzed cytokine production of IL-2 and IFN-γ on day 6. Dot plots show one representative result of five independent experiments ($n = 5$, box and whiskers, medians ± min/max, * $p < 0.05$, ** $p \leq 0.01$, and n.s. determined by one-way ANOVA).

Appendix E.

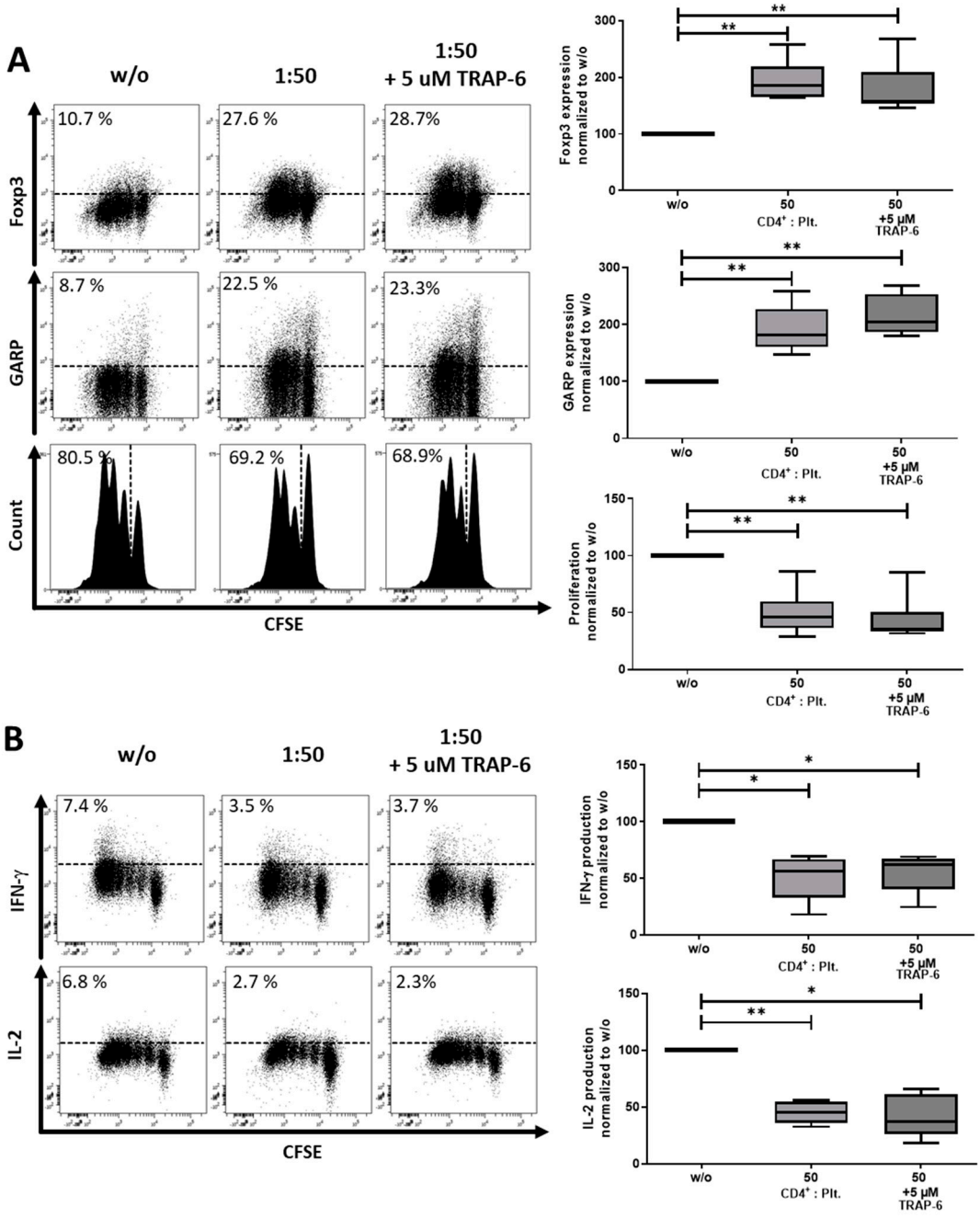

Figure A5. TRAP-6-activated platelets induced a regulatory phenotype in $CD4^+CD25^-$ T cells. 1×10^6 $CD4^+CD25^-$ T cells were stimulated with 0.5 µg/mL anti-CD3 mAb and 1.0 µg/mL anti-CD28 mAb with or without 50×10^6 platelets for 6 days and treated with or without 5 µM TRAP-6. (**A**) Foxp3 and GARP expression and proliferation were determined at day 3 via flow cytometry. (**B**) Using intracellular flow cytometry, we analyzed cytokine production of IL-2 and IFN-γ on day 6. Dot plots show one representative result of five independent experiments ($n = 5$, box and whiskers, medians ± min/max, * $p < 0.05$, ** $p \leq 0.01$, and n.s. determined by one-way ANOVA).

Appendix F.

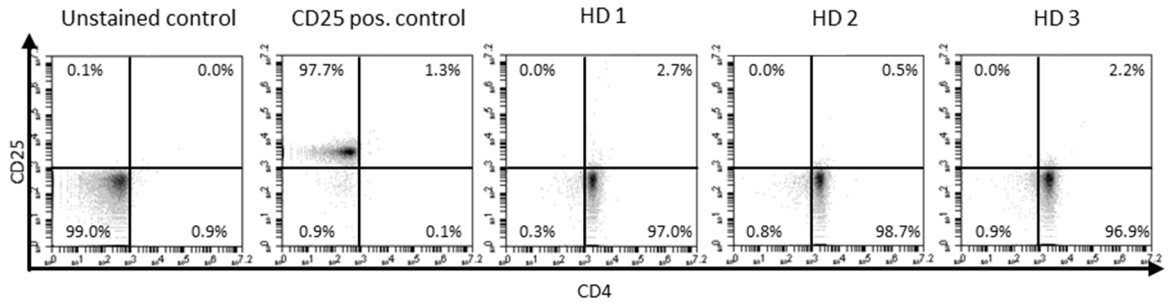

Figure A6. Flow cytometric analysis of T cell purity. $CD4^+CD25^-$ cells showed a purity of around 98% after isolation. $CD4^+CD25^-$ T cells were isolated as described in the manuscript. Shown are the unstained control, the CD25-positive staining control, and successful $CD4^+CD25^-$ isolations of three different healthy donors.

Appendix G.

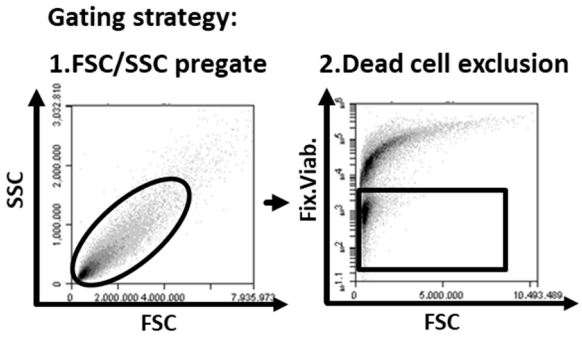

Figure A7. Gating strategy. Cells were pregated via forward- and side scatter (FSC/SSC) following a dead cell exclusion via fixable viability dye.

References

1. Schupp, J.; Krebs, F.K.; Zimmer, N.; Trzeciak, E.; Schuppan, D.; Tuettenberg, A. Targeting myeloid cells in the tumor sustaining microenvironment. *Cell. Immunol.* **2019**, *343*, 103713. [CrossRef] [PubMed]
2. Yap, M.L.; McFadyen, J.D.; Wang, X.; Ziegler, M.; Chen, Y.-C.; Willcox, A.; Nowell, C.J.; Scott, A.M.; Sloan, E.K.; Hogarth, P.M.; et al. Activated platelets in the tumor microenvironment for targeting of antibody-drug conjugates to tumors and metastases. *Theranostics* **2019**, *9*, 1154–1169. [CrossRef] [PubMed]
3. Huong, P.T.; Nguyen, L.T.; Nguyen, X.-B.; Lee, S.K.; Bach, D.-H. The Role of Platelets in the Tumor-Microenvironment and the Drug Resistance of Cancer Cells. *Cancers* **2019**, *11*, 240. [CrossRef] [PubMed]
4. McAllister, S.S.; Weinberg, R.A. The tumour-induced systemic environment as a critical regulator of cancer progression and metastasis. *Nat. Cell Biol.* **2014**, *16*, 717–727. [CrossRef] [PubMed]
5. Palumbo, J.S.; Talmage, K.E.; Massari, J.V.; La Jeunesse, C.M.; Flick, M.J.; Kombrinck, K.W.; Jirousková, M.; Degen, J.L. Platelets and fibrin(ogen) increase metastatic potential by impeding natural killer cell-mediated elimination of tumor cells. *Blood* **2005**, *105*, 178–185. [CrossRef] [PubMed]
6. Camerer, E.; Qazi, A.A.; Duong, D.N.; Cornelissen, I.; Advincula, R.; Coughlin, S.R. Platelets, protease-activated receptors, and fibrinogen in hematogenous metastasis. *Blood* **2004**, *104*, 397–401. [CrossRef]
7. Orellana, R.; Kato, S.; Erices, R.; Bravo, M.L.; Gonzalez, P.; Oliva, B.; Cubillos, S.; Valdivia, A.; Ibañez, C.; Brañes, J.; et al. Platelets enhance tissue factor protein and metastasis initiating cell markers, and act as chemoattractants increasing the migration of ovarian cancer cells. *BMC Cancer* **2015**, *15*, 290. [CrossRef]
8. Karpatkin, S.; Pearlstein, E.; Ambrogio, C.; Coller, B.S. Role of adhesive proteins in platelet tumor interaction in vitro and metastasis formation in vivo. *J. Clin. Invest.* **1988**, *81*, 1012–1019. [CrossRef]

9. Stone, R.L.; Nick, A.M.; McNeish, I.A.; Balkwill, F.; Han, H.D.; Bottsford-Miller, J.; Rupairmoole, R.; Armaiz-Pena, G.N.; Pecot, C.V.; Coward, J.; et al. Paraneoplastic thrombocytosis in ovarian cancer. *N. Engl. J. Med.* **2012**, *366*, 610–618. [CrossRef]
10. Sierko, E.; Wojtukiewicz, M.Z. Platelets and angiogenesis in malignancy. *Semin. Thromb. Hemost.* **2004**, *30*, 95–108. [CrossRef]
11. Schumacher, D.; Strilic, B.; Sivaraj, K.K.; Wettschureck, N.; Offermanns, S. Platelet-derived nucleotides promote tumor-cell transendothelial migration and metastasis via P2Y2 receptor. *Cancer Cell* **2013**, *24*, 130–137. [CrossRef] [PubMed]
12. Wojtukiewicz, M.Z.; Sierko, E.; Hempel, D.; Tucker, S.C.; Honn, K.V. Platelets and cancer angiogenesis nexus. *Cancer Metastasis Rev* **2017**, *36*, 249–262. [CrossRef] [PubMed]
13. Waldmann, T.A. Cytokines in Cancer Immunotherapy. *Cold Spring Harb. Perspect. Biol.* **2018**, *10*. [CrossRef] [PubMed]
14. Wang, S.; Li, Z.; Xu, R. Human Cancer and Platelet Interaction, a Potential Therapeutic Target. *Int. J. Mol. Sci.* **2018**, *19*, 1246. [CrossRef] [PubMed]
15. Li, N. Platelets in cancer metastasis: To help the "villain" to do evil. *Int. J. Cancer* **2016**, *138*, 2078–2087. [CrossRef] [PubMed]
16. Buergy, D.; Wenz, F.; Groden, C.; Brockmann, M.A. Tumor-platelet interaction in solid tumors. *Int. J. Cancer* **2012**, *130*, 2747–2760. [CrossRef]
17. Labelle, M.; Begum, S.; Hynes, R.O. Platelets guide the formation of early metastatic niches. *Proc. Natl. Acad. Sci. USA* **2014**, *111*, E3053-61. [CrossRef]
18. Mezouar, S.; Frère, C.; Darbousset, R.; Mege, D.; Crescence, L.; Dignat-George, F.; Panicot-Dubois, L.; Dubois, C. Role of platelets in cancer and cancer-associated thrombosis: Experimental and clinical evidences. *Thrombosis Research* **2016**, *139*, 65–76. [CrossRef]
19. Zhang, N.; Zhang, W.-J.; Cai, H.-Q.; Liu, H.-L.; Peng, L.; Li, C.-H.; Ye, L.-Y.; Xu, S.-Q.; Yang, Z.-H.; Lou, J.-N. Platelet adhesion and fusion to endothelial cell facilitate the metastasis of tumor cell in hypoxia-reoxygenation condition. *Clin. Exp. Metastasis* **2011**, *28*, 1–12. [CrossRef]
20. Marcolino, E.; Siddiqui, Y.H.; van den Bosch, M.; Poole, A.W.; Jayaraman, P.-S.; Gaston, K. Blood platelets stimulate cancer extravasation through TGFβ-mediated downregulation of PRH/HHEX. *Oncogenesis* **2020**, *9*, 10. [CrossRef]
21. Ballerini, P.; Dovizio, M.; Bruno, A.; Tacconelli, S.; Patrignani, P. P2Y12 Receptors in Tumorigenesis and Metastasis. *Front. Pharmacol.* **2018**, *9*, 66. [CrossRef]
22. Li, W.-H.; Qiu, Y.; Zhang, H.-Q.; Liu, Y.; You, J.-F.; Tian, X.-X.; Fang, W.-G. P2Y2 receptor promotes cell invasion and metastasis in prostate cancer cells. *Br. J. Cancer* **2013**, *109*, 1666–1675. [CrossRef] [PubMed]
23. Labelle, M.; Begum, S.; Hynes, R.O. Direct signaling between platelets and cancer cells induces an epithelial-mesenchymal-like transition and promotes metastasis. *Cancer Cell* **2011**, *20*, 576–590. [CrossRef] [PubMed]
24. Novitskiy, S.V.; Pickup, M.W.; Chytil, A.; Polosukhina, D.; Owens, P.; Moses, H.L. Deletion of TGF-β signaling in myeloid cells enhances their anti-tumorigenic properties. *J. Leukoc. Biol.* **2012**, *92*, 641–651. [CrossRef] [PubMed]
25. Pang, Y.; Gara, S.K.; Achyut, B.R.; Li, Z.; Yan, H.H.; Day, C.-P.; Weiss, J.M.; Trinchieri, G.; Morris, J.C.; Yang, L. TGF-β signaling in myeloid cells is required for tumor metastasis. *Cancer Discov.* **2013**, *3*, 936–951. [CrossRef] [PubMed]
26. Leblanc, R.; Peyruchaud, O. Metastasis: new functional implications of platelets and megakaryocytes. *Blood* **2016**, *128*, 24–31. [CrossRef] [PubMed]
27. Cravioto-Villanueva, A.; Luna-Perez, P.; La Gutierrez-de Barrera, M.; Martinez-Gómez, H.; Maffuz, A.; Rojas-Garcia, P.; Perez-Alvarez, C.; Rodriguez-Ramirez, S.; Rodriguez-Antezana, E.; Ramirez-Ramirez, L. Thrombocytosis as a predictor of distant recurrence in patients with rectal cancer. *Arch. Med. Res.* **2012**, *43*, 305–311. [CrossRef]
28. Weber, M.R.; Zuka, M.; Lorger, M.; Tschan, M.; Torbett, B.E.; Zijlstra, A.; Quigley, J.P.; Staflin, K.; Eliceiri, B.P.; Krueger, J.S.; et al. Activated tumor cell integrin αvβ3 cooperates with platelets to promote extravasation and metastasis from the blood stream. *Thromb. Res.* **2016**, *140*, S27–S36. [CrossRef]

29. Heinmöller, E.; Weinel, R.J.; Heidtmann, H.H.; Salge, U.; Seitz, R.; Schmitz, I.; Müller, K.M.; Zirngibl, H. Studies on tumor-cell-induced platelet aggregation in human lung cancer cell lines. *J. Cancer Res. Clin. Oncol.* **1996**, *122*, 735–744. [CrossRef]
30. Honn, K.V.; Tang, D. Hemostasis and malignancy: an overview. *Cancer Metastasis Rev.* **1992**, *11*, 223–226. [CrossRef]
31. Wilson, E.B.; El-Jawhari, J.J.; Neilson, A.L.; Hall, G.D.; Melcher, A.A.; Meade, J.L.; Cook, G.P. Human tumour immune evasion via TGF-β blocks NK cell activation but not survival allowing therapeutic restoration of anti-tumour activity. *PLoS ONE* **2011**, *6*, e22842. [CrossRef] [PubMed]
32. Nieswandt, B.; Hafner, M.; Echtenacher, B.; Männel, D.N. Lysis of tumor cells by natural killer cells in mice is impeded by platelets. *Cancer Res.* **1999**, *59*, 1295–1300. [PubMed]
33. Guo, S.-W.; Du, Y.; Liu, X. Platelet-derived TGF-β1 mediates the down-modulation of NKG2D expression and may be responsible for impaired natural killer (NK) cytotoxicity in women with endometriosis. *Hum. Reprod.* **2016**, *31*, 1462–1474. [CrossRef] [PubMed]
34. Placke, T.; Örgel, M.; Schaller, M.; Jung, G.; Rammensee, H.-G.; Kopp, H.-G.; Salih, H.R. Platelet-derived MHC class I confers a pseudonormal phenotype to cancer cells that subverts the antitumor reactivity of natural killer immune cells. *Cancer Res.* **2012**, *72*, 440–448. [CrossRef]
35. Wang, R.; Zhu, J.; Dong, X.; Shi, M.; Lu, C.; Springer, T.A. GARP regulates the bioavailability and activation of TGFβ. *Mol. Biol. Cell* **2012**, *23*, 1129–1139. [CrossRef]
36. Zimmer, N.; Kim, E.; Sprang, B.; Leukel, P.; Khafaji, F.; Ringel, F.; Sommer, C.; Tuettenberg, J.; Tuettenberg, A. GARP as an Immune Regulatory Molecule in the Tumor Microenvironment of Glioblastoma Multiforme. *Int. J. Mol. Sci.* **2019**, *20*, 3676. [CrossRef]
37. Hahn, S.A.; Stahl, H.F.; Becker, C.; Correll, A.; Schneider, F.-J.; Tuettenberg, A.; Jonuleit, H. Soluble GARP has potent antiinflammatory and immunomodulatory impact on human $CD4^+$ T cells. *Blood* **2013**, *122*, 1182–1191. [CrossRef]
38. Hahn, S.A.; Neuhoff, A.; Landsberg, J.; Schupp, J.; Eberts, D.; Leukel, P.; Bros, M.; Weilbaecher, M.; Schuppan, D.; Grabbe, S.; et al. A key role of GARP in the immune suppressive tumor microenvironment. *Oncotarget* **2016**, *7*, 42996–43009. [CrossRef]
39. Koupenova, M.; Clancy, L.; Corkrey, H.A.; Freedman, J.E. Circulating Platelets as Mediators of Immunity, Inflammation, and Thrombosis. *Circ. Res.* **2018**, *122*, 337–351. [CrossRef]
40. Gaertner, F.; Massberg, S. Patrolling the vascular borders: platelets in immunity to infection and cancer. *Nat. Rev. Immunol.* **2019**, *19*, 747–760. [CrossRef]
41. Metelli, A.; Wu, B.X.; Riesenberg, B.; Guglietta, S.; Huck, J.D.; Mills, C.; Li, A.; Rachidi, S.; Krieg, C.; Rubinstein, M.P.; et al. Thrombin contributes to cancer immune evasion via proteolysis of platelet-bound GARP to activate LTGF-β. *Sci. Transl. Med.* **2020**, *12*. [CrossRef] [PubMed]
42. Erpenbeck, L.; Schön, M.P. Deadly allies: the fatal interplay between platelets and metastasizing cancer cells. *Blood* **2010**, *115*, 3427–3436. [CrossRef] [PubMed]
43. Cao, W.; Yao, X.; Cen, D.; Zhi, Y.; Zhu, N.; Xu, L. Prognostic role of pretreatment thrombocytosis on survival in patients with cervical cancer: a systematic review and meta-analysis. *World J. Surg. Oncol.* **2019**, *17*, 132. [CrossRef] [PubMed]
44. Vermeersch, E.; Denorme, F.; Maes, W.; de Meyer, S.F.; Vanhoorelbeke, K.; Edwards, J.; Shevach, E.M.; Unutmaz, D.; Fujii, H.; Deckmyn, H.; et al. The role of platelet and endothelial GARP in thrombosis and hemostasis. *PLoS ONE* **2017**, *12*, e0173329. [CrossRef] [PubMed]
45. Palacios-Acedo, A.L.; Mège, D.; Crescence, L.; Dignat-George, F.; Dubois, C.; Panicot-Dubois, L. Platelets, Thrombo-Inflammation, and Cancer: Collaborating With the Enemy. *Front. Immunol.* **2019**, *10*, 1805. [CrossRef]
46. Rachidi, S.; Metelli, A.; Riesenberg, B.; Wu, B.X.; Nelson, M.H.; Wallace, C.; Paulos, C.M.; Rubinstein, M.P.; Garrett-Mayer, E.; Hennig, M.; et al. Platelets subvert T cell immunity against cancer via GARP-TGFβ axis. *Sci. Immunol.* **2017**, *2*. [CrossRef]
47. Wang, Z.; Fang, M.; Li, J.; Yang, R.; Du, J.; Luo, Y. High Platelet Levels Attenuate the Efficacy of Platinum-Based Treatment in Non-Small Cell Lung Cancer. *Cell. Physiol. Biochem.* **2018**, *48*, 2456–2469. [CrossRef]
48. Mercier, J.; Voutsadakis, I.A. The platelets-neutrophils to lymphocytes ratio: a new prognostic marker in metastatic colorectal cancer. *J. Gastrointest. Oncol.* **2018**, *9*, 478–486. [CrossRef]

49. Takenaka, Y.; Oya, R.; Kitamiura, T.; Ashida, N.; Shimizu, K.; Takemura, K.; Yamamoto, Y.; Uno, A. Platelet count and platelet-lymphocyte ratio as prognostic markers for head and neck squamous cell carcinoma: Meta-analysis. *Head Neck* **2018**, *40*, 2714–2723. [CrossRef]
50. Brockmann, M.A.; Giese, A.; Mueller, K.; Kaba, F.J.; Lohr, F.; Weiss, C.; Gottschalk, S.; Nolte, I.; Leppert, J.; Tuettenberg, J.; et al. Preoperative thrombocytosis predicts poor survival in patients with glioblastoma. *Neuro-oncology.* **2007**, *9*, 335–342. [CrossRef]
51. Hefler-Frischmuth, K.; Grimm, C.; Gensthaler, L.; Reiser, E.; Schwameis, R.; Hefler, L.A. Prognostic value of preoperative hyponatremia and thrombocytosis in patients with epithelial ovarian cancer. *Wien. Klin. Wochenschr.* **2018**, *130*, 575–580. [CrossRef] [PubMed]
52. Davis, A.N.; Afshar-Kharghan, V.; Sood, A.K. Platelet effects on ovarian cancer. *Semin. Oncol.* **2014**, *41*, 378–384. [CrossRef] [PubMed]
53. Ho-Tin-Noé, B.; Carbo, C.; Demers, M.; Cifuni, S.M.; Goerge, T.; Wagner, D.D. Innate immune cells induce hemorrhage in tumors during thrombocytopenia. *Am. J. Pathol.* **2009**, *175*, 1699–1708. [CrossRef] [PubMed]
54. Kopp, H.-G.; Placke, T.; Salih, H.R. Platelet-derived transforming growth factor-beta down-regulates NKG2D thereby inhibiting natural killer cell antitumor reactivity. *Cancer Res.* **2009**, *69*, 7775–7783. [CrossRef] [PubMed]
55. Labelle, M.; Hynes, R.O. The initial hours of metastasis: the importance of cooperative host-tumor cell interactions during hematogenous dissemination. *Cancer Discov.* **2012**, *2*, 1091–1099. [CrossRef]
56. Kumm, E.J.; Pagel, O.; Gambaryan, S.; Walter, U.; Zahedi, R.P.; Smolenski, A.; Jurk, K. The Cell Cycle Checkpoint System MAST(L)-ENSA/ARPP19-PP2A is Targeted by cAMP/PKA and cGMP/PKG in Anucleate Human Platelets. *Cells* **2020**, *9*, 472. [CrossRef]
57. Tuettenberg, A.; Huter, E.; Hubo, M.; Horn, J.; Knop, J.; Grimbacher, B.; Kroczek, R.A.; Stoll, S.; Jonuleit, H. The role of ICOS in directing T cell responses: ICOS-dependent induction of T cell anergy by tolerogenic dendritic cells. *J. Immunol.* **2009**, *182*, 3349–3356. [CrossRef]
58. Kotecha, N.; Krutzik, P.O.; Irish, J.M. Web-based analysis and publication of flow cytometry experiments. *Curr. Protoc. Cytom.* **2010**, *Chapter 10*, Unit10.17. [CrossRef]